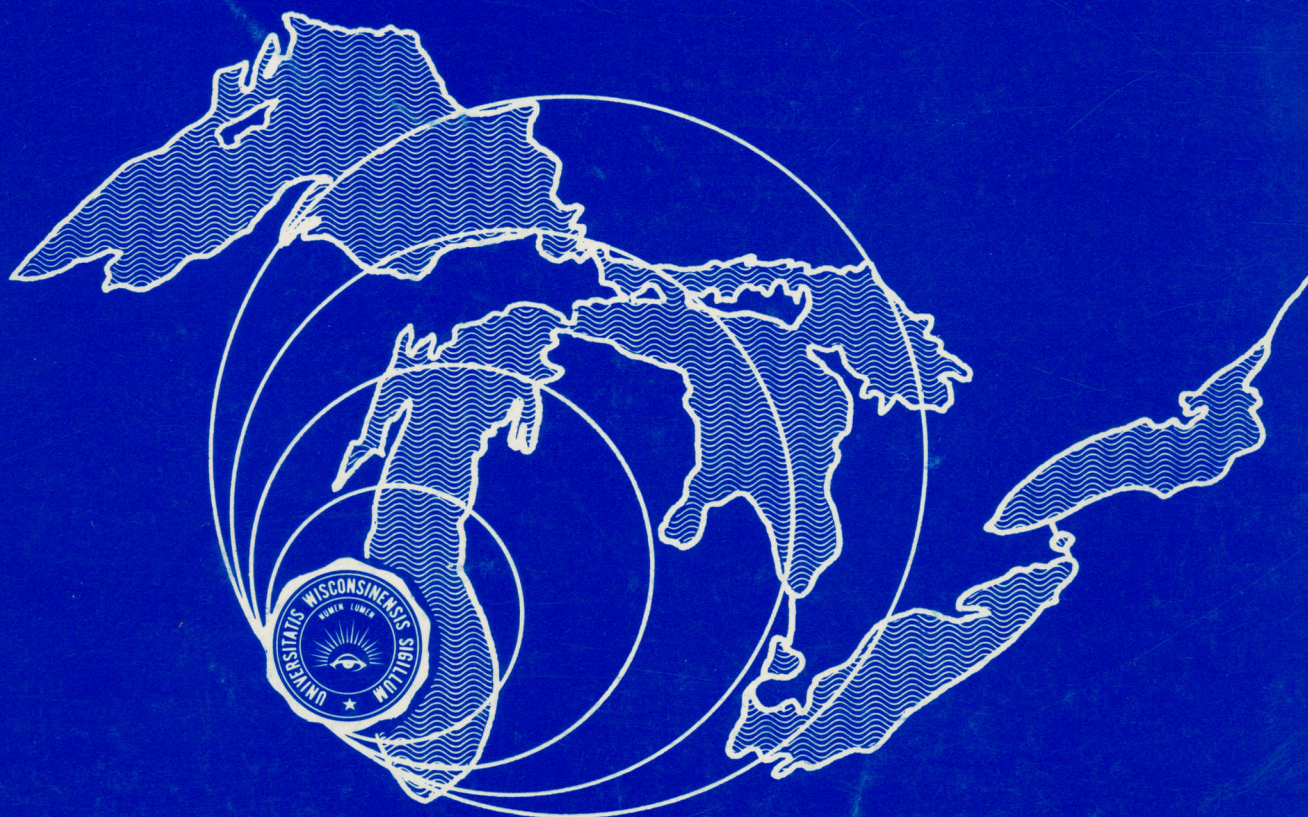


THE UNIVERSITY OF WISCONSIN—MILWAUKEE

CENTER  
FOR  
GREAT LAKES STUDIES



MILWAUKEE, WISCONSIN 53201 U.S.A.



AEC - Mortimer  
144-C039

C00-2158-12

INVESTIGATION OF THE INFLUENCE OF THERMAL DISCHARGE  
FROM A LARGE ELECTRIC POWER STATION  
ON THE TEMPERATURE AND NEAR-SHORE CIRCULATION  
OF LAKE MICHIGAN

FINAL REPORT

Special  
Report  
#22

by

G. K. SATO\* and C. H. MORTIMER (Principal Investigator)

Center for Great Lakes Studies  
The University of Wisconsin--Milwaukee  
Milwaukee, Wisconsin, USA 53201

1 August 1971 - 31 August 1974

PREPARED FOR THE U. S. ATOMIC ENERGY COMMISSION  
UNDER CONTRACT NO. AT (11-1)-2158

\*Present address: Canada Centre for Inland Waters, Burlington, Ontario.

**SPECIAL REPORT NO. 22**

**Lake Currents and Temperatures  
Near the Western Shore  
of Lake Michigan**

**by**

**G. K. SATO and C. H. MORTIMER**

**Center for Great Lakes Studies  
The University of Wisconsin--Milwaukee  
Milwaukee, Wisconsin, USA 53201**

**MARCH, 1975**

## Table of Contents

	<u>Page No.</u>	
Acknowledgements	iv	
Abstract and Conclusions	v	
Chapter 1. <u>Introduction</u>	1	
Rationale for this investigation	1	
Other investigations relevant to this study	2	
"Lake Michigan Basin; Lake Currents" (U.S. Dept. Interior 1967)	7	
The importance of upwelling	12	
The influence of near-inertial internal waves on offshore and nearshore currents	17	
Lake Ontario (IFYGL) investigations	24	
General conclusions from this review	29	
General plan and scope of this investigation	31	
Chapter 2. <u>Experimental design; instruments and methods used; field experience</u>	35	
Data recording -- current speed, current direction and water temperature	35	
Braincon Type 573 digital current meter	38	
Taut-line mooring system	38	
Sedar release mechanism	42	
Field experience with the current meters and their mooring systems	45	
Data processing and analysis of instrument malfunctions	50	
Wind measurements	55	
Data analysis	55	
Chapter 3. <u>The observations: monthly plots of wind, current, and temperature</u>	61	
Chapter 4. <u>Analysis of current records and current-wind relationships</u>	157	
	Page Nos. in	
	<u>Cha. 3</u>	<u>Cha. 4</u>
Survey I, 3 April to 5 June 1972	62	159
Survey II, 5 June to 25 August 1972	77	180
Survey III, 25 August to 7 December 1972	105	201
Survey IV, 12 April to 17 July 1973	120	219
Survey V, 17 July to 13 August 1973	136	234
Survey VI, 15 August to 7 November 1973	136	235

## Table of Contents, Continued

	<u>Page No.</u>
Chapter 5. <u>Sinking plumes</u>	259
Discussion of sinking plumes	271
Chapter 6. <u>Summarizing discussion and analysis</u>	273
Persistence factors	273
Response to wind, particularly to wind reversals	276
The rotary, near-inertial current component; definition of the "nearshore" zone	285
Water temperature	287
Spectral and cross-spectral analyses of currents (deferred from Chapter 4)	288
References	308
Figure legends and table headings	313

## Acknowledgements

The field work and report preparation for this investigation proved to be more arduous and complicated than envisioned at the outset. We are therefore grateful to the Atomic Energy Commission for supporting this study, but also for their patience in awaiting the published results. Our special thanks are also due to Mr. Donald Mraz, the crew of R/V NEESKAY, Mr. Robert Scott (machinist) and Mr. David Baumgartner (instrument specialist) for considerable help in construction, field work, and data reduction. For the preparation of figures and report drafts we are also grateful to Mr. Ratko Ristic and Mrs. Kathie Lehnhardt, respectively.

## ABSTRACT AND CONCLUSIONS

The objective of this investigation, planned to provide the physical background for a biological study (Beeton and Barker 1974) was a description of the variability of nearshore current regimes and temperature fields in the neighbourhood of the Wisconsin Electric Company's fossil-fueled, lake-cooled power plant at Oak Creek, Wisconsin. Attention was paid, not to plume geometry and behaviour in the near field (except for a study of sinking plumes in winter, Chapter 5), but to the ambient Lake motions into which the plumes are being discharged.

An array of recording current meters and thermographs was moored in an area of approximately 15 km alongshore, and the same distance offshore, to provide 10-minute readings of current speed, current direction, and temperature. Up to 10 stations were occupied, although not all at the same time, from April 1972 and April to November 1973 (figure 2.1 and table 2.1). Water depths ranged from 12 to 46 m and, at the four deepest stations, instruments were placed at two depths, typically 12 and 23 m. At other stations the depth of single instruments ranged from 10 to 17 m.

The total body of current and temperature data, and wind data from the nearby Milwaukee airport, is presented with descriptive text in monthly diagrams in Chapter 3 and is further analyzed by means of vector frequency and progressive vector diagrams in Chapter 4, with summarizing discussion in Chapter 6. Chapter 5 -- self-contained with discussion -- presents results of five sinking plume surveys made when the plume-receiving lake water was at a temperature below 4°C.

The currents in the coastal region here investigated proved to be mainly responsive to the direction of the wind (Chapter 3). Because the general orientation of the shoreline and bottom contours at Oak Creek is SSE-NNW, with Wind Point, Racine, providing some protection from winds from due south, our measurements amply confirmed the expectation that the currents

would respond most strongly to winds from the sector N to SE -- i. e. winds with the maximum overwater path (fetch) and least strongly to winds from SW to W, with the least fetch. The adjustment of the current to wind stress, shoreline orientation, and the Coriolis force resulted in a generally shore-parallel current regime, with flows toward SSE for most of the time, but frequently interrupted by periods of northgoing currents and by episodes of very weak currents. The latter were associated with weak or westerly winds. Although not confirmed by water level measurements, we must infer from the shore-parallel flow patterns that the wind-initiated currents often approached geostrophic equilibrium, as did also the currents accompanying upwelling and downwelling motions disclosed by the temperature records discussed below.

At the shallow-water stations, current speeds were generally greater, and responses to changes in wind regime were more rapid and more frequent, than at the deeper-water stations. Large changes or reversals in wind direction were generally followed, after a lag interval, by reversals in current direction. The lag length differed with station depth -- being least in shallowest stations -- and with current and wind strength before the wind reversed. The lag length varied from 2 to 69 hours (tables 6.4 and 6.5) with average values of 6.8 and 10.9 hours for north to south reversals in 1972 and 1973, respectively, and 7.4 and 10.6 hours for south to north reversals during 1972 and 1973, respectively. At the deeper-water stations the current sometimes failed to reverse after a wind reversal, even though currents in shallow water had done so. In such cases, large horizontal shears were generated.

Vector frequency diagrams and progressive vector diagrams for monthly or shorter intervals (Chapter 4) confirmed the predominantly shore-parallel current patterns with greater flow tendency towards SSE. Current speeds were very variable, monthly means were commonly as low as  $5 \text{ cm sec}^{-1}$ , but such means included episodes of very weak currents (less than  $4 \text{ cm sec}^{-1}$ ) which in total may have occupied half the month. The current speeds in the other half ranged from 4 to over  $30 \text{ cm sec}^{-1}$ . A commonly observed response to the onset of strong winds was a rapid rise in current speed, followed by a slower decrease after the winds had abated. This, we

believe, is an important property of coastal currents in the Great Lakes, which could provide the basis for estimating frictional forces, not attempted here (see figure 6.1).

Mean monthly current vectors were computed, as were also per-  
sistence factors (defined and tabulated in Chapter 6, table 6.1, 6.2), to provide an index of the persistence of flow in the direction of the resultant vector. On a scale from zero to unity, the monthly persistence factors varied from 0.3 to 0.75, with resultant vectors conforming to the shore-parallel, predominantly southward flow. Persistence factors were lowest for station 3, located near Wind Point, Racine, reflecting the greater variability at that station.

Before stratification had become established in June, temperature records showed steady increases and no large variations, but after stratification the effects of upwelling and downwelling events became apparent, associated with north-going and south-going currents, respectively. The onset of upwelling and downwelling was signalled by a respective drop or rise in temperature, often sudden and commonly associated with a reversal in current flow. As soon as stratification had become strongly established in July and August, temperature "waves", accompanied by synchronized rotation of the current vectors at near-inertial frequency, were observed at the deeper, but not at the shallowest stations. This behaviour was the consequence of the generation of internal Poincaré waves of near-inertial frequency (Mortimer 1974). These waves and their rotary currents become the most conspicuous feature of motion in offshore waters during summer, but are masked or suppressed by predominantly shore-parallel unidirectional currents as the shoreline is approached. Since even our deepest stations showed a dominance of unidirectional flow, or a transitional mixture of unidirectional and rotational flow on some occasions, the nearshore zone at Oak Creek is therefore about 10 to 15 km wide, if defined as the zone within which unidirectional flow dominates. The similarly defined zone on the north shore of Lake Ontario

is estimated by Blanton (1974) to be 8 km wide. The fact that deeper water is nearer shore in Lake Ontario may account for this difference.

In spite of the general correlation between onshore wind and near-shore current, cross-spectral comparisons of wind and current show surprisingly low coherence when all wind directions are included (figure 6.2). Spectral and cross-spectral analyses for current and for temperature, between station pairs and between instrument pairs at the deeper stations, showed that most of the variance and the highest interstation coherences were confined to a frequency range below one cycle per day (Chapter 6). Station 3, because of its position, showed low coherence with other stations. No major oscillations were disclosed in any spectrum, although recognizable peaks were found near the inertial frequency in current and temperature spectra from deeper stations during the season of stratification.

The results of the plume surveys during winter and early spring 1972/3 are discussed at the end of Chapter 5. As anticipated, the plume was found to sink when discharged into receiving water of temperature less than 4°C. The sinking "skirt" of the plume consisted of water at temperatures near 4°C (maximum density) formed by mixing of plume and receiving waters. The extent and shape of the plume, bounded by the shoreline and the sinking skirt, varied considerably with wind and lake current conditions, although we were unable to explore the full variability because our surveys were confined to relatively calm and ice-free conditions. An impression of the variability can be gained by comparing the plume diagrams in Chapter 5. Our conclusion is that sinking at the plume's periphery represents an active offshore transport mechanism which prevents build-up or trapping of heat and materials in the plume area.

## CHAPTER ONE

### INTRODUCTION

#### Rationale for this investigation

The investigation reported here was originally proposed to provide a physical background for a study of the effects, on Lake Michigan water quality and biological populations, of a large fossil-fueled electric power plant which uses lake water for cooling. The proposal was prompted by the need to assess the nature and extent of biological damage in the Great Lakes arising from the industrial use of lake water for cooling, the largest present and projected users being fossil-fueled and nuclear power stations. While scenarios of potential biological damage by "thermal pollution" are easy to write, facts to support or refute them are much more difficult to obtain. Therefore, the existence on Lake Michigan of a large power station (Oak Creek Plant, Wisconsin Electric Power Company, generating capacity 1760 megawatts, electrical) which had been using Lake Michigan for once-through cooling for many years, prompted the Center for Great Lakes Studies to propose a combined physical and biological investigation. Although, as it turned out, the two components of the study were funded by separate branches of the Atomic Energy Commission and have been reported separately (Beeton and Barker 1974, Part A. Biology, under Contract No. AT (11-1) 2160; and this report) they may be regarded as complementary, representing interacting components of the complex physical/biological coastal system. Superimposed upon the extreme variability of this system is the pollution load from the Milwaukee metropolitan area and the localized heat load from the power station. It was anticipated at the outset that "noise" from the metropolitan pollution load would probably mask "signals" from the thermal load; and this is the general conclusion from the Beeton/Barker report.

In order to predict the influence of a cooling water effluent on a lake system it is necessary to understand not only the hydrodynamics of the "plume", but also the natural variability of the receiving water, particularly long-term

and short-term variations in the temperature and current regimes. As surveying, modelling, and verification of plume behavior is being competently and actively pursued in many institutions, for example the Argonne National Laboratory, we decided to devote most of our effort to filling the largest knowledge gap, namely the natural variance in temperature and flow regimes in the "far field" region of plume dispersal. We therefore concentrated our observations on the current and temperature patterns and their response to wind and seasonal cycles of heat flux in a zone extending not more than 10 miles (16 km) from the nearest shore point (see Table 2.1). In other words, this study is concerned, not with the geometry and hydrodynamics of the Oak Creek plume (surveys of which were made during 1972 and 1973 by Limnetics, Inc., 1974, commissioned by the Wisconsin Electric Power Company) but of the variability of the underwater "weather" into which the plume is injected and dissipated. But, as little is known as yet about the behavior of large power plant plumes in Lake Michigan in winter, we looked for and found a sinking plume at Oak Creek and surveyed its principal features in Chapter 5.

#### Other investigations directly relevant to this study

Until recently, investigations of currents in Lake Michigan have not been concentrated in nearshore zones, but have been more concerned with whole-basin patterns of surface currents (Harrington 1894, van Oosten 1963, Johnson 1960, Ayers et al. 1958) or with large-scale circulation patterns in specific sub-regions or sections of the basin (Bellaire 1963, Noble et al. 1968). All the above studies dealt principally with wind-driven currents. Thermally-driven circulations in Lake Michigan were the subject of a paper by Huang (1971). The general knowledge of circulation patterns derived from the above investigations, applying as they do to the whole basin, nevertheless provides some indication of currents near the shore, although with coarse resolution only. It became evident, however, that nearshore currents are likely to be highly variable, generally shore-parallel, and subject to frequent reversals depending on changes in the wind.

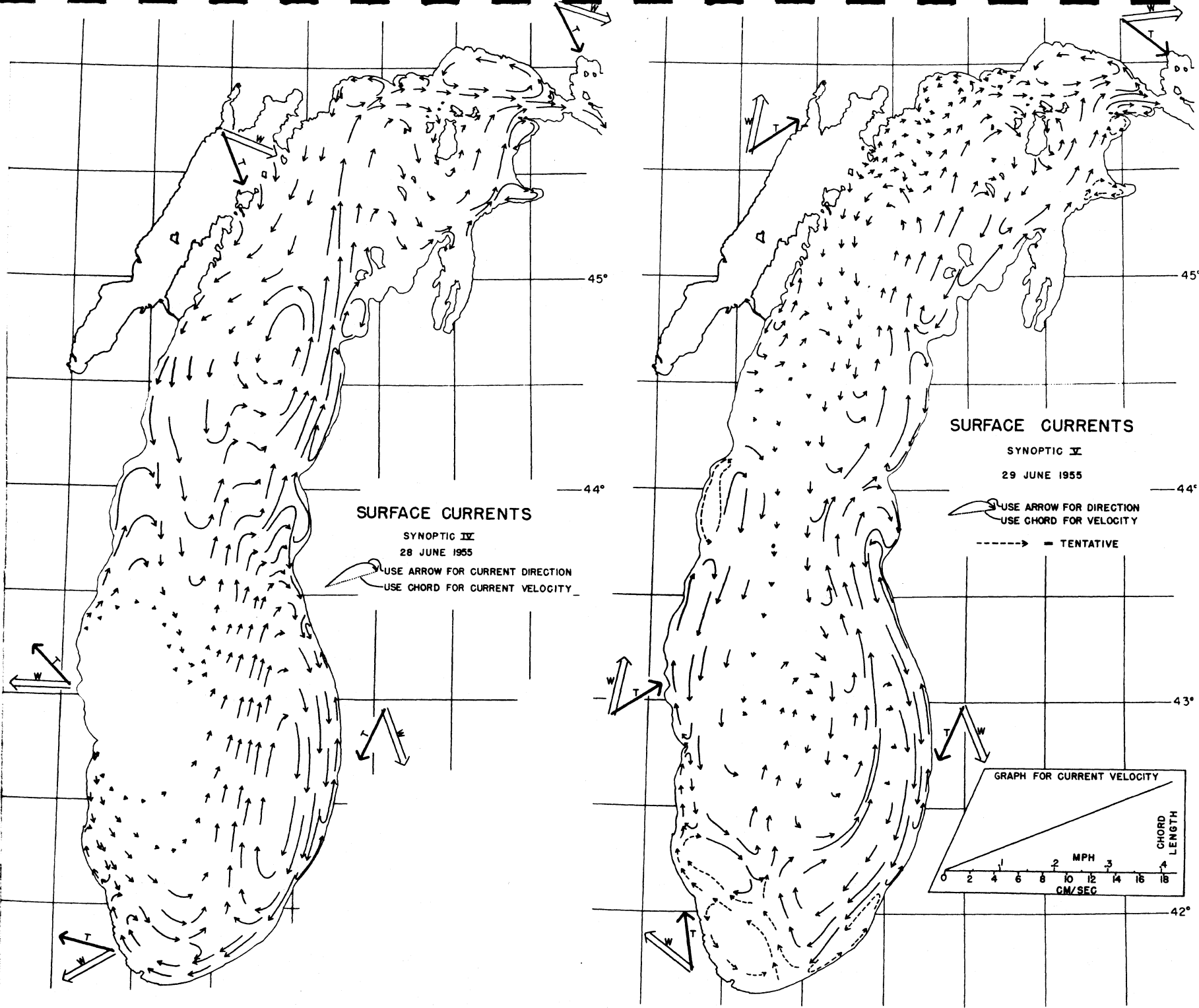


Figure 1.1 Surface currents in Lake Michigan 28 and 29 June 1955 computed by Ayers et al. (1958).

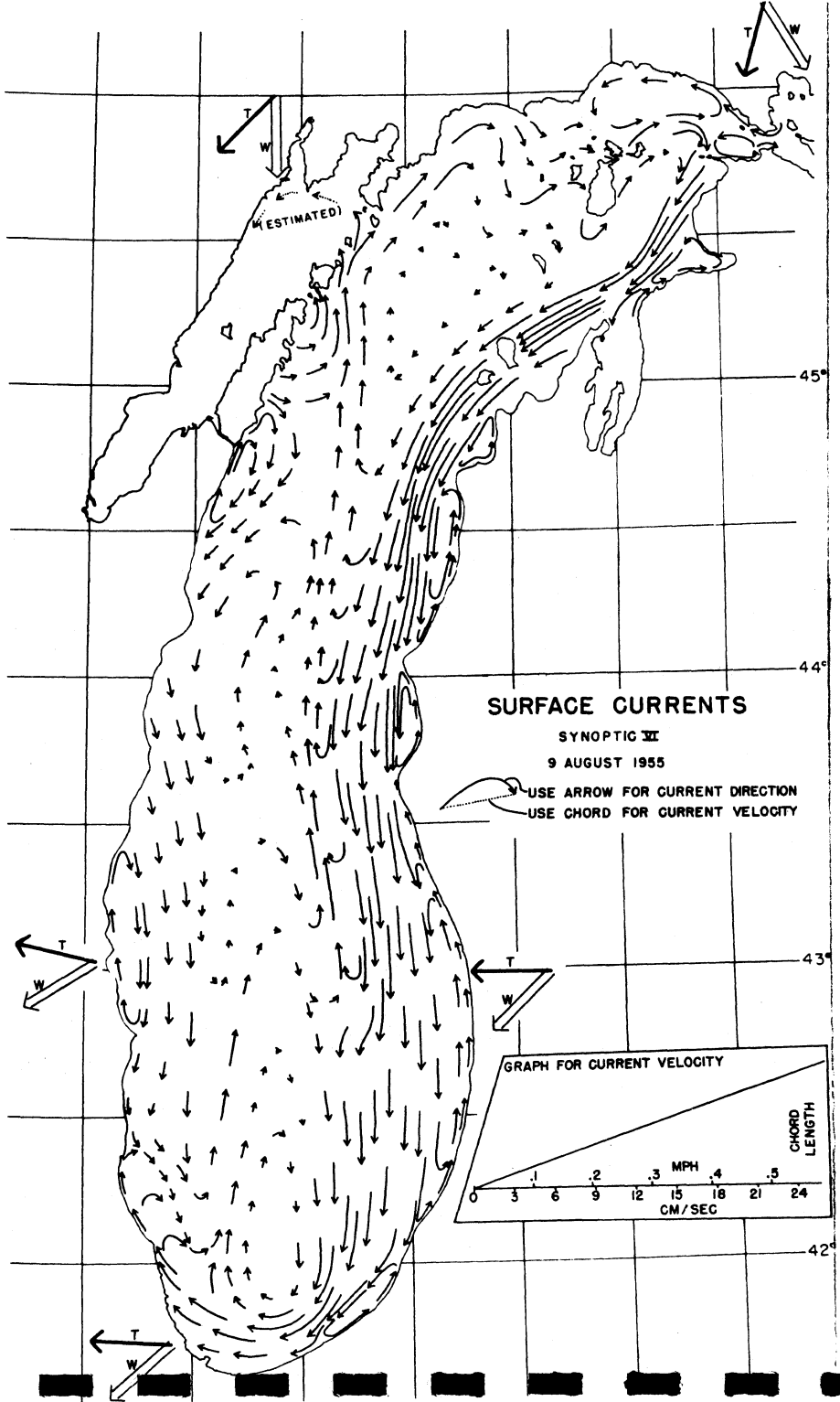
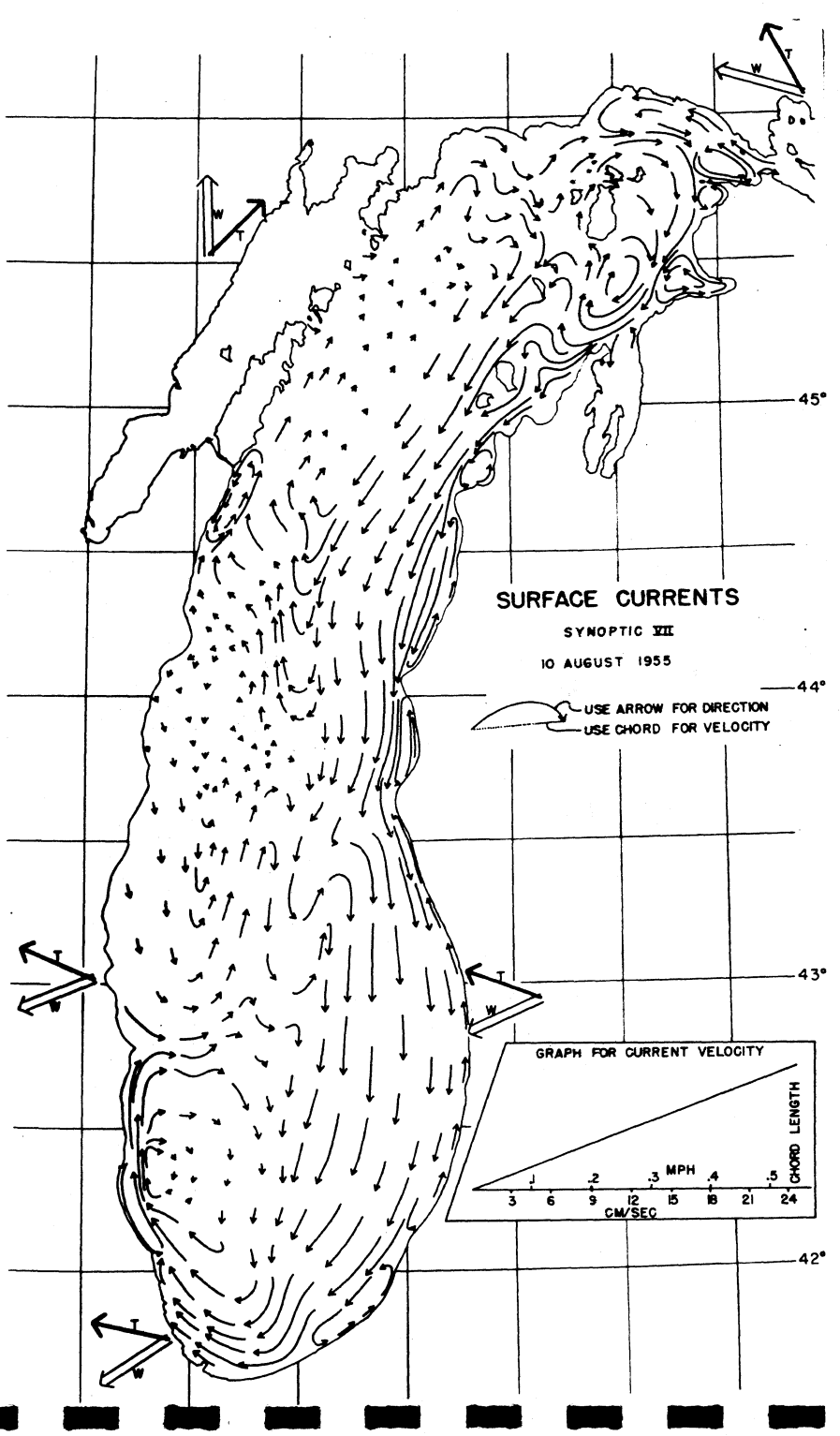


Figure 1.2 Surface currents in Lake Michigan 9 and 10 August 1955 computed by Ayers et al. (1958).

The current patterns (figs. 1.1 and 1.2) computed by Ayers et al. (1968) -- using the classic oceanographic dynamic height method, based on the depth distribution of temperature in Lake Michigan cross-sections obtained by seven simultaneous (synoptic) research vessel cruises -- show a high variability from day to day, particularly nearshore. If, for example, we examine the currents near the Oak Creek Plant, (marked O in figs. 1.1 and 1.2) we see considerable changes from day to day; 28 and 29 June 1955 in figure 1.1, and 9 and 10 August 1955 in figure 1.2. Between one day and the next, in both examples, the computed current direction at Oak Creek had reversed. Because of the assumptions made in the method, the pictures presented in figures 1.1 and 1.2 can represent only mean circulation patterns, derived from the density distribution in the basin, as illustrated in the later figure 1.6 for example, and do not take account of perturbations arising from internal waves -- shown to be important and even dominant during summer circulation in Lake Michigan (Mortimer 1971) -- or from local wind changes which exert a considerable influence on nearshore currents. Figure 1.2 incorporated some degree of averaging of internal wave effects and short-term wind episodes; and the current pattern it displays is the result of the spectacular upwelling event along the eastern shore, illustrated in figure 1.3, arising from strong northerly winds during preceding days. The frequent and often sudden onsets of upwelling, along either shore depending on the direction of the wind stress modified by the deflecting force of the earth's rotation, exert a large influence on nearshore temperature and current patterns during summer and fall, when the lake is stratified. Indeed, strong upwelling responses to wind stress are characteristic of the Great Lakes, and further examples are discussed later in this report.

A closer look at nearshore current patterns in the Great Lakes was first taken in basins other than Michigan: the Keweenaw current in Lake Superior (Ragotzkie 1966); in the Toronto region of Lake Ontario (Hamblin and Rodgers 1967); and near Douglas Point, Lake Huron (Csanady 1963, particularly p. 367, and the review by Csanady 1970). These measurements and those of Gunwaldsen et al., (1971) near Oswego confirm that the

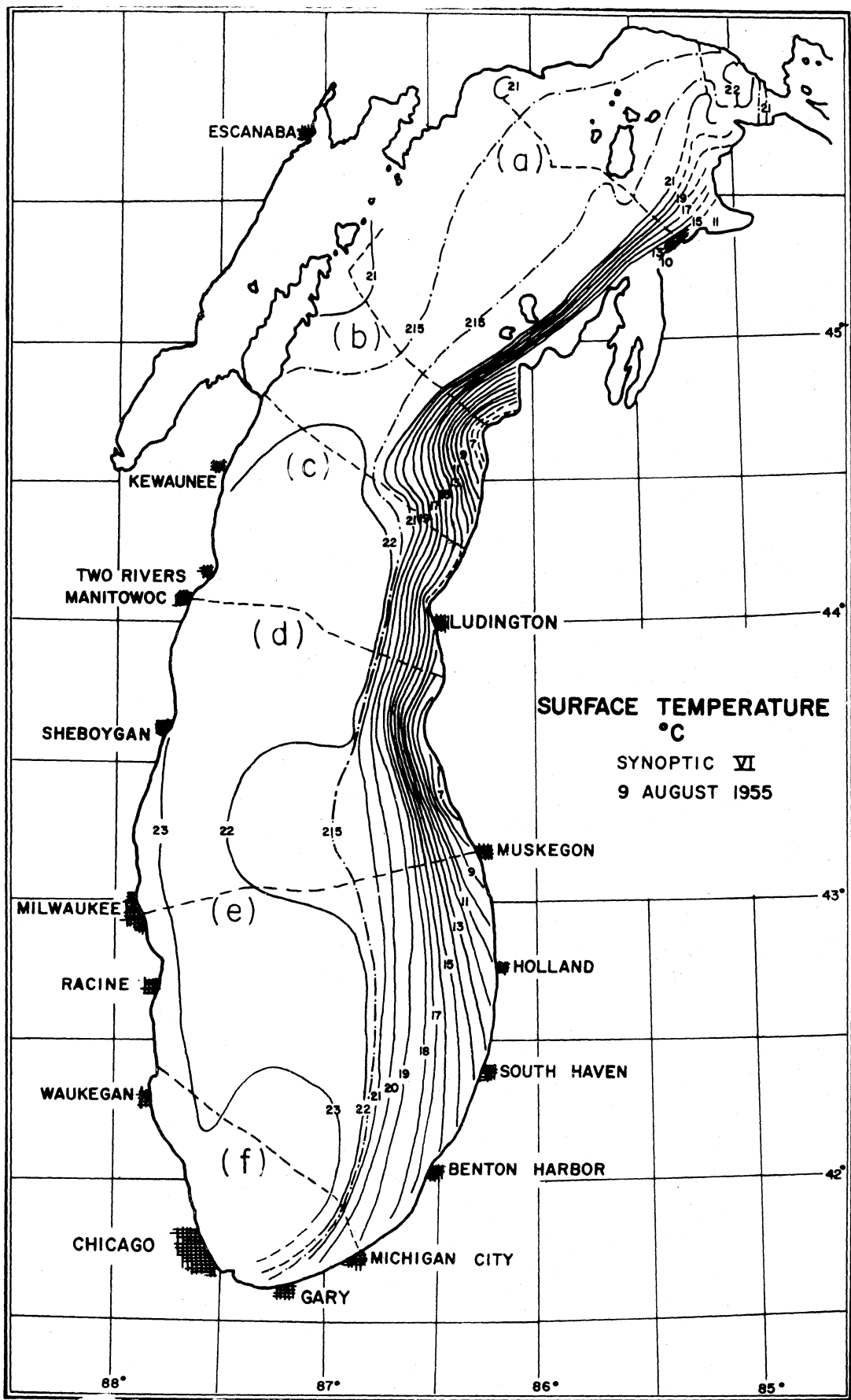


Figure 1.3 Lake Michigan, 9 August 1955. Distribution of surface temperature, °C, derived from seven "synoptic" temperature surveys by Ayers et al. (1958). Vessel tracks are shown as broken lines.

nearshore currents are complex, predominantly shore-parallel, and subject to rapid and frequent reversals associated with changes in the wind. The fact that these investigations are so few is an illustration of the remarkable lack of direct current measurements in lakes in general, as opposed to those inferred from changes in the temperature structure. The infrequency of attempts at direct current measurement is the direct result of a serious instrumentation gap not yet satisfactorily filled. If the flow field, and in particular the interacting gradients of density and velocity (shear), had been as easy to measure as temperature, we should know a great deal more about lake dynamics than we do at the present time.

In Lake Michigan, examples of nearshore current measurements are even more scanty, although an increasing effort has been devoted to filling this gap recently, for example, Monahan (1973) in Grand Traverse Bay, Michigan, and Terrell and Green (1972) who demonstrated a technique of aerial photography of floating poster boards off Point Beach, Wisconsin.

"Lake Michigan Basin: Lake Currents" (U.S. Department of the Interior, 1967).

By far the most ambitious, comprehensive, and therefore costly study of currents in Lake Michigan was that undertaken by the U.S. Public Health Service, later transferred to the Department of the Interior, Federal Water Pollution Control Administration (FWPCA). Some of the results were published in a substantial report referenced here as Department of the Interior (1967) and titled "Lake Michigan Basin: Lake Currents" Great Lakes and Illinois Basin River Basins Project. Current speed, current direction, and temperature were recorded by instruments moored at various depths at thirty-four stations, occupied in some cases for a two-year period from 1962 to 1964. Instruments originally developed for deep ocean measurements were employed, and the moorings were spaced relatively uniformly over the southern half of the basin with a smaller number of instruments in the northern half. Very few of the stations were closer than three miles (5 km) from shore. A major objective of the study was to "determine the net circulation of the Lake and relate this to wind movement for prediction purposes." Some drifting drogue studies were also made in shallow water particularly in the Chicago area. In the

above mentioned report, Okubo and Verber drew some inferences concerning the intensity and scales of turbulence, although they noted that "more than half of the groups of drogues showed a regular pattern of turbulence dispersion, whereas a few groups exhibited a depression or reversal of diffusion caused primarily by convergences." Generally the surface drift (at 1.5 m depth) followed the wind direction closely; but deeper drogues (at 6.1 m depth) often moved against the wind, demonstrating the existence of a vertical shear. Typical velocities were  $4 \text{ cm. sec}^{-1}$  at 1.5 m and  $2 \text{ cm. sec}^{-1}$  at 6.1 m.

Although this FWPCA investigation as a whole represented a monumental effort compared with any study made before, it only partially succeeded in the objective of developing a picture of the "net circulation" and devising a predictive model. As it turned out, the net circulation pattern was often masked or even completely obscured by short-term perturbations, particularly upwelling events and large amplitude internal waves during the season of stratification. These perturbations, predicted by Mortimer (1963), are described in later paragraphs and are interpreted with the help of simple models, which take the stratification and the earth's rotation into account (Mortimer 1971, 1974).

The general results of the FWPCA study were summarized for the stratified and non-stratified seasons on pp. 118, 119, of U.S. Department of the Interior (1967). In offshore water the following patterns were found.

"During stratified conditions the short-term analysis of data does not indicate a wind-driven current system. The hour-to-hour currents are dominated by the internal wave regime which receives its principal energy from the wind. The internal wave regime is also affected by the Earth's rotation which tends to obscure the direct relationship between winds as the driving force and currents produced by internal waves. The internal wave rotation, with a period close to the inertial frequency, is often altered by sudden wind inputs. This regime lasts from late spring (April) into November or early December. The rotating influence is normally not found in the inshore waters.

"By contrast, the winter circulation is less complex and almost entirely wind-driven. The major exception appears when an ice cover occurs or a reverse (winter type) thermocline develops in the central basin."

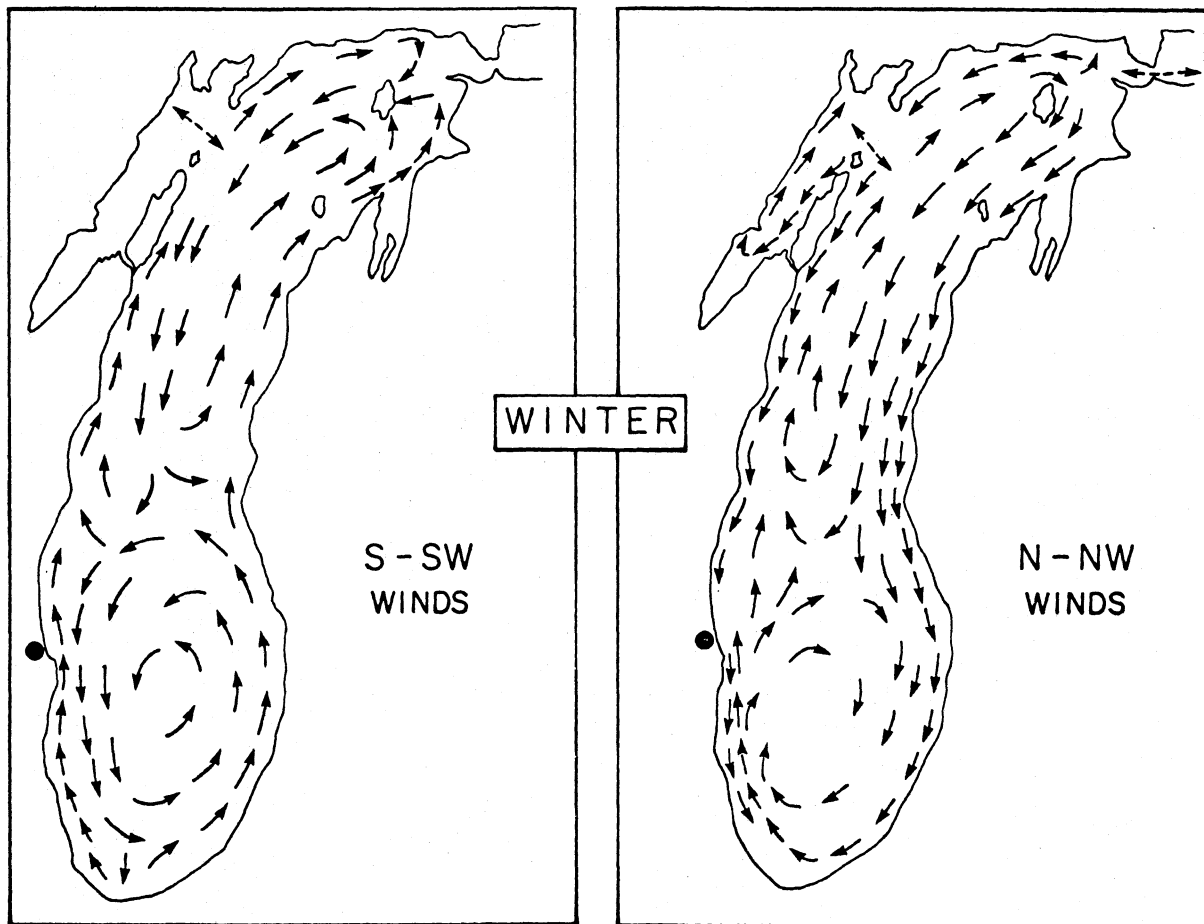


Figure 1.4 Prevailing current pattern in Lake Michigan in winter, deduced by U. S. Department of the Interior (1967).

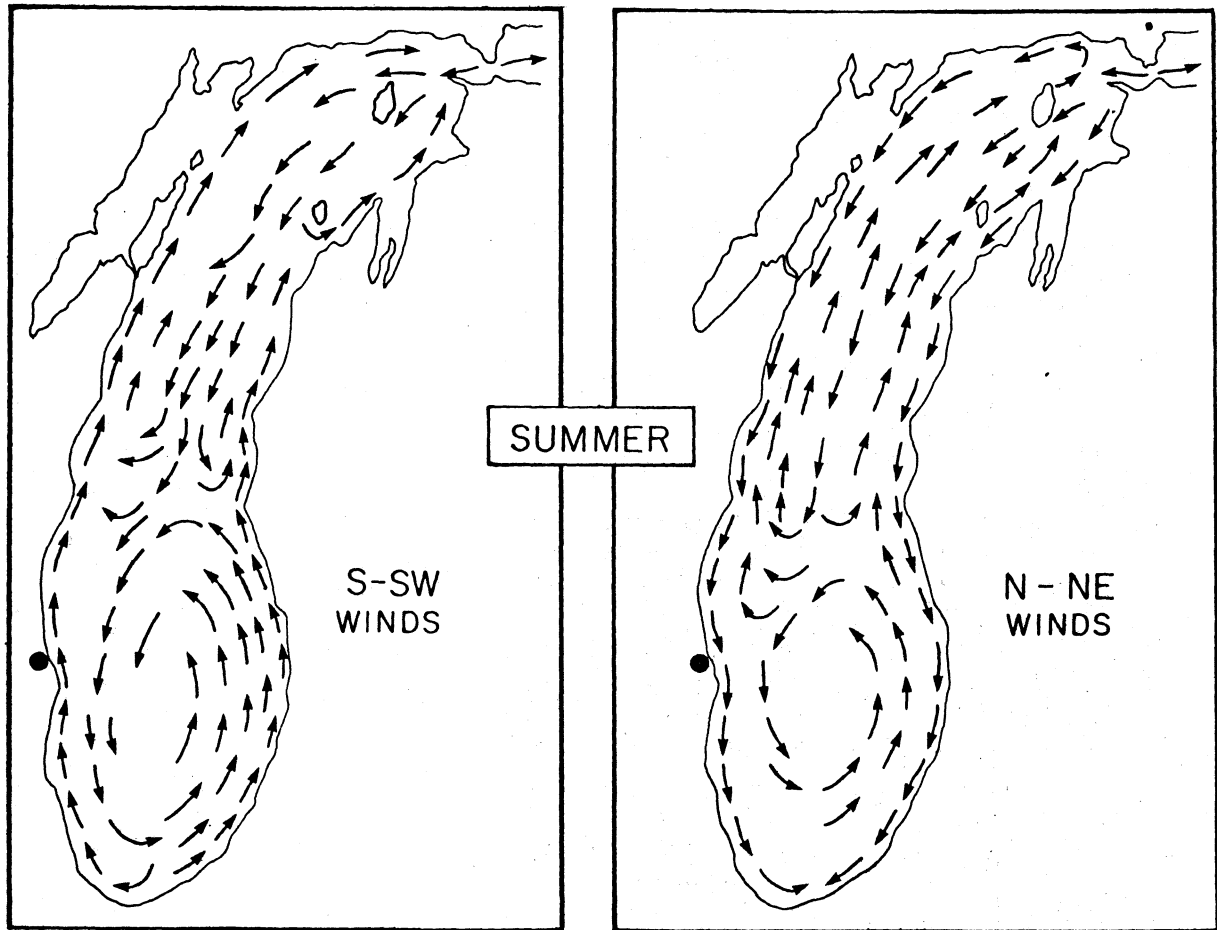


Figure 1.5 Prevailing current patterns in Lake Michigan in summer, deduced by U. S. Department of the Interior (1967).

"A straight prediction model, based on wind, is not valid for summer (stratified) conditions in mid-lake. Inshore current patterns in the upper 5 m appear to have a wind-driven circulation throughout the year. The response to this system appears in about 1 hour under moderate wind conditions.

"The inshore zone varies in width and probably extends as much as 10 miles from the shore during the most favorable conditions and as little as 2 miles during periods of upwelling. Mid-lake circulation patterns in winter are not under the influence of internal waves except under very special conditions. Spectral analysis of current meter data, for the winter period, gives no evidence of a dominant frequency which could control current patterns. Winter patterns in mid-lake are, similar to the inshore areas during summer, wind-driven. The response time of the mid-lake portion is probably the same as the inshore waters.

"Although the winds are the primary driving force in winter, other forces exist which complicate the pattern. When a wind reversal occurs in one sector of the Lake, the remainder of the Lake is at or attempting to maintain equilibrium under the prevailing wind regime. No steady-state system can exist while external conditions are constantly changing. For this reason, Lake Michigan probably never achieves a steady-state or equilibrium condition everywhere at one time. However, large sectors, such as the southern basin, do achieve a near-equilibrium condition. Under these conditions, during the nonstratified period, a prediction model is applicable."

In spite of the variability just described, the FWPCA team attempted to derive "net residual" flow by displaying averaged monthly data in  $10^\circ$  intervals of direction and  $3 \text{ cm. sec}^{-1}$  intervals of speed for each station, smoothing out minor differences between stations and using "conformal flow along the boundaries". By this means, averaged patterns of water movement were developed for the upper layers, one in summer and one in winter, for winds from the two dominant directions during those seasons. The two surface patterns predicted to be dominant in winter are shown in figure 1.4. Under the influence of N to NW, i. e. southward to southeastward winds, the "near-shore" flow near Oak Creek (near the large dot in the figures) is southerly, whereas under a northward to northeastward (i. e. S to SW) winds "occur normally from January to April, but on an intermittent basis". In summer (fig. 1.5) "nearshore" currents also reflect the influence of prevailing winds, suggesting

that a wind change from the S-SW sector to the N-NE sector (a frequent occurrence with the passage of weather fronts in summer) will be associated with a current reversal of the shore-parallel flow. "The break between the inshore and offshore circulation appears to occur at or near where the thermocline intersects with the bottom of the Lake. This means that the location will vary as the thermocline gets deeper."

### The importance of upwelling

Nearshore currents, with which we are principally concerned in the present report, are strongly influenced not only directly by wind as just described, but also by another mechanism not treated in detail in U.S. Department of the Interior (1967), namely, coastal upwelling and the long-period internal (Kelvin-type) waves which can be generated as a result of that disturbance (Mortimer 1963). Because of their low phase speed, commonly between 35 and 45 cm. sec<sup>-1</sup>, the motions associated with these waves are usually indistinguishable from "steady" currents; and this may be the explanation of examples noted later in this report, in which the current direction predicted from local wind did not agree with that observed.

The upwelling phenomenon, common on either the eastern or western shore of Lake Michigan in summer depending on wind direction, is confined to a coastal band not wider than 20 km. For example, the depth distribution of temperature on three of the sections from which the figure 1.3 upwelling picture was derived is illustrated in figure 1.6. The upward tilt of the isotherms occurs close to the coast; and the remainder of the thermocline shows the influence of near-inertial internal waves mentioned above and treated in Mortimer (1971). A common pattern is one in which upwelling on one shore is accompanied by downwelling (a depression of the thermocline isotherms) in a coastal strip on the other shore (see fig. 1.8).

Clues to the occurrence and extent of coastal upwelling during the summer are given by temperature records at the water intakes of municipal filtration plants. An example for the year 1955, i. e., including the upwelling event illustrated in figures 1.3 and 1.6, is shown in figure 1.7 with a display

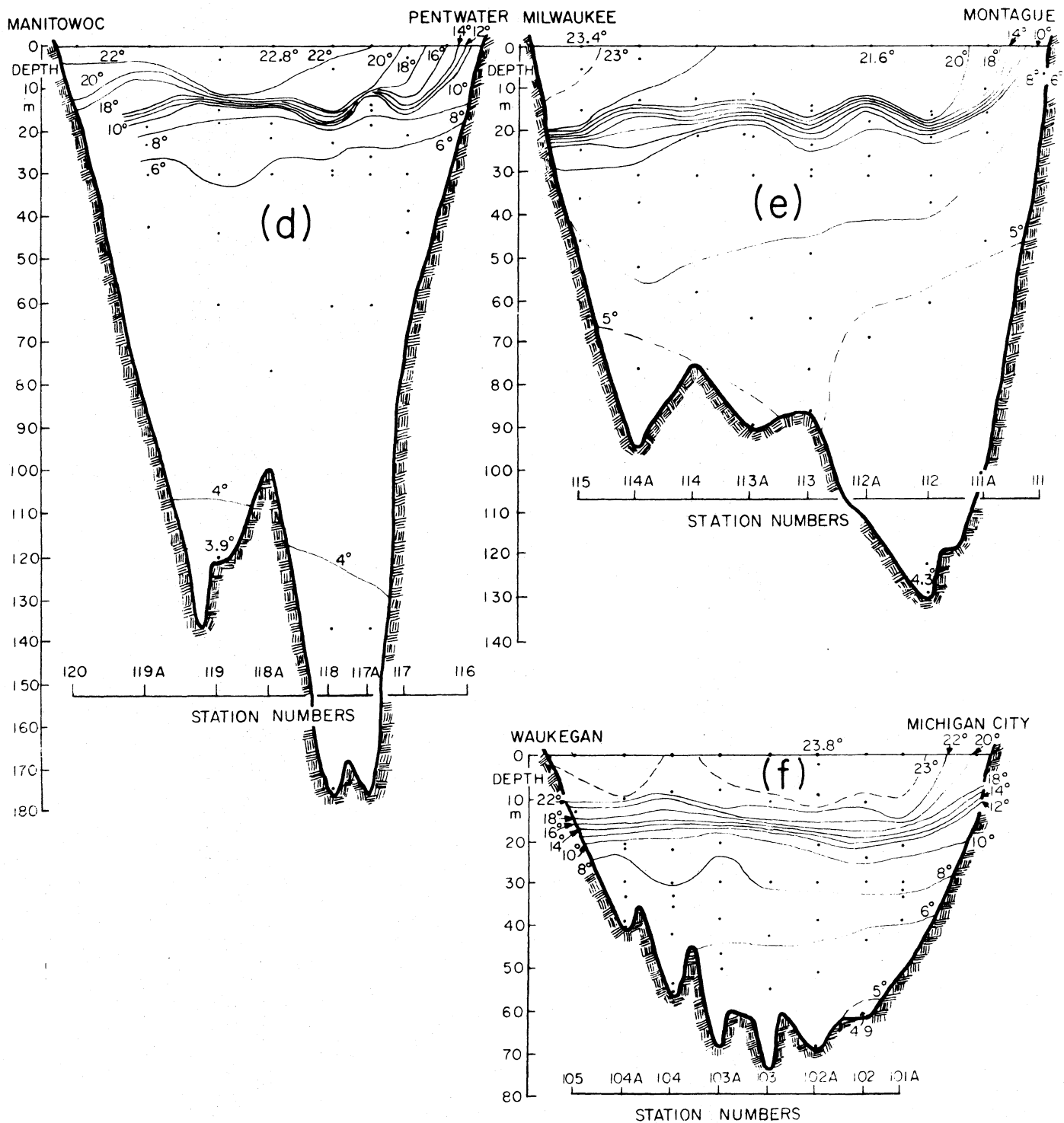


Figure 1.6 Lake Michigan, 9 August 1955. Distribution of temperature, °C, observed on research vessel transects (d), (e), and (f), shown as broken lines in figure 1.3 (re-drawn from data in Ayers, *et al.* 1958).

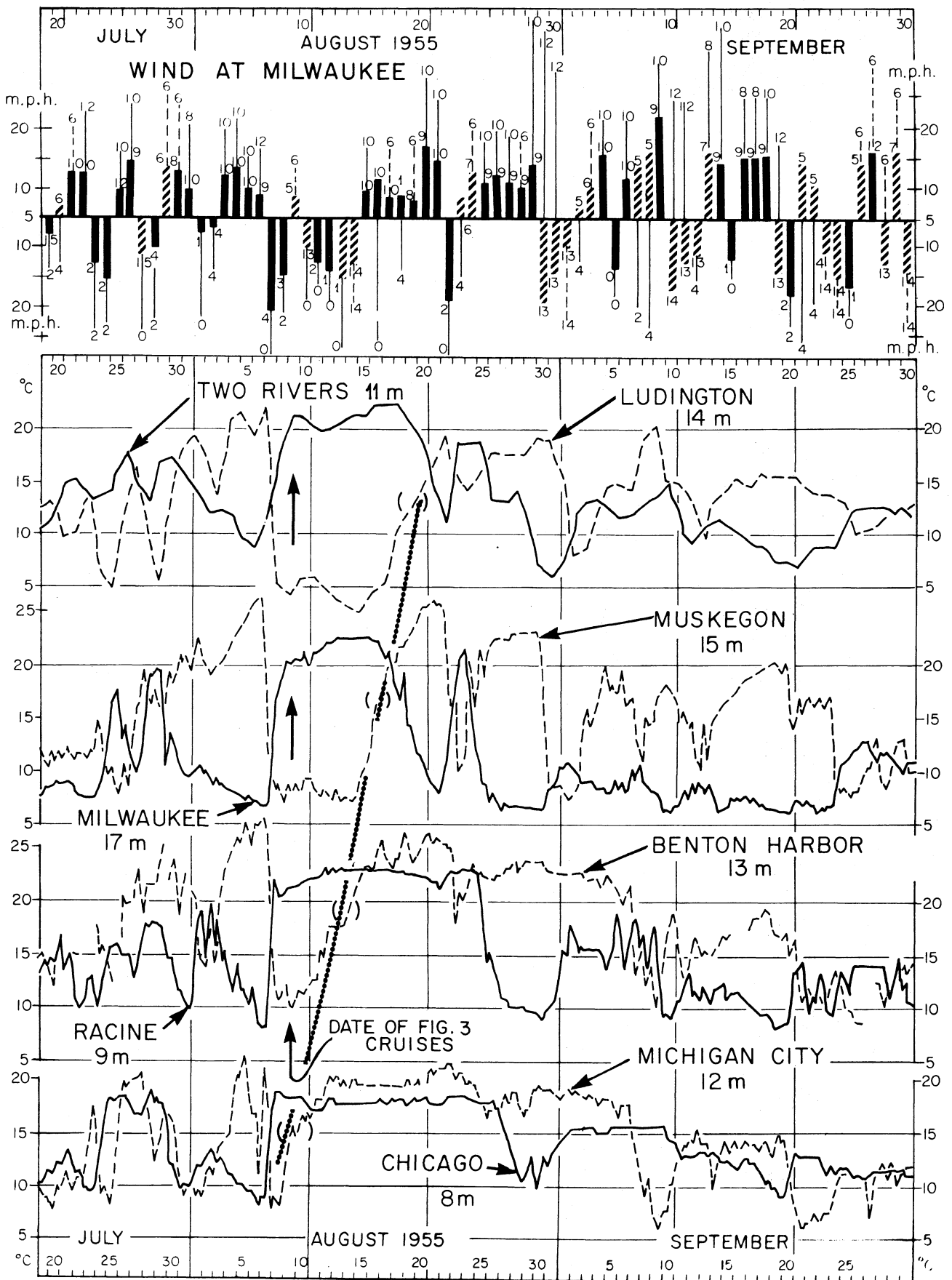


Figure 1.7 Temperatures, °C, at Lake Michigan municipal water intakes (depths shown) July-September 1955 (re-drawn from Mortimer 1964), 6-hr means at Milwaukee and Racine, otherwise daily. Also shown is daily mean and "faster mile" wind at Milwaukee; details of the coding, numbered clockwise in 1/4 compass quadrants from 0 at N (see Mortimer 1971).

of daily mean and maximum winds and with eastern and western intake stations paired to show the out of phase "flip-flop" behavior of the temperature records at stations lying on approximately the same latitude. Contributing to the interpretation of the upwelling event illustrated in figure 1.3, figure 1.7 shows that a reversal from S-W winds to strong E winds occurred on 7 August and that this led to a sharp reversal of intake temperatures at all four pairs of stations, indicating strong upwelling on the eastern shore and downwelling on the western shore, confirmed by the August 9 and 10 surveys (figure 1.6). Continued southward to westward winds on 11 and 12 August maintained the extreme temperature differences between the eastern and western members of each intake pair (except for Chicago-Michigan City at the southern end of the basin); and the subsequent temperature changes at the eastern intakes (linked by heavy dotted line in figure 1.7) were interpreted by Mortimer (1963) as evidence of a slow, coast-bound, Kelvin-type internal wave.

What may appear to be our pre-occupation with upwelling is deliberate and designed to emphasize the strong modifying action which such motions have on coastal currents, sometimes masking local wind responses entirely, as we show in later examples. The Milwaukee temperature record in figure 1.7 shows features similar to those found in other years; and its similarity to the Racine record makes it a good guide to conditions at Oak Creek. During the months of stratification, periods of upwelling frequently alternate with periods of downwelling depending on wind direction, the principal action being confined to a nearshore strip of 15 to 20 km wide.

Upwelling/downwelling events are examples of the influence of whole-basin motions on the nearshore zone and represent also a large source of potential energy for the generation of conspicuous internal waves involving the whole of the Lake thermocline. A typical early summer picture of thermocline topography across the Milwaukee-Muskegon section is illustrated in the left-hand section of figure 1.8. Weak winds, mainly from the south during preceding

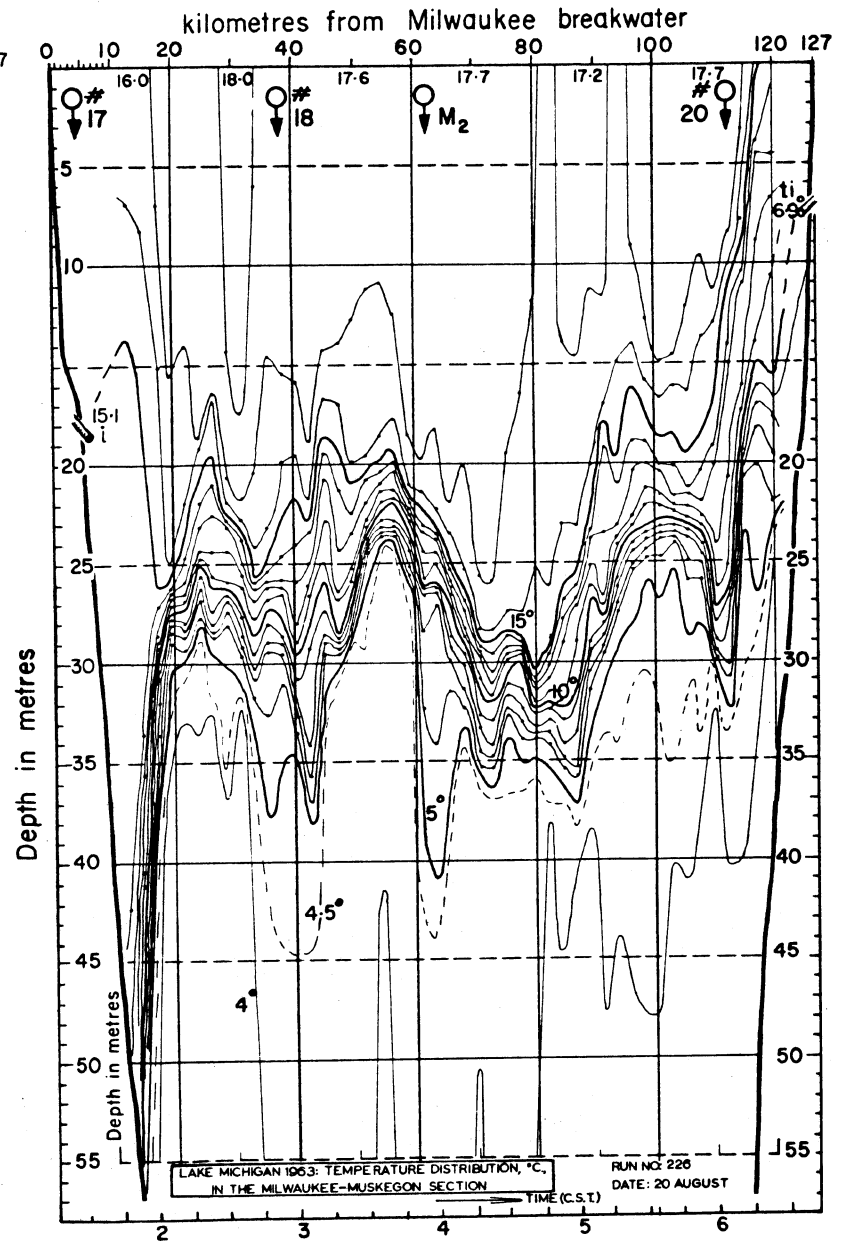
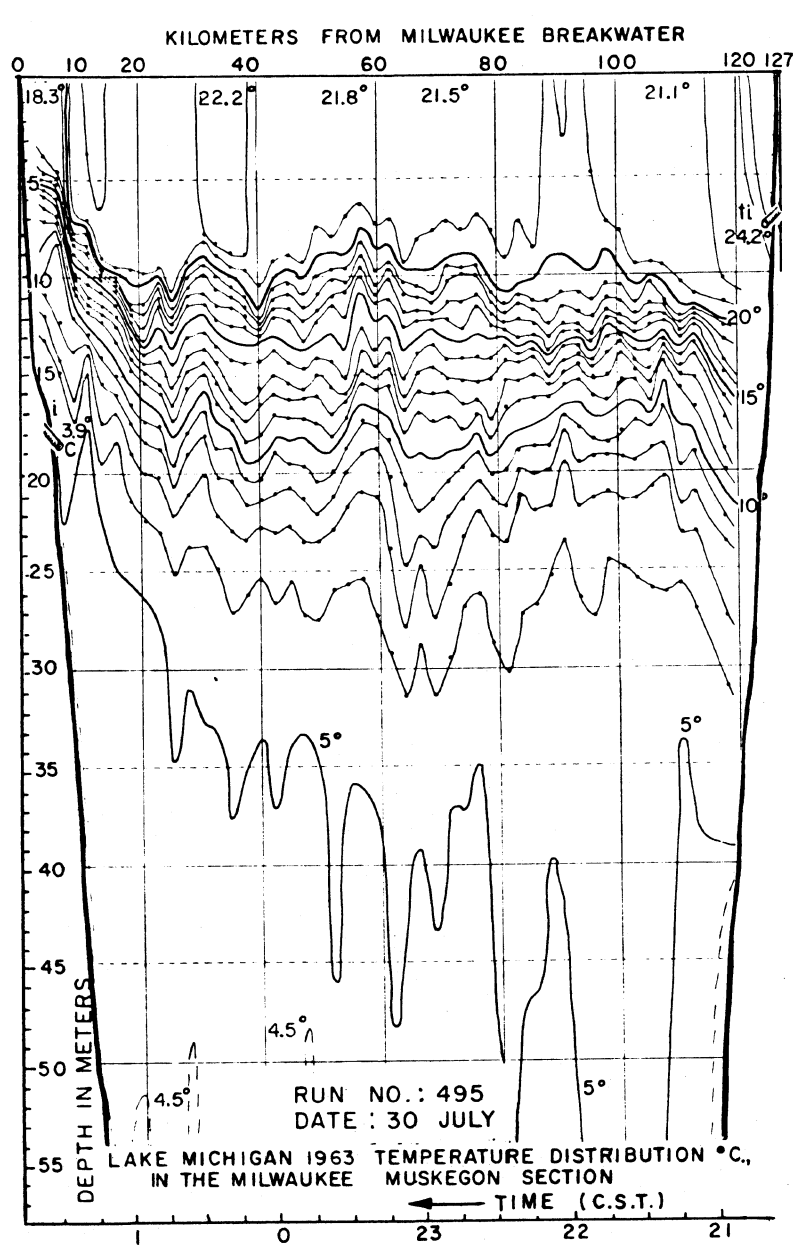


Figure 1.8 Lake Michigan, 1963: depth distribution of temperature, °C, in the Milwaukee-Muskegon section on 30 July after weak southerly winds and on 20 August after strong northerly winds.

weeks, had led to upwelling on the Milwaukee shore and weak downwelling on the Michigan side. By contrast, the right-hand section of figure 1.8 shows that strong southward winds on 17 August 1963 had generated strong downwelling off Milwaukee with corresponding upwelling off Muskegon. These downwelling and upwelling motions, constituting large perturbations of the thermocline from its equilibrium level, were confined to the 20 km-wide nearshore portions of the section. Over the remainder of the thermocline a conspicuous wave-like topography was evident.

#### The influence of near-inertial internal waves on offshore and nearshore currents

We shall not discuss the nature of these waves further here (they are interpreted in terms of simple models in Mortimer 1971, 1974) except to say that they represent a strong resonant response of the basins with a dominant periodicity of 16 to 17 hours, a little less than the local inertial period of 17.5 hours. From the point of view of this report, the most significant property of these "near-inertial" waves is that the currents associated with them rotate clockwise once every wave period. In offshore waters during stratification, this rotary "inertial" or "near inertial" current often dominates the circulation pattern, making the observation of "steady" residual currents very difficult at least with fixed instruments. This was one of the reasons why the massive effort of U. S. Department of the Interior (1967) did not achieve its objective.

Under these circumstances, there are two ways of presenting the current pattern, either as a "current rose", for example top left in figure 1.9 -- in which two-hourly current vectors of a 16-hour near-inertial wave are shown emanating from one point with no unidirectional current component -- or as a "progressive" vector diagram, in which a current track is reconstructed by placing successive current vectors head to tail. (Note that this reconstruction accurately depicts the real current track only if the flow field behaves uniformly over the area covered by the track. The actual track can only be measured by an instrument floating with the current -- a Lagrangian measurement -- not by a fixed instrument -- Eulerian measurement.) If there is no unidirectional current component ( $r = \infty$  in the top left example, figure 1.9) the progressive vector diagram is a closed figure, a circle in the illustrated example.

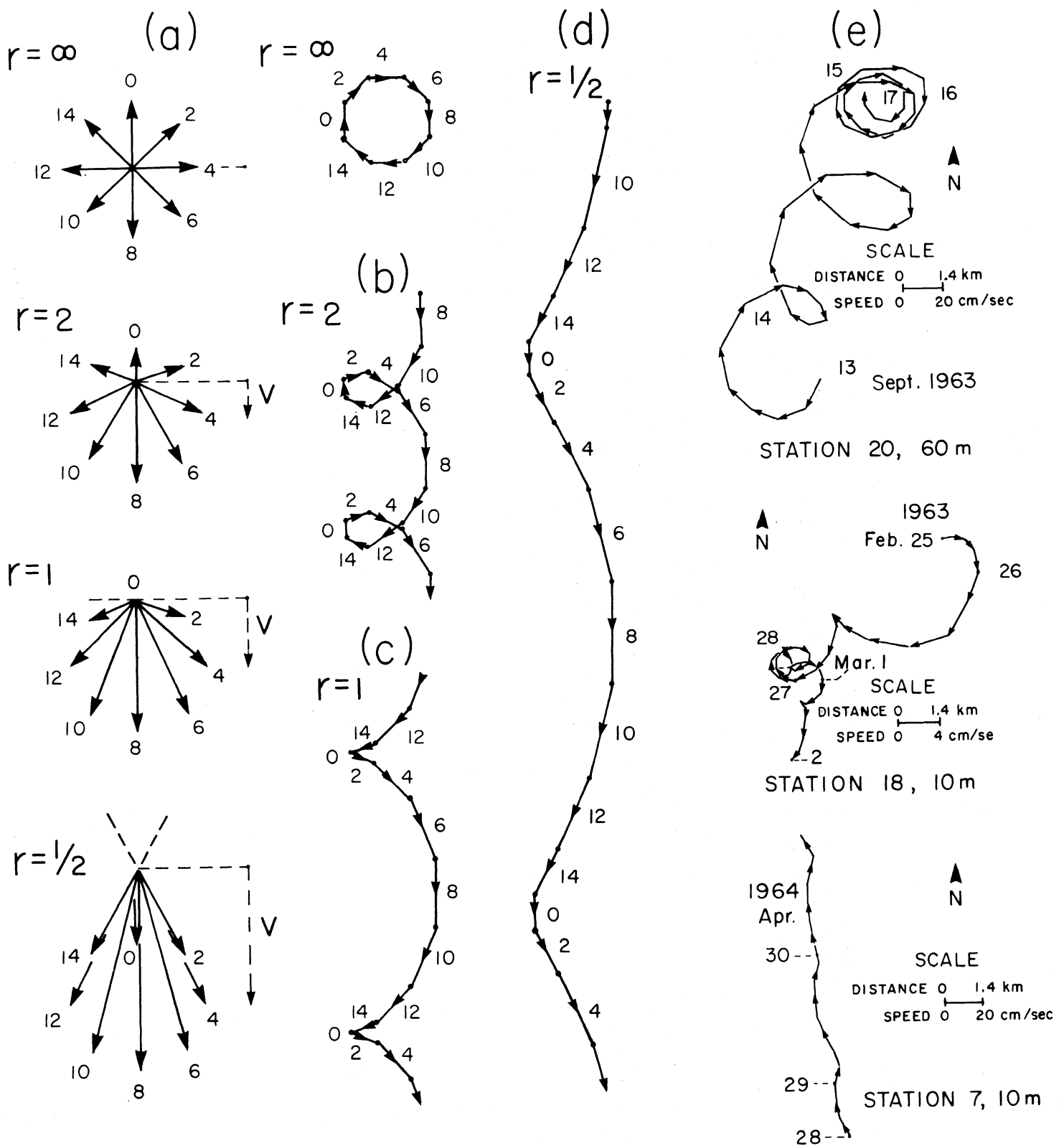


Figure 1.9 (a) Current "roses" in which a rotating (Poincare wave) current component of constant speed,  $\underline{u}$ , is combined with unidirectional current components of speeds 0,  $\underline{u}/2$ ,  $\underline{u}$ , and  $2\underline{u}$ , to yield respective rotating/unidirectional speed ratios,  $r = \underline{u} = \infty, 2, 1, 1/2$ . (b), (c), and (d) Combined current trajectories corresponding to  $r = 2, 1$ , and  $1/2$ , respectively. (e) Observed current trajectories in Lake Michigan (progressive vector diagrams from Verber 1966).

The remainder of the left-hand half of figure 1.9 shows combinations of the same rotating, wave-induced current vectors with increasing proportions of unidirectional current components, with ratios  $r$  (speed ratios of rotational and unidirectional components) of 2, 1, and 1/2. The corresponding progressive vector diagrams are shown in figure 1.9(b), (c), and (d). These are models of types of current trajectory frequently observed (also by us in later examples) and may be respectively termed "looping", "cusping", and "meandering" currents. Some Lake Michigan examples from Verber (1966) are shown in figure 1.9(e).

These models, elementary though they are, have their uses in interpreting more complex current patterns including those near shore, particularly when it is remembered that rotation dominates in offshore waters during stratification, while the unidirectional components become increasingly important as the shores are approached. As we shall show in later examples, rotational motion is not entirely suppressed even nearshore, although it clearly becomes less important there; and examples of looping, cusping, and meandering progressive vector diagrams can all be found.

The current patterns in which shore-parallel motions dominate -- wind-driven current, geostrophic currents associated with upwelling/downwelling events and the progressive (Kelvin-type) internal waves which follow -- are confined to a nearshore band about 15 km wide. Therefore in the region 5 to 25 km offshore there is, characteristically in summer and fall, a transition between the nearshore shore-parallel patterns and the offshore rotary motions of near-inertial period, (15 to 17 hr Poincaré waves, Mortimer 1971, 1974). Figure 1.10 is an artist's attempt to portray that transition in a simple model of uniform depth. It shows (i) a portion of a long Kelvin wave with shore-parallel currents, maximum at the shore and decreasing exponentially away from the shore (to  $1/e$  or 37% of the onshore value at distance  $d_e$ ), and (ii) clockwise rotary currents produced by a cellular pattern of standing Poincaré waves of relatively short wavelength. Looping, cusping, and meandering currents are produced in the transition region.

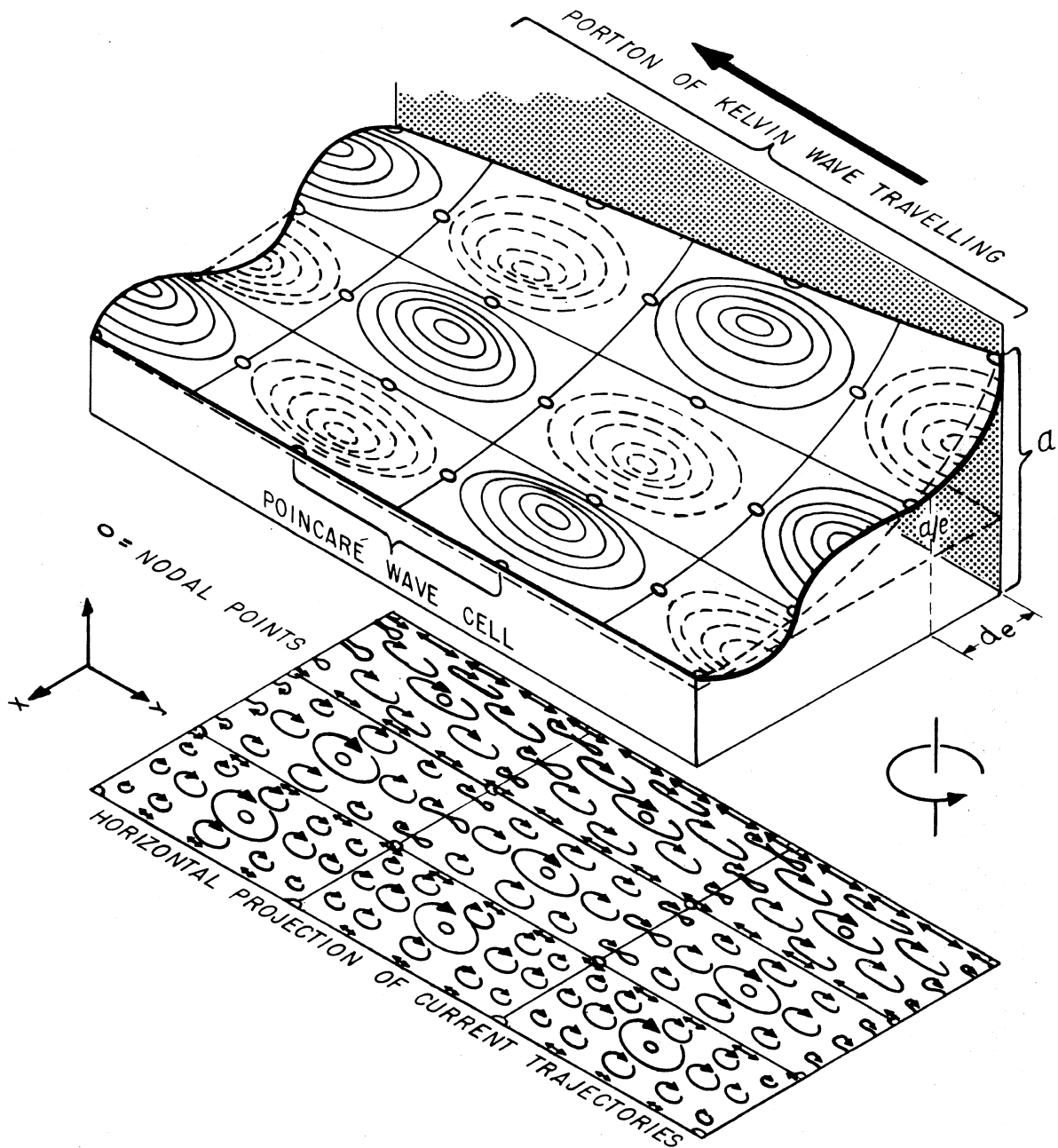


Figure 1.10 Thermocline topography and horizontal current patterns produced in a wide channel (only one side of which is shown) by a combination of near-inertial standing waves (Mortimer 1971, 1974), generating rotary currents and extending over the whole of the thermocline, and near-shore progressive Kelvin waves generating nearshore shore-parallel currents. From Mortimer (1971).

The dominance of rotating currents at offshore stations during stratification is clearly demonstrated by spectra of energy density; an example for a Lake Michigan station 20 km offshore is shown in figure 1.10. Bearing in mind that the energy density scale is logarithmic, almost all the kinetic energy at that station during early summer was concentrated close to the inertial period. This was true both for the 15 m layer above the thermocline and for the 90 m layer below, although at the latter depth the current speeds and therefore kinetic energy densities were considerably less than those in surface layers. By contrast, at the same station during the unstratified phase in April, energy density was spread more evenly across the spectrum with no concentration at the inertial frequency.

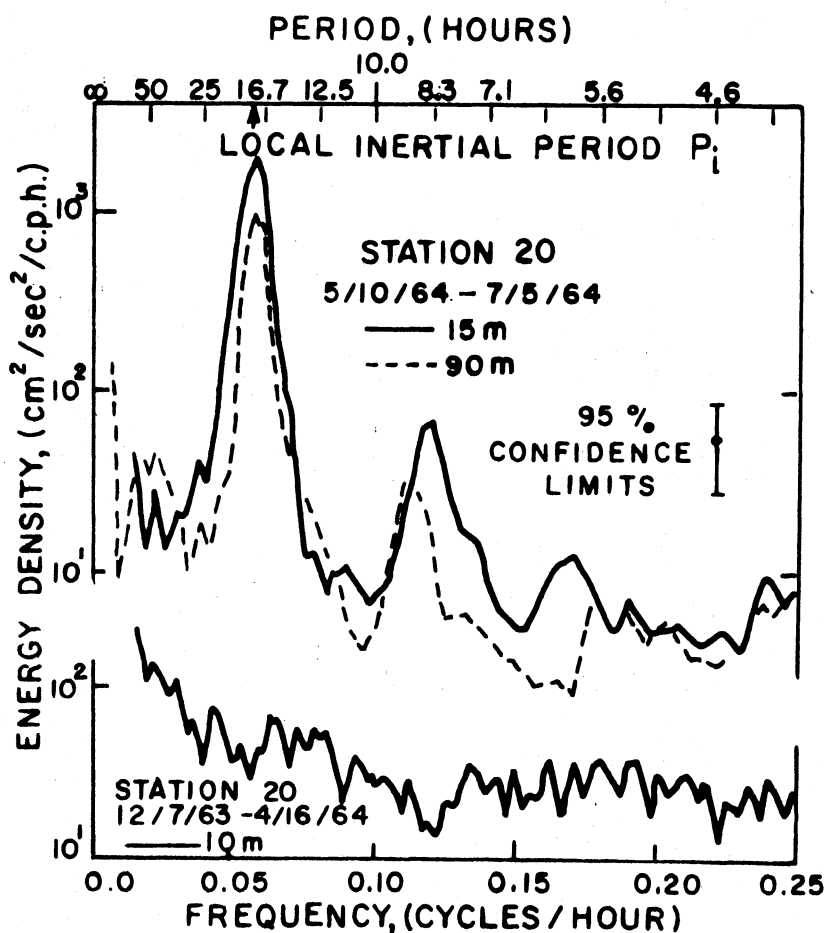


Figure 1.11 Spectra of the N-S component of current at station 20, Lake Michigan, for depths and dates shown (Malone 1968).

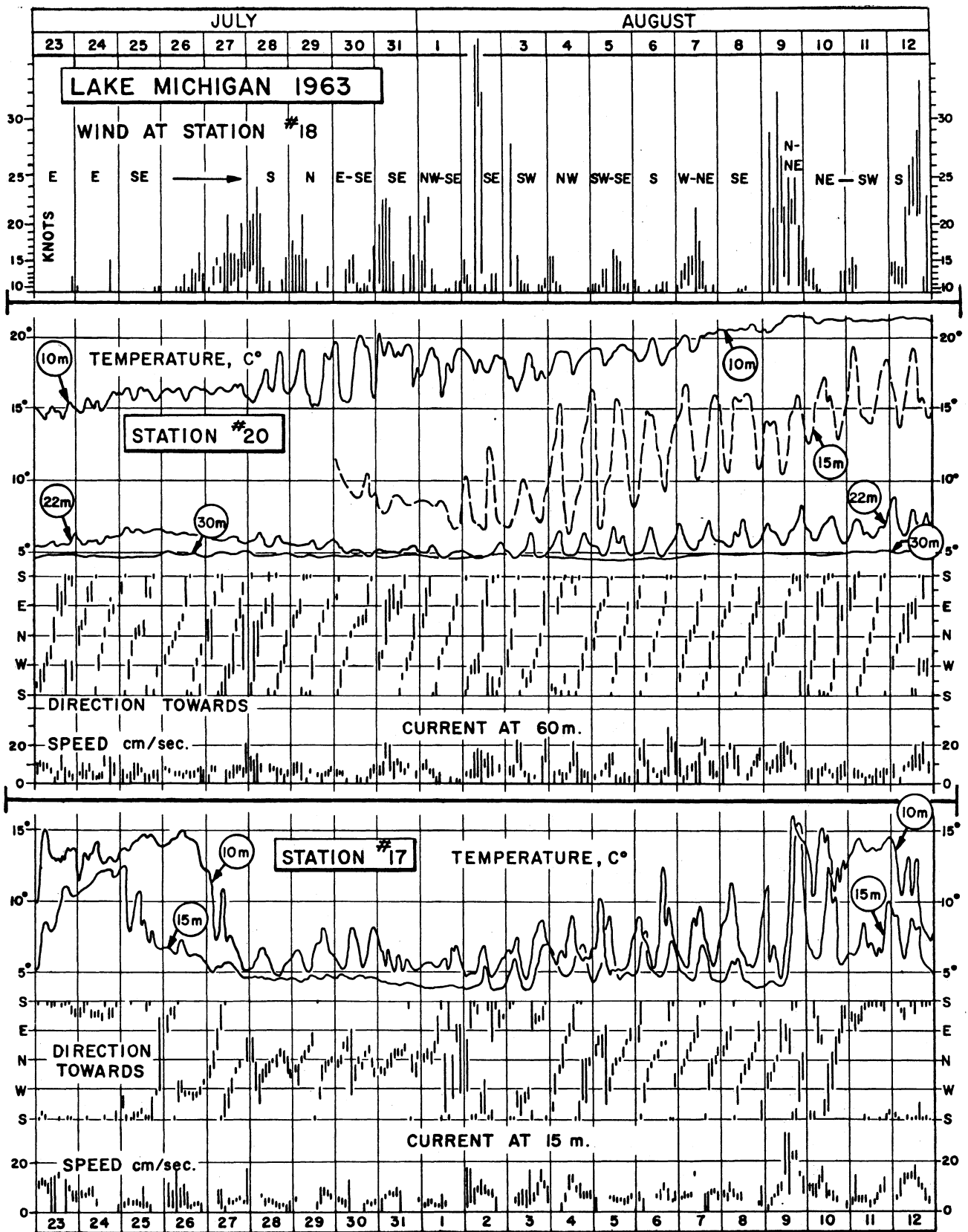


Figure 1.12 Lake Michigan, 23 July to 12 August 1973; records of wind at a mid-lake station 18 and of temperature and two-hourly ranges of current directions and speeds at various depths at an offshore station 20 and a nearshore station 17, see figure 1.8 for positions (from U. S. Dept. Interior, 1967, in which station locations are given).

Figure 1.9(e) also illustrates the typical contrast in progressive current vector diagrams derived from records at offshore stations 18 and 20 and a nearshore station 7 (4 km from shore, Verber 1966). The contrast between rotary patterns at offshore stations and predominantly shore-parallel unidirectional patterns at nearshore stations is also well illustrated in figure 1.12 which compares records of temperature, current speed and direction, at two of the U.S. Department of the Interior (1967) stations near the Milwaukee-Muskegon section over the time interval 23 July to 12 August 1963. Station 20, referred to earlier (figure 1.11), was approximately 20 km from the eastern shore and 6 km south of the figure 1.8 section and, although not a mid-lake station, was more influenced by offshore than by inshore motions. Station 17, 4 km from the western shore and 12 km north of the section, can be regarded as a nearshore station by our definition. The "wind stress" diagram at the top of figure 1.12 (2-hourly ranges of wind speed squared) was obtained at station 18 near mid-lake on the figure 1.8 section. The strong northwestward wind pulse on 2 August set large near-inertial waves in motion at station 20, illustrated by the 15 m temperature record near thermocline depth. The waves persisted with great regularity for ten days, until disturbed by another storm. As predicted by Mortimer's (1963) models, the period was close to 17 hours and the thermocline wave was coupled in the predicted phase relationship with a regular 17-hour clockwise rotation of the current vectors both (a) above and (b) below the thermocline, with (a) and (b) always opposed in direction. The regularity of this rotation is demonstrated by the repeated diagonal progressions of the 2-hourly ranges in current direction across the direction diagram in the middle of figure 1.12.

At the nearshore station 17, by contrast, the temperature wave on the thermocline was less conspicuous and, more significantly, the current directions showed a strong unidirectional component, generally towards north or south, with direction reversals on 26 July, and 1, 4, and 10 August. During the relatively calm intervals 28 July to 1 August, and 4 to 8 August, the current was predominantly north-going but with some rotational component superimposed upon it, generating a looping or cusping current trajectory. By virtue of its position, station 17 provides records which can be compared with those presented in this report.

One consequence of the monumental effort by U.S. Department of the Interior (1967) was the creation of more interest in Lake Michigan currents on whole-basin scales. This led to further analysis (Malone 1968, see figure 1.11), to testing of simple conceptual and analytical models (Mortimer 1971, 1974), to a more detailed analysis of coastal currents (Davidson and Birchfield 1967), and to several attempts at numerical modelling of wind-driven currents (Birchfield 1969, Kizlauskas and Katz 1973).

#### Lake Ontario (IFYGL) investigations

As mentioned above, work on coastal currents in the Great Lakes was initiated and has principally continued in basins other than Michigan, notably in Lake Ontario. We refer particularly to the planning studies, the 1972 field operations, and the analysis now in progress for IFYGL (International Field Year for the Great Lakes). It would be out of place here to deal with the IFYGL Lake Ontario material in detail, but we shall briefly mention some of the planning inputs and some of the emerging findings directly relevant to interpretation of Lake Michigan's nearshore currents.

We have already referred to Csanady's interest in coastal circulation and diffusion in Lake Huron. That led to a series of theoretical papers combined with field investigations (Csanady 1967, 1971, 1972a, 1973, 1974), more recently directed to Lake Ontario (Csanady 1972b, 1974). Baroclinic coastal currents, well developed along the southern shore of Lake Ontario, had also been the subject of a series of studies by J. T. Scott and his associates (Scott and Lansing 1967, Scott and Landsberg 1969, Scott, Jekel, and Fenlon 1971). Csanady, Scott, and associates carried out repeated measurements of the temperature (density) and current fields on sections normal to the shore, using "coastal chains" of moored buoys at which the temperature and current profiles were measured from a boat. The temperature (density) and current fields were correlated to determine the degree of geostrophic equilibrium. A growing number of such coastal chain observations in the Great Lakes (the Csanady and Scott publications already referred to, also Smith and Ragotzkie 1970) provided evidence that in certain regions the baroclinic coastal currents sometimes assume the nature of "coastal jets", attaining maximum velocities some distance offshore.

Coastal chain measurements formed a substantial part of the IFYGL field operations in 1972. Five coastal chains in all were manned, two on the northern (Canadian) shore of Lake Ontario by Csanady's group and three on the southern (U.S.) shore by Scott's group. Data reports on these projects have been produced (Csanady and Pade 1972, Scott, Fenlon, Jekel, Landsberg, and Lemmin 1973) analysis of which is continuing. This analysis and the analysis of current measurements covering wider regions of Lake Ontario, made by the Canada Centre for Inland Waters before and during the IFYGL Program is leading to the following important general conclusions.

From a dynamic viewpoint, a nearshore zone of about 10 km in width plays a major role in the energy transfer from wind to total basin motion and contains the greater part of the Lake's total kinetic energy. As we have seen, it is in this zone that massive upwelling and downwelling occurs, generating long internal waves. The zone contains a complex mixture of shore-trapped boundary waves of long period -- often indistinguishable from "steady" baroclinic geostrophic currents -- and directly wind-driven flows, which show lagging correlations with changes in direction and magnitude of the wind stress. Some of these emerging findings have been treated by Blanton (1974a, 1974b), Blanton and Murthy (1974) and reviewed by Boyce (1974).

Blanton performed spectral analysis on records from fixed current meters placed at 3, 6, 11, and 16 km from the northern Lake Ontario shore near Oshawa. For selected intervals representative of spring, summer and fall, (during 1970 with comparisons with IFYGL episodes in 1972) Blanton partitioned the total kinetic energy (mean speed squared plus the variance) into different frequency regions, of which two are selected for presentation in figure 1.13: frequency region (A), energy associated with periods greater than 3 days; and frequency region (B), energy associated with the narrow near-inertial range 16 to 18 hours period, i. e. rotary motion produced by near-inertial internal waves referred to above. Expressed as percent of the total kinetic energy of the whole spectrum, the distribution of portions (A) and (B) with distance from

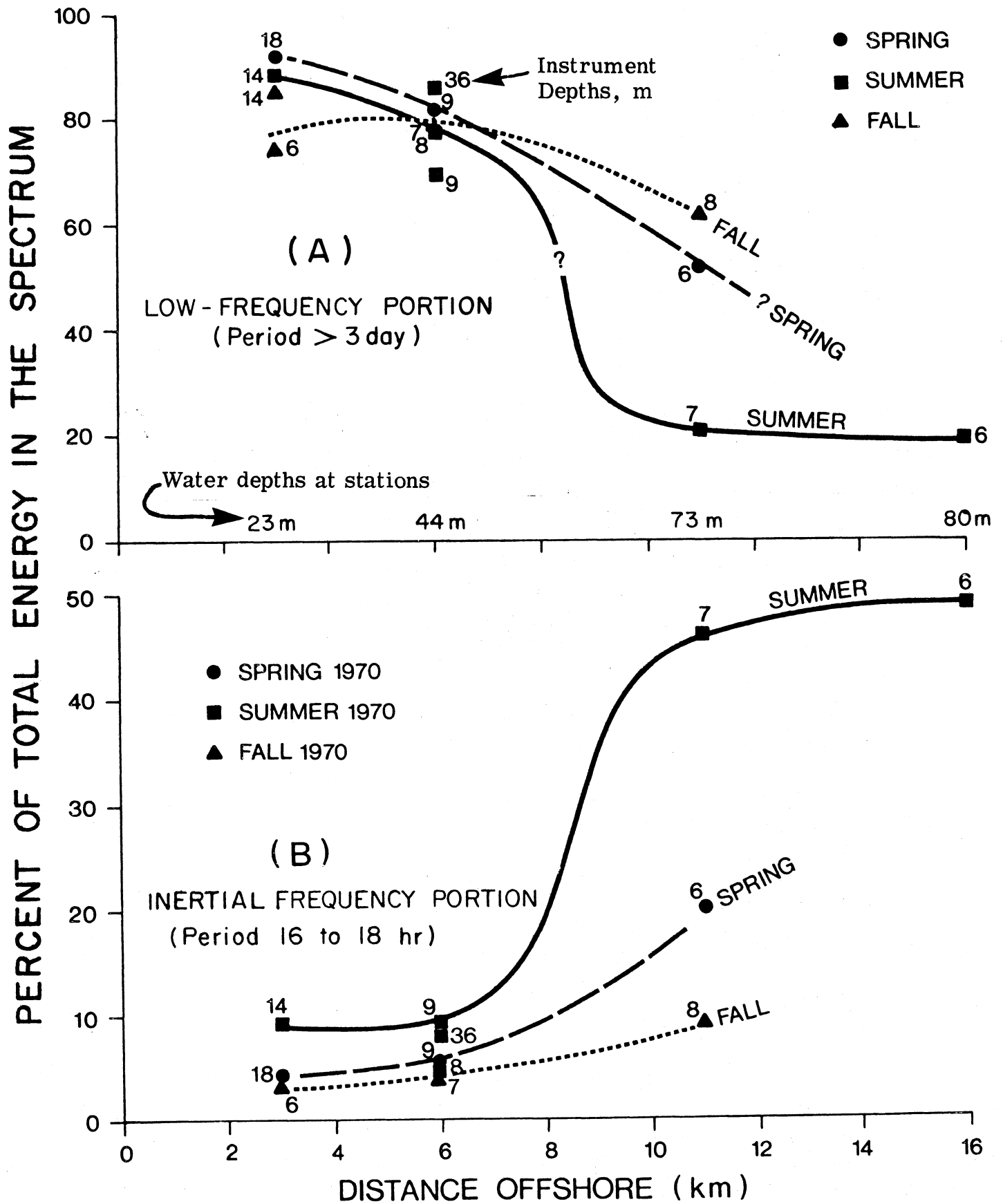


Figure 1.13 Percent of total kinetic energy found during three seasons, in motions with periods (A) in excess of 3 days, and (B) between 16 and 18 hr, determined by Blanton (1974a) at four distances from the northern shore of Lake Ontario.

shore is plotted for the three seasons in figure 1.13. It is immediately evident that in the low-frequency band, most of the energy is found within 7 or 8 km from the shore, while at distances greater than 10 km offshore, the proportion of inertial motion increases, very markedly during summer. These results suggest that the transition between the nearshore and offshore regimes is relatively abrupt in northern Lake Ontario, and this conclusion is further illustrated in figure 1.14 by spectra of the kinetic energy attributable to horizontal currents measured at 7-8 m depths at stations respectively 6 km and 11 km from shore (Boyce 1974, from unpublished data by J. O. Blanton). Spectra from both stations contain a peak near the inertial frequency, but the relative energy density at that frequency shows a ratio of about 10 to 1 in favor of the "offshore" station. On the other hand, in the lower frequency range corresponding to (A) in figure 1.13, the "nearshore" spectrum shows the greater energy density. This confirms the conclusion we demonstrated previously by visual comparison of current directions at an offshore and a near-shore station in figure 1.12.

Blanton (1974a) also describes a decrease in total kinetic energy of horizontal motions with increasing distance from shore and notes a general tendency for a corresponding difference in total variance. In other words, the nearshore zone represents a more turbulent boundary layer, at least in some regions of the eddy spectrum. Total energy at any given distance offshore was found to be lowest in spring and highest in the fall, with predominantly westward flow off Oshawa in all seasons. Superimposed on this were reversals in current direction occurring after changes in wind direction; and Blanton characterizes the time dependence of these events as follows: "Nearshore currents reverse from west to east flow about 6 hours after the wind changes, but farther offshore the reversals lagged to the wind by about 12 hours in summer and 36 hours in fall."

This conclusion, that the nearshore zone takes on the characteristics of a turbulent boundary layer, is supported by horizontal turbulence spectra measured by Palmer (1973), using mechanical and hot-film current meters and also comparing a station 1 km offshore in Lake Ontario with one "well offshore". His nearshore spectrum contained more energy at high frequencies

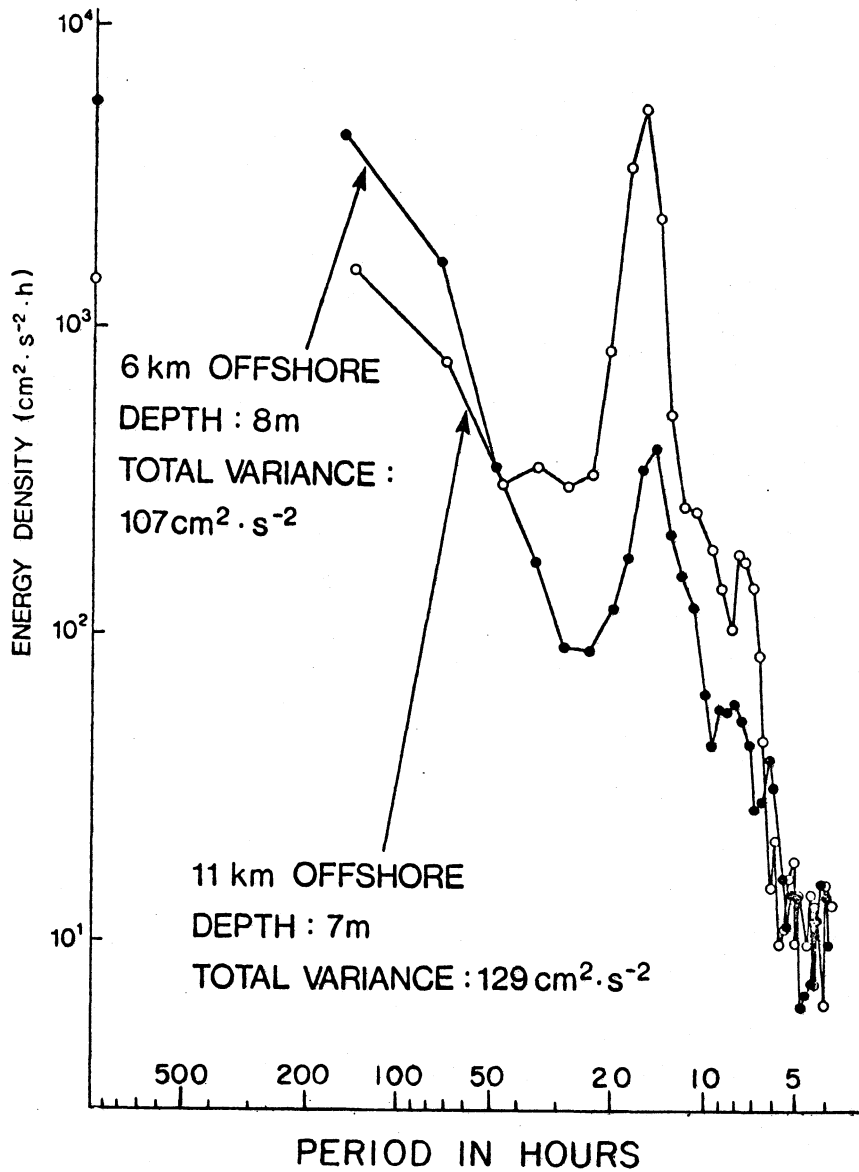


Figure 1.14 Spectra of kinetic energy density at two stations, one at 5 km and the other at 11 km from the northern shore of Lake Ontario (from Boyce 1974, from Blanton's unpublished data). Note the spectral valley between the large energy density at periods greater than 50 hr and the conspicuous energy peak near the inertial period (16 hr), greatest for the offshore station (open circles).

and was reminiscent of spectra found in turbulent boundary layers. Csanady and Mekinda (1970) also examined turbulent spectra based on rapid fluctuations of current direction at a nearshore station in Lake Huron, noting energy density maxima in the range 0.1 to 1 cycles per minute, with a rapid falloff in the range 1 to 10 cycles per minute.

#### General conclusions from the review

In the foregoing review we have attempted to cover, although not in detail, the principal findings to date relating to coastal currents in the Great Lakes. Some familiarity with this background is essential if the reader is to interpret the Lake Michigan observations now to be presented. We may expect, for example, that the field of motion in coastal waters will respond more strongly to the component of wind along the main axis of the basin and that each major storm involving large changes in stress or stress direction, will be reflected in large adjustments in the coastal current regime after some lag period, the length of which will depend on the strength of the preceding current, on water depth, and on the time history of the changing stress. During summer stratification, for example, there will be frequent upwelling-downwelling (downwelling-upwelling) changeovers, in which the thermocline rises (falls) and the surface layers move offshore (onshore). Superimposed on these complex and little understood processes is the variability of bottom topography and of wind stress.

Because the momentum flux from air to water takes place at the surface, the average wind-derived stress per unit volume of fluid in a mixed layer is inversely proportional to the depth of that layer. Therefore, shallow near-shore water masses will respond more quickly to changes in wind force than deeper layers further offshore. At the same time, the momentum of the deeper currents will develop a degree of persistence; and large horizontal shears are to be expected in coastal regions during the periods of changing wind (Blanton and Murthy 1974). If vertical density differences are present -- in the form of a thermocline or less distinct stratification -- internal waves

add to the complexity as mentioned earlier; and rotary motions principally of near-inertial frequency will combine with predominantly shore-parallel unidirectional motions to produce even more complex patterns than those illustrated for simple cases and models in figures 1.9 and 1.10.

To demonstrate the complexity of the coastal regime is easy -- and perhaps that is the principal result of the foregoing review -- but to design investigations and models to reveal the key mechanisms and their interactions is difficult. Boyce, in the conclusions to his 1974 review, addresses this problem.

"An area of research of great practical importance is the study of lake coastal zones. In these studies we can no longer rely on assumptions that local vertically acting processes can be distinguished from processes driven by the interaction of lake-basin-scale motions with an irregular shoreline. The prospects of a deterministic modelling approach to the scales of motion affecting biological and chemical interactions in the coastal zone are less bright than for the larger-scale motions offshore. From a numerical modelling point of view alone, the increased horizontal and vertical resolution needed near the coast and the requirement to simulate the driving large-scale motions, together tax the finite memory capacity of the largest computers, let alone the task of assembling even more complex programs. In a sense, this situation is analogous to the problem of meteorological predictions wherein it is possible to forecast accurately the evolution of large-scale weather systems, at the same time being quite uncertain concerning the predictions of daily local surface conditions. For the immediate future, a statistical or climatological approach seems to be warranted. In a given area, the kinds of information useful to water resource management are seasonal temperature structure of the coastal zone average values, extremes, and standard deviations, the width of the coastal current zone and strength of the currents, the nature of the inner coastal boundary with reference to the phenomenon of coastal entrapment, and most important, the statistics of major current reversals and of periods of stagnation in the coastal zone."

It is our hope that the present report may be a substantial contribution to such a "climatological" approach, more specifically to the development of a climatology of coastal currents in Lake Michigan.

## General Plan and Scope of This Investigation

Our plan was to establish an array of current meters in Lake Michigan near the Oak Creek Plant of the Wisconsin Electric Power Company for intervals of several months covering a two-year period. During 1972 instruments were installed at eight of the stations shown in figure 2.1 (next chapter) in an array designed to investigate the current characteristics along the Oak Creek coastline. During 1973 more effort was made to explore inshore/offshore differences. Unfortunately, the study was plagued by instrument loss in 1972 and by instrument malfunctions leading to serious data loss, particularly during 1973. Without wishing to present excuses or apportion blame, we believe our conclusion -- that much more reliability needs to be built into expensive oceanographic instrumentation -- to be an understatement. In spite of these setbacks, we obtained sufficient data to permit description of the temporal and spatial characteristics of coastal currents in that region. We investigated the variation of currents with time at each of the stations, and we explored some of the features of the current field as a function of depth and distance from shore.

Relationships between current and wind were also studied; and the total information gained on temporal and spatial current variability and on wind stress variability contributes to a definition of the scales and the statistics of the "underwater weather" into which cooling water or other effluents disperse, under conditions reasonably representative of those along the western shore of the Lake Michigan basin. For example, when current activity is low, the dispersion rate of an effluent will be correspondingly low; but during upwelling and downwelling episodes, or after strong storm disturbances, massive exchanges between the inshore and offshore regions -- including the development of transient and rapidly changing horizontal shear zones -- will increase the dispersion rate by many orders of magnitude.

An additional, smaller part of our study included a search for and a description of "sinking plumes", to be expected in winter when the plume is discharged into ambient lake water of temperatures less than 4°C. As this phenomenon is related to the "thermal bar", this will be described briefly in the following paragraph. Of particular interest to us, and to those concerned with possible effects of cooling water on biology of Lake Michigan, was to explore whether the artificial thermal bar represented by the sinking plume would increase or decrease dispersion near the plume area. A definite answer to that question could not be found, but we conclude that the sinking plume will persist during the later winter months, with a variable form and size determined by local topography and atmospheric conditions.

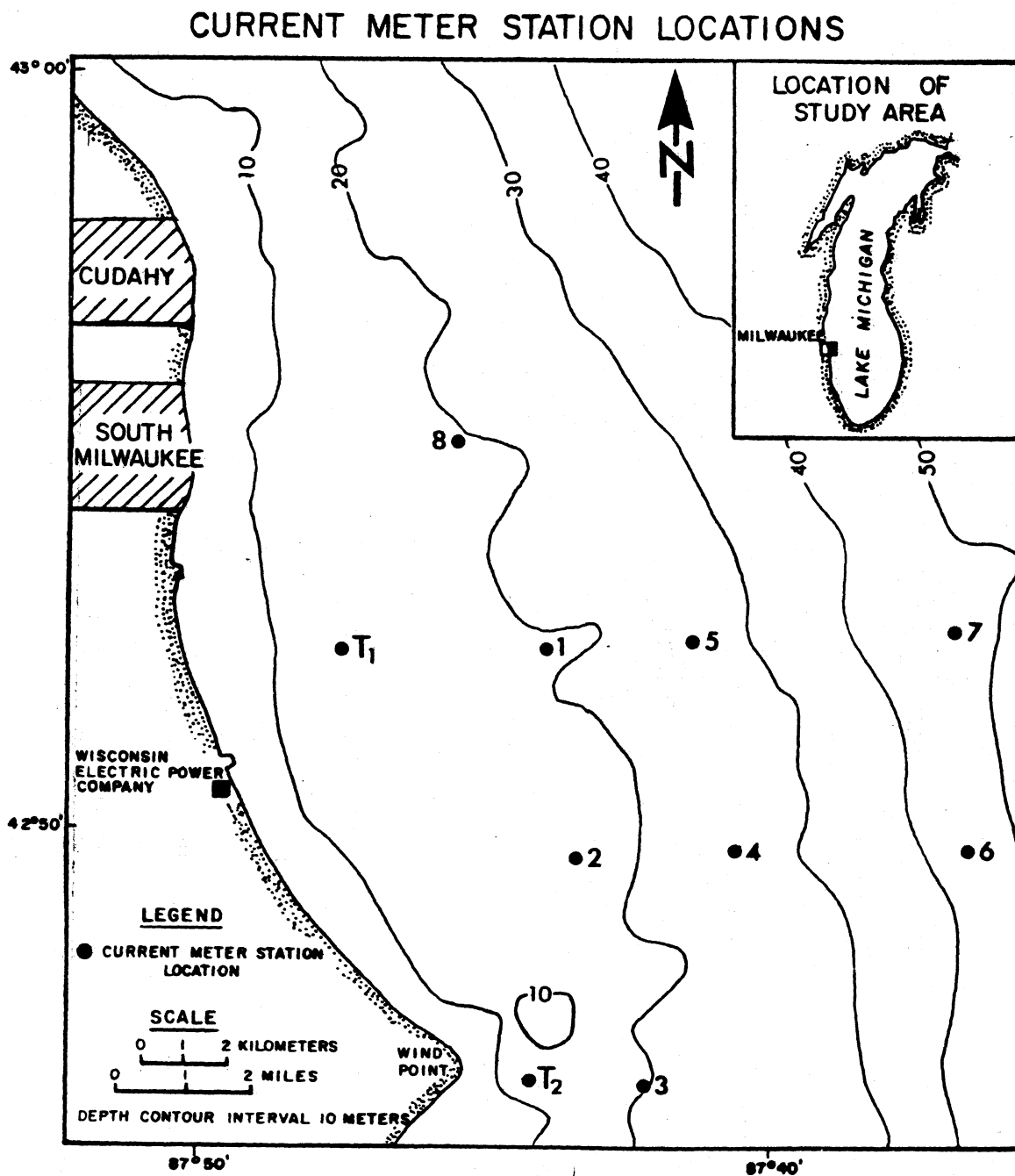
Formation of a (spring) thermal bar is seen in lakes which cool below 4°C in winter, but which are large enough and wind-blown enough to keep the offshore water mass unfrozen and well-mixed, to yield a temperature of well below that of maximum density by the end of the winter.

Thermal bars are formed under circumstances in which the offshore whole water mass cools down below the temperature of maximum density, 4°C. If, under these circumstances, heat is added to the shallow nearshore waters -- by initial warming in spring or by a heated effluent -- the inshore temperatures rise above 4°C and thermal stratification typically becomes established there. Between the inshore stratified water and the offshore unstratified colder water (< 4°C) a narrow transition zone is formed and is marked by a nearly vertical 4°C isotherm. This transition zone is known as the "thermal bar", and was interpreted by Tikhomirov (1963) as a convergence produced by inshore/offshore mixing, creating a mixed water mass of temperature near 4°C, and therefore denser than either of the parent masses. Consequent sinking of that mixture forms the thermal bar. As heat input increases with advancing spring, the bar moves progressively offshore until thermal stratification is established over the whole basin. This process, described in detail for Lake Ontario by Rodgers (1966) and Sato (1969) occupies several weeks.

In the Great Lakes the principal dynamic characteristic of the thermal bar is not the convergence, but a geostrophic coastal current on the shore side of the bar. That current is driven in a counterclockwise direction by the combined action of the thermal gradient and the earth's rotation, as predicted (although not yet measured) by the models of Bennett (1971) and Huang (1971). In Bennett's model, a weaker circulation, associated with upwelling in shallow water and a broad zone of sinking in the region of the 4° isotherm, redistributes the heat gain through the surface.

When the ambient lake conditions are those in which a thermal bar would form -- i. e. well-mixed offshore water at temperatures below 4°C -- a heated effluent will form its localized thermal bar, sinking at the fringes; and this is the pattern we observed, although no measurements of the currents associated with this phenomenon were made. This matter is discussed further in Chapter 5. The near-vertical topography of the 3° and 4° isotherms forms an extensive skirt-like boundary to the plume. This must constitute -- as in Bennett's (1971) model a broad zone of sinking water, thereby transporting heat and materials away from the plume area toward deeper regions of the Lake. This does not suggest that a concentration of materials would build up in the plume area. The natural thermal bar, on the other hand, is characterized by a shore-bound geostrophic current in addition to a sinking convergence. Therefore, during certain phases of evolution of the thermal bar, materials introduced at the shore would tend to stay nearshore, perhaps for some weeks.

Figure 2.1 Locations of Lake Michigan current measuring stations, near Oak Creek, Wisconsin: 1 to 8 moorings; T<sub>1</sub> and T<sub>2</sub> towers.



## CHAPTER TWO

### EXPERIMENTAL DESIGN: INSTRUMENTS AND METHODS USED; FIELD EXPERIENCE

#### Data Recording -- Current Speed, Current Direction, and Water Temperature

Braincon Type 573 Digital Current Meters were deployed at 10 stations, numbered 1 to 8 and  $T_1$  and  $T_2$  positions shown in figure 2.1, arranged to monitor the ambient lake current and temperature and to detect nearshore/offshore differences up to distance of approximately 10 miles (16 km) from shore and 10 miles (16 km) alongshore in the neighborhood of the Wisconsin Electric Power Company's fossil-fueled power plant at Oak Creek. The alongshore extent ranged from South Milwaukee to Wind Point, Racine. Station data and the dates of occupation are listed later in Table 2.1. As figure 2.1 shows, the general arrangement of stations was along two eastward lines from Oak Creek. But, because of the curvature of shoreline, station distances from the Oak Creek plant (tabulated in brackets) were in most cases greater than the distances from the nearest shoreline, tabulated outside the brackets.

At Stations 1 to 8 the instruments were suspended on taut wire moorings, illustrated in figure 2.3 and described below. At the shallow-water Stations  $T_1$  and  $T_2$  the instruments were mounted on a fabricated metal framework or "tower" (fig. 2.4). Stations  $T_1$  and  $T_2$  were approximately 2 miles and 1 mile (3.2 and 1.6 km) from shore respectively. Water depths, instrument depths, and distances from shore are given for each station in Table 2.1 in the following section (Field Experience).

Figure 2.2 The Braincon Type 573 Digital Current Meter (Braincon Corp., Marion, Mass. 02738). Specifications (19 May 1969) are on opposite page.

**GENERAL**

The Braincon 573 Digital Current Meter is an internal recording, self-contained instrument which measures current speed, current direction in relation to magnetic north, and instrument tilt, recording their values periodically on 4 channel magnetic tape. Optional sensors for depth, temperature and time may be incorporated. The 573 Digital Current Meter incorporates the most advanced technology yet applied to "in-situ" oceanographic instrumentation. It is one of a series of digital products resulting from a company sponsored development program begun in 1965. This instrument features small size, light weight, cartridge magnetic tape loading, computer compatible tape formatting and solid state TTL logic. The 573 Digital Current Meter represents the most cost-effective approach to oceanographic measurements available as a standard product.

**TECHNICAL DESCRIPTION**

The 573 Digital Current Meter consists of four basic assemblies; the sensor assembly, the data acquisition assembly, the battery assembly, and the pressure case assembly.

The sensors provide a standardized output (nominally 0 to 1v dc), which is interfaced with an analog to digital converter. The data is programmed and recorded in digital form by a 4-channel incremental digital recorder. A time base generator provides the primary time reference to initiate sensing and recording cycles. Data can be recorded every 5, 10, 20, 30 or 60 minutes. (Sampling period is specified at time of order.)

**CURRENT SPEED SENSOR**

Current speed from .05 to 5 knots is sensed with a Savonius rotor. The rotor is mounted within a standard cage on tungsten carbide bearings. The rotor is magnetically coupled through the instrument pressure case to a gear train and turns a potentiometer which generates 0 to 1 volt dc output for a 0-360° rotation.

**CURRENT DIRECTIONAL SENSOR**

Current direction is sensed using a 9.25 sq. ft. vane which aligns the instrument in the direction of current flow. Its position is measured in reference to a magnetic compass. The design of the vane has been chosen to be detuned over the vortex shedding frequencies encountered in the speed range of interest. Its response time closely matches that of the Savonius rotor.

**TILT SENSOR**

Instrument tilt in the plane of the direction vane is sensed with a viscous damped pendulum coupled to a micro-torque potentiometer.

**TEMPERATURE SENSOR (Optional)**

Ambient temperature is sensed using a precision thermistor mounted in the instrument end cap.

**PRESSURE SENSOR (Optional)**

Pressure is sensed using a pressure operated, high-resolution potentiometer.

**TIME SENSOR (Optional)**

A twelve or twenty-four hour index on the record can be provided by an Accutron\*.

\*Trade Mark of Bulova Watch Co.

**DATA ACQUISITION ASSEMBLY**

The data acquisition assembly accepts the output of the sensors and digitizes, programs, records, and stores the data in digital form on 4-channel, 4-track, 1/4" magnetic tape at a packing density of 100 BCD digits per inch.

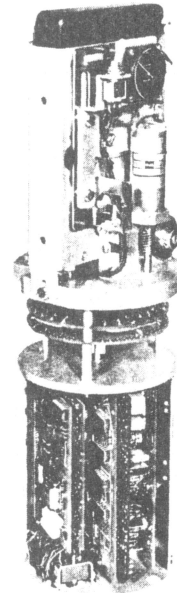
The data acquisition assembly incorporates a magnetic tape transport and programmer (DATA SHEET 41), an analog to digital converter (DATA SHEET 47), an analog multiplexer, a power regulation component, and an Accutron time base generator for sampling control.

The tape transport is cartridge loaded. The cartridge contains 375' of magnetic tape, which can record 450,000 BCD digits.

**DATA PROCESSING**

The data recorded on the magnetic tape is in a computer compatible format which permits digit by digit translation of the data for computer analysis. Five options are available:

1. Directly into a computer memory using a Braincon 622 Digital Output coupler.
2. Storage on 1/2", 566 bit per inch IBM compatible magnetic tape using a Braincon 595MT7 Magnetic Tape Data Processor (DATA SHEET 48).
3. Storage on 9-channel, 800 bit per inch IBM system 360 compatible magnetic tape using a Braincon 595MT9 Magnetic Tape Data Processor.
4. Storage on 8-channel punched paper tape using a Braincon 595PT Magnetic Tape Data Processor.
5. Utilization of Braincon Corporation's Data Processing Service to translate the data to 8-channel punched paper tape.



The Digital Data Module shown above is basic to all Braincon digital data acquisition systems. This compact package contains the tape recorder, Accutron, analog/digital converter, output register, programmer and multiplexer.

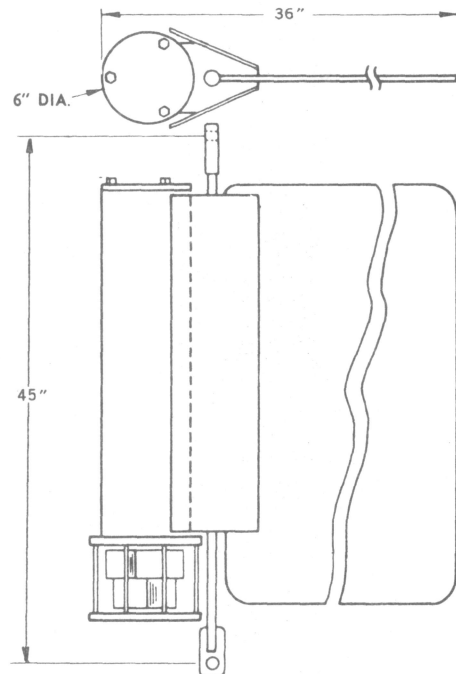


## Figure 2.2 (continued) Specifications of the Braincon Type 573 Digital Current Meter.

### CURRENT SPEED SENSOR

**Type:** Savonius rotor (balanced in air) 2/3 size  
**Range:** 0.05 to 5 knots  
**Calibration Threshold:** 0.05 knots (minimum)  
**Sensitivity:** 132 RPM/knot (nominal)  
**Mounting:** Tungsten Carbide pivot bearing to instrument pressure case.  
**Accuracy:**  $\pm 3\%$  of full scale

### CURRENT DIRECTION SENSOR

**Type:** 9.25 sq. ft. (approx.) vane (balanced in water to be insensitive to tilt) is referenced to a magnetic compass.  
**Range:** 0 to 360° continuous  
**Vane Sensitivity:**  $\pm 5^\circ$  at 0.05 knots  
**Vane Mounting:** Integral with pressure case.  
**Vane Bearing Materials:** Teflon and #300 Series Stainless Steel.  
**Compass Type:** Viscous Damped permanent magnet compass.  
**Current Direction Accuracy:**  $\pm 2\%$ .

### INSTRUMENT TILT SENSOR

**Type:** Viscous damped pendulous inclinometer with potentiometric output.  
**Tilt Range:**  $\pm 30^\circ$   
**Accuracy:**  $\pm 2^\circ$

### PRESSURE SENSOR (optional)

**Sensor Type:** Pressure operated potentiometer with oil filled isolator.

<b>Pressure Range:</b>	0- 15 psi	0- 400 psi
	0- 30 psi	0- 600 psi
	0- 60 psi	0-1000 psi
	0-100 psi	0-2000 psi
	0-200 psi	0-3000 psi
		0-5000 psi

**Accuracy:**  $\pm 2\%$

### TEMPERATURE SENSOR (optional)

**Sensor Type:** Precision Thermistor.  
**Temperature Range:**  $-2^\circ$  to  $30^\circ\text{C}$   
**Accuracy:**  $\pm .25^\circ\text{C}$

### TIME SENSOR (optional)

**Type:** Accutron  
**Range:** Time index every 12 or 24 hours.  
**Accuracy:**  $\pm 2$  sec/day.

### ANALOG TO DIGITAL CONVERTER

**Type:** Solid State Voltage—frequency to count converter with BCD output.

**Output:** 3 BCD digit output directly proportional to the analog input voltage.

**Sensitivity:** .001 volts.

**Accuracy:**  $\pm .1\%$

**Input Range:** 0.000 to 0.999 volts dc

### RECORDER AND PROGRAMMER

**Sensor Sampling Period:** Selectable at time of order for every 1, 5, 10, 15, 20, 30 or 60 minutes using Accutron.

**Programming Mechanism:** Sensor input lines are automatically sequenced and synchronized to the magnetic tape advance mechanism.

**Tape word formatting:** The complement of BCD is recorded in one row across 4 channels.

**Tape Cartridge Capacity:** 450,000 BCD digits.

**Packing Density:** 100 BCD digit/inch.

**Tape Cartridge:**  $\frac{1}{4}$ " wide, 375' long, 1.0 mil thick magnetic tape in endless loop cartridge.

**Recording Mode:** magnetic Tape Saturation.

**Recording Speed:** 10 BCD digits/sec. asynchronously.

### INSTRUMENT POWER SUPPLY

**Type:** Rechargeable, Nickel-Cadmium battery pack.

### OPERATING ENVIRONMENT

**Operating Temp. Range:**  $-2^\circ$  to  $40^\circ\text{C}$

**Storage Temp. Range:**  $-34^\circ$  to  $+65^\circ\text{C}$

**Shock:** Will withstand 6" drop on wood surface.

### INSTRUMENT HOUSING

**Operating Medium:** Sea Water

**Maximum Pressure:** 7000 psi

**Max. Tensile Load:** 7000 lbs. across instrument suspension bar.

**Material:** Aluminum

**Finish:** Anodized

**Coating:** Baked-on Paint

**Color:** Blue Green

**Hardware:** 300 series stainless steel, welded where necessary.

**Anti-Corrosion Protection:** Sacrificial Magnesium Anode

**Condensation Control:** Replaceable Dessiccant

**Maximum Length:** 45" between top and bottom mooring eyes.

**Maximum Instrument O.D.:** 6"

**Max. Weight in Air:** 70 lbs. (approximately)

**Max. Weight in Sea Water:** 50 lbs. (approximately)

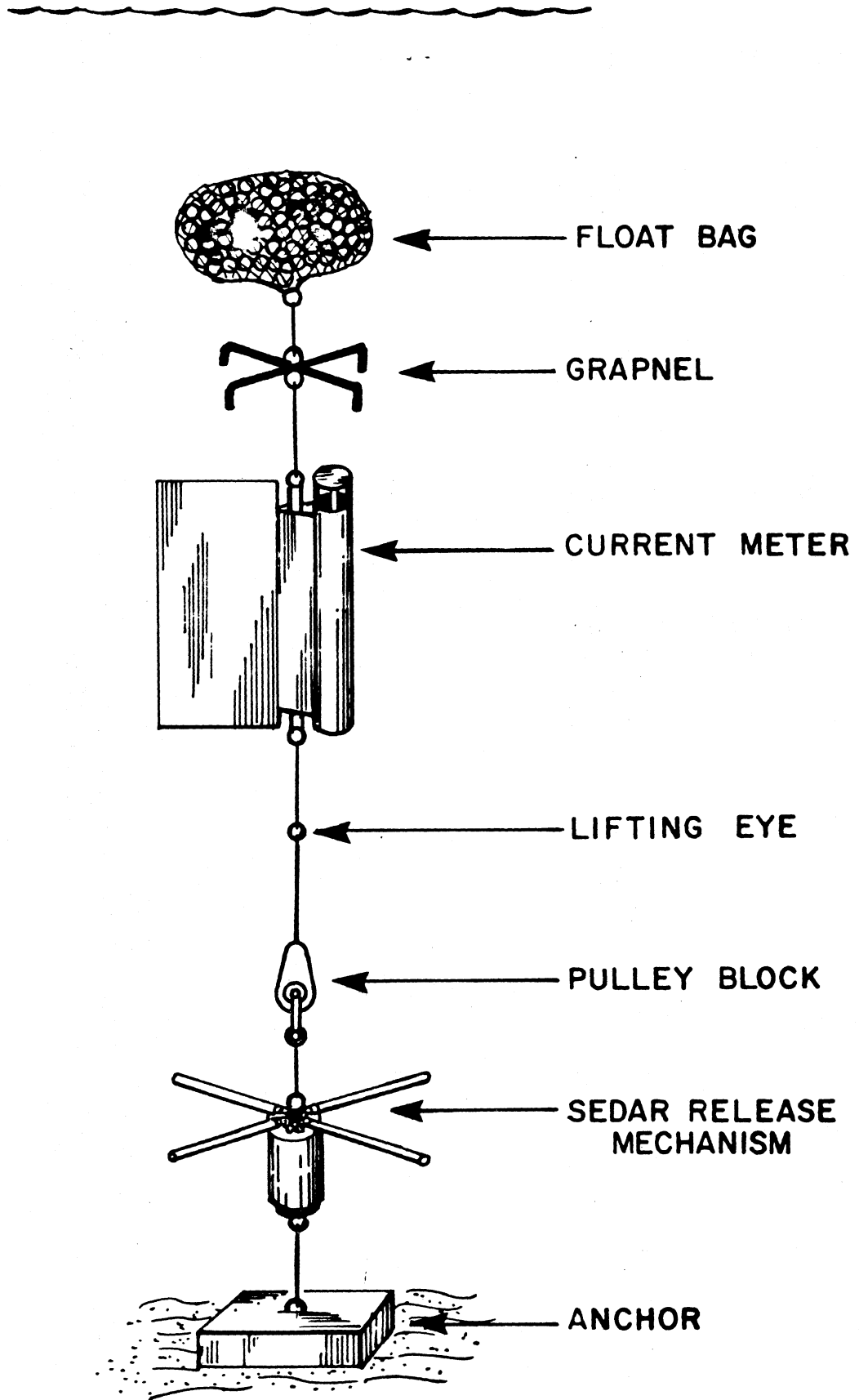
## Braincon Type 573 Digital Current Meter

Summarized specifications are given, in a description supplied by the manufacturer, in figure 2.2. Current is sensed by a Savonius rotor over a range from 2.5 cm. sec<sup>-1</sup> claimed (actual minimum closer to 4 cm. sec<sup>-1</sup>) to 250 cm. sec<sup>-1</sup>. Current direction is sensed by a vane referenced to a magnetic compass, and the vane sensitivity is given as  $\pm 5^\circ$  at 2.5 cm. sec<sup>-1</sup>. The combined accuracy of compass and vane is given as  $\pm 2\%$  in direction. Recording is on 4-channel quarter-inch magnetic tape, coded as the complement of BCD in one row across the four channels. Current speed, current direction, and water temperature are each recorded as 3-digit numbers at 10-minute intervals. With a tape cartridge capacity of 450,000 BCD digits at 100 digits per inch, maximum recording duration at the 10-minute interval is 125 days, which somewhat exceeds the battery life (rechargeable, nickle-cadmium battery pack). The anticipated (Accutron) clock error is  $\pm 5$  minutes over 125 days.

## Taut-line mooring system

This is illustrated in figure 2.3. To maintain the current meter at desired depth and in a position within  $5^\circ$  of the vertical, a submerged float was used, consisting of hollow, water-tight plastic balls contained in a strong nylon net bag. The float was placed at approximately 30 feet (9 m) from the surface to avoid interference with navigation and to minimize the influence of surface waves on current meter motion. Two tilt sensors were available and these were used on different instruments from time to time, confirming that the angle of tilt did not exceed  $5^\circ$ . Therefore, no correction for tilt was made in the current speed reading.

Figure 2.3 The taut-line mooring system, with submerged float, Type 573 current meter, and release mechanism.



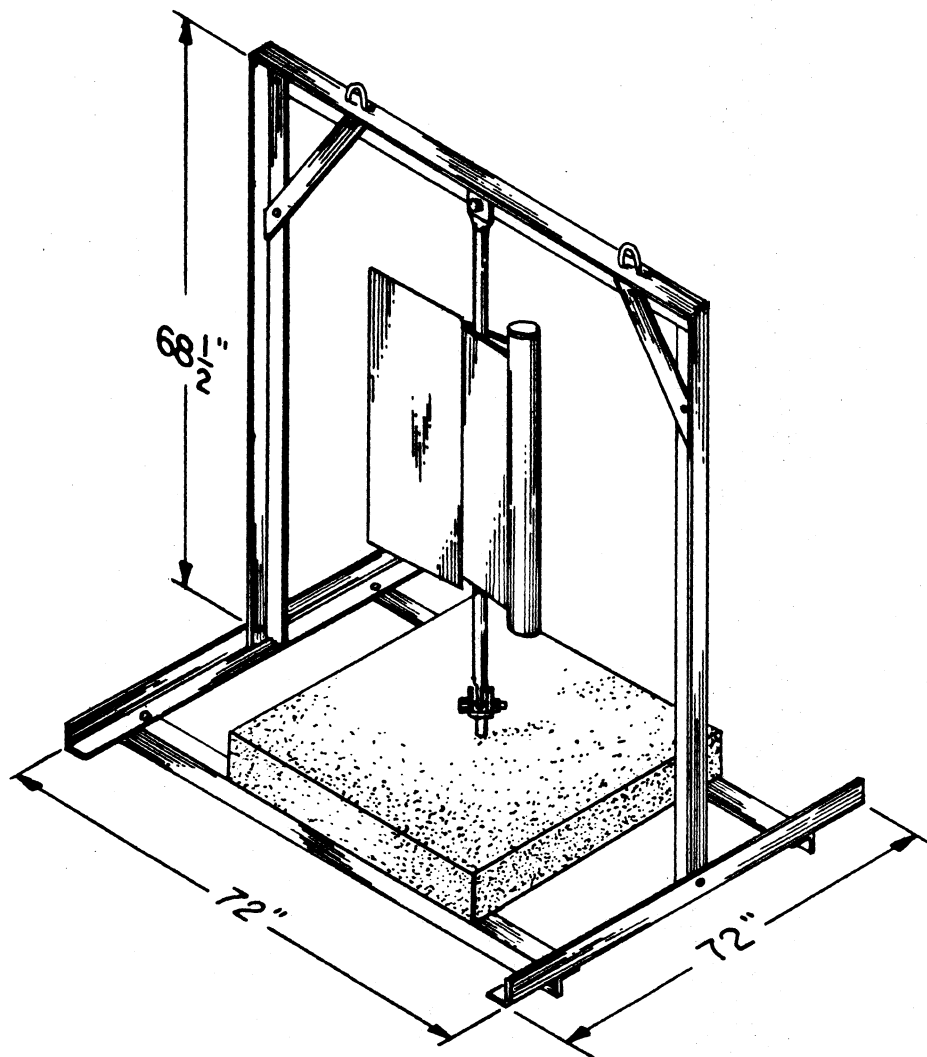


Figure 2.4 Tower mounting for the current meter in shallow water.

The mooring cable, 3/8 inch (9.5 mm) diameter steel wire rope, was made up in sections to connect the following components, here listed in descending order: float bag; inverted grapnel -- a device to facilitate recovery by dragging in an emergency -- current meter; lifting eye; pulley block for lowering as described below, a Braincon SEDAR Release mechanism described below; and an expendable concrete sinker.

The mooring system was installed from the Center for Great Lakes Studies' research vessel, first connecting the SEDAR to the sinker with a chain and then attaching the wire cable to the top of the SEDAR. This whole bottom section was lifted by the winch at the lifting eye and placed in the water by the side of the vessel. A one-inch nylon rope was put through the pulley block and used to support the bottom section of the mooring system. The top section of the mooring line was then connected to the bottom section. One end of the nylon rope was held in place while the other end was slacked slowly in order to allow the sinker to descend gently to the bottom of the lake. The secured end was then released and pulled through the pulley block and retrieved.

As already mentioned, fixed frames not moorings were used on the two shallow stations T1 and T2. These frames or towers were fabricated from aluminum angle and were approximately two meters in height (fig. 2.4). Specially modified current meters, with the Savonius rotor at the top of the instrument instead of the bottom, were used and the framework gave ample clearance for the current meter to swing through 360°. The structure, with the current meter installed, was lowered to the bottom from the research vessel by winch. Divers were then sent down to disconnect the lowering cable; and the procedure was reversed on recovery.

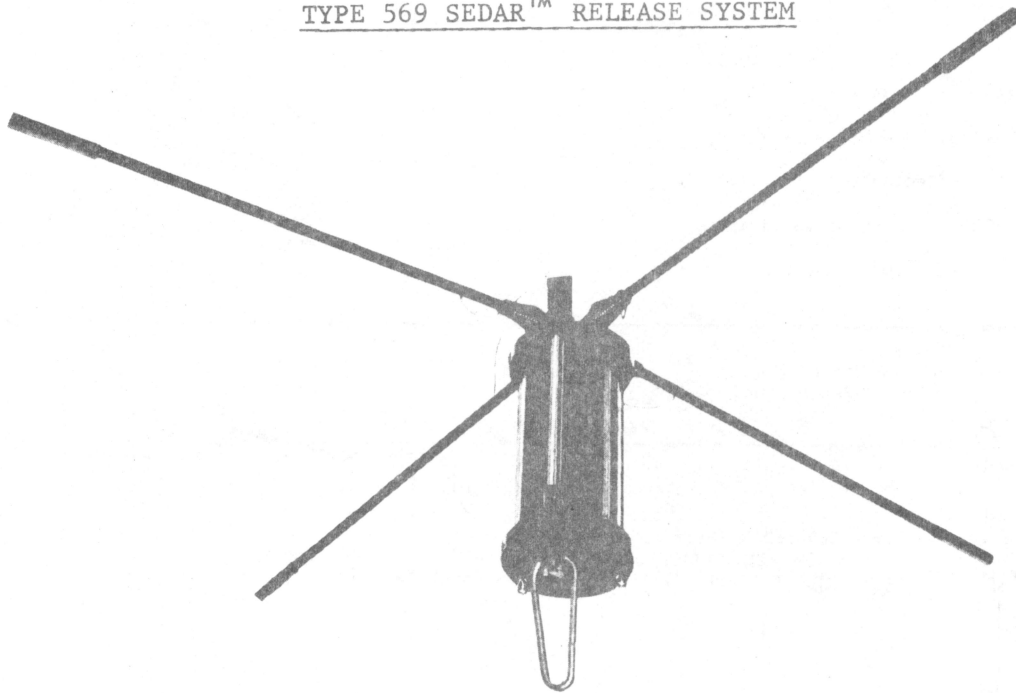
## SEDAR release mechanism

The SEDAR (Submerged Electrode Detection And Ranging) System was chosen in place of the more commonly used acoustic release mechanisms, because we believed that the sometimes abrupt thermoclines in Lake Michigan could mask acoustic commands, when these were not delivered from directly above the instrument. Reflection or diffraction of the signal could not occur with SEDAR. We had previously tested this system in Lake Michigan and it had been successfully used on various occasions in operations in the northern part of the Lake and in Green Bay. However, our field experience at Oak Creek included several premature releases during thunderstorms, which caused considerable delay and reorganization in the program. These events and the precautions which we took as a consequence of them are described in the next section.

SEDAR (fig. 2.5) responds to modulated, coded electric field radiation "injected" into the water by towed electrodes connected to a transmitter on the research vessel. This release mechanism consists of a sensitive receiver tuned to a selected frequency in the range 600 to 1000 Hz, low enough to give useful ranges underwater. When the signal is received for 20 seconds, an explosive squib is fired which releases a link at the bottom of the mechanism, permitting a float to carry the equipment to the surface and leaving the sinker on the bottom. The claim by the manufacturer that "natural and man-made interference is virtually obscured" was not borne out by our experience; but with appropriate precautions the system has merit in avoiding the effects of density discontinuities in the water on the reliability of acoustic systems. Each instrument was tuned to a known frequency and could be recalled to the surface without releasing the others.

Figure 2.5 Description and mode of operation of the Braincon Corporation's Type 569 SEDAR release mechanism. Further details on the following page.

TYPE 569 SEDAR™ RELEASE SYSTEM



THE SEDAR (Submerged Electrode Detection And Ranging) SYSTEM IS A TECHNIQUE WHICH UTILIZES UNDERWATER ELECTRIC FIELD RADIATION TRANSMITTED FROM A VESSEL TO A SUITABLE UNDERWATER RECEIVER.

IT OPERATES ON THE PRINCIPLE OF IONIC CONDUCTION AND IS COMPLETELY UNRELATED TO ACOUSTIC SYSTEMS.

TYPE 569 SEDAR RELEASE SYSTEM

The Type 569 SEDAR Release System offers an effective alternate to acoustic systems in shallow or continental depth waters. The use of modulated electric field radiation with coding eliminates the effects of thermal structures or salinity discontinuities which limit the reliability of acoustic instrumentation. In addition, natural and man-made interference is virtually obscured.

DESCRIPTION

The Type 569 is a versatile, highly reliable device capable of releasing loads at Continental Shelf depths. Dependable operating ranges are obtained with a surface towed transmitter array, and receiver moored in depths to 600 feet. The SEDAR technique permits a compact receiver package with low power consumption. The unit will operate continuously for a 90-day period.

The release mechanism consists of a SEDAR receiver coupled to the same mechanism used in Braincon's Type 620 Release. Receipt of the SEDAR signal for 20 seconds fires a chemically charged piston, tripping the release mechanism. This combined action causes the bottom mounting bar to fall away, releasing the anchor or mooring.

The Type 569 SEDAR release system may be used in any mooring configuration where tension and range specifications are not exceeded. A typical field application is illustrated (back) in which a Type 569 SEDAR release system is attached to a subsurface float 50 ft. below the surface. When the interrogation signal is received, the subsurface float rises to the surface with the stored 100 ft. 5/8" plaited line pulling from the optional line storage case adjacent to the receiver. The mooring string may then be recovered by a surface ship.

The technique of transmission, design of the circuitry, mechanical release, and material selection, have been chosen to provide a reliable, reusable remote release at low cost. The method has been proven through field use in extreme weather and sea conditions, and is ideally suited for every day marine use in the oceanographic, offshore petroleum, marine, and fishing industries.

Other applications of the SEDAR technique include ships positioning, diver underwater communication, telemetry and remote control, guidance, and navigation.

For further information on the Type 569 SEDAR release system or other SEDAR system applications, contact the Sales Department, Braincon Corporation.

Figure 2.5 (continued) Specifications of the Type 569 SEDAR release system.

SPECIFICATIONS

SYSTEM

Max. Slant Range at Continental Shelf Depths: 3000 Ft.

TRANSMITTER

Transmitter Array: See below

Typical Installation: See below

Coded Channels: 5 Selectable in the field

Output Power: 115v ac, 1000 watts minimum

Operating Temperature: 10° to 40°C

RECEIVER

Receiving Array: See below

Typical Installation: See below

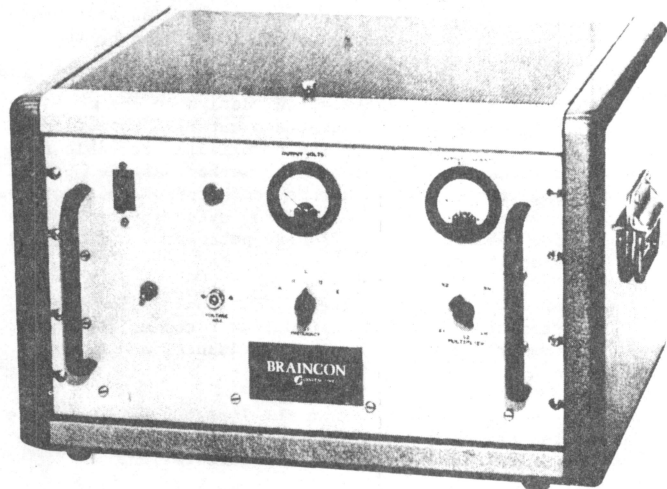
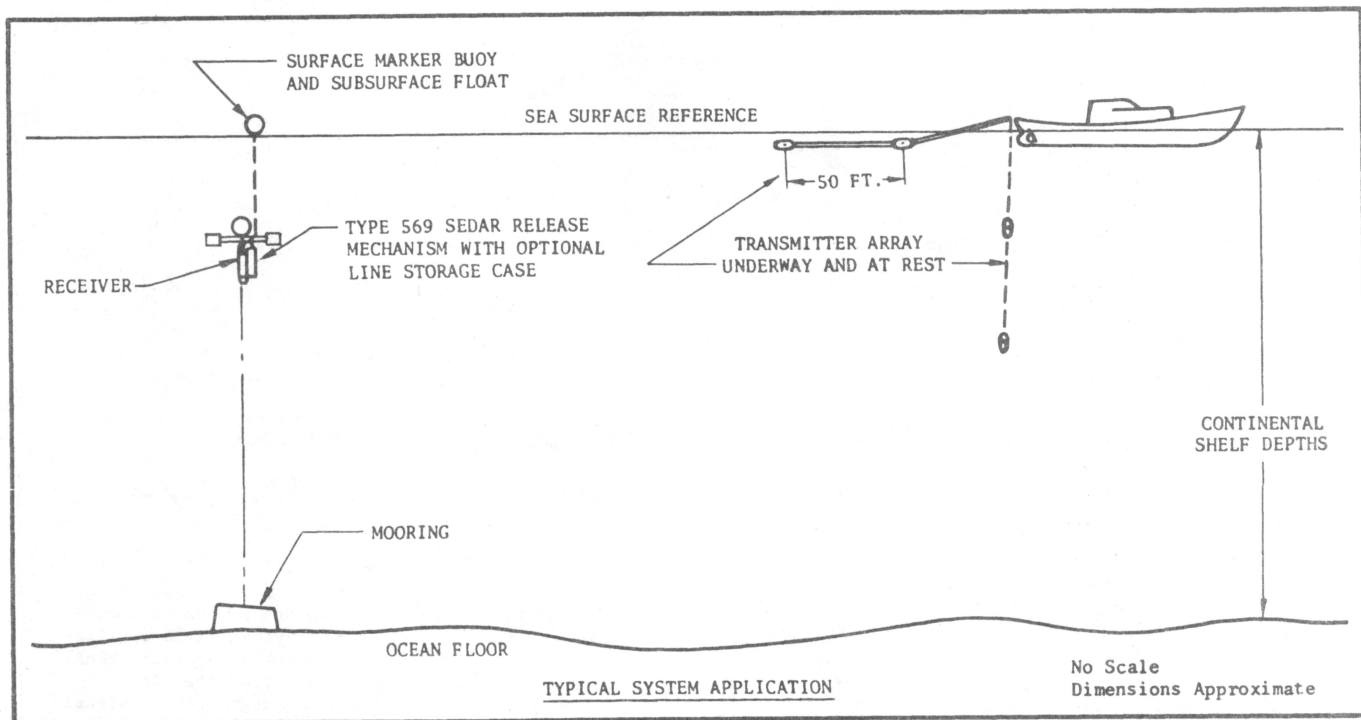
Battery Life: 90 days standard

Operating Temperature: -2° to 35°C

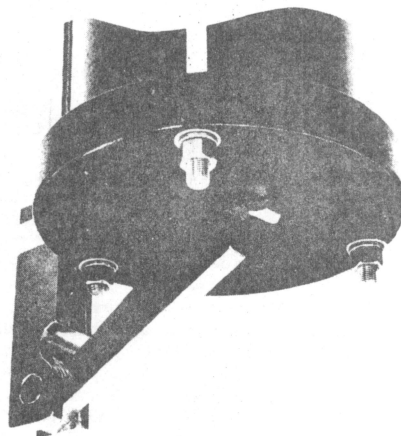
Max. Operating Tension: 10,000 lbs.

Max. Depth: 600 Ft.

Decoder Combinations: 5 (preset at factory)



SEDAR SYSTEM TRANSMITTER



SEDAR RELEASE, BOTTOM VIEW

## Field Experience with the Current Meters and Their Mooring Systems

Six surveys were conducted between April 1972 and November 1973 (Table 2.1). The nearshore stations were usually single current meter moorings whereas the deeper stations consisted of two meters, one in the upper and the other in the lower part of the water column. Plans to install current meters at all of the Figure 2.1 stations for the same periods of time were hampered by unfavorable lake and weather conditions, as the instruments could not be set more than two or three at a time. Quite often in the early summer months calm lake conditions were accompanied by poor visibility which made sighting of landmarks for station positions impossible. To overcome this problem, the Center for Great Lakes Studies purchased a Motorola Mini-Ranger System to determine accurately station positions during the 1973 surveys.

Of the five current meters used for Survey I, two were installed in early April 1972; inclement weather delayed the setting of the other three meters until early May 1972. All the meters from this survey were successfully recovered on June 5 and 6, 1972. Whereas Survey I had used exclusively taut-line mooring systems, Survey II consisted of two tower structures at the nearshore stations T1 and T2 and eight current meters using taut-line moorings. Because good visibility and calm lake conditions occurred only rarely, it was not possible to install current meters at stations 5 and 7 as planned.

During Survey II (see Table 2.1) premature release of the SEDAR mechanisms occurred on 14 July 1972 during a severe local thunderstorm. Our previous experience and that of the manufacturer and other users gave no warning of this, but it proved not to be an isolated incident at the Oak Creek site; and

Table 2.1

## LIST OF STATIONS AND LAKE MICHIGAN CURRENT SURVEYS

Survey	No.	Station		Meter Depth (m)	Date Set	Date Retrieved	No. of Days of Record in Water		Comments
		Distance from shore (km)*	Water Depth (m)				Expected	Obtained	
I	1	8.0 (8.4)	20	15	3 April 1972	5 June 1972	69	69	Parity error
	2	5.3 (7.2)	22	17	3 April 1972	5 June 1972	64	64	
	3	4.2	19	13	2 May 1972	5 June 1972	36	35	
	4	8.0 (10.8)	28	15	4 May 1972	6 June 1972	36	35	
				23	4 May 1972	6 June 1972	36	35	
II	1	8.0 (8.4)	20	15	5 June 1972	Lost			
	2	5.3 (7.2)	22	17	5 June 1972	Lost			
	3	4.2	19	13	5 June 1972	29 July 1972 in Sheboygan Harbor	54	32	Tape torn
	4	8.0 (10.8)	28	15	6 June 1972	17 August 1972 south of Terry	72	55	Tape cut
				23		Andrae Park	72	24	Tape unwound
	6	12.8 (16.3)	46	15	21 June 1972	3 September 1972	81	0	Tape cut
				23		near Ludington	81	80	
				15	14 June 1972	4 August 1972 at Terry Andrae Park	48	48	
	T <sub>1</sub>	3.5 (3.7)	13	11	14 June 1972	25 August 1972	71	71	
	T <sub>2</sub>	1.7	12	10	15 June 1972	25 August 1972	71	71	

\*Bracketed: distance from shore along E-W line in Fig. 2.1. Unbracketed: distance from nearest shoreline.

Table 2.1 (continued)

## LIST OF STATIONS AND LAKE MICHIGAN CURRENT SURVEY

Survey	Station No.	Station Distance from shore (km)*	Water Depth (m)	Meter Depth (m)	Date Set	Date Retrieved	No. of Days of Record in Water		Comments	
							Expected	Obtained		
III	T <sub>1</sub>	3.5 (3.7)	13	10	25 August 1972	27 October 1972	63	63		
	T <sub>2</sub>	1.7	12	10	25 August 1972	7 December 1972	104	92		
	T <sub>1</sub>	3.5 (3.7)	13	10	27 October 1972	Unrecovered				
IV	1	8.0 (8.4)	18	14	12 April 1972	17 July 1973	96	0	Faulty battery pack - no data	
	2	5.3 (7.2)	18	14	12 April 1973	17 April 1972	5	0	36 sec cycle - no data	
	2	5.3 (7.2)	18	15	14	17 April 1973	26 June 1973	5	5	36 sec cycle - no data
				73				0		
	4	8.0 (10.8)	28	12	23	13 April 1973	4 June 1973	52	52	No temperature data, hourly current speed & direction readings
				23				0		
	4	8.0 (10.8)	28	12	23	4 June 1973	19 June 1973	15	15	Erratic readings
				23				0		
	5	11.0 (12.0)	28	12	23	13 April 1973	17 July 1973	95	72	Zero speed readings
				23				41		
7	15.2 (18.1)	46	13	26	13 April 1973	4 June 1973	52	26	" " "	
			26				20			
7	15.2 (18.1)	46	13	26	7 June 1973	19 June 1973	15	15	Bad temp. readings	
			26				15			
									Zero speed readings	

\*Bracketed: distance from shore along E-W line in Fig. 2.1. Unbracketed: distance from nearest shoreline.

Table 2.1 (continued) LIST OF STATIONS AND LAKE MICHIGAN CURRENT SURVEYS

Survey	Station No.	Distance from shore (km)*	Water Depth (m)	Meter Depth (m)	Date Set	Date Retrieved	No. of Days of Record in Water		Comments
							Expected	Obtained	
V	1	8.0 (8.4)	18	14	17 July 1973	8 August 1973	22	5	36 sec cycle
				15			22	22	
	2	5.3 (7.2)	18	14	19 July 1973	8 August 1973	20		Zero speed readings Unrecoverable parity errors
				15			20		
	4	8.0 (10.8)	28	12	18 July 1973 (Prematurely released)	4 September 1973	20	20	Erratic readings Unrecoverable parity errors
				23			20	0	
5	11.0 (12.0)	28	12	17 July 1973	13 August 1973	27	0	Unrecoverable parity errors	
			23			27	27		
6	12.8 (16.3)	46	13	18 July 1973	13 August 1973	26	21	Erratic direction readings Erratic readings - bad temp. readings	
			26			26	26		Erratic readings in both meters
VI	1	8.0 (8.4)	18	14	15 August 1973	7 November 1973	84		Zero speed No data
				15			84		
	5	11.0 (12.0)	28	12	16 August 1973	19 September 1973	34	34	Erratic readings - bad temp. readings
				23			34	34	
	6	12.8 (16.3)	46	13	15 August 1973 (Prematurely released)	29 August 1973	14	14	Zero speed readings Erratic readings
				26			14	0	

\*Bracketed: distance from shore along E-W line in Fig. 2.1. Unbracketed: distance from nearest shoreline.

future users are warned that precautions have to be taken. All the moorings were released, and extensive searches were then conducted to recover the instruments in different parts of the lake; all but two were found, as a result of information from the Coast Guard, boat and beach property owners, railroad ferries and fishing vessels, and as a result of wide advertisement. At stations 4 and 8 the sudden increase in temperature caused by the upward motion of current meters from the cold lower layer to the warm upper layers of the lake indicated the release date to be 14 July 1972. No conclusion could be drawn from the other meters recovered due to faulty tape cartridges which did not provide complete data for the period during which the current meters were in operation.

During the drift away from the Oak Creek site, the floats were on the surface and the current meters were suspended in the upper layer above the thermocline. The instruments at the deeper stations, the mooring cable and release mechanism formed a drag line which extended through the thermocline into the lower layer. The resultant "current" recorded by the meter showed beautifully clear but uninterpretable examples of inertial motion, because of the opposition in flow between the upper and lower layers (see figs. 3.29, 3.30, 4.36).

After the July 1972 disaster, the use of taut-line mooring systems was temporarily discontinued until safety devices could be constructed and tested. In Survey III only instruments supported on the tower frameworks were used. When operations were resumed with 10 current meters during Survey IV (1973) preset mechanical timers were installed in the SEDAR Release Mechanisms, putting them into the activated mode only for a limited pre-determined time at the end of the measurement interval. Also, as a further precaution, a slack tethering line was attached between the pulley block and anchor (sinker) in

Figure 2.3 so that, if premature release occurred, as it did on some occasions, the float would rise to the surface but not drift away. On recovery, the tethering line was released and discarded. Further work is continuing at the Center for Great Lakes Studies designed to increase the reliability of the release mechanisms without sacrificing undue sensitivity and range. These steps include reduction of amplifier gain and (possibly later) shortening of the receiving antennae. Also, a more reliable pre-set mechanical timer is being installed to cut down the period in which the instrument would be subject to pre-release. This step, of course, also restricts the time during which it can be deliberately released. Previously employed mechanical timers had failed in one or two instances, so that release did not occur on command. Fortunately, at this shallow station, divers could be sent down to retrieve the instruments.

#### Data Processing and Analysis of Instrument Malfunctions

A summary of the data reduction steps is given in Figure 2.6. After the current meters were recovered from the lake, they were brought back to the Center for Great Lakes Studies, where the data were translated from 1/4 inch current meter tape to 1/2 inch computer compatible tape, using the Braincon Digital Magnetic Tape Processor. The computer tape was then sent to the Madison Campus Computer Center for cataloguing for use in the computer. The data were converted from free format form to card image form for use in the UNIVAC 1110. In order to perform this conversion, a tape dump of the "raw" data was obtained to determine the nature of the data. After the conversion to card image form, the data were converted to calibrated values of speed, direction and temperature.

# FLOW CHART FOR DATA REDUCTION

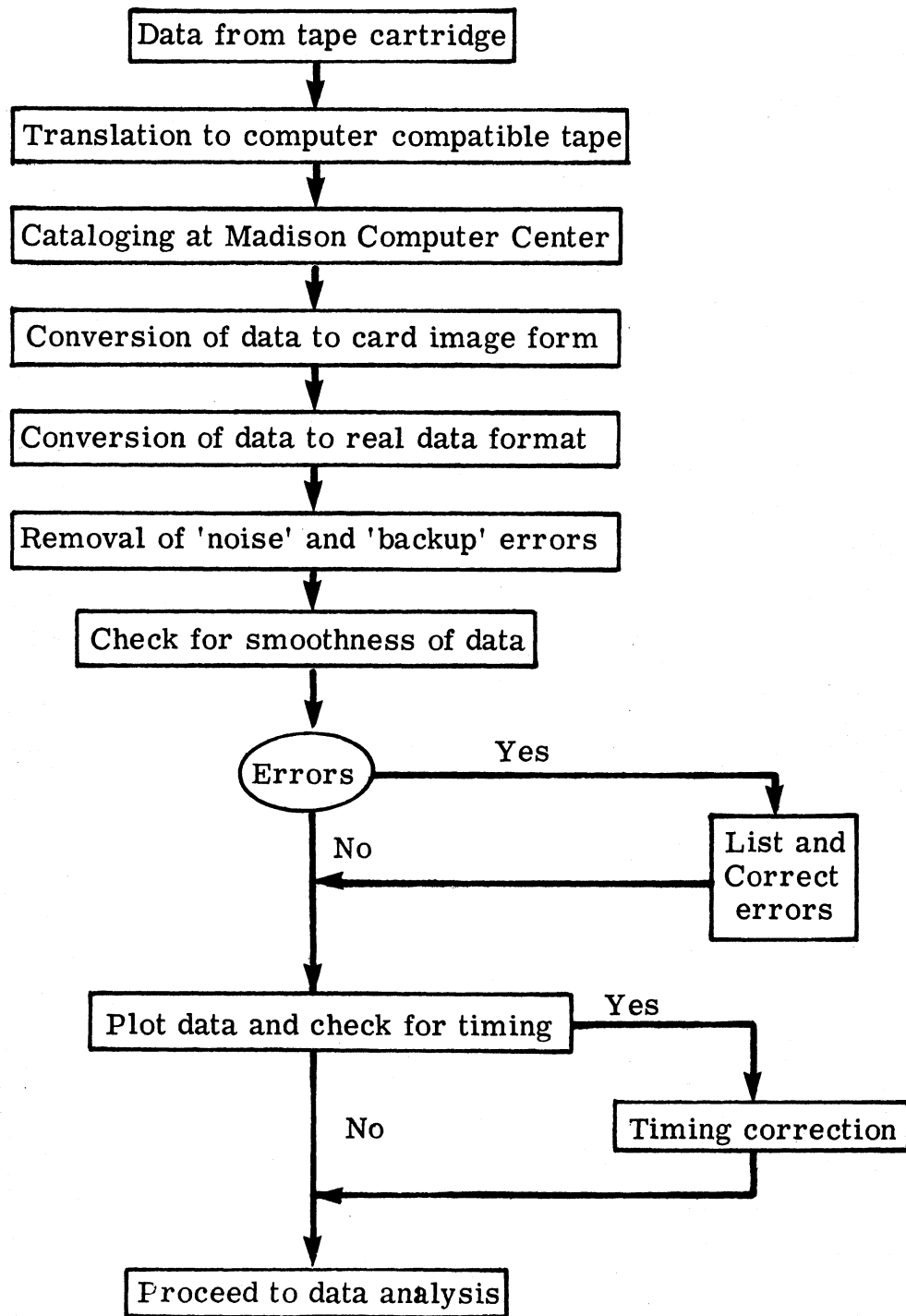


Figure 2.6 Steps in the data reduction process.

In addition to the steps described under data reduction, the data had to be corrected for machine errors, some of which were recoverable and the rest unrecoverable. The following is a list of the problems encountered with the instruments or in data reduction.

(i) 'Noise' Error:

'Noise' errors were found in the data in the form of alphanumeric data where numeric data should have been recorded. These were caused by the dropping of 'bits' in the recording cycle. 'Noise' errors were corrected by substituting an average value of the three readings before and after the incorrect readings.

(ii) 'Backup' Errors:

These speed reading errors occurred in all of the current meter data and were caused by an error in the potentiometer measurement used to measure the Savonius rotor revolutions. Instead of the potentiometric readings decreasing, they occasionally increased with the result that extremely high speed values were recorded. These errors were corrected using the method for correcting 'Noise' errors.

(iii) 'Peak' Values:

Sudden increases in current speed followed by a zero value in speed were caused by a malfunction in the recording cycle of the meter. These values were substituted with corrected values calculated using the method described above.

(iv) 'Short Sequences':

Each ten-minute reading was supposed to consist of 23 characters. However, when instrument error resulted in fewer than 23 characters being recorded, the missing characters were substituted by corrected values.

(v) 'Erratic' Readings:

Large amounts of data were lost through erratic readings which occurred with great frequency during the 1973 surveys. As noted in Table 2.1 some of the meters had zero speed readings while others had erratic speed and direction readings caused by the potentiometric wipers not making contact with the speed and direction potentiometers at every ten-minute interval. Some of the data were so affected as to be useless while the others were corrected by passing them through a filter and substituting the incorrect values with averaged values. For those with many erratic readings, a digitizer was used to obtain hourly values.

(vi) Parity Errors:

Parity errors occurred in several of the current meter data as noted in Table 2.1. These errors are unrecoverable because the computer rejects data with parity errors. In an attempt to recover the data, they were retranslated onto another computer tape but the fact that the parity errors occurred again indicated the source of the problem to be in the recording cycle of the current meter.

(vii) Faulty Tape Cartridges

In a couple of the current meters during Survey II faulty tape cartridges were encountered. The tapes did not wind properly and large sections of the tape were found in the meter outside its cartridge.

To overcome this problem which resulted in the loss of data, another type of tape cartridge with a bracket to keep the tape more efficiently on its spool was used.

(viii) Faulty Magnetic Reed Switch:

In two current meters used during Survey II magnetic reed switches in the battery packs which remained in the closed position caused a loss of data. This problem was overcome by carefully checking the reed switches in the battery packs in subsequent surveys.

(ix) Faulty Battery Packs:

Whereas no problems were encountered with the batteries during the 1972 surveys, there were numerous occurrences of the batteries not providing enough power for the expected period of 120 days in the 1973 surveys. Some of the meters did not record for the entire period that the meters were deployed in the lake and others had too many erratic readings to make the data unreliable.

To get away from the problem of unreliable battery packs, investigations are being made to use other types of batteries such as lead acid which may be more reliable. In the meantime the battery recharging procedure has been modified to obtain better-charged battery packs.

## Wind Measurements

The principal wind data used in this report were obtained as hourly readings from the Standard Meteorological Station at Mitchell Field Airport, Milwaukee. These are hourly readings of speed and direction at standard anemometric height (10 m). Unfortunately, it was not possible to make comparisons with wind speed and directions over the water.

## Data Analysis

An outline of methods used to analyze the data is shown in figures 2.7 and 2.8. Current speed and direction diagrams, temperature diagrams, vector frequency diagrams and spectral analyses were based on ten-minute readings, whereas the progressive vector diagrams and wind data were based on hourly readings.

### Speed and direction diagrams (presented in Chapter Three)

Current speed and direction values were plotted on a monthly basis to illustrate the general nature of current structure and to compare the data from different stations for any gross discrepancies. Wind speed and direction were also plotted on the same diagram as a basis of comparison with the current data. Wind speed was plotted as wind speed squared to express it as a function of wind stress. All speeds below 7 mph (11 km/hr) were ignored since winds of lower speed seemed to have very little effect on the currents. Generally the currents correlated well with winds; high current speeds corresponded with high wind speeds. The currents were mostly shore parallel with very few directly onshore or offshore.

Figure 2.7

FLOW CHART FOR ANALYSIS OF CURRENT AND WIND DATA

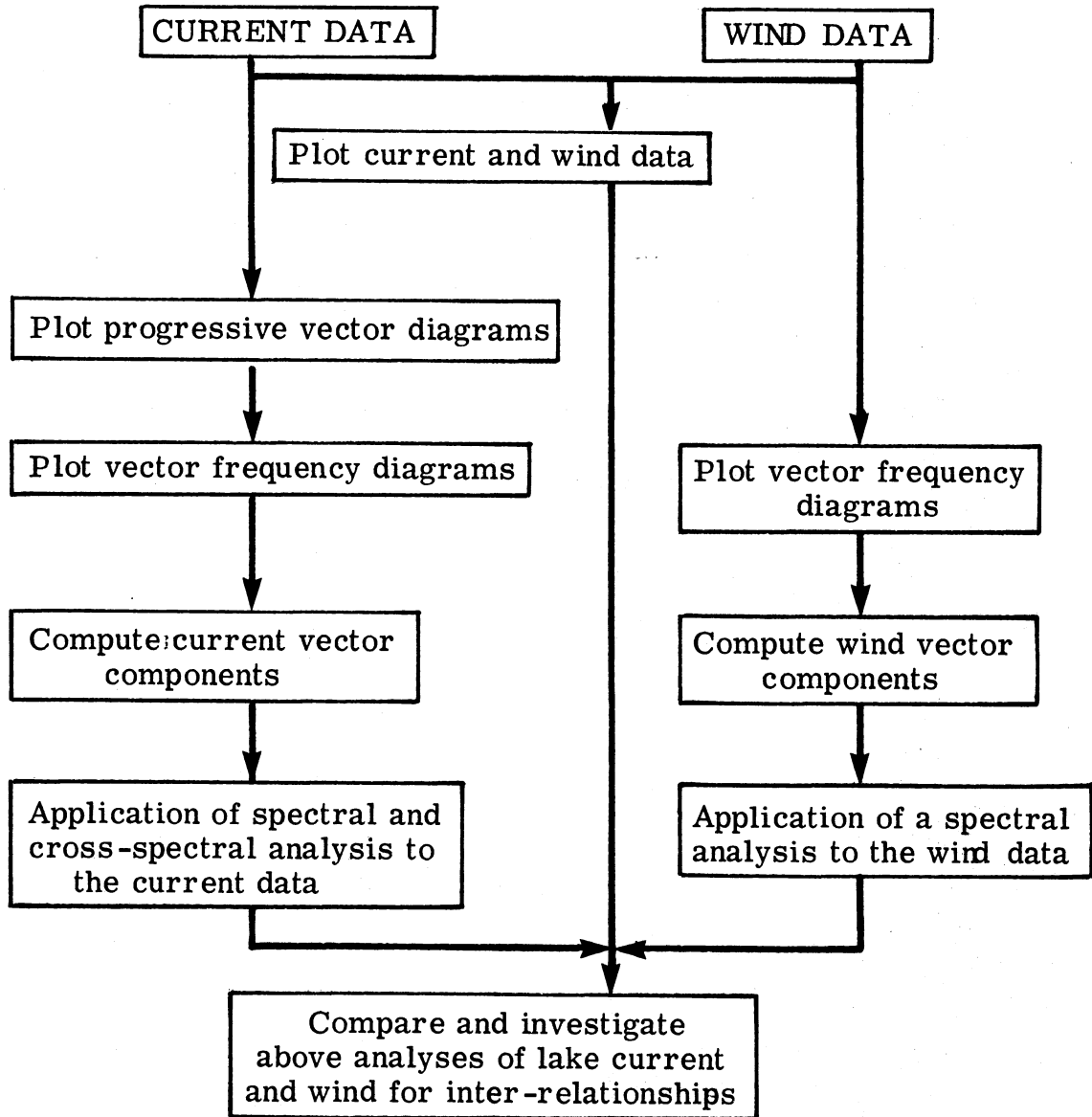
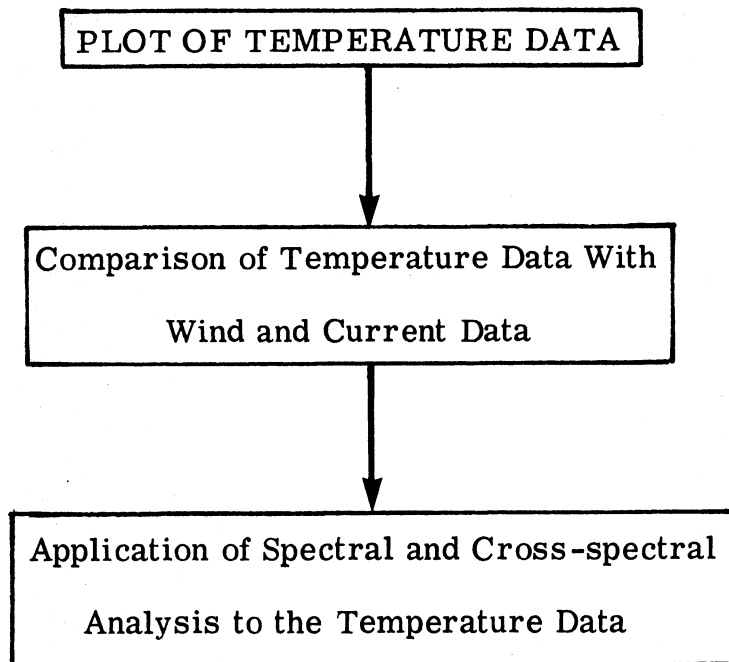


Figure 2.8  
FLOW CHART FOR ANALYSIS  
OF TEMPERATURE DATA



### Temperature diagrams (presented in Chapter 3)

Monthly temperature diagrams were used to illustrate the temperature pattern at different stations as a function of time. Near-inertial oscillations were not observed on most of the records. After the lake began to stratify, upwelling and downwelling episodes occurred, associated with north-going and south-going currents, respectively. Using visual comparisons and cross-spectral techniques; correlations between temperature and current records were explored (fig. 2.8 ).

### Progressive vector diagrams (presented in Chapter 4)

Progressive vector diagrams were used to illustrate the general flow pattern of currents past the current meters. The diagrams were developed by adding consecutive hourly averaged current data in vector form. Straight line patterns indicate the dominance of persistent non-oscillatory currents, whereas circular patterns indicate the presence of inertial-type motions. Since progressive vector diagrams are based on currents following past fixed current meters, the progressive vectors do not necessarily represent current flow elsewhere, although this is quite often inferred. Most of the current patterns were found to have straight-line characteristics.

### Vector frequency diagrams (presented in Chapter 4)

Vector frequency diagrams were used to present speed and direction characteristics of current data in polar coordinate form, based on ten-minute readings. This type of diagram is more useful than histograms for speed and direction because it shows the distribution of the currents with respect to both

speed and direction simultaneously. The data were classified into thirty-six  $10^\circ$  directional arcs and 4 cm/sec speed intervals.

The percent frequency of occurrence of the recorded 10-minute data points in each speed and direction interval was determined and plotted in polar coordinate form. Contours of equal percent frequency of occurrence were then drawn to present the major direction and speed intervals.

A similar vector frequency diagram was also developed for wind vectors by classifying them according to thirty-six  $10^\circ$  directional arcs and 3 m/sec speed intervals.

#### Persistence factors (tabulated in Chapter 6)

Persistence factors were calculated on a monthly basis for each current meter in an attempt to quantify and to display the persistence found in the currents, using the relationship:

$$\text{Persistence factor } P = \frac{\text{Resultant mean current vector}}{\text{Mean current speed}}$$

Persistence would be unity if the current were to travel in the same direction for the entire month. The minimum persistence factor of zero would be obtained if the currents were to travel equally in all directions, or half in one direction and half in an exactly opposite direction.

#### Spectral analysis (discussed in Chapter 6, and based on method of Munk et al. 1959)

Spectral and cross-spectral analyses were applied to the current and temperature data. Spectral analysis determines the frequency distribution of the energy (or variance) of the record over a defined frequency range. Peaks in the

spectra at particular frequencies indicate a higher content of energy (or variance) than in the neighboring frequency bands and thus disclose the presence of periodic motion. Cross-spectral analysis of two time series can be used to determine coherence and phase relationships between them.

Relationship between winds and currents (discussed in Chapters 3, 4, and 6)

The relationship between wind and current was studied by applying cross-spectral analysis to the wind and current data. Also the time lag between current and wind reversals, and the response of current to wind as a function of depth and distance from shore were qualitatively investigated by comparing wind and current diagrams.

CHAPTER THREE  
THE OBSERVATIONS: MONTHLY PLOTS OF WIND,  
CURRENT, AND TEMPERATURE

In this chapter the complete data set, forming the body of this report, is assembled as compactly as possible in the form of monthly time series plots (figures 3.1 to 3.77, time scaled in days from the midnight on which the month began). For each station, depth, and month, the current speeds and directions (10-minute readings,  $\text{cm. sec}^{-1}$ ) are combined in one figure with the corresponding hourly values of wind direction and speed squared ( $\text{m. sec}^{-1}$ ) at Mitchell Field, 8 miles (13 km) from our site. In the absence of better over-water estimates, wind speed squared at Mitchell Field is assumed to be approximately proportional to the wind stress on the water in our area of study. In most cases, for convenient reference, the monthly record of water temperature (10-minute readings) is placed to face the corresponding monthly wind/current diagram. Where this is not possible, the corresponding current plot appears on the following page. In the interests of readability, the figures are interspersed in the text.

To facilitate wind and current comparisons we have adopted the same direction convention for both, i. e. always "direction toward". We therefore refer, for example, to northward or northgoing (or southward or southgoing) currents and winds. For the winds this is, of course, the opposite of the usual meteorological convention. Before examining the records month-by-month and station-by-station, we draw some brief conclusions from a general inspection and defer more detailed discussion to Chapter 6.

Strong coupling of wind and current is evident; during spells of weak winds the currents are generally also weak. Episodes of stronger wind are usually accompanied, after a lag, by episodes of stronger current with or without reversals in direction, depending on the current structure before the wind commenced. The result in most but not all of such episodes was a general correspondence between wind and current, strongly modified, however, by the boundary constraint of the shore, and by differences in fetch for winds from different directions. For example, during periods of northeastward winds (small fetch)

or weak winds, currents were weak; whereas strong southward or southwestward winds (large-fetch) produced strong SSE shore-parallel currents. We have taken a speed of  $4 \text{ cm. sec}^{-1}$  as the threshold speed below which the Savonius rotor will not respond reliably to a steady current. Responses below  $4 \text{ cm. sec}^{-1}$  were, however, sometimes recorded for decelerating currents; and at such low speeds the inertia of the relatively massive rotor introduces errors. The direction vane is more sensitive and will continue to respond to currents of less than  $4 \text{ cm. sec}^{-1}$ . In later discussion readings of  $4 \text{ cm. sec}^{-1}$  or less are referred to as "very weak currents", the recorded direction of which may be significant, but the recorded speed of which cannot be reliably distinguished from zero. Certain sections of the record presented below show a rather confusing picture of current direction oscillating between northeastward and northwestward. Such oscillations were not usually present with southward currents.

Upwelling and downwelling episodes are illustrated, respectively, by sudden decreases and increases in temperature. While the sudden increase in temperature made the recognition of downwelling easy, upwelling episodes were more difficult to observe, especially during spring, because the temperature of water layers below the instruments did not differ greatly from the temperature of the water surrounding them. Upwelling and downwelling episodes were associated with northward and southward currents respectively. Some current reversals were accompanied by upwelling or downwelling, depending upon the strength and persistence of the current after reversal. Frequently these current reversals were associated with wind reversals. During the spring season, current reversals were easy to identify; however, during summer, after stratification had set in, the presence of oscillatory, near-inertial motions made reversal identification more difficult.

The general characteristics of current and temperature variance are discussed month-by-month and station-by-station in the following sections.

#### Survey I, 3 April to 4 June 1972:

We shall describe the results from this survey in sufficient detail to instruct the reader what to look for in figures of later surveys, treated in less detail. Station positions were shown earlier in figure 2.1; and the details of

instrument settings and recording dates are given in the following extract from Table 2.1.

Station No.	1	2	3	4	
Distance from shore (km)*	8.0 (8.4)	5.3 (2.2)	4.2	8.0 (10.8)	
Water depth (m)	20	22	19	28	
Instrument depth (m)	15	17	13	15	23
Date set	3 April	3 April	2 May	4 May	4 May
Date retrieved	5 June	5 June	5 June	6 June	6 June
No. of days of record in water: expected	69	64	36	36	36
obtained	69	64	35	35	35
Comments	Parity error				

\*Bracketed: distance from shore along E-W line in Fig. 2.1.

Unbracketed: distance from nearest shoreline.

During April, temperature and current records were obtained only at Station 1 (15 m) and Station 2 (17 m). The monthly picture of current speed and direction was very similar at the two stations (figures 3.2 and 3.3) with speeds slightly higher at Station 2. Temperature (figure 3.1) increased steadily during the month from 1.1° to 3.6° C at both stations. There was a brief rise to 4°C at 22.6\*days at Station 1 and at 23.3 days at Station 2. The cause of this rise may have been temporary downwelling of warmer upper layers or -- a remote possibility -- advection of water from the power plant's sinking plume.

Comparison of current speed and direction disclosed six episodes of currents peaking at speeds 15-20 cm.sec<sup>-1</sup> all of which except one were directed toward the S to E quadrant. The exception, centered on 20.8 days on the time scale, was a northgoing current following a moderately strong burst of westgoing wind starting 20.0 days and peaking at 20.7 days. The wind reverted to eastward at about 21.0 days and was moderately strong for a day thereafter, during which time the current direction changed to southwestward. The speed however was

\*Footnote: Add 1.0 to convert this time scale to calendar days.

Figure 3.1

APRIL 1972: WATER TEMPERATURE

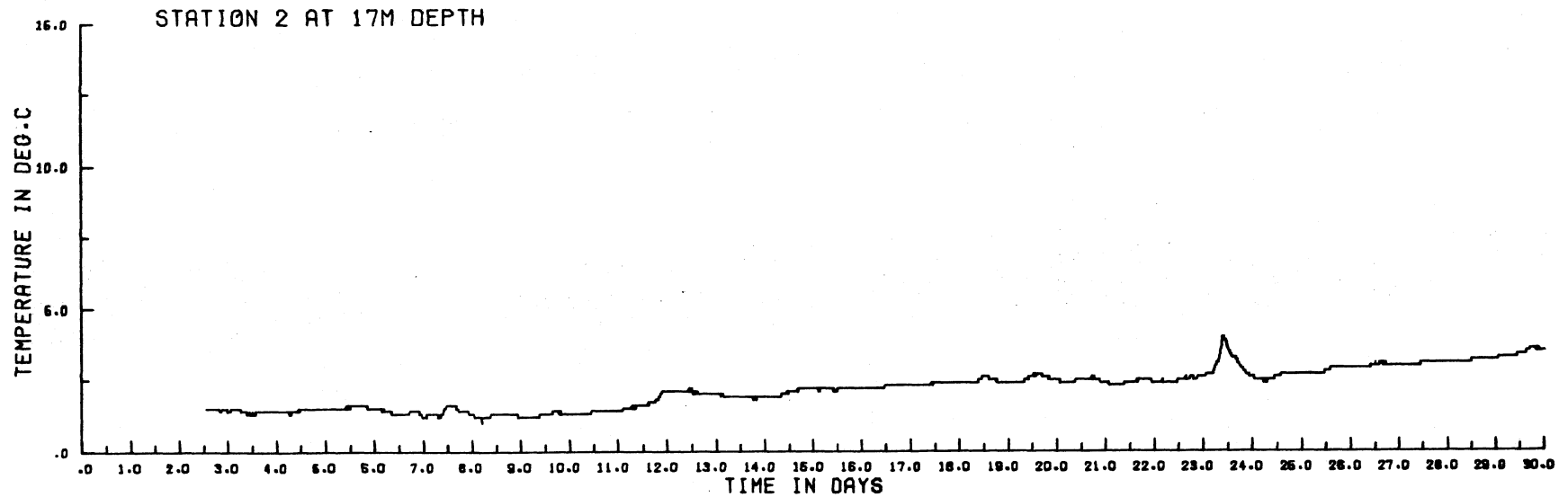
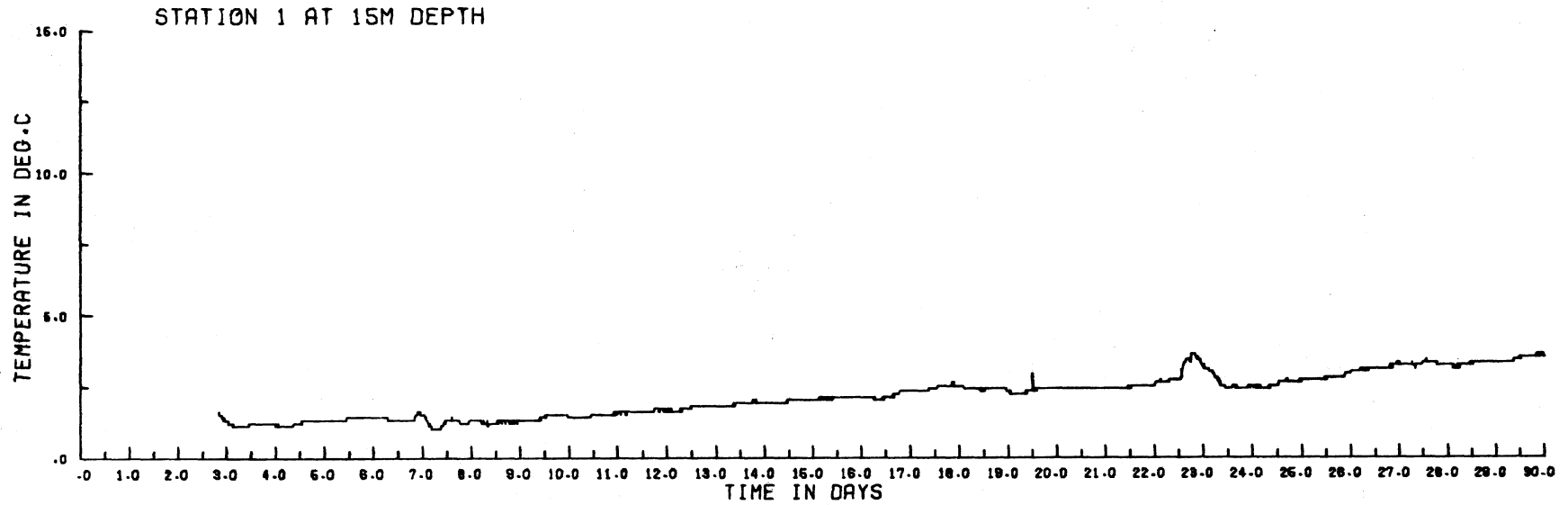


Figure 3.2

APRIL 1972 : WIND (MITCHELL FIELD) COMPARED WITH STATION 1 CURRENT AT 15M DEPTH

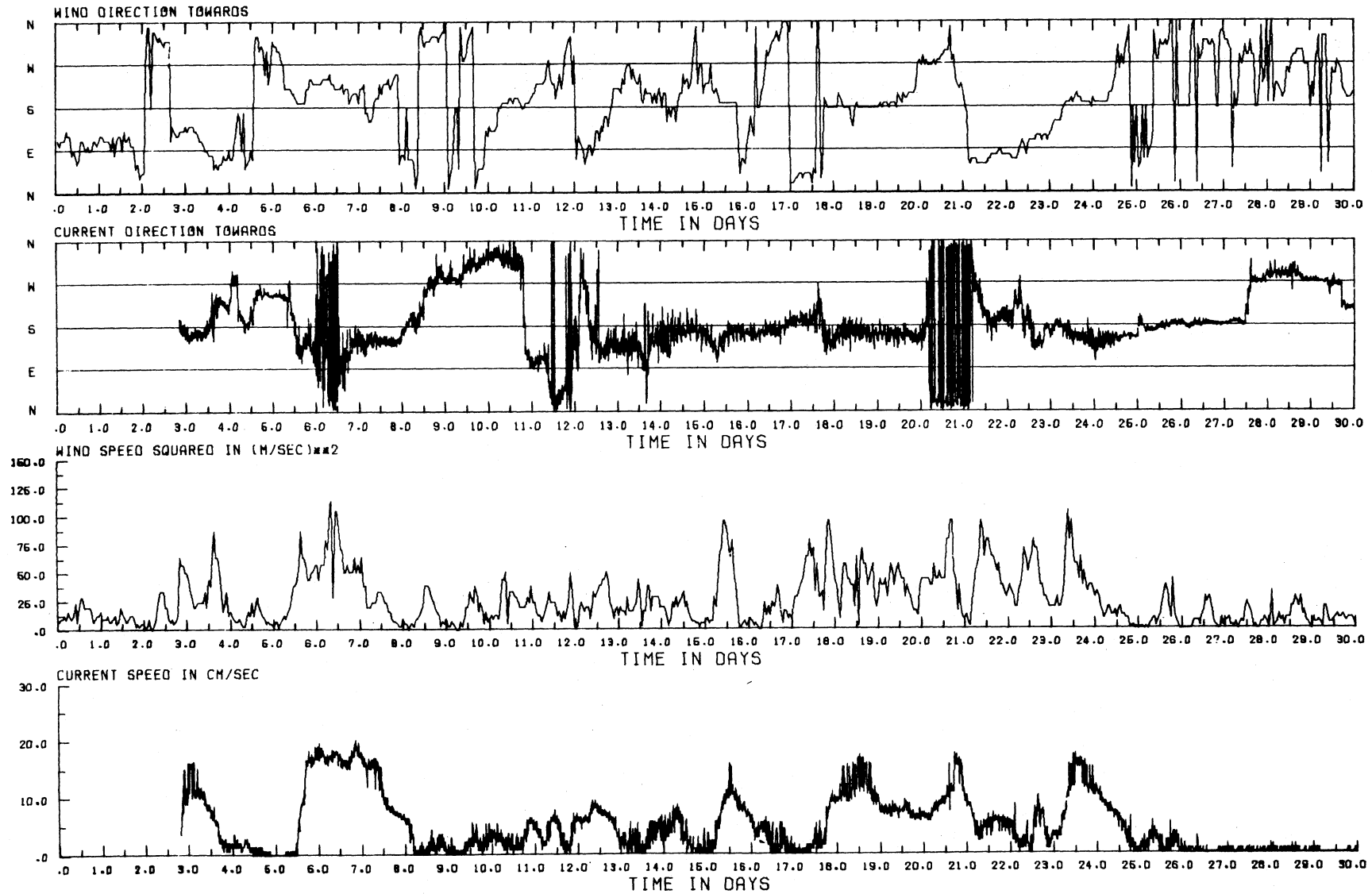
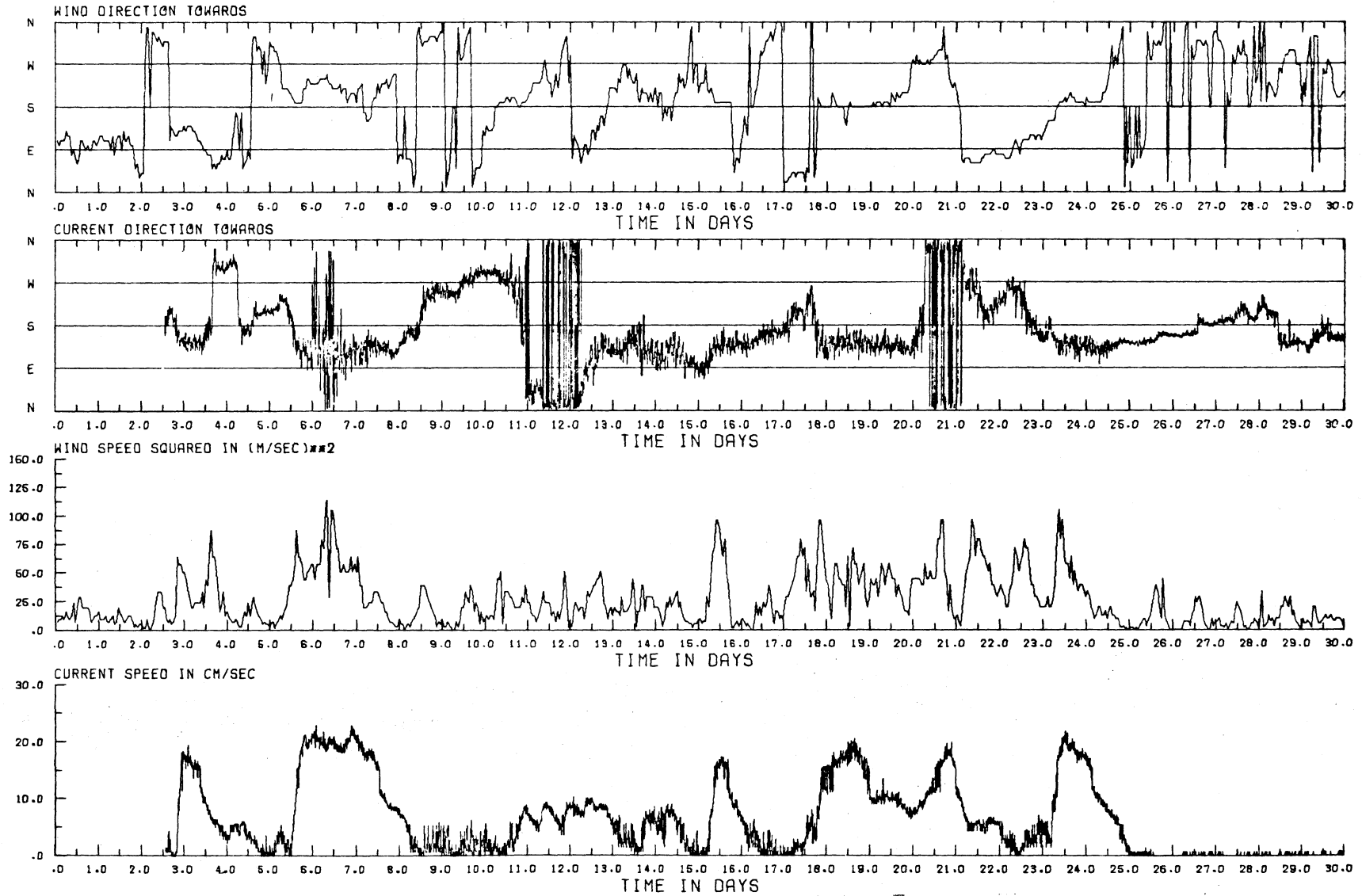


Figure 3.3

APRIL 1972: WIND (MITCHELL FIELD) COMPARED WITH STATION 2 CURRENT AT 17M DEPTH



low because of the short fetch of the eastward wind. A similar sequence of wind and current directions is seen between 11.0 and 13.0 days, but both the wind speed and current speed were low.

Except during eastward wind pulses (3.6 to 4.2 days, and the 21.3 to 21.8 day pulse already mentioned) the "envelope" of current speed shows considerable similarity to that of wind speed squared, for example, the pulses centered on 3.2, 6.5, 15.6, 18.2, 20.8, and 23.6 days. As expected, the current start-up and peak current speeds lagged by a few hours behind the wind start-up and peak wind speeds. The lag times of the two distinct southward to northward current reversals were 4 to 6 hours, while the lag time of the single distinct northward to southward reversal (at 12.0 days) was about 11 hours.

During the month of May 1972 current meters were installed at stations 1, 2, 3, and 4. The current directions for stations 1 and 2 (figs. 3.5, 3.6) were very similar during episodes of strong persistent currents and intervening intervals of weak currents. During the latter intervals, current directions at station 3 (fig. 3.8) exhibited greater variation than at other stations. This variation was probably a result of station three's location near Wind Point, where it was probably reacting to the current regimes in the bays to the north and south of the station.

At all four stations during May, episodes of strong, steady, south-going winds (6.0 to 9.0, 29.0 to 30.3 days) produced the strongest currents also southgoing, while an episode of northwestward wind, persisting from about 11.4 to 12.4 days, was followed by a northward current pulse of lesser magnitude centered on 12.5 days at all four stations. The preceding reversal in current direction, however, did not follow the same course at all stations. At stations 1 and 2 (figures 3.5 and 3.6) it gradually changed from southward to northward over the interval 9.6 to 12.0 days; while at station 3 (fig. 3.8) the change started more suddenly at 9.7 days and was completed by 10.5 days, and at station 4 (fig. 3.10) the change did not begin until 11.4 days and was completed about one day later.

Figure 3.4

MAY 1972: WATER TEMPERATURE

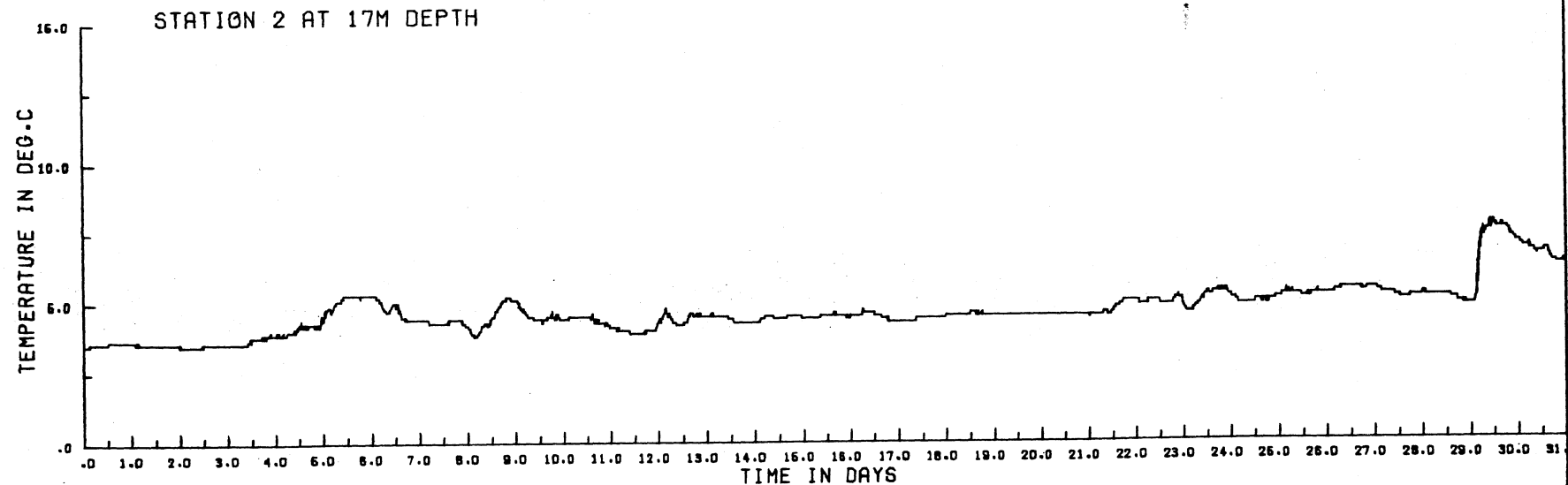
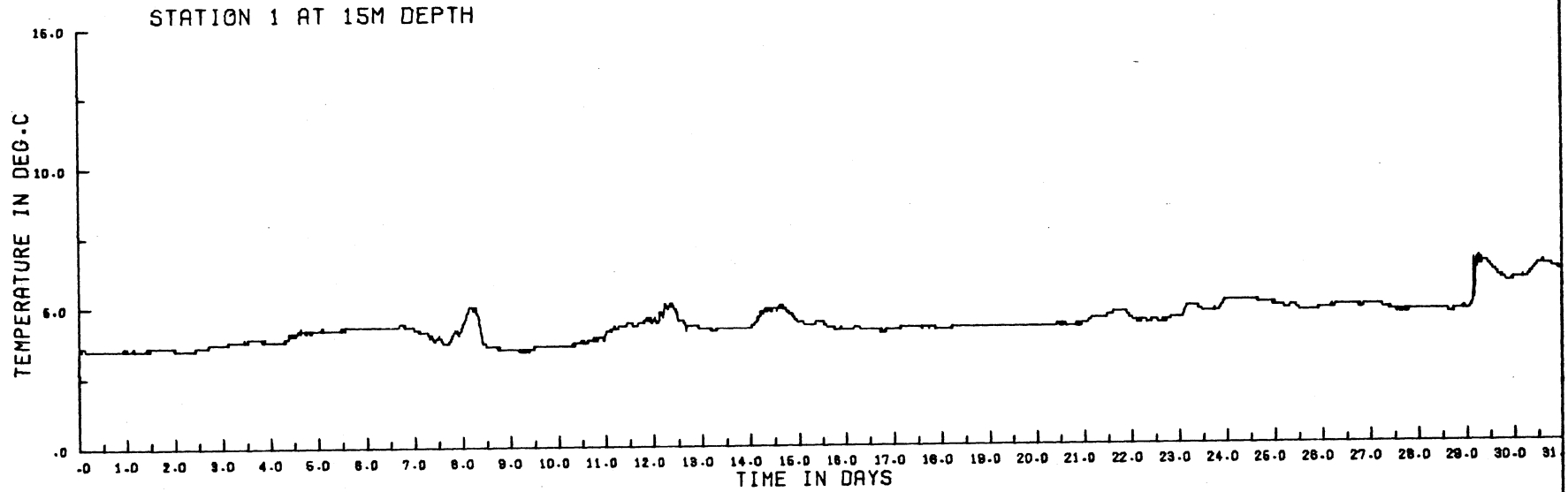


Figure 3.5

MAY 1972 : WIND (MITCHELL FIELD) COMPARED WITH STATION 1 CURRENT AT 15M DEPTH

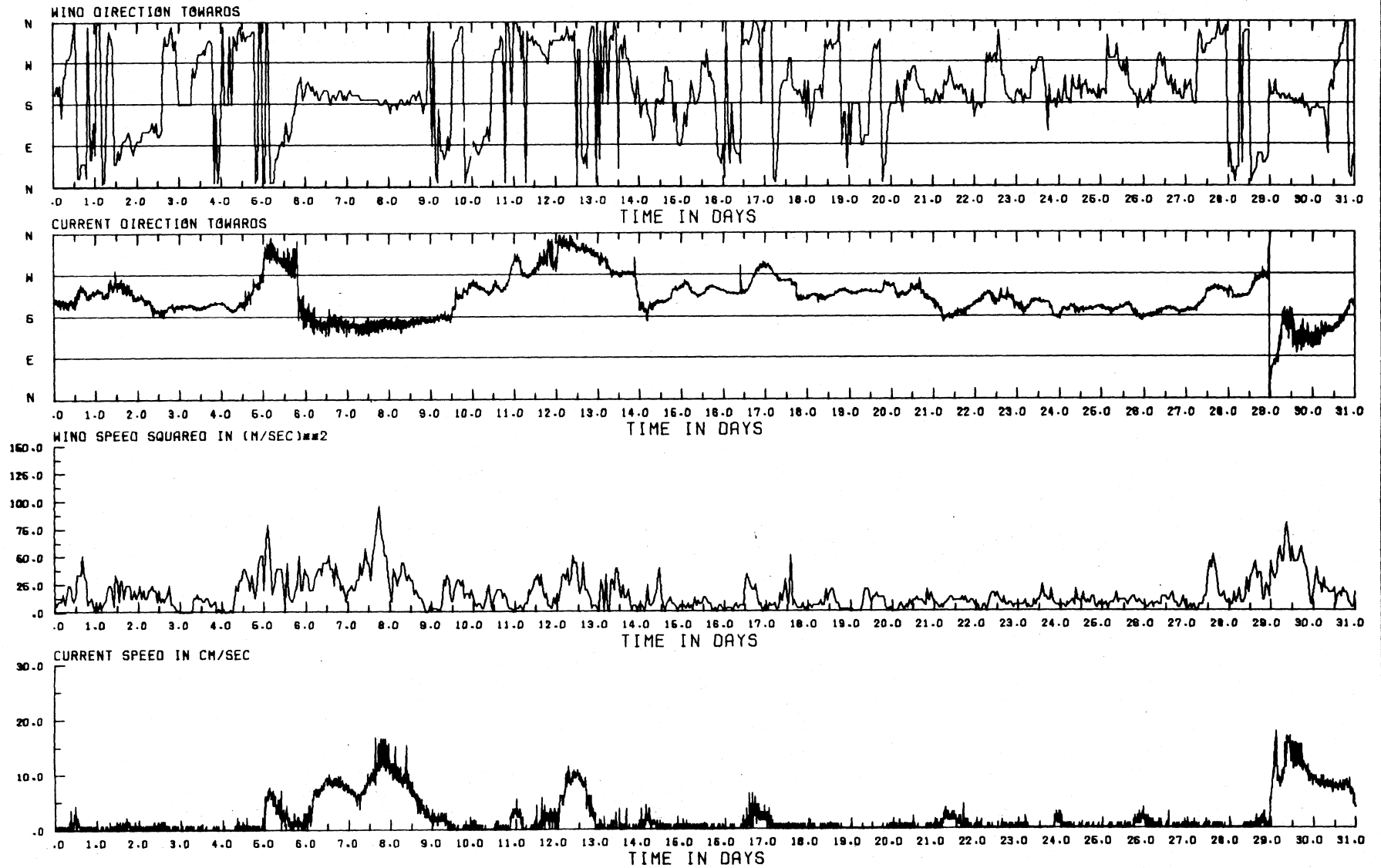
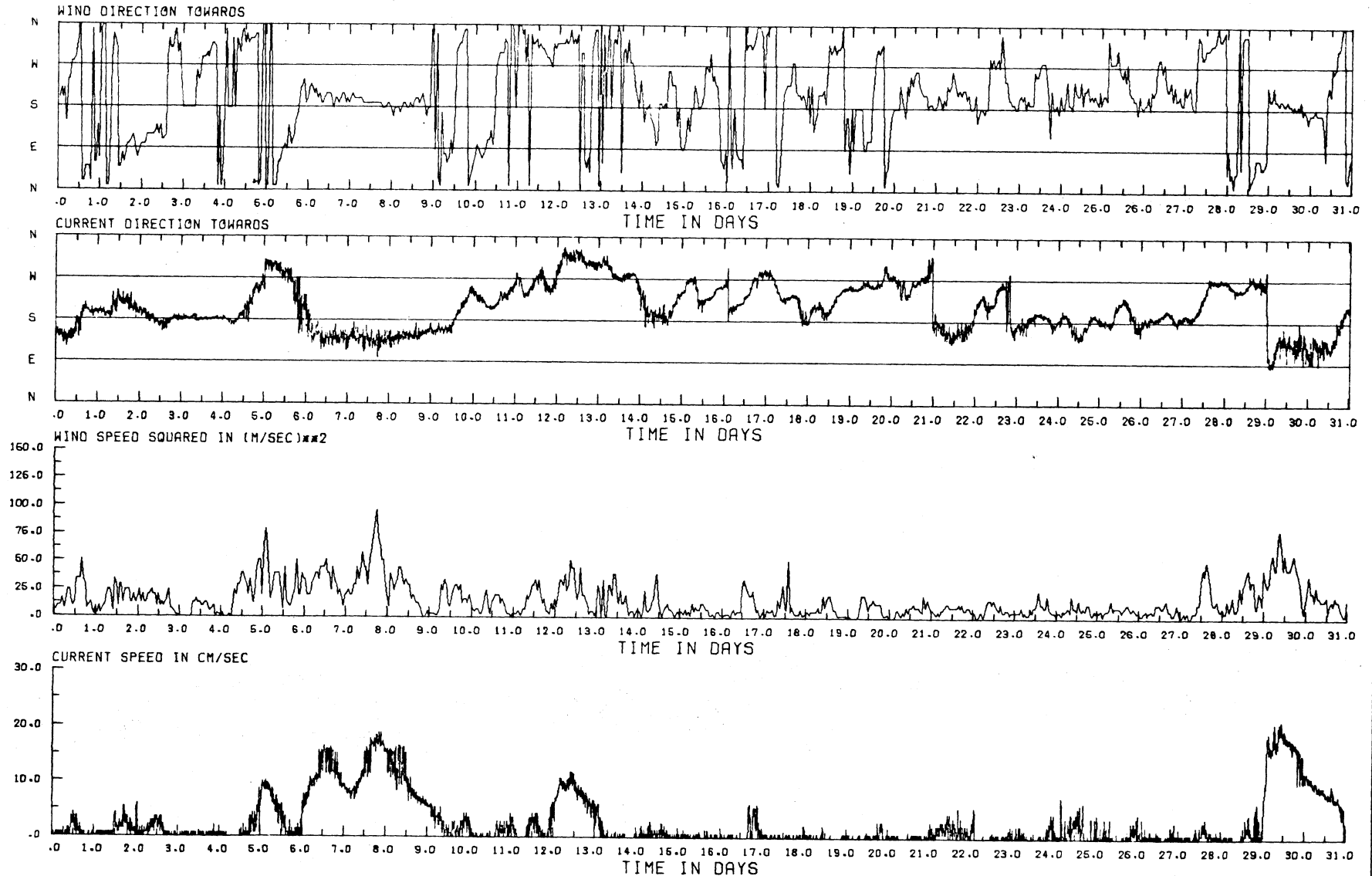


Figure 3.6

MAY 1972: WIND (MITCHELL FIELD) COMPARED WITH STATION 2 CURRENT AT 17M DEPTH



There were also station differences during intervals of weaker current. Whereas the nearshore stations exhibited generally southward flow during the intervals of weak current, the station 4 instruments recorded generally north-eastward flow. Distinct current reversals occurred most often at station 3 (fig. 3.8, 13 reversals with lag times from 1 to 12 hours) while the other stations showed only three distinct reversals with lag times of 4 to 16 hours; and these reversals took place more rapidly at the nearshore stations than at the offshore ones. As already noted, current reversals occurred during some episodes at the nearshore stations 1 and 2 but not at the offshore station 4, because of the presence there of an already established persistent current which maintained its direction despite wind reversal.

Upwelling and downwelling episodes were generally not very noticeable on the temperature records during May (figs. 3.4, 3.7, 3.9). An exception was the downwelling episode starting at 29.2 days and observed at all four stations. The lake was not sufficiently stratified at that time to exhibit large temperature changes during upwelling or downwelling episodes. The downwelling event at 29.2 days was the result of strong southgoing wind and coincided with the current reversal already noted.

The June portion of Survey I consists of the first four days only (figures 3.12 and 3.13); the remainder of the month is covered in Survey II. A downwelling episode starting at 3.4 days was recorded at the shallow-water stations 1, 2, and 3, but not at the deeper station 4 (fig. 3.12). The downwelling was associated with a reversal in current-direction from northward to southward (fig. 3.13); and again current direction was more variable in direction at station 3 (Wind Point) than at the other stations. Also the peak speeds were higher at both depths at station 4, the deepest station, where a steadier southgoing current was recorded that at the other stations, over the interval 0.5 to 2.0 days. However, the current pulse following the wind change at 3.3 days was confined to the lower instrument (23 m, fig. 3.13). In general, the close correspondence between wind and current directions was also evident during the short June record.

Figure 3.7

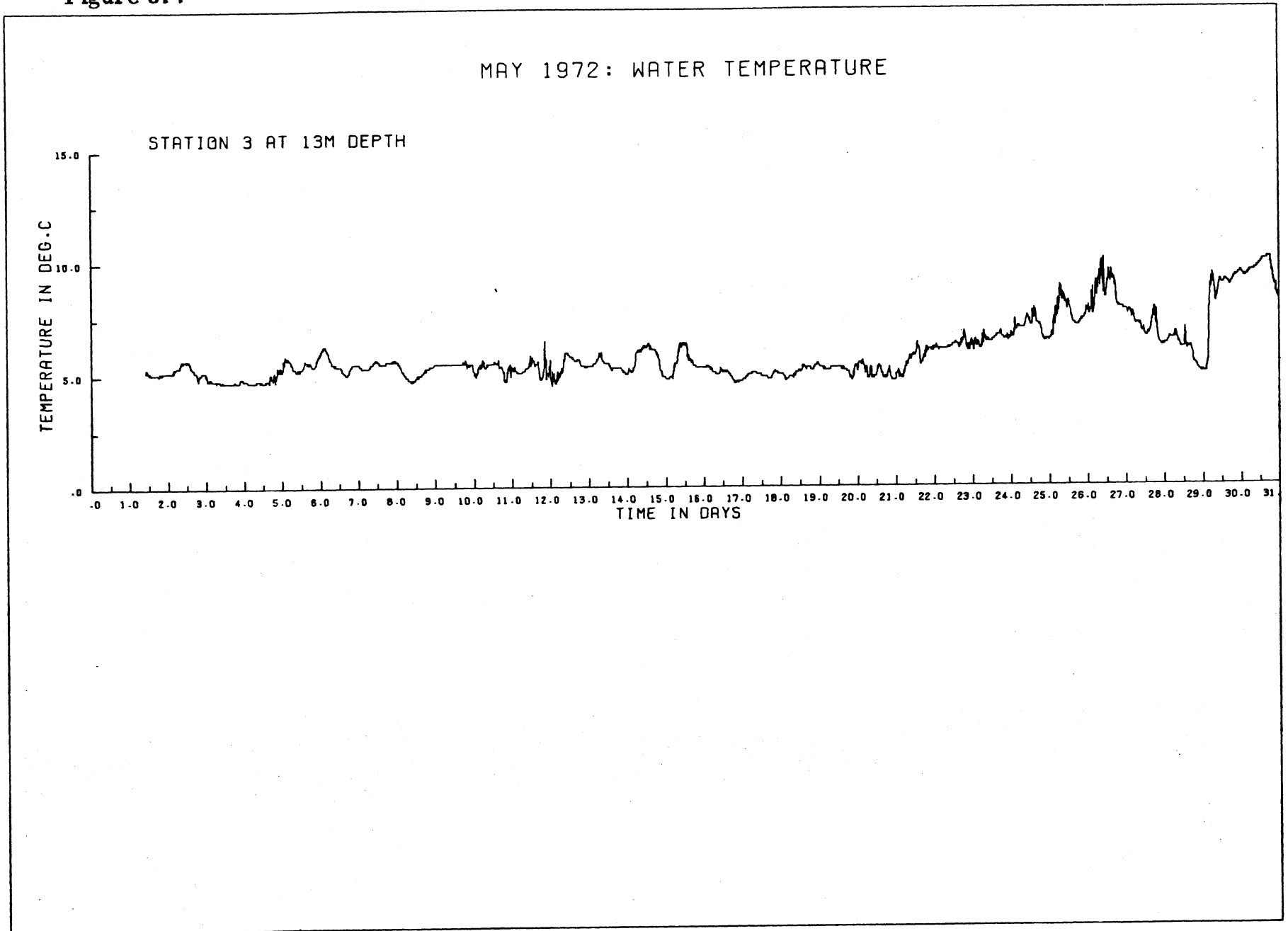


Figure 3.8

MAY 1972: WIND (MITCHELL FIELD) COMPARED WITH STATION 3 CURRENT AT 13M DEPTH

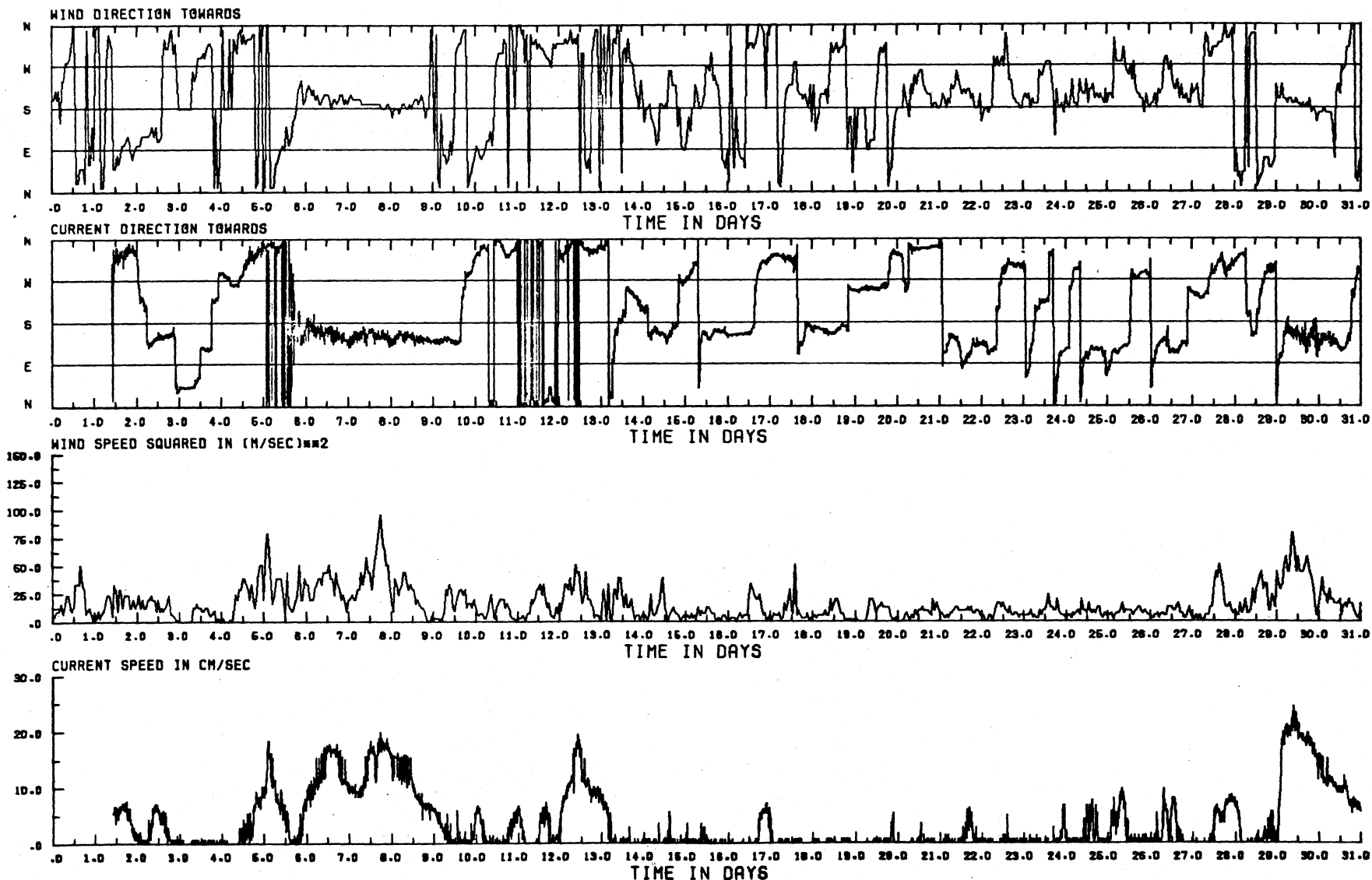


Figure 3.9

MAY 1972: WATER TEMPERATURE

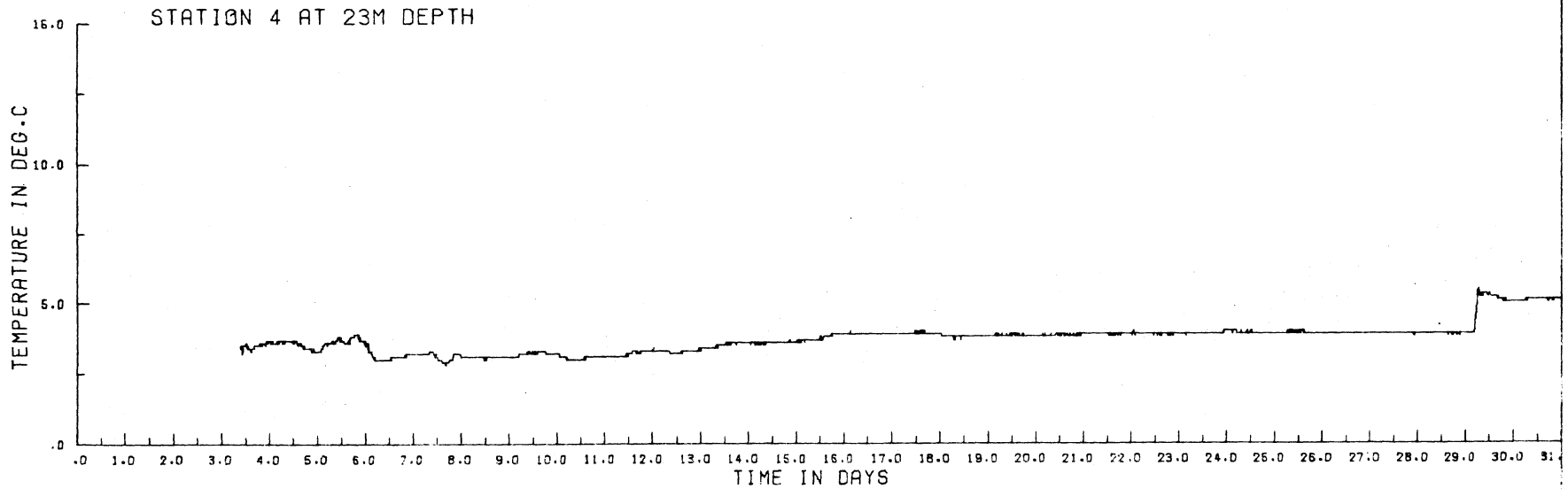
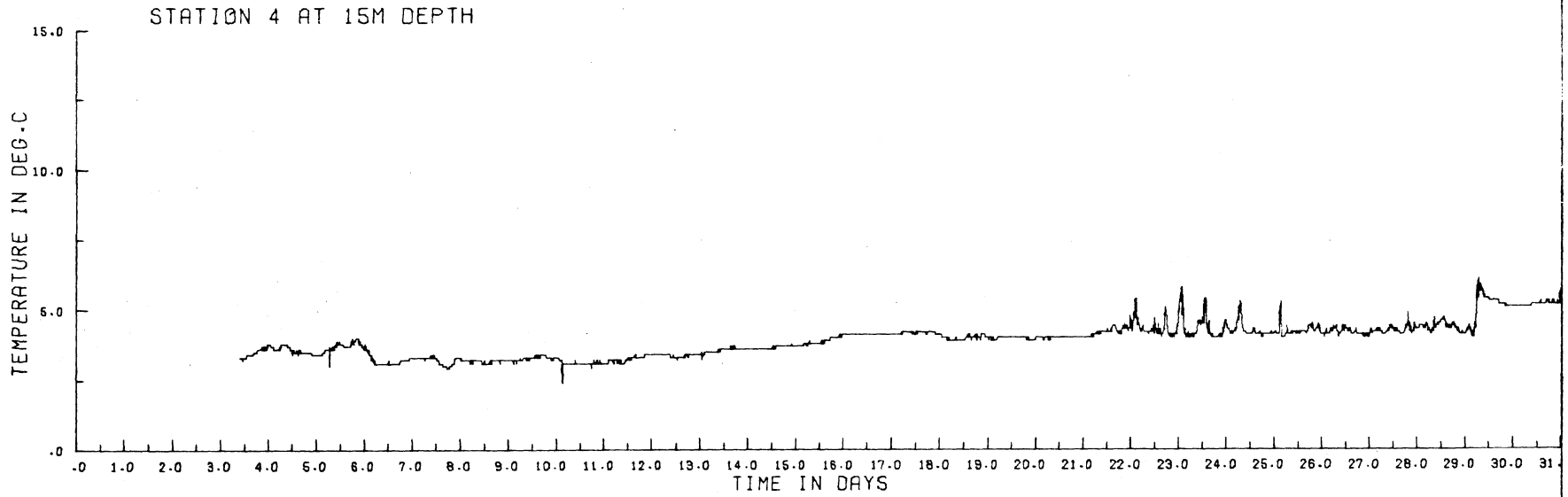


Figure 3.10

MAY 1972: WIND (MITCHELL FIELD) COMPARED WITH STATION 4 CURRENT AT 15M DEPTH

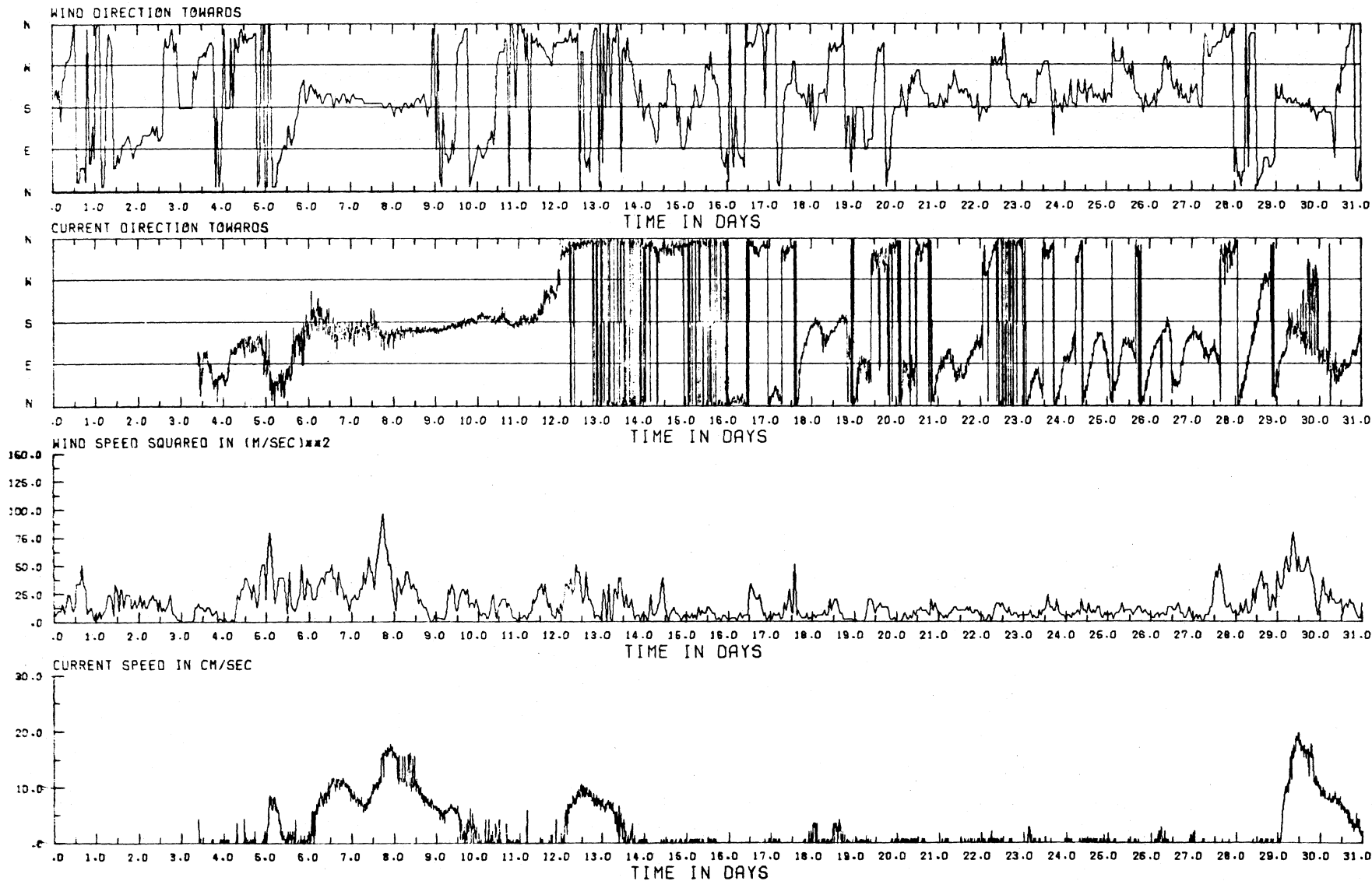
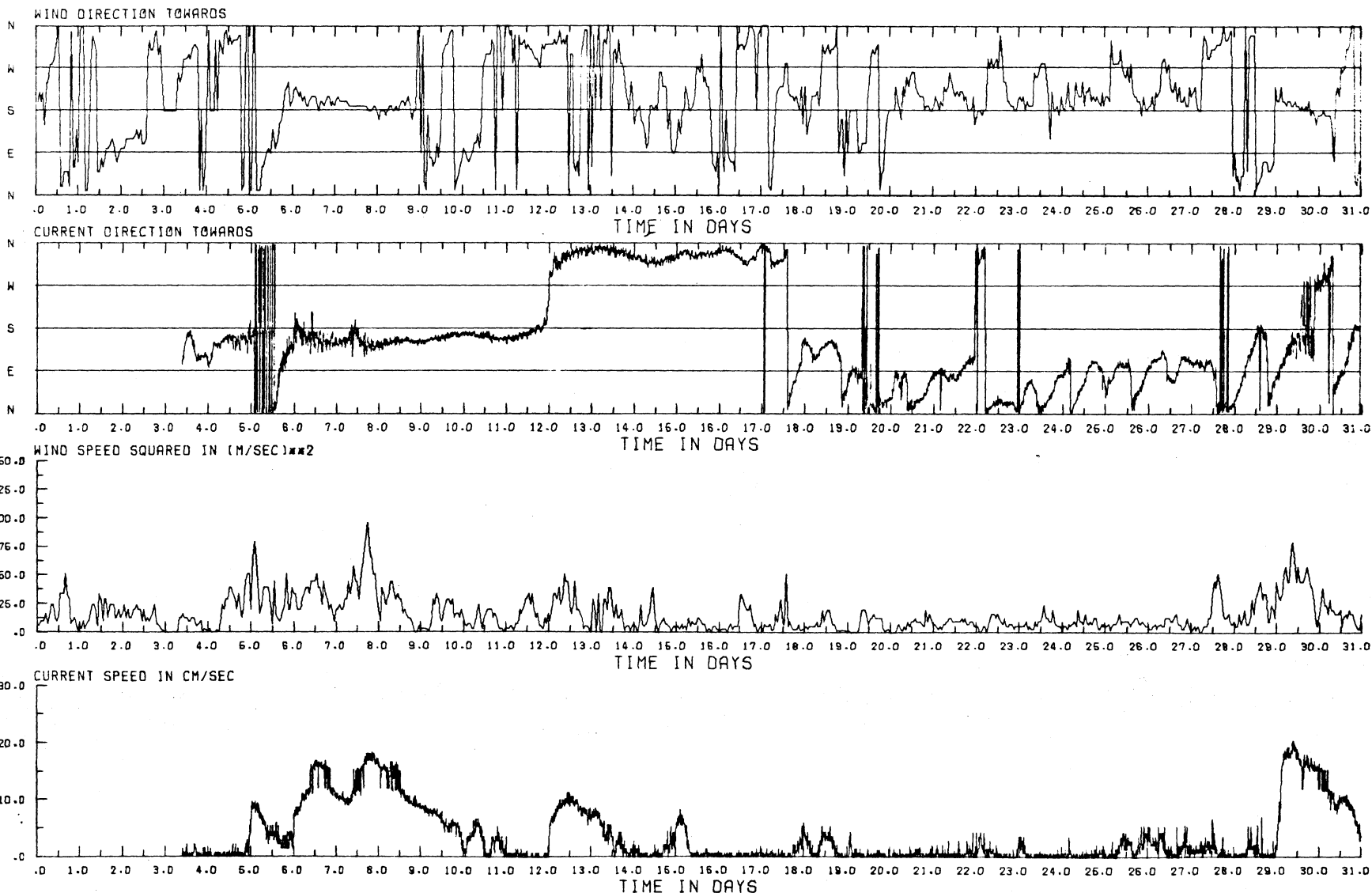


Figure 3.11

MAY 1972: WIND (MITCHELL FIELD) COMPARED WITH STATION 4 CURRENT AT 23M DEPTH



An important and we believe new result arising from this study is already well illustrated in the foregoing figures (for example, 3.3 and 3.11) for Survey I. The most common form of a current speed "pulse" is a steep initial rise in speed followed by a more or less steady phase of varying length, depending on wind persistence, followed by a fall in speed which is much more gradual than the initial rise. If this behaviour proves to be typical of wind-driven coastal currents in general, it must be related to the balance between the inertia of the moving water and the frictional braking applied. This may provide a route to realistic estimates of the magnitude of coastal frictional forces, estimates which are needed for improvement in hydrodynamical modelling.

Survey II - 5 June to 25 August 1972 (see Table 2.1 extract on p. 91)

Current meters were set at stations 1, 2, 3, 4, 6, and 8, but no data were obtained from stations 1 and 2 (lost after the premature release on 14 July) and from the upper meter at station 6 because of a faulty tape cartridge.

The June records (figures 3.14 - 3.24) again show a high correlation between wind and current with the strongest responses to southgoing winds. Those responses were most rapid at the tower stations ( $T_1$  and  $T_2$ , figures 3.23 and 3.24) with a less abrupt response at the deeper stations. Distinct current reversals took place eight times at station 3 with lag times of 1 to 8 hours and three times at each of stations 4 and 6 with lag times of 2 to 12 hours. Downwelling and upwelling episodes were noted in the temperature records at all of the stations. Again, station 3 recorded the highest frequency of these episodes. Near-inertial oscillations were not observed in these temperature records.

Instrument malfunctions were detected in some current meters. No current was recorded by the station 4 upper meter on 7 and 8 June and between 17 - 20 June; and at station  $T_1$  the meter direction sensor appeared to remain "stuck" on June 23 and 24 and the temperature sensor appeared to be faulty on June 15 and 16.

[the text continues on page 92]

# JUNE 1972: WATER TEMPERATURE

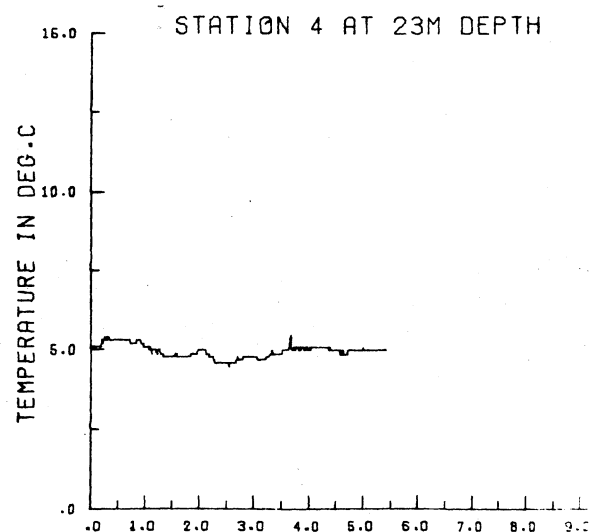
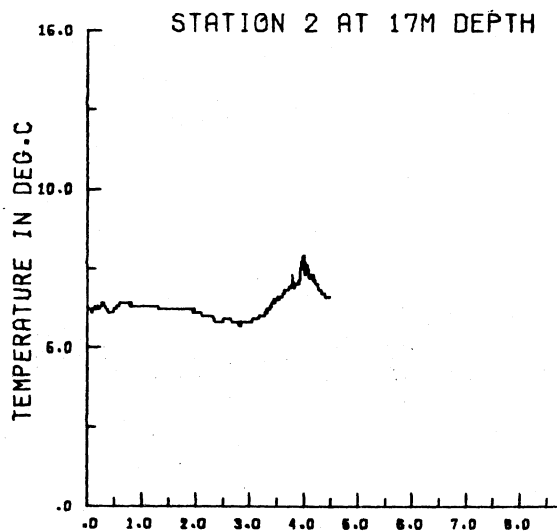
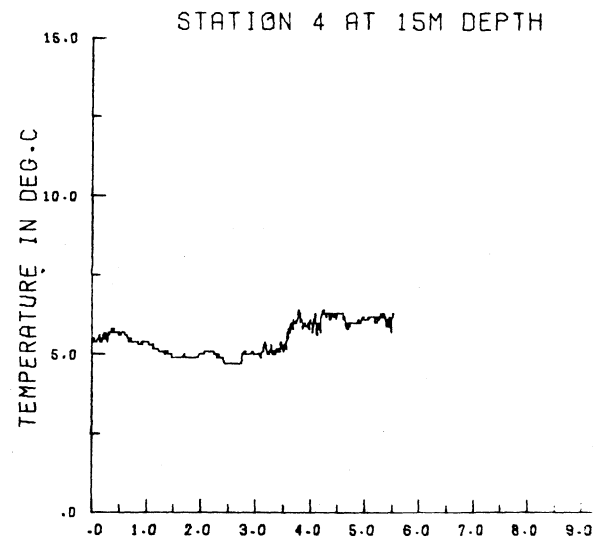
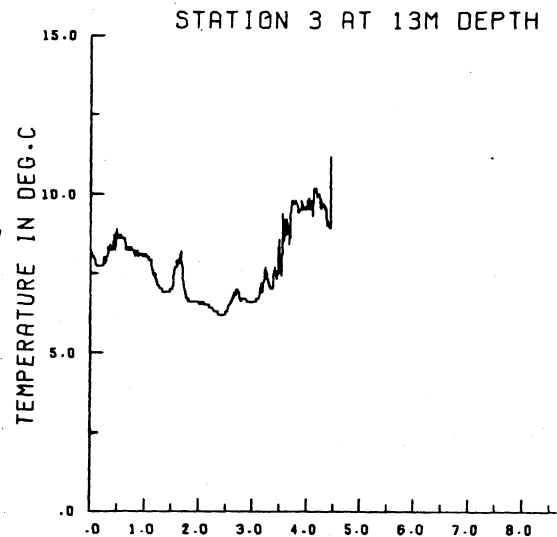
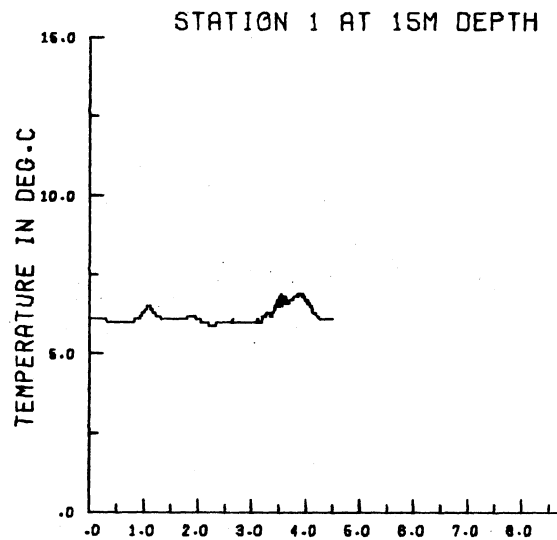
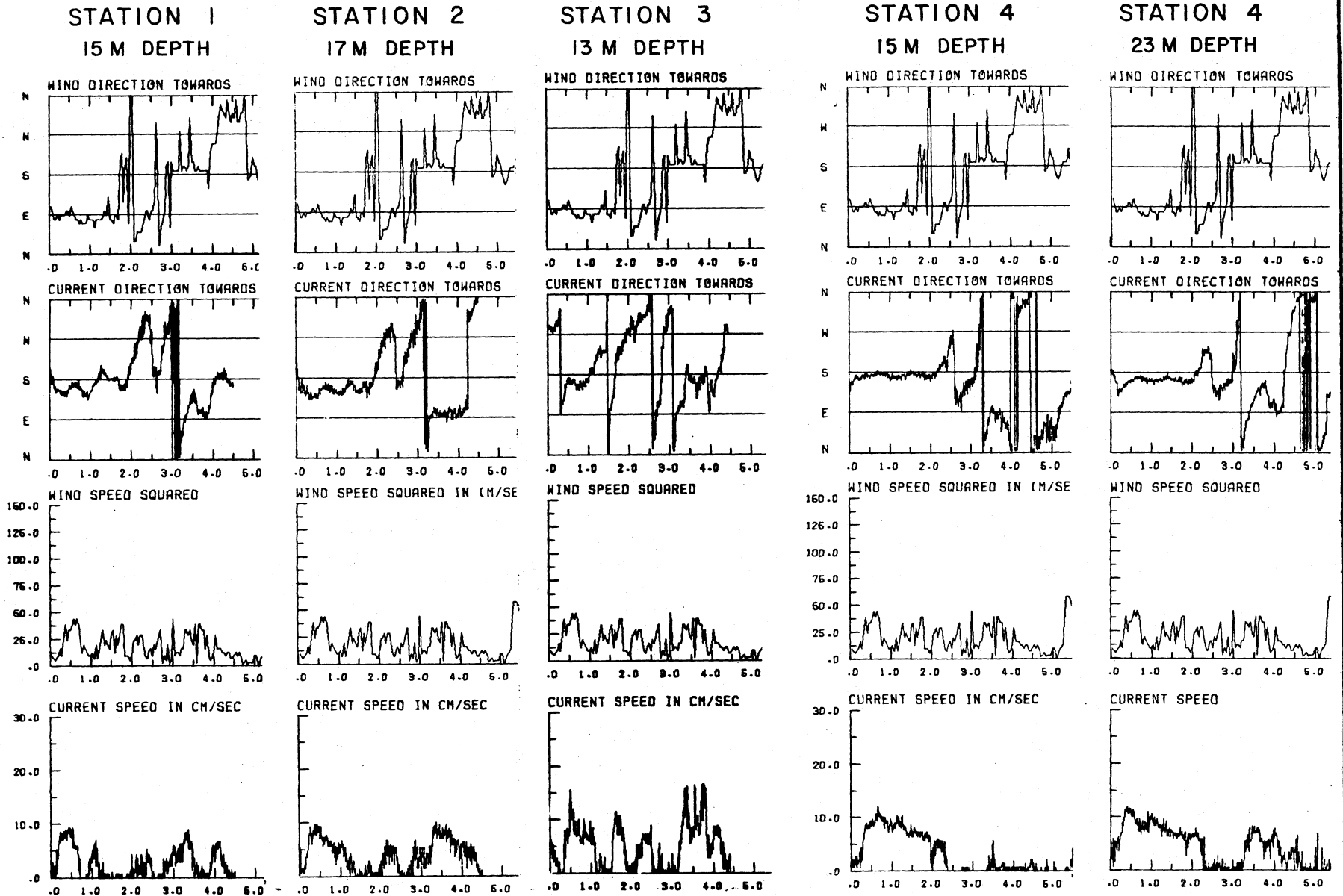


Figure 3.12

Figure 3.13

JUNE 1972 : WIND (MITCHELL FIELD) COMPARED WITH CURRENT AT :



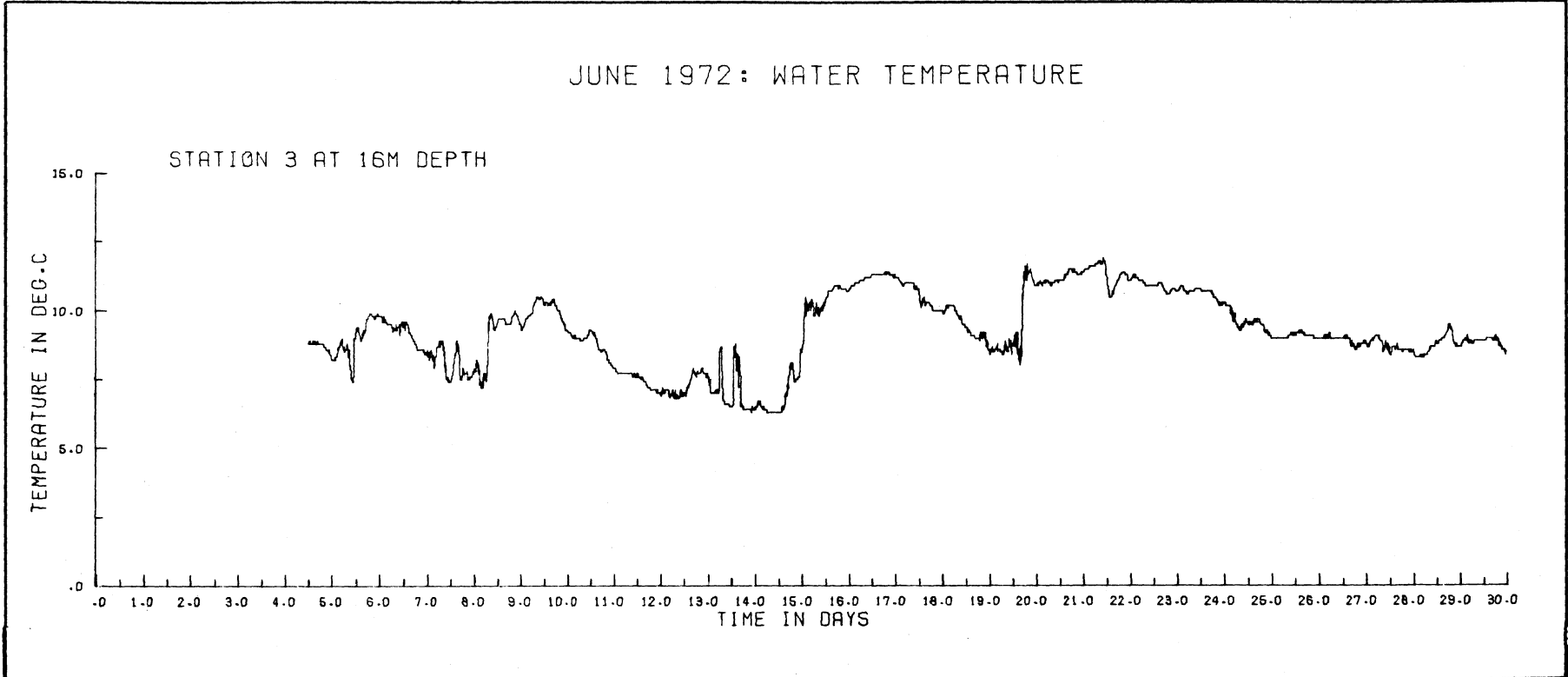


Figure 3.14

Figure 3.15

JUNE 1972: WIND (MITCHELL FIELD) COMPARED WITH STATION 3 CURRENT AT 16M DEPTH

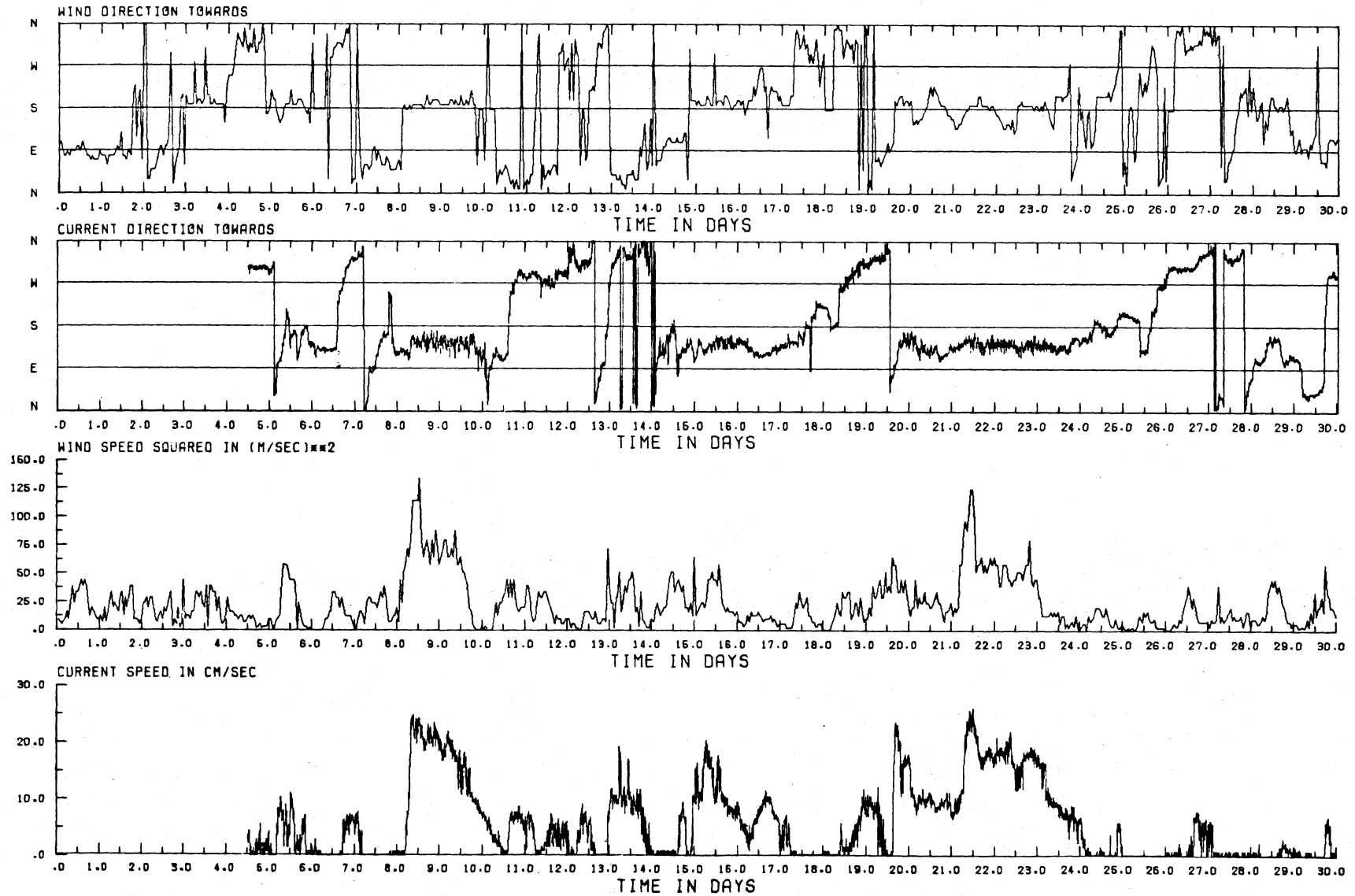


Figure 3.16

JUNE 1972: WATER TEMPERATURE

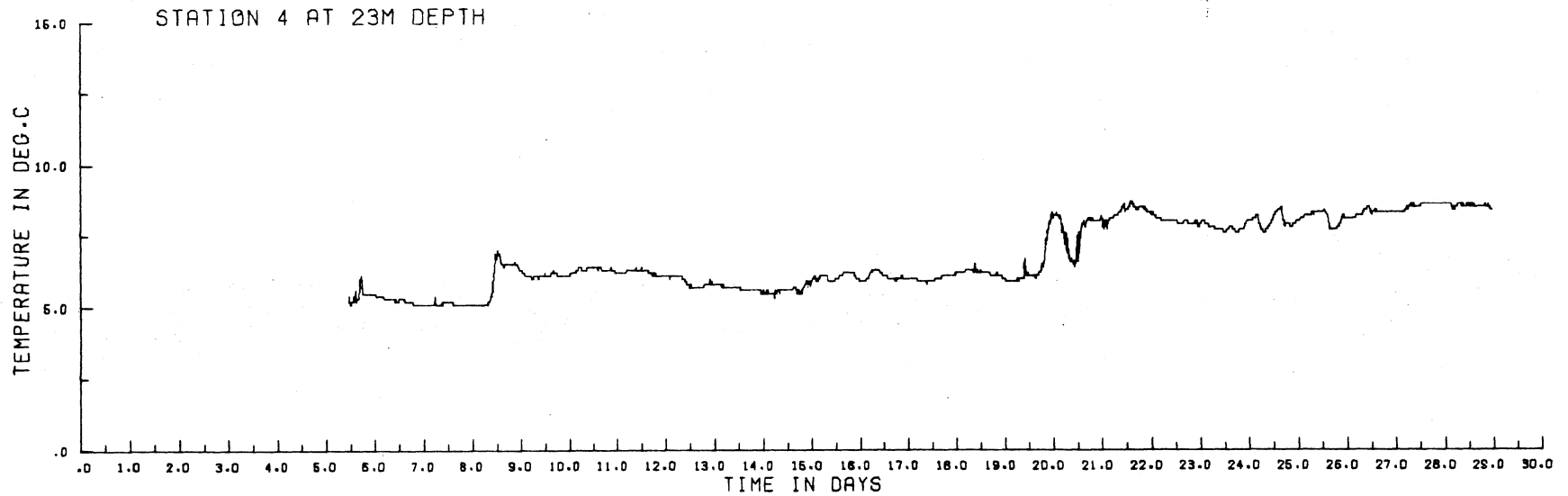
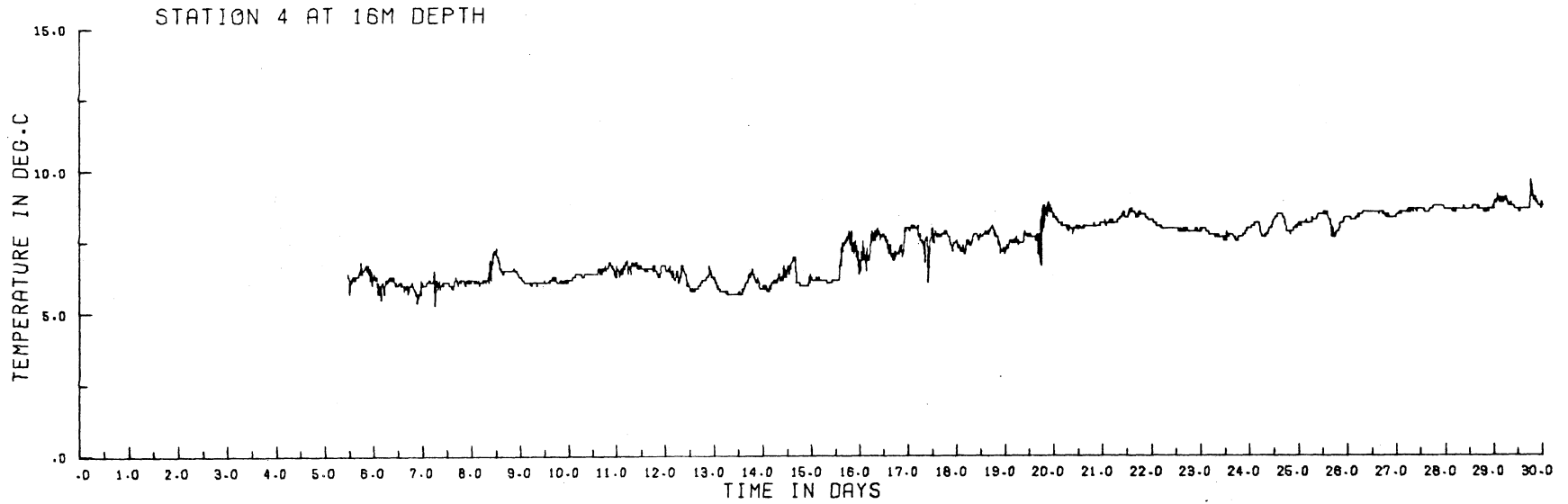


Figure 3.17

JUNE 1972: WIND (MITCHELL FIELD) COMPARED WITH STATION 4 CURRENT AT 16M DEPTH

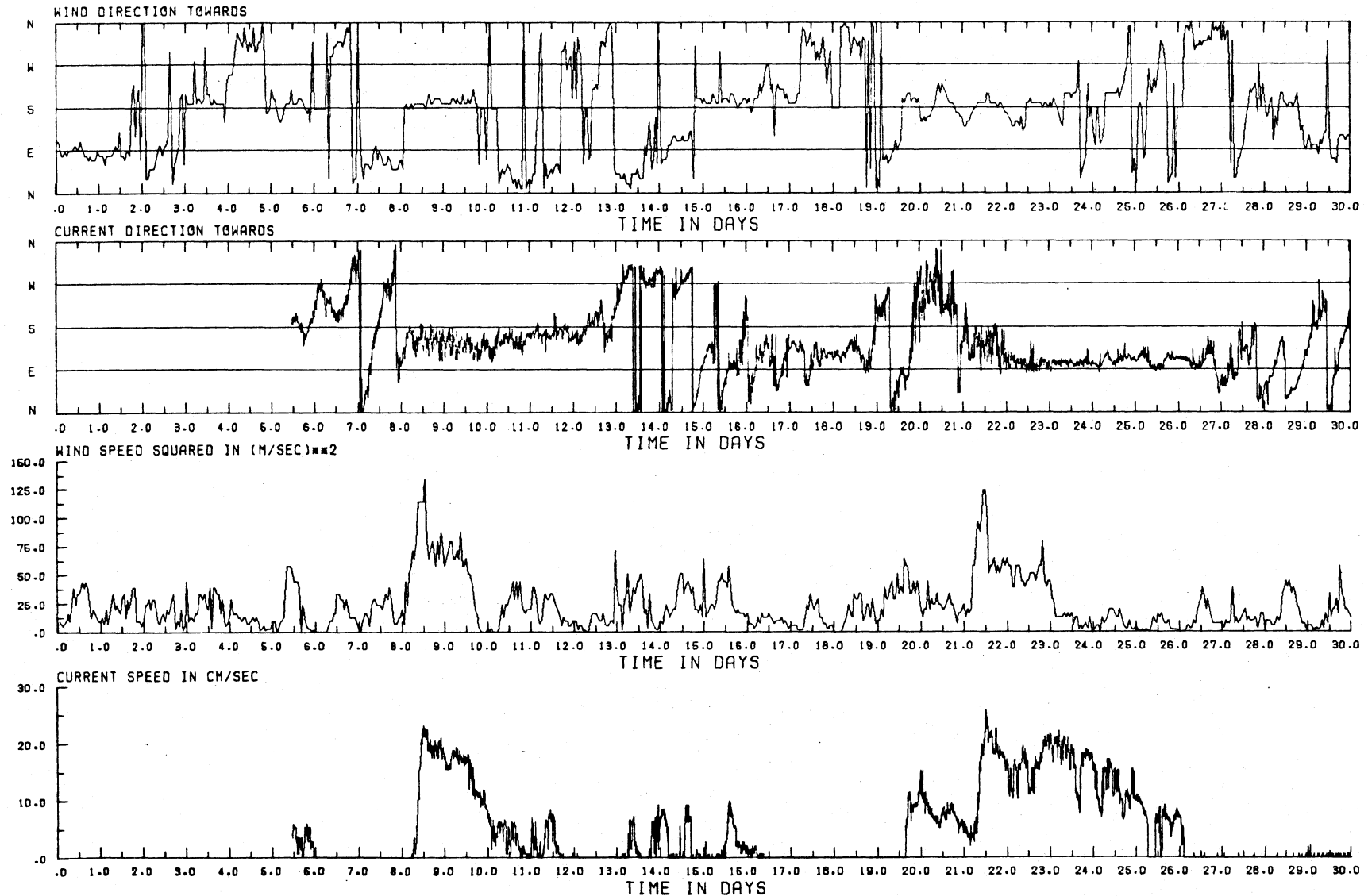


Figure 3.18

JUNE 1972: WIND (MITCHELL FIELD) COMPARED WITH STATION 4 CURRENT AT 23M DEPTH

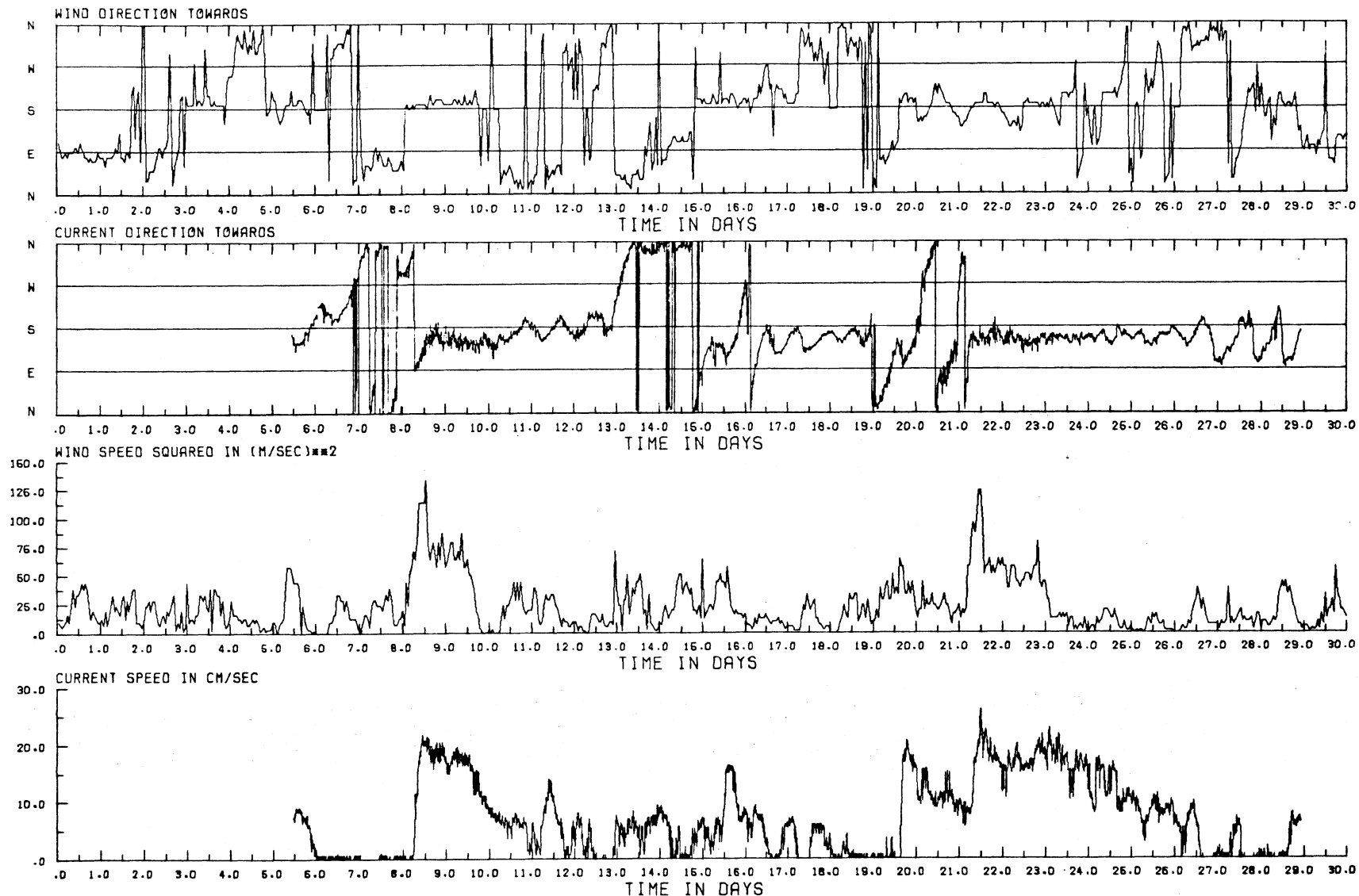
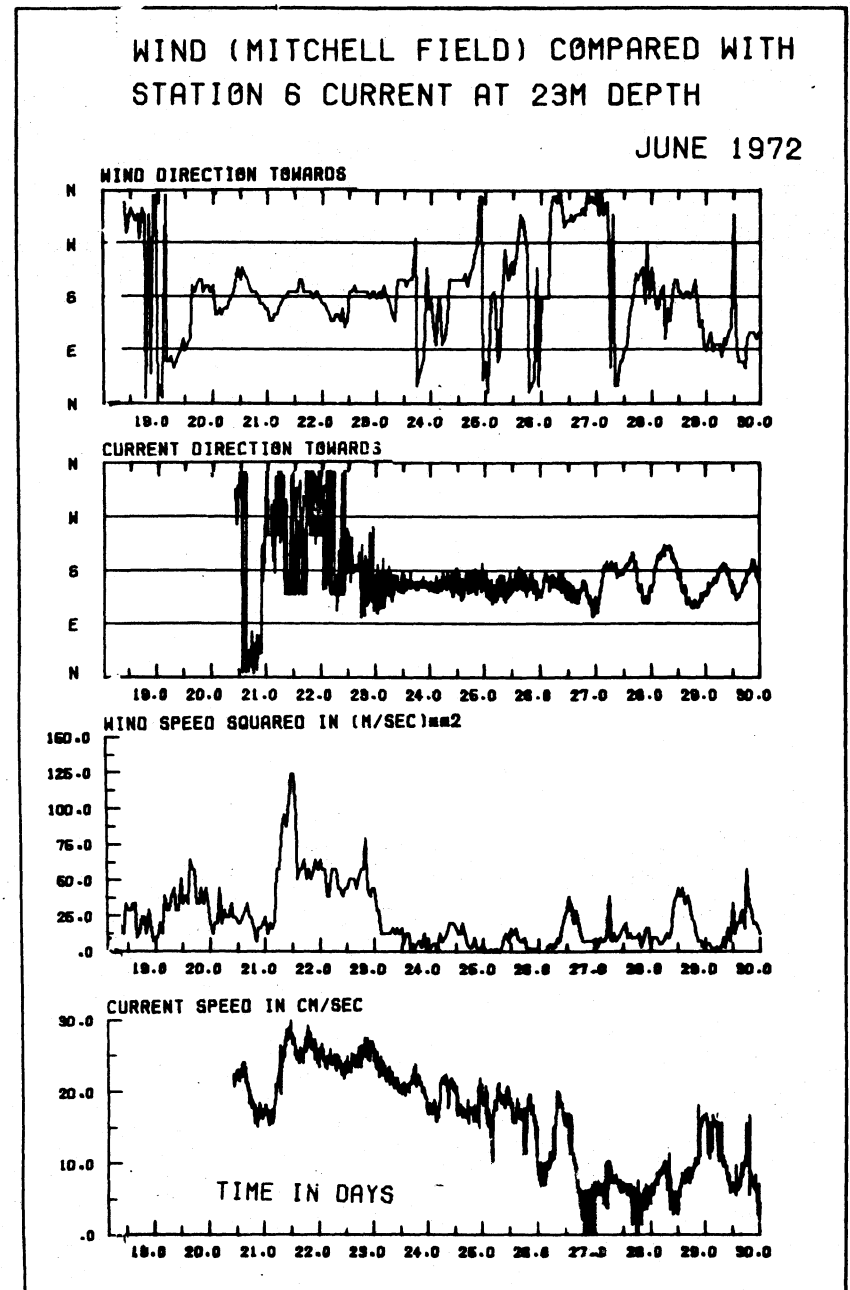
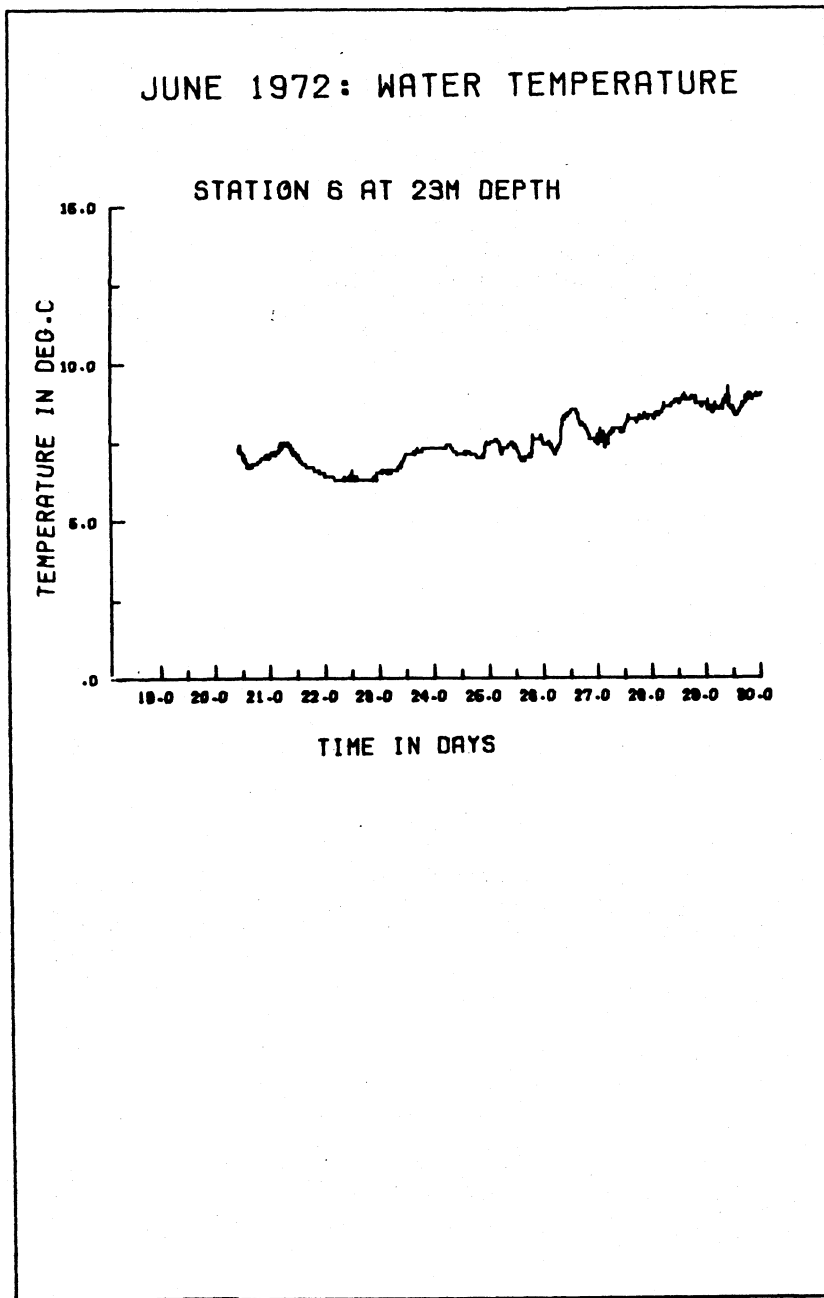


Figure 3.19



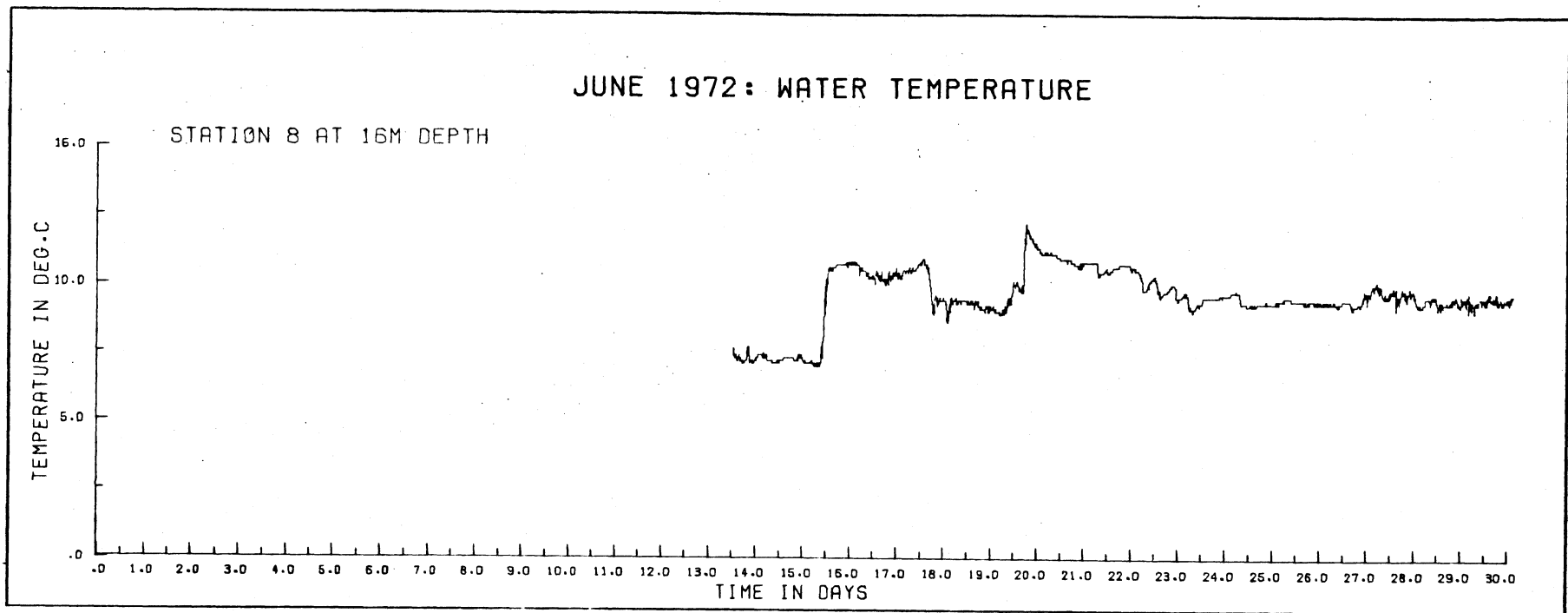


Figure 3.20

Figure 3.21

JUNE 1972: WIND (MITCHELL FIELD) COMPARED WITH STATION 8 CURRENT AT 16M DEPTH

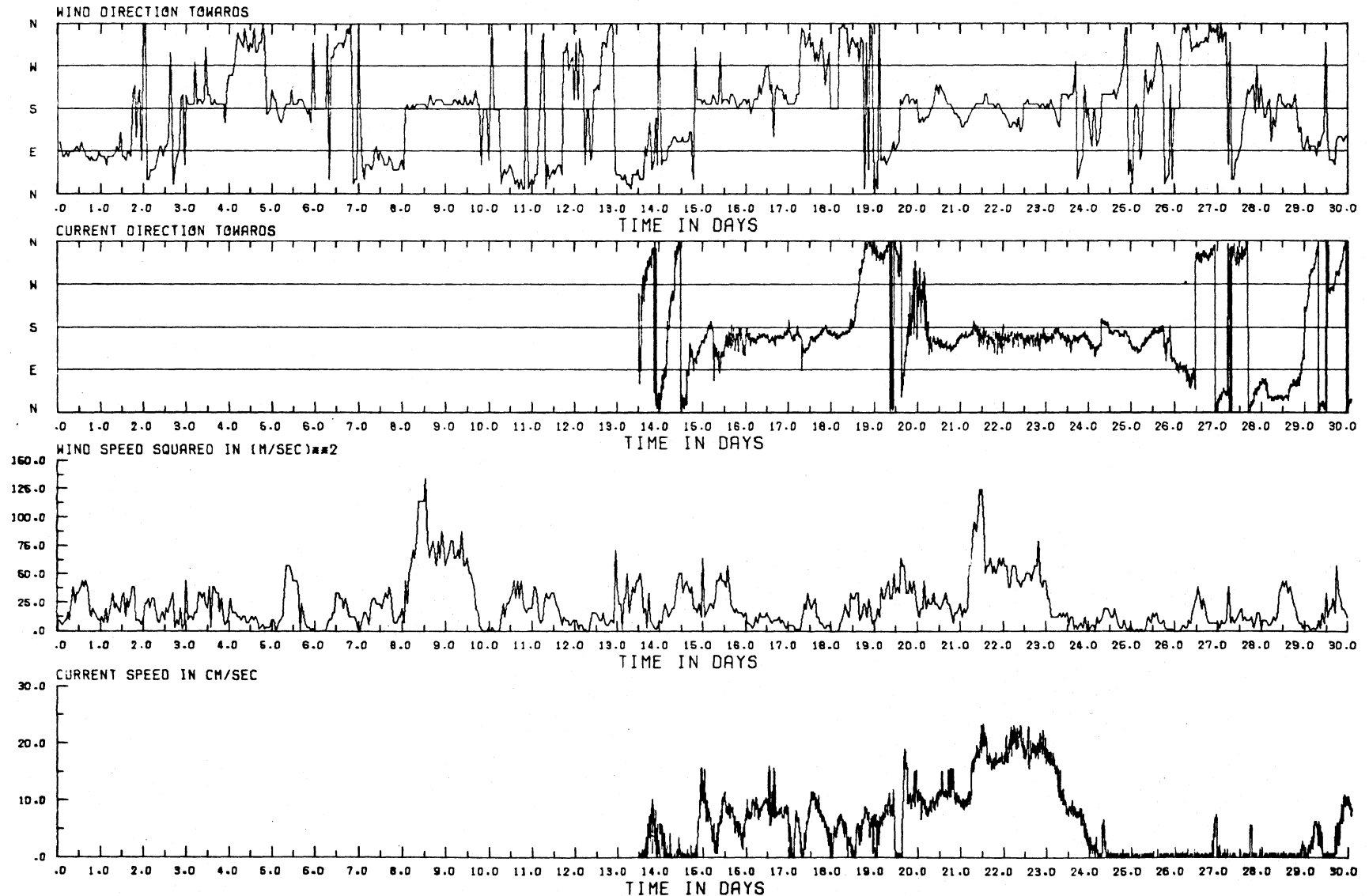
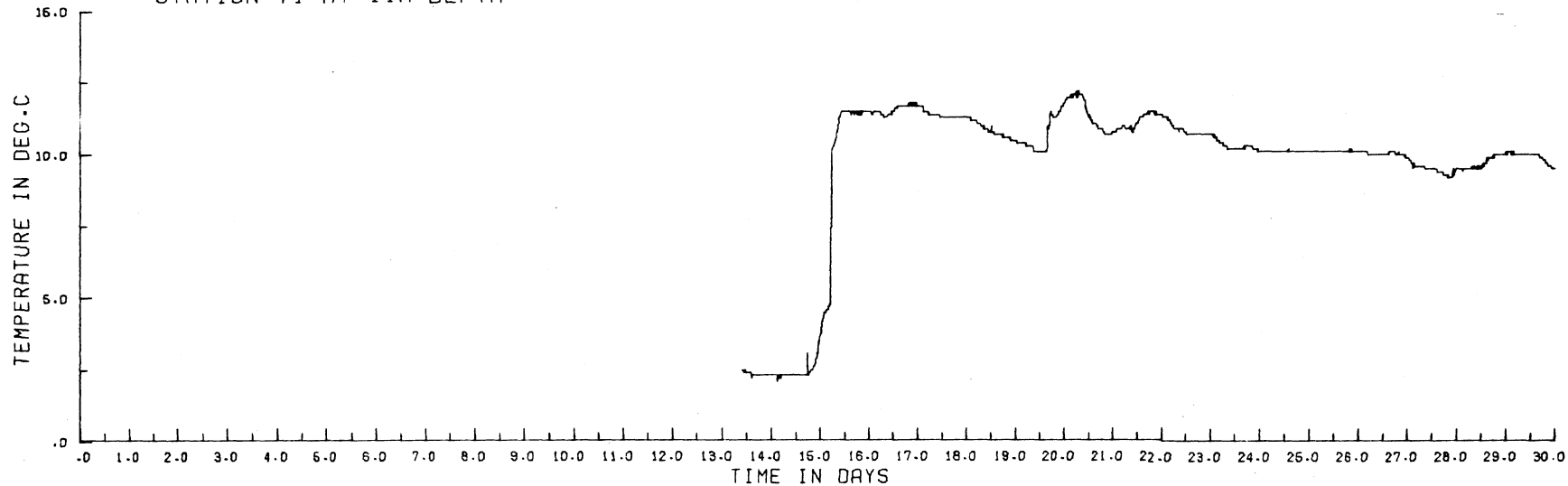


Figure 3.22

JUNE 1972: WATER TEMPERATURE

STATION T1 AT 11M DEPTH



STATION T2 AT 10M DEPTH

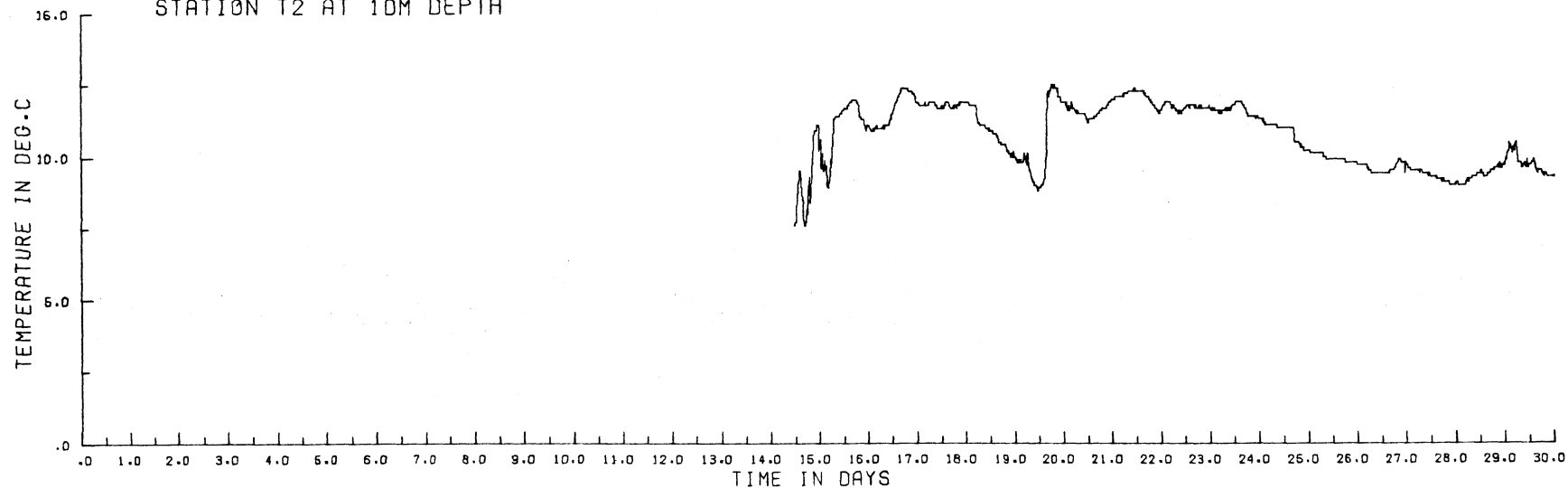


Figure 3.23

JUNE 1972: WIND (MITCHELL FIELD) COMPARED WITH STATION T1 CURRENT AT 11M DEPTH

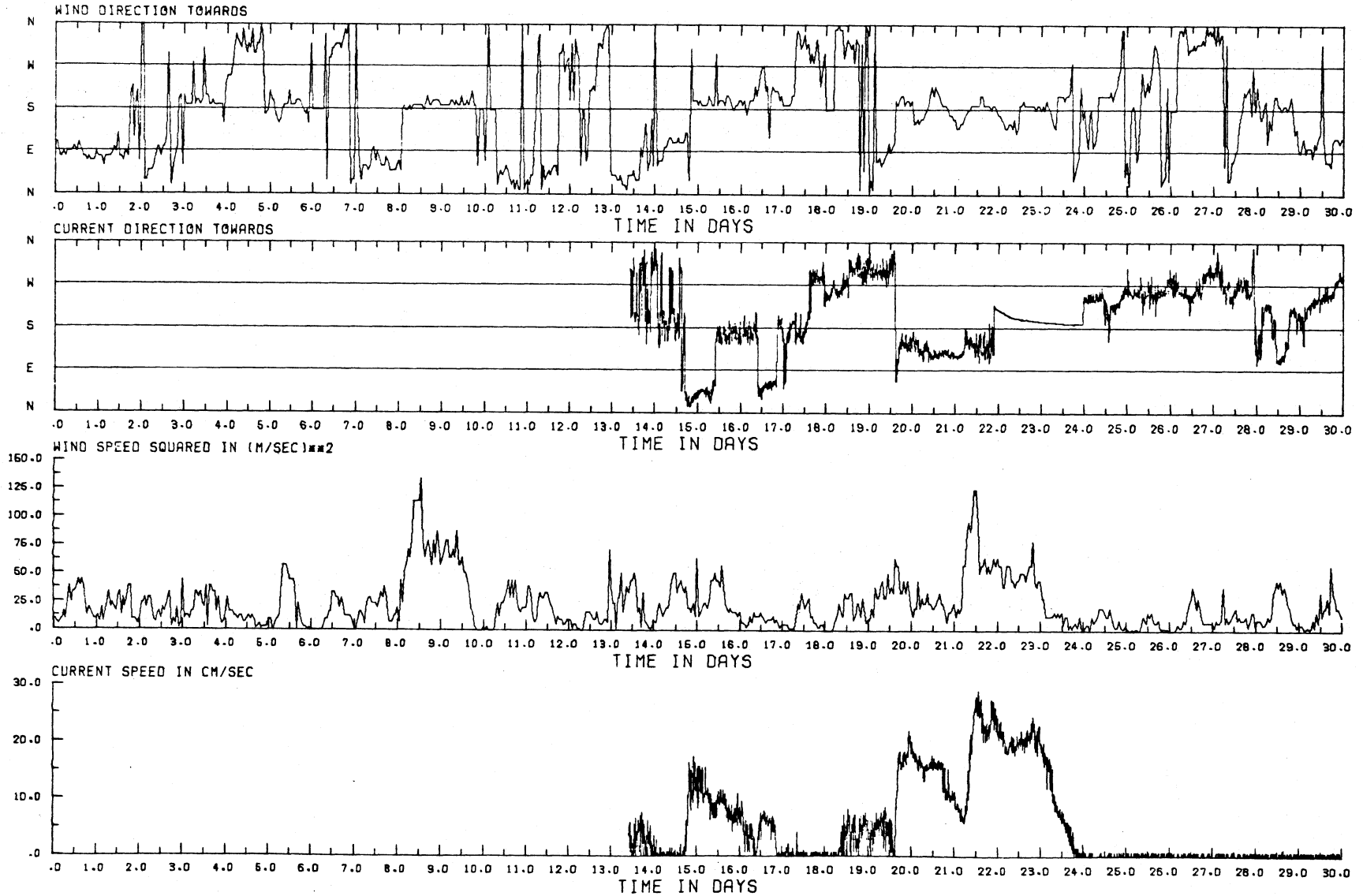
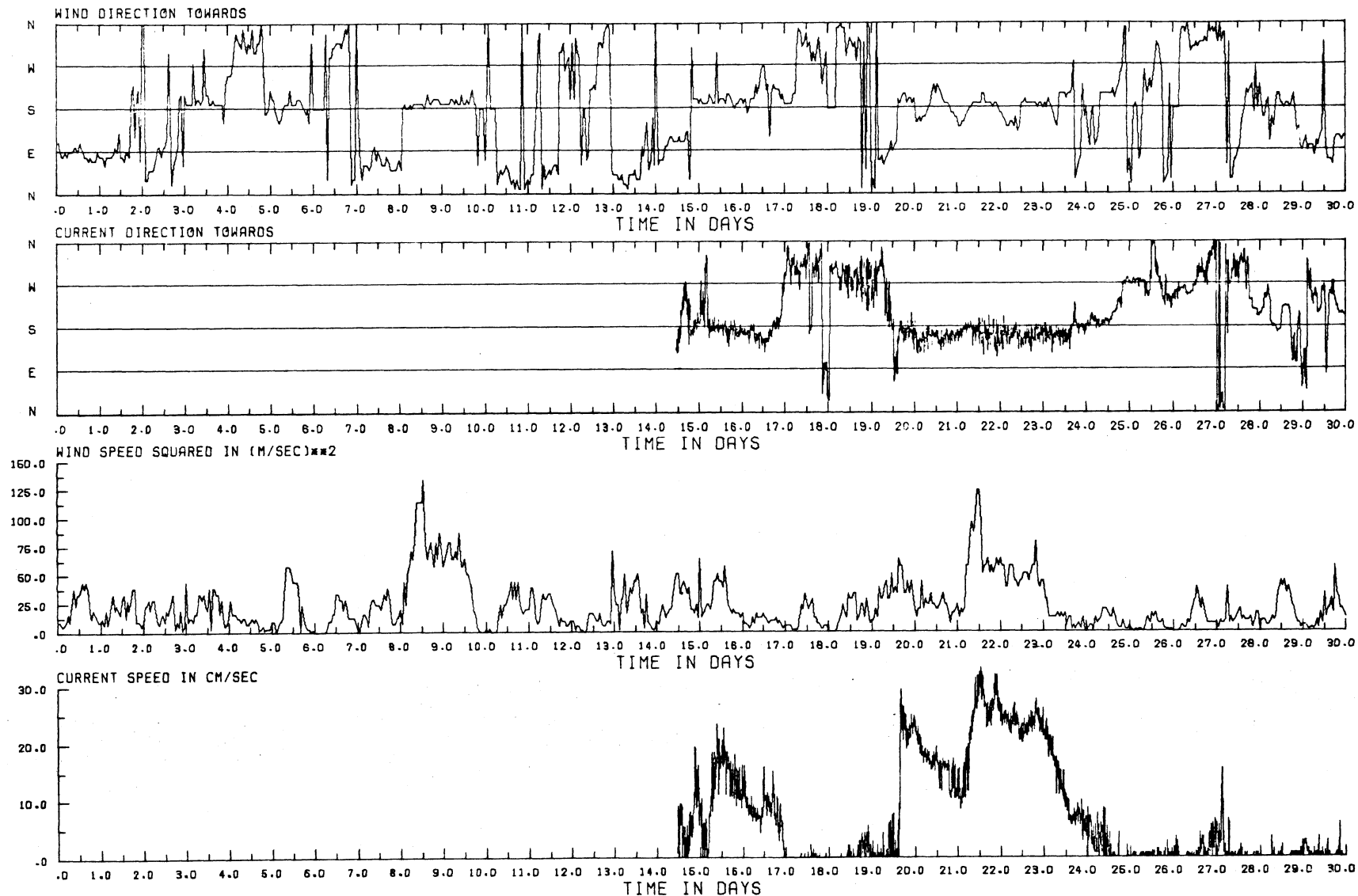


Figure 3.24

JUNE 1972: WIND (MITCHELL FIELD) COMPARED WITH STATION T2 CURRENT AT 10M DEPTH



Extract from Table 2.1

Station and date list for Survey II

Survey	Station No.	Distance from shore (km)*	Water Depth (m)	Meter Depth (m)	Date Set	Date Retrieved	No. of Days of Record in Water		Comments
							Expected	Obtained	
II	1	8.0 (8.4)	20	15	5 June 1972	Lost			
	2	5.3 (7.2)	22	17	5 June 1972	Lost			
	3	4.2	19	13	5 June 1972	29 July 1972 in Sheboygan Harbor	54	32	Tape torn
	4	8.0 (10.8)	28	15	6 June 1972	17 August 1972 south of Terry Andrae Park	72	55	Tape cut
	6	12.8 (16.3)	46	15	21 June 1972	3 September 1972 near Ludington	81	0	Tape unwound
	8	6.0	20	15	14 June 1972	4 August 1972 at Terry Andrae Park	81	80	Tape cut
	T <sub>1</sub>	3.5 (3.7)	13	11	14 June 1972	25 August 1972	48	48	
	T <sub>2</sub>	1.7	12	10	15 June 1972	25 August 1972	71	71	

\*Bracketed: distance from shore along E-W line in Fig. 2.1. Unbracketed: distance from nearest shoreline.

At the beginning of the July-August period, i. e. from the 2nd to the 5th of July, currents were generally southeasterly at all stations under the influence of southgoing winds (figs. 3.25 to 3.35). At the tower stations and at the shallower moorings a downwelling episode occurred between 2.0 and 2.5 days at the tower stations (fig. 3.33) station 3 (fig. 3.25) and station 8 (fig. 3.31) but was not evident at the other stations. This was followed by a speed-up of the southeasterly current at station 3 and then by a short-lived current reversal (fig. 3.25); at station 4 the current was maintained in a southeasterly direction until 6.2 days (fig. 3.27) and the same was true at station 6 (23 m depth, fig. 3.29). At stations  $T_1$  and  $T_2$  the current, after the southeasterly pulse associated with the downwelling on 2.5 days, remained relatively slow and variable in direction for the remainder of the month except for another pulse of southgoing current on 26.0 days (figs. 3.34 and 3.35). This behavior was presumably the result of the light variable winds which persisted for most of that month.

The July records show the first influence of rotary-near inertial motion associated with fully developed stratification, for example from 6.5 to 11.0 days at station 6 (fig. 3.29) and from 4.7 to 8.0 days at station 8 (16 m, fig. 3.32). This type of motion was not observed at the shallowest stations (station 3, fig. 3.25, and stations  $T_1$  and  $T_2$ , figs. 3.34 and 3.35), whereas at station 4 (fig. 3.27) the current direction between 7.0 and 12.0 days showed a "looping" behaviour (compare fig. 1.9b) intermediate between the absence of rotation at the shallower stations and the steadier rotation at station 6 and station 8. Similar differences will be illustrated later in the progressive vector diagrams. Rotary motion, when and where it appeared, made the wind-induced current reversals more difficult to detect.

The premature release of the moored current array, as a result of a severe local thunderstorm on 14 July, could be detected on the records of some of the instruments later recovered. There were sudden jumps in temperature (for example at stations 4 and 8, figs. 3.26 and 3.31) or jumps in current speed (station 4, fig. 3.27, and station 8, fig. 3.32).

[the text continues on page 98]

Figure 3.25

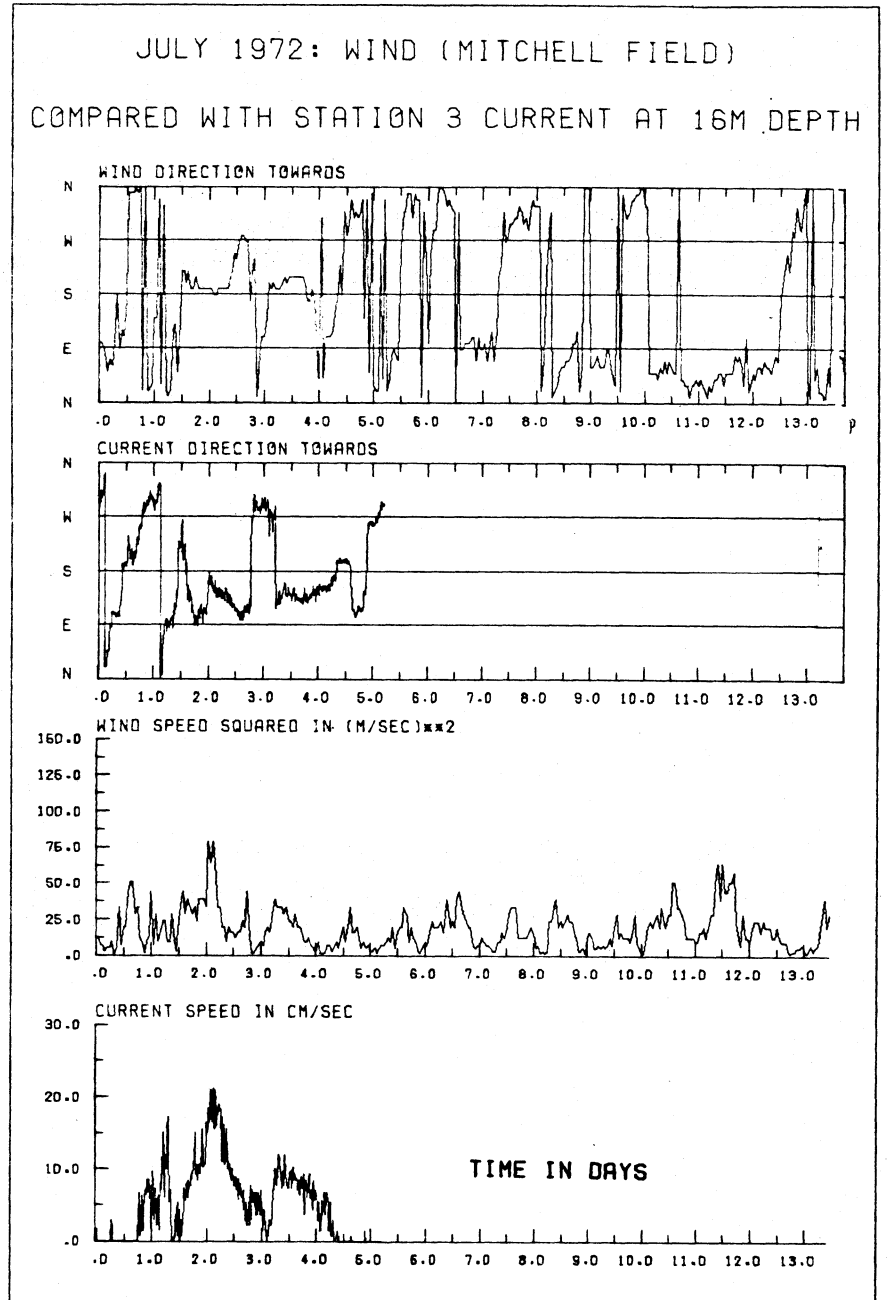
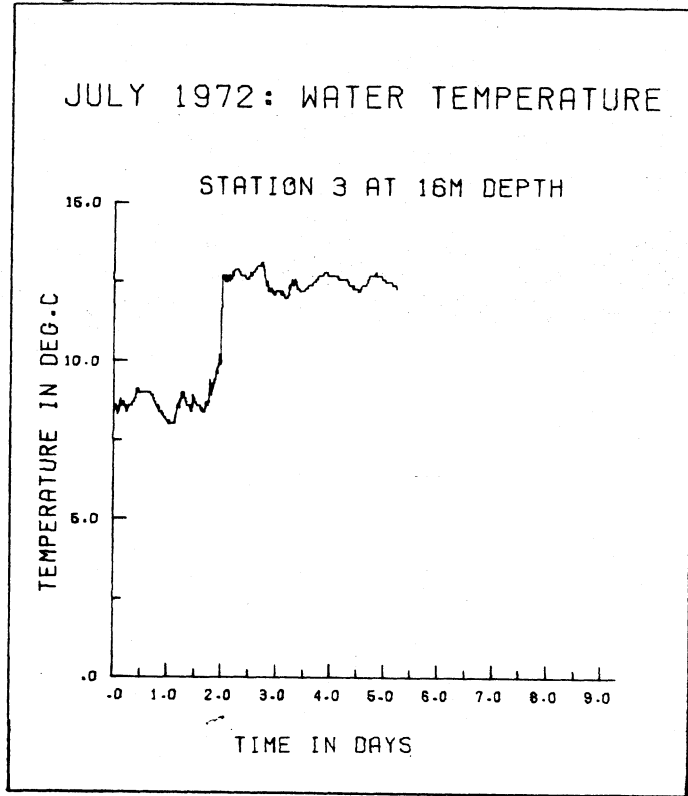


Figure 3.26

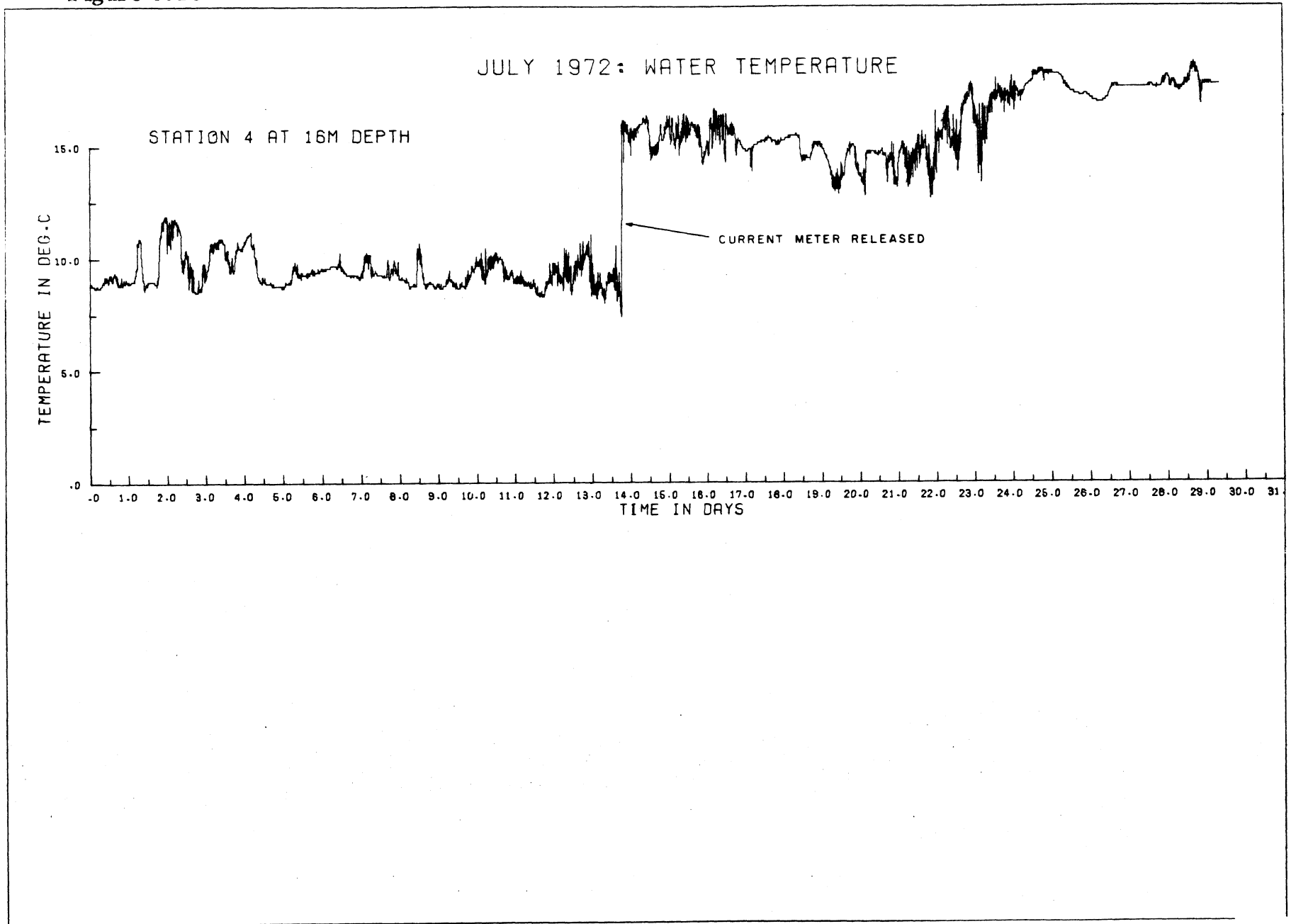


Figure 3.27

JULY 1972: WIND (MITCHELL FIELD) COMPARED WITH STATION 4 CURRENT AT 16M DEPTH

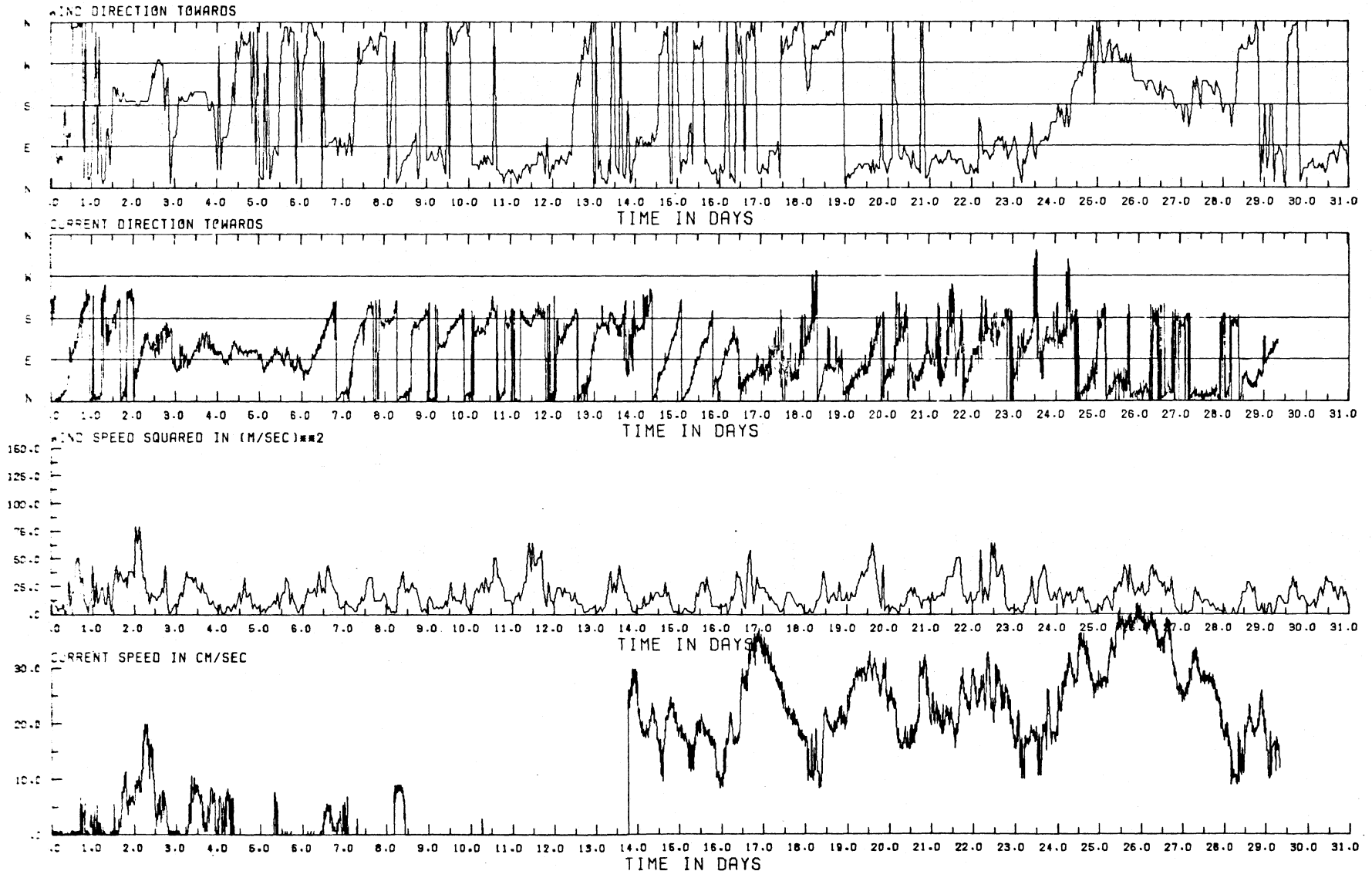


Figure 3.28

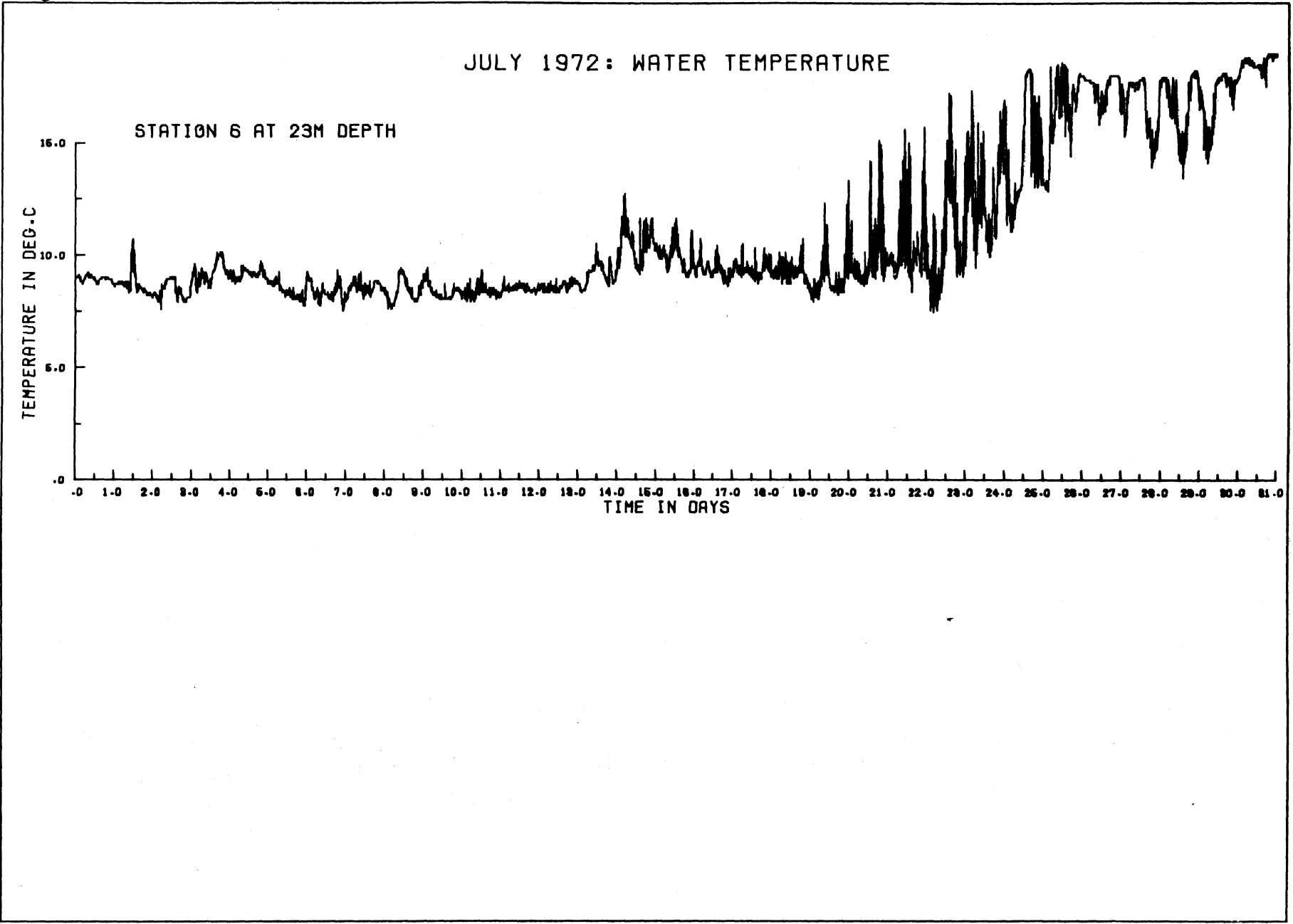
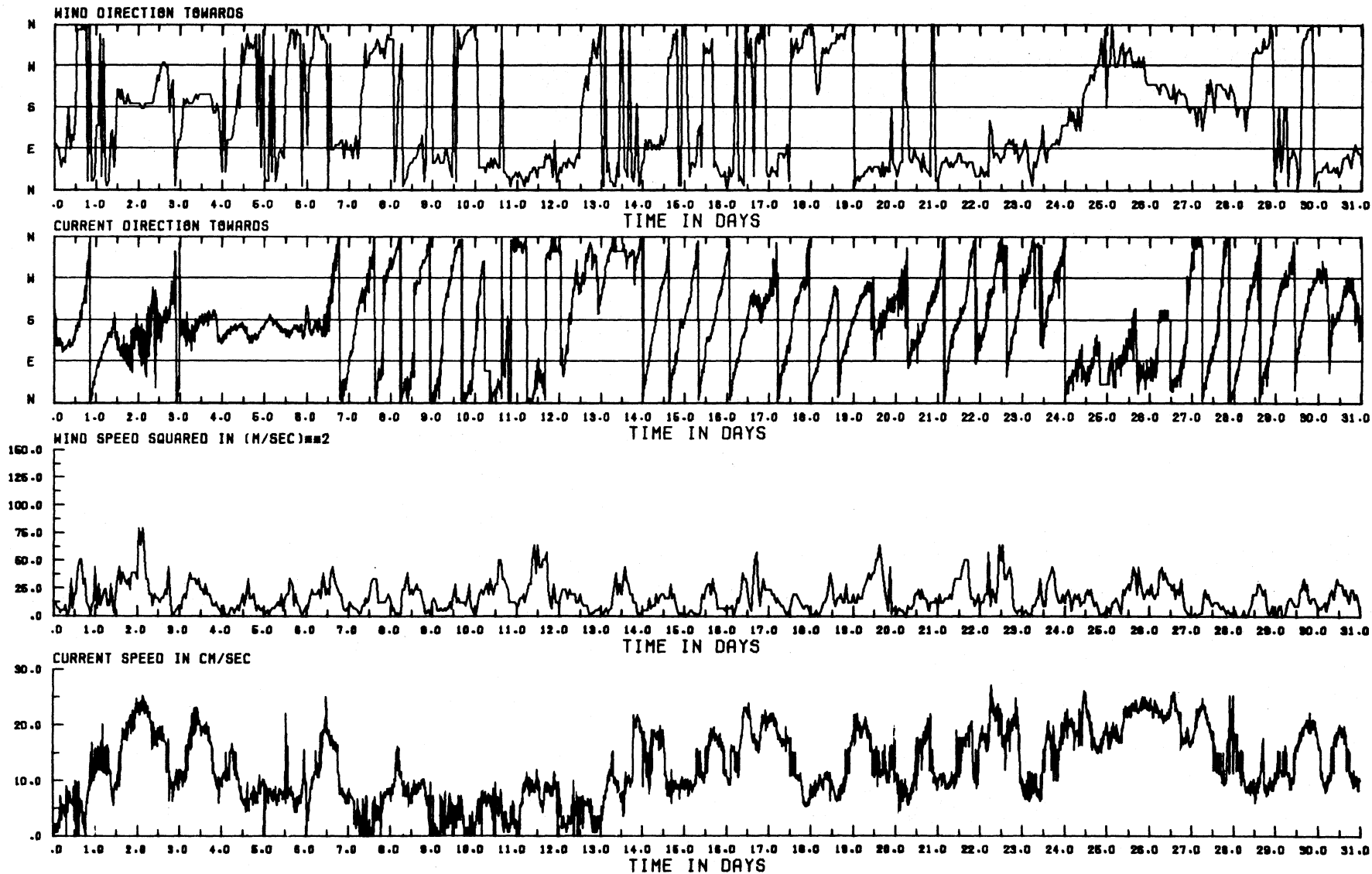


Figure 3.29

JULY 1972: WIND (MITCHELL FIELD) COMPARED WITH STATION 6 CURRENT AT 23M DEPTH



After their release, the station 4 and 8 meters showed a generally southeasterly 'residual' direction indicating that the meters floated northwestward. The station 6 meter travelled first northwesterly and then northeasterly. These directions explain why the station 4 and 8 meters were found near Sheboygan (located north of Oak Creek) and why the station 6 meters were found across the lake near Ludington. The above predominant directions can be more clearly seen in the progressive vector diagram (figs. 4.36, 4.38).

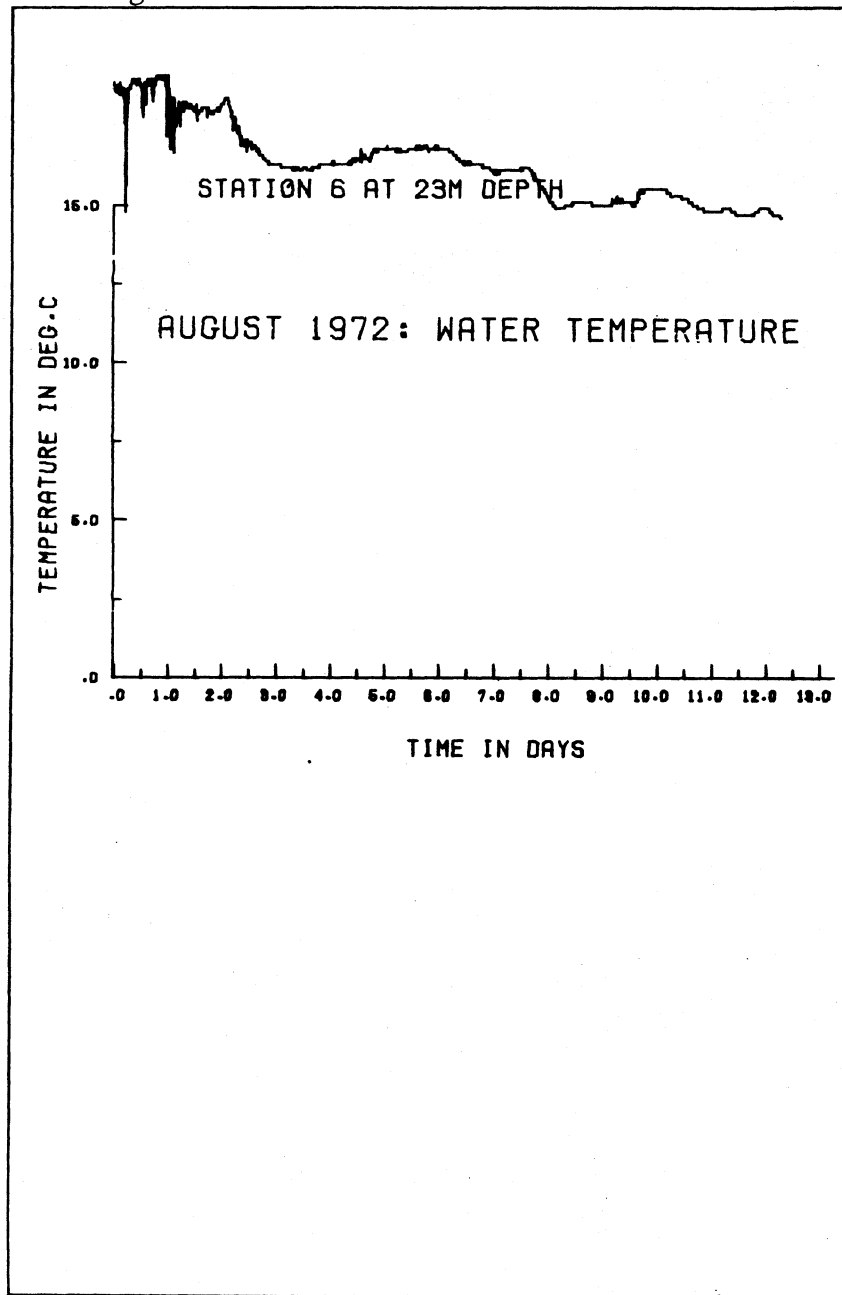
For several days after the release, two of the instruments (station 4, 14 to 16 July; and station 6, 14 to 24 July, 27 July to 12 August; see figs. 3.27, 3.29, and 3.30) showed a regular rotation of current direction with near-inertial period superimposed on the general drift. The drifting instrument presumably recorded the interaction of the drag (i. e. wind drag on the float, then at the surface, and also the drag of the sub-thermocline currents on the mooring cable and released SEDAR mechanism) and the near-inertial rotating current pattern in the upper layer, through which the instrument was being dragged.

As summarized in the extract from table 2.1 on p. 91, the station 3 instrument ceased recording on 6 July, i. e. a week before the premature release, and was recovered on 29 July in Sheboygan Harbor. The station 4 instrument ceased recording on 30 July and was recovered south of Terry Andrae Park on 17 August, having registered "current speeds" in excess of 30 cm. sec.<sup>-1</sup> during the previous week. The station 6 instrument continued to record until 13 August (figs. 3.28, 3.29 for July, and 3.30 for August inserted with the July set for convenience) and apparently remained drifting in the lake until its recovery on 3 September near Ludington. During its 30-day drift in the open lake, from 14 July to 13 August, the station 6 instrument was subjected to almost continuous near-inertial rotary motion. The station 8 instrument ceased recording on 25 July (figs. 3.31 and 3.32) when it probably went aground at Terry Andrae Park where it was recovered on 4 August.

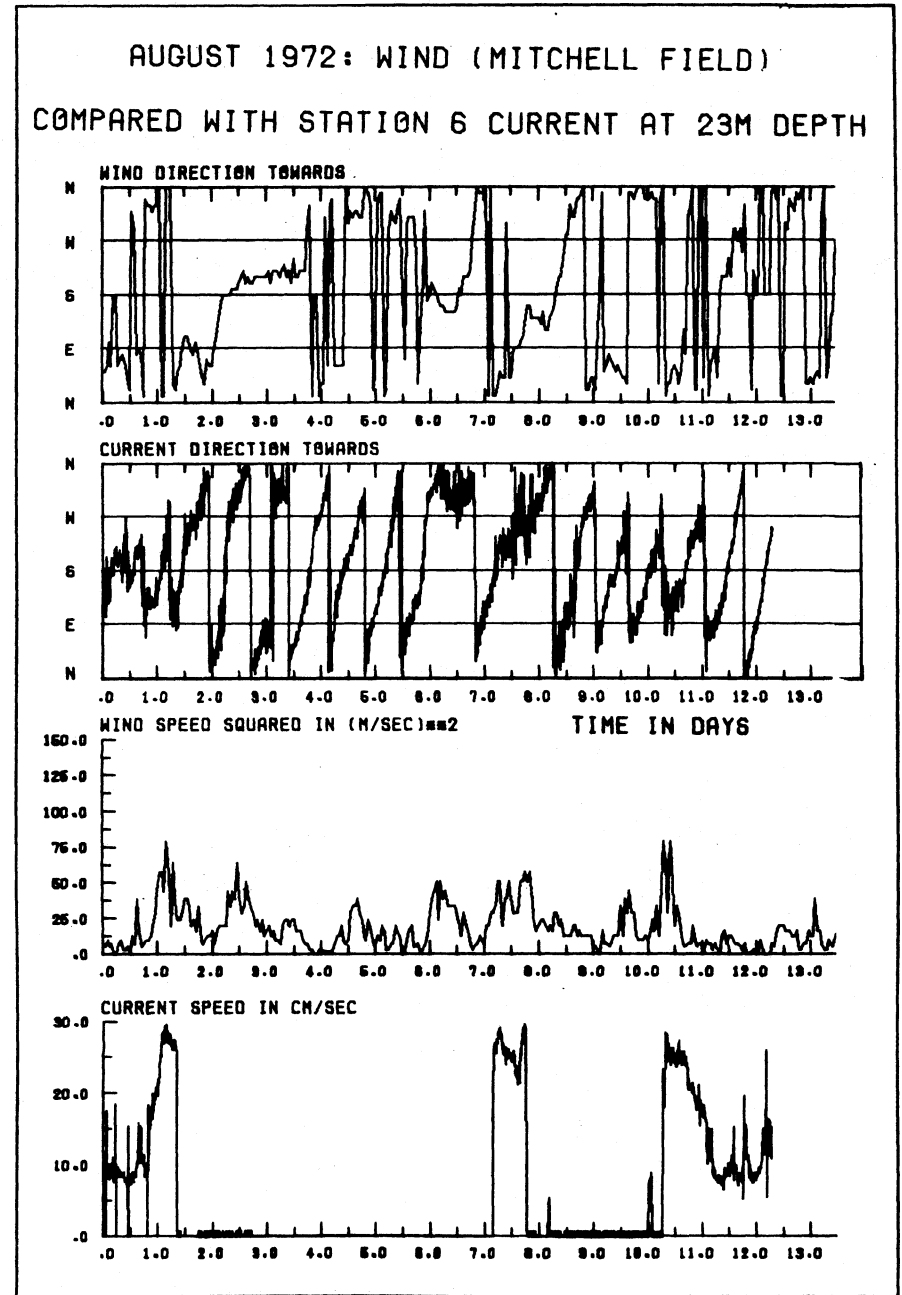
Since the station  $T_1$  and  $T_2$  meters were unaffected by the storm of 14 July, the meters continued to operate until the latter part of August. Although the currents were generally weak (figs. 3.34, 3.35, 3.37, 3.38) there

[the text continues on page 105]

Figure 3.30



- 66 -



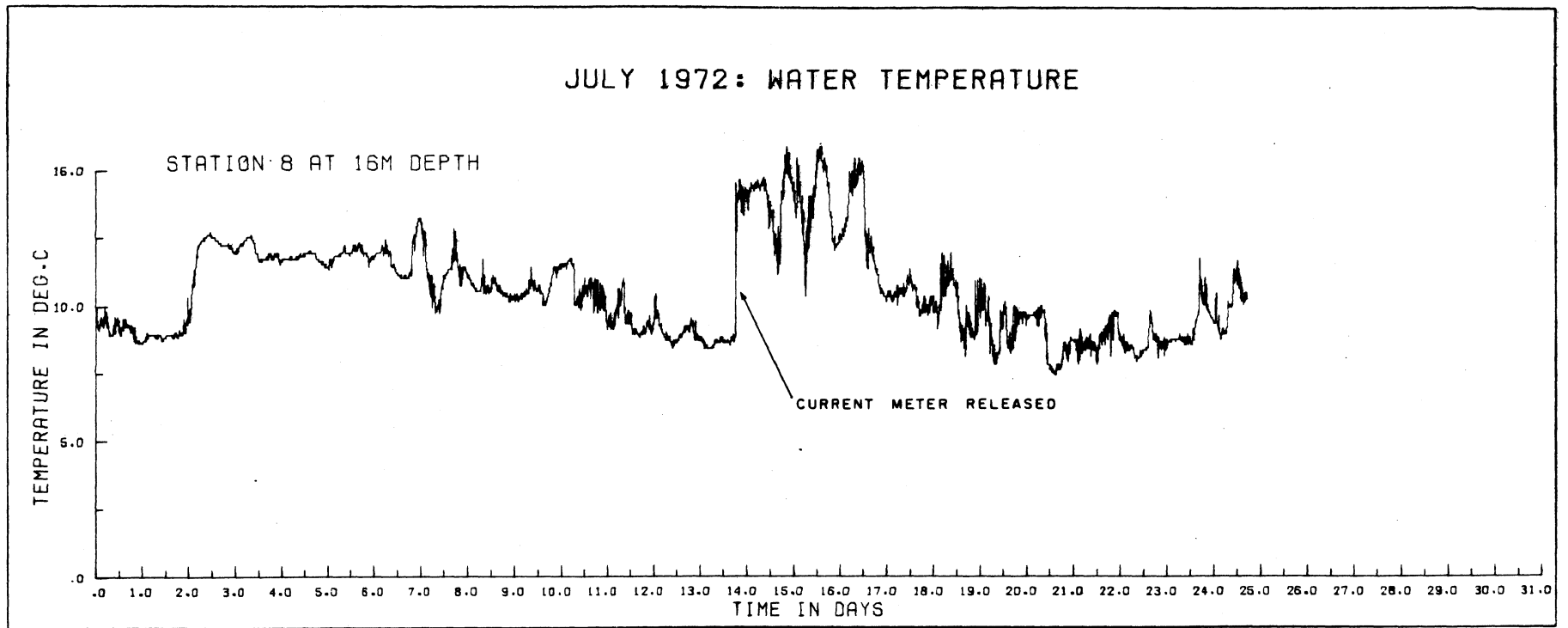


Figure 3.31

Figure 3.32

JULY 1972: WIND (MITCHELL FIELD) COMPARED WITH STATION 8 CURRENT AT 16M DEPTH

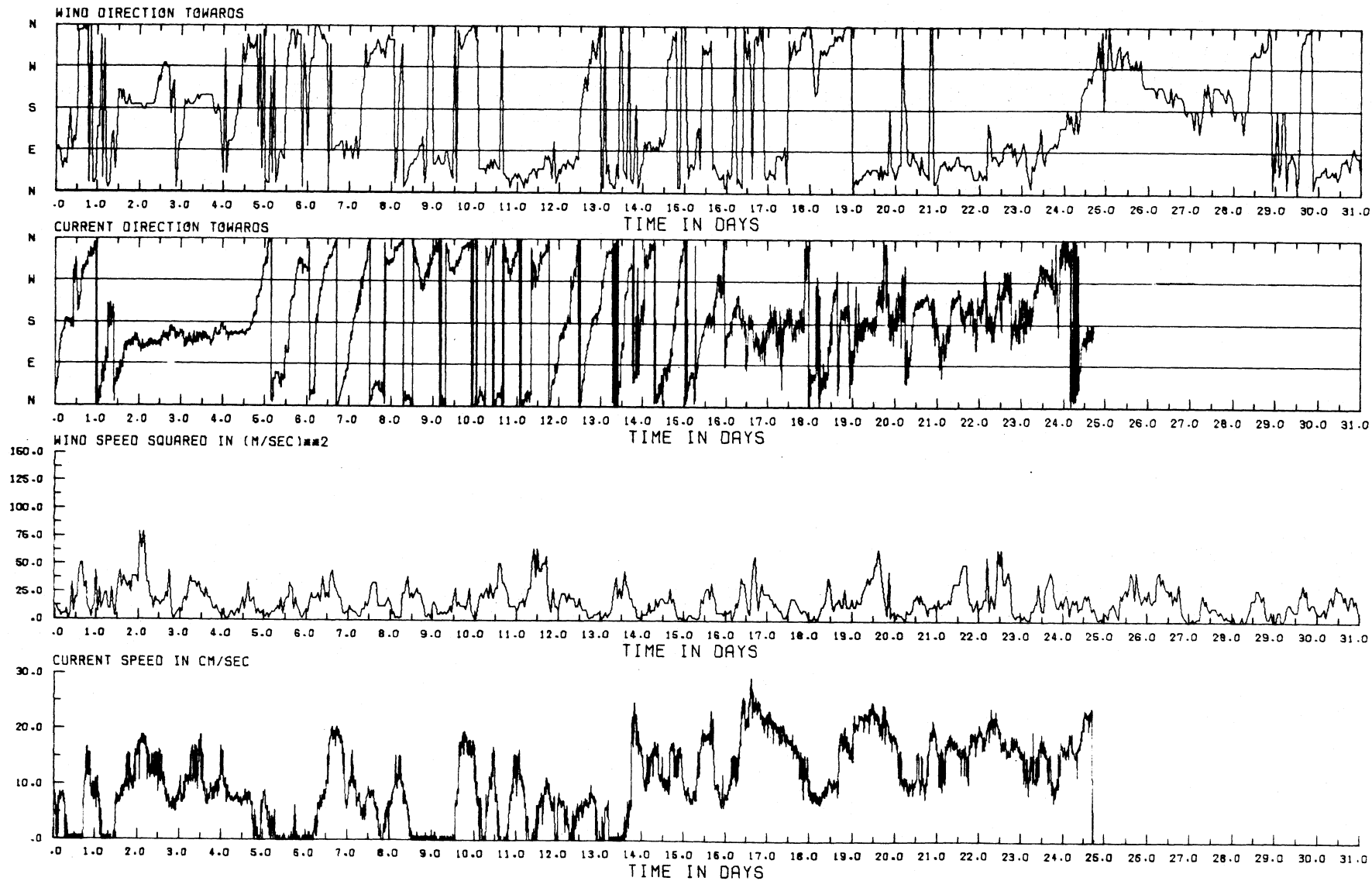


Figure 3.33

JULY 1972: WATER TEMPERATURE

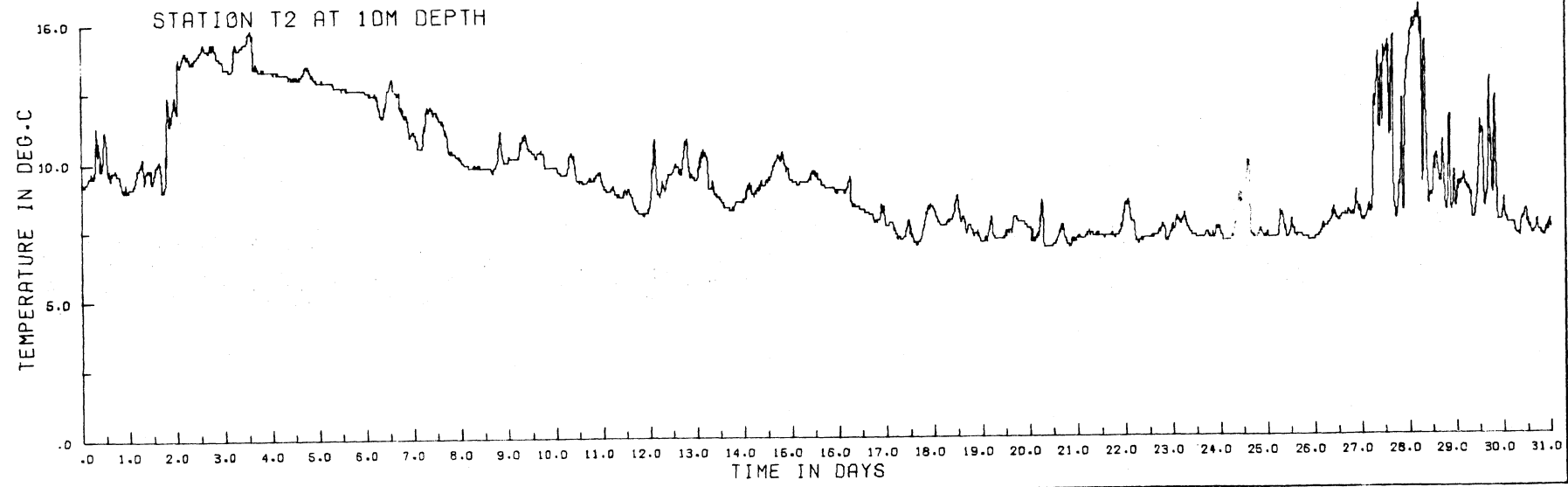
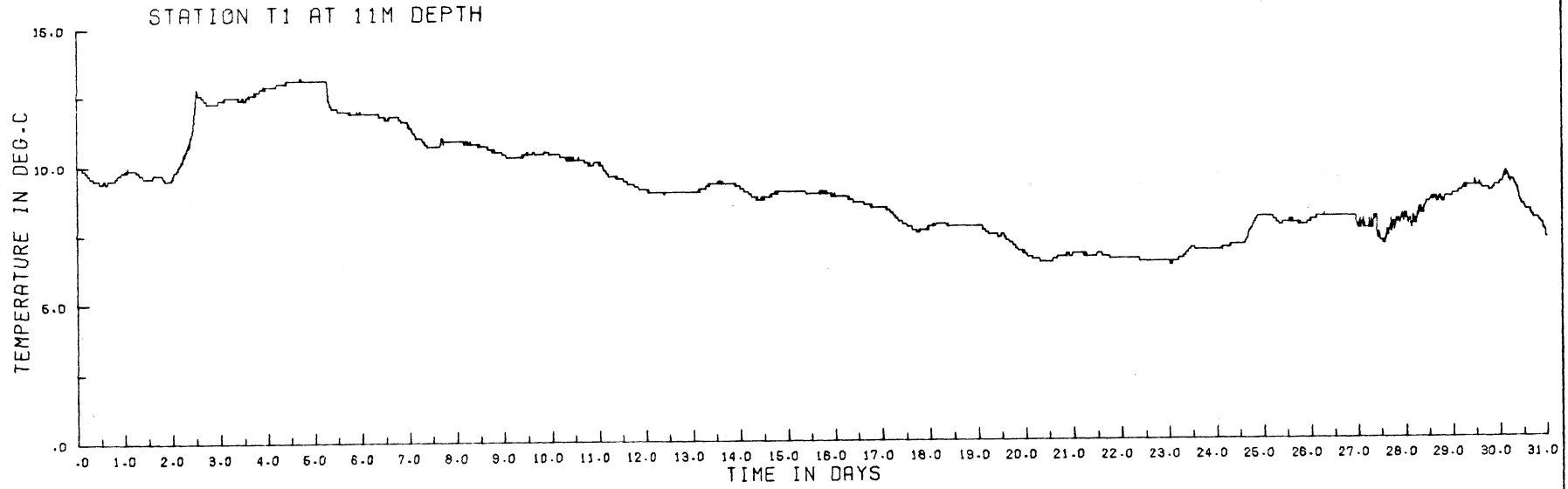


Figure 3.34

JULY 1972: WIND (MITCHELL FIELD) COMPARED WITH STATION T1 CURRENT AT 11M DEPTH

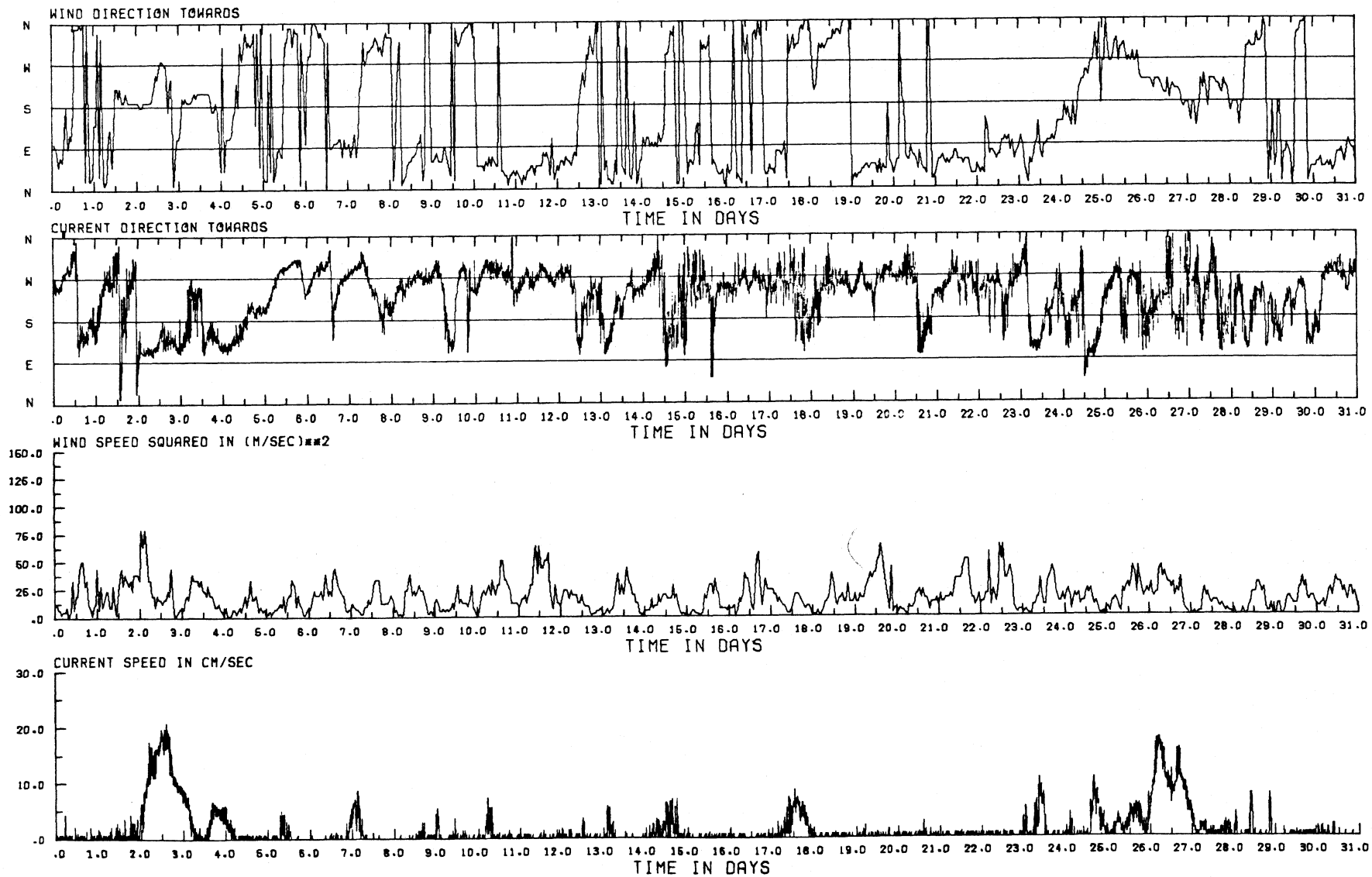
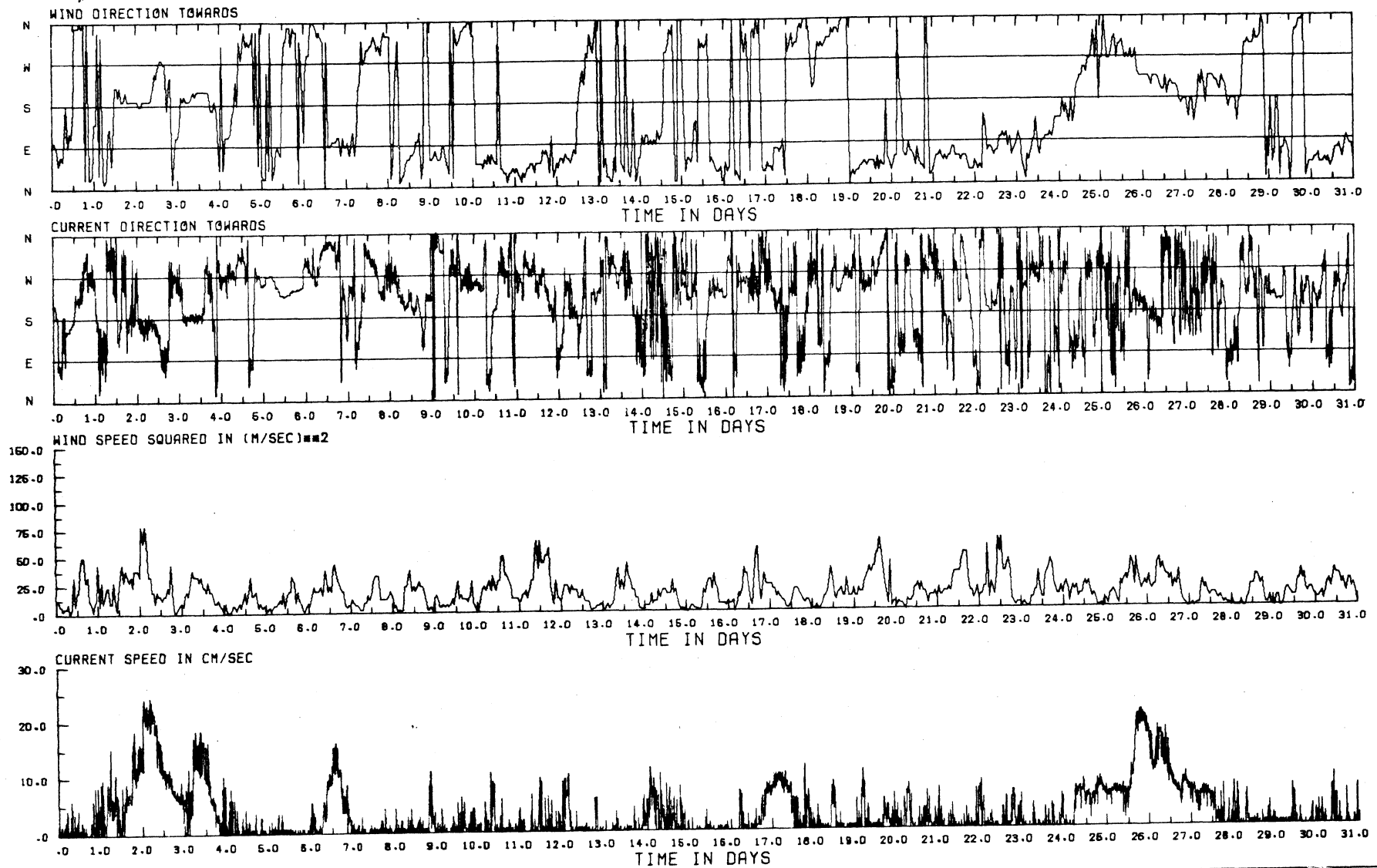


Figure 3.35

JULY 1972: WIND (MITCHELL FIELD) COMPARED WITH STATION T2 CURRENT AT 10M DEPTH



were a few exceptions: (July 17-18, 26, 27 and August 2, 4, 7-11, 14-15, and 23). Strong currents were found to flow generally in the southerly direction and current reversals were found to occur between 1 and 24 hours after wind reversals. The current readings were rather erratic for some periods indicating that these readings may have been affected by surface winds. Some near-inertial period oscillations were noticed at station  $T_1$  between July 16 and 20.

Strong upwelling and downwelling episodes which could be associated with northerly and southerly currents respectively were observed in the temperature records at these two stations (fig. 3.33). Temperature values ranged from  $7.2^{\circ}\text{C}$  to  $16^{\circ}\text{C}$ .

Survey III. 25 August to 30 September 1972

Extract from Table 2.1

Station and date list for Survey III

Station No.	$T_1$	$T_2$	$T_1$
Distance from shore (km)*	3.5 (3.7)	1.7	3.5 (3.7)
Water depth (m)	13	12	13
Instrument depth (m)	10	10	10
Date set (1972)	25 August	25 August	27 October
Date retrieved	27 October	7 December	Unrecovered
No. of days of record in water			
expected:	63	104	-----
obtained:	63	92	-----

\*Bracketed: distance from shore along E-W line in Fig. 2.1.

Unbracketed: distance from nearest shoreline.

During this survey only the tower-mounted instruments were operating: station  $T_1$  from 25 August (fig. 3.36, 3.37) to 27 October (figs. 3.39, 3.40, 3.42, and 3.43). On that date the meter at  $T_1$  was replaced, but that instrument still has to be recovered. The meter at station  $T_2$  recorded from 25 August to 25 November, i. e. for an uninterrupted period of 3 months (figs. 3.38, 3.41, 3.44, and 3.46) and the instrument was recovered on 7 December.

[the text continues on page 108]

Figure 3.36

AUGUST 1972: WATER TEMPERATURE

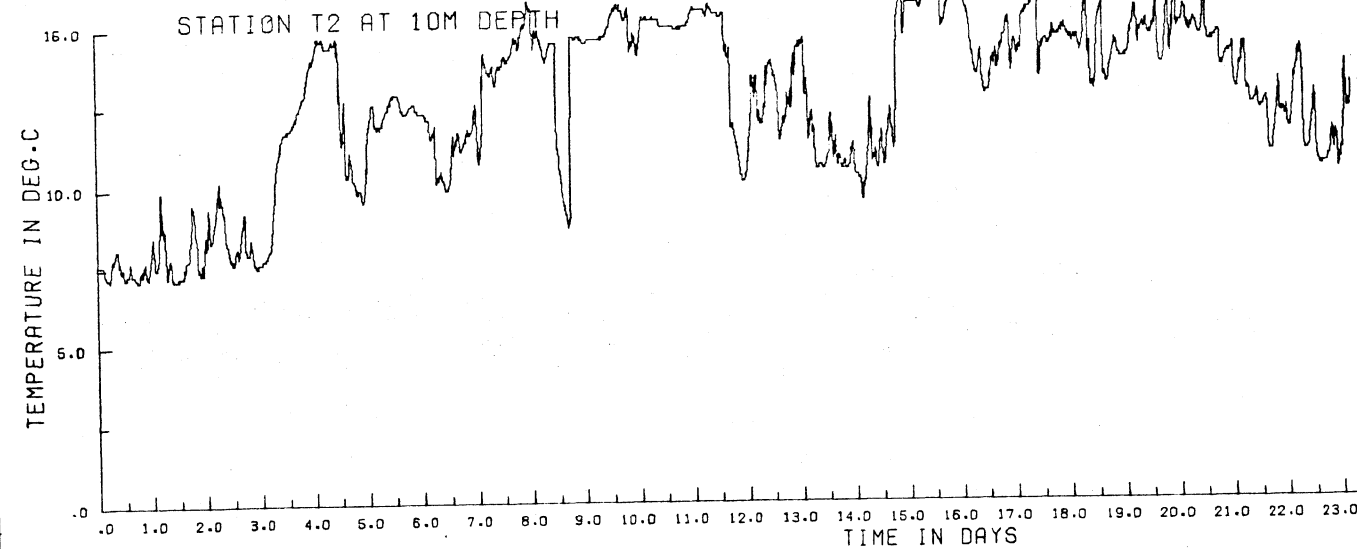
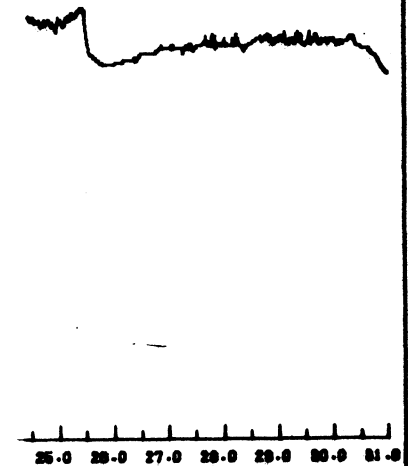
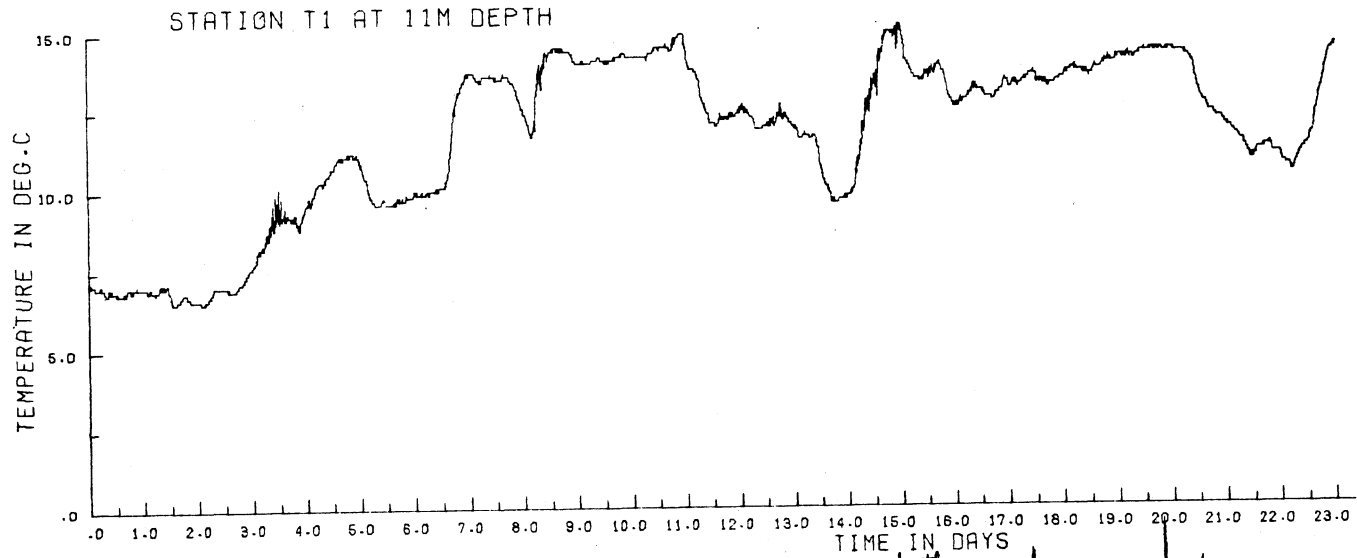
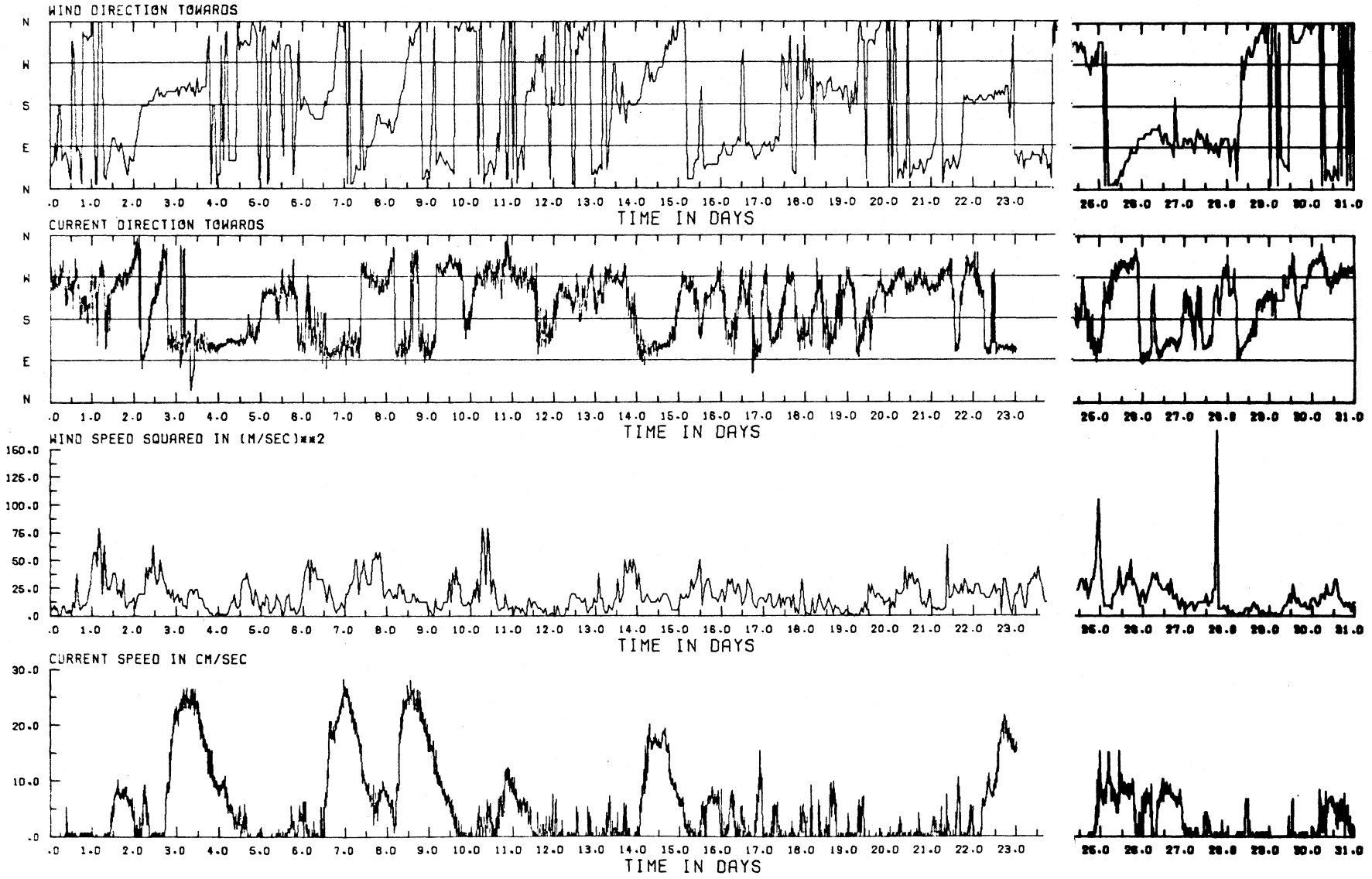


Figure 3.37

AUGUST 1972: WIND (MITCHELL FIELD) COMPARED WITH STATION T1 CURRENT AT 11M DEPTH



- 107 -

During September a conspicuous upwelling episode at 9.4 days followed a reversal in wind direction from southgoing to northgoing and was accompanied by a pulse of southgoing current (figs. 3.40, 3.41), whereas the strongest current pulse of the month also southgoing, was accompanied by a sharp rise of temperature at both stations (fig. 3.39). This and other temperature changes during that month do not find simple explanations, except in general terms of horizontal advective movements. Current direction was apparently steadier at station  $T_1$  than at  $T_2$ . During August and September, current reversals occurred five times at each of the stations with lags ranging from 3 to 6 hours for north-south reversals and from 2-12 hours for south-north reversals. The response time at station  $T_1$  was faster than at station  $T_2$ . The lower temperatures fell to  $5.1^\circ\text{C}$  during the end of the month, particularly during periods of northgoing winds, probably associated with an upwelled condition.

During October the temperature records were much steadier (fig. 3.42) as were also the current directions (figs. 3.43, 3.44). Current speeds were high, exceeding  $30 \text{ cm. s}^{-1}$  on two occasions during that month. The episodic or pulse-like nature of the currents correlated with southgoing or northgoing winds is very evident in the records for this month. There were four major episodes of northgoing currents with rapid reversals to southgoing. Weak currents were confined to the short interval 3.5 to 5.5 October. In all, there were seven marked current reversals, but in contrast to previous months the current changes were not always clearly associated with wind reversals. The increase in temperature at station  $T_1$  on 3 October was associated with predominantly westgoing currents -- in other words warmer water was being advected toward the shore -- but the decrease in temperature on 5 October is difficult to explain during an interval of very weak currents.

During November only the instrument at station  $T_2$  was in operation, and this showed a more persistent current pattern, in terms of direction, than found during previous months. While, as a partial explanation for this, the winds were mainly southgoing for most of the month, there were some sharp reversals in wind direction, but the initial responses of the current to these reversals were generally more sluggish than those seen on previous records.

[the text continues on page 120]

Figure 3.38

AUGUST 1972: WIND (MITCHELL FIELD) COMPARED WITH STATION T2 CURRENT AT 10M DEPTH

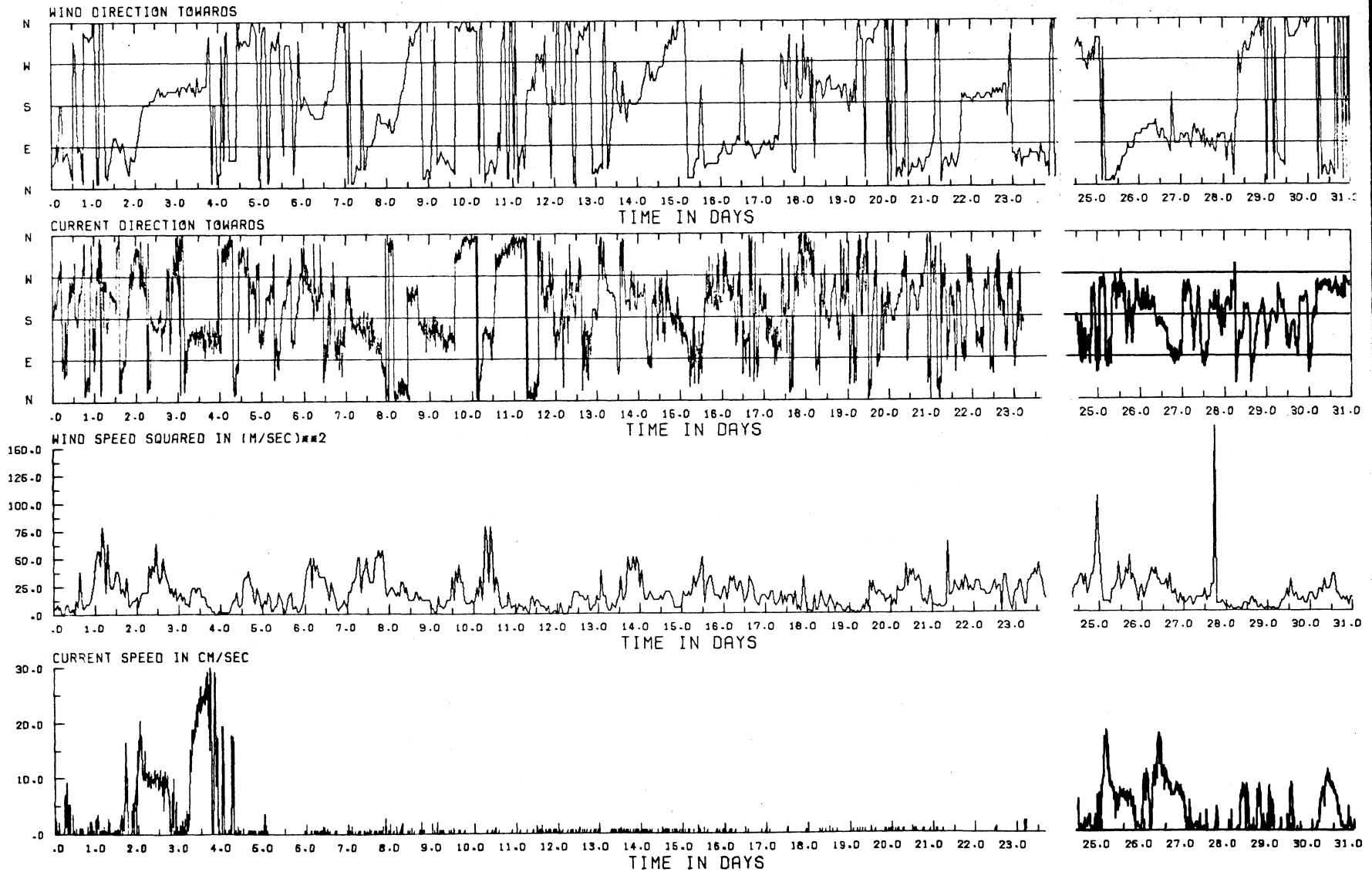


Figure 3.39

SEPTEMBER 1972: WATER TEMPERATURE

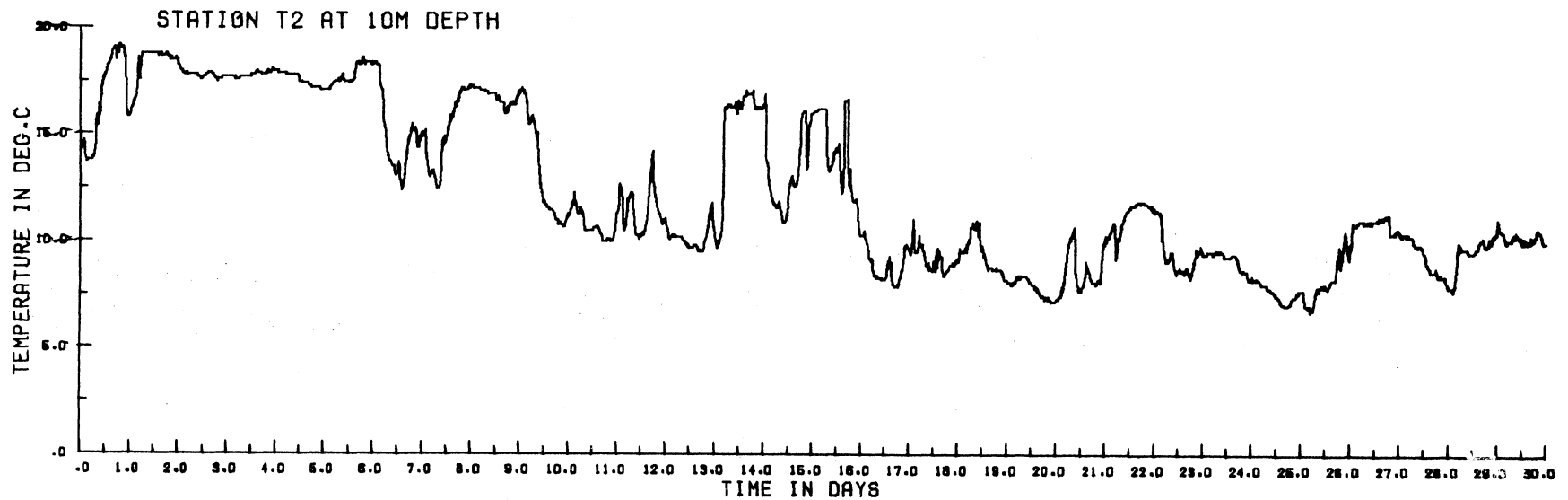
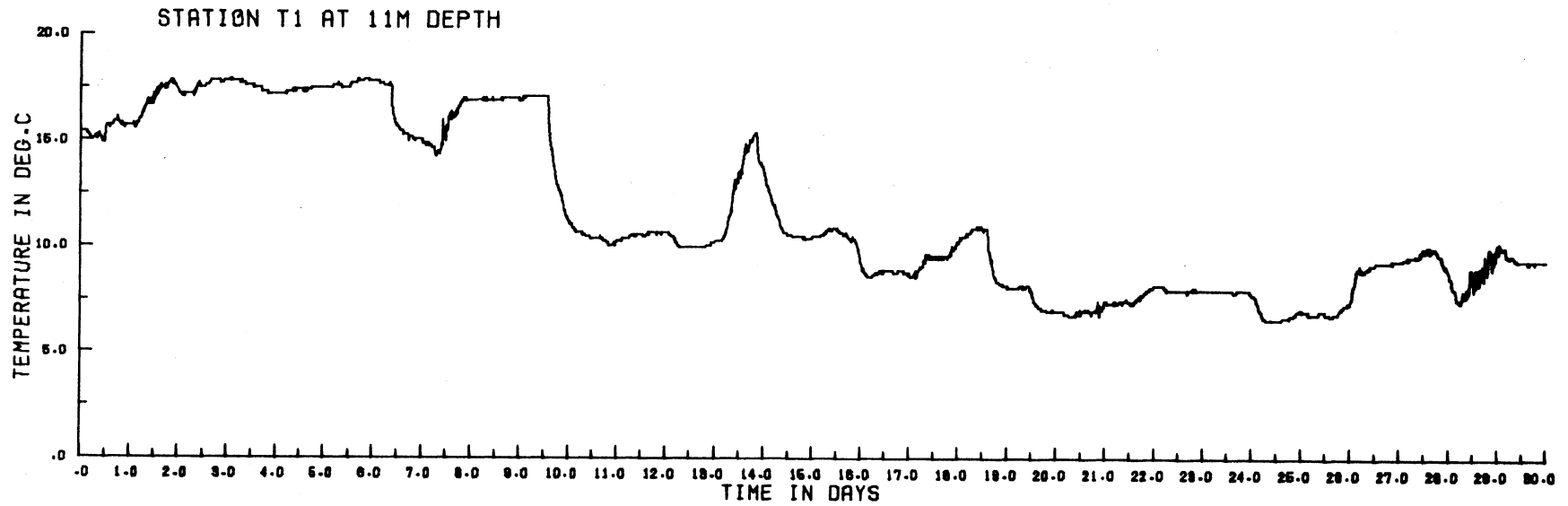
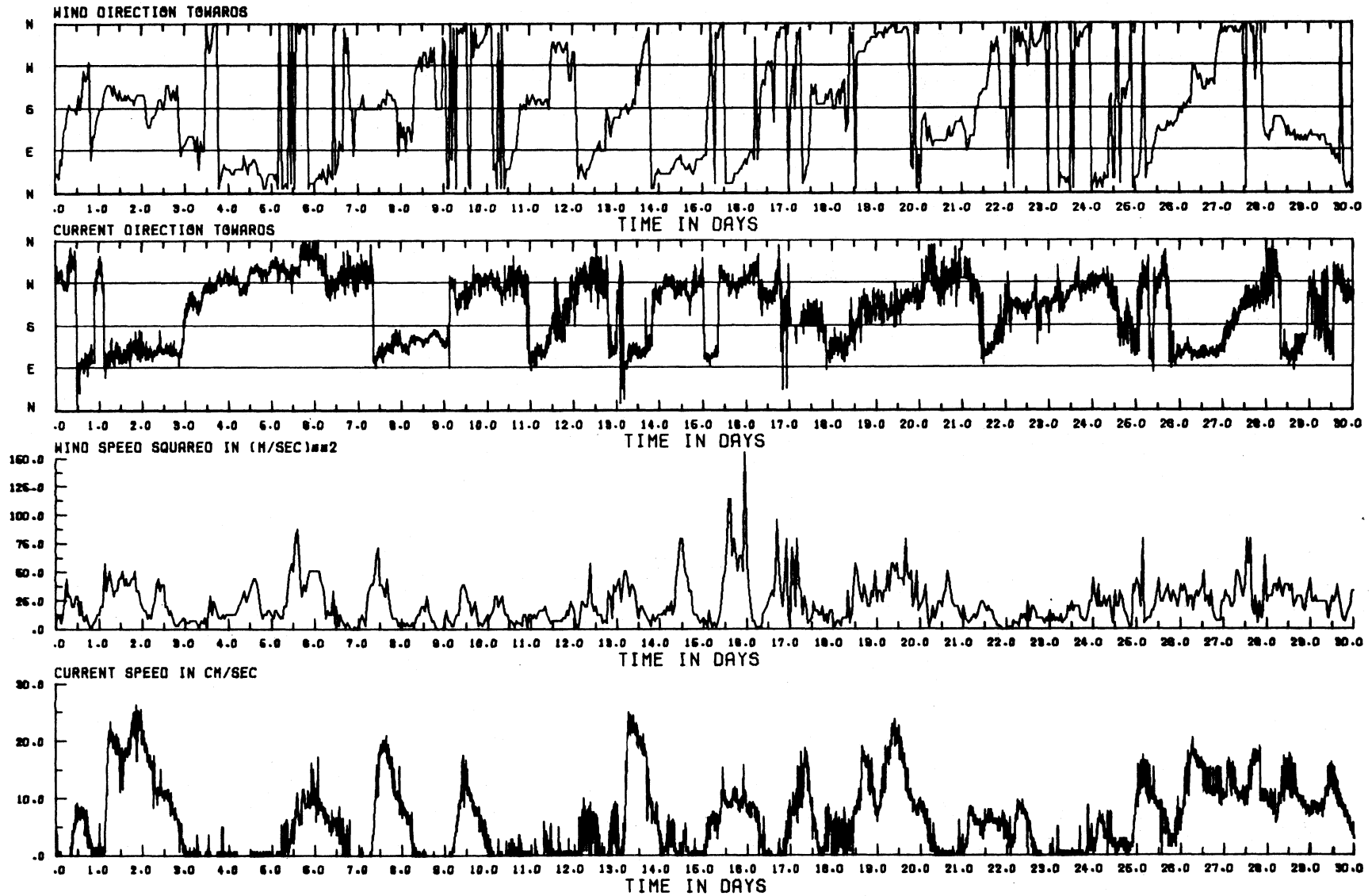


Figure 3.40

SEPTEMBER 1972: WIND (MITCHELL FIELD) COMPARED WITH STATION T1 CURRENT AT 11M DEPTH



This page is left blank to optimize the order of the following pages.

Figure 3.41

SEPTEMBER 1972: WIND (MITCHELL FIELD) COMPARED WITH STATION T2 AT 10M DEPTH

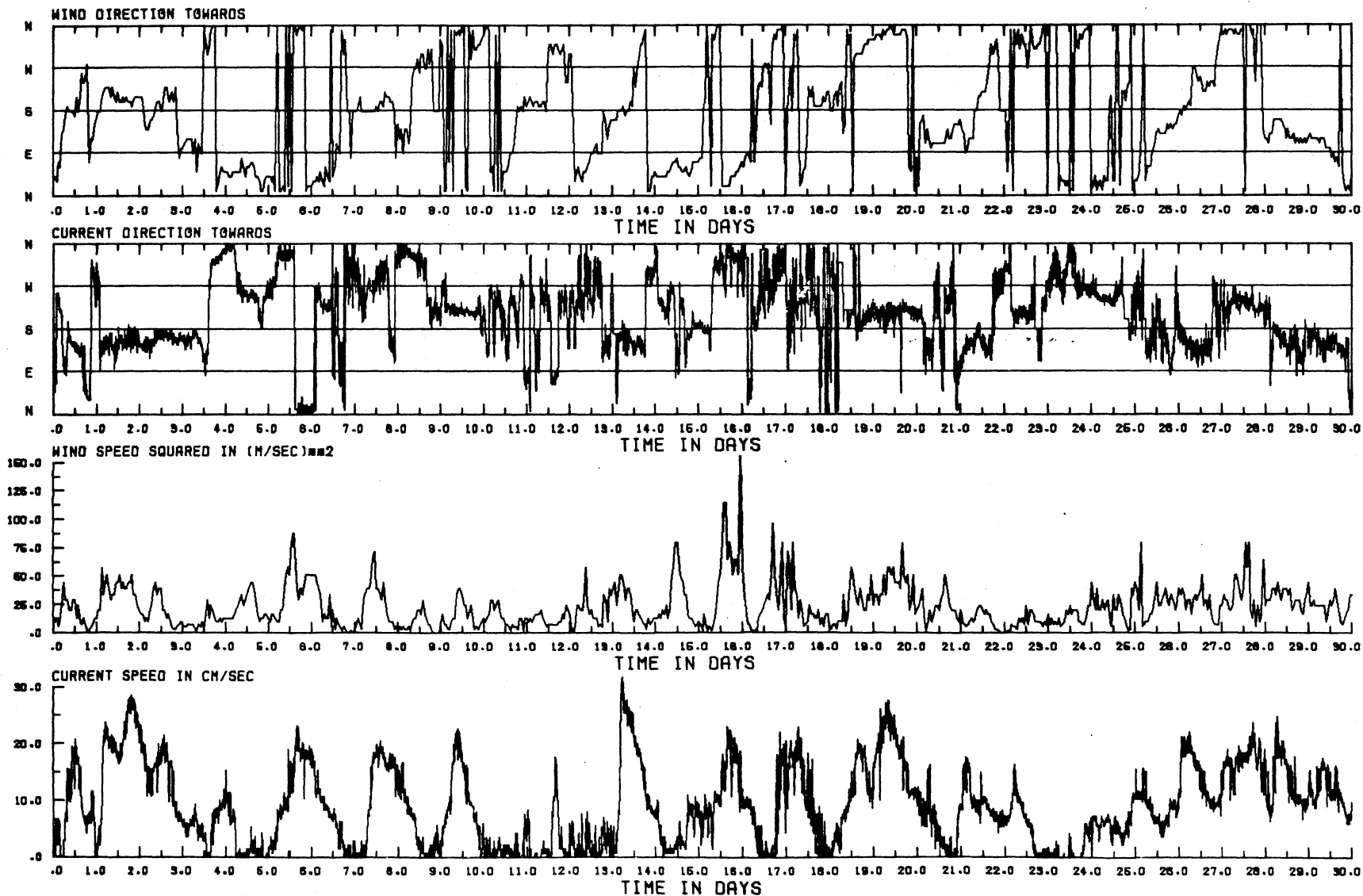


Figure 3.42

OCTOBER 1972: WATER TEMPERATURE

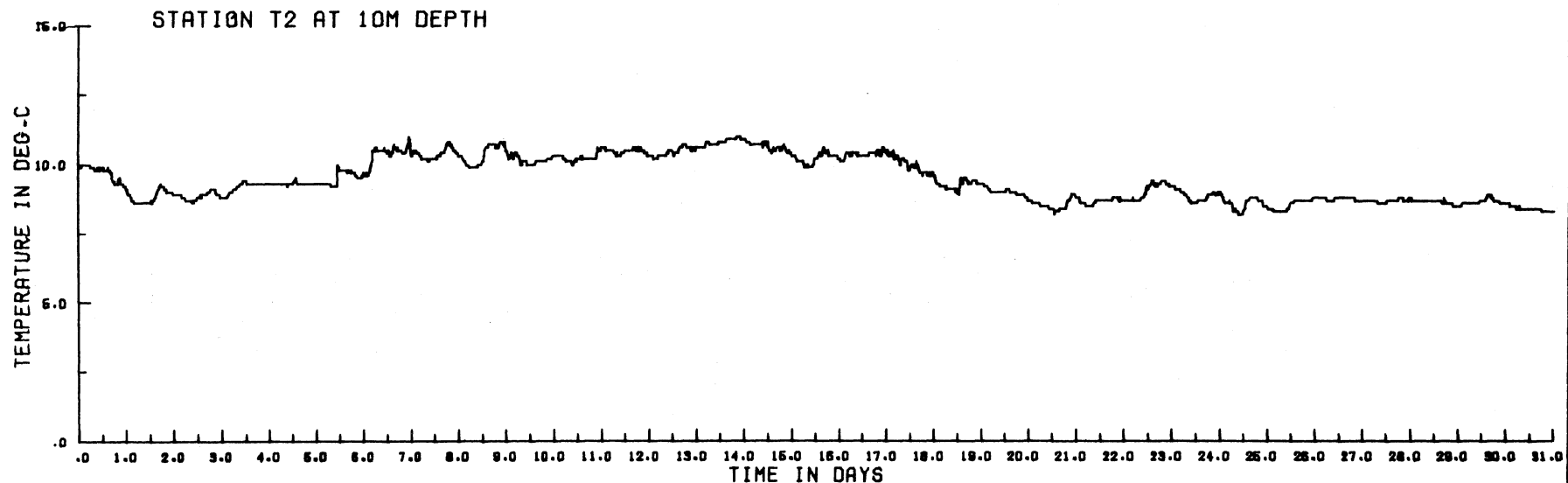
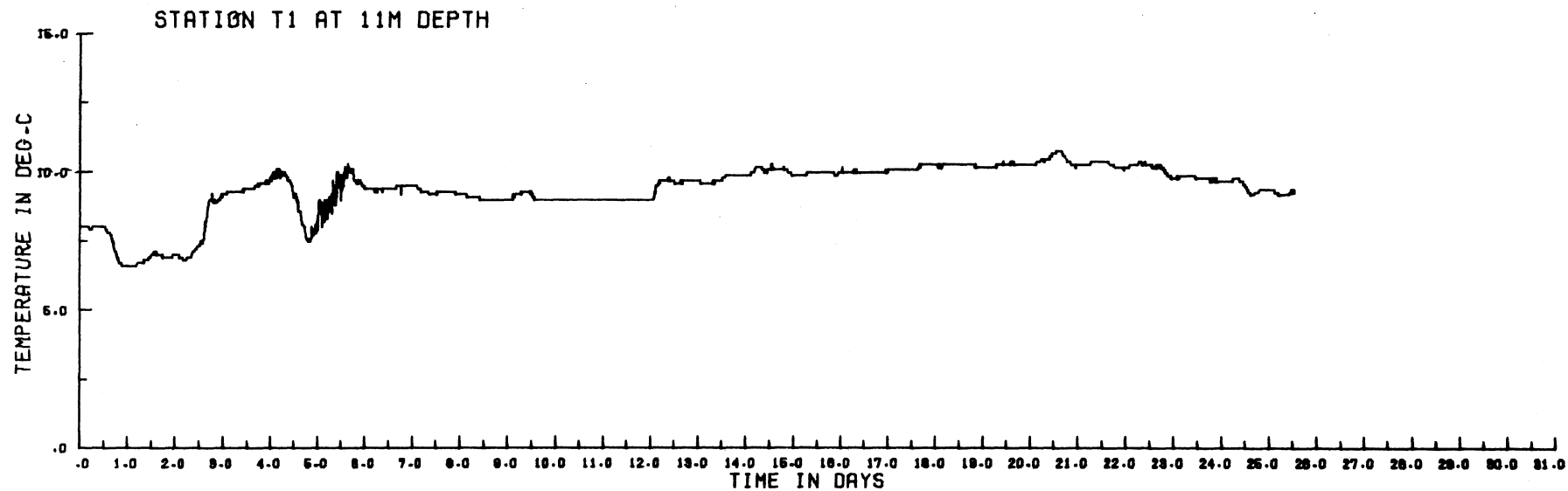
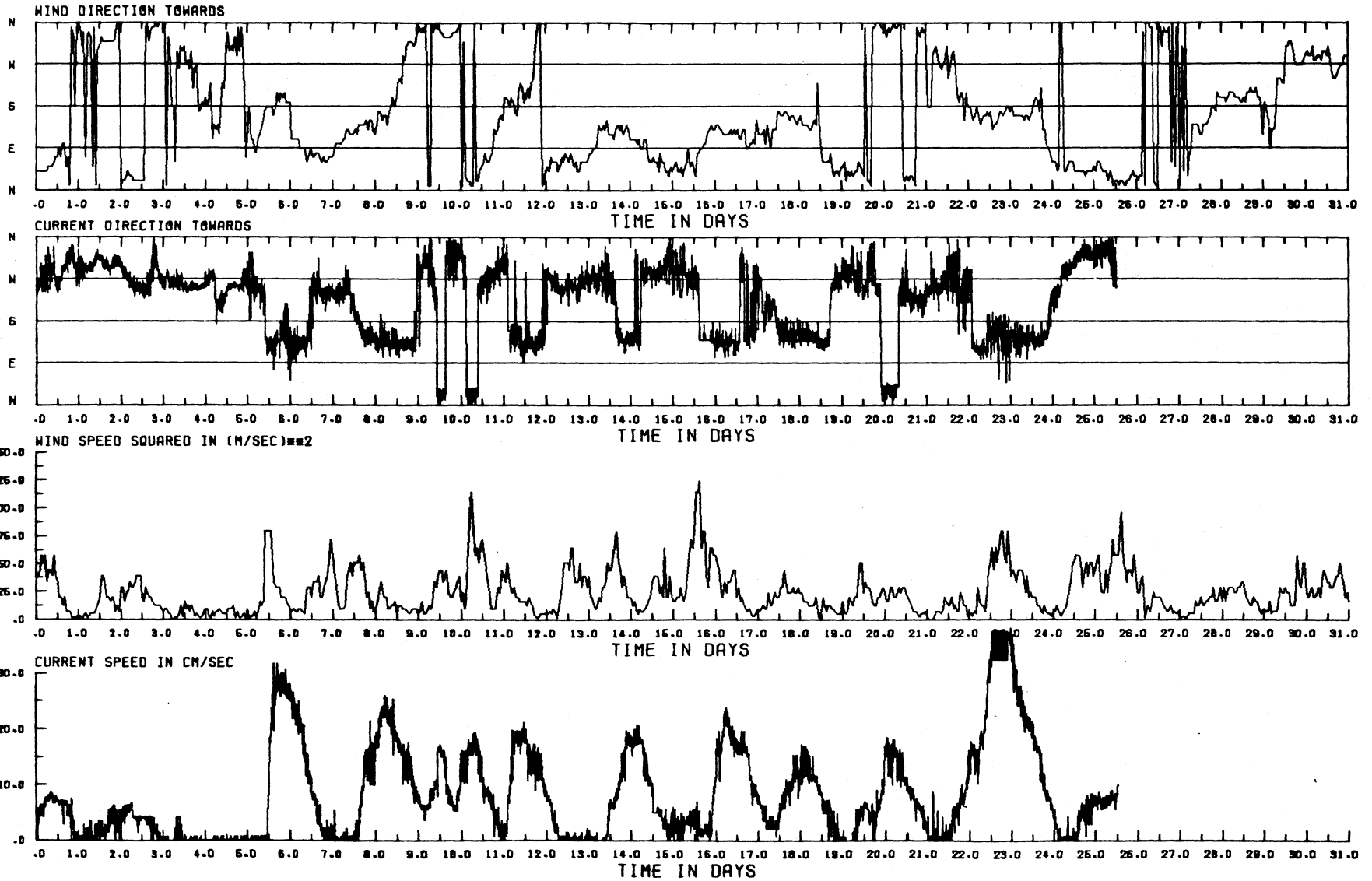


Figure 3.43

OCTOBER 1972: WIND (MITCHELL FIELD) COMPARED WITH STATION T1 CURRENT AT 11M DEPTH



Extract from Table 2.1

Station and date list for Survey IV

Survey	Station No.	Distance from shore (km)*	Water Depth (m)	Meter Depth (m)	Date Set	Date Retrieved	No. of Days of Record in Water		Comments
							Expected	Obtained	
IV	1	8.0 (8.4)	18	14	12 April 1972	17 July 1973	96	0	Faulty battery pack - no data
	2	5.3 (7.2)	18	14	12 April 1973	17 April 1972	5	0	36 sec cycle - no data
	2	5.3 (7.2)	18	15 14	17 April 1973	26 June 1973	5 73	5 0	36 sec cycle - no data
							73	71	No temperature data, hourly current speed & direction readings
	4	8.0 (10.8)	28	12 23	13 April 1973	4 June 1973	52 52	52 0	No data
	4	8.0 (10.8)	28	12 23	4 June 1973 (Prematurely released)	19 June 1973	15 15	15 0	Erratic readings No data
	5	11.0 (12.0)	28	12 23	13 April 1973 (Prematurely released)	17 July 1973	95 95	72 41	Zero speed reading Erratic direction readings
	7	15.2 (18.1)	46	13 26	13 April 1973 (Prematurely released)	4 June 1973	52 52	26 20	" " " " " "
	7	15.2 (18.1)	46	13 26	7 June 1973 (Prematurely released)	19 June 1973	15 15	15 15	Bad temp. readings Zero speed reading

\*Bracketed: distance from shore along E-W line in Fig. 2.1. Unbracketed: distance from nearest shoreline.

Figure 3.44

OCTOBER 1972: WIND (MITCHELL FIELD) COMPARED WITH STATION T2 CURRENT AT 10M DEPTH

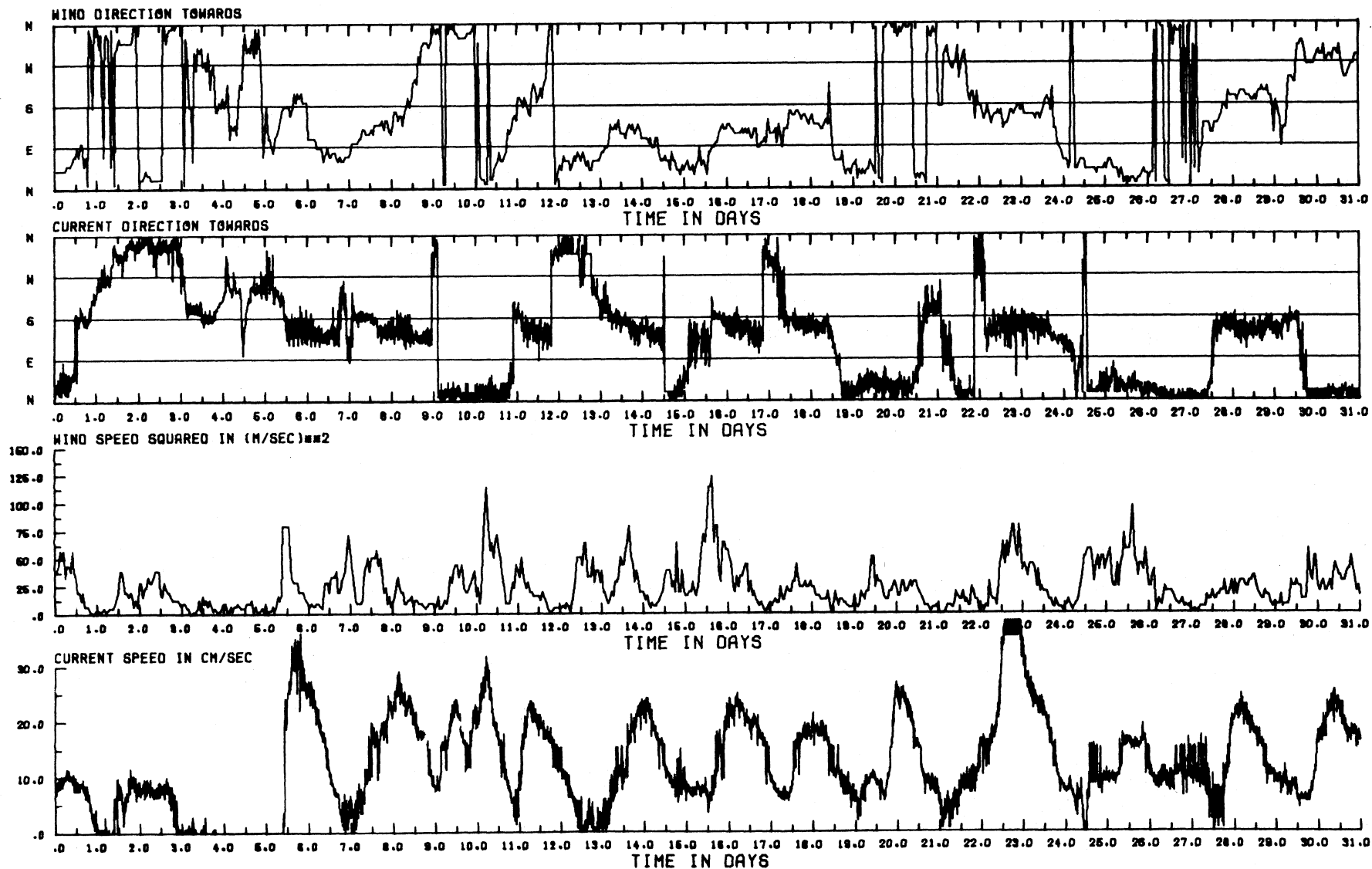


Figure 3.45

NOVEMBER 1972: WATER TEMPERATURE

STATION T2 AT 10M DEPTH

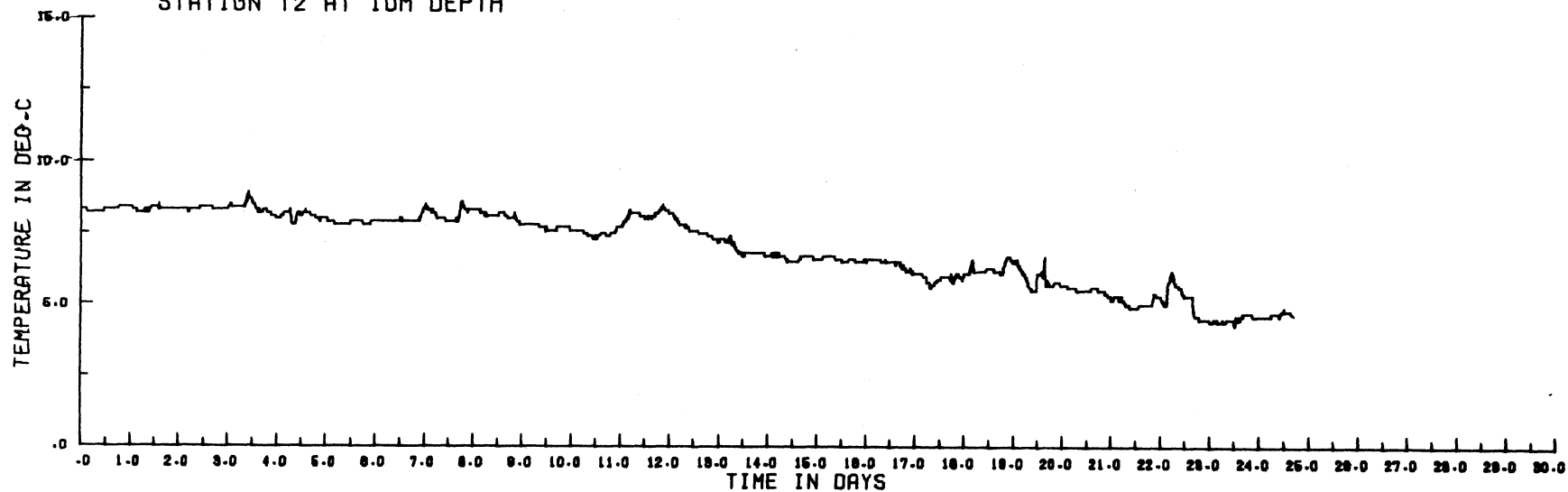
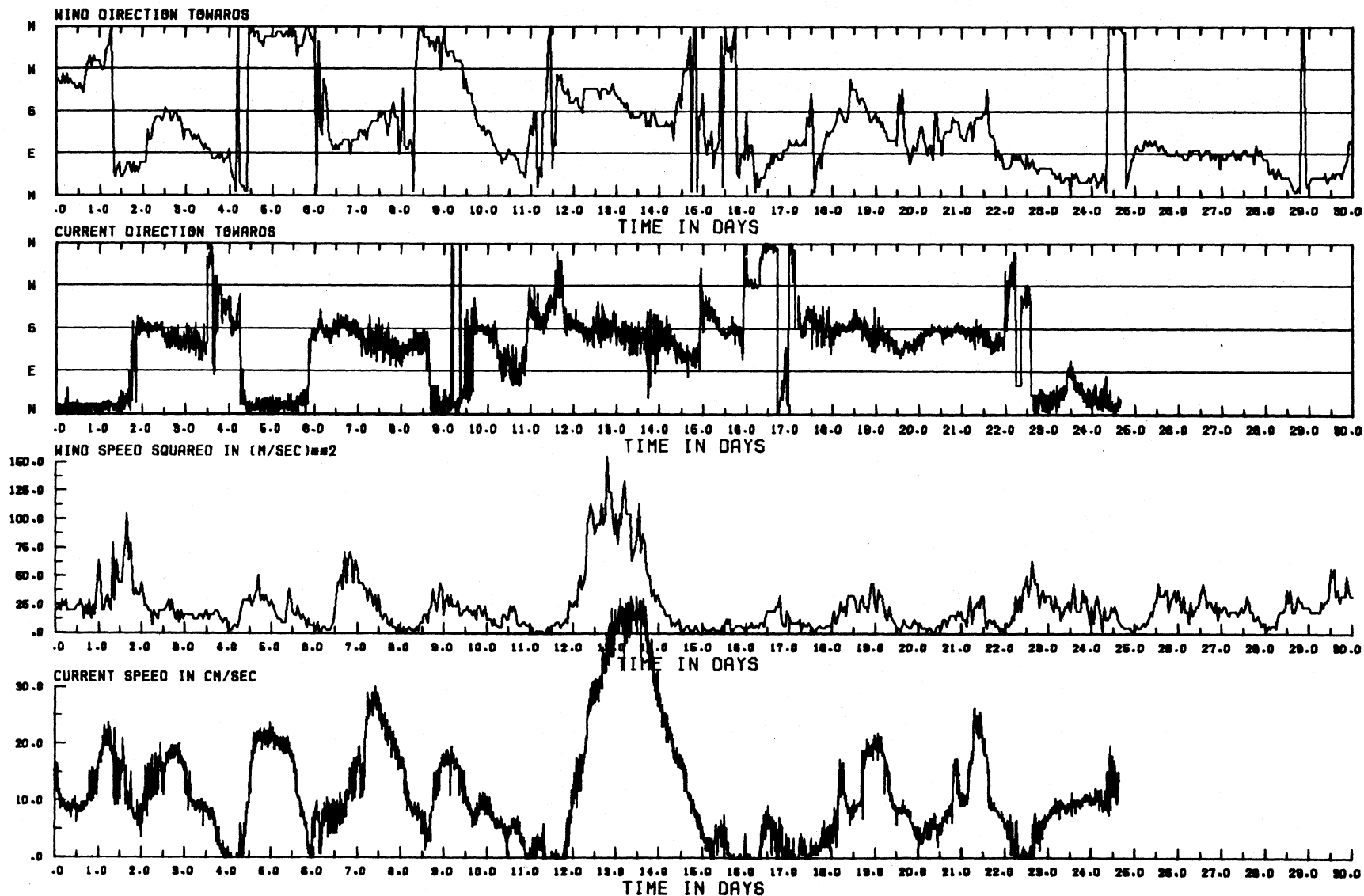


Figure 3.46

NOVEMBER 1972: WIND (MITCHELL FIELD) COMPARED WITH STATION T2 CURRENT AT 10M DEPTH



Note, for example, the relatively sluggish response of currents to the onset and decay of wind stress in the interval 12 to 15 days (fig. 3.46). In November, the main lake thermocline was at much greater depths than in summer -- in any case in much deeper water than was the  $T_2$  instrument -- so the records probably reflect a greater persistence in current pattern in a much deeper upper layer. Temperatures (fig. 3.45) ranged from  $8.5^\circ$  to  $4.5^\circ\text{C}$ . The downward trend toward the end of the month indicates the beginning of the main cooling cycle in the lake.

Survey IV. 12 April to 26 June 1973 (see extract of table 2.1 on page 116)

The history of this survey, representing an attempt to recoup some of the losses of the previous year, is summarized in the extract from Table 2.1 on p. 116. In this year also, four of the station moorings were found to have been prematurely released, one (station 7) before 4 June and the others probably by a severe thunderstorm on 16 June (see evidence of records discussed later) -- but did not drift away because tethering lines had been fitted.

During April, instruments were installed at stations 1, 2, 4, 5, and 7, but no current records were obtained from station 1, station 2, upper instrument, and station 4, lower instrument. The current speed record at station 5 (upper instrument) was defective as was also the temperature record at station 2. Since the current speed and direction readings at that station were very erratic, the digitizer was used to obtain hourly averages -- as described in the data processing section of Chapter 2 -- and this is the explanation of the relative smoothness of the plots during April and succeeding months (figs. 3.47, 3.54, and 3.60).

As in April 1972, current direction was mainly shore-parallel with no oscillatory motion evident, and current speeds were strongly correlated with wind speeds with the greatest effect again observed for southgoing winds. For example, in figure 3.51, stronger northgoing winds from 13 to 21 days produced currents which were not appreciably faster than those produced by weaker southgoing winds at the end of the month. Reversals in current direction related to wind reversals were again found, although the response was much slower at the deepest

[the text continues on page 128]

Figure 3.47

APRIL 1973: WIND (MITCHELL FIELD) COMPARED WITH STATION 2 CURRENT AT 15M DEPTH

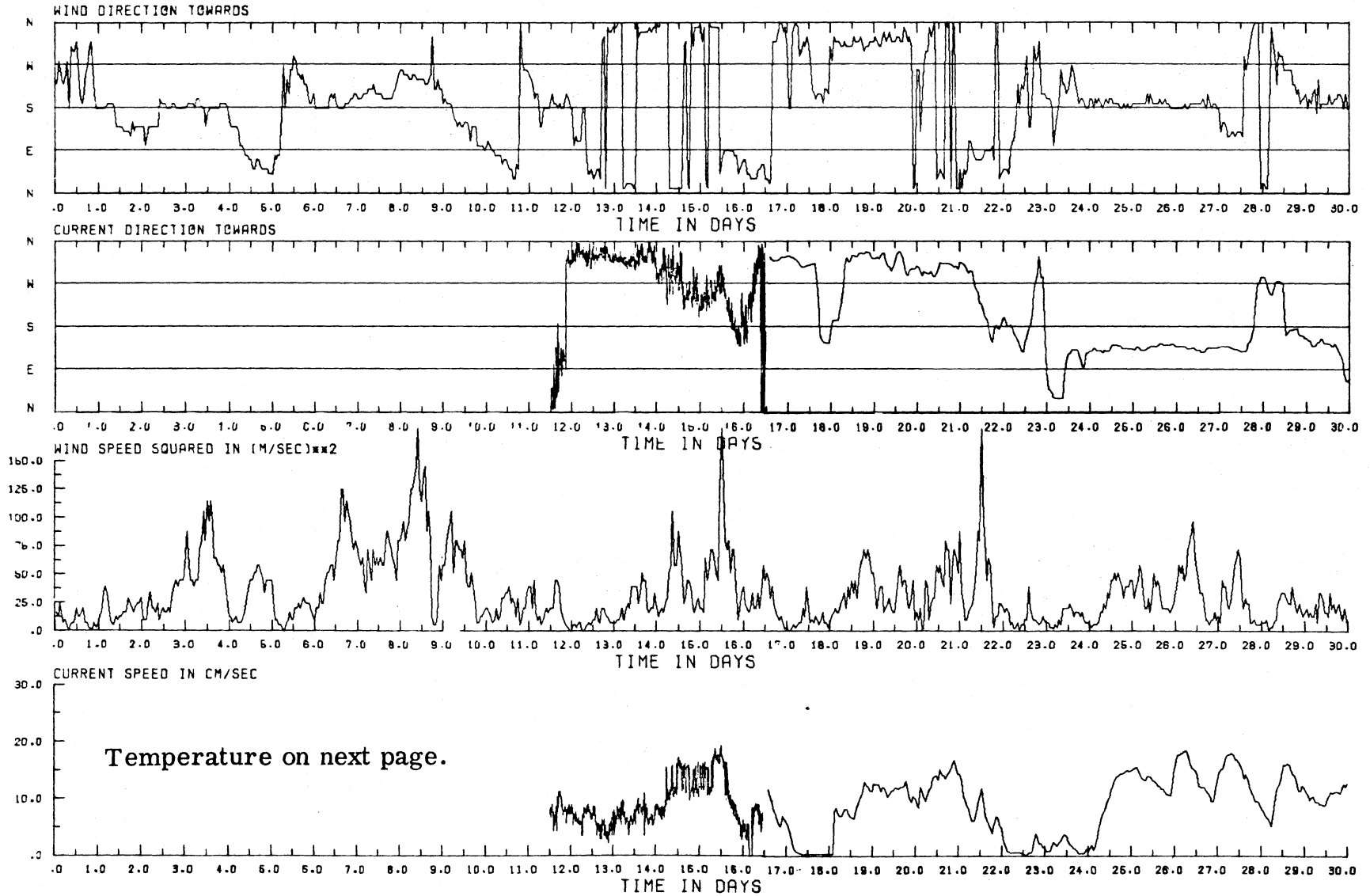


Figure 3.48

APRIL 1973: WATER TEMPERATURE

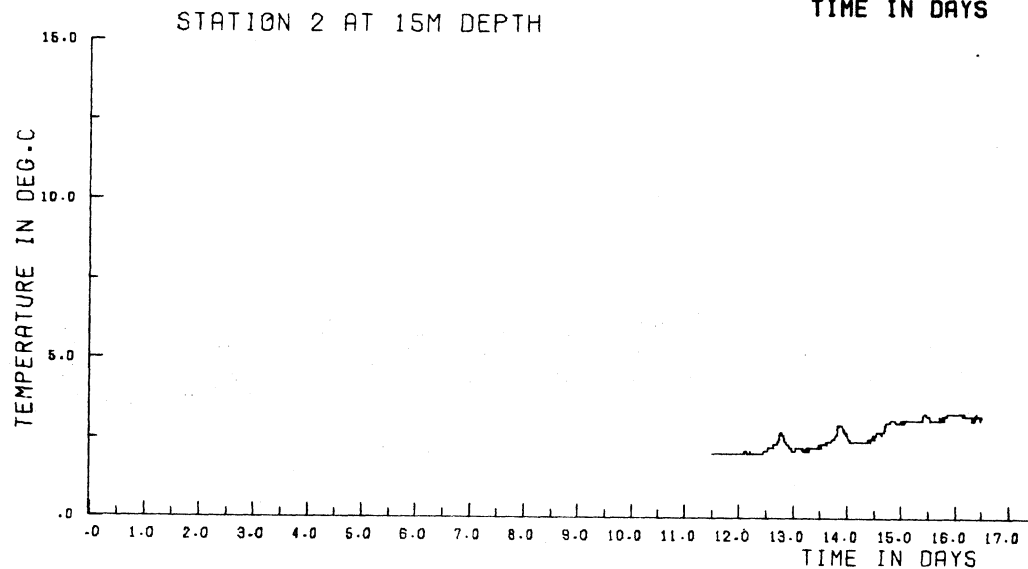
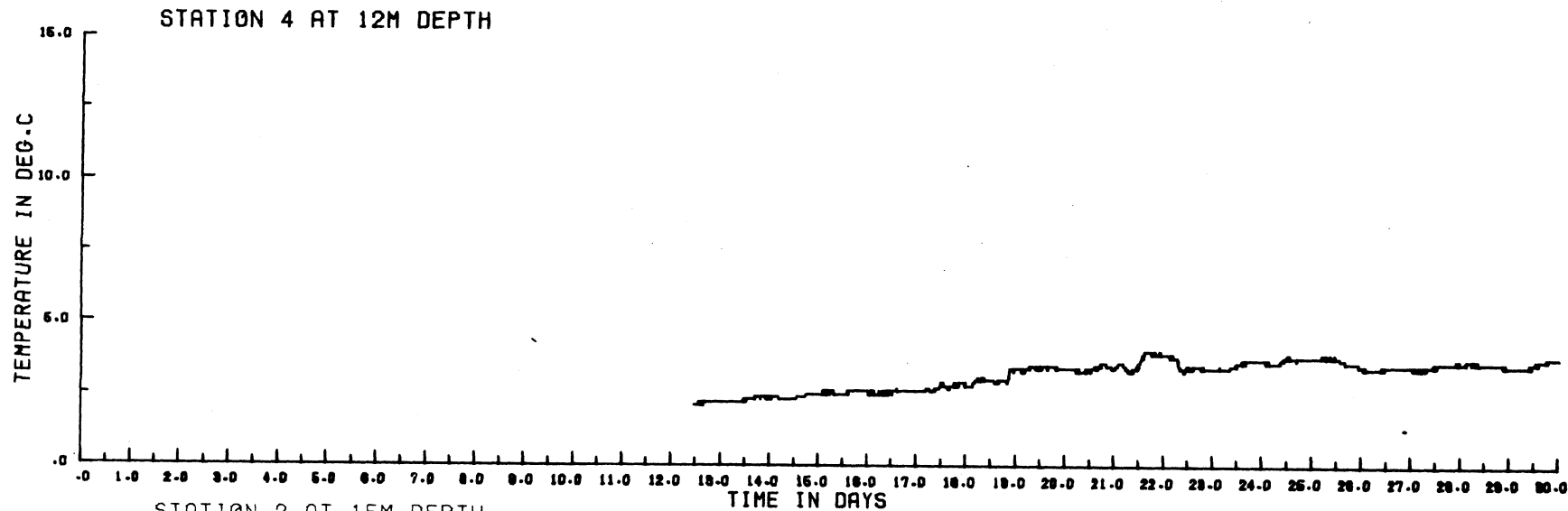


Figure 3.49

APRIL 1973: WIND (MITCHELL FIELD) COMPARED WITH STATION 4 CURRENT AT 12M DEPTH

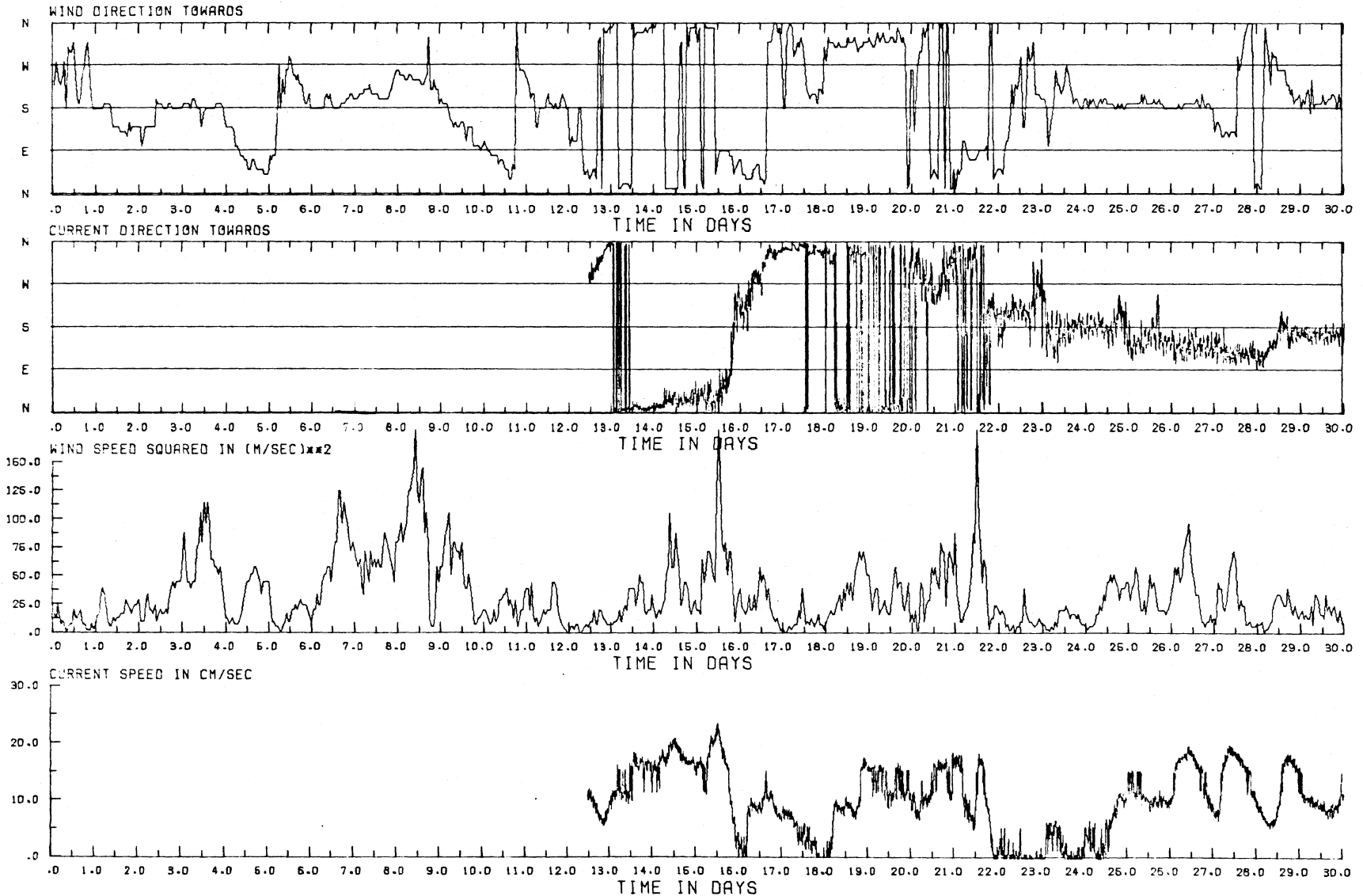


Figure 3.50

APRIL 1973: WATER TEMPERATURE

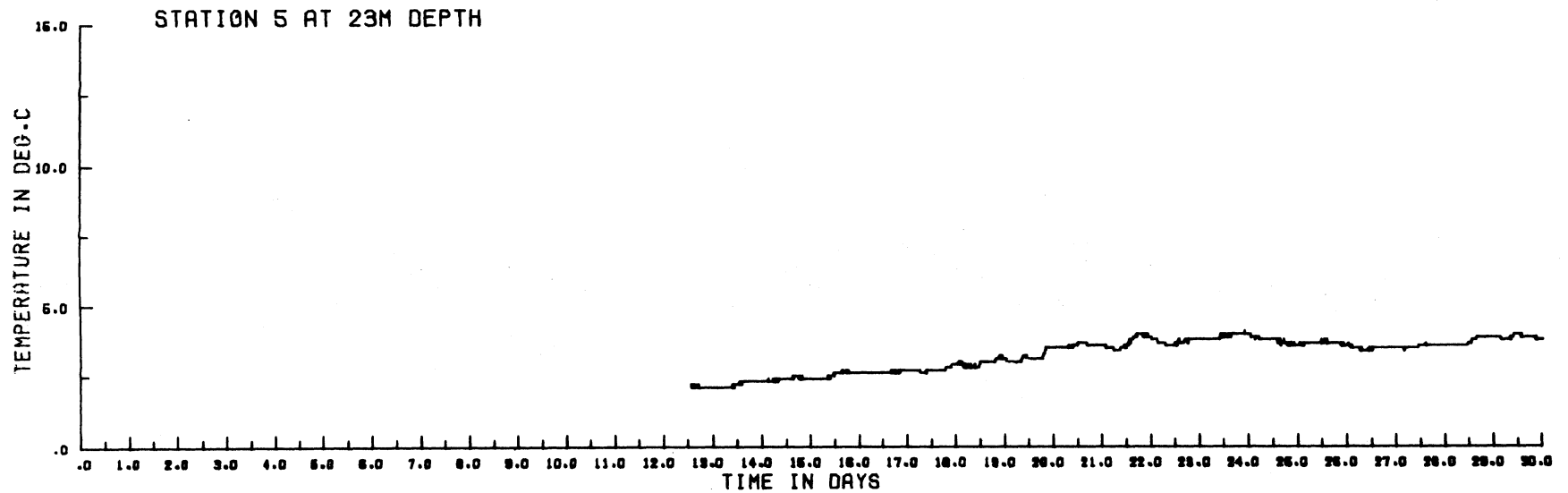
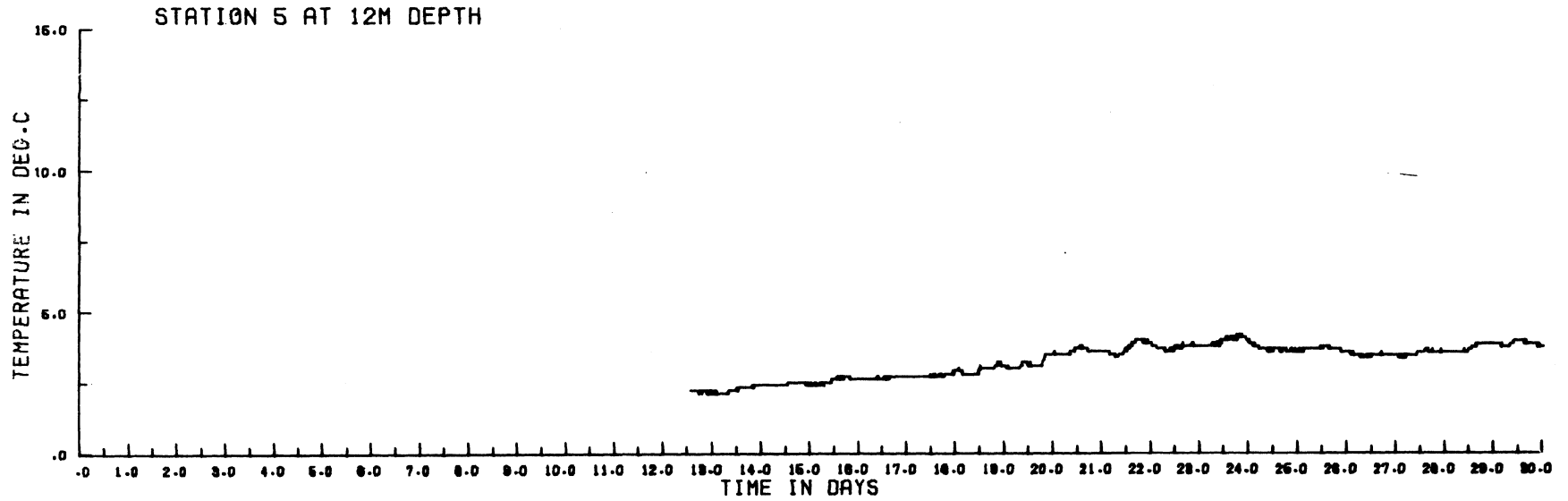


Figure 3. 51

APRIL 1973: WIND (MITCHELL FIELD) COMPARED WITH STATION 5 CURRENT AT 23M DEPTH

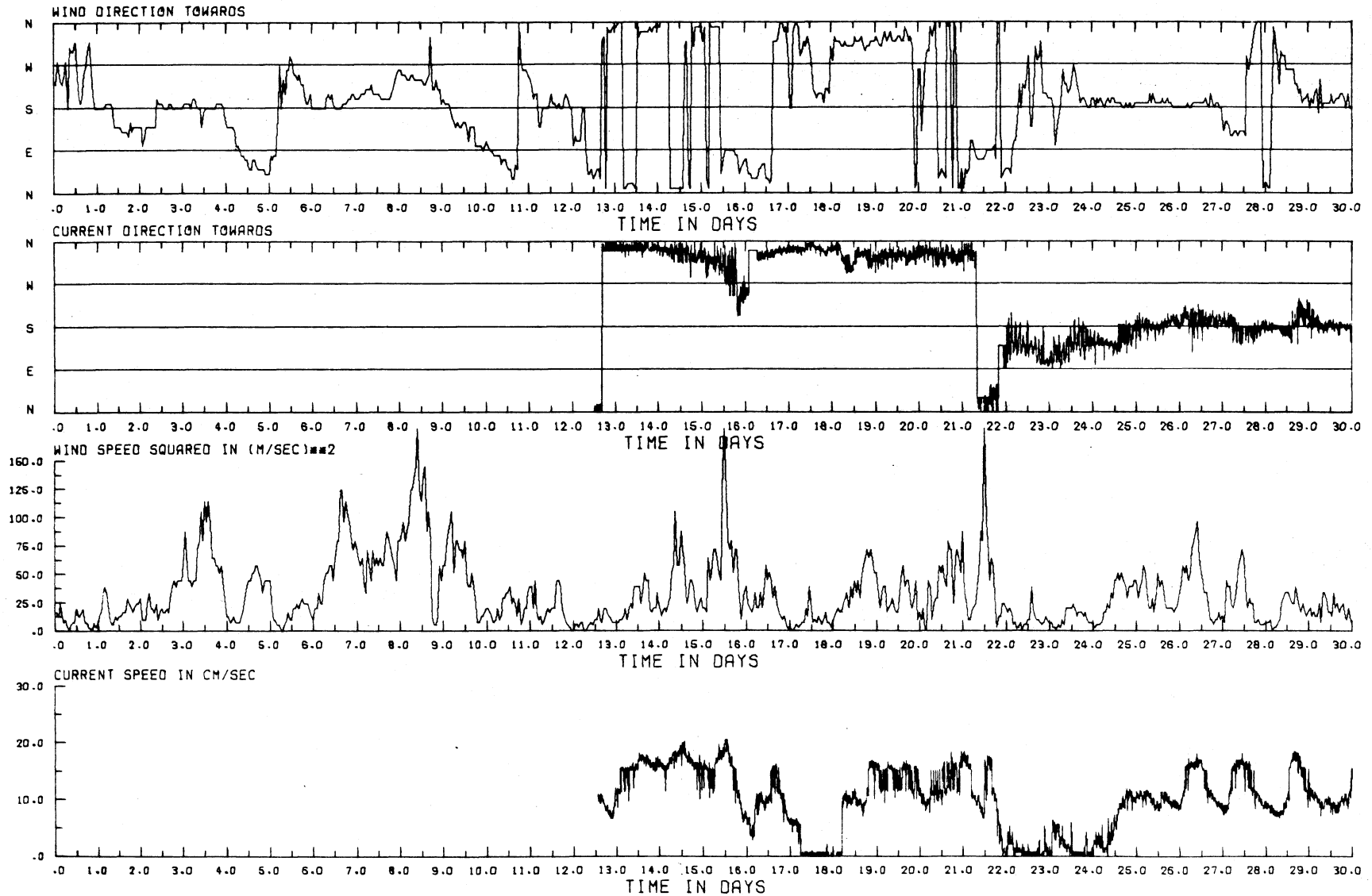


Figure 3.52

APRIL 1973: WATER TEMPERATURE

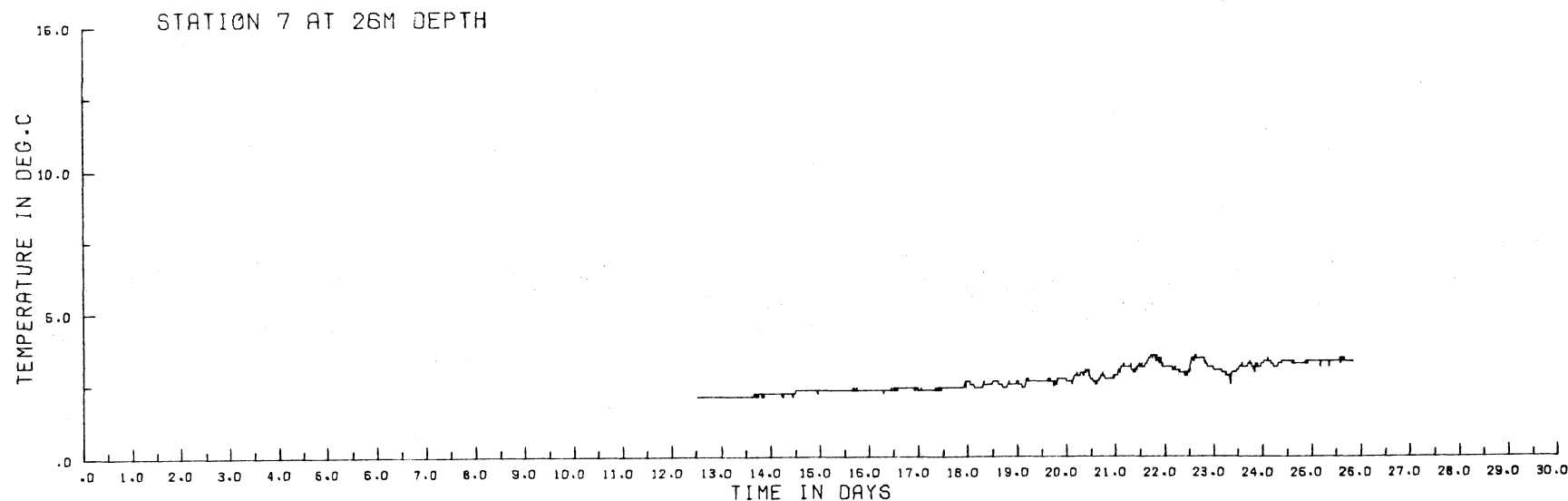
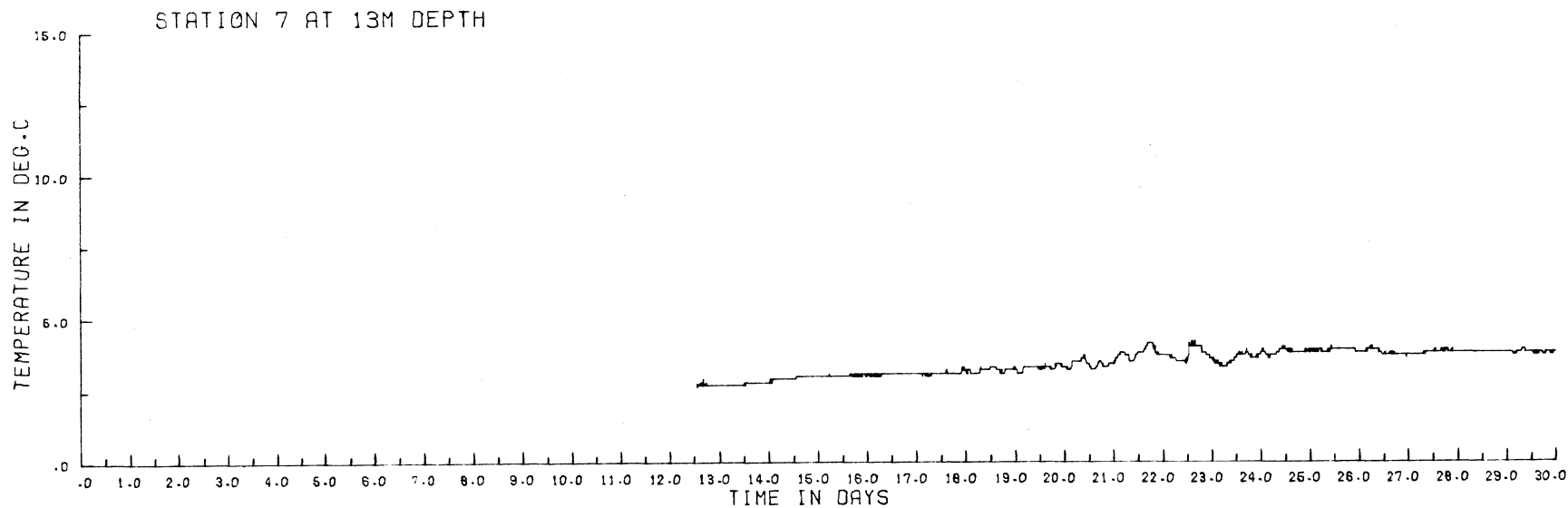
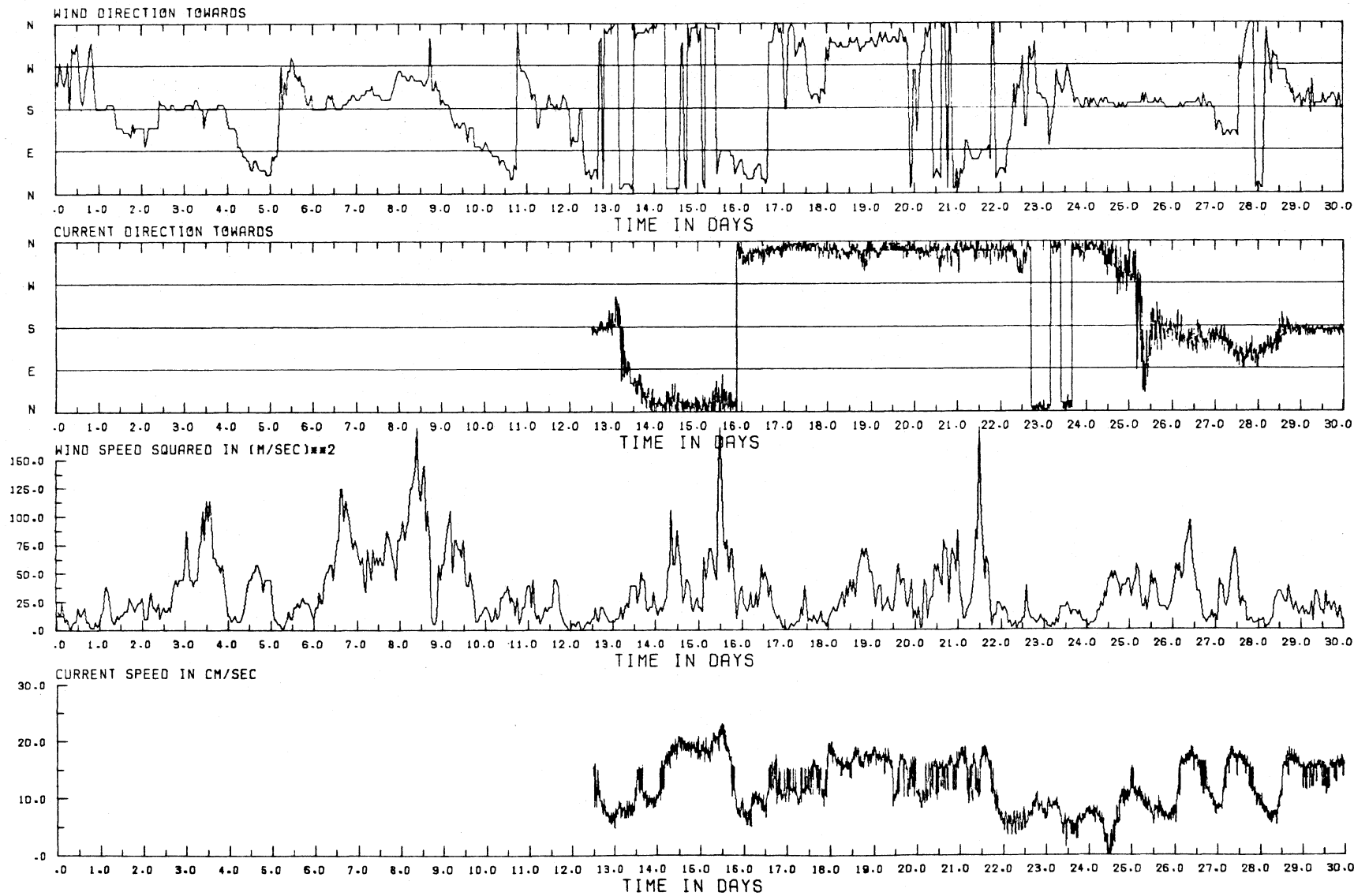


Figure 3.53

APRIL 1973: WIND (MITCHELL FIELD) COMPARED WITH STATION 7 CURRENT AT 13M DEPTH



station (7, fig. 3.53) where the northgoing current persisted for several days after the wind direction had reversed on 23.0 days, at which time the winds were weak. It was not until stronger winds appeared after 25.0 days that the current reversed, showing peaks in speed correlated with peaks in wind speed.

There were no distinct temperature patterns or events, and the record showed a general warming trend from  $2.2^{\circ}$  to  $4.1^{\circ}\text{C}$ .

During May, distinct current reversals were observed on several occasions, with lag times ranging from 3 to 34 hours. The longest lag occurred at station 4 (fig. 3.56) where a steady northgoing current persisted at about  $17 \text{ cm. s}^{-1}$  from 6.0 to 7.5 days, at which time the wind changed in direction from northwest-going to eastgoing. The current slowed down, but did not change its direction until 9.0 days. The records from stations 2 and 4 showed some shorter, quasi-periodic changes in current direction, for example from 12.5 to 14.5 and 20.0 to 22.0 days at station 2 (fig. 3.54) and from 21 to 24 days at station 4 (fig. 3.56). The periodicity and the clockwise rotation suggest the influence of inertial motion on a southgoing current, although at that time stratification had not become established, and the near-inertial motion associated with internal waves cannot be invoked as an explanation.

Except for the strong current peak associated with westgoing winds from 26.0 to 26.5 days, producing northgoing current (figs. 3.54 and 3.55), the other strong current pulses (up to  $20 \text{ cm. s}^{-1}$ ) during the month were southgoing and associated with generally southgoing winds.

Temperature fluctuations were small, showing some minor episodes of downwelling, for example at 18.0 days at station 4 (fig. 3.55) and the temperature ranged from  $4.0^{\circ}$  to  $8.2^{\circ}\text{C}$ .

During June, current speed records were only available from stations 2 and 4, and not for the whole month in either case (figs. 3.60 and 3.62). Winds were generally weak during the month with the exception of two brief pulses, one of northeast-going winds peaking at 7.7 days (associated with a northwest-going current at station 2) and a northgoing wind pulse at 15.8 days. The high current speeds shown during and after that pulse at station 4 must be discounted, because when recovered the instrument was found to have been prematurely released,

[the text continues on page 136]

Figure 3. 54

MAY 1973: WIND (MITCHELL FIELD) COMPARED WITH STATION 2 CURRENT AT 15M DEPTH

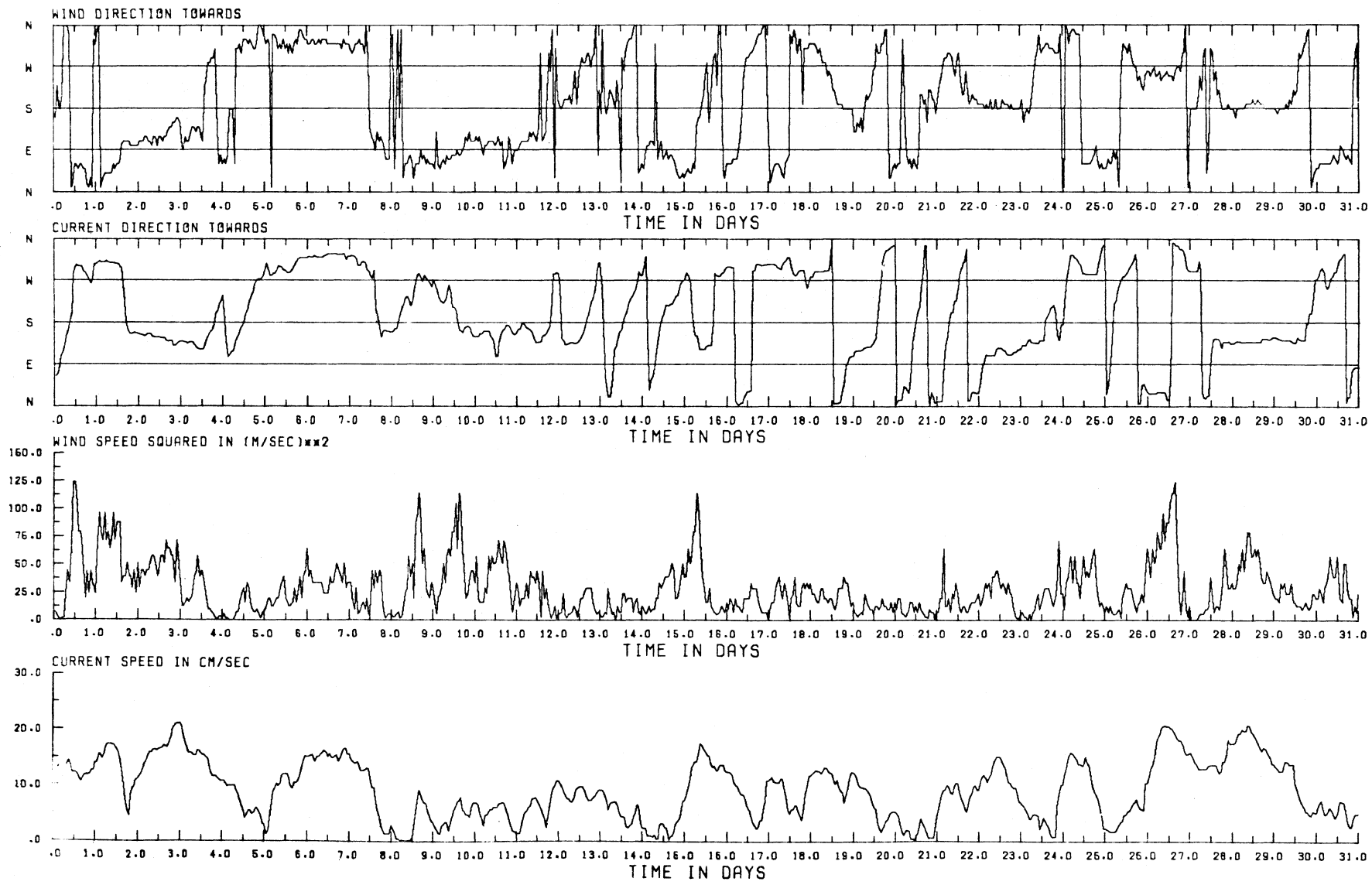


Figure 3.55

MAY 1973: WATER TEMPERATURE

STATION 4 AT 12M DEPTH

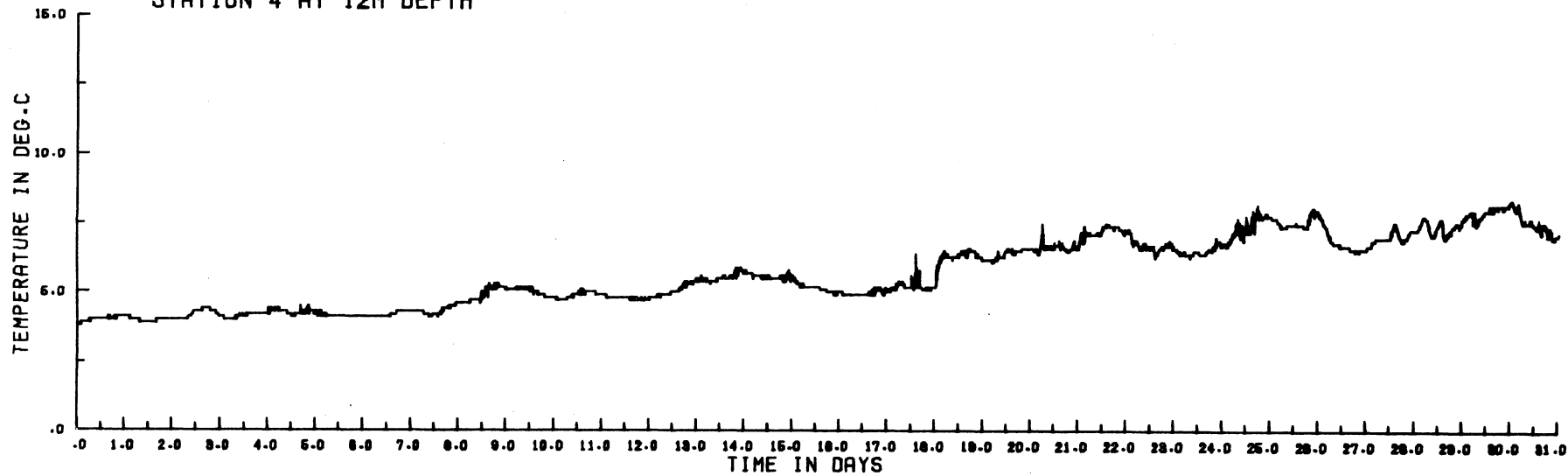


Figure 3.56

MAY 1973: WIND (MITCHELL FIELD) COMPARED WITH STATION 4 CURRENT AT 12M DEPTH

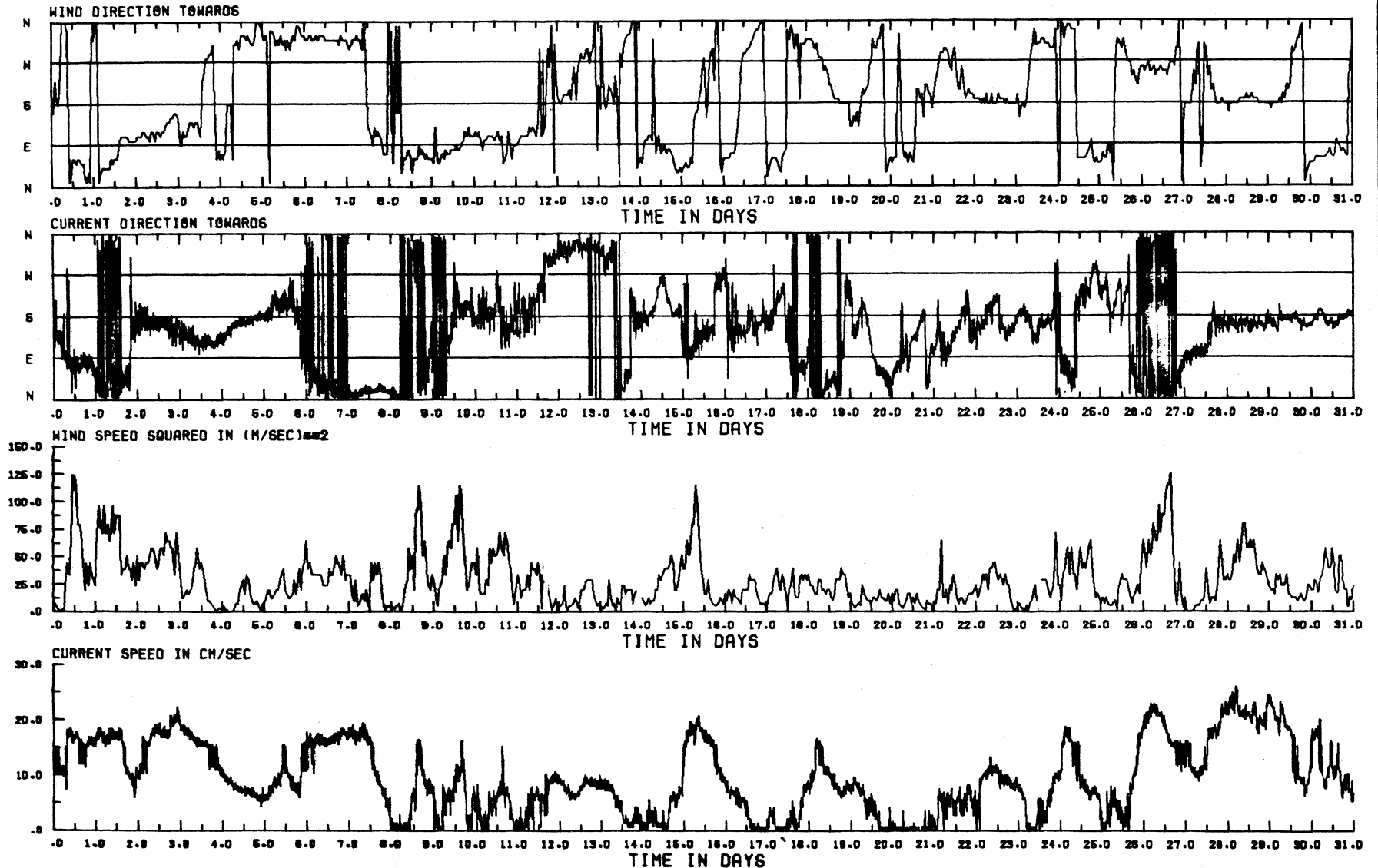
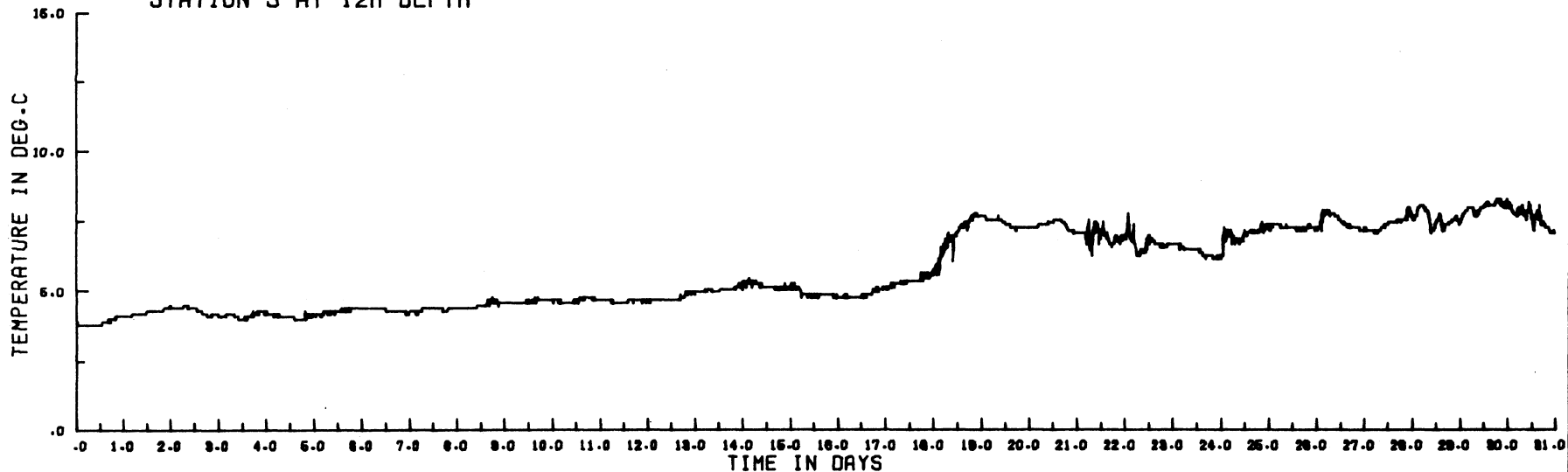


Figure 3.57

MAY 1973: WATER TEMPERATURE

STATION 5 AT 12M DEPTH



STATION 5 AT 23M DEPTH

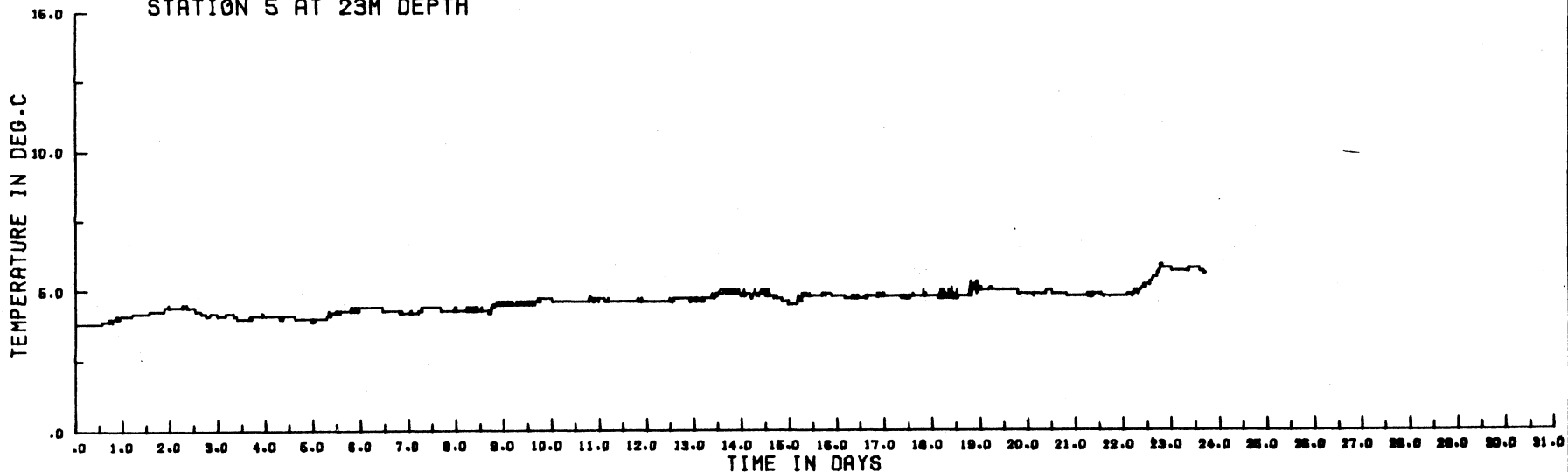


Figure 3.58

MAY 1973: WIND (MITCHELL FIELD) COMPARED WITH STATION 5 CURRENT AT 23M DEPTH

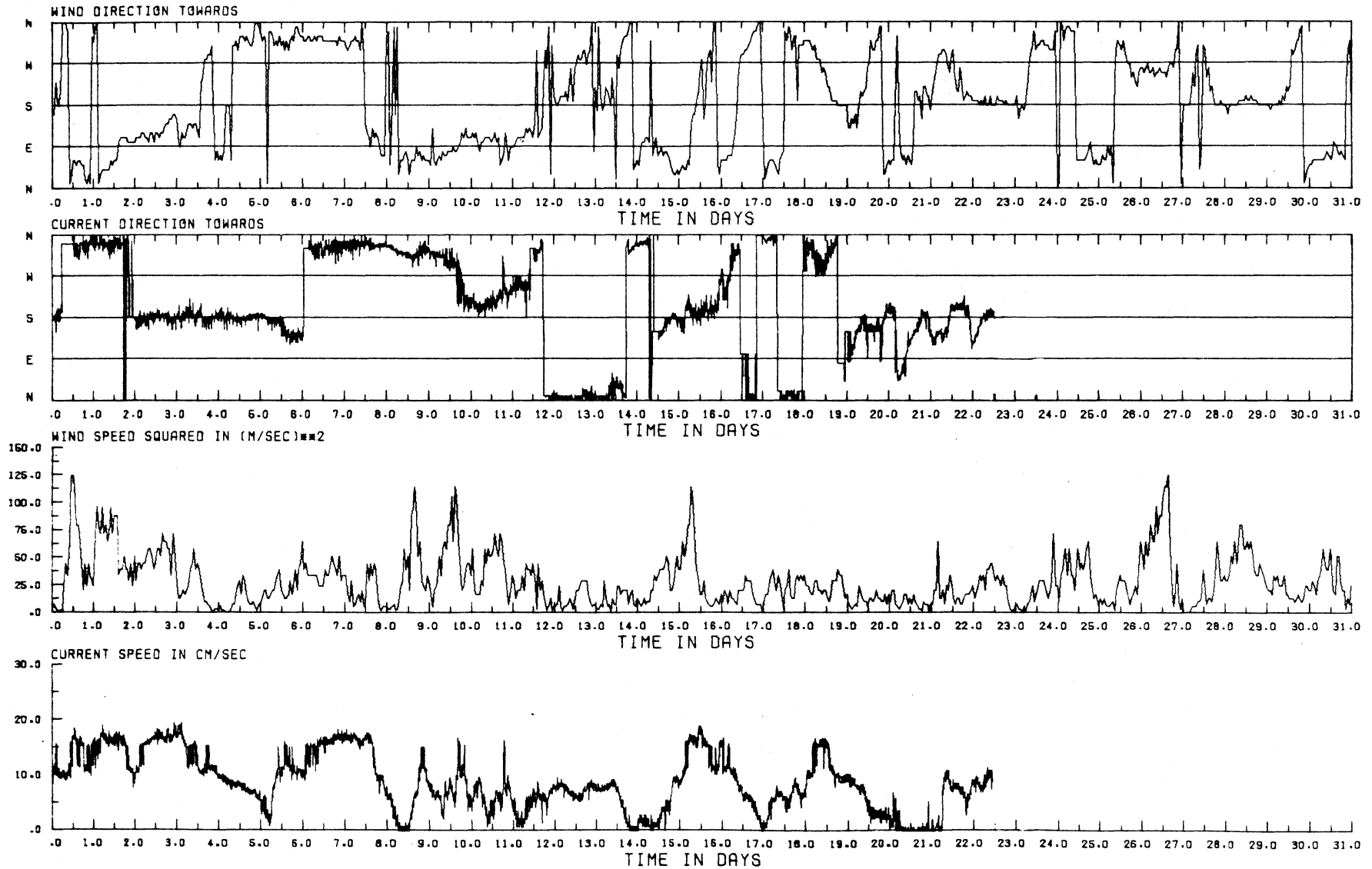
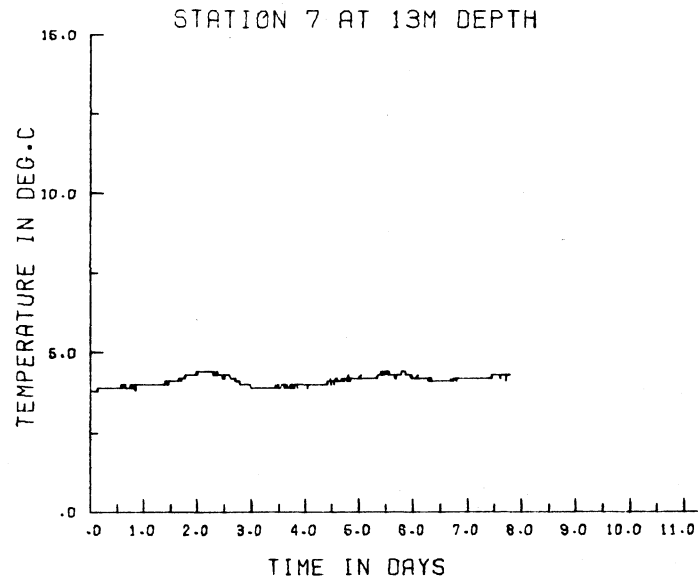


Figure 3.59

MAY 1973: WATER TEMPERATURE



MAY 1973: WIND (MITCHELL FIELD)

COMPARED WITH STATION 7 CURRENT AT 13M DEPTH

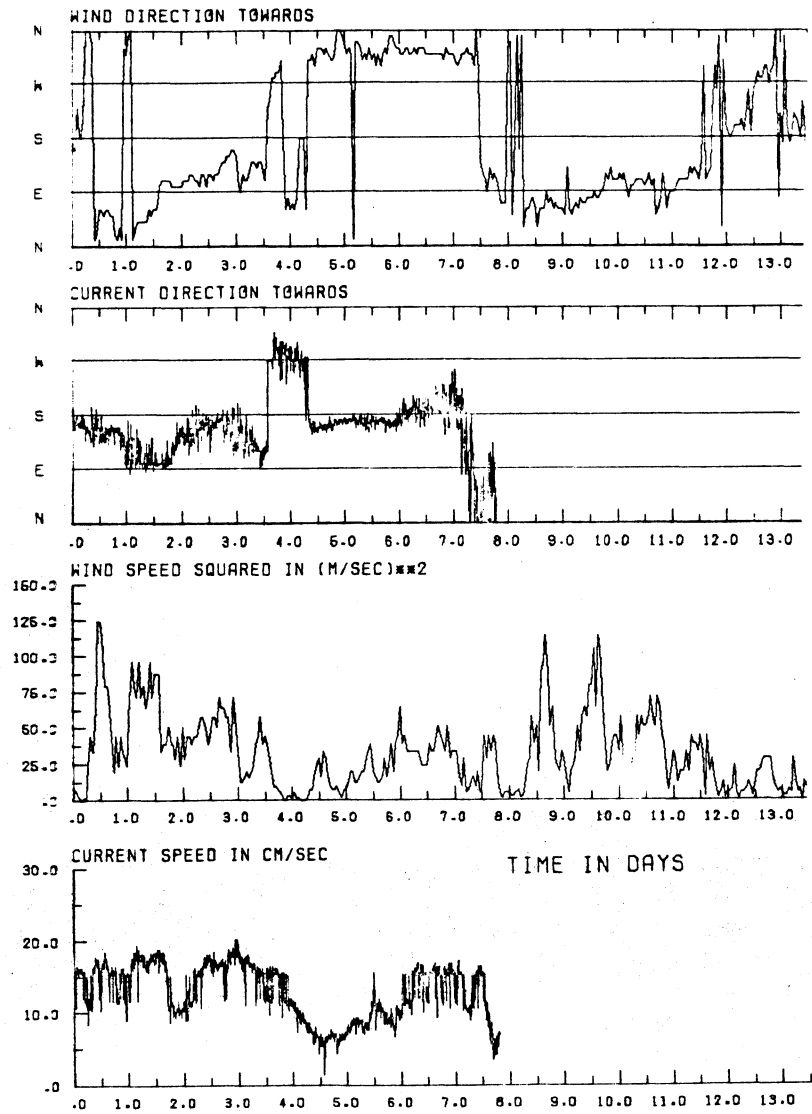
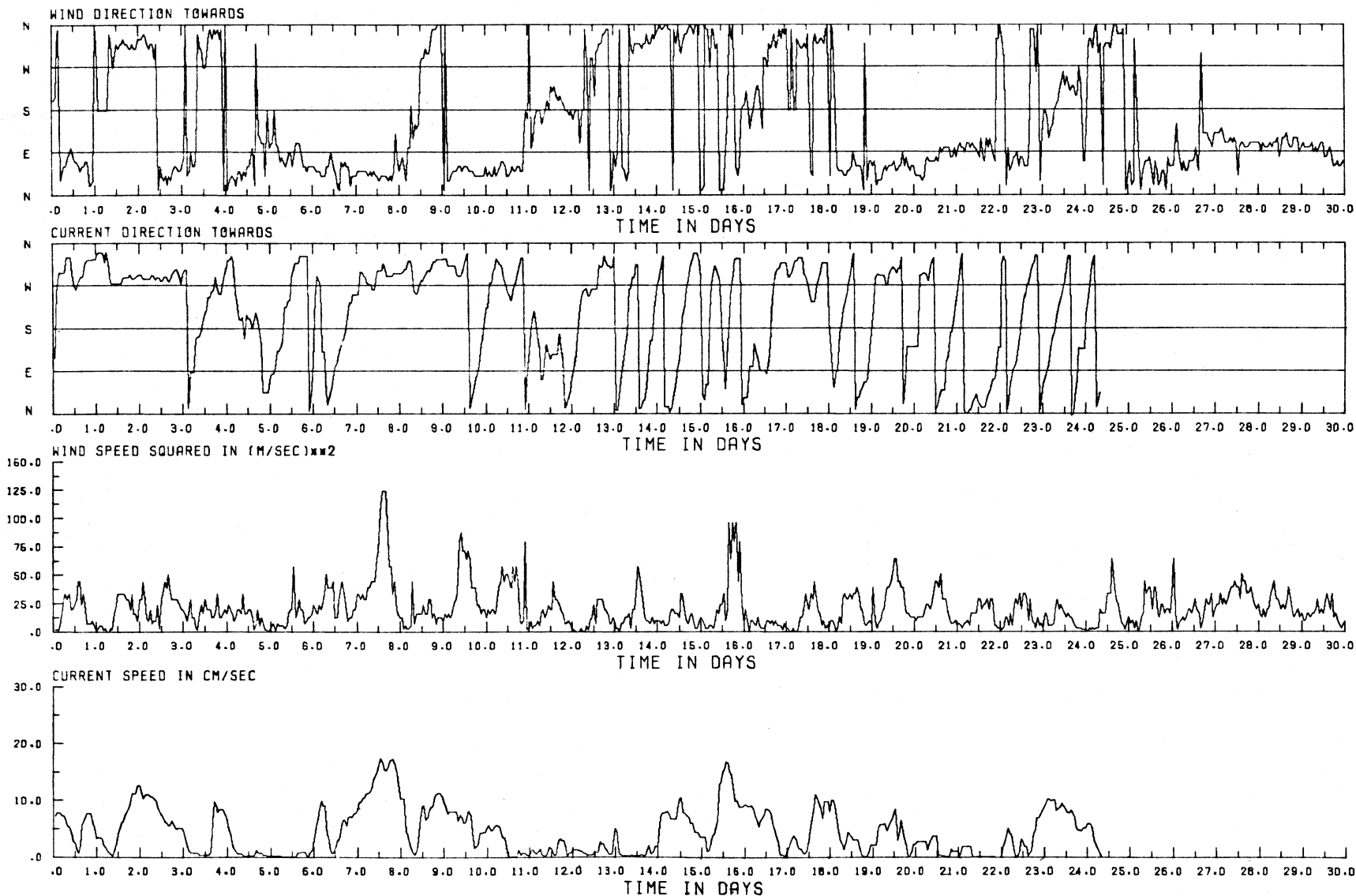


Figure 3.60

JUNE 1973: WIND (MITCHELL FIELD) COMPARED WITH STATION 2 CURRENT AT 15M DEPTH



probably at about 15.5 days. In general associated with the weaker winds, strong persistent southerly currents were not observed during June, in fact, the predominant current direction was northwesterly in response to generally northgoing winds.

The striking feature of the current pattern during the middle third of the month was a very regular near-inertial motion shown clearly in the temperature records at station 5 (fig. 3.61) and in the current direction record at station 7 (figs. 3.63, 3.64). The 18 regular rotations in direction at station 7 correspond to a period of close to 17 hours, clear evidence of the presence of internal Poincaré-type waves.

It is not clear from the station 5 and 7 records when the instruments were prematurely released, but apparent disturbances on the figure 4 record (fig. 3.62) suggests 15.8 days as the most probable time. There were severe thunderstorms on that day. If, however, the instruments were released earlier, the recordings after release relate to depths about 9 m higher than originally set.

Survey V. 17 July to 13 August 1973.

Survey VI. 15 August to 7 November 1973. (see table opposite)

During Survey V, instruments were placed at 14 and 15 m at stations 1 and 2 (to test coherence) at 12 and 23 m at stations 4 and 5 and at 13 and 26 m at station 6. The data from stations 1, 2, 4, and 5 were plotted from the 10-minute values, while the "erratic" data from station 6 was smoothed to hourly averages, using a digitizer. Although station 2 recorded current directions only, these were plotted for comparison with directions at other stations.

Both the temperature records and the current records showed strong influence of near-inertial rotary motions, conspicuous at station 1 during July (figs. 3.65 and 3.66) and at station 4 in August (figs. 3.72 and 3.73) up to the premature release of that instrument probably at about 19.5 days in August. Both the station 4 and station 5 instruments (fig. 3.68) show a meandering south-going current during a downwelling spell (21 to 24 days, fig. 3.67), with weak westward and northwestward winds at the time. A change to northeastward winds at 24.2 days was followed by strong rotary currents at station 5, but with

[the text continues on page 148 ]

Survey	Station No.	Distance from shore (km)*	Water Depth (m)	Meter Depth (m)	Date Set	Date Retrieved	No. of Days of Record in Water		Comments
							Expected	Obtained	
V	1	8.0 (8.4)	18	14	17 July 1973	8 August 1973	22	5	36 sec cycle
				15			22	22	
	2	5.3 (7.2)	18	14	19 July 1973	8 August 1973	20		Zero speed readings Unrecoverable parity errors
				15			20	20	
	4	8.0 (10.8)	28	12	18 July 1973 (Prematurely released)	4 September 1973	20	20	Erratic readings Unrecoverable parity errors
				23			20	0	
5	11.0 (12.0)	28	12	17 July 1973	13 August 1973	27	0	Unrecoverable parity errors	
			23			27	27		
6	12.8 (16.3)	46	13	18 July 1973	13 August 1973	26	21	Erratic direction readings Erratic readings - bad temp. readings	
			26			26	26		
VI	1	8.0 (8.4)	18	14	15 August 1973	7 November 1973	84		Zero speed No data
				15			84		
	5	11.0 (12.0)	28	12	16 August 1973	19 September 1973	34	34	Erratic readings - bad temp. readings
				23			34	34	
	6	12.8 (16.3)	46	13	15 August 1973 (Prematurely released)	29 August 1973	14	14	Zero speed readings Erratic readings
				26			14	0	

\*Bracketed: distance from shore along E-W line in Fig. 2.1. Unbracketed: distance from nearest shoreline.

Figure 3.61

JUNE 1973: WATER TEMPERATURE

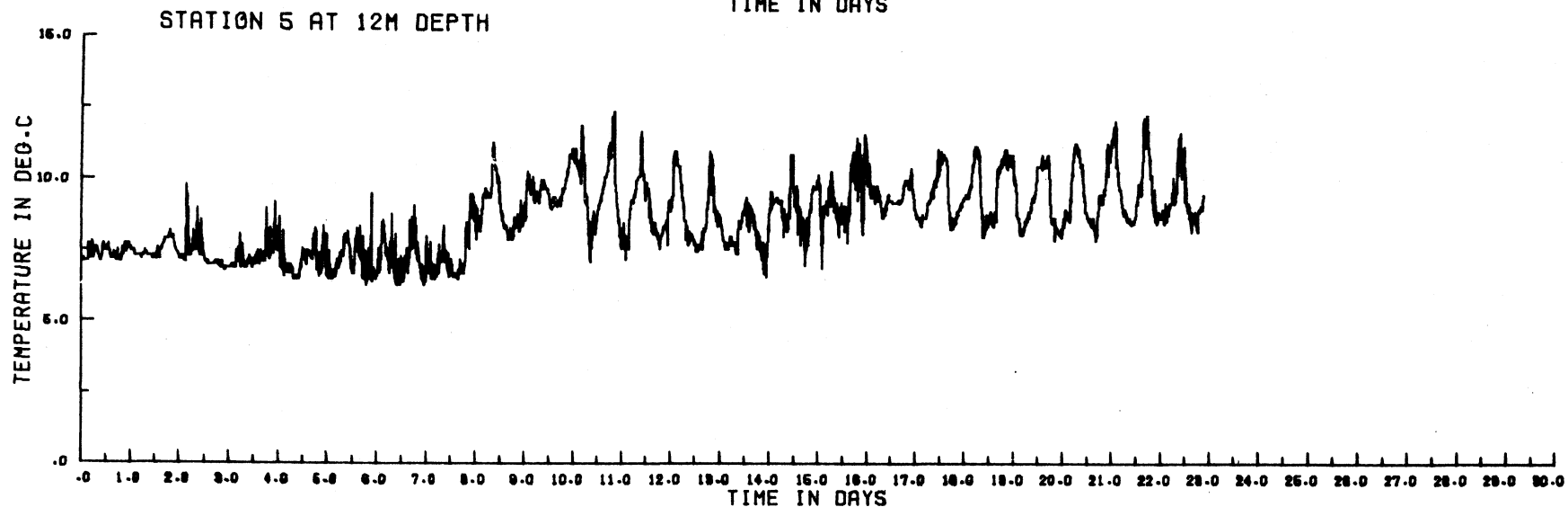
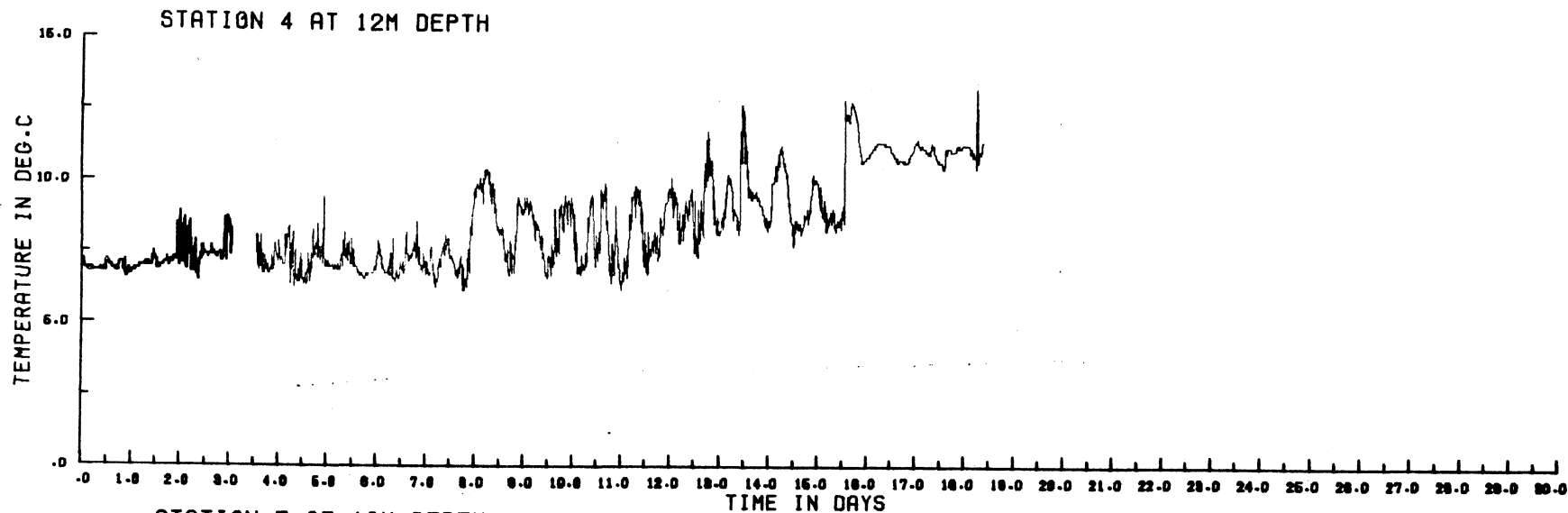


Figure 3.62

JUNE 1973: WIND (MITCHELL FIELD) COMPARED WITH STATION 4 CURRENT AT 12M DEPTH

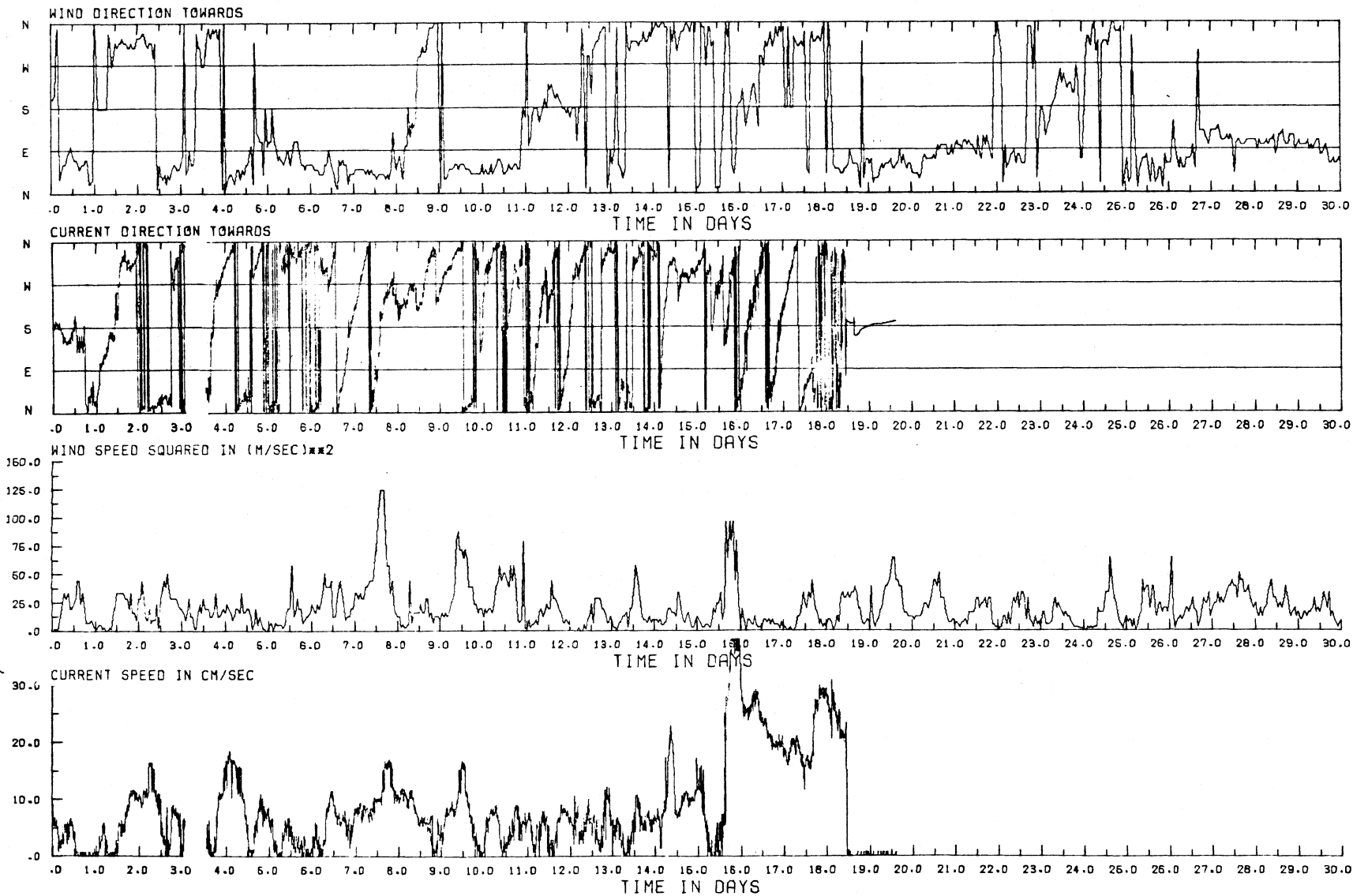


Figure 3.63

JUNE 1973: WIND (MITCHELL FIELD) COMPARED WITH STATION 7 CURRENT AT 13M DEPTH

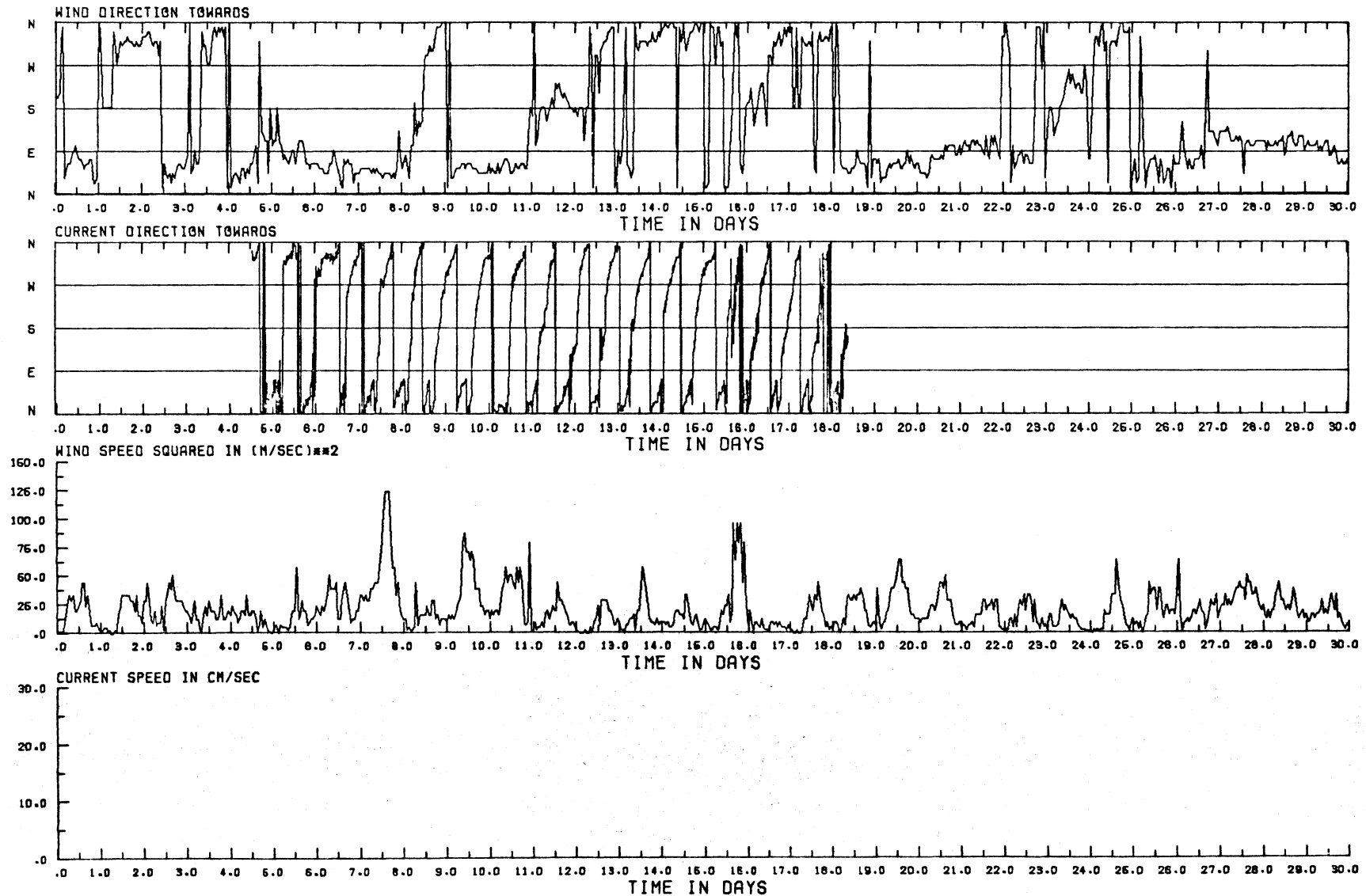


Figure 3.64

JUNE 1973: WIND (MITCHELL FIELD) COMPARED WITH STATION 7 CURRENT AT 26M DEPTH

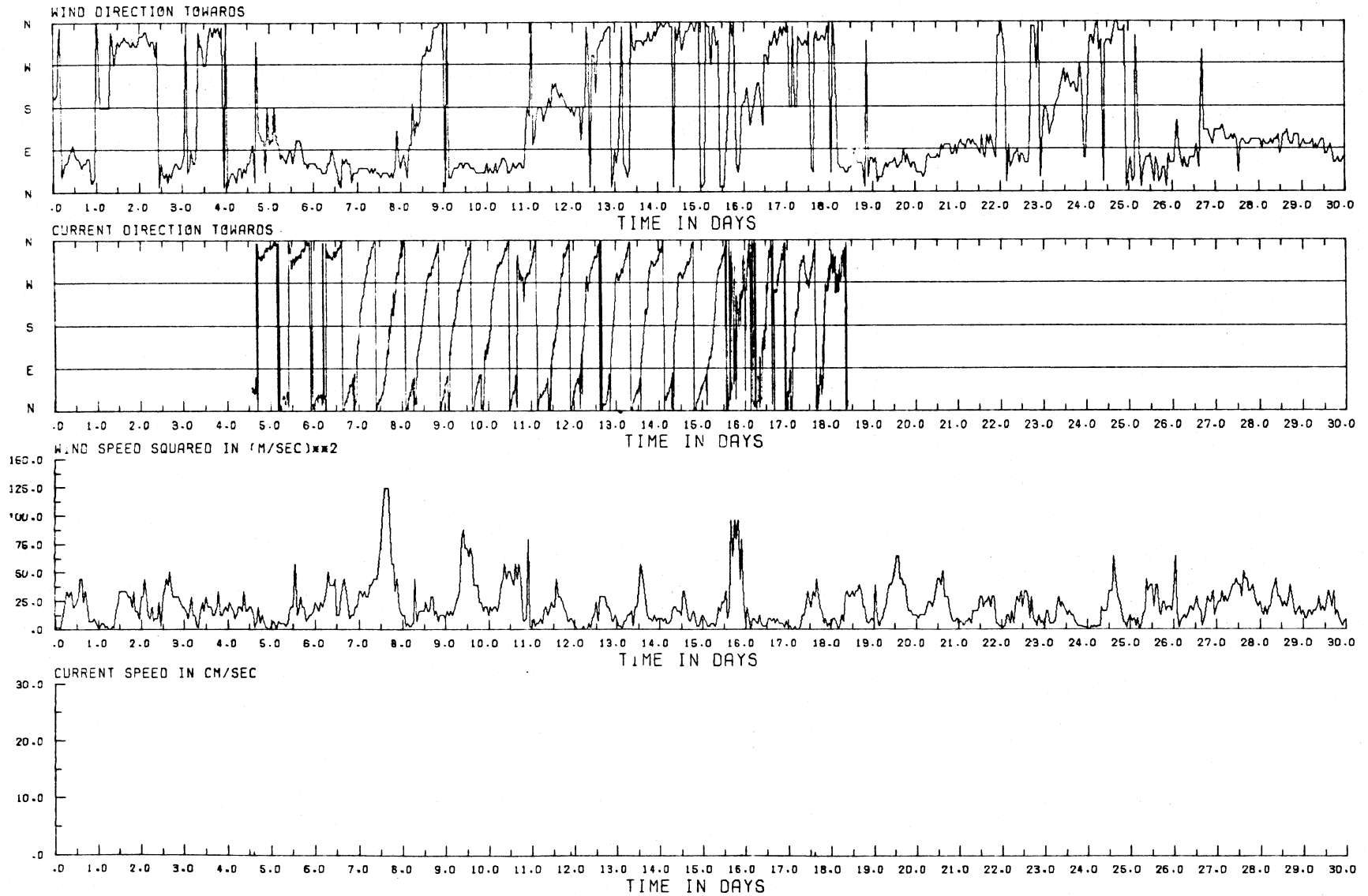


Figure 3.65

JULY 1973: WATER TEMPERATURE

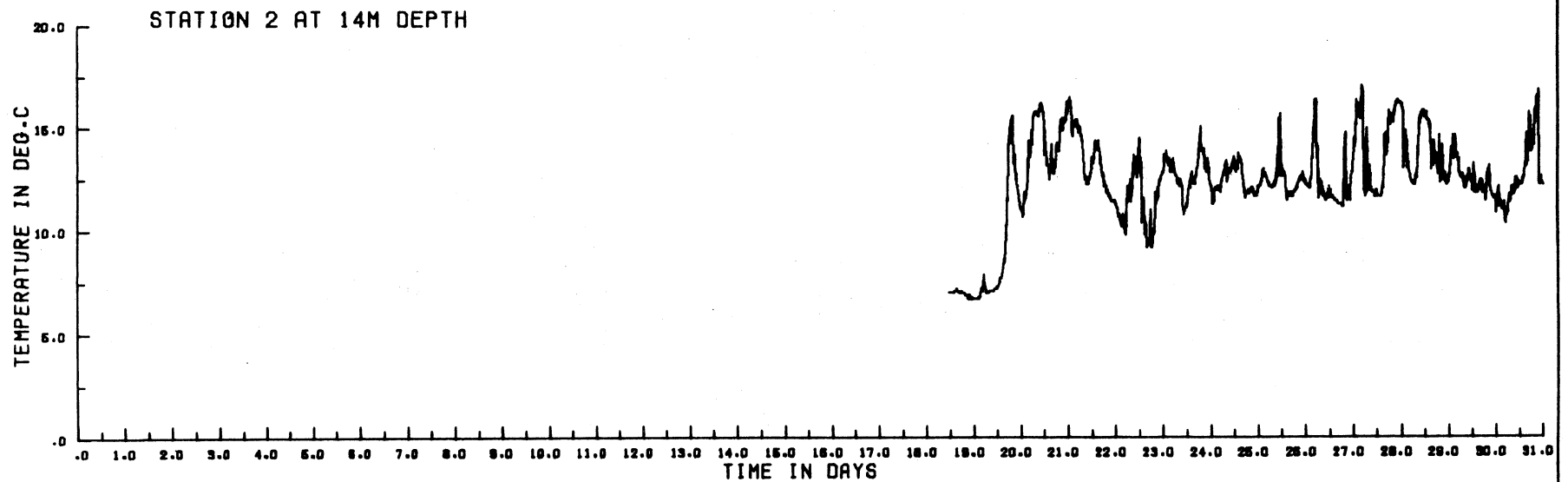
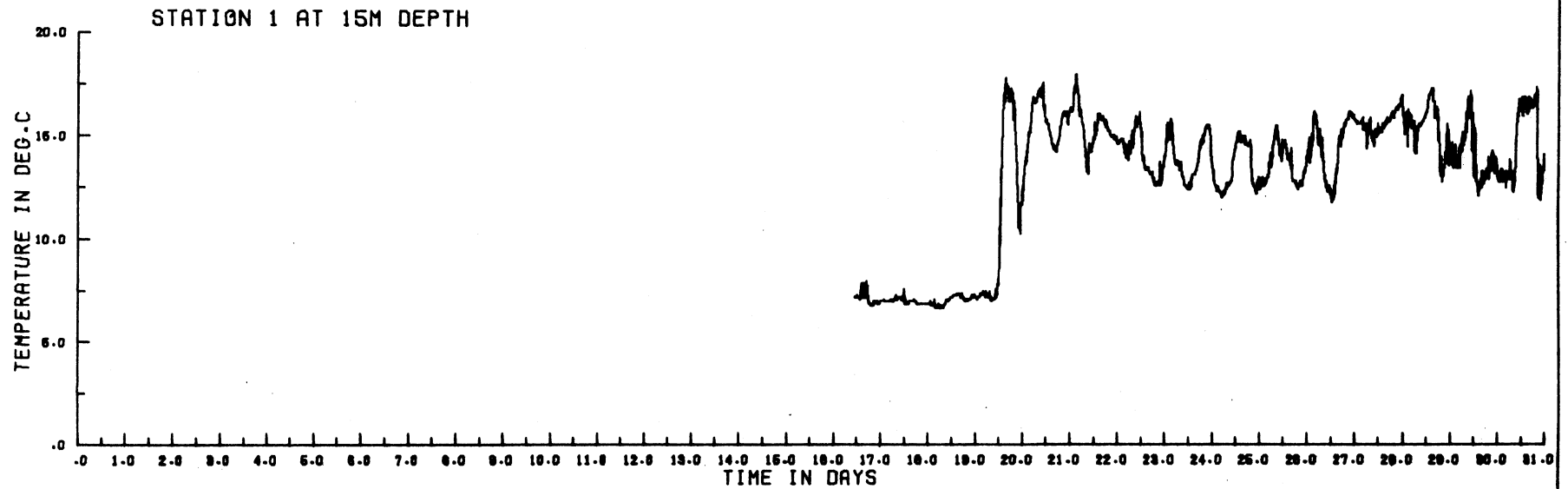


Figure 3.66

JULY 1973: WIND (MITCHELL FIELD) COMPARED WITH

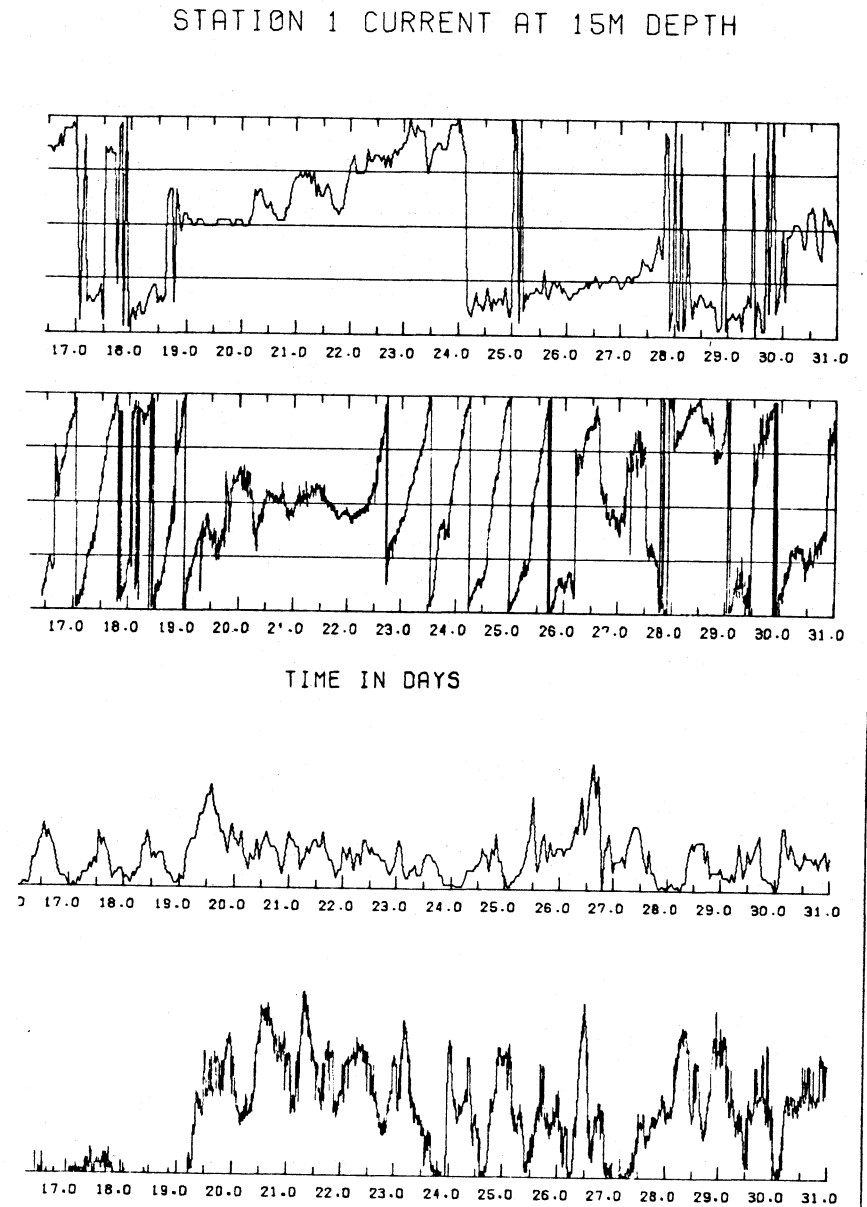
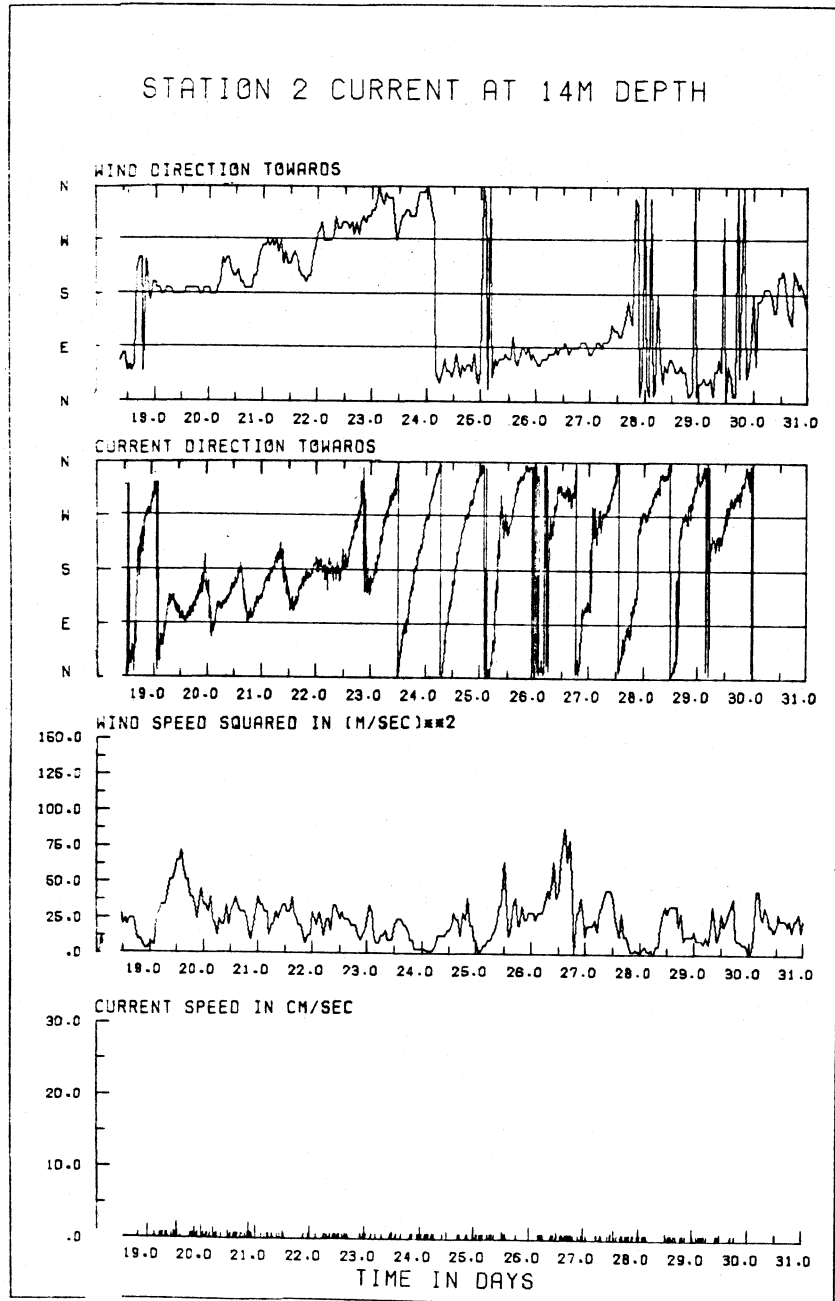


Figure 3.67

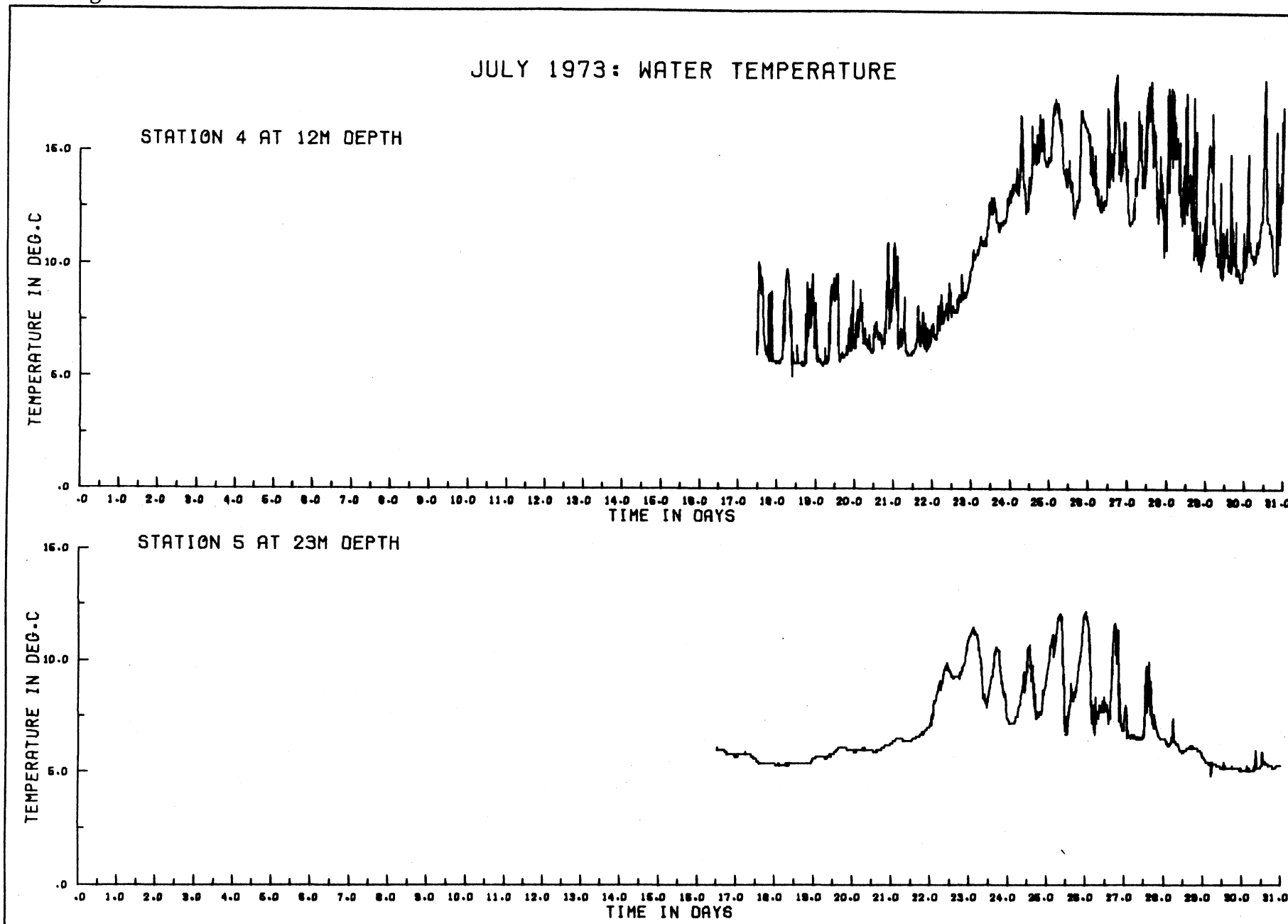


Figure 3.68

JULY 1973: WIND (MITCHELL FIELD) COMPARED WITH

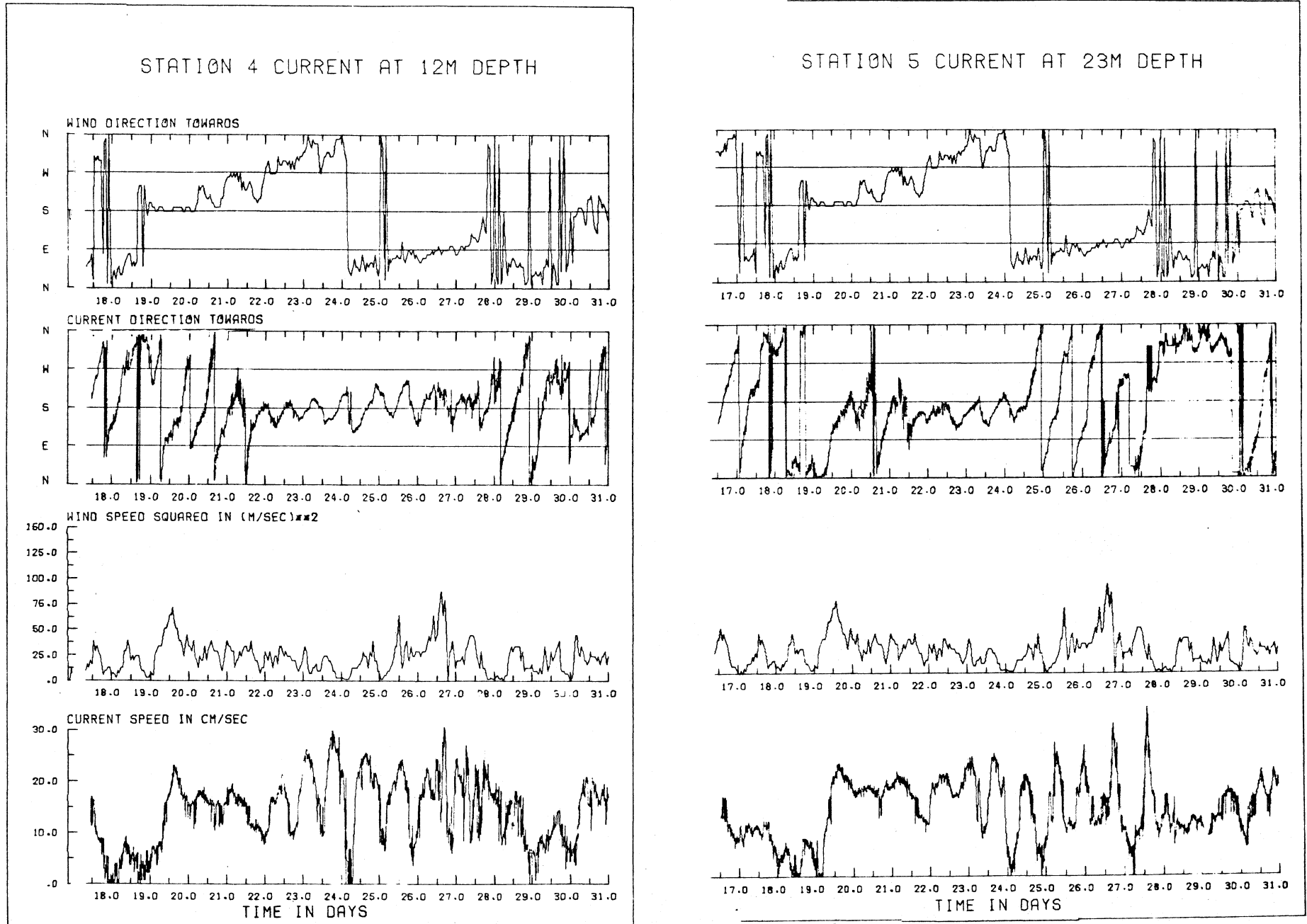


Figure 3.69

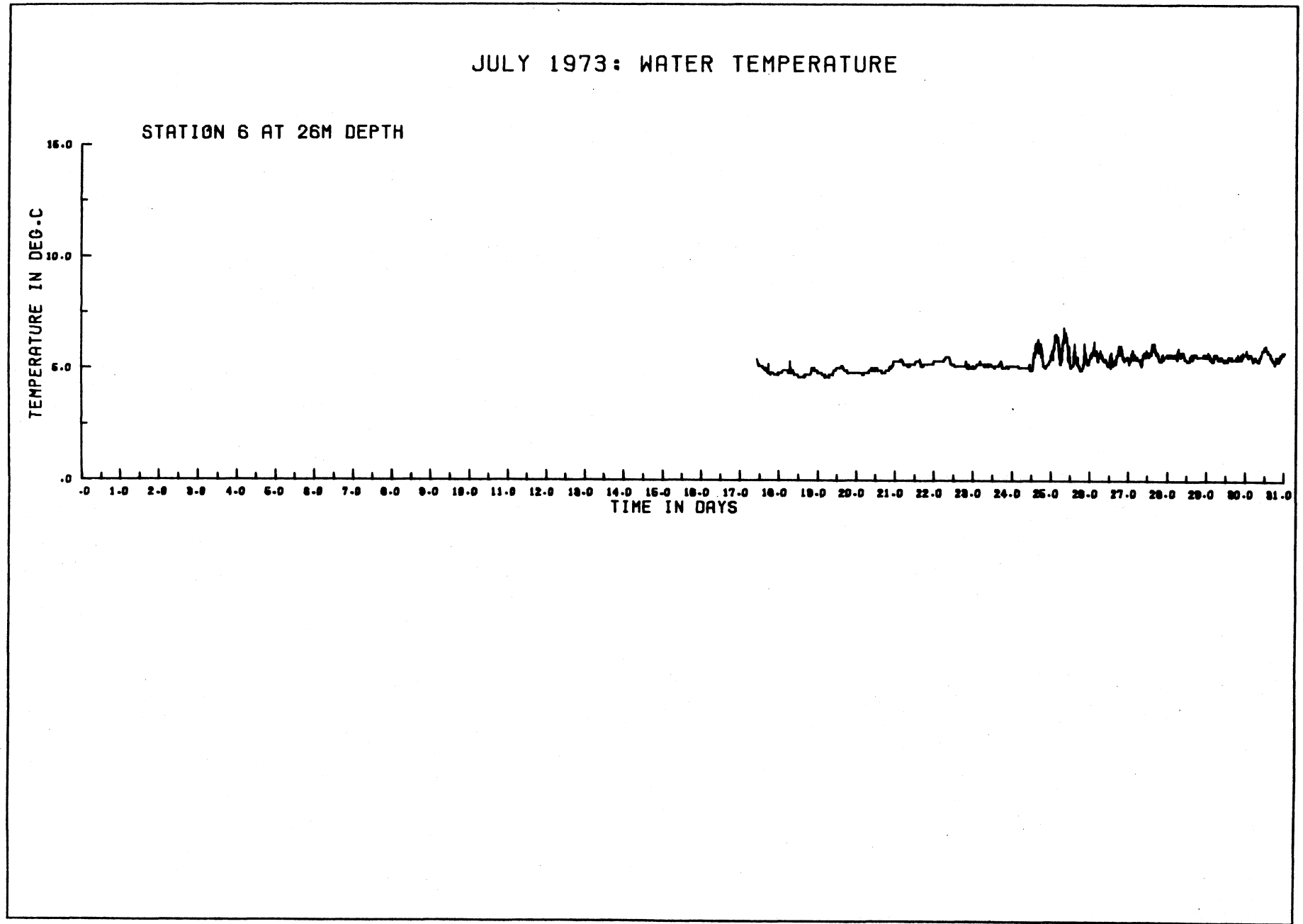
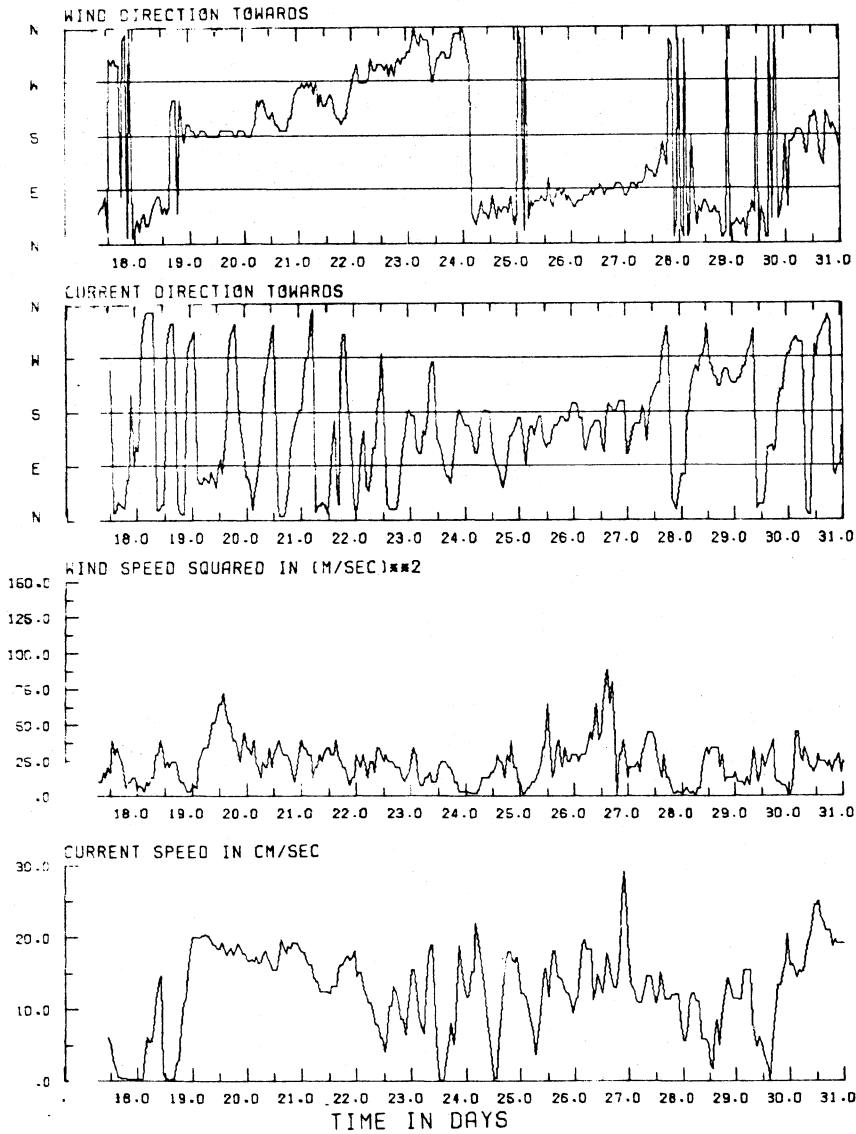


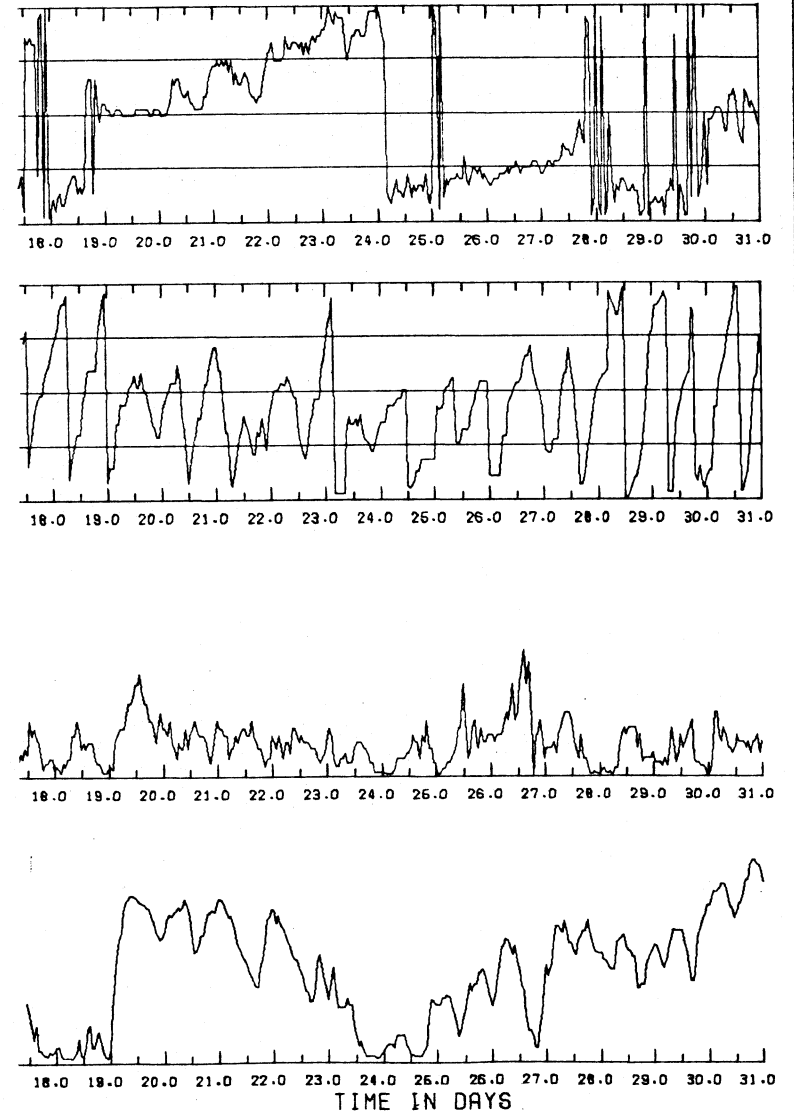
Figure 3.70

JULY 1973: WIND (MITCHELL FIELD) COMPARED WITH

STATION 6 CURRENT AT 13M DEPTH



STATION 6 CURRENT AT 26M DEPTH



a continuation of the meandering southgoing current at station 4 and with strong near-inertial temperature oscillations at both stations. The latter finding is perhaps surprising because, with a somewhat stronger eastward winds, an upwelling situation could have been expected. Station 6 also shows influence of near-inertial rotation of current direction, although at 26 m the temperature (fig. 3.69) remained fairly uniform between 5° and 6°C.

During August the temperature at station 4 (fig. 3.72) remained fairly high, with oscillations which became very marked and of near-inertial frequency between 12.0 and 19.0 days, after which time the current velocities (fig. 3.73) became very high, with very erratic current direction and with uniformly high temperature at about 20°C. It seems likely that the station 4 instruments, later found with the buoy at the surface, were prematurely released at that time. Fortunately, however, they were retained on station by the tethering rope.

During the interval 1.0 to 5.0 days in August, stations 4, 5, and 6 showed strong southgoing currents, which later became strongly rotary at station 5 (fig. 3.74, with no record after 10.3 days), but more meandering at station 4 (fig. 3.73) continuing so until 19.0 days. At station 6 the current records were unusable after 6.0 days, but the temperature record continued for 5 days more (fig. 3.75) and showed clear near-inertial oscillations. In general, as observed in previous records, the shallower water stations reacted more rapidly to changes in the wind than did the offshore stations.

The results from Survey VI (started on 15 August, see extract from Table 21 on p.137) were fragmentary. Only the data from the upper instrument at station 5 was usable, and then only after deriving hourly averages by digitizing. Records were obtained from station 4 at 12 m depth only for the first day of September, which represents only a minor extension of the August figure 3.73. Therefore the September figure for station 4 (12 m) has been omitted. The current on that day was southeastward in direction and fairly steady about 18 cm. s<sup>-1</sup>.

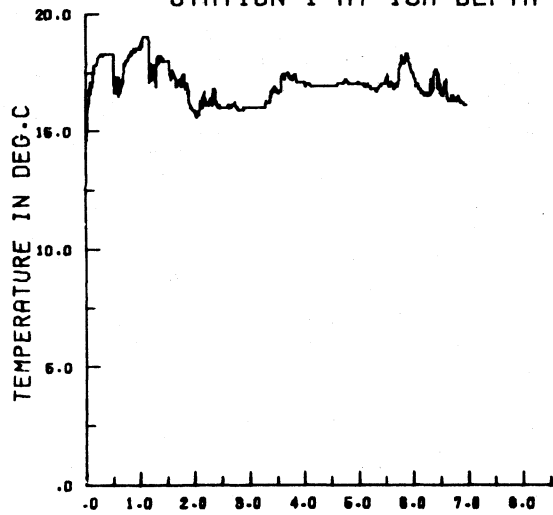
[the text continues on page 156]

Figure 3.71

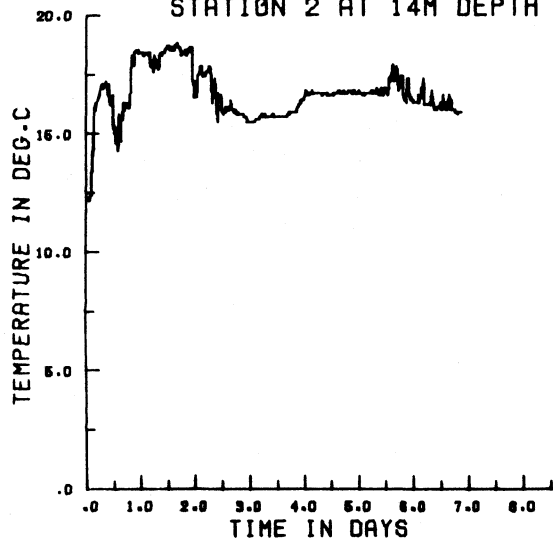
AUGUST 1973:

WATER TEMPERATURE

STATION 1 AT 15M DEPTH

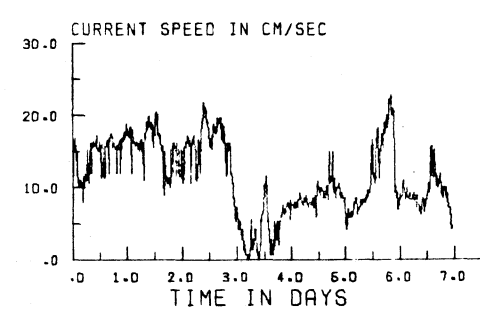
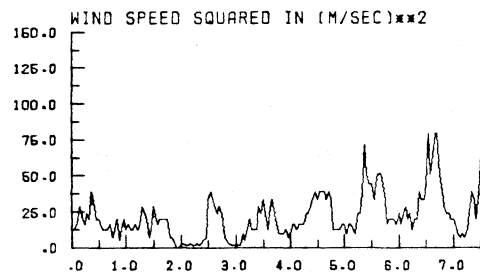
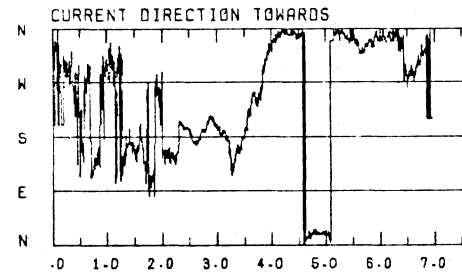
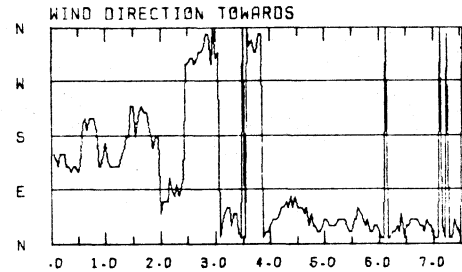


STATION 2 AT 14M DEPTH



AUGUST 1973: WIND (MITCHELL FIELD) COMPARED WITH

STATION 1 CURRENT AT 15M



STATION 2 CURRENT AT 14M

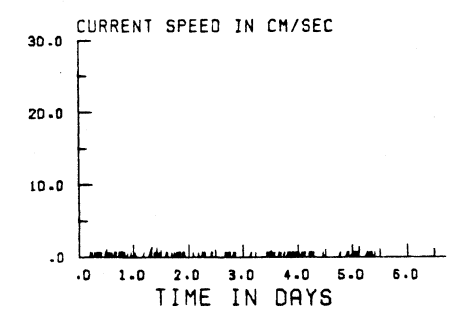
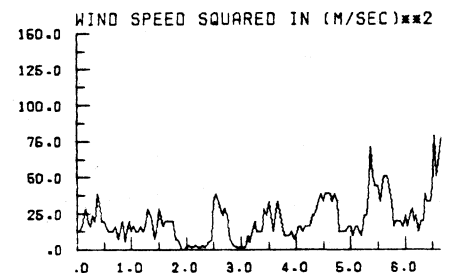
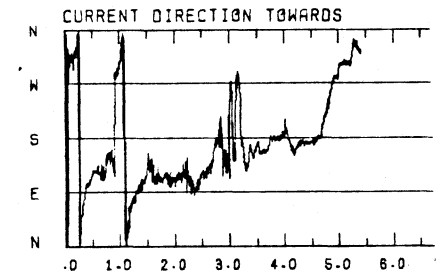
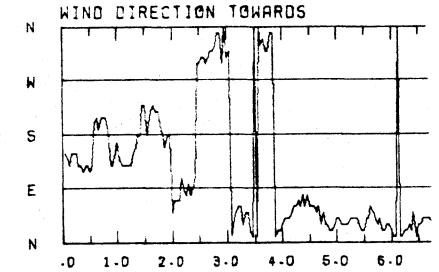


Figure 3.72

AUGUST 1973: WATER TEMPERATURE

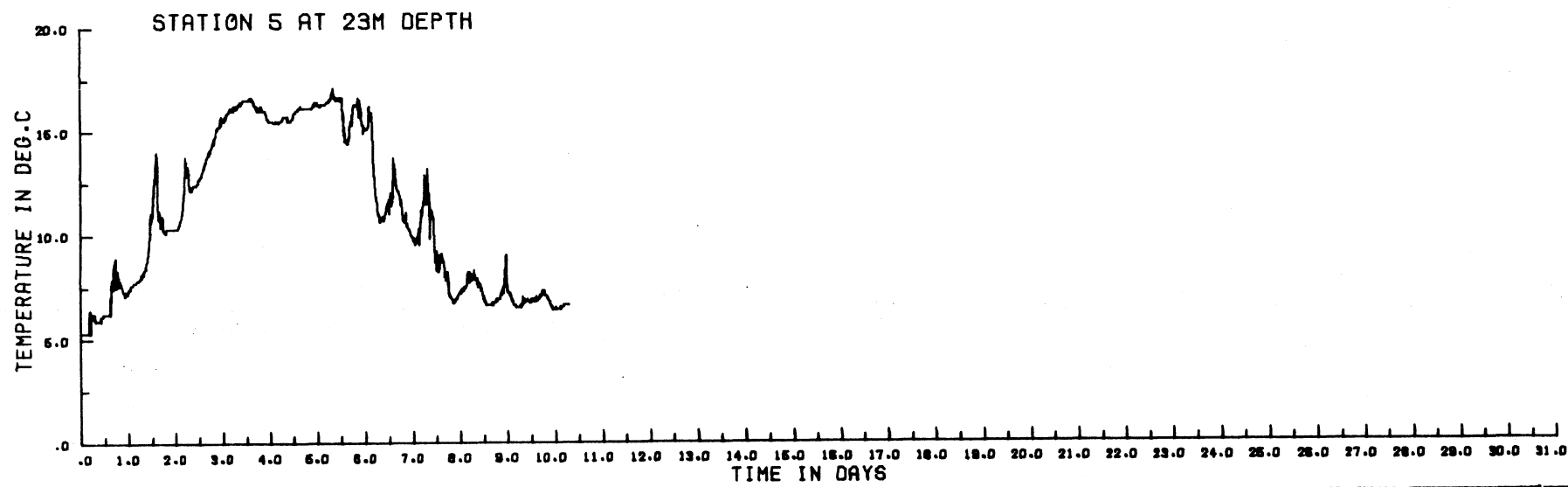
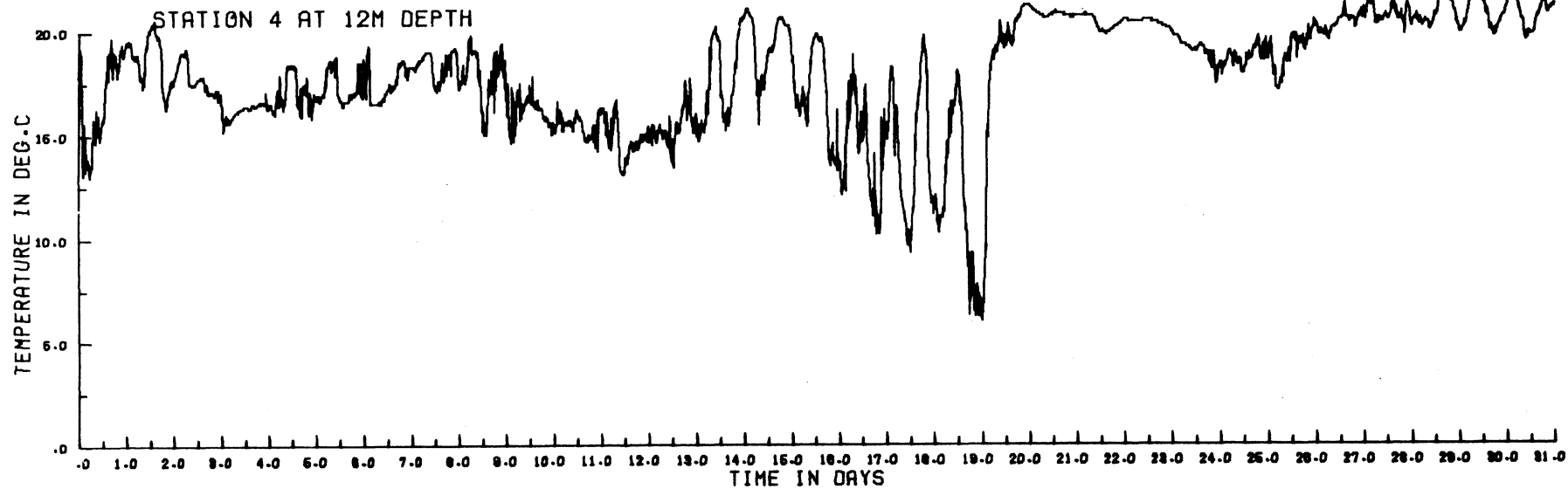


Figure 3. 73

AUGUST 1973: WIND (MITCHELL FIELD) COMPARED WITH STATION 4 CURRENT AT 12M DEPTH

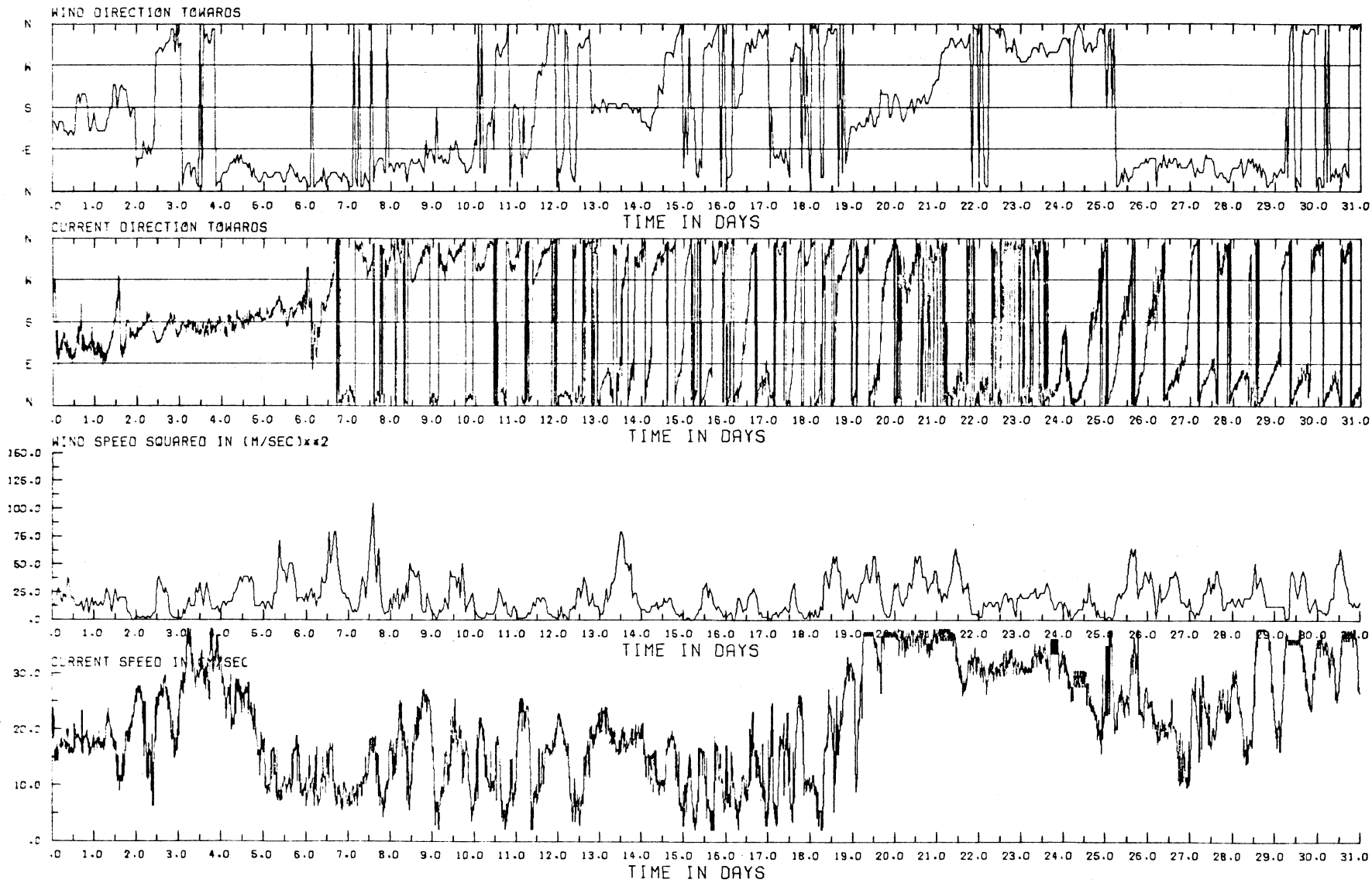


Figure 3.74

AUGUST 1973: WIND (MITCHELL FIELD) COMPARED WITH STATION 5 CURRENT AT 23M DEPTH

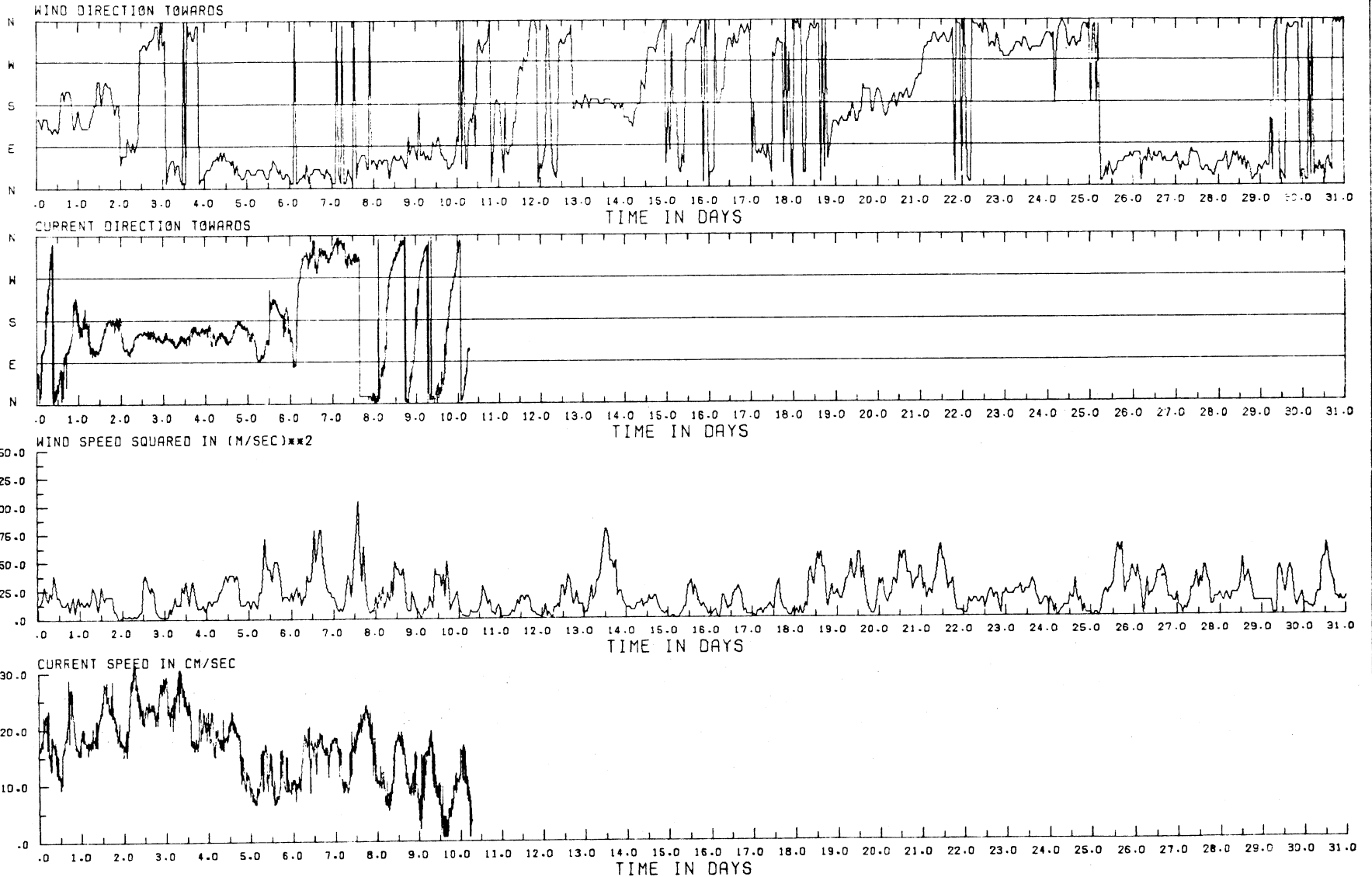
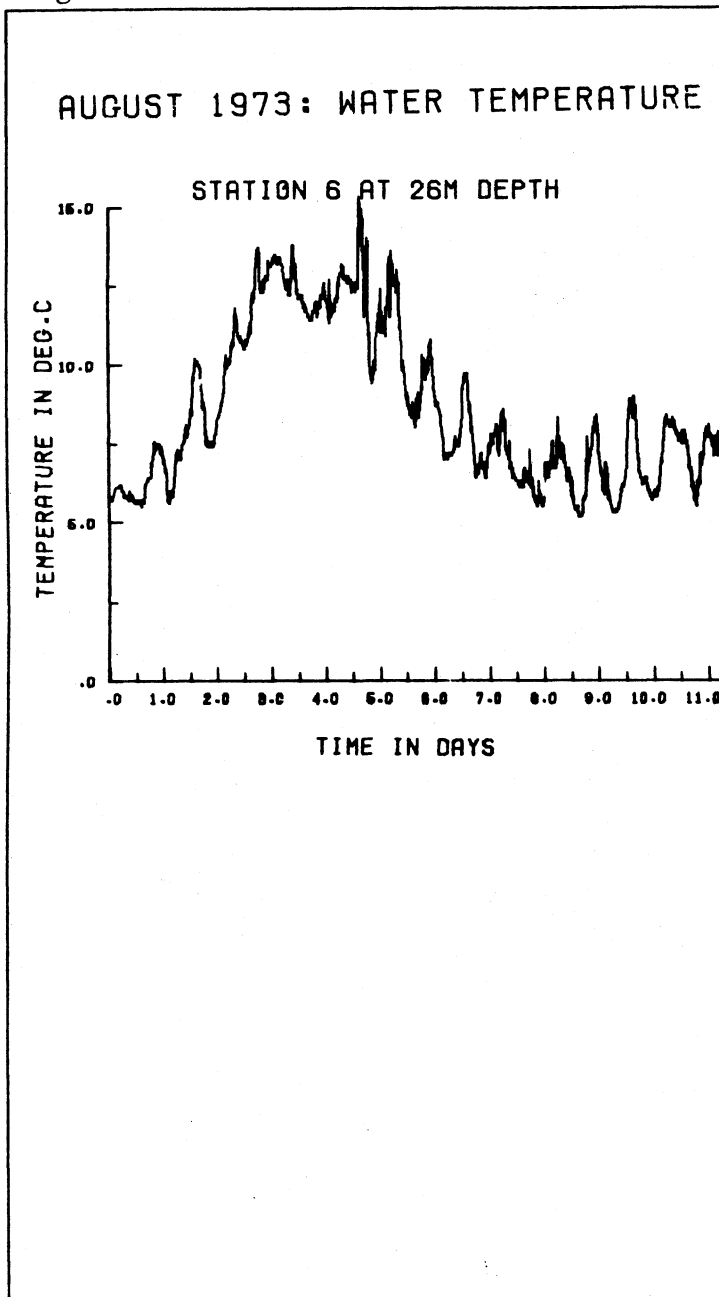
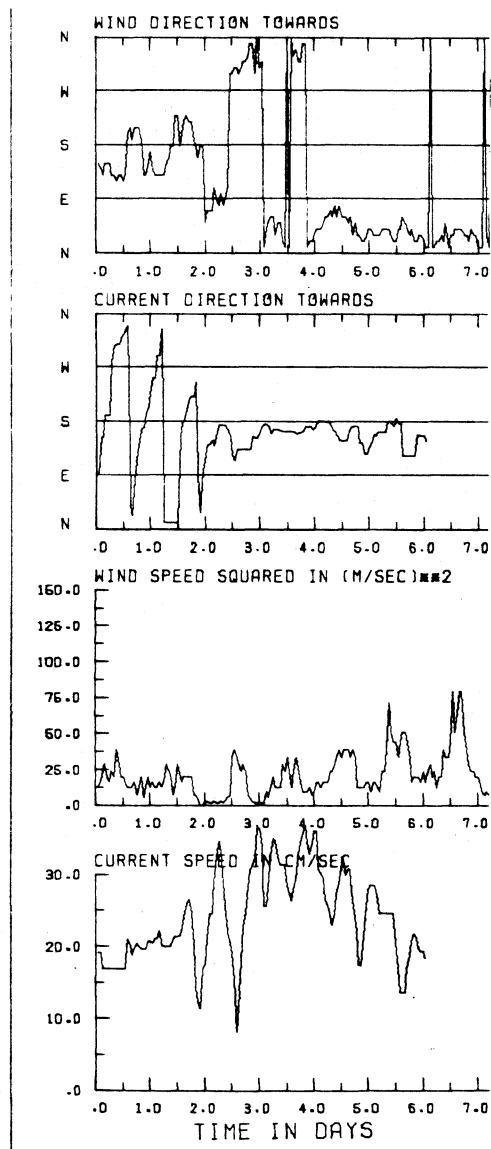


Figure 3.75



AUGUST 1973: WIND (MITCHELL FIELD) COMPARED WITH  
STATION  
6 CURRENT AT 13M DEPTH



STATION  
6 CURRENT AT 26M DEPTH

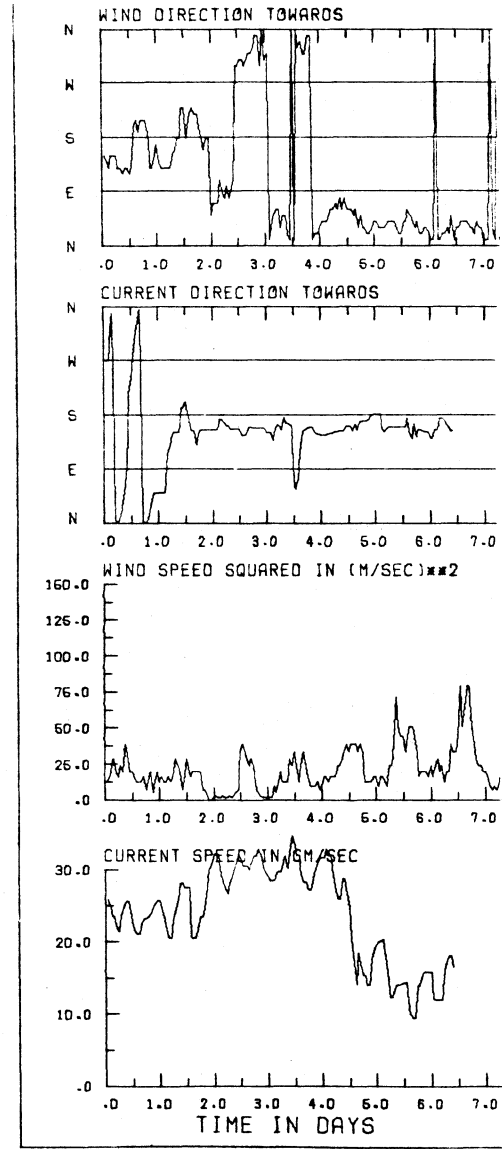


Figure 3.76

AUGUST 1973: WIND (MITCHELL FIELD) COMPARED WITH STATION 5 CURRENT AT 12M DEPTH

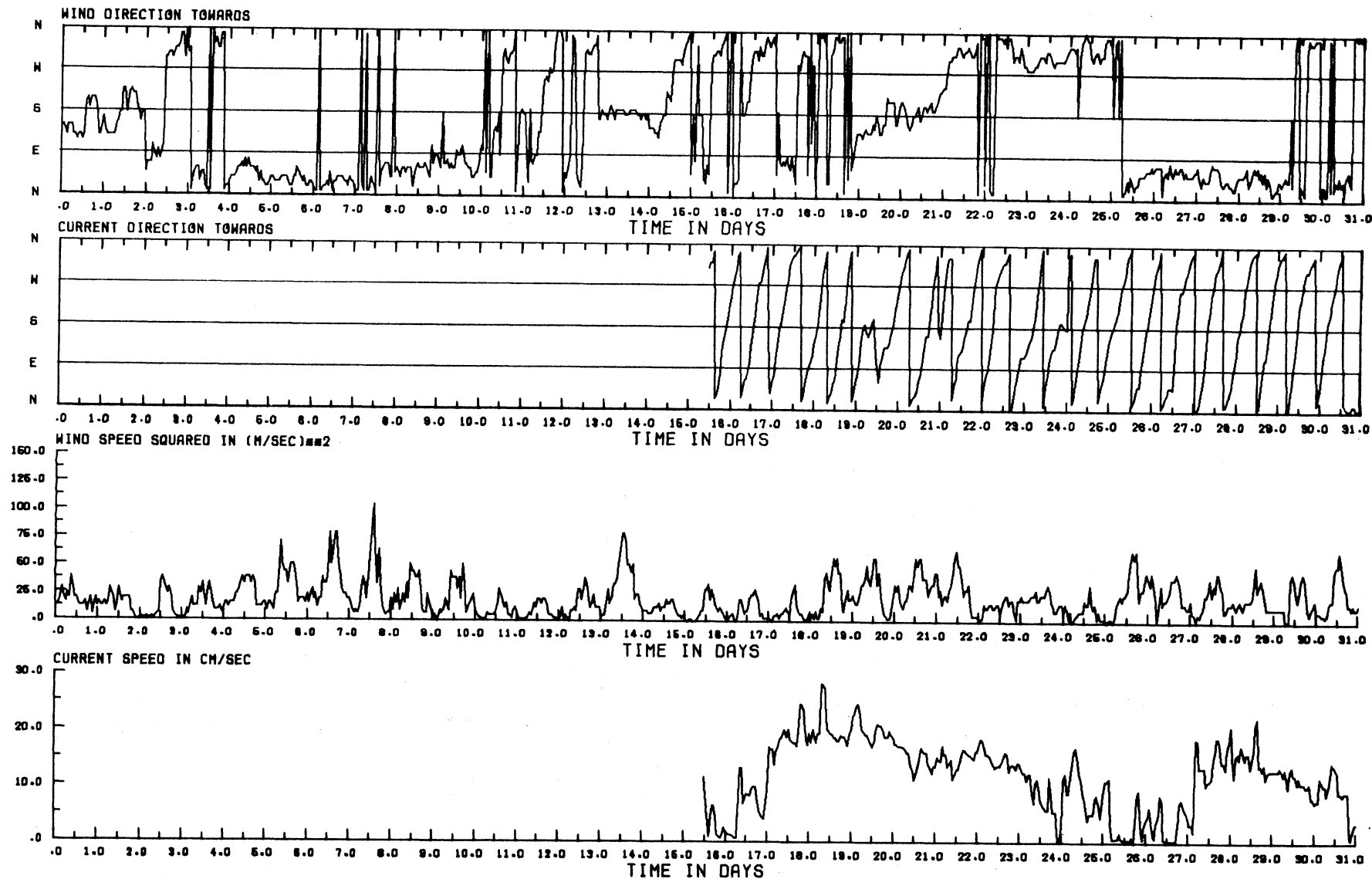
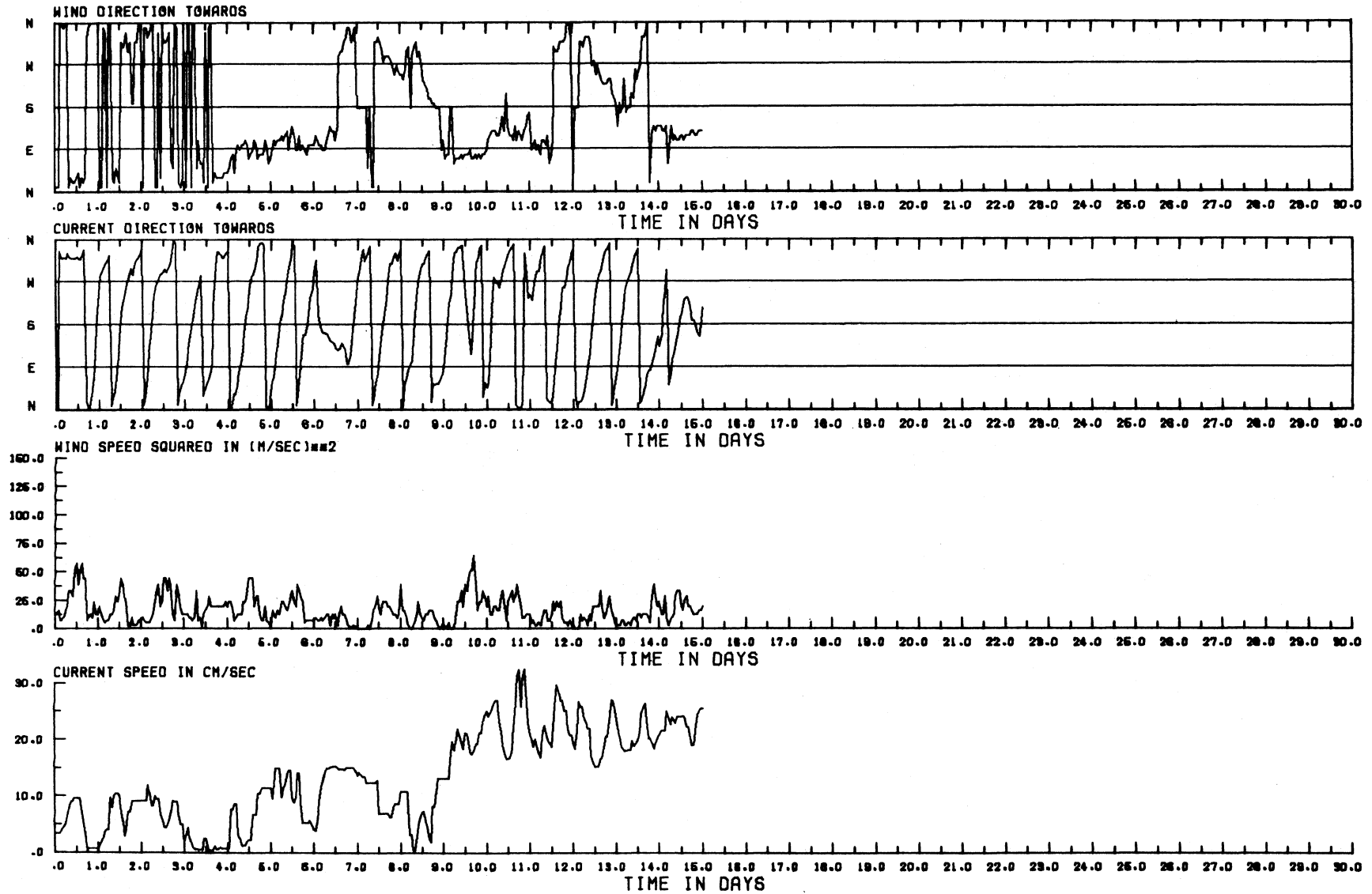


Figure 3.77

SEPTEMBER 1973: WIND (MITCHELL FIELD) COMPARED WITH STATION 5 CURRENT AT 12M DEPTH



The 12 m instrument at station 5 ran for about a month after 15 August and showed extremely regular rotation of current direction, totalling 42 "waves" in 29.5 days, an average period of 16.9 hours. At the same time the currents were relatively strong, although there were no very strong winds at Mitchell Field during the recording interval (figs. 3.76 and 3.77).

## CHAPTER FOUR

### ANALYSIS OF CURRENT RECORDS AND CURRENT-WIND RELATIONSHIPS

Although all the information we gained on current, wind, and temperature is contained in the seventy-seven monthly diagrams of Chapter Three, it is instructive to summarize and analyze that mass of data by compressing it in the form of vector frequency and progressive vector diagrams, then proceeding to a second stage of analysis in which are computed: persistence factors; spectra of current and temperature records at individual stations; and co-spectra to disclose coherence and phase relationships between pairs of stations or (in one example) between wind and current.

The vector frequency diagrams are based on a polar array of compartments bounded by "direction spokes" at  $10^\circ$  intervals and by concentric "speed circles" at  $4 \text{ cm. sec}^{-1}$  intervals ( $2 \text{ m. sec}^{-1}$  for wind speed). For the selected time interval -- varying from a few days to a month or more -- each 10-minute speed/direction vector was allocated to its appropriate compartment. Then contours of percentage frequency of occurrence were drawn, yielding a clearer presentation than the conventional paired direction and speed histograms.

The progressive vector diagrams were formed by first condensing six successive sets of 10-minute readings of current speed and direction into average hourly vectors, each represented by an arrow indicating direction (relative to N at the top of the page) and speed (proportional to arrow length). The hourly vector arrows were then joined successively tail to head to form a "current track". This is likely to represent the true current track only in the neighbourhood of the current meter, i. e. only within the area in which current speed and direction is everywhere the same, although varying in time. Comparison of progressive vector diagrams for the same time interval, but for different stations, serves to show how accurately and over what area the progressive vector diagrams represent the current field. A straight-line track indicates a uni-directional current; meandering, cusping, or looping tracks respectively indicate increasing proportions of rotary current components as explained in Chapter One.

Persistence factors were calculated on a monthly basis for each current meter using the relationship:

$$\text{Persistence factor } P = \frac{\text{Resultant monthly mean current vector}}{\text{monthly mean current speed.}}$$

P, a measure of the directional persistence of the currents, will be discussed in Chapter 6 and presented in Tables 6.1 and 6.2. The azimuth angles of the mean current vector are also given in those tables.

The persistence factor would be 1.0 if the current had travelled in the same direction for the entire month. The minimum persistence factor of zero would be obtained if the currents had travelled with equal speed and frequency in all directions or if the vector frequency diagram for the month was exactly symmetrical about any diameter, reflecting the fact that flow in any given direction was balanced by flow of the same magnitude in the opposite direction.

As already noted in Chapter 3, the vector frequency diagrams confirm that winds blowing off the land do not have sufficient fetch to exert much influence on the nearshore current regime, whereas winds blowing toward S-SW or towards NW-N exert the maximum effect in setting currents in motion or reversing existing patterns. Currents were clearly constrained to run roughly shore-parallel; currents directed normal to the shore were rare.

It should be noted that the vector frequency diagrams for both wind and current always indicate the direction toward which the flow is going. Depending on the availability and continuity of the data, the results summarized in the vector frequency and progressive vector diagrams are presented for intervals which may be more or less than a month. Where possible, vector frequency and progressive vector diagrams which cover the same or overlapping time intervals are placed on facing pages for each of comparison. The progressive vector diagram presents a time history of the measurements at a particular station -- and also an approximation to the real current track, subject to the qualifications noted earlier -- and the vector frequency diagram summarizes the same information by means of percentage frequency contours. These diagrams, it should be noted, include a high percentage (often over 50%) of "very weak" current readings, i. e. of speeds

4 cm.s<sup>-1</sup> or less, treated in later discussion. Thus an average current speed for the whole interval covered by a vector frequency diagram may be only 5 cm.s<sup>-1</sup>, whereas the average taken over "active" current intervals only may be 10 cm.s<sup>-1</sup> or more. Most of the data points in the diagram will therefore be crowded close to the origin. The progressive vector diagrams also differentiate between periods of active currents, when progress along the "track" is relatively fast, and weak currents when little progress is made. This draws attention to the episodic nature of the wind and current interactions, now to be described for each survey.

### Survey I, 3 April to 5 June 1972

During the month of April, winds were mainly toward SSW for speeds greater than 5 m/sec (fig. 4.1). There were some episodes of winds to the northwestward and northeastward but very little activity toward the southeast. The vector frequency diagrams for Stations 1 and 2 (figs. 4.2 and 4.3) showed a strong tendency toward the southeast and a little toward the northwest. The southeastward currents were associated with SSW-going winds and the northwestward currents with northwest-going winds. Wind along these two directions had the greatest fetch, since both came from across the lake. In contrast, northeastward winds, with little fetch, had little influence on the current regime.

The progressive vector diagrams (figs. 4.6 and 4.8, upper two-thirds) showed very similar patterns during the active periods, although they differed during periods of weak current. Station 2 currents tended to be more southeastward, probably a result of shoreline configuration.

Although the overall distribution pattern of the vector frequency diagram for Stations 1 and 2 during May and the first four days of June was similar to that for April, there were fewer episodes of strong wind toward SSW (fig. 4.4). The currents were correspondingly less strong, as shown by the vector frequency figures 4.5 and 4.7 and the progressive vector figures 4.6 and 4.8 (bottom one-third). All the vector frequency diagrams for May (figs. 4.5, 4.7, 4.9, 4.11, and 4.13) as well as the progressive vector diagrams (figs. 4.6, 4.8, 4.10, 4.12, and 4.14) show that the two main directions of flow for the strongest

[the text continues on page 180]

Figure 4.1

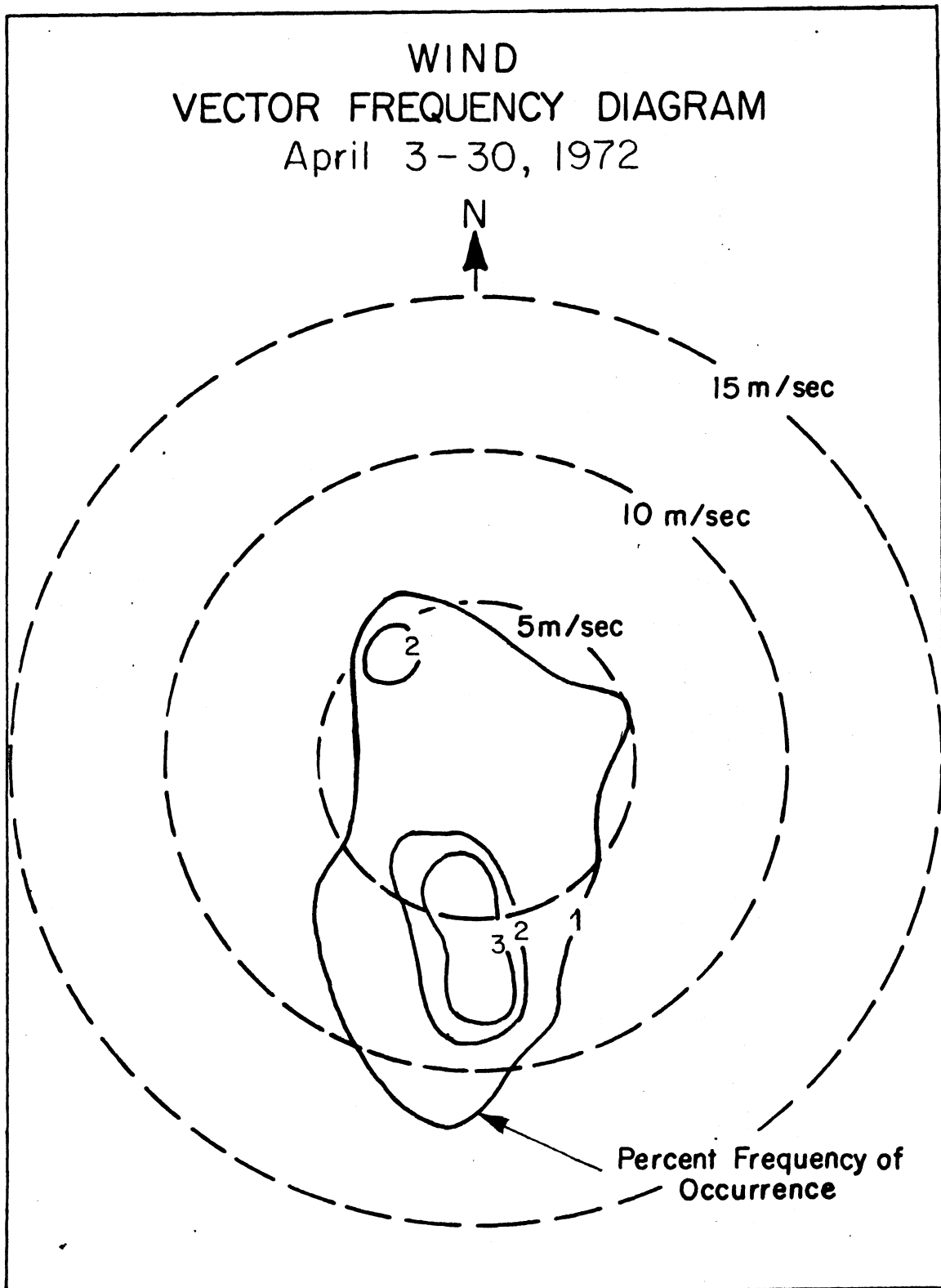


Figure 4.2

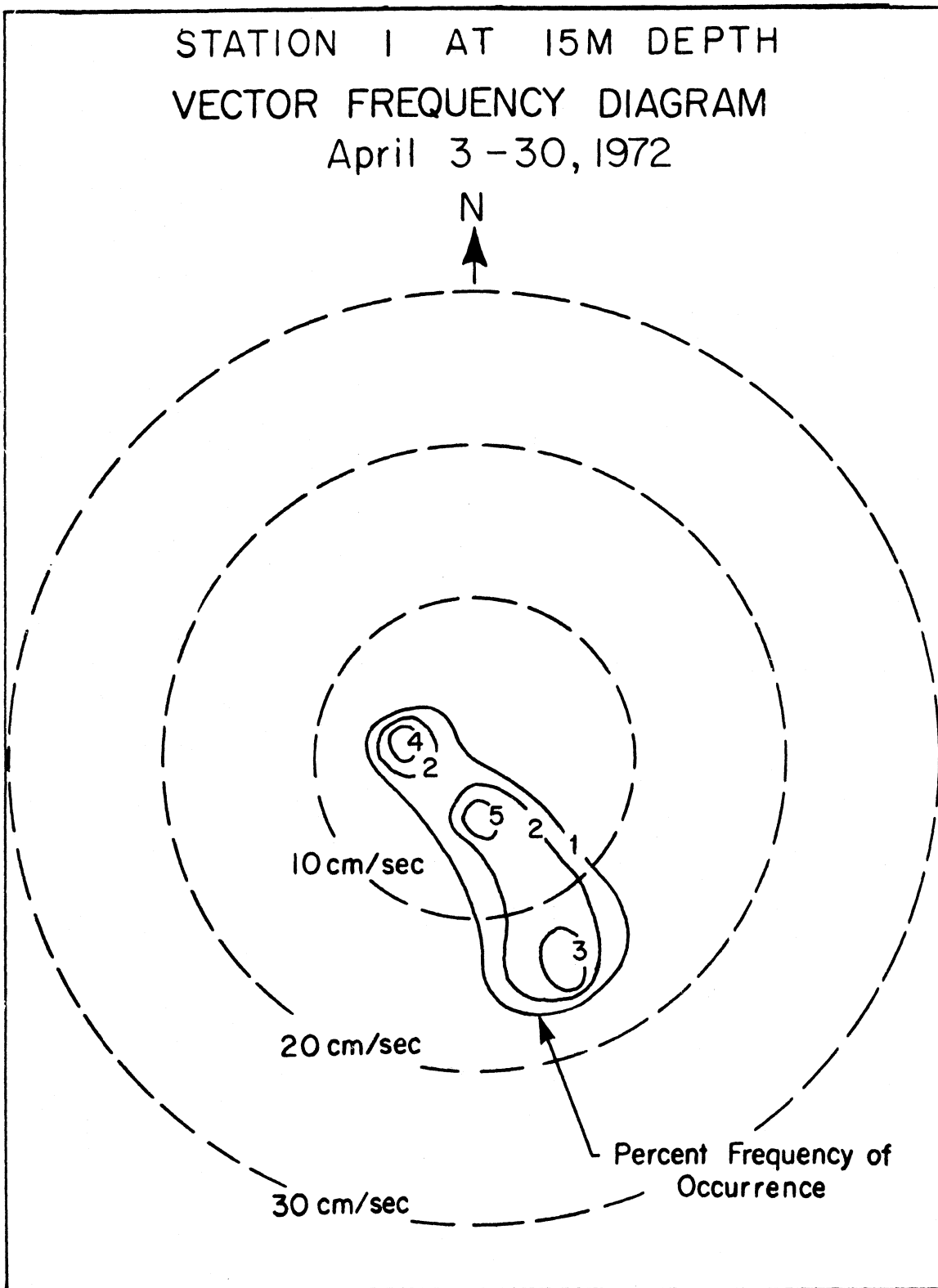


Figure 4.3

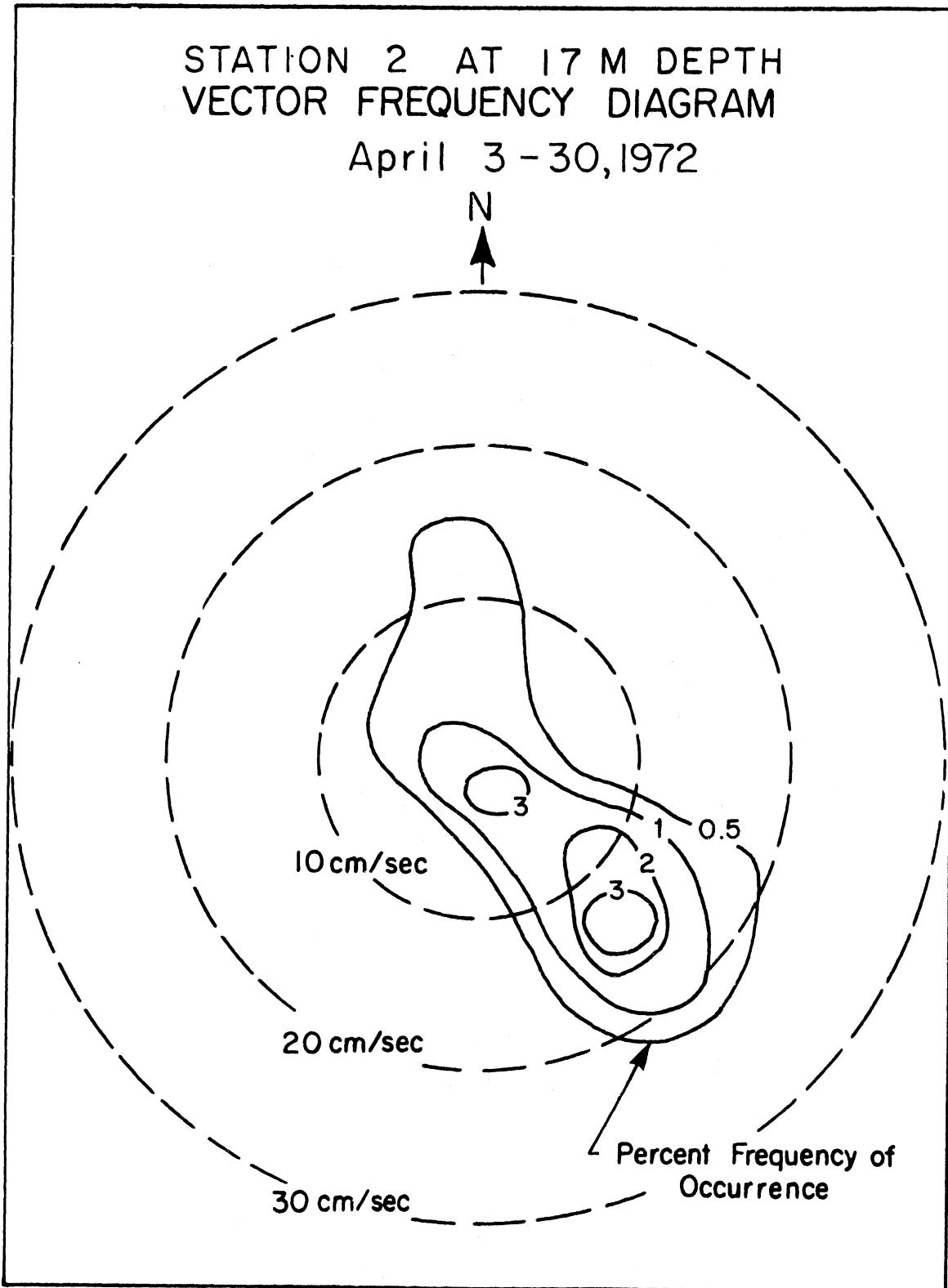


Figure 4.4

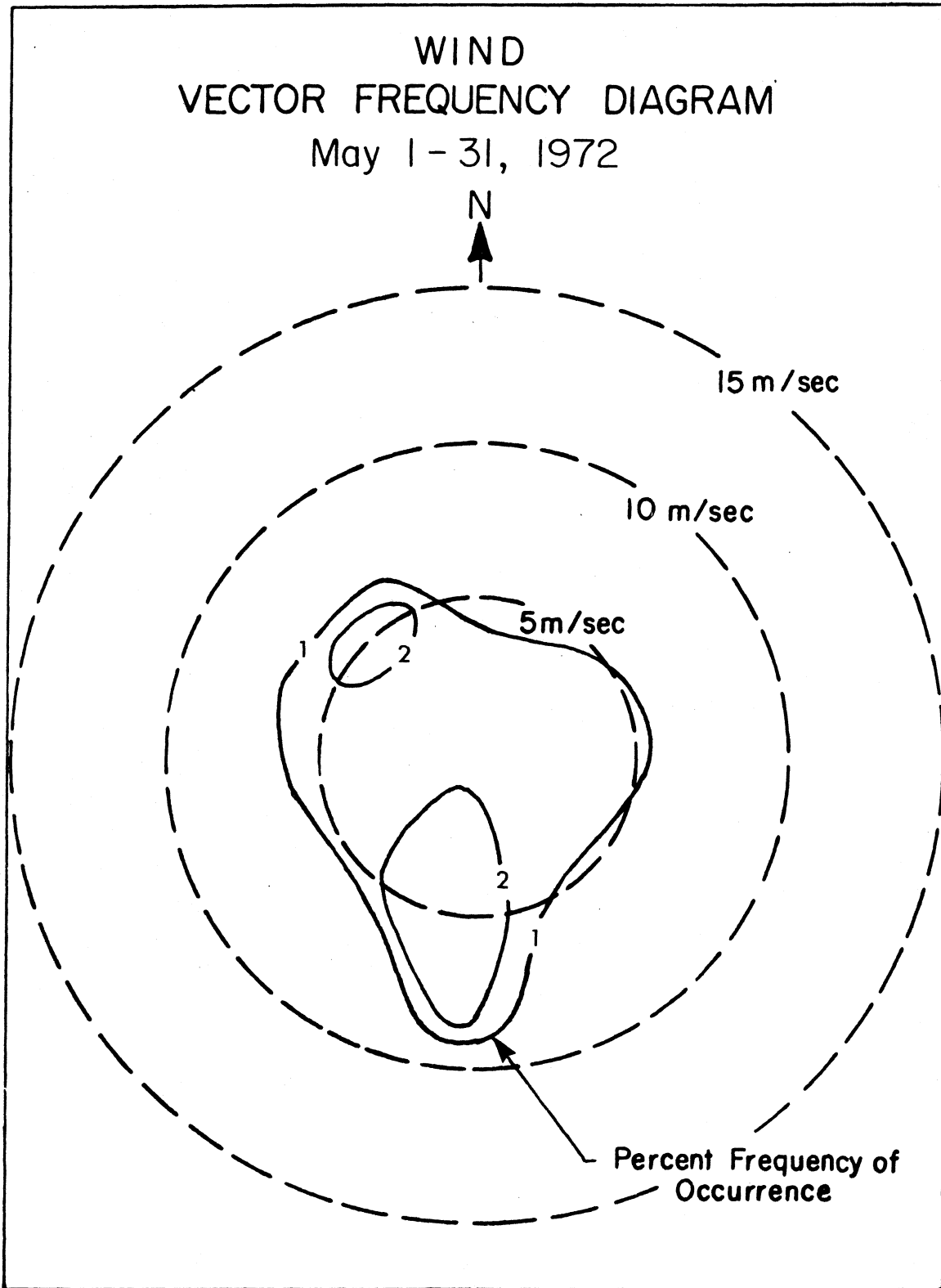


Figure 4.5

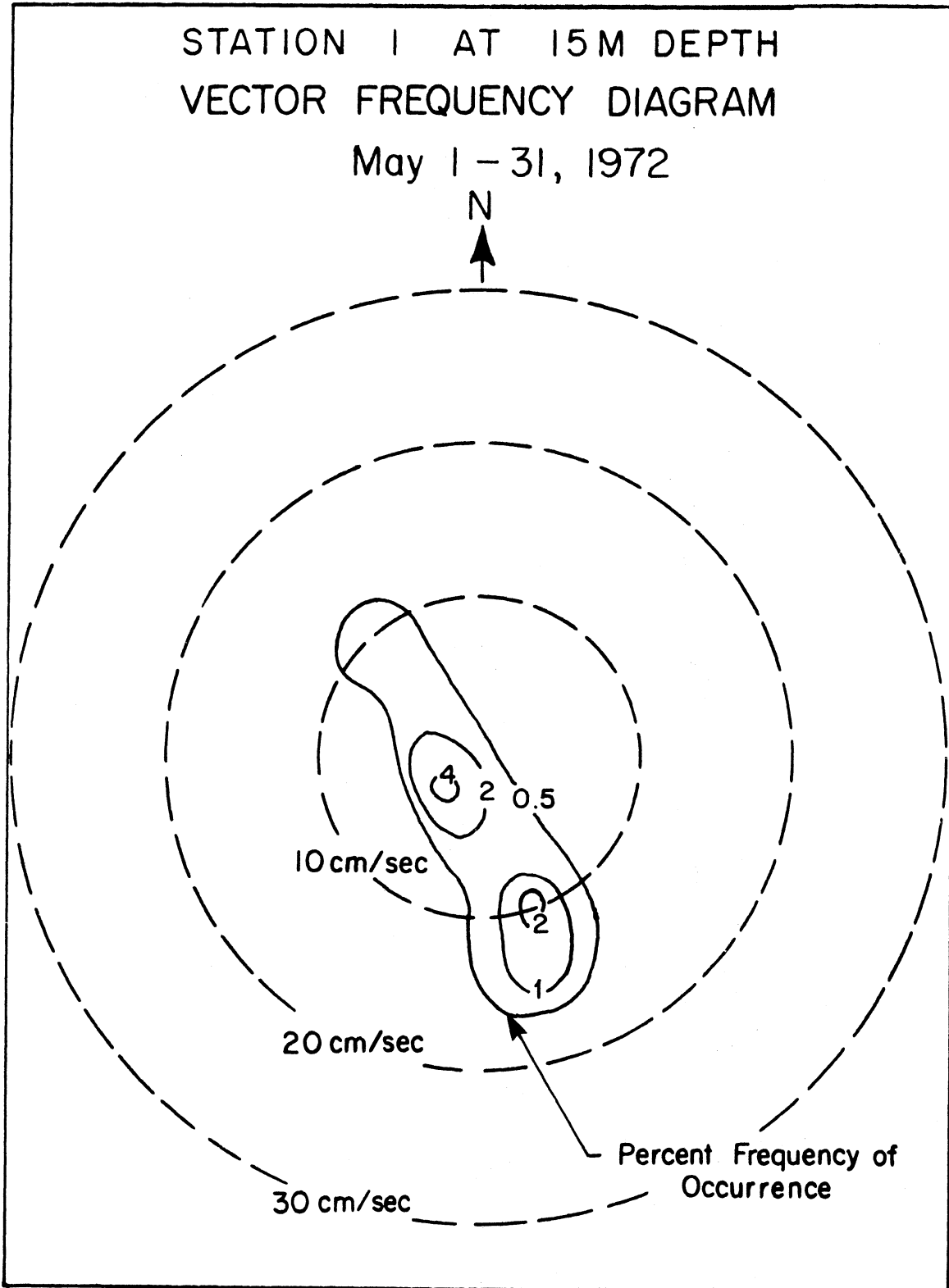


Figure 4.6

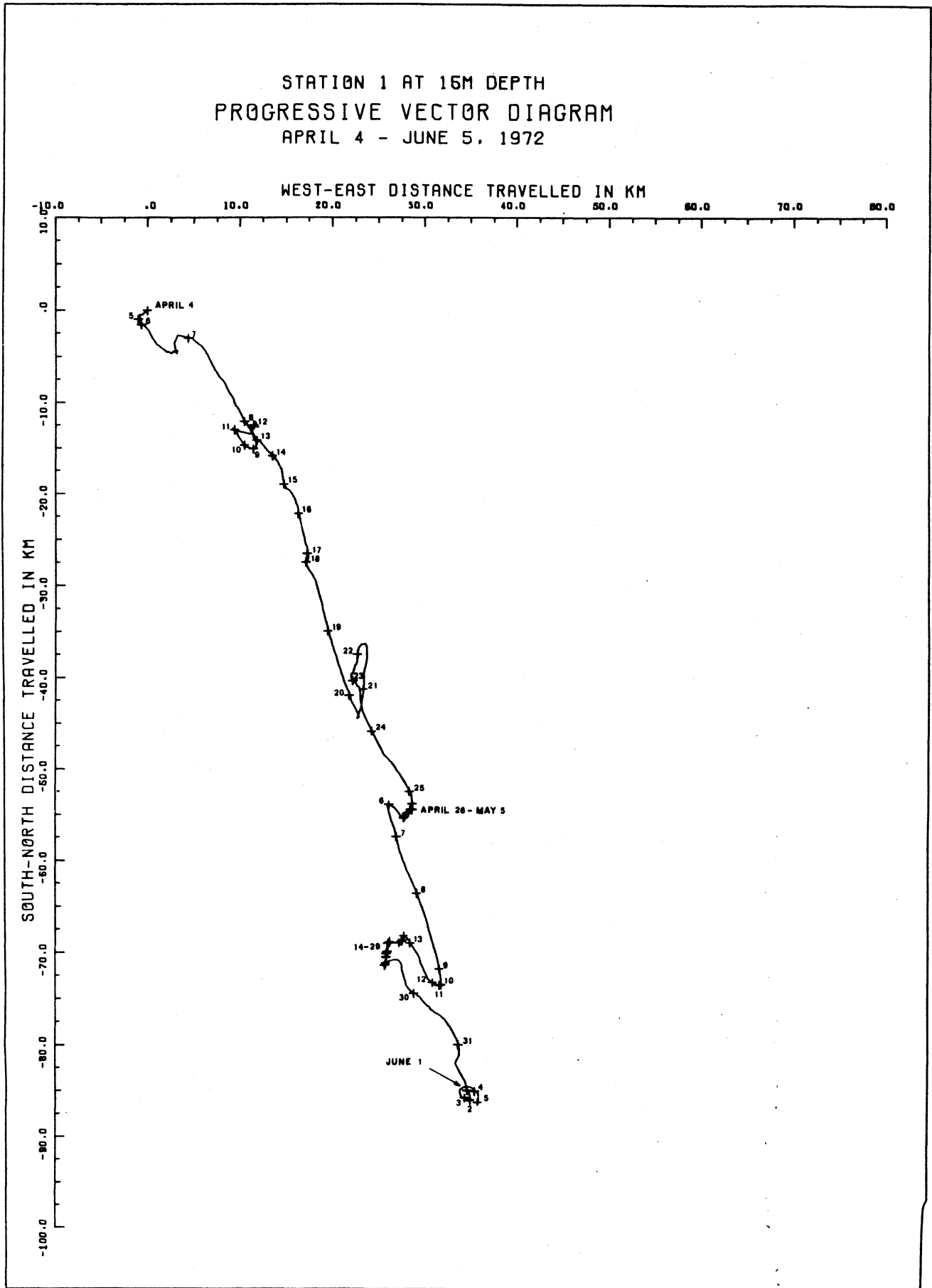


Figure 4.7

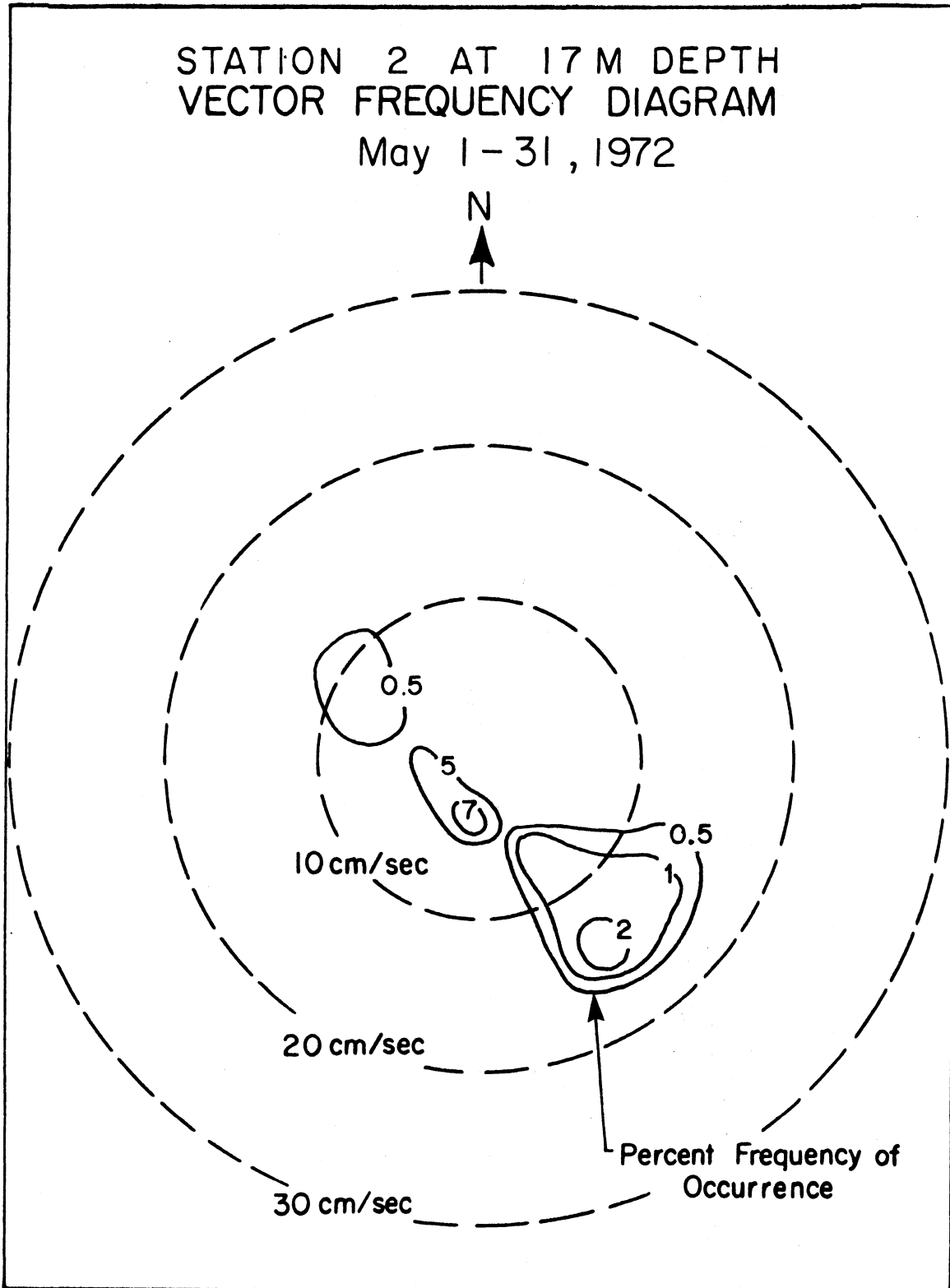


Figure 4.8

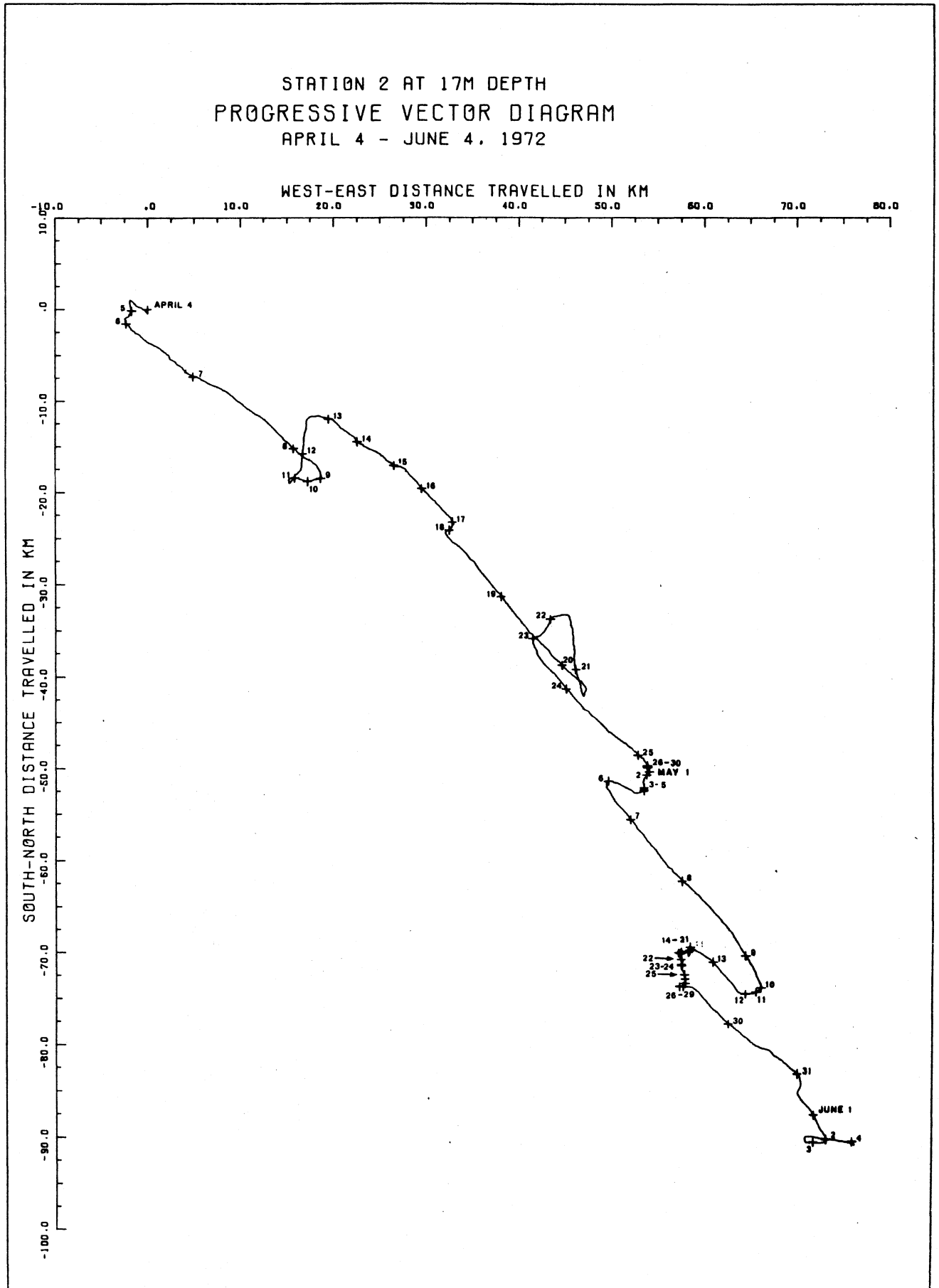


Figure 4.9

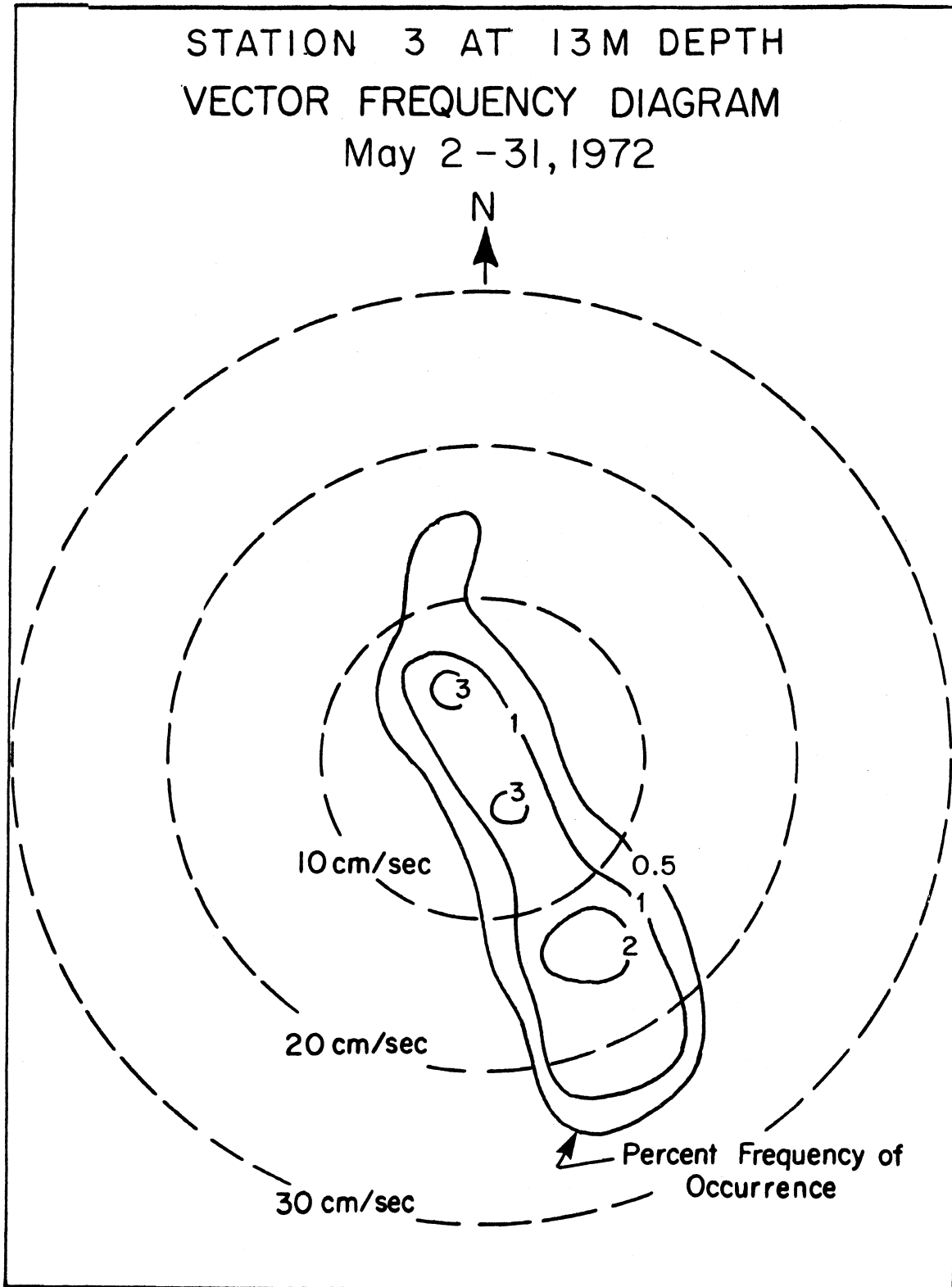


Figure 4.10

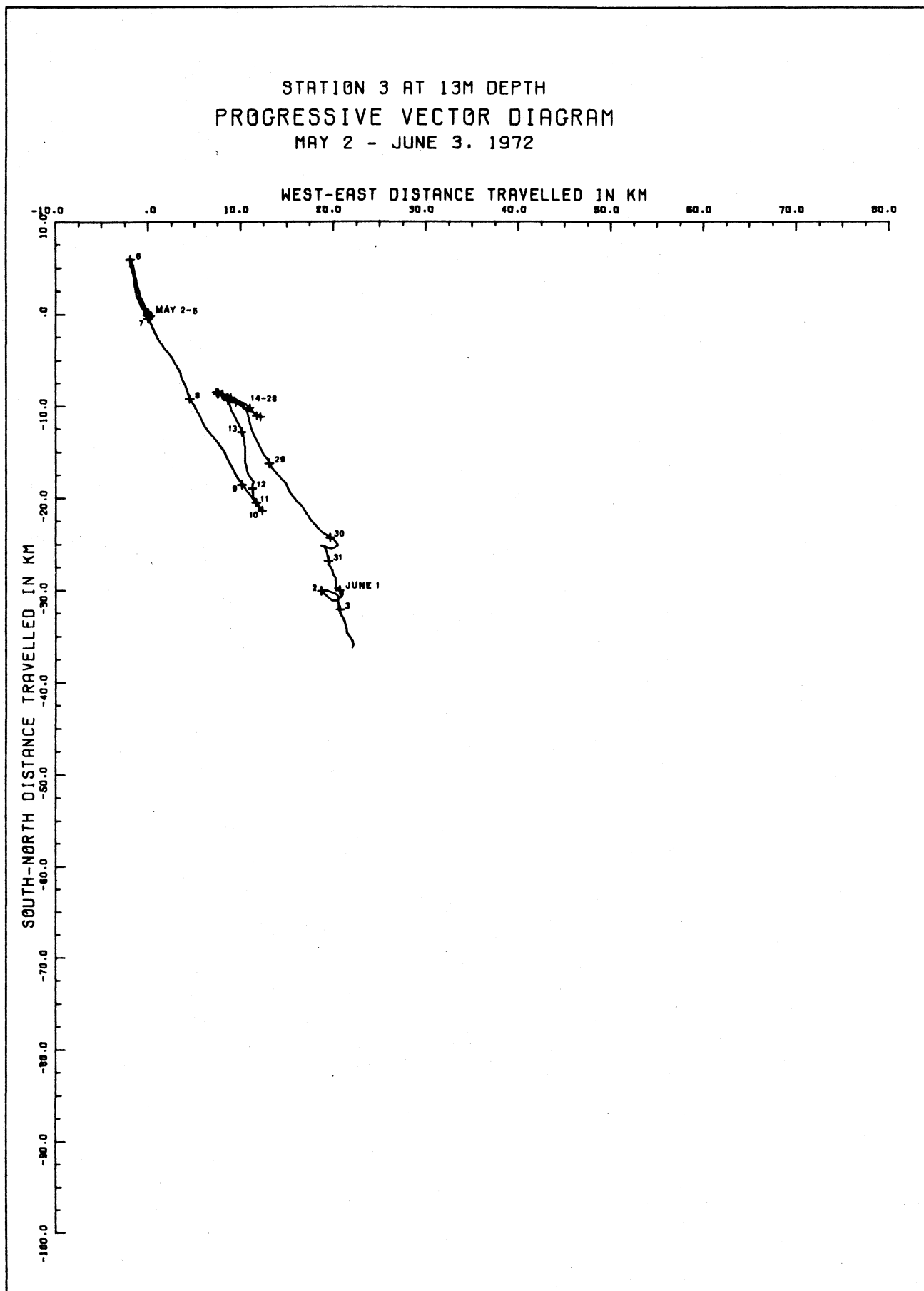


Figure 4.11

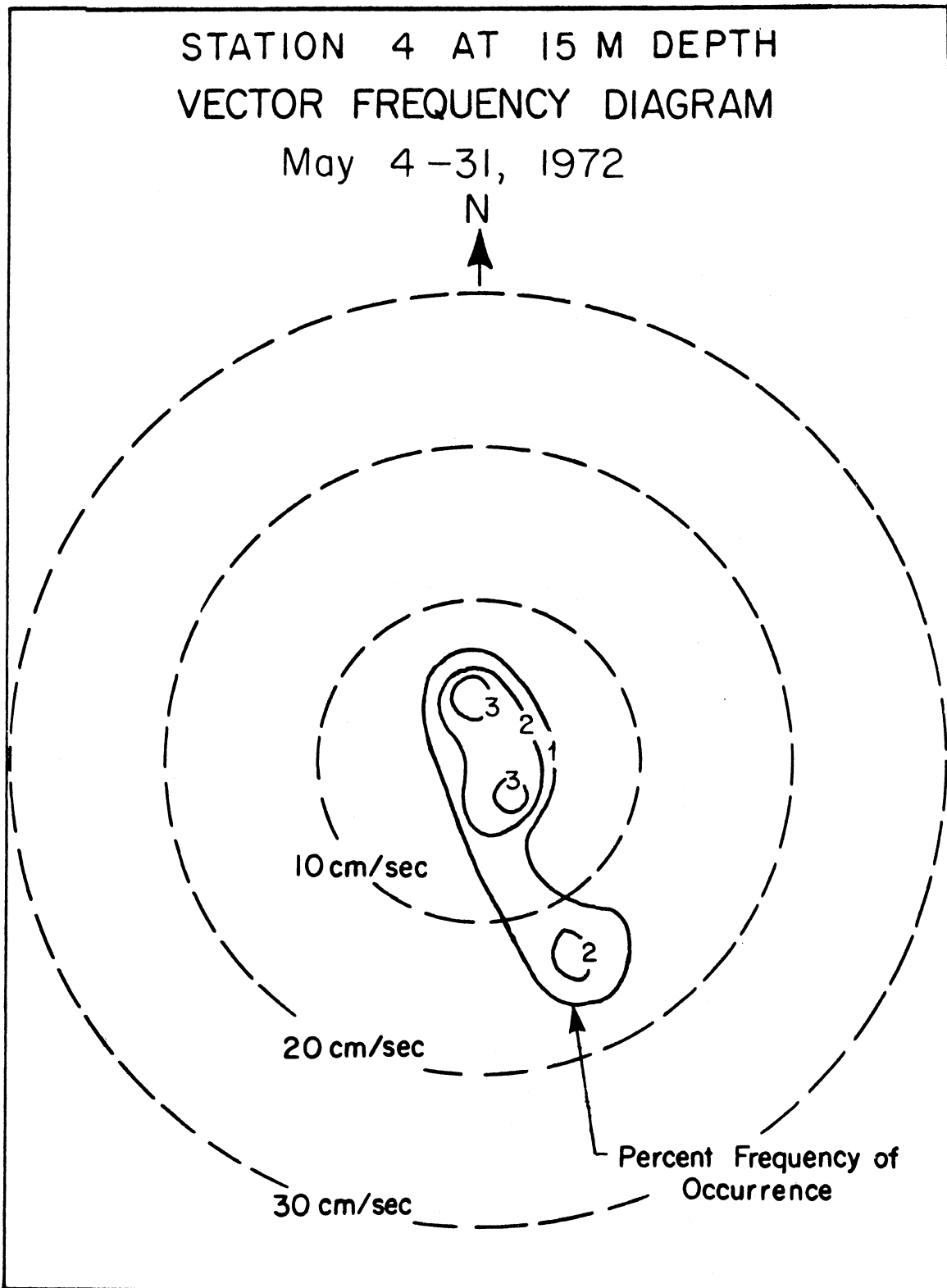


Figure 4.12

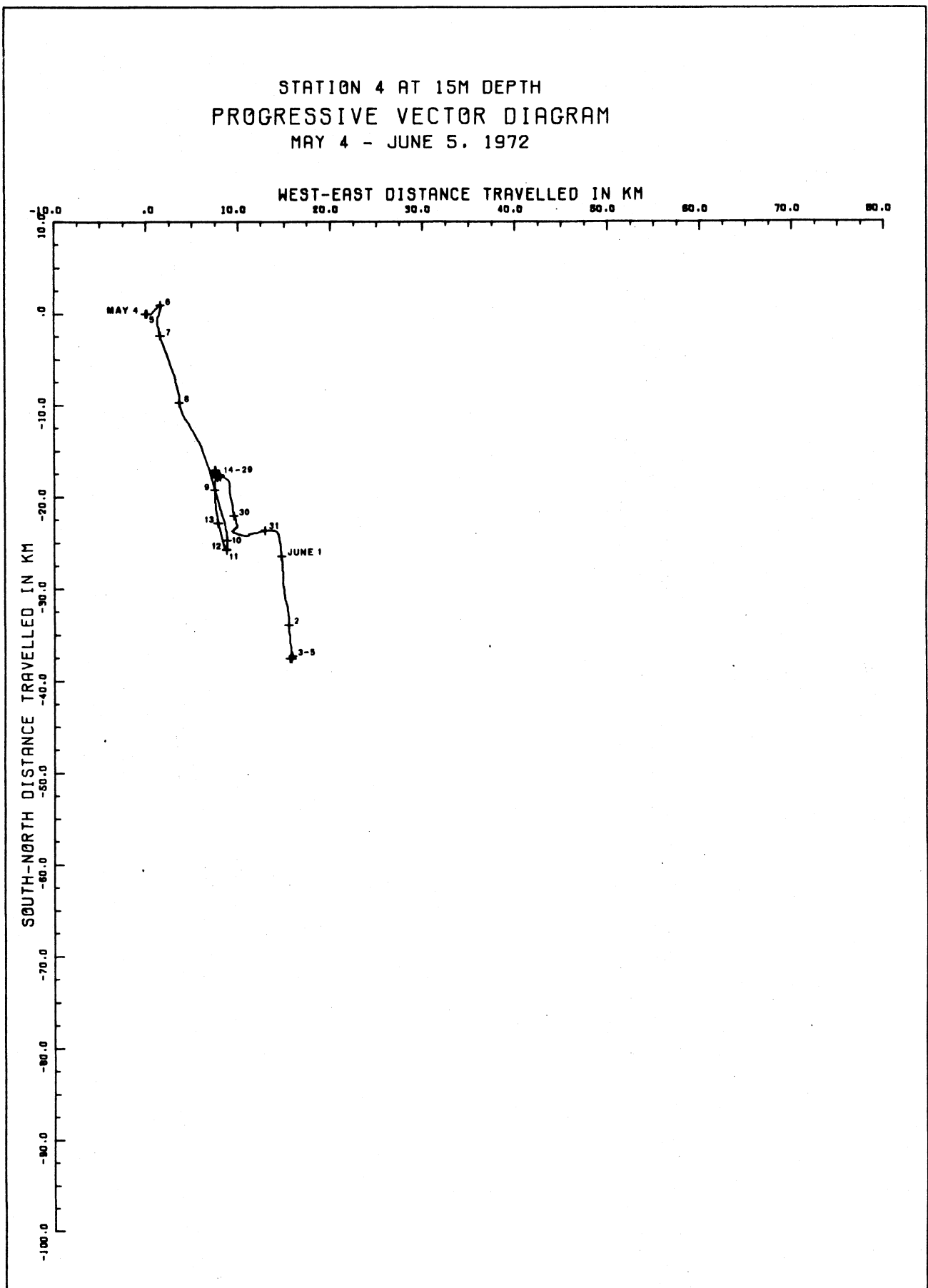


Figure 4.13

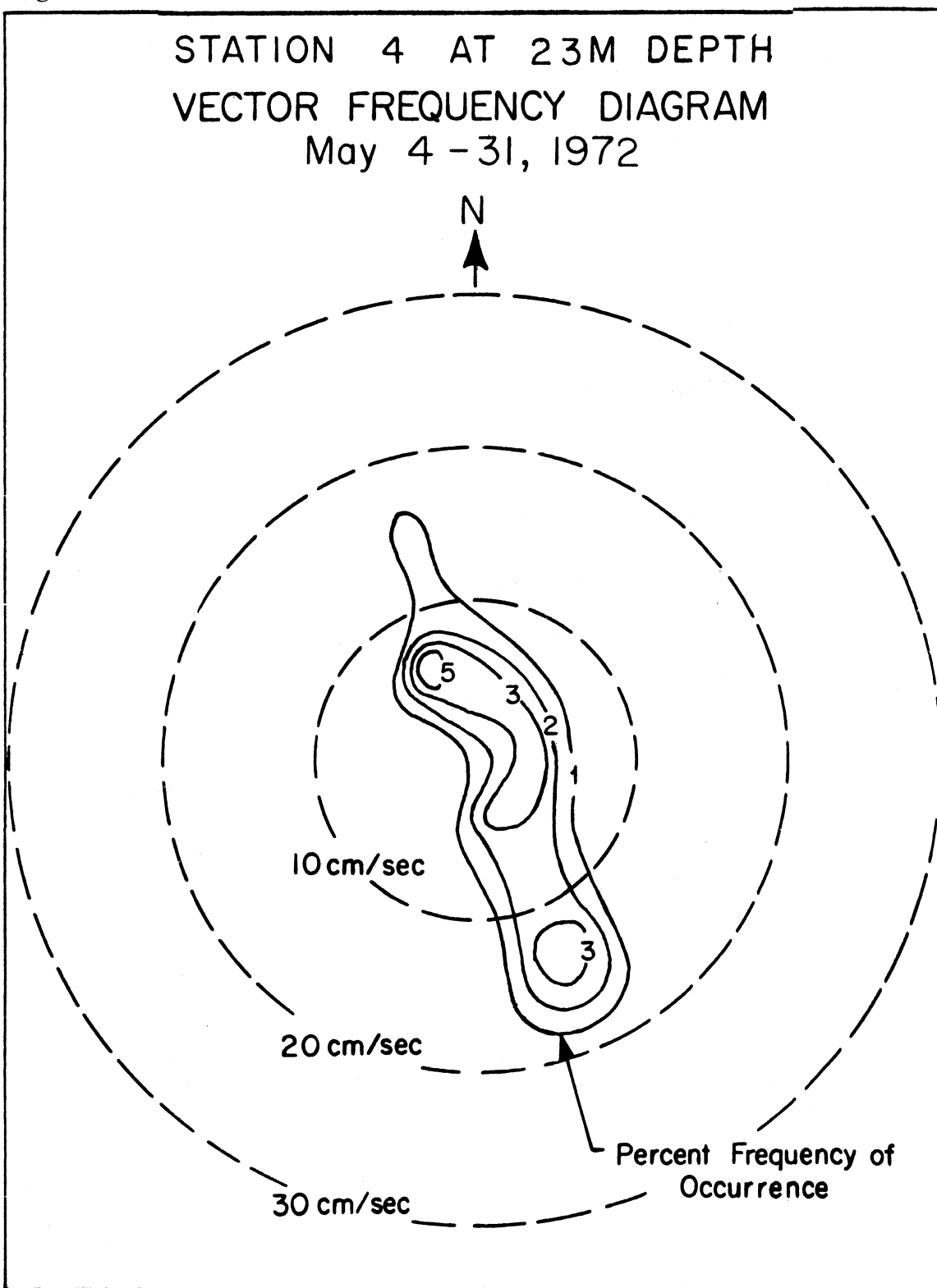


Figure 4.14

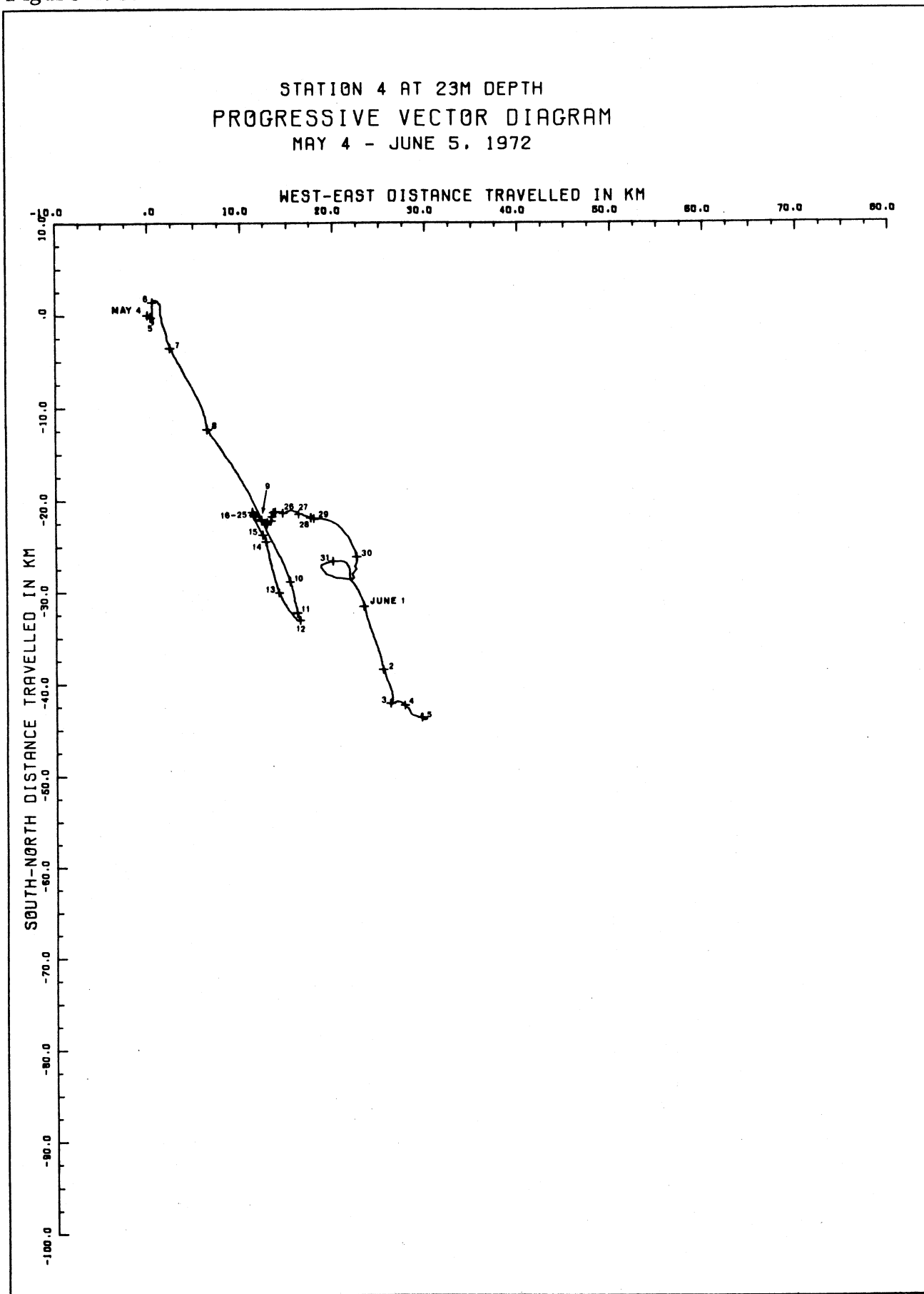


Figure 4.15

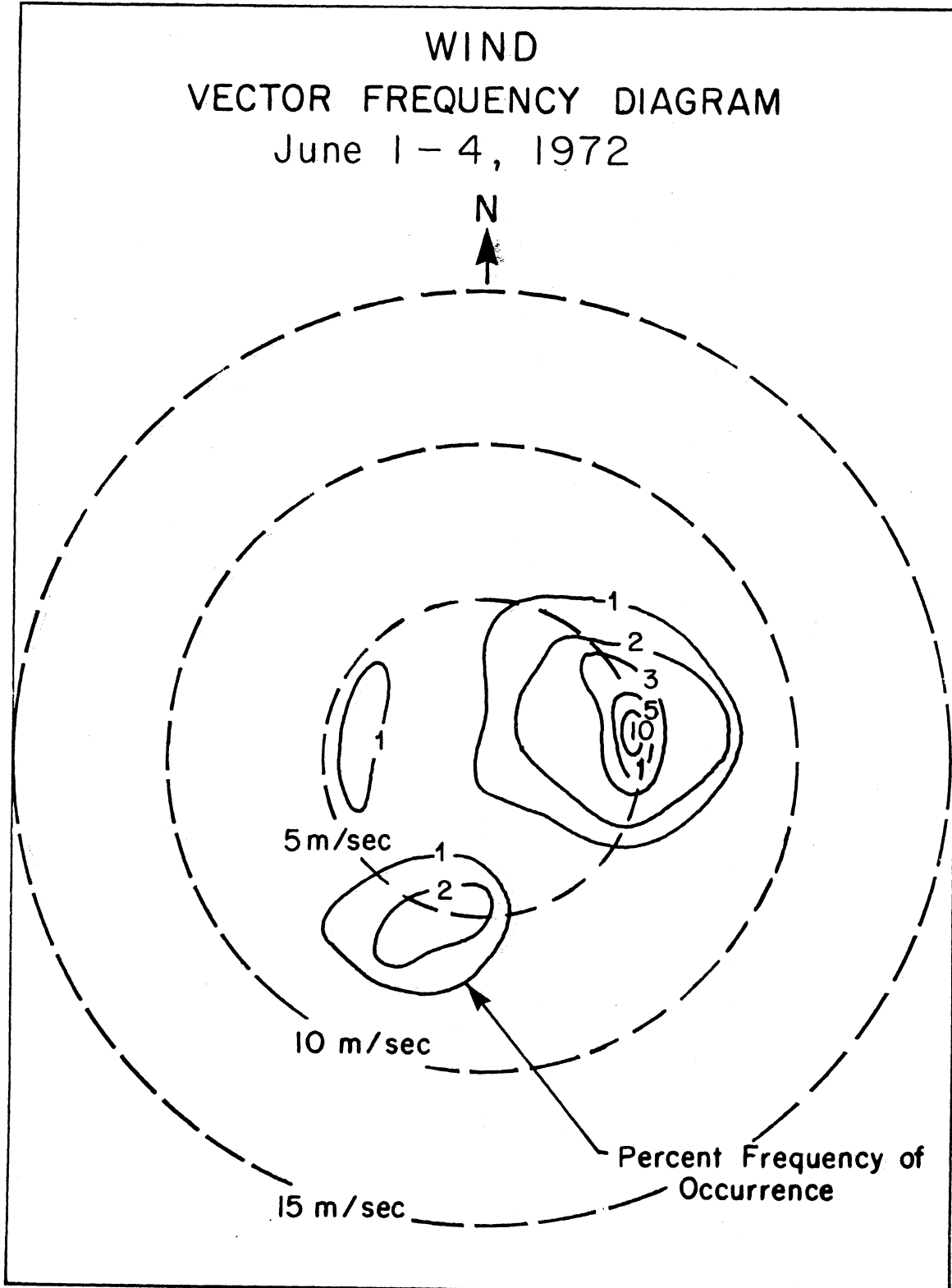


Figure 4.16 The corresponding progressive vector diagram is on page 165.

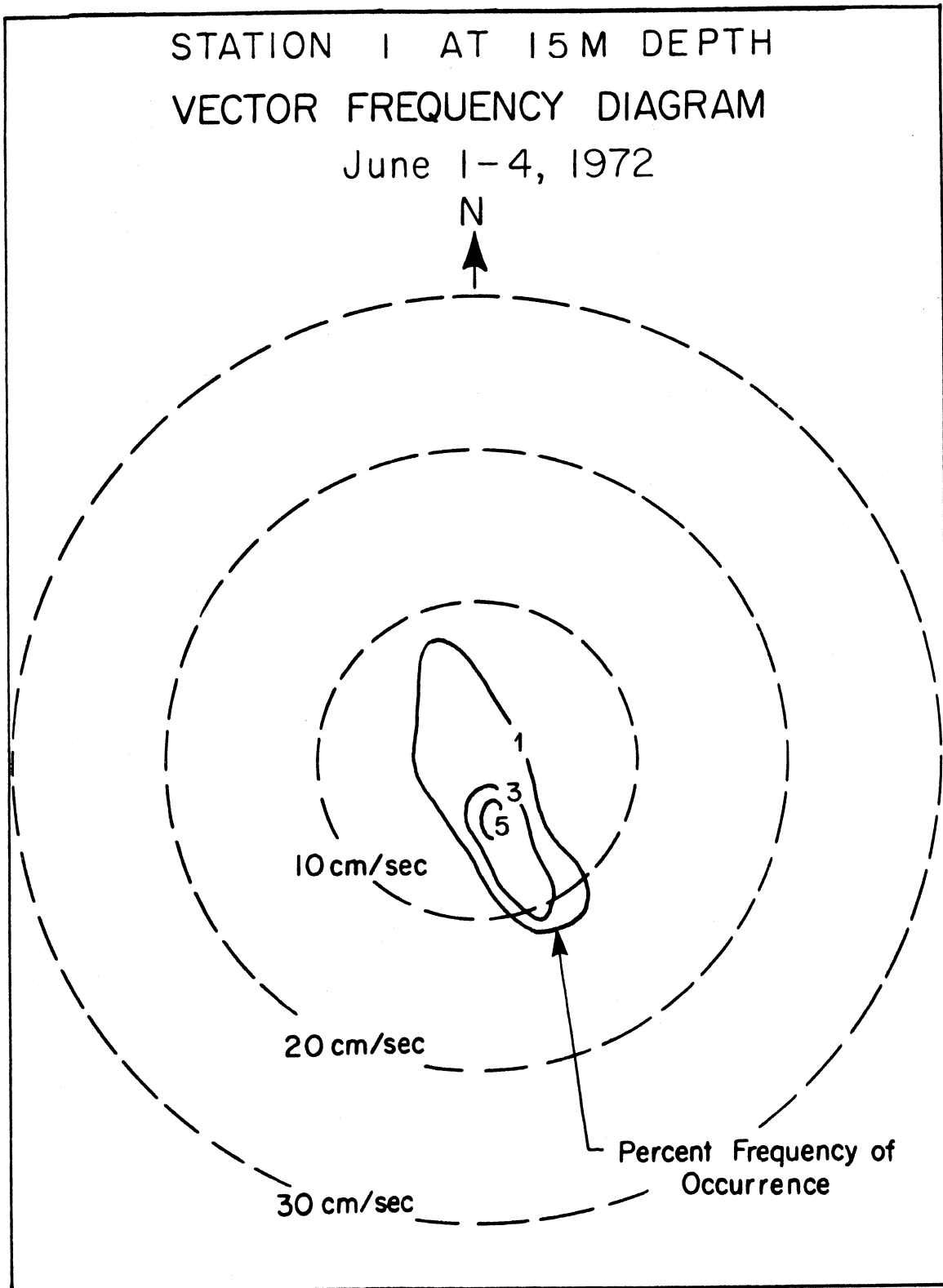


Figure 4.17 The corresponding progressive vector diagram is on page 167.

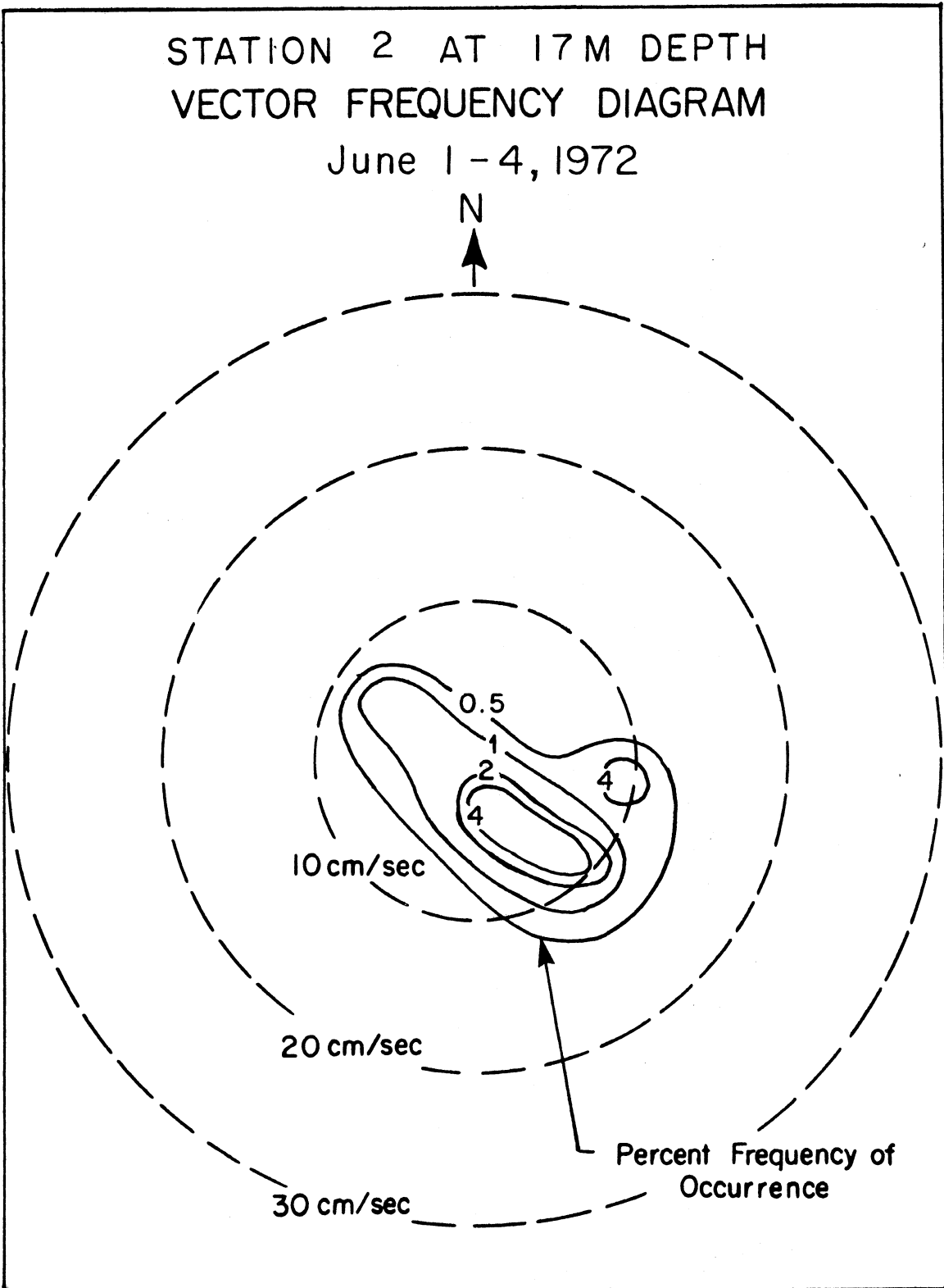


Figure 4.18 The corresponding progressive vector diagram is on page 169.

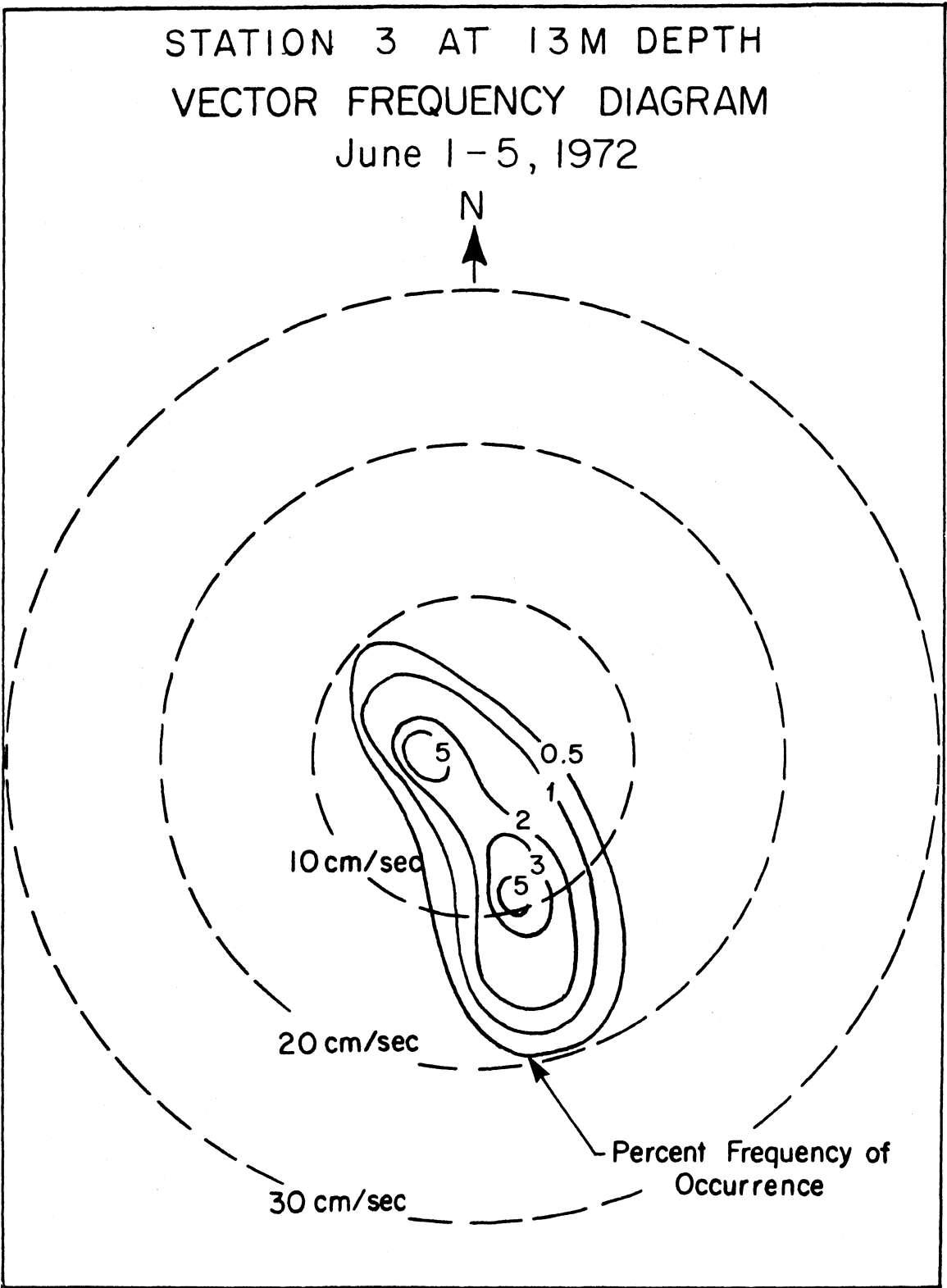


Figure 4.19 The corresponding progressive vector diagram is on page 171.

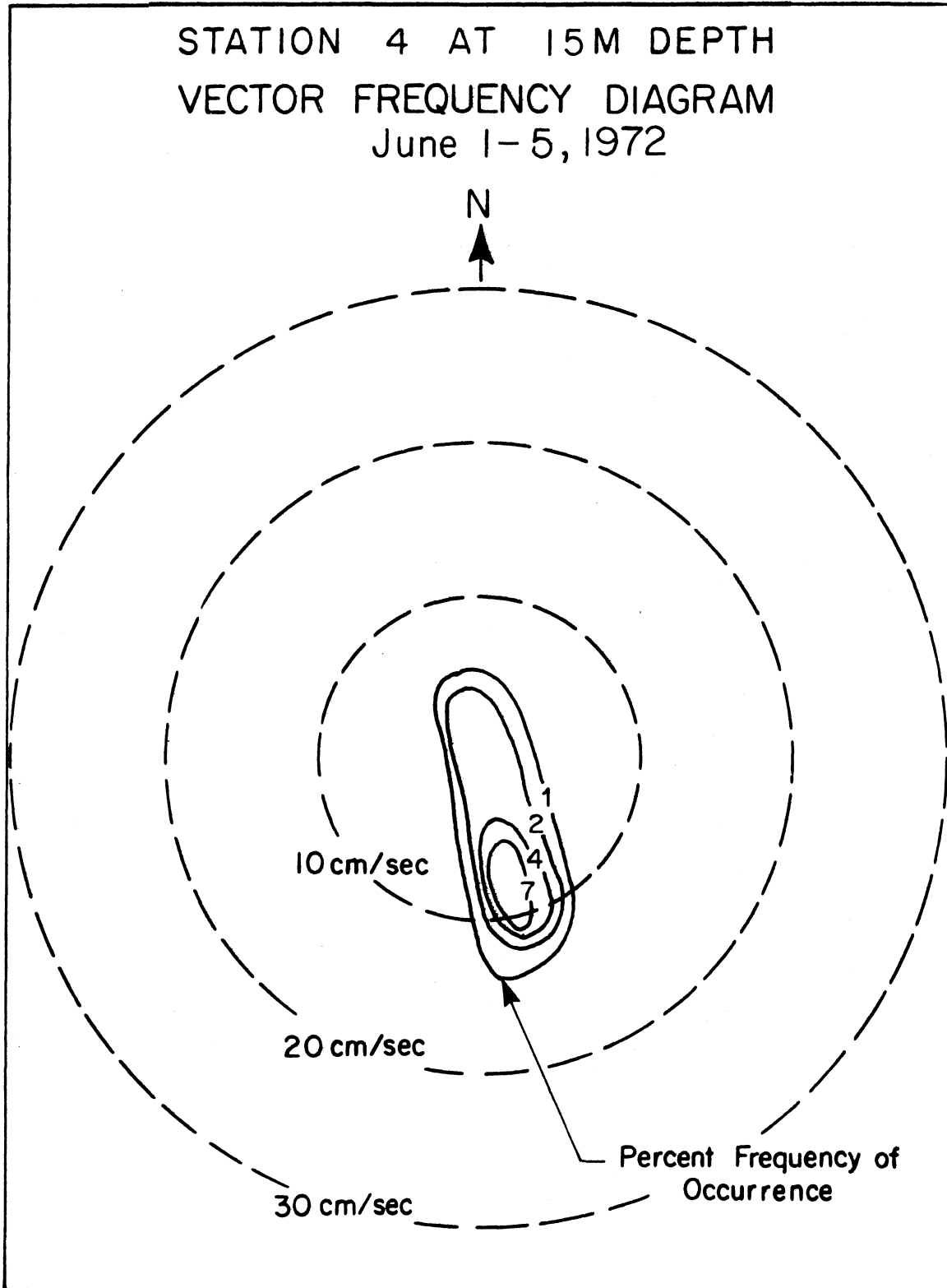
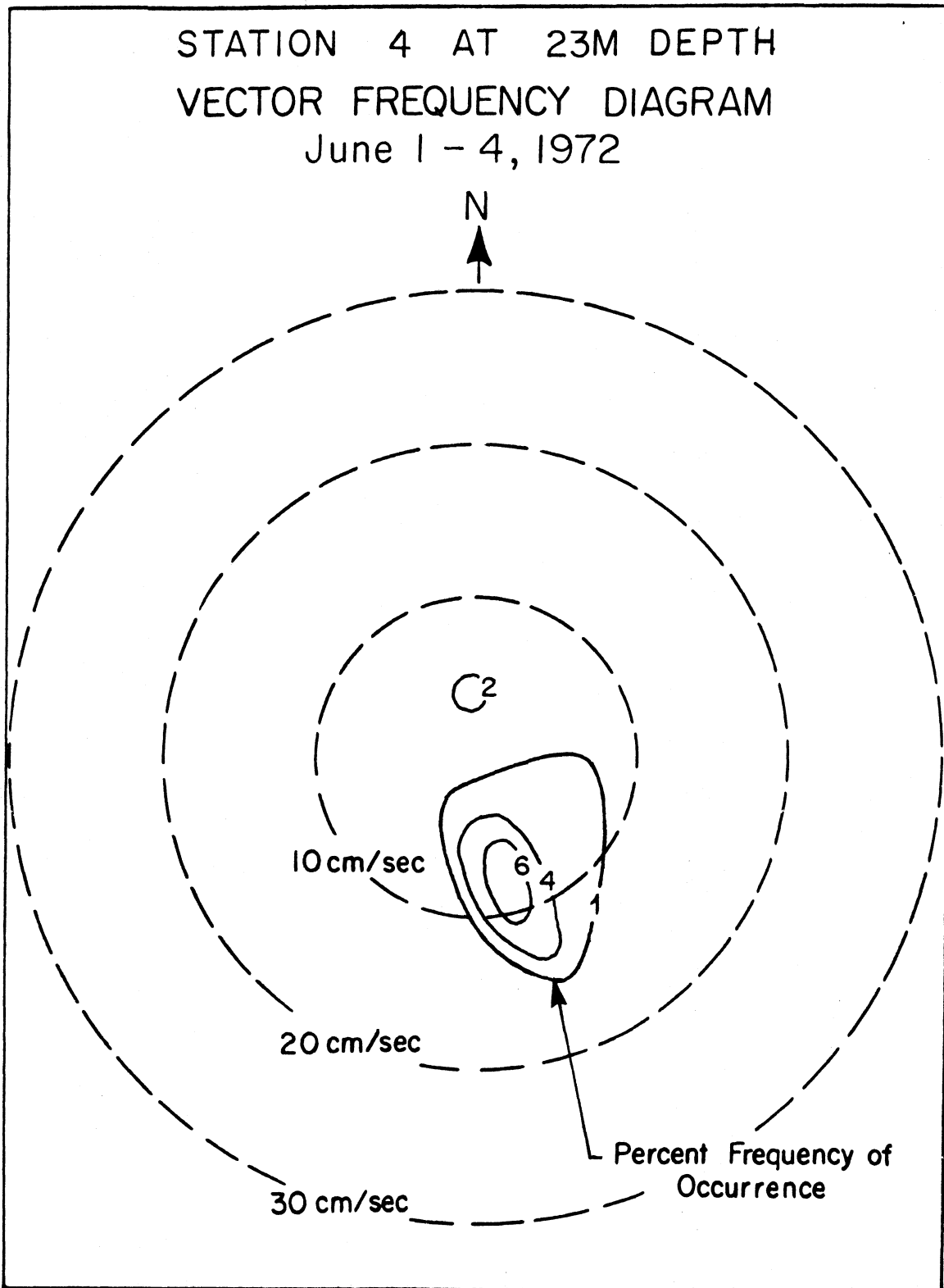


Figure 4.20 The corresponding progressive vector diagram is on page 173.



currents were toward SSW or NNW and shore-parallel. Station 3 showed the strongest currents, with an 0.5% frequency isopleth as high as  $25 \text{ cm. s}^{-1}$  (fig. 4.9). Greater between-station variability was found in the weak current range,  $0-5 \text{ cm. s}^{-1}$ .

During the first four days of June the strongest winds were eastward (fig. 4.15), but the currents at Stations 1, 3, and 4 persisted toward SSE (figs. 4.16, 4.18, 4.19, and 4.20), with a more southeasterly trend at Station 2 (fig. 4.17).

#### Survey II, 5 June to 25 August 1972

For the remainder of June the strongest winds were directed slightly west of south, with weaker episodes toward northeast (fig. 4.21). Currents at Station 3 were strongly bi-directional, southeastward and northwestward (fig. 4.22) showing reversals 10 and 15 June (fig. 4.23). A southeastward trend continued for that station during the first five days of July (fig. 4.32). The same trend, during June, with less northeastward current, was shown at Stations 6 (fig. 4.28), 8 (fig. 4.29) and 4 (figs. 4.26 and 4.27) 23 m depth; but the instrument at 16 m depth at that station recorded more easterly currents (toward ESE) after 22 June (figs. 4.24 and 4.25). This throws doubt on the reliability of that particular instrument at least during the last week of June. Station  $T_2$  (fig. 4.31) showed dominance of current toward SSE with the 0.5% frequency isopleth reaching  $30 \text{ cm. s}^{-1}$ . At Station  $T_1$ , on the other hand, current directions are more variable (fig. 4.30, see also the progressive vector diagrams for these two stations in figures 4.41 and 4.43).

Because the moored instruments at Stations 3, 4, 6 and 8 were prematurely released on 14 July and drifted from their positions, the vector frequencies are presented here only for the interval 0 to 14 July (figs. 4.33 to 4.35, and 4.37), although for the purposes of later discussion some of the progressive vector diagrams have been extended beyond the release date, e.g. figures 4.36 and 4.38. Except for the 16 m instrument at Station 4 (fig. 4.34), the records of which we had reason to question for the latter half of June, the flow at the other moored stations (figs. 4.33, 4.35, and 4.37) was directed predominantly toward SSE during the 1 to 14 July interval, with a smaller response

[the text continues on page 195]

Figure 4.21

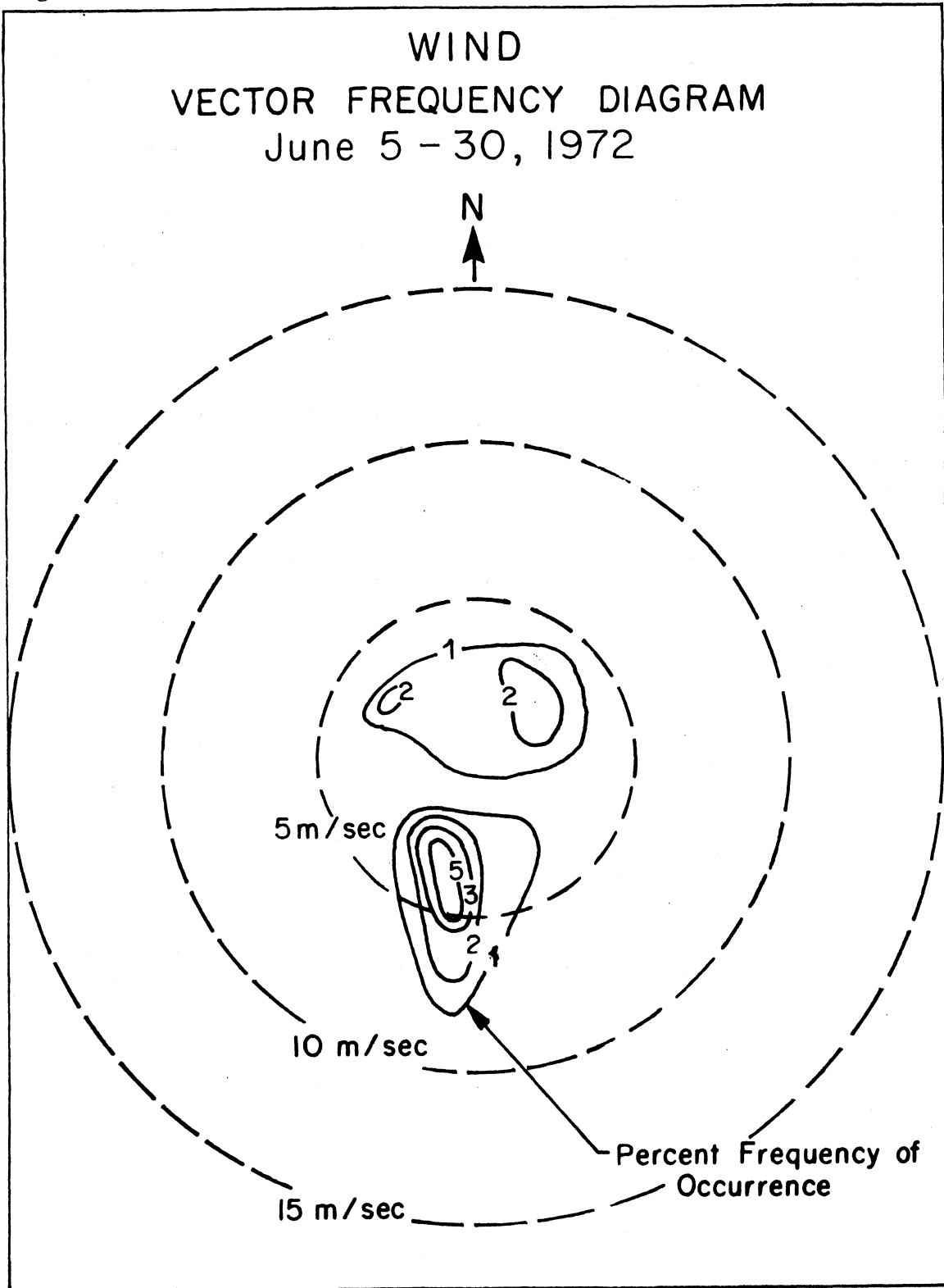


Figure 4.22

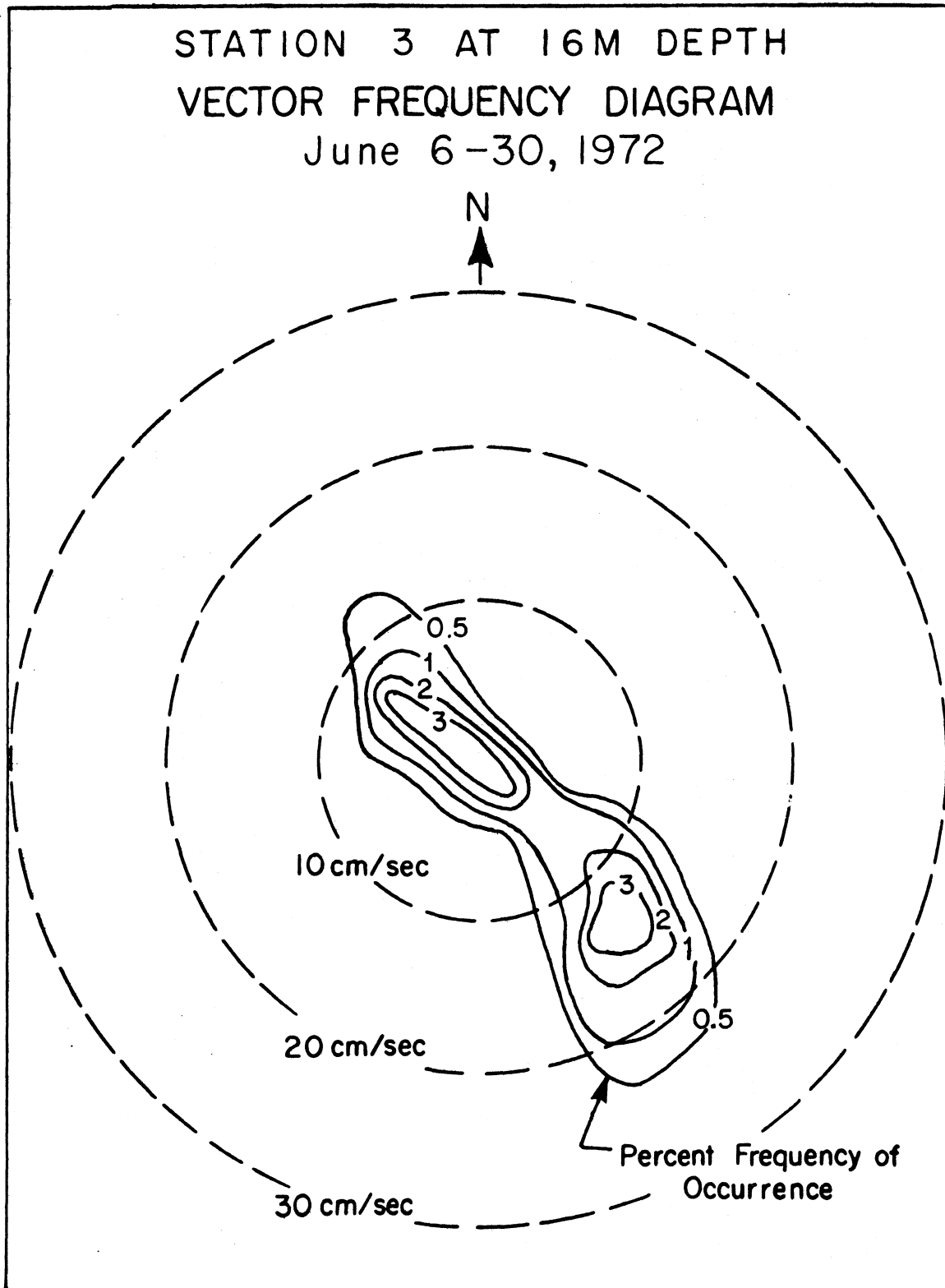


Figure 4.23

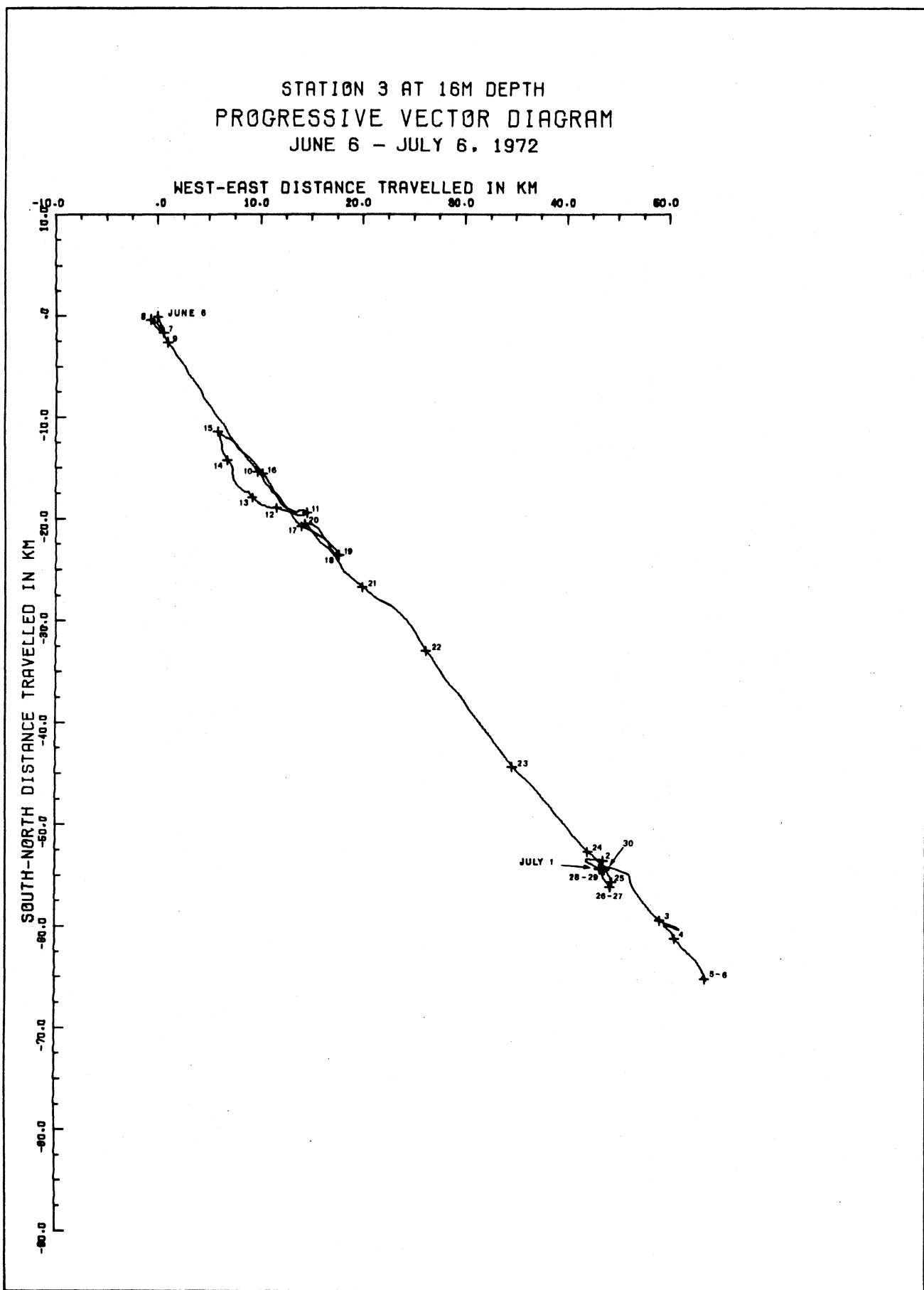


Figure 4.24

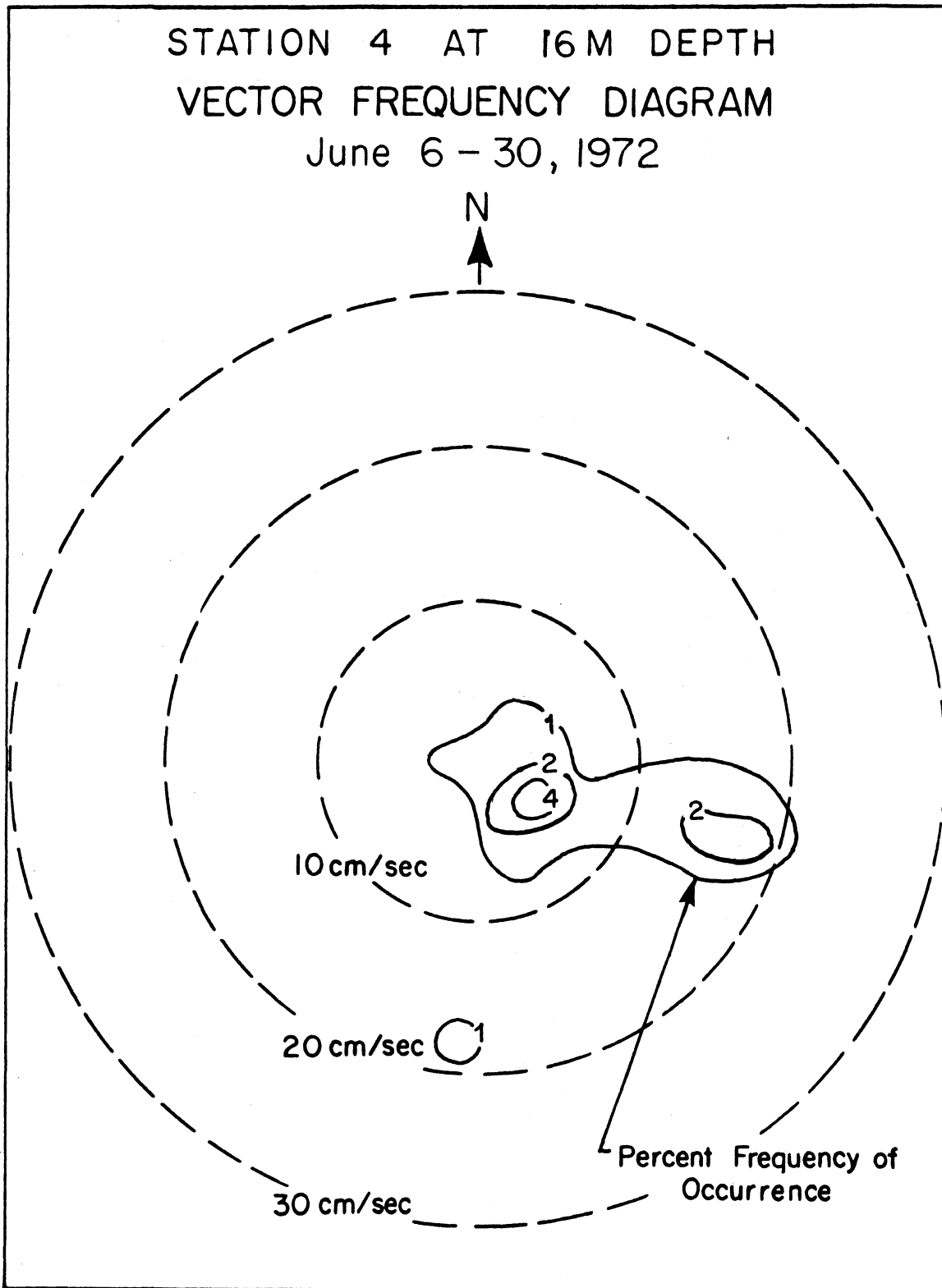


Figure 4.25

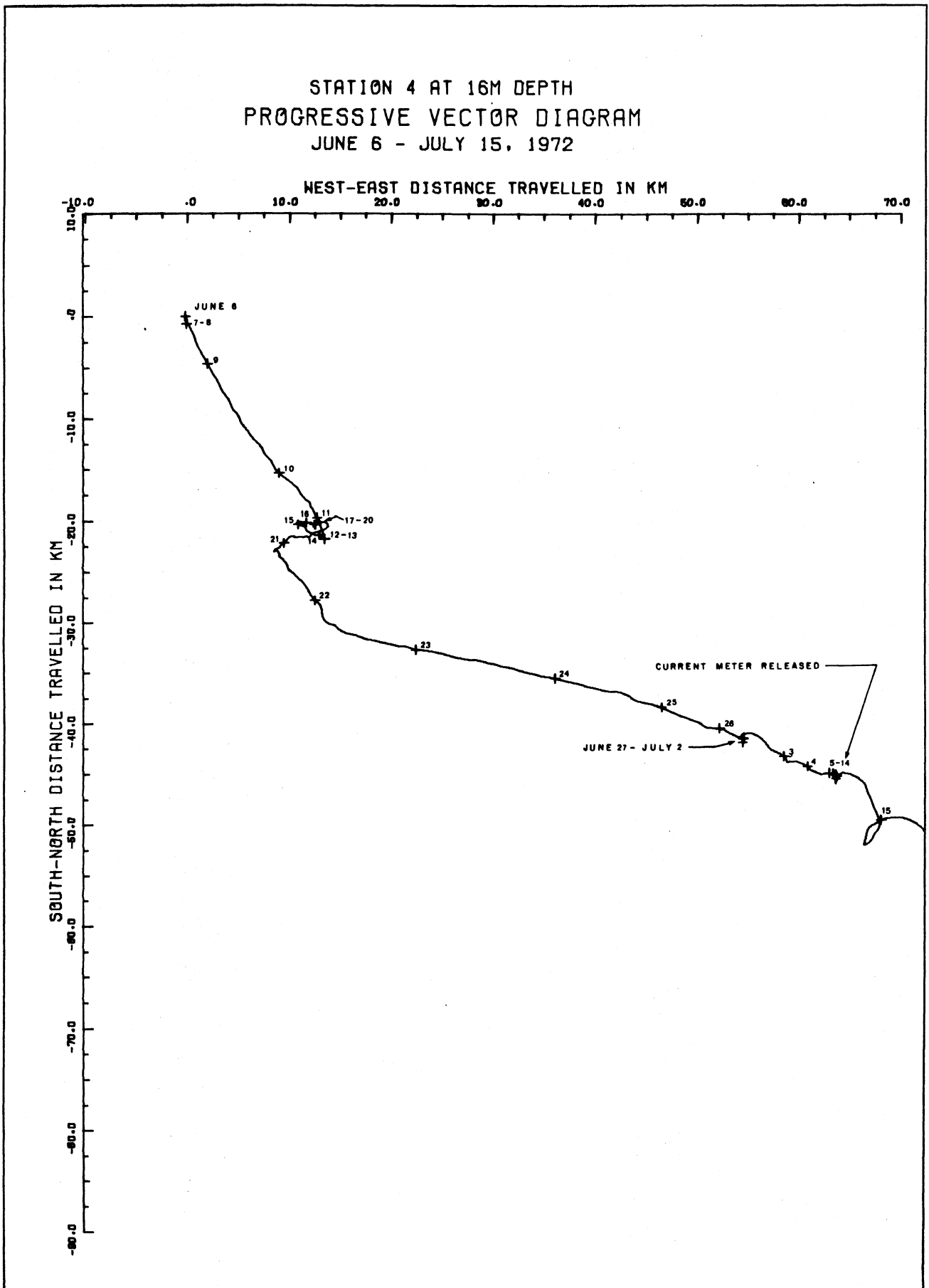


Figure 4.26

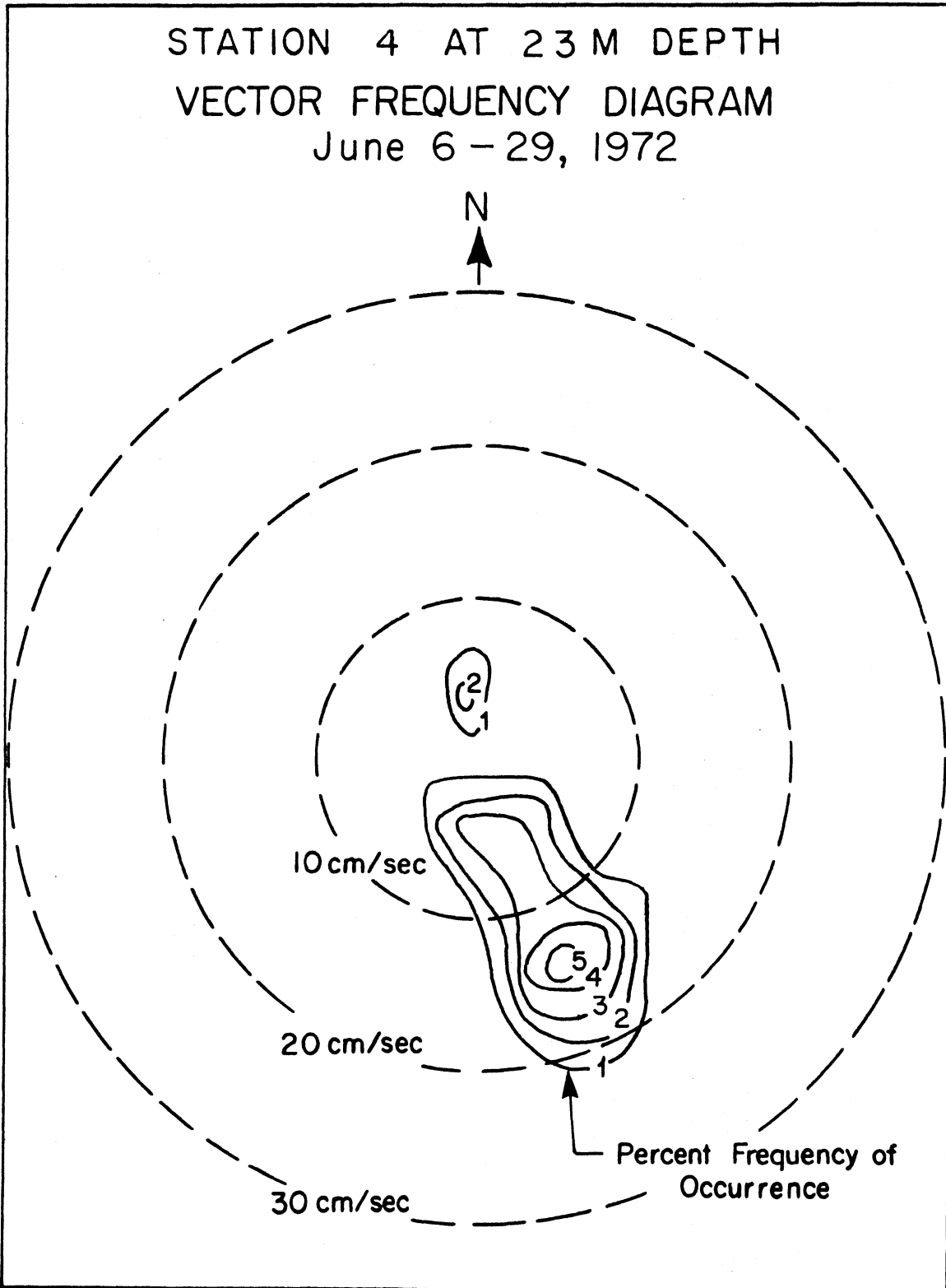


Figure 4.27

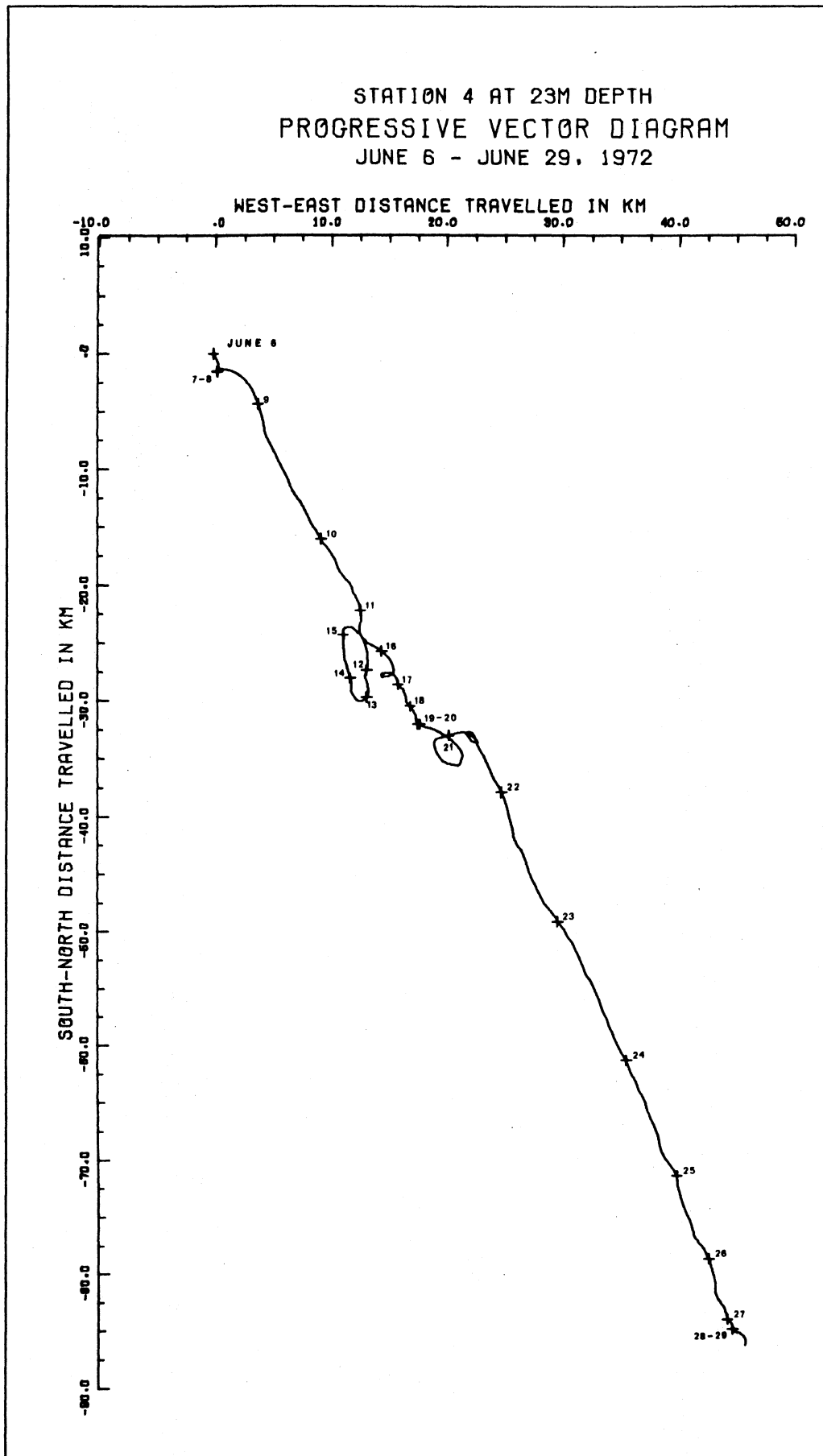


Figure 4.28 Corresponding progressive vector diagram is on page 197.

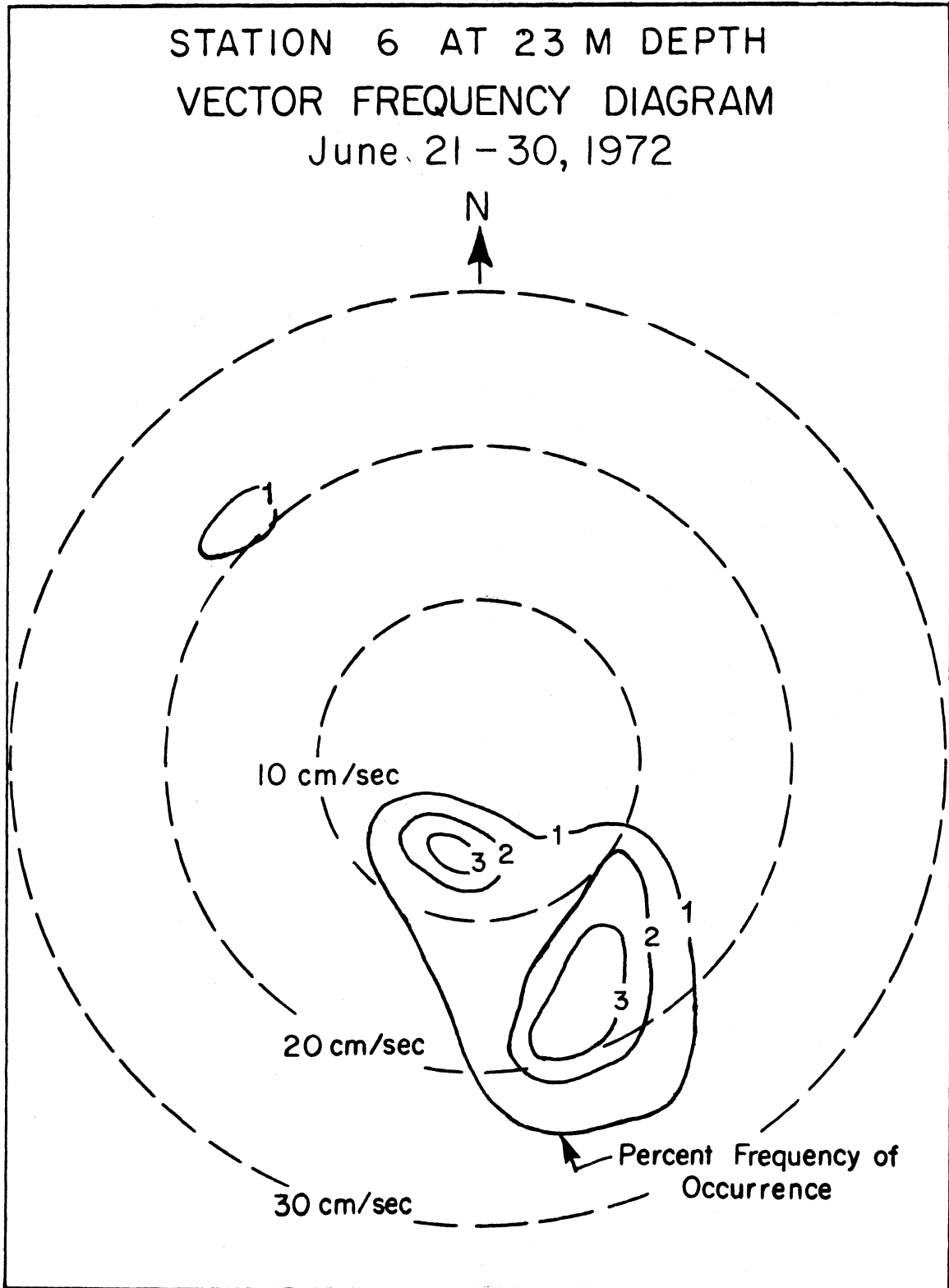


Figure 4.29 Corresponding progressive vector diagram is on page 199.

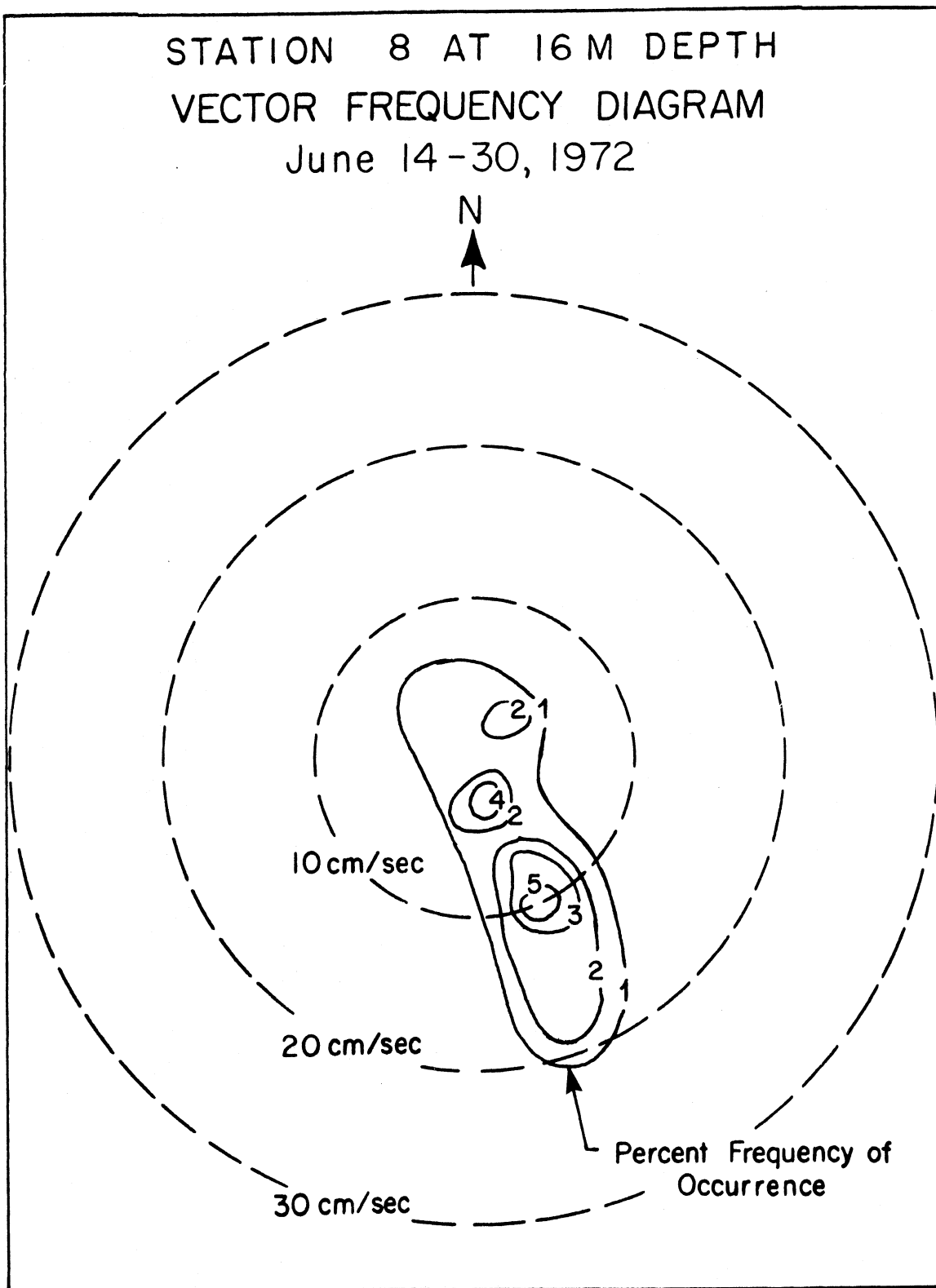


Figure 4.30 The corresponding progressive vector diagram is on page 203.

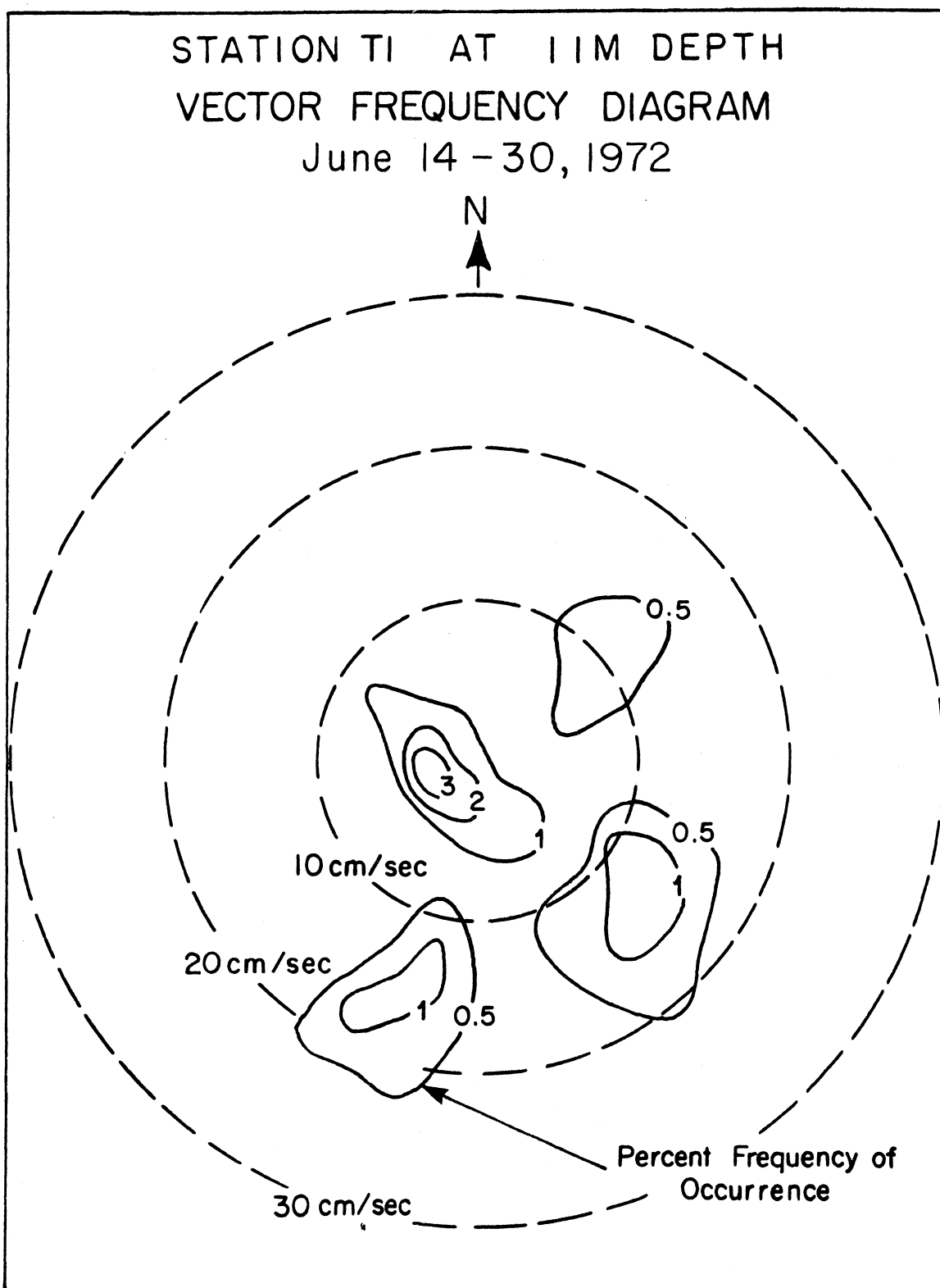


Figure 4.31 The corresponding progressive vector diagram is on page 205.

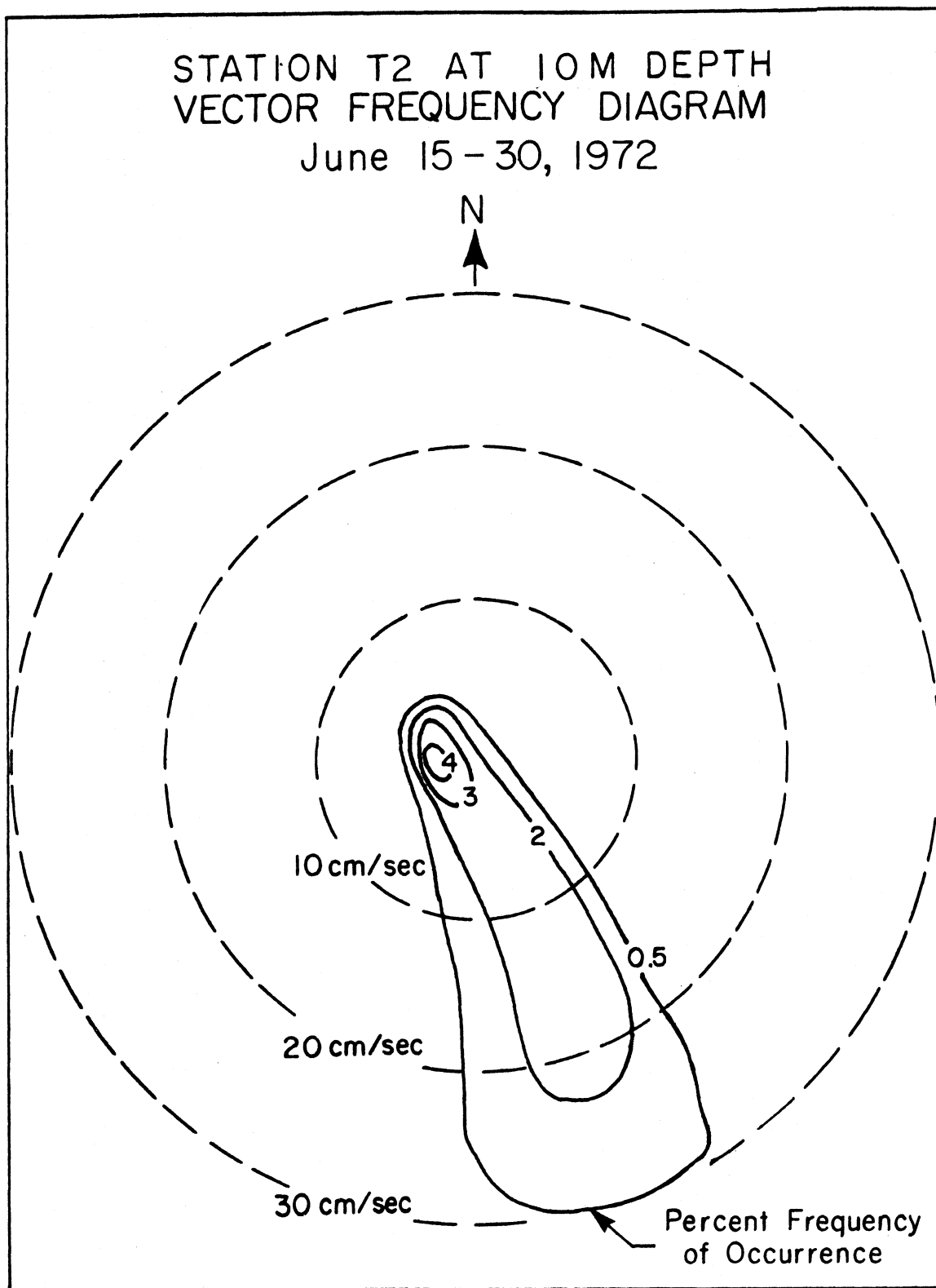


Figure 4.32

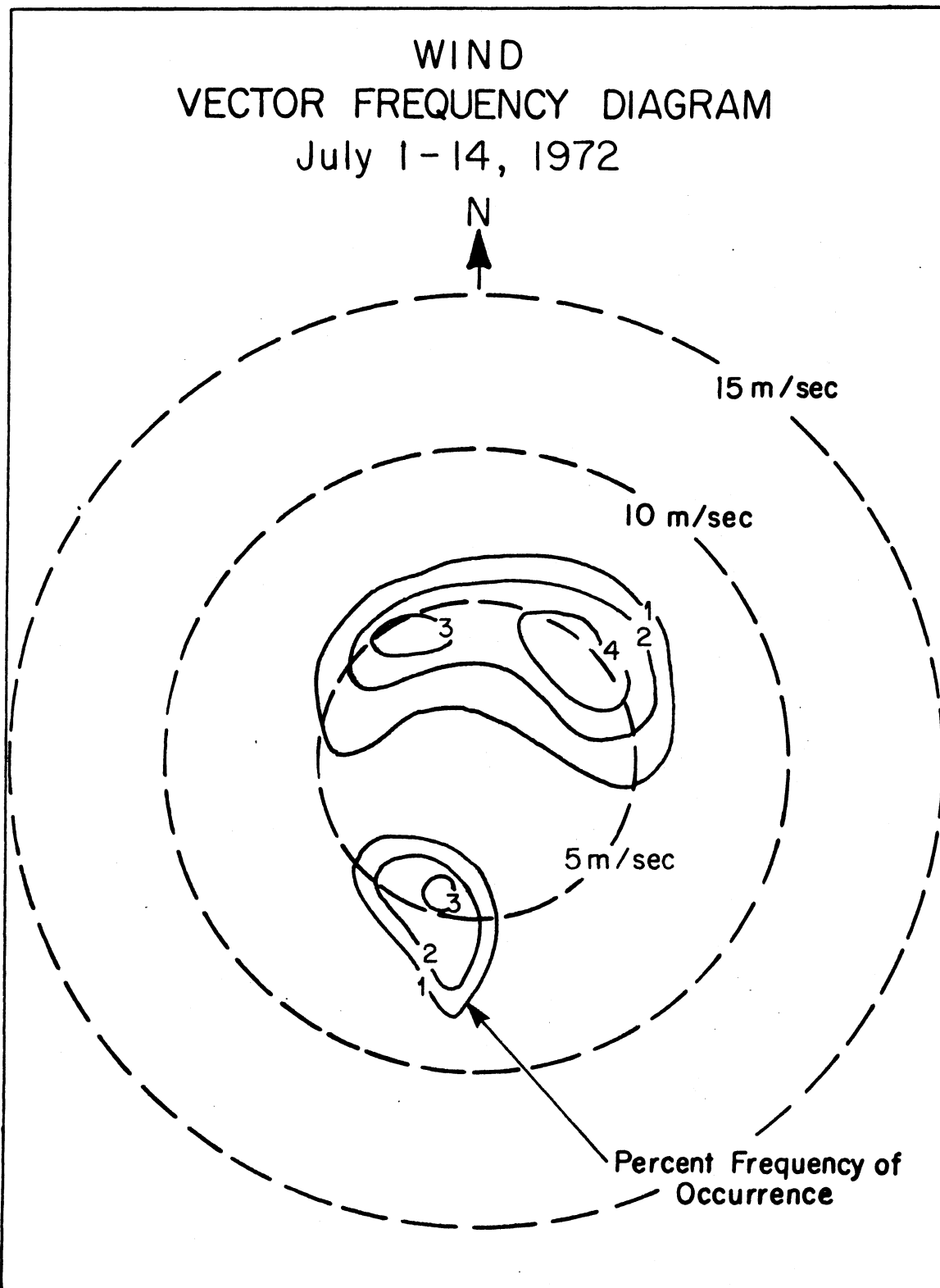


Figure 4.33 Corresponding progressive vector diagram is on page 183.

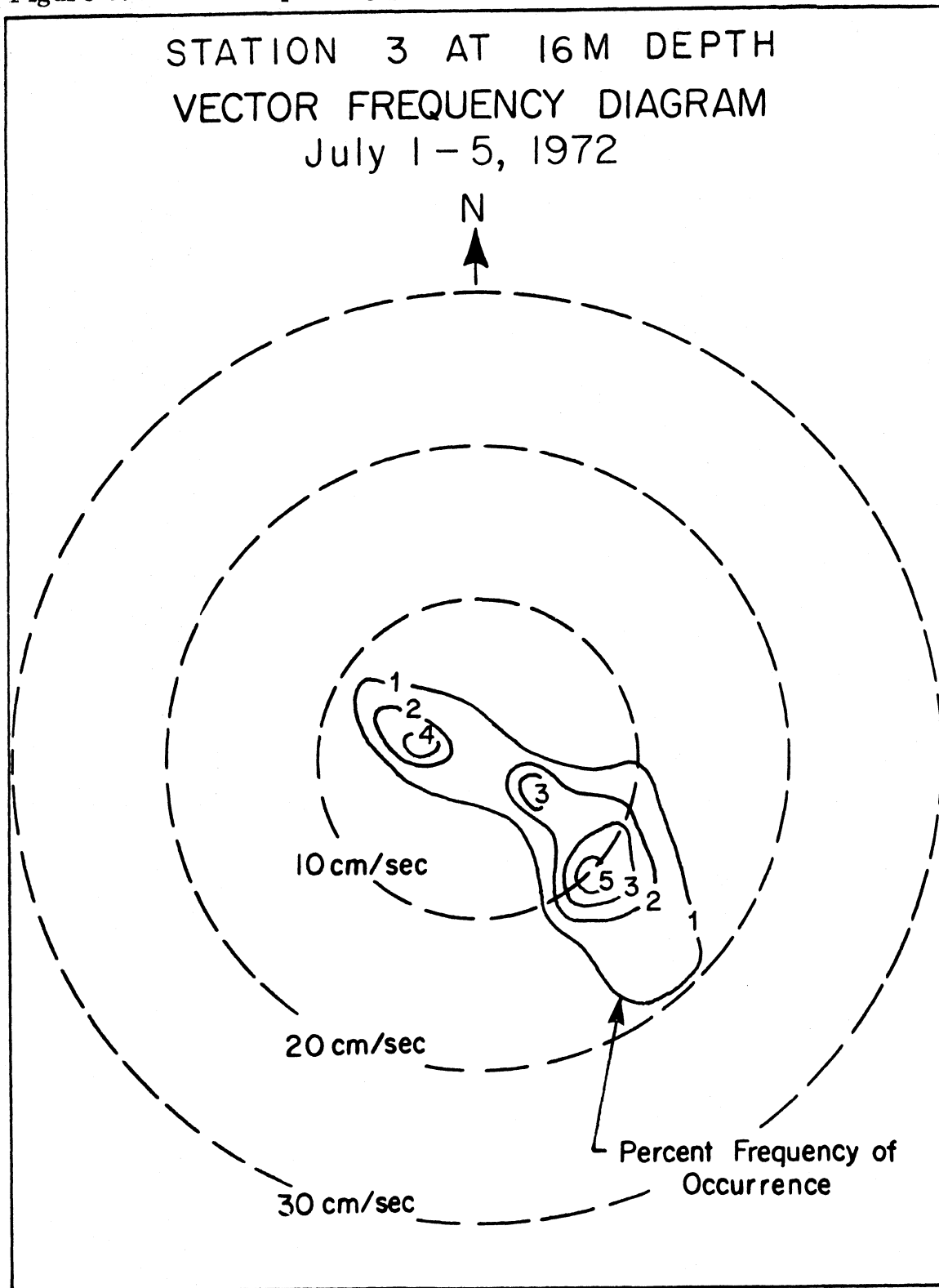
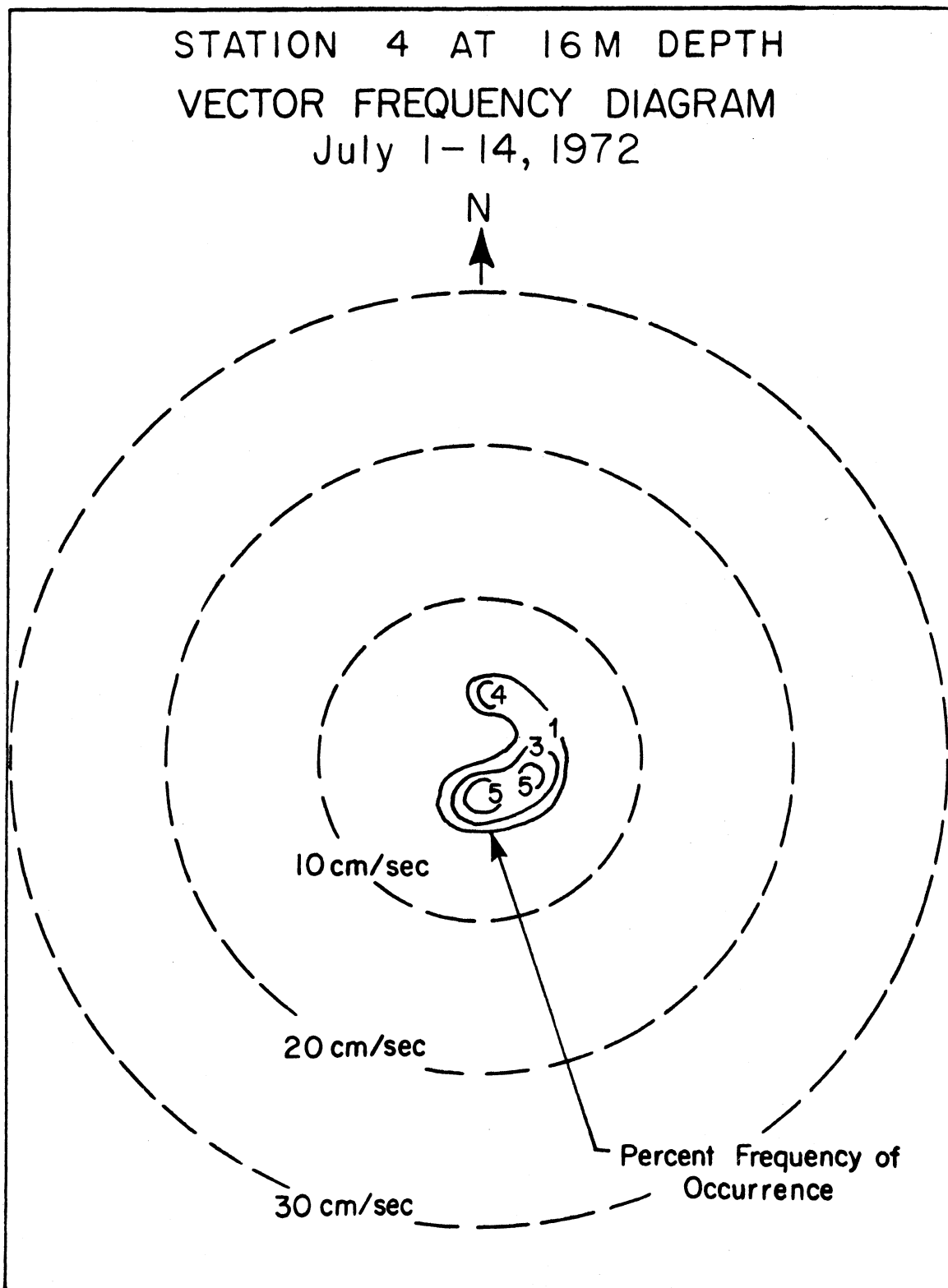


Figure 4.34 The corresponding progressive vector diagram is on page 185.



toward NNW. The corresponding wind diagram (fig. 4.32), on the other hand, exhibited a southward, a NNW-ward, and a northeastward component; but because of the smaller fetch of the latter component it produced little current response.

The wind diagram for the whole of July (figure 4.39) is similar to that described above for the first half of the month; and the corresponding current records from the tower stations ( $T_1$ , fig. 4.40 and  $T_2$ , fig. 4.42) show generally weak currents with a southeasterly trend, particularly at  $T_2$ .

Before the premature release, the progressive vector diagrams for Stations 6 and 8 (figs. 4.36 and 4.38) showed predominance of flow toward SSE but with some flow in the reverse direction. After the release on 14 July, the directions recorded were the resultant of (a) the drift of the mooring away from its earlier fixed position and (b) the motion of the water mass through which the instrument was being dragged, mainly by wind stress on the float, then at the surface. Component (a) is therefore  $180^\circ$  opposed to the direction in which the mooring was drifting -- predominantly northerly for both Station 6 and Station 8, but with some more easterly excursions for the former. As a consequence, the Station 8 instrument (and some others) were recovered near Sheboygan, Wisconsin, whereas the Station 6 instrument was picked up in the eastern part of the lake near Ludington, Michigan. In both cases the diagram for the stations shows evidence of rotary motion beginning after the release on 16 July and probably a contribution from component (b), i. e. Poincaré wave rotating currents in the upper layer, through which the instrument was being dragged, by a combination of wind drag on the surface float and the drag of sub-thermocline layer on the lower part of the mooring wire and SEDAR cylinder. The effect of rotary motion is most marked in the case of instrument 6 (fig. 4.36) the drift of which, as inferred, crossed the central region of the lake from its point of recovery.

For the remainder of 1972 only the tower instruments were operating. During August there were intervals of strong wind both in a northward and southward direction (fig. 4.44), but the current response at  $T_1$  was strongest toward the SE and less strong toward NW (fig. 4.45). The generally

[the text continues on page 201]

Figure 4.35

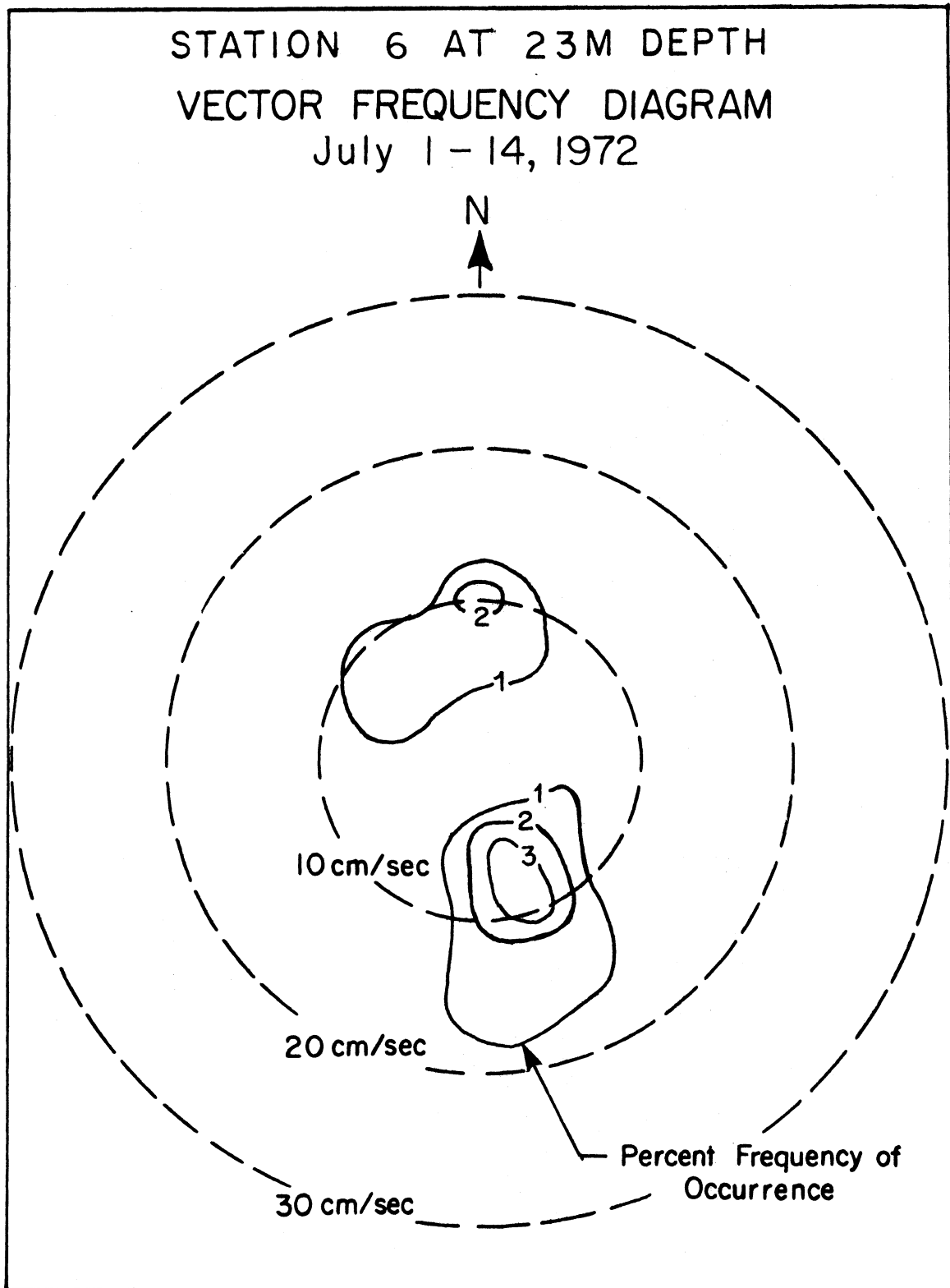


Figure 4.36

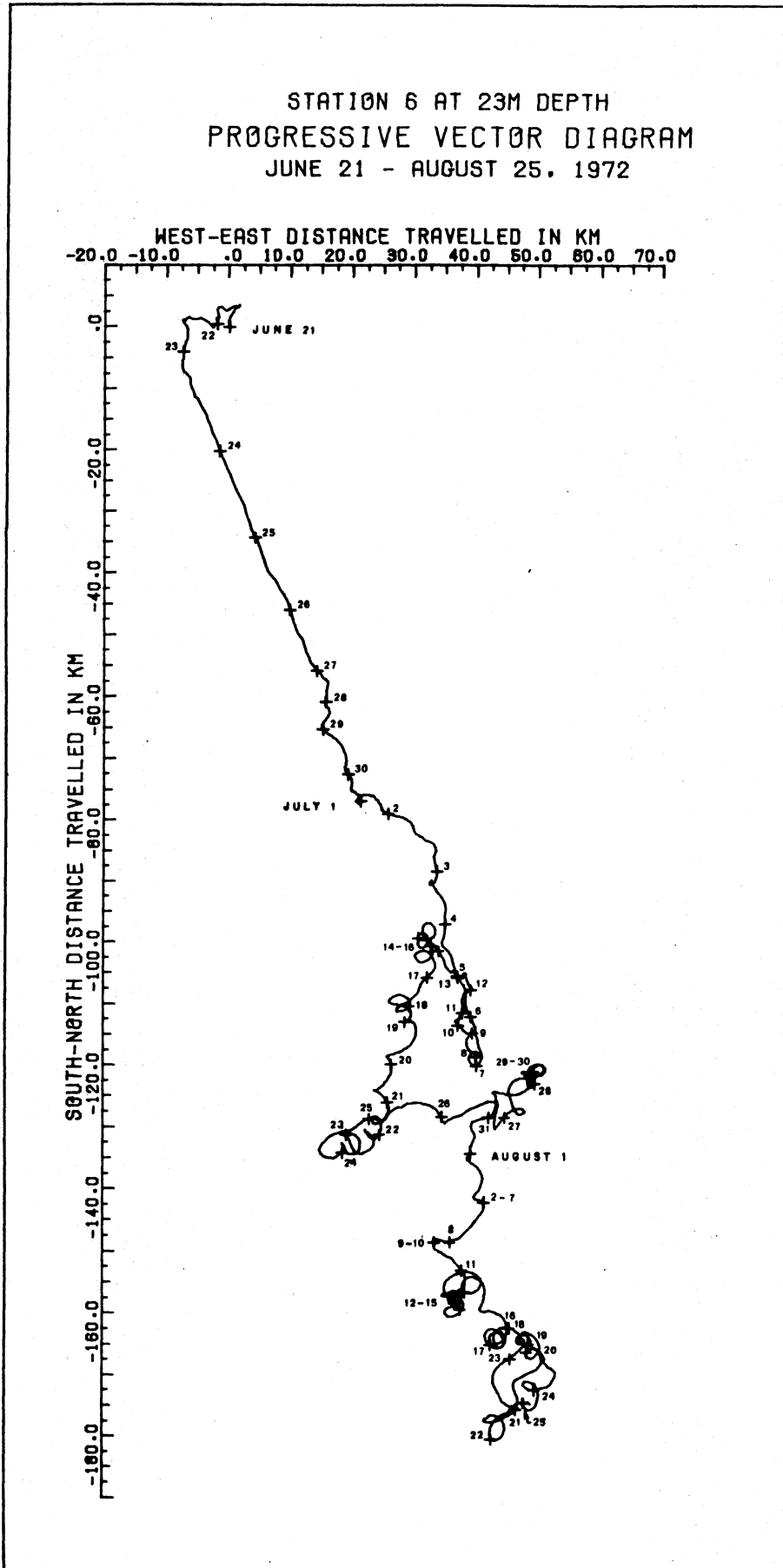


Figure 4.37

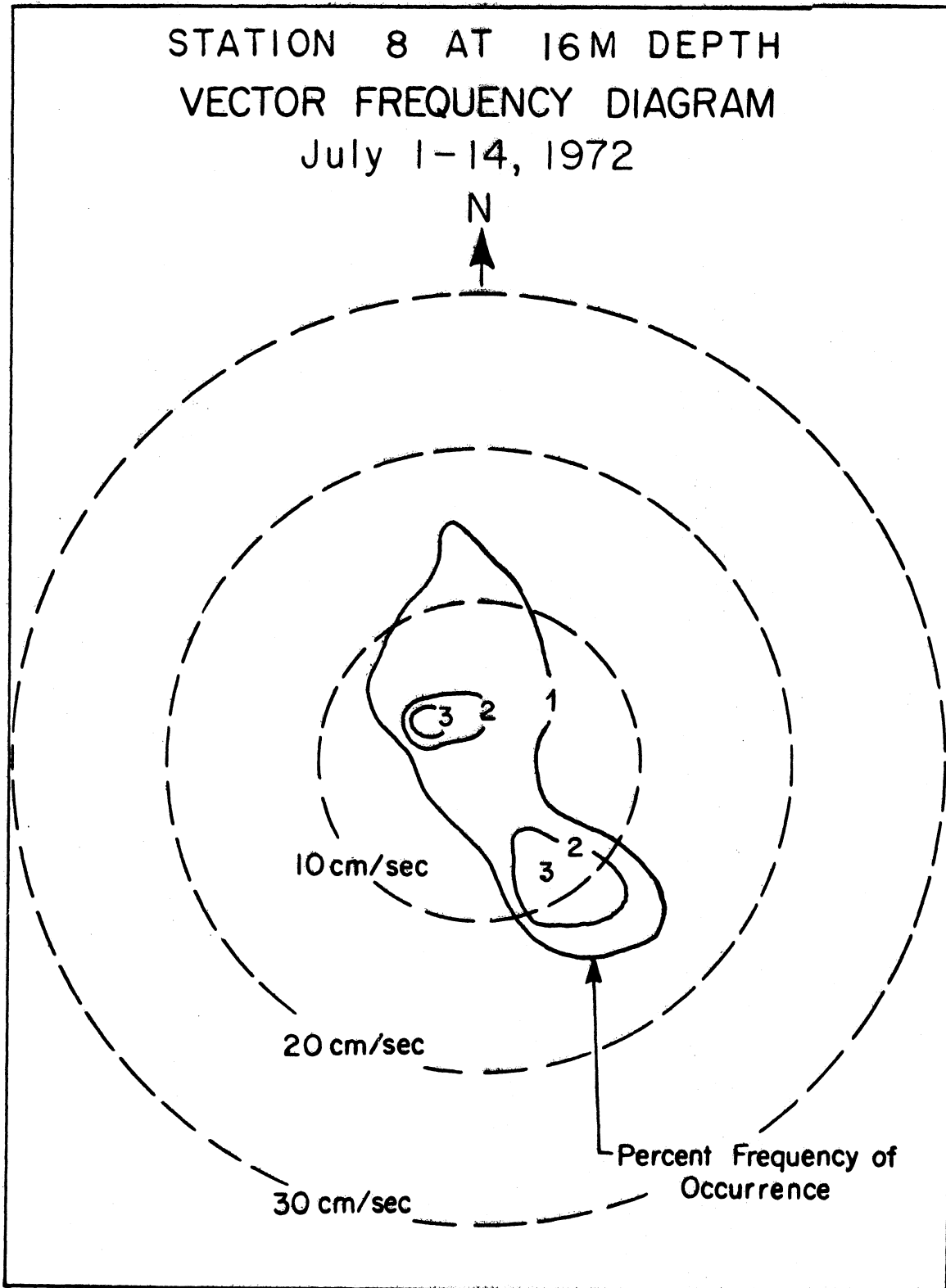
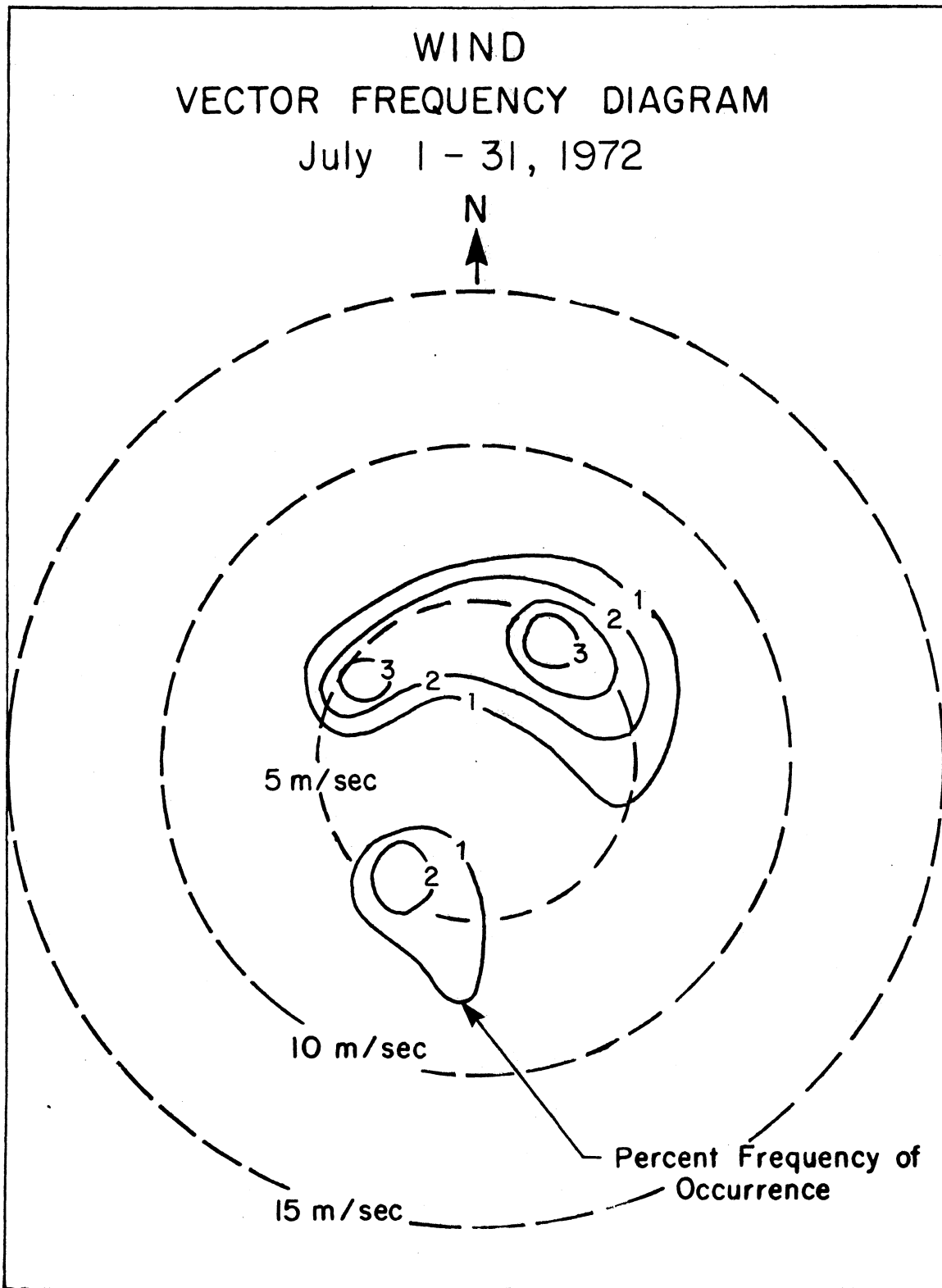




Figure 4.39



low speeds shown for Station  $T_2$  (fig. 4.46, and for the corresponding monthly plot in Chapter 3) are the result of failure of the speed sensor during August, also clearly shown by comparison of the  $T_1$  and  $T_2$  progressive vector diagrams for 3 to 22 August (figs. 4.41 and 4.43). The  $T_1$  diagram must be considered representative for August with predominantly southeastward flow with northwestward reversals of short duration.

### Survey III, 25 August to 25 November 1972

The strongest winds during September were toward SSE and less strong toward NNE (fig. 4.47). The corresponding response at Station  $T_1$  took the form of predominantly southeastward or southward currents (figs. 4.48 and 4.49). The 0.5% frequency isopleth for this station included southeastward currents with speeds as high as  $22 \text{ cm. s}^{-1}$ . At Station  $T_2$ , (figs. 4.50 and 4.51) because of its more exposed position, the current directions were more variable than at  $T_1$ .

During October, winds were directed mainly toward SE or NE (fig. 4.52), a pattern not seen in previous months. As expected, strong southeastward and northeastward current responses were found at the more exposed Station  $T_2$  (figs. 4.54 and 4.51) whereas at the more sheltered Station  $T_1$  only the southeastward response was conspicuous (figs. 4.53 and 4.49).

During November the vector frequency diagram for wind included a wider range of directions than in previous months but with the highest frequencies in the eastward to southward sector (fig. 4.55). The strongest current response at Station  $T_2$  was southward, with a weaker component toward NNE (fig. 4.56).

Comparison of the progressive vector diagrams for Station  $T_1$  and Station  $T_2$  for the whole of the Survey III period (figs. 4.49 and 4.51) shows that, whereas the patterns were similar during episodes of active currents, the current behaviour at the two stations differed greatly during intervals of weak currents. Although both stations exhibited predominantly southerly or northerly flow, the  $T_2$  currents were generally found to be more active with a greater frequency of current reversals.

[text continues on page 219]

Figure 4.40

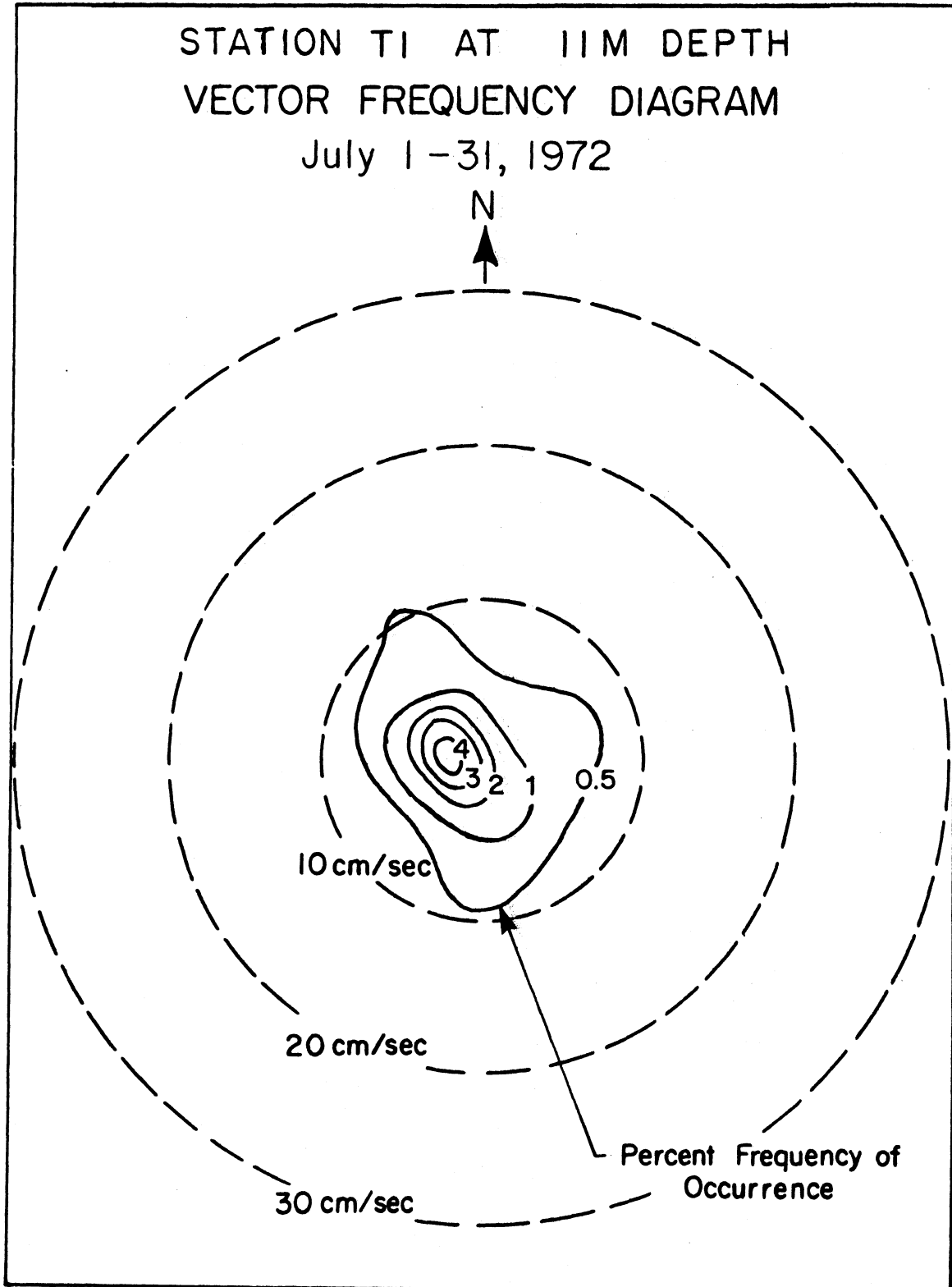


Figure 4.41

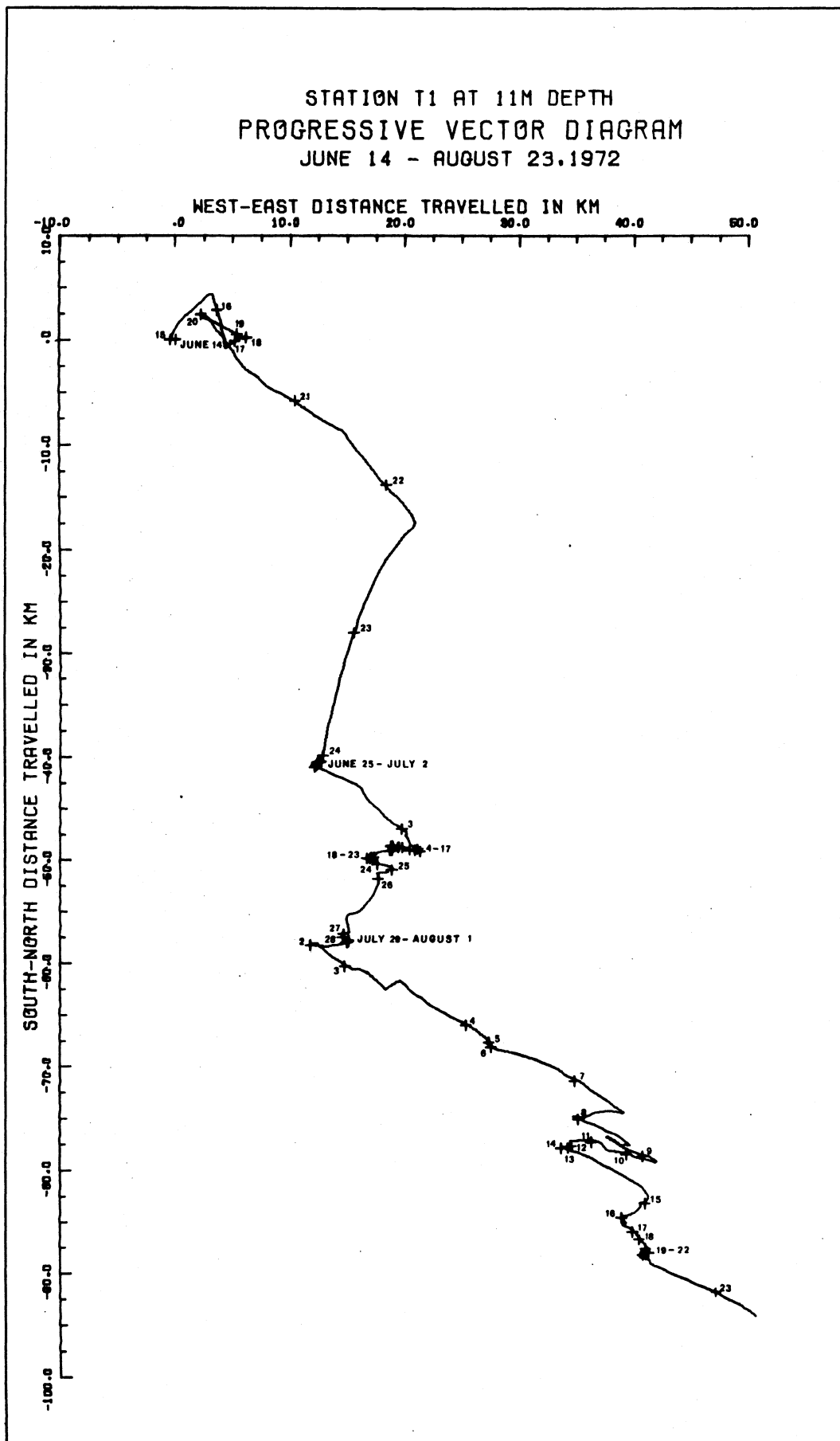


Figure 4.42

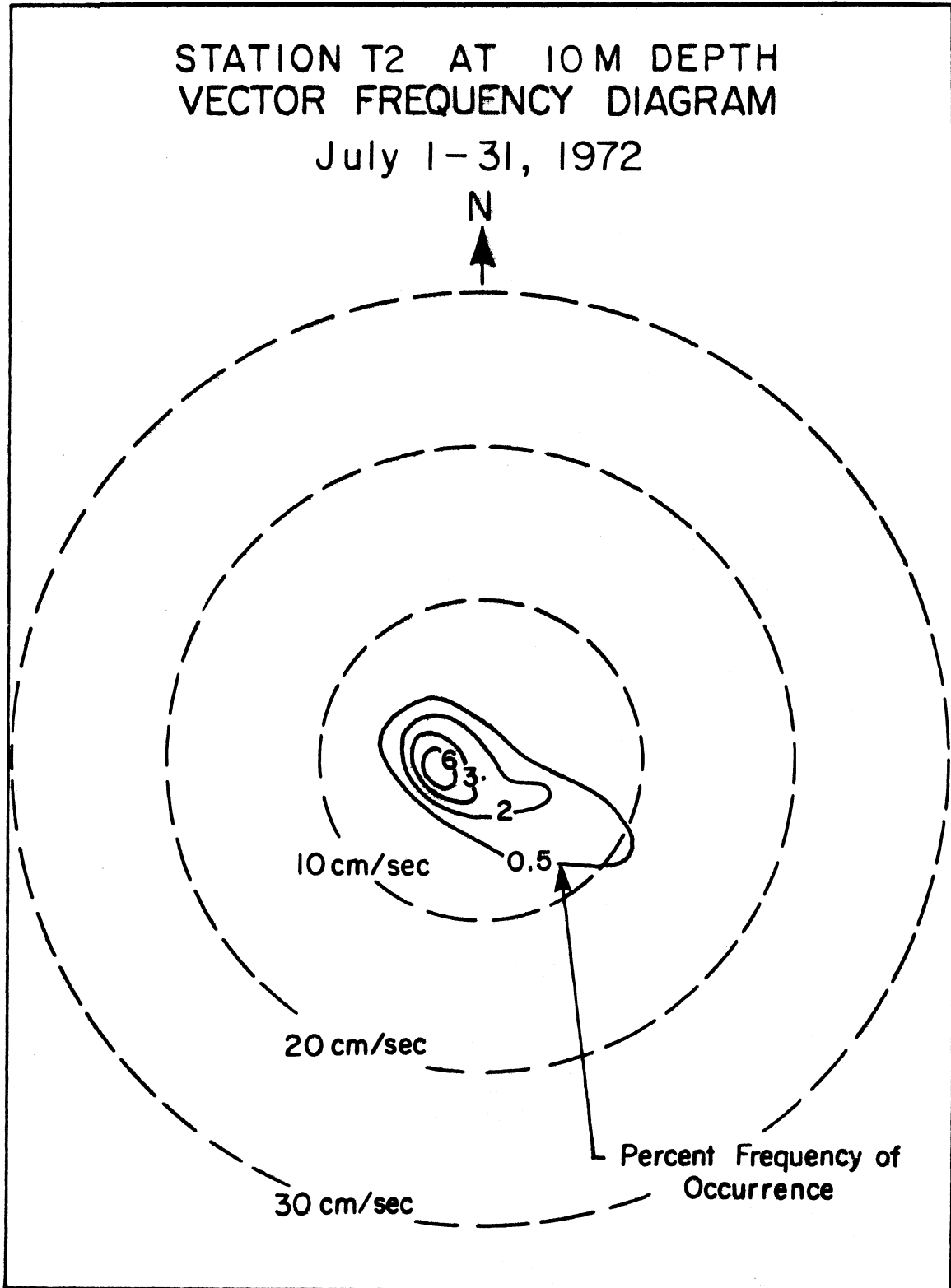


Figure 4.43

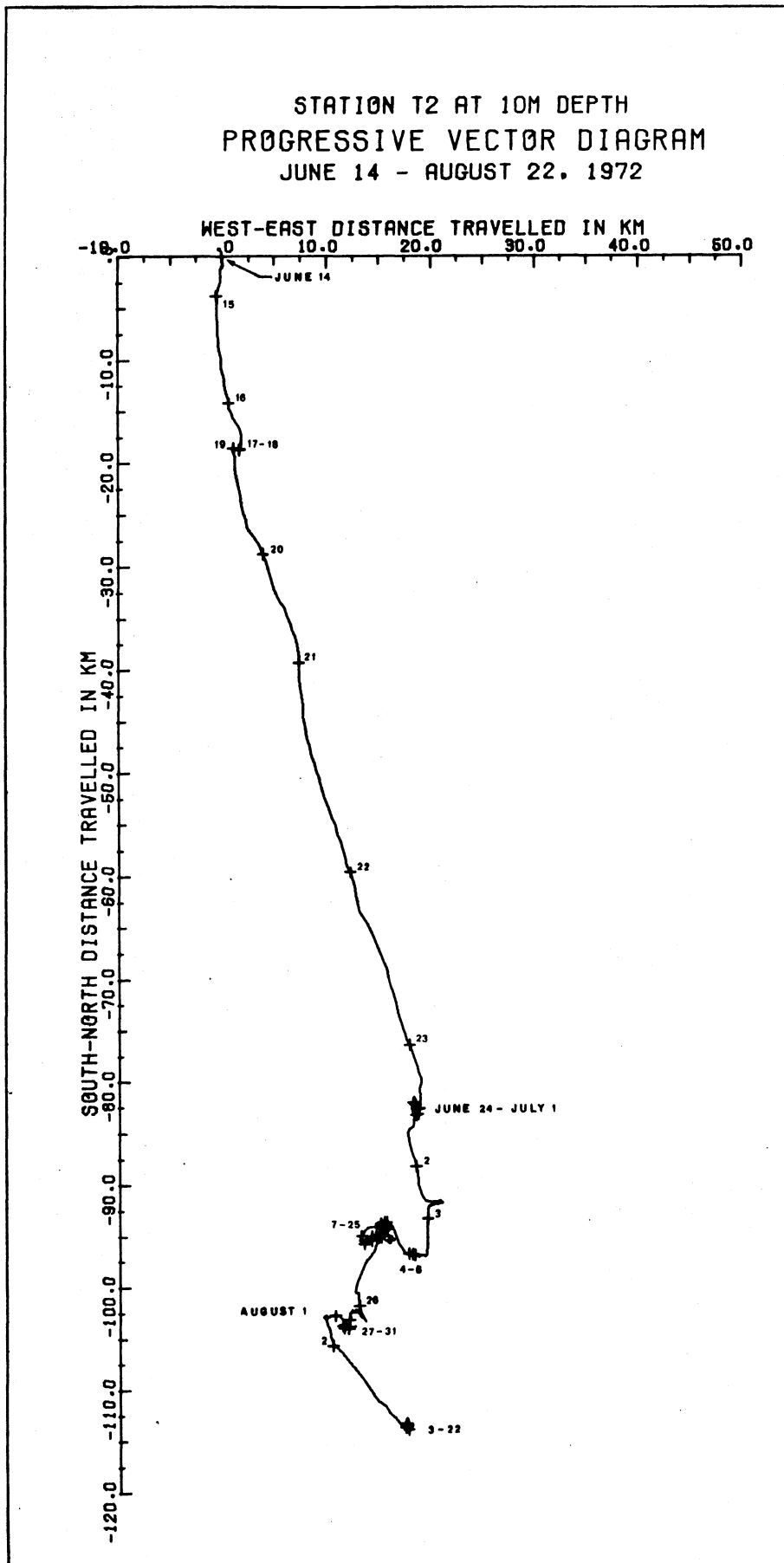


Figure 4.44

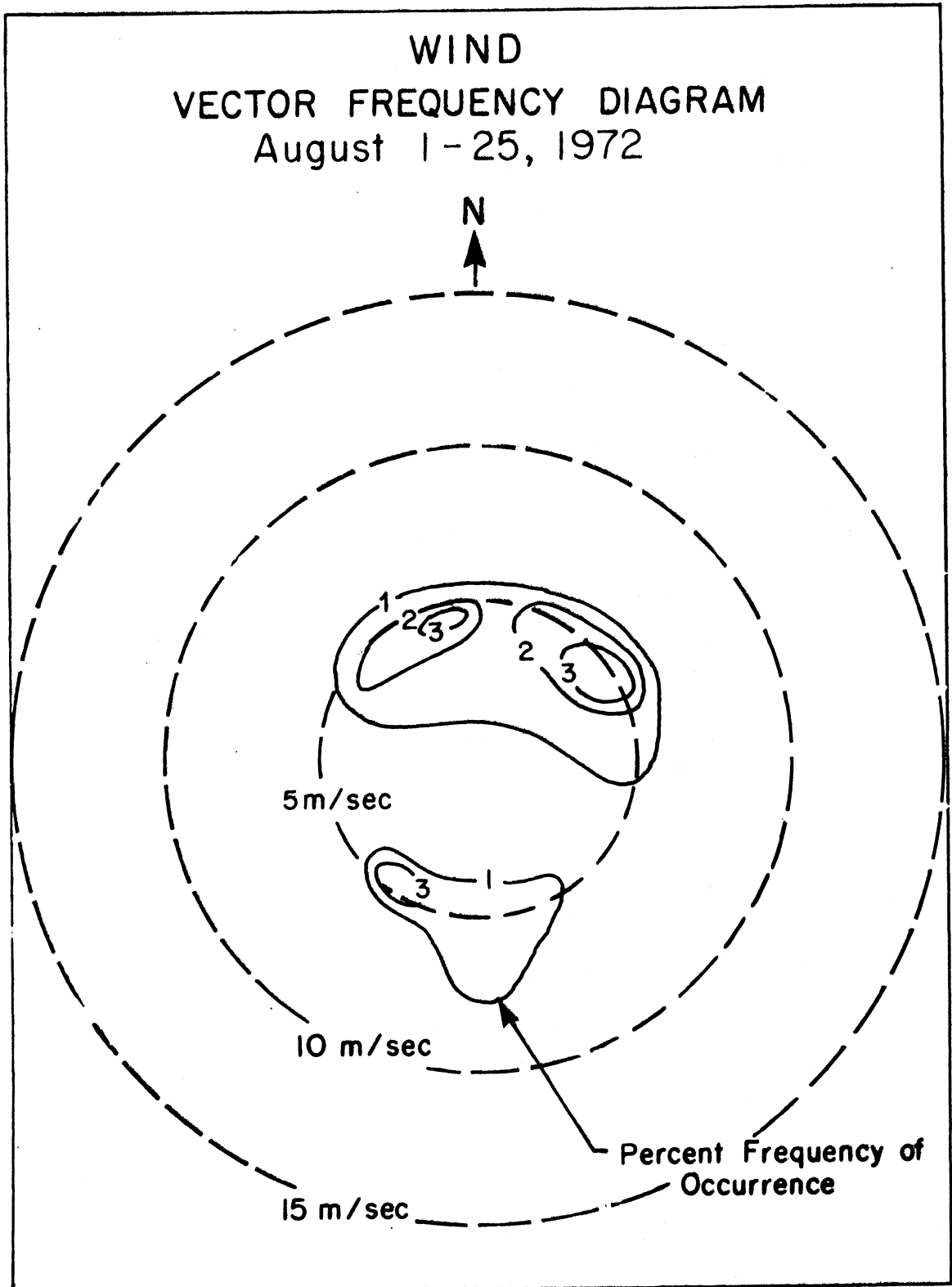


Figure 4.45 The corresponding progressive vector diagram is on page 203.

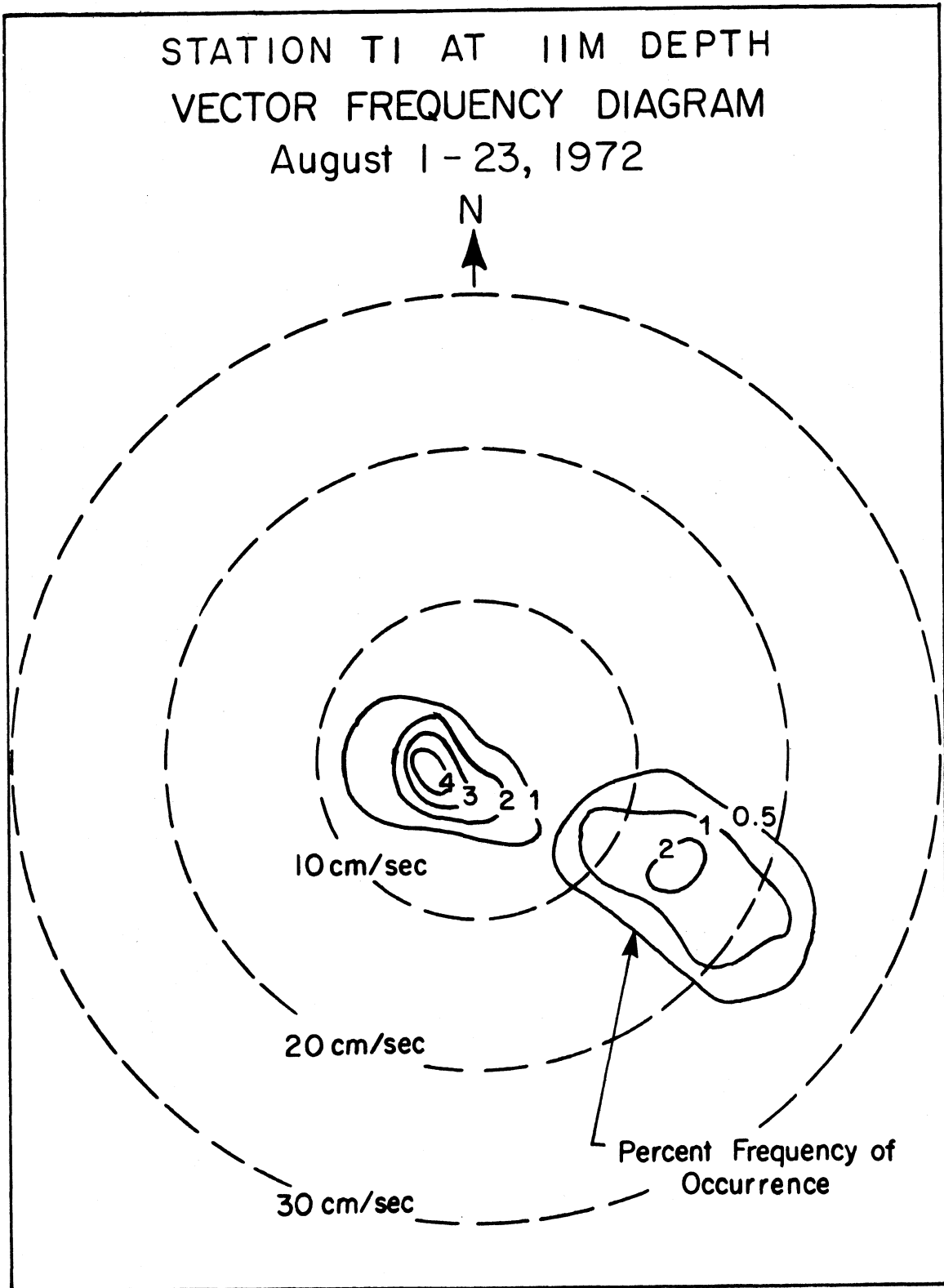


Figure 4.46 The corresponding progressive vector diagram is on page 205.

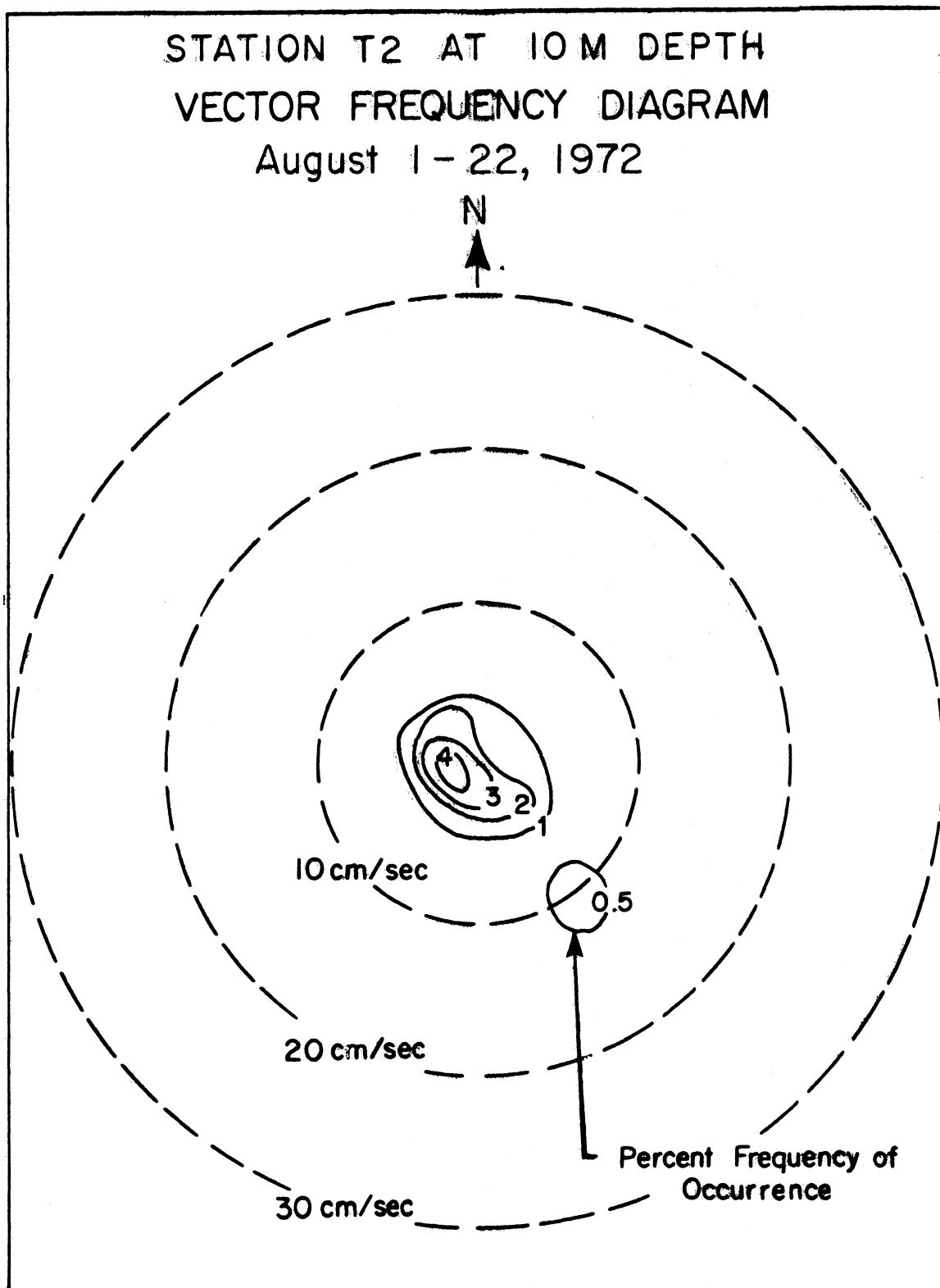


Figure 4.47

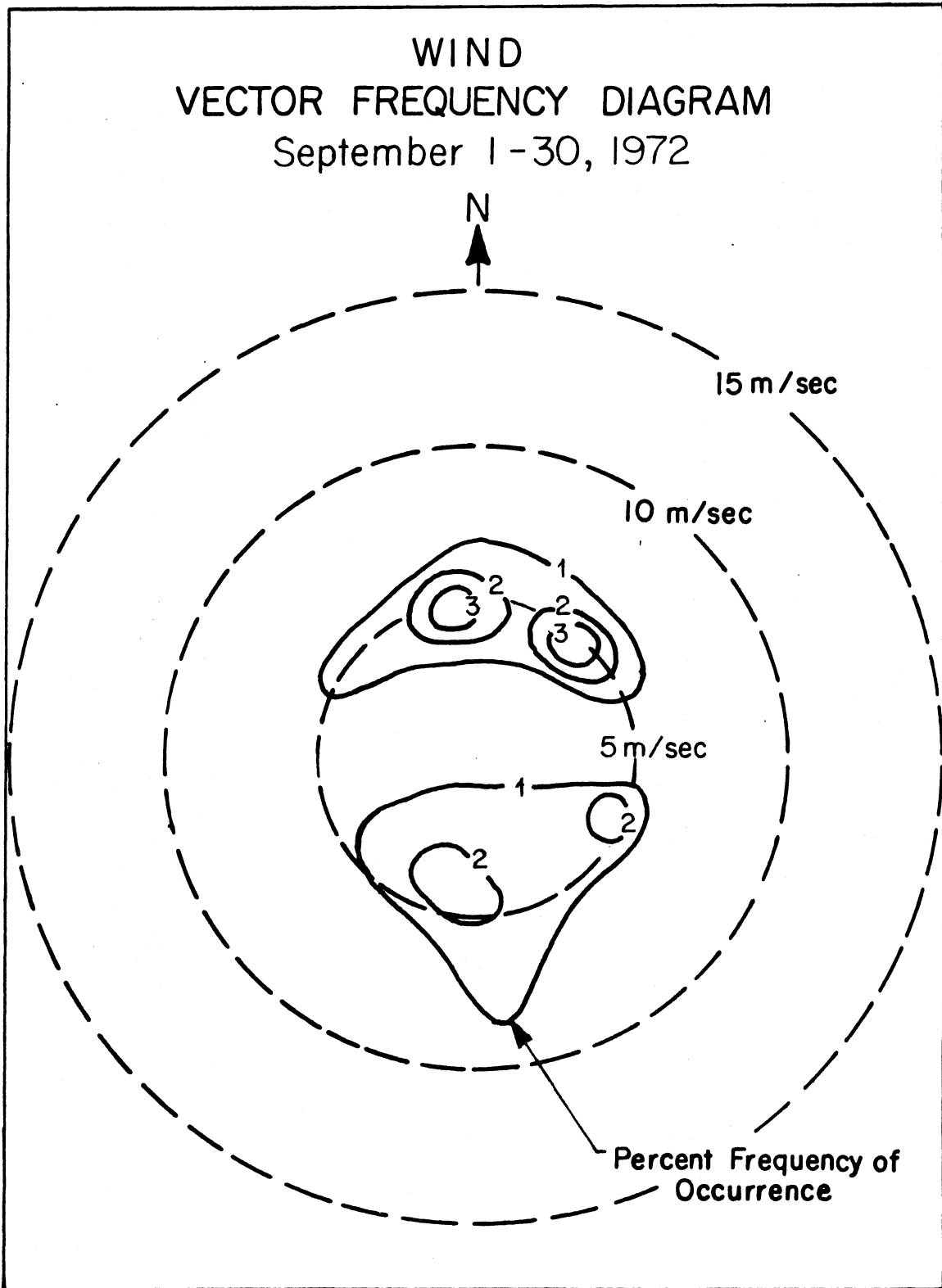


Figure 4.48

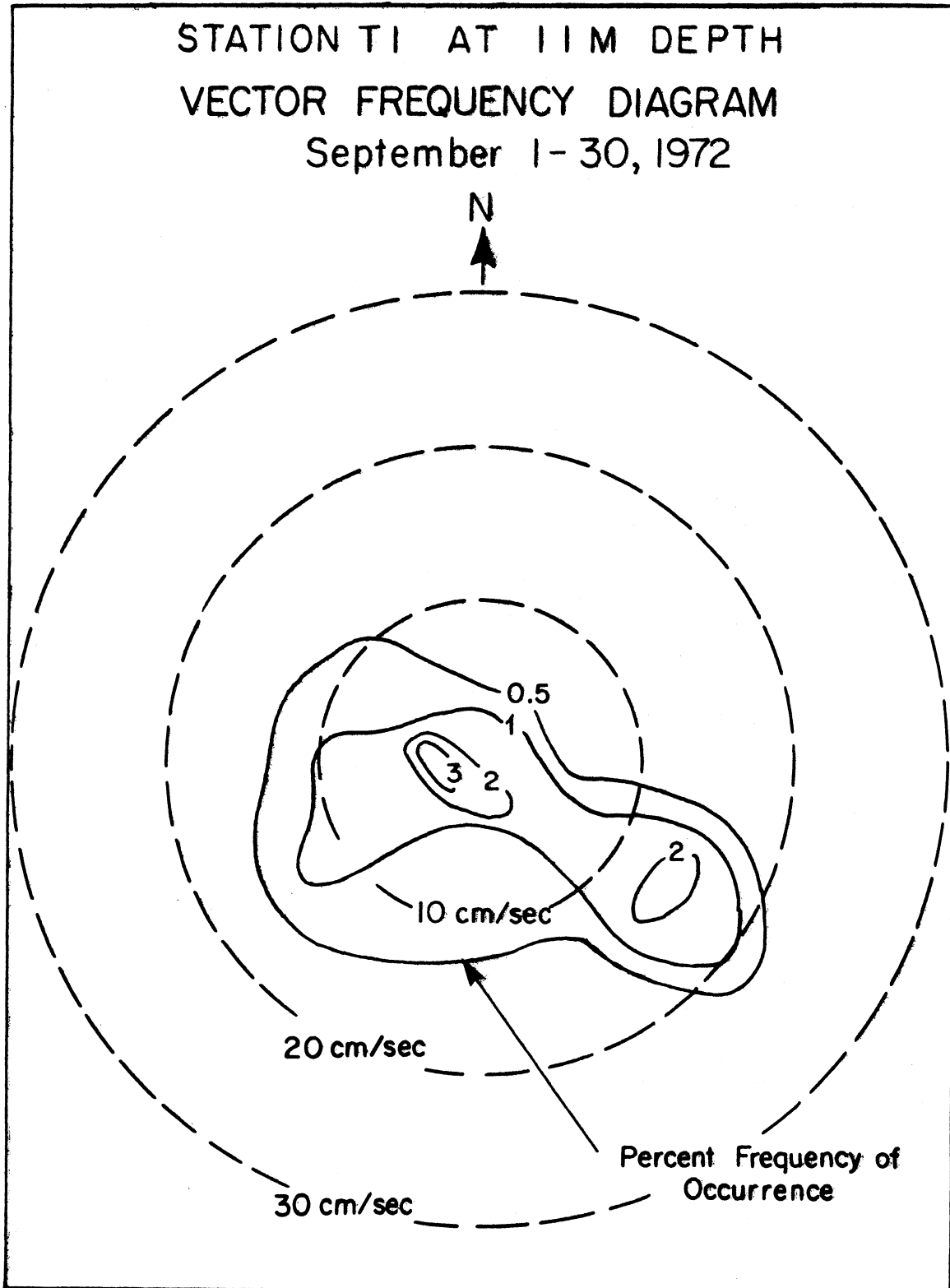


Figure 4.49

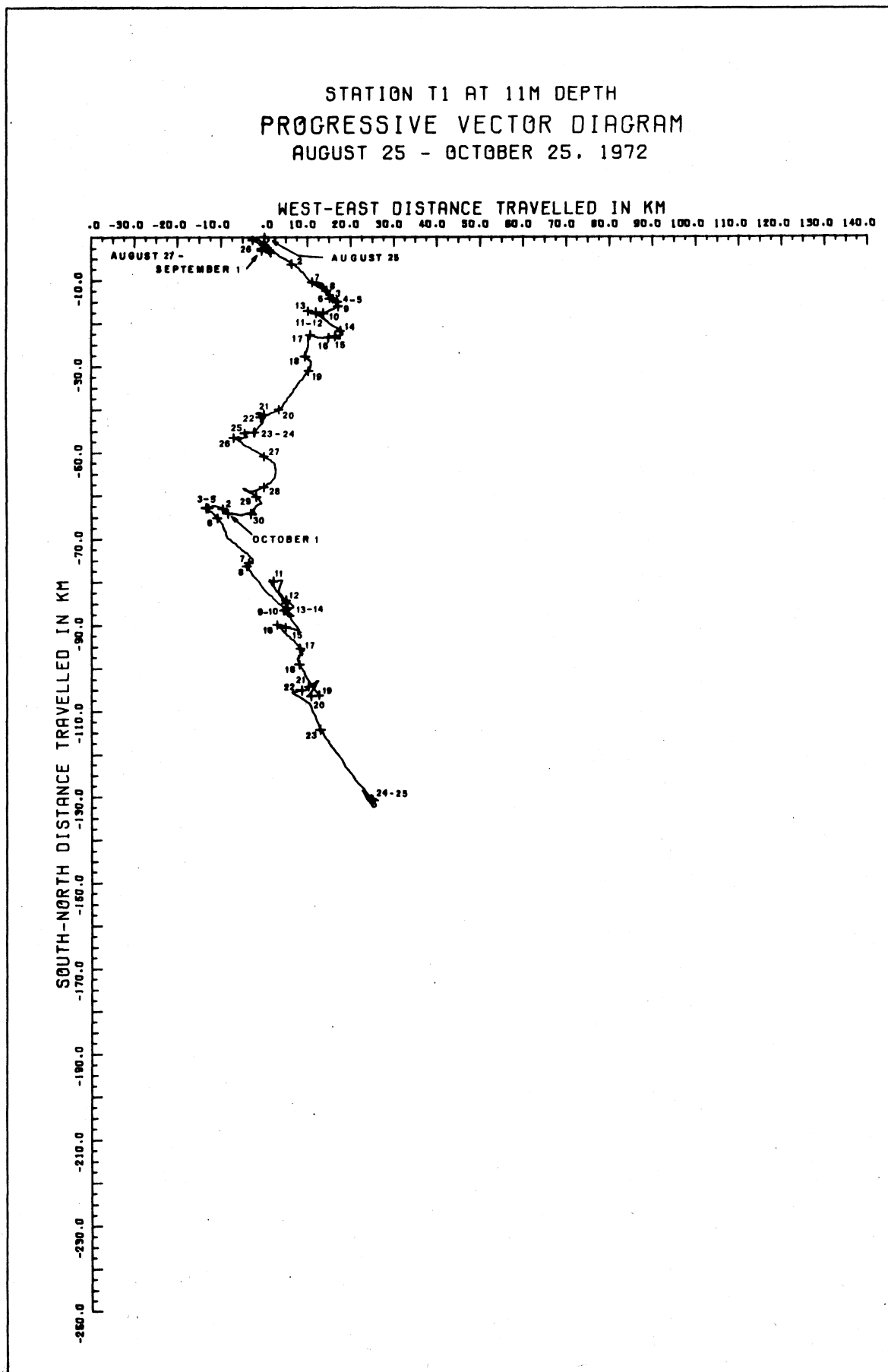


Figure 4.50

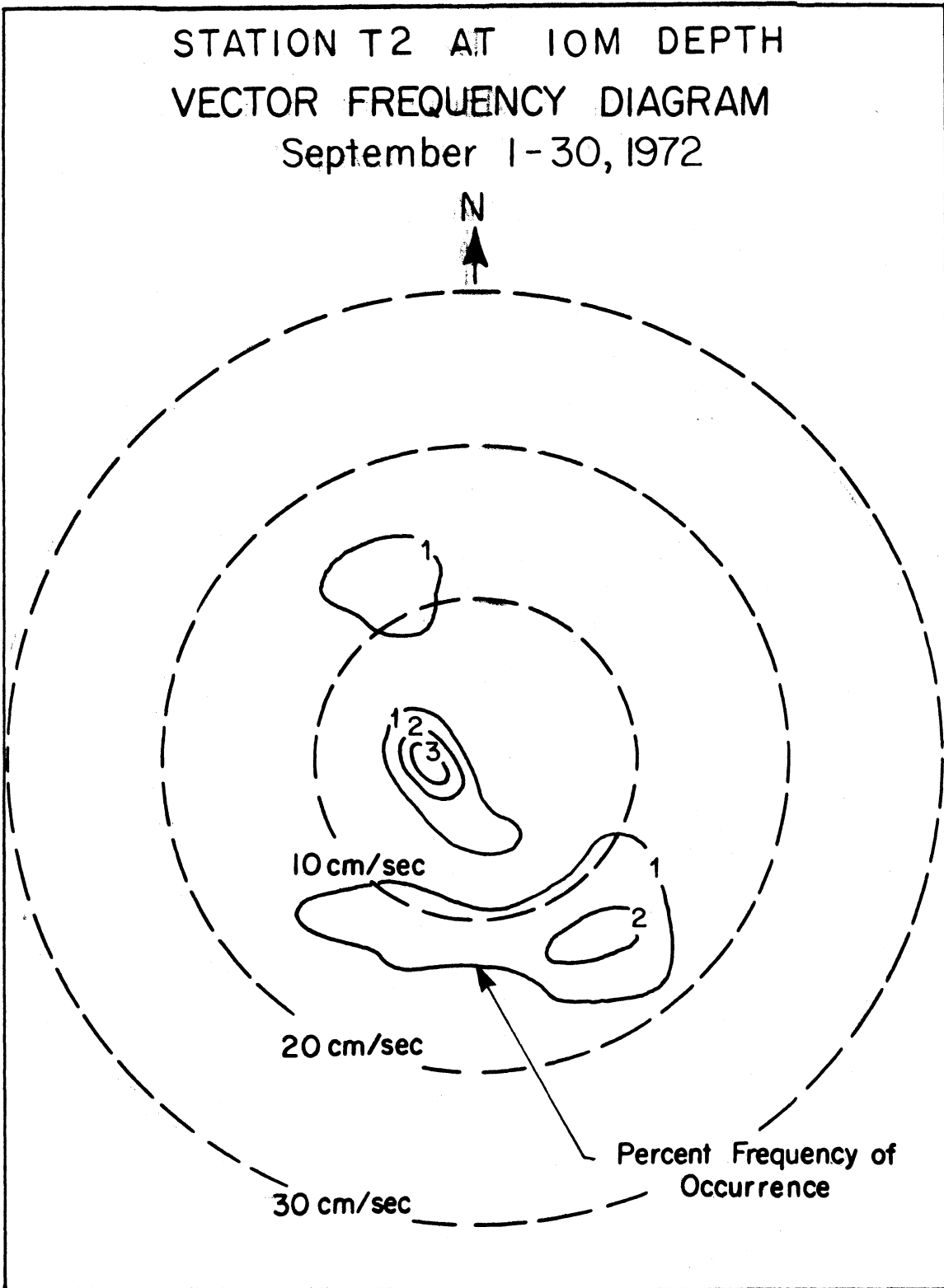


Figure 4.51

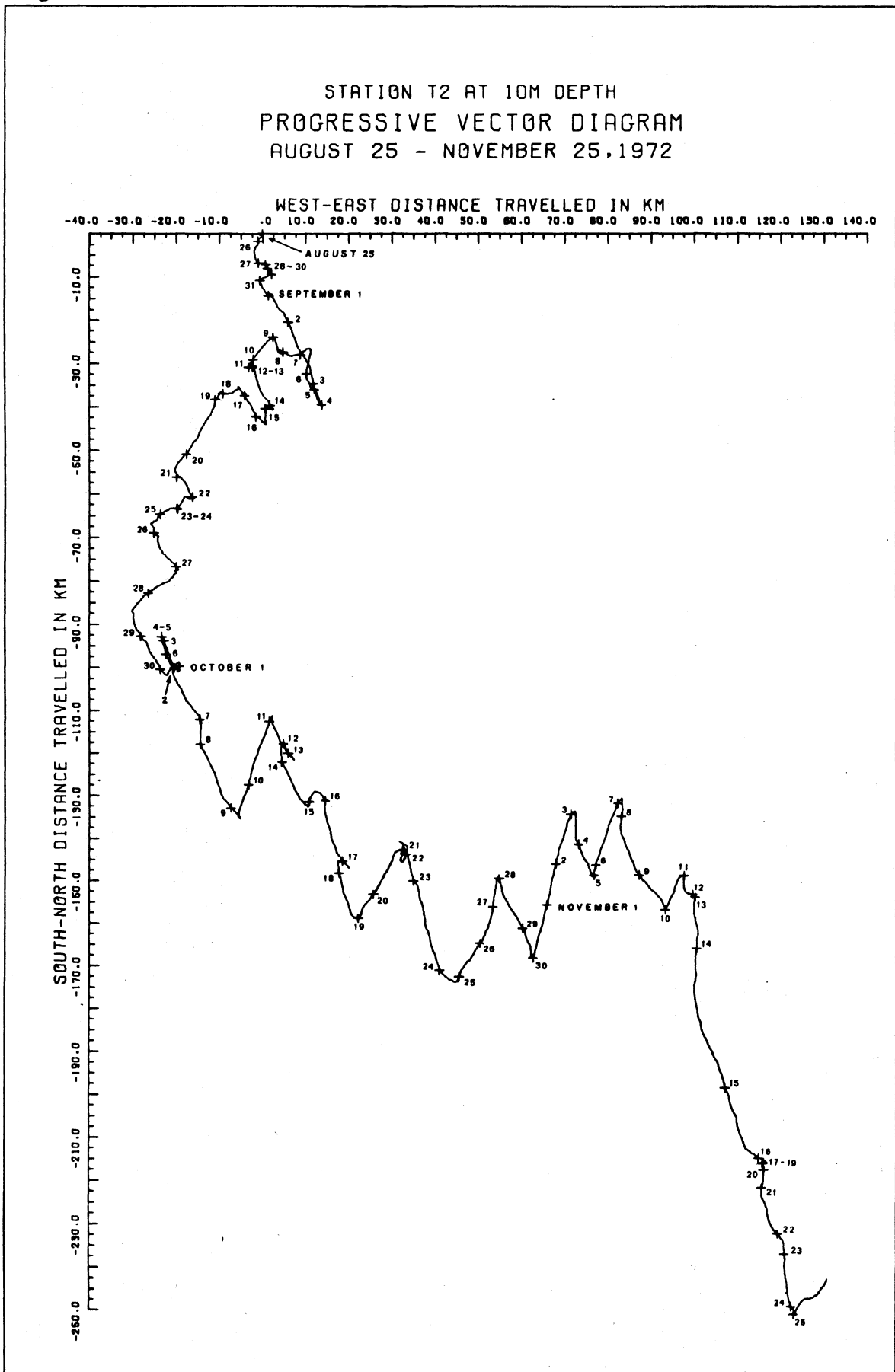


Figure 4.52

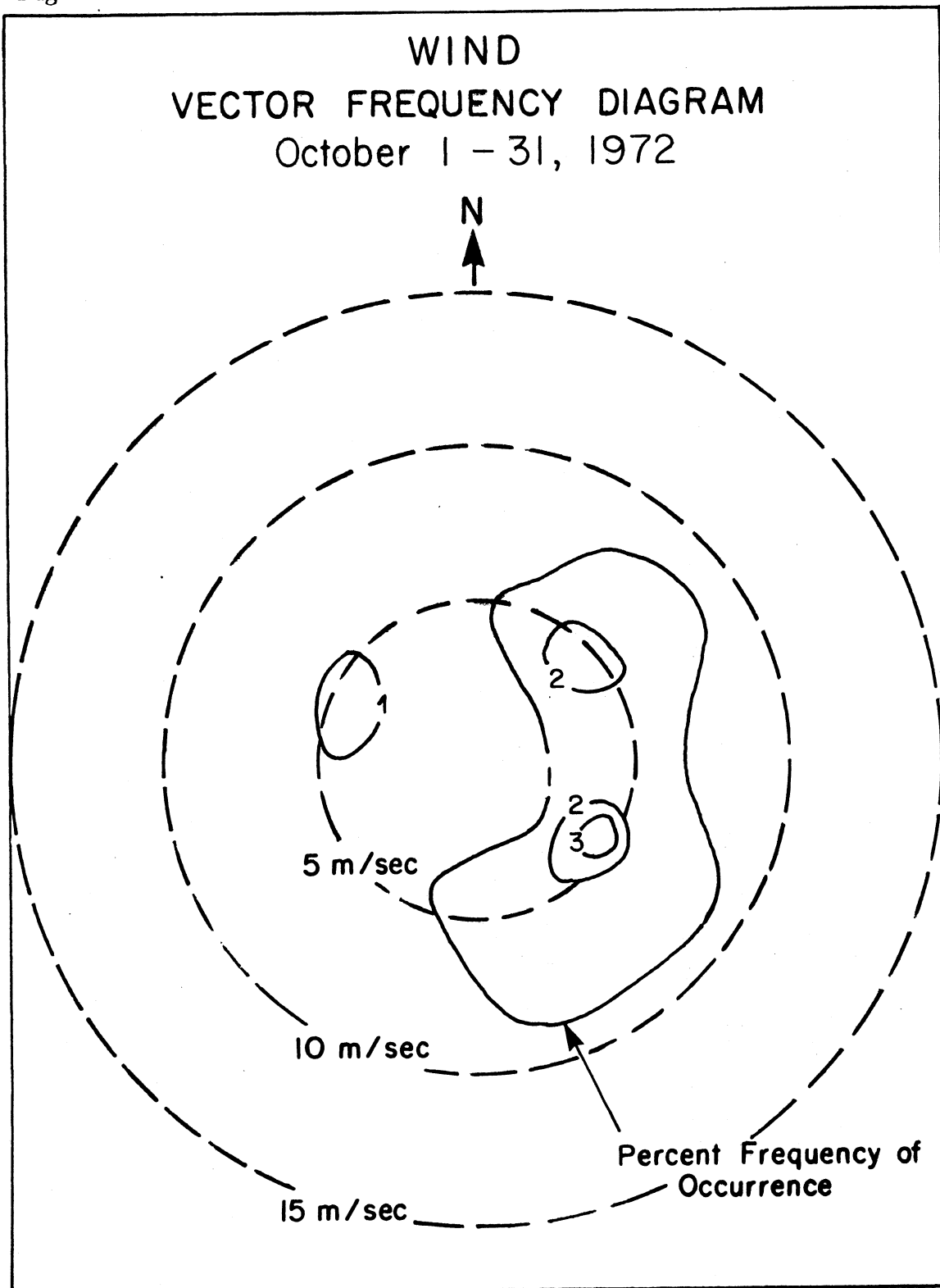


Figure 4.53 The corresponding progressive vector diagram is on page 211.

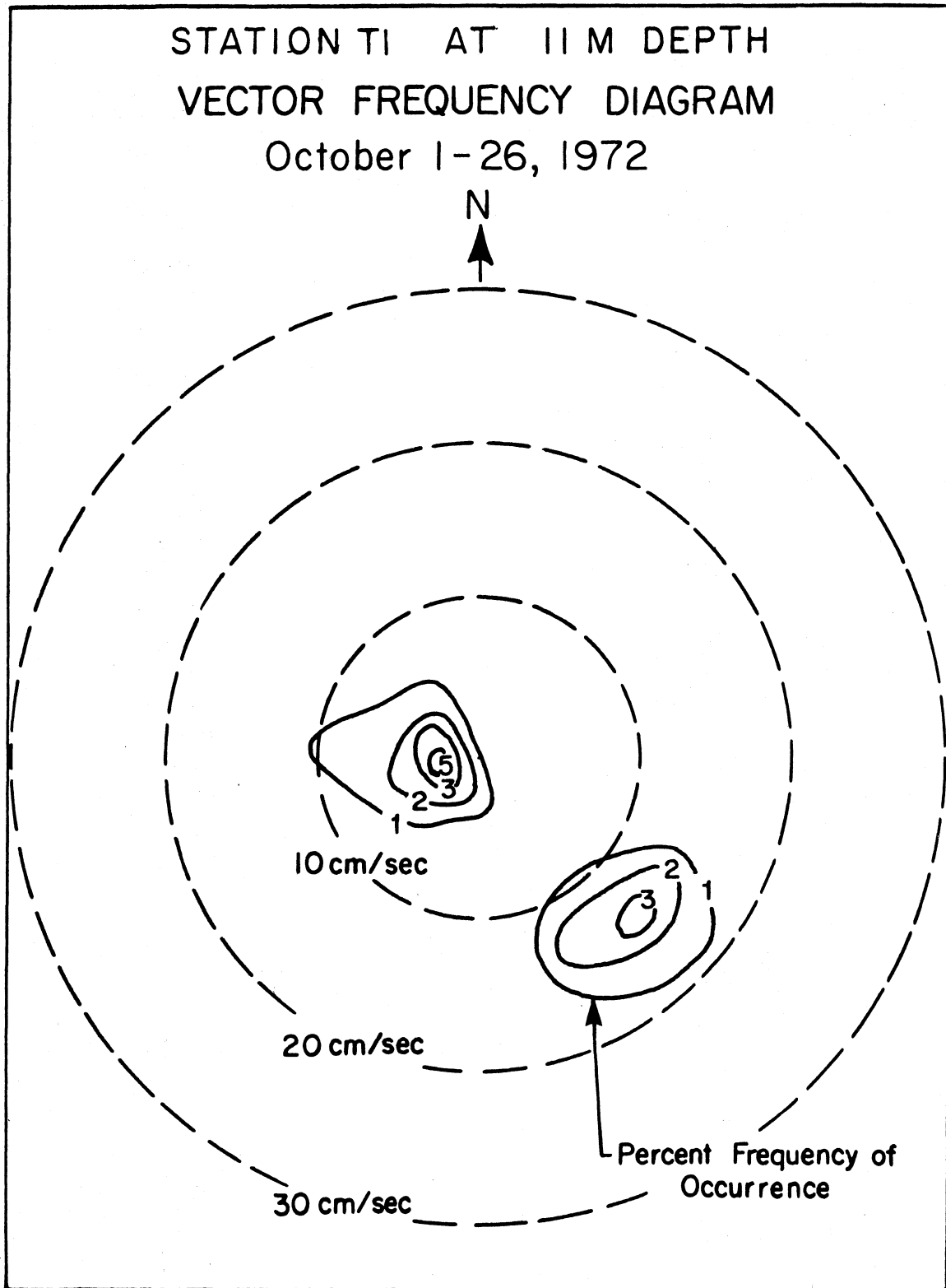


Figure 4.54 The corresponding progressive vector diagram is on page 213.

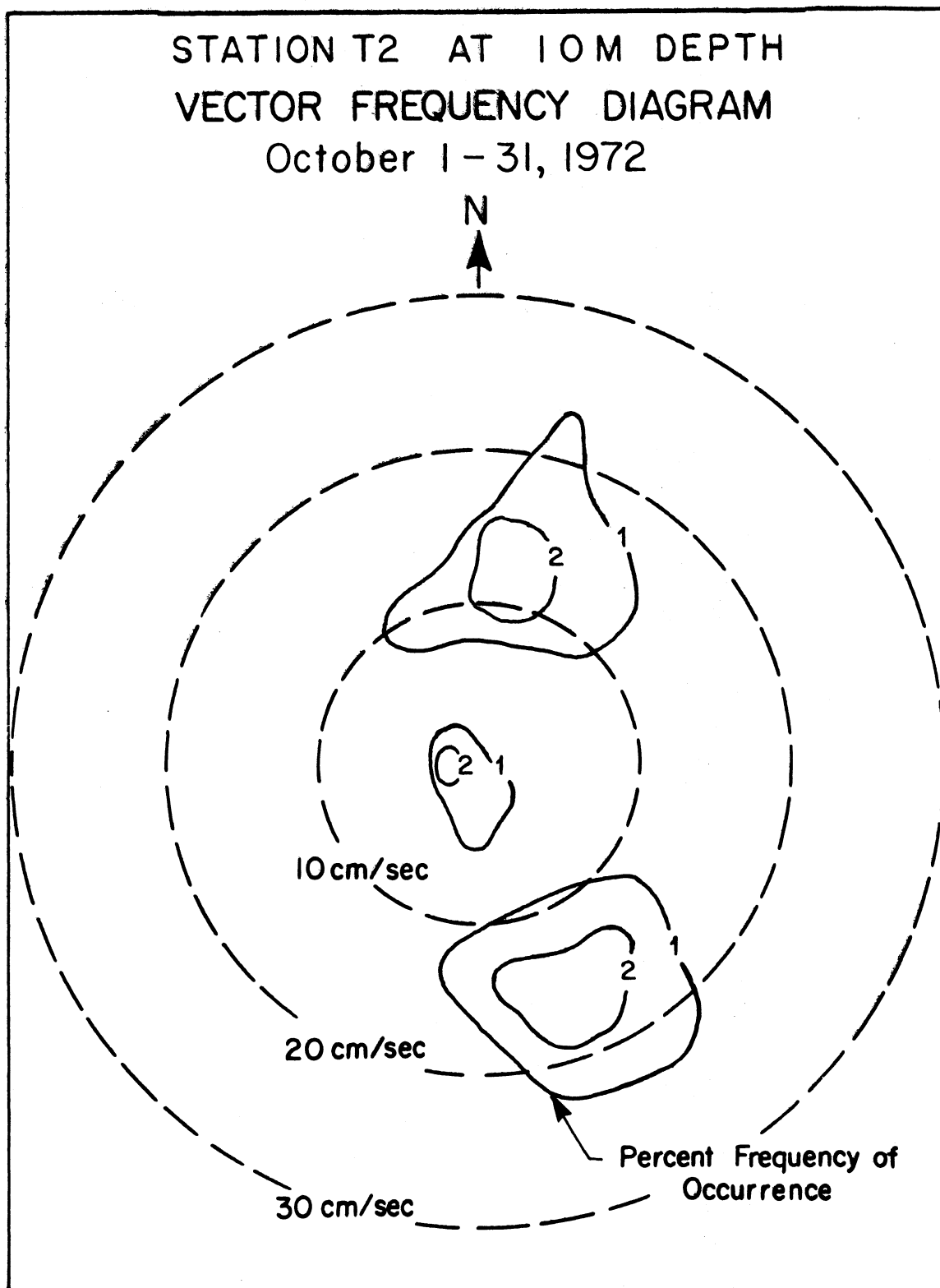


Figure 4.55

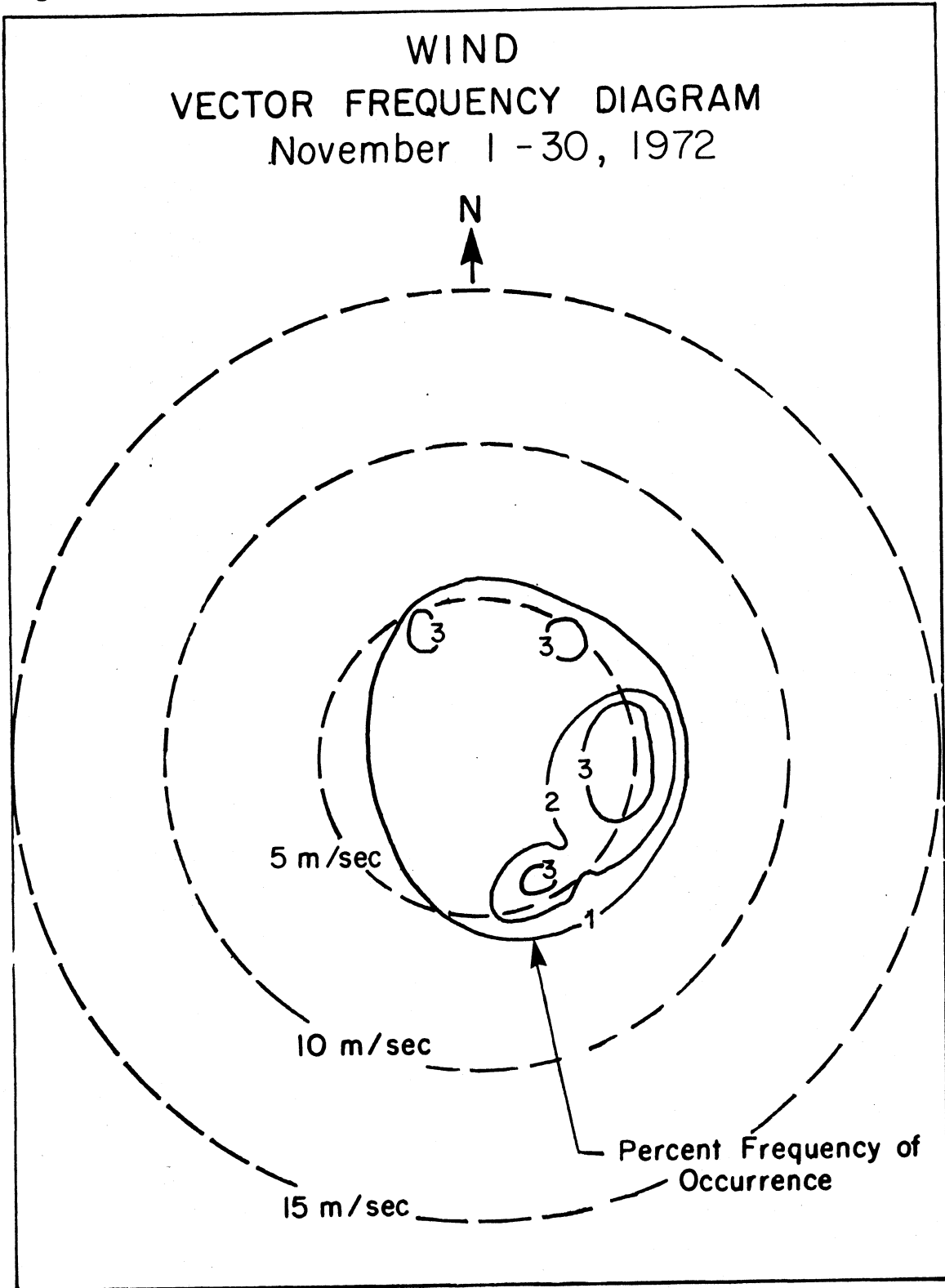
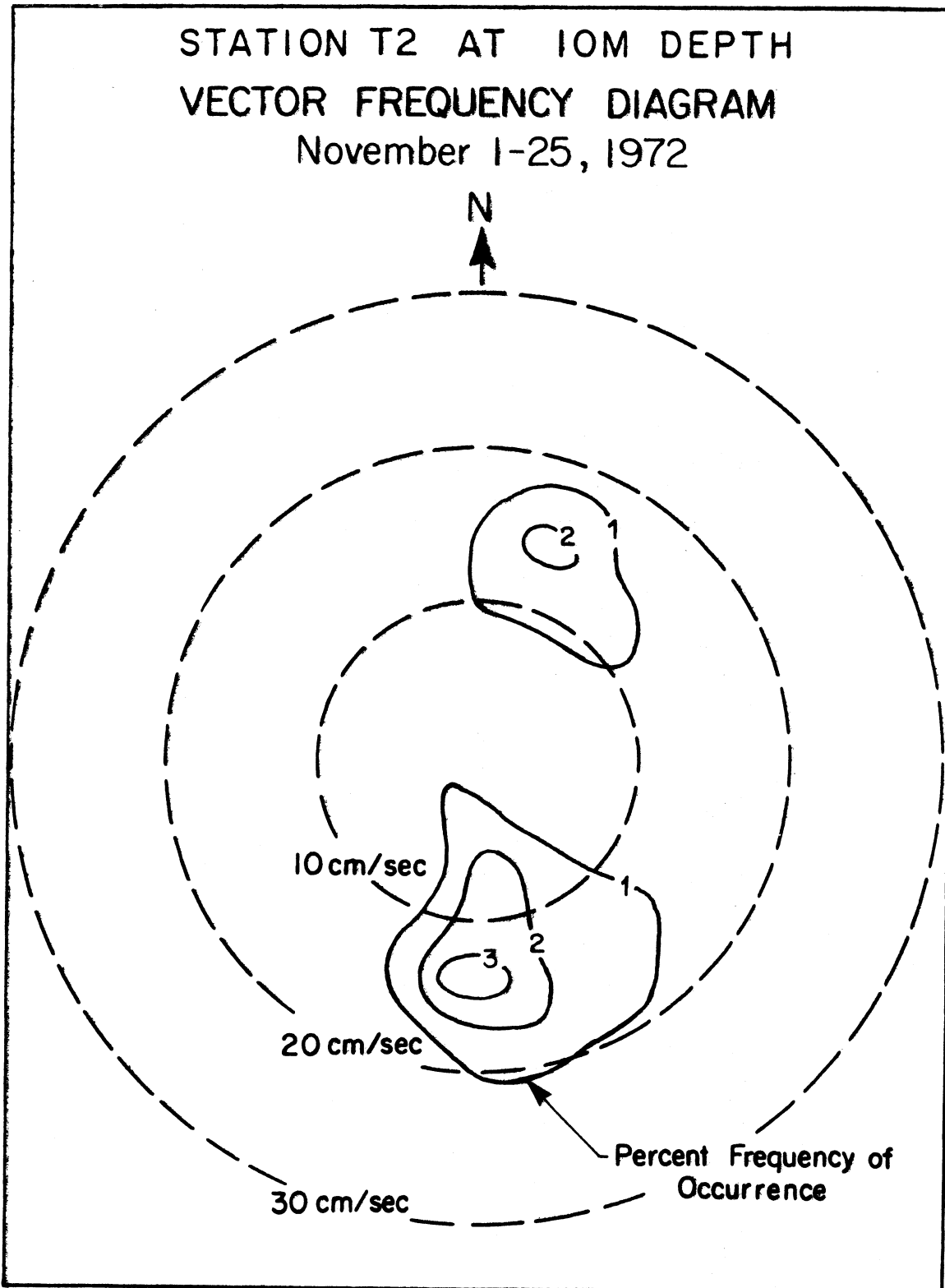


Figure 4.56 The corresponding progressive vector diagram is on page 213.



## Survey IV, 12 April - 26 June 1973

During April 1973, winds were most persistent toward the NNW and SSE and strongest in the latter direction (fig. 4.57). The vector frequency diagrams were similar for all the stations (2, 4, 5, and 7; figs. 4.58 to 4.61). As expected from the dominant wind directions and fetch, the two dominant directions of flow were toward the southeast and northwest. The greater persistence of northwestward currents at the deeper station (7, fig. 4.61) was the result of events during 22-26 April when the currents maintained that direction even after the shallow station currents had changed direction on 22 April.

The general pattern of the progressive vector diagram for April is repeated, with individual variations, at all stations (fig. 4.64 on a more open scale than the others, figs. 4.66, 4.68, and 4.70). From 14 to 17 April the current was toward NNE at Stations 4 and 7, but toward NNW at Station 5. From 17 to 22 April the flow was toward NNW at all stations, reversing toward S at Station 5 and toward SE at Stations 2 and 4 on 22 April. But at Station 7 that reversal, toward SSE, was delayed until 25 April. After each reversal, the current persisted toward S to SE until the end of the month.

During May 1973 winds were distributed around the compass, with almost equal frequency concentrations toward S, NW, NE, and SE (fig. 4.62). The vector frequency diagrams for current, however, confirm that there was little response to the northeastward winds because of small fetch at that site. Station 2 (fig. 4.63) shows a bipolar frequency distribution toward NW and SE. At Station 4 (fig. 4.65) the distribution was toward N and SSE; and at Station 5 (fig. 4.67) it was toward NNW and S. At Station 7 (fig. 4.69) for the interval 1 to 10 May only, the current was confined to the sector southward to southeastward with high frequencies toward SSE. The speed was also relatively steady at about  $15 \text{ cm. s}^{-1}$ .

The progressive vector diagrams (figs. 4.64, 4.66, 4.68, and 4.70) illustrate variation between the flow patterns at the different stations. Station 2, in the shallowest water, shows the greatest variability, while Station 7, in the deepest water, exhibits the greatest persistence in current direction.

[the text continues on page 234]

Figure 4.57

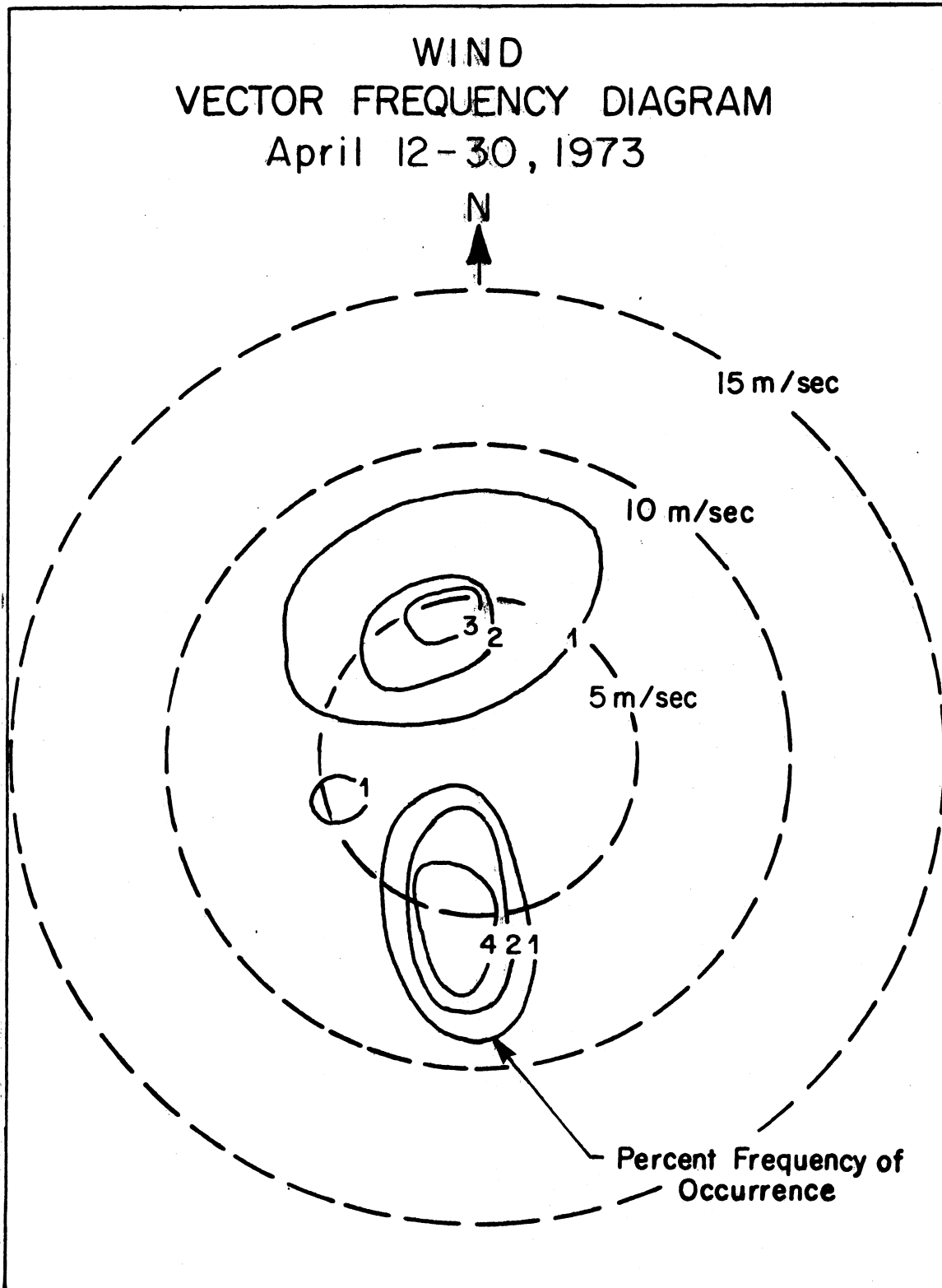


Figure 4.58 The corresponding progressive vector diagram is on page 227.

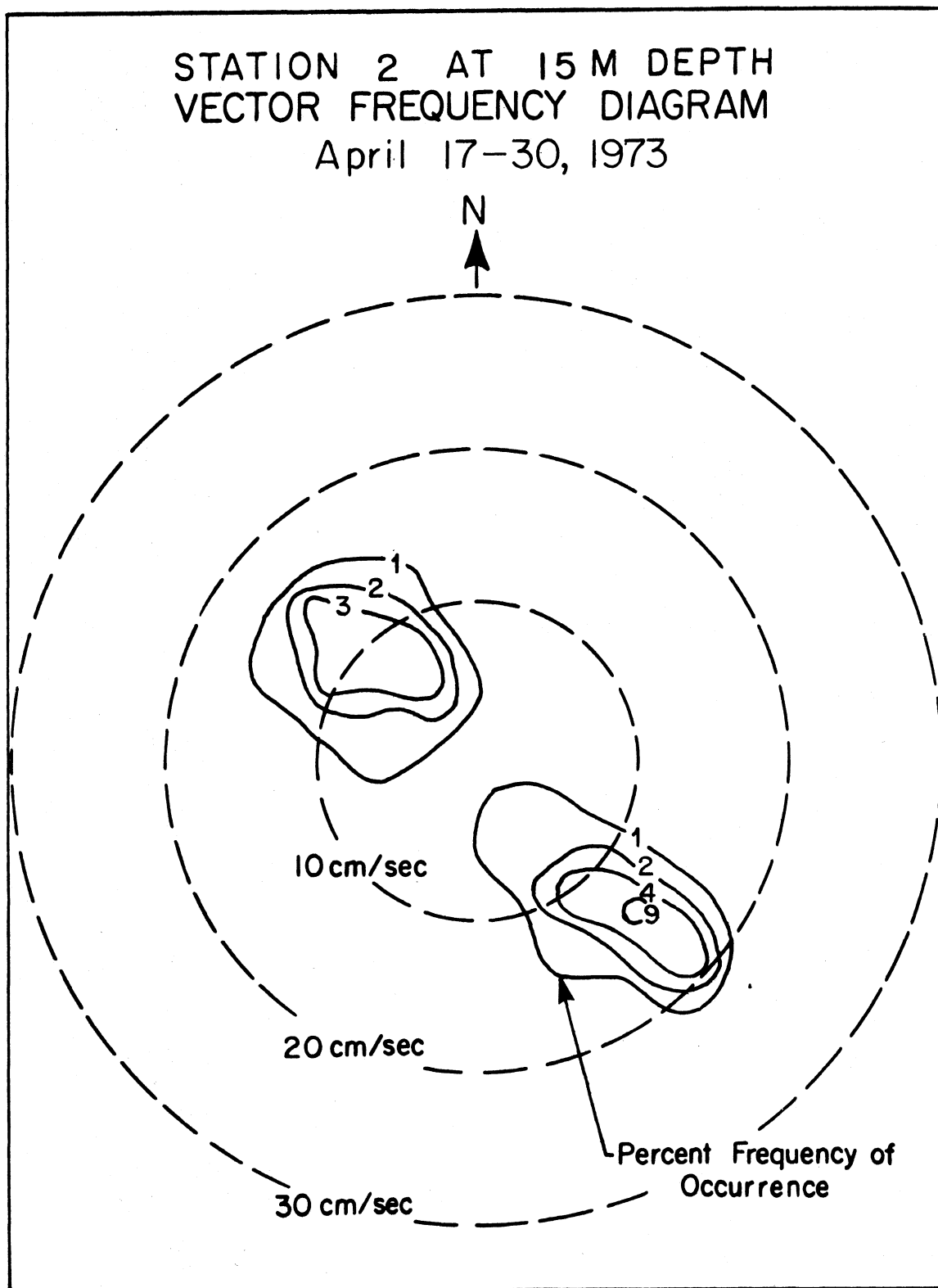


Figure 4.59 The corresponding progressive vector diagram is on page 229.

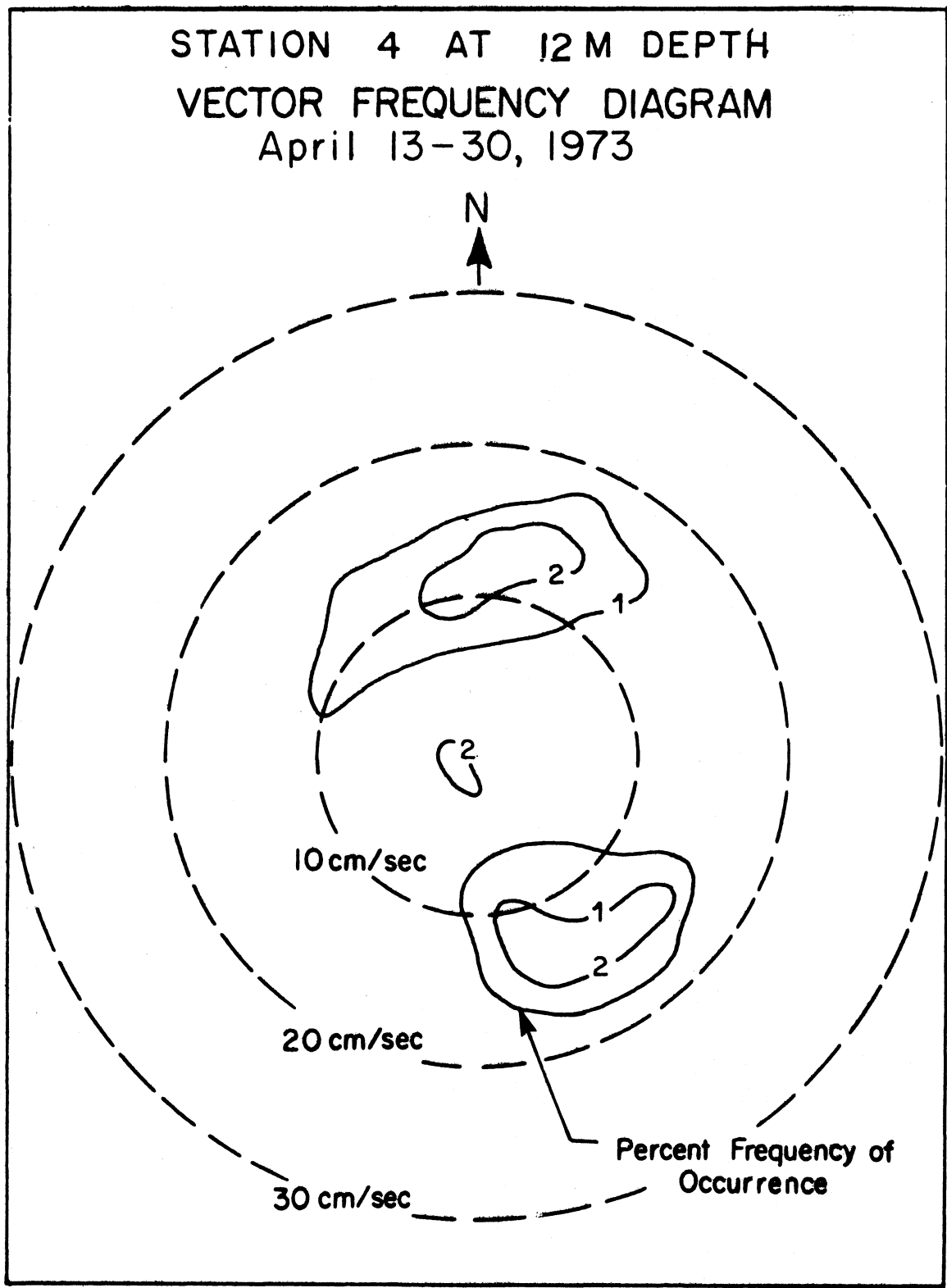


Figure 4.60 The corresponding progressive vector diagram is on page 231.

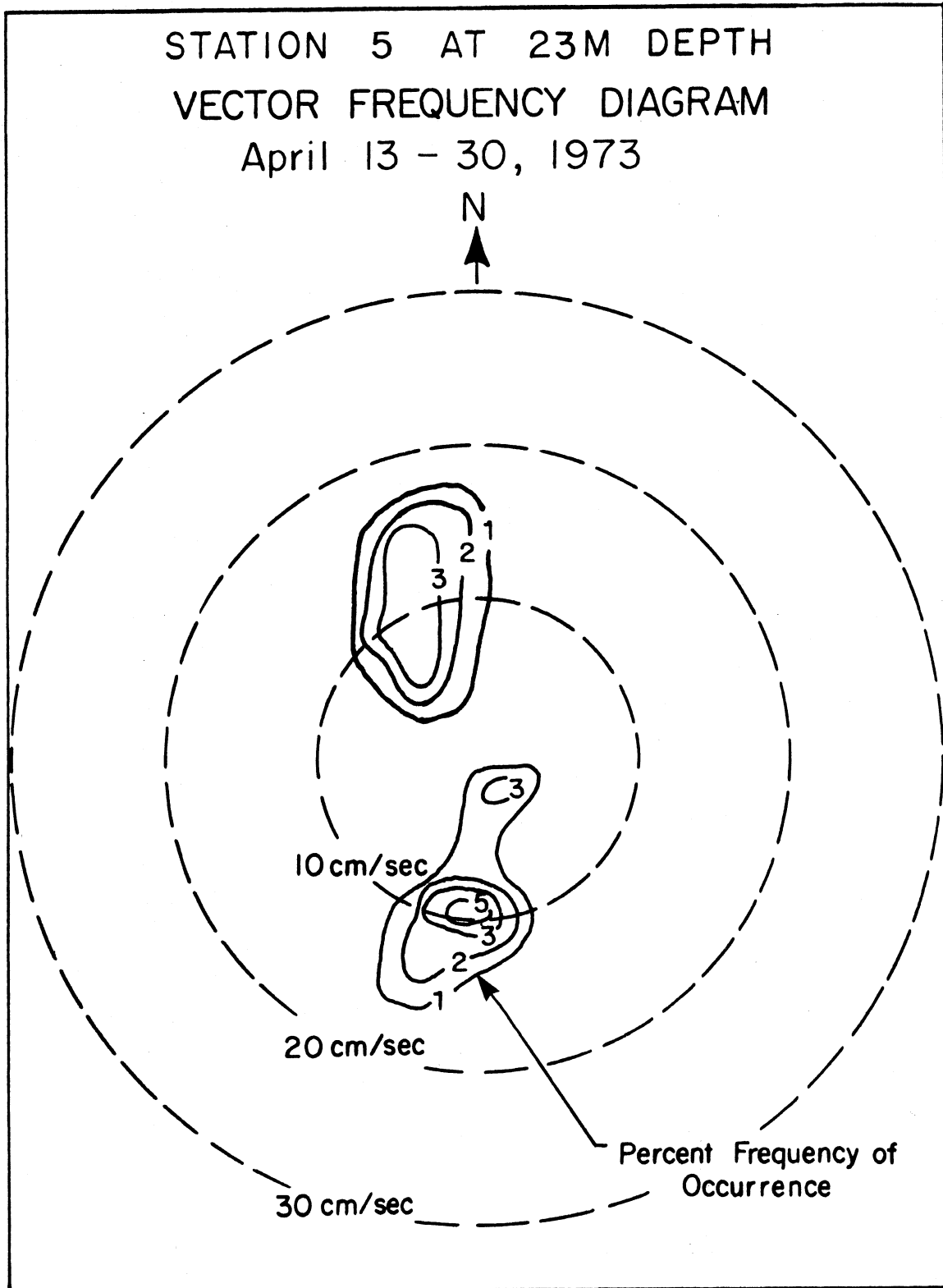


Figure 4.61 The corresponding progressive vector diagram is on page 233.

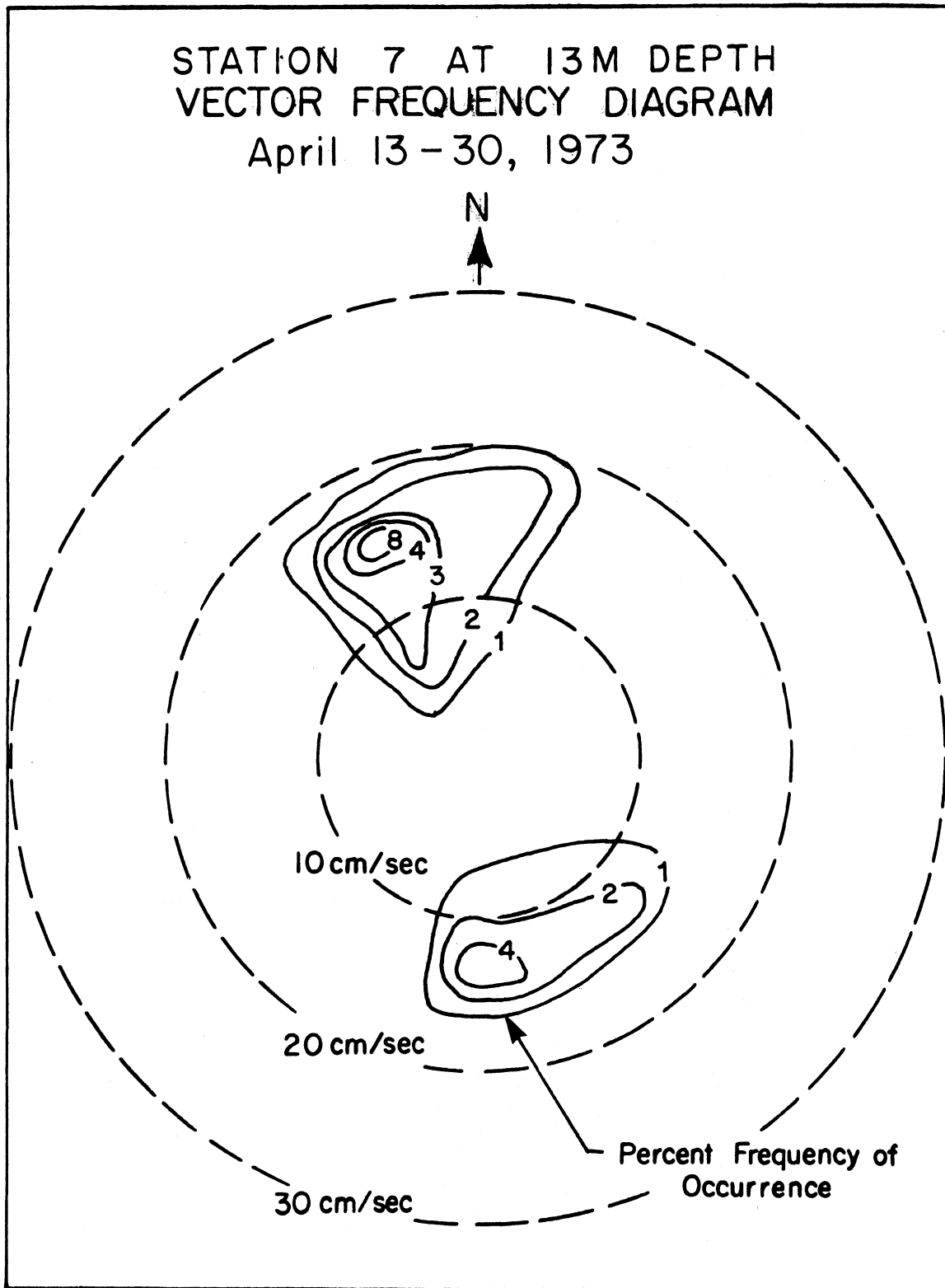


Figure 4.62

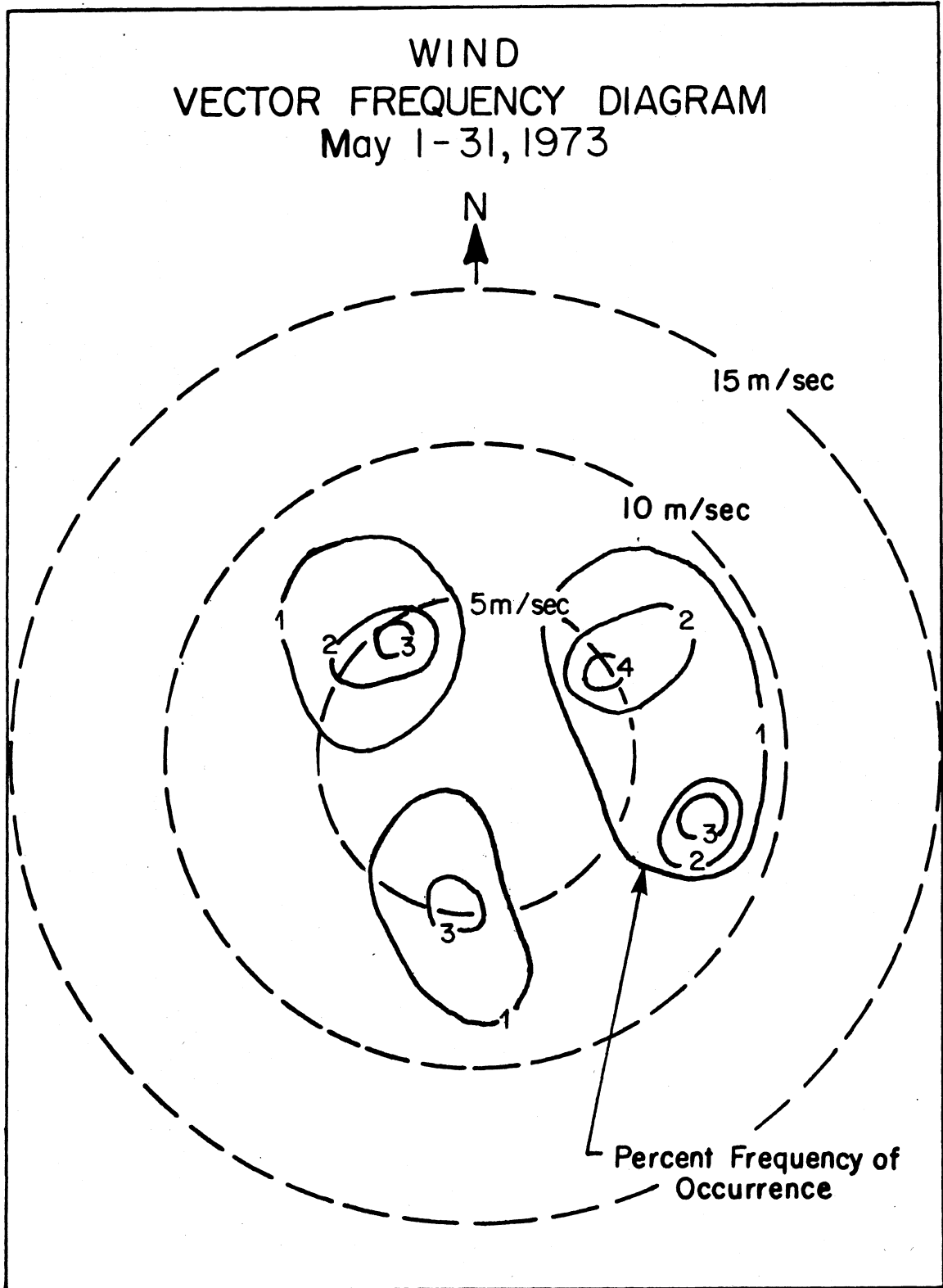


Figure 4.63

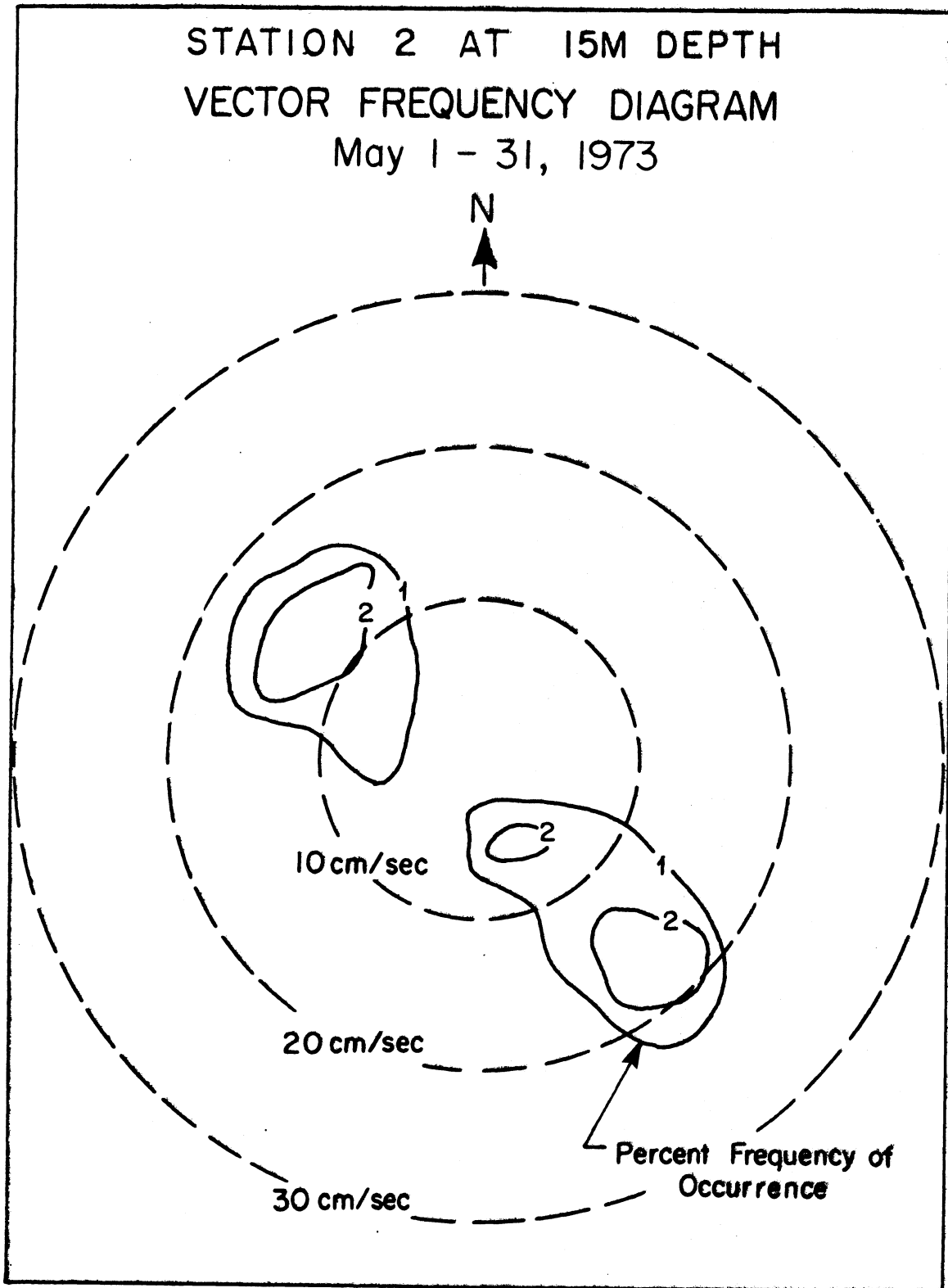


Figure 4.64

STATION 2 AT 15M DEPTH  
PROGRESSIVE VECTOR DIAGRAM  
APRIL 18 - JUNE 22, 1973

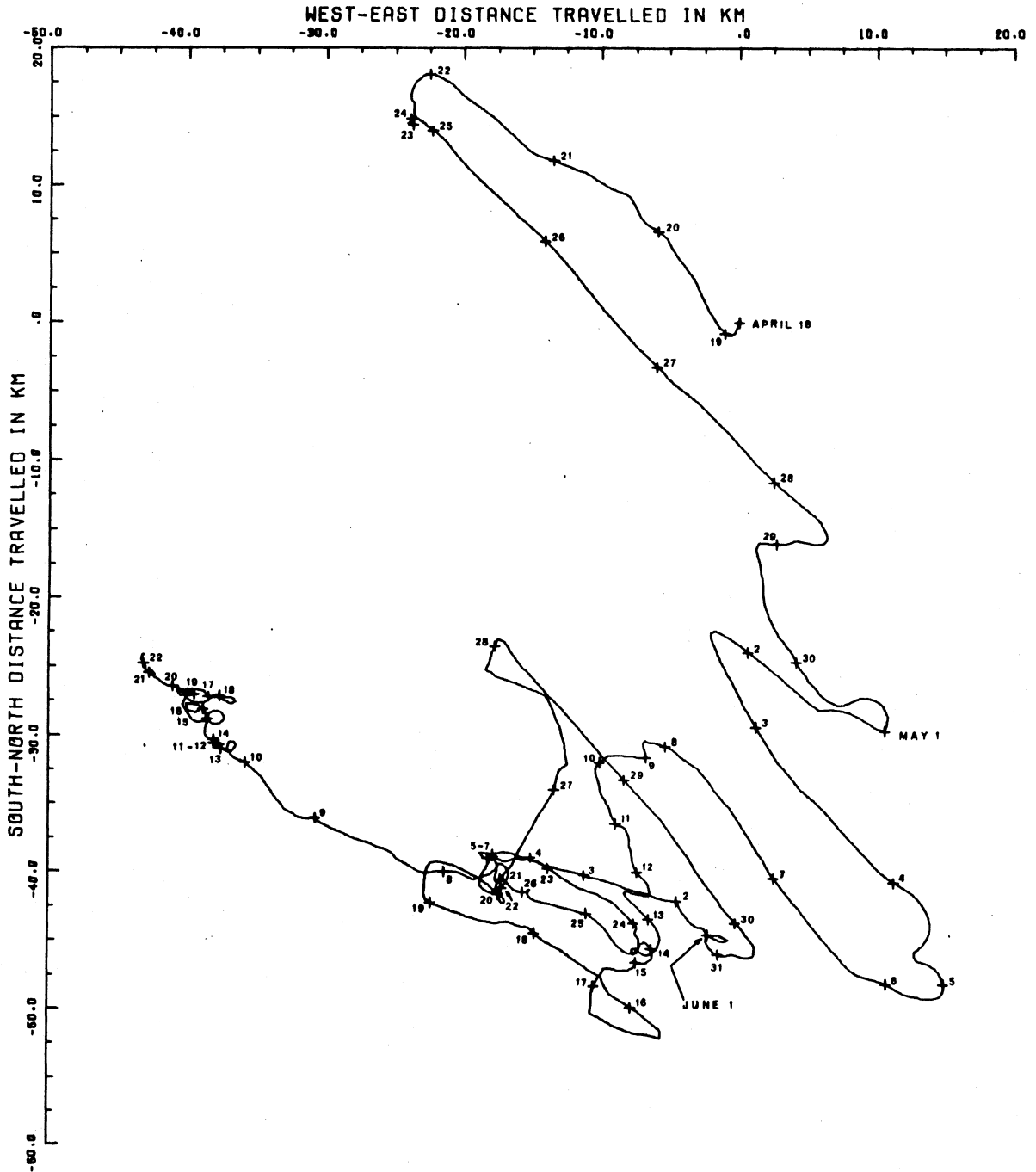


Figure 4.65

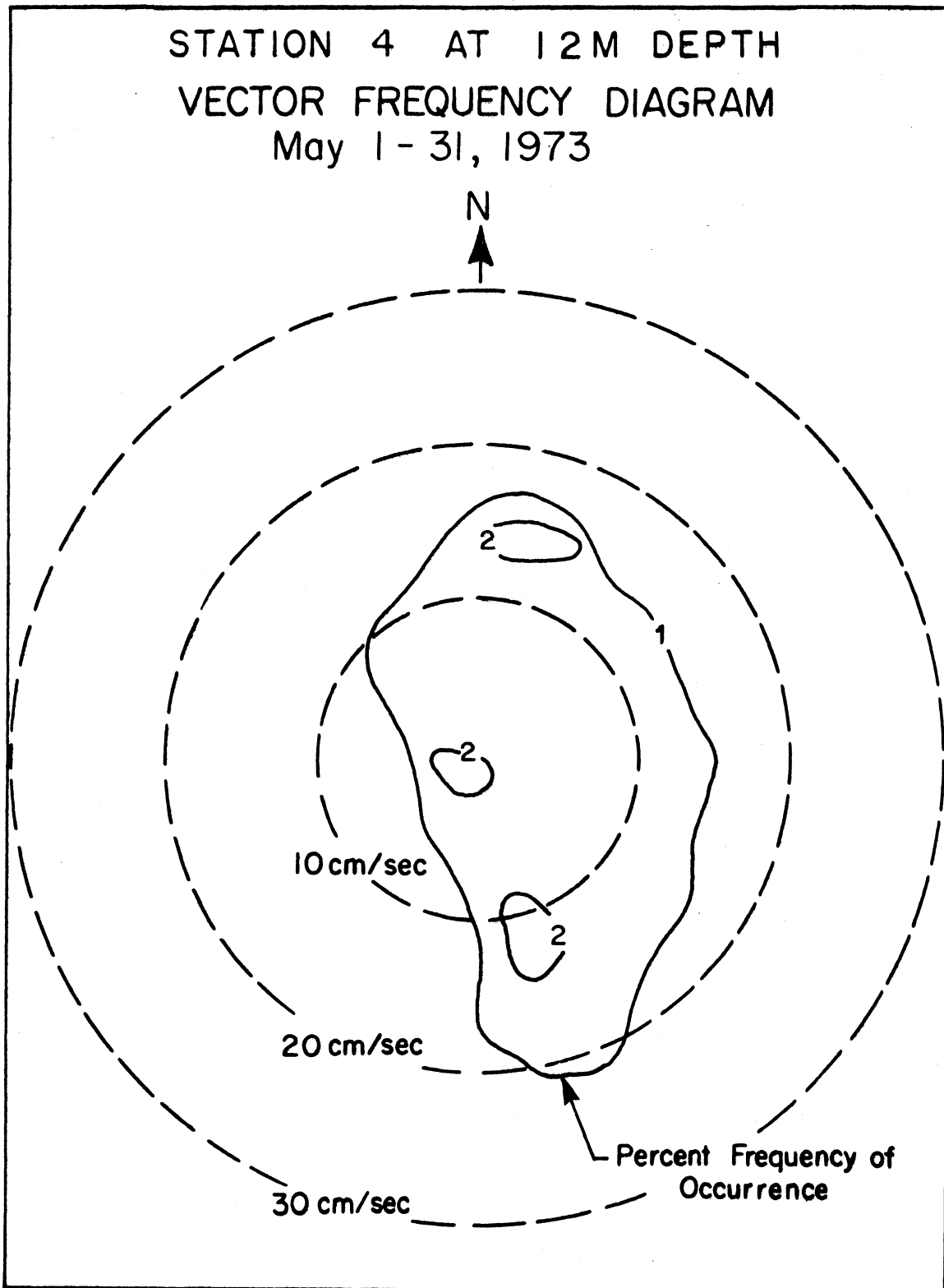


Figure 4.66

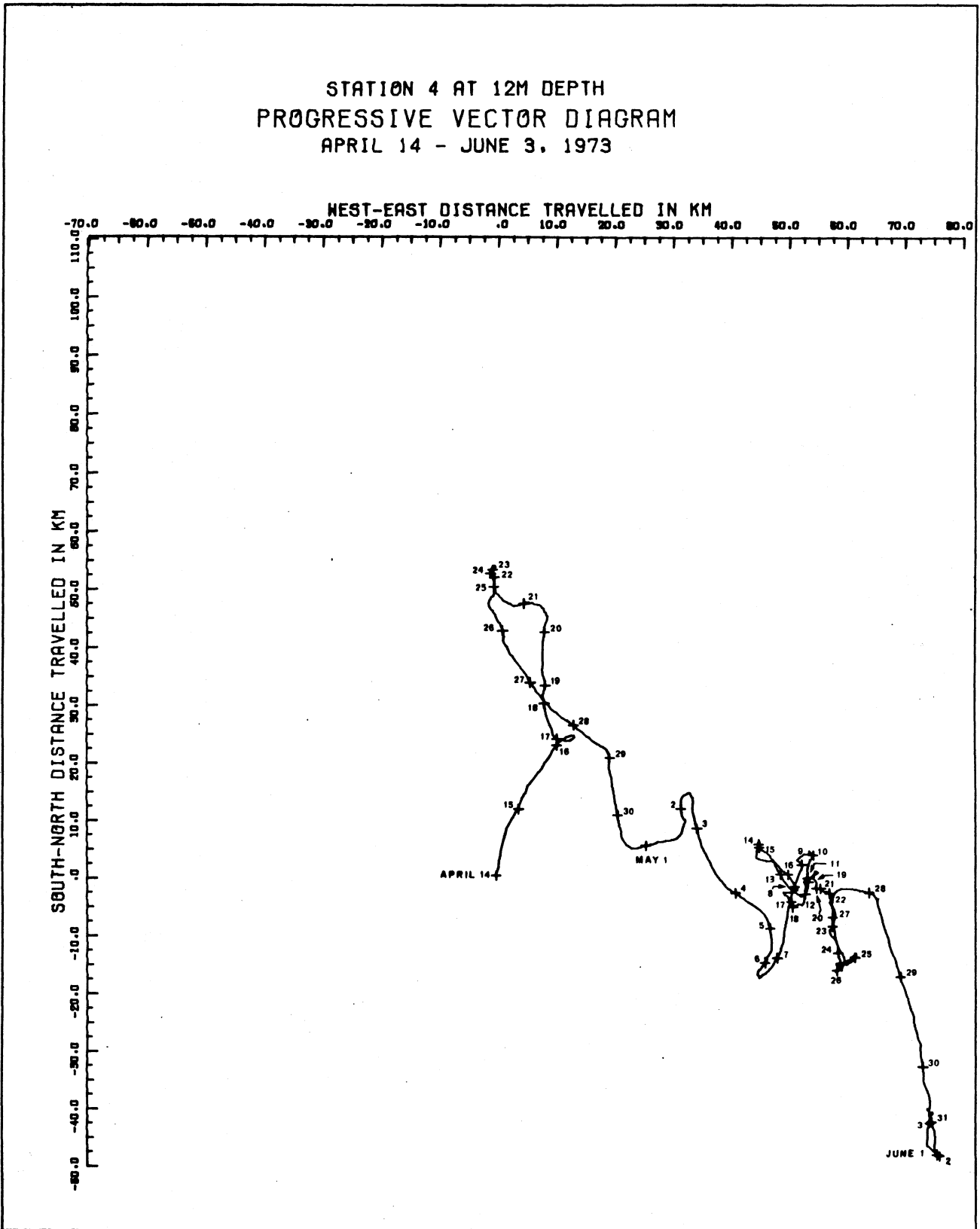


Figure 4.67

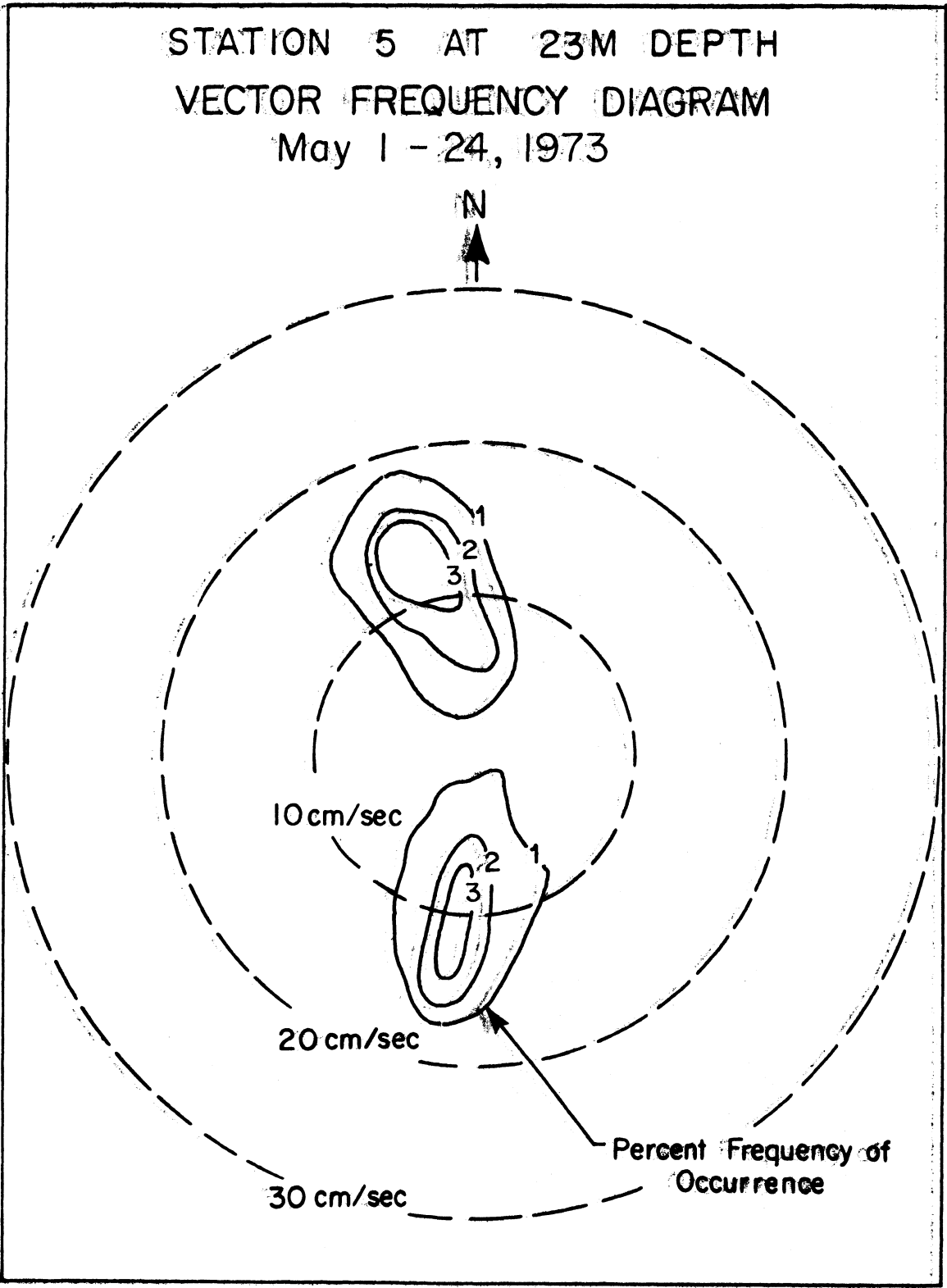


Figure 4.68

STATION 5 AT 23M DEPTH  
PROGRESSIVE VECTOR DIAGRAM  
APRIL 14 - MAY 24, 1973

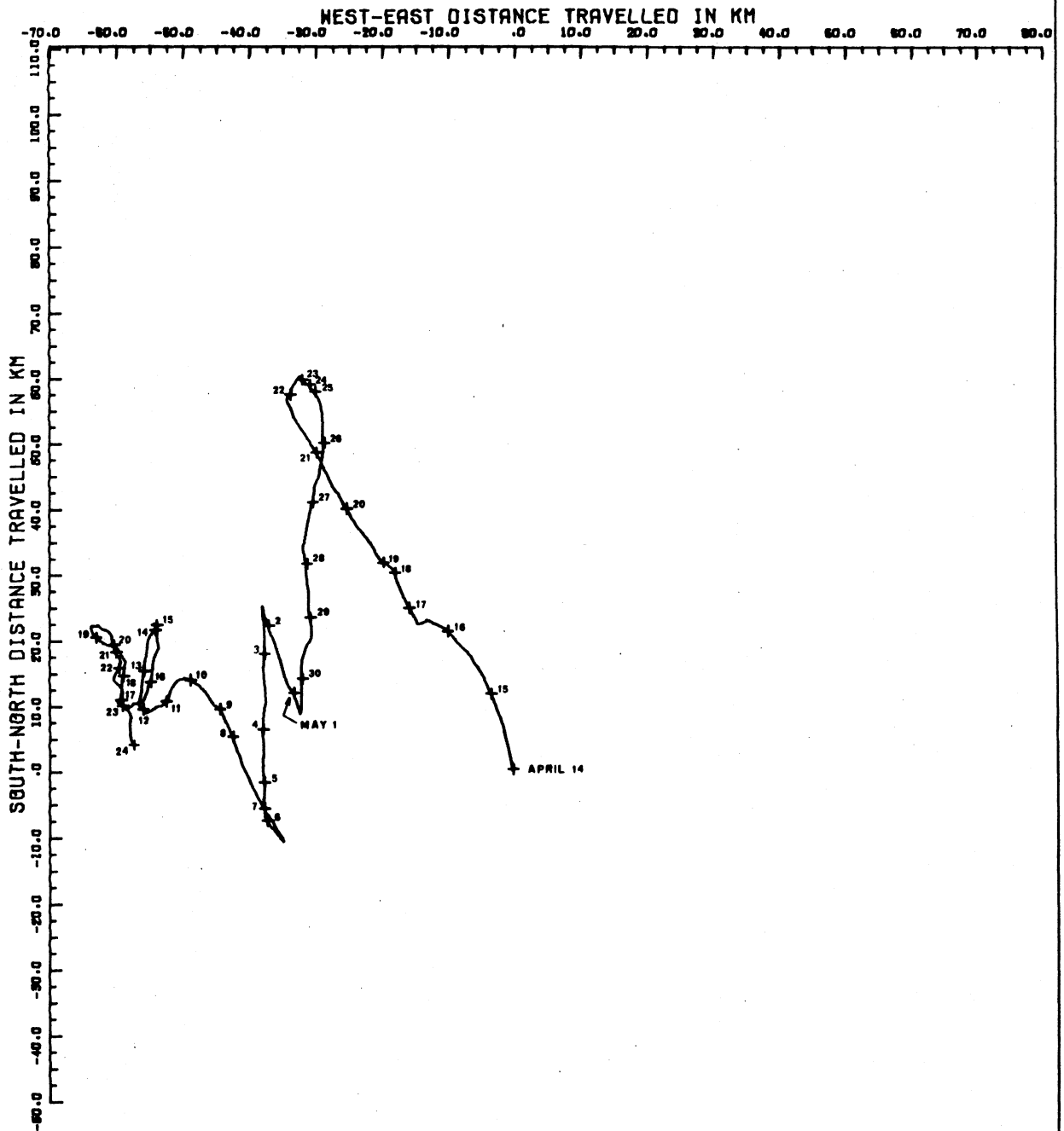


Figure 4.69

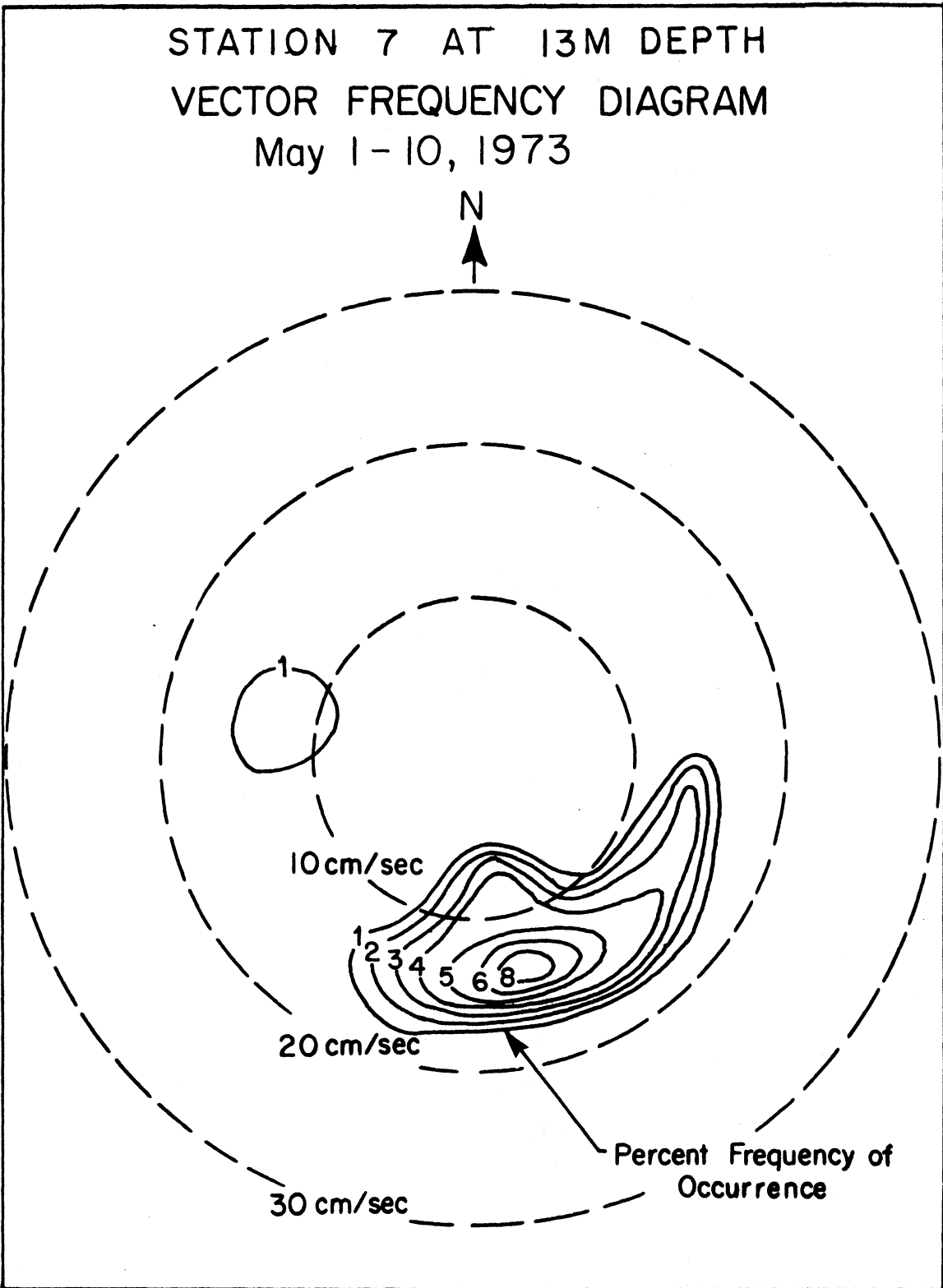
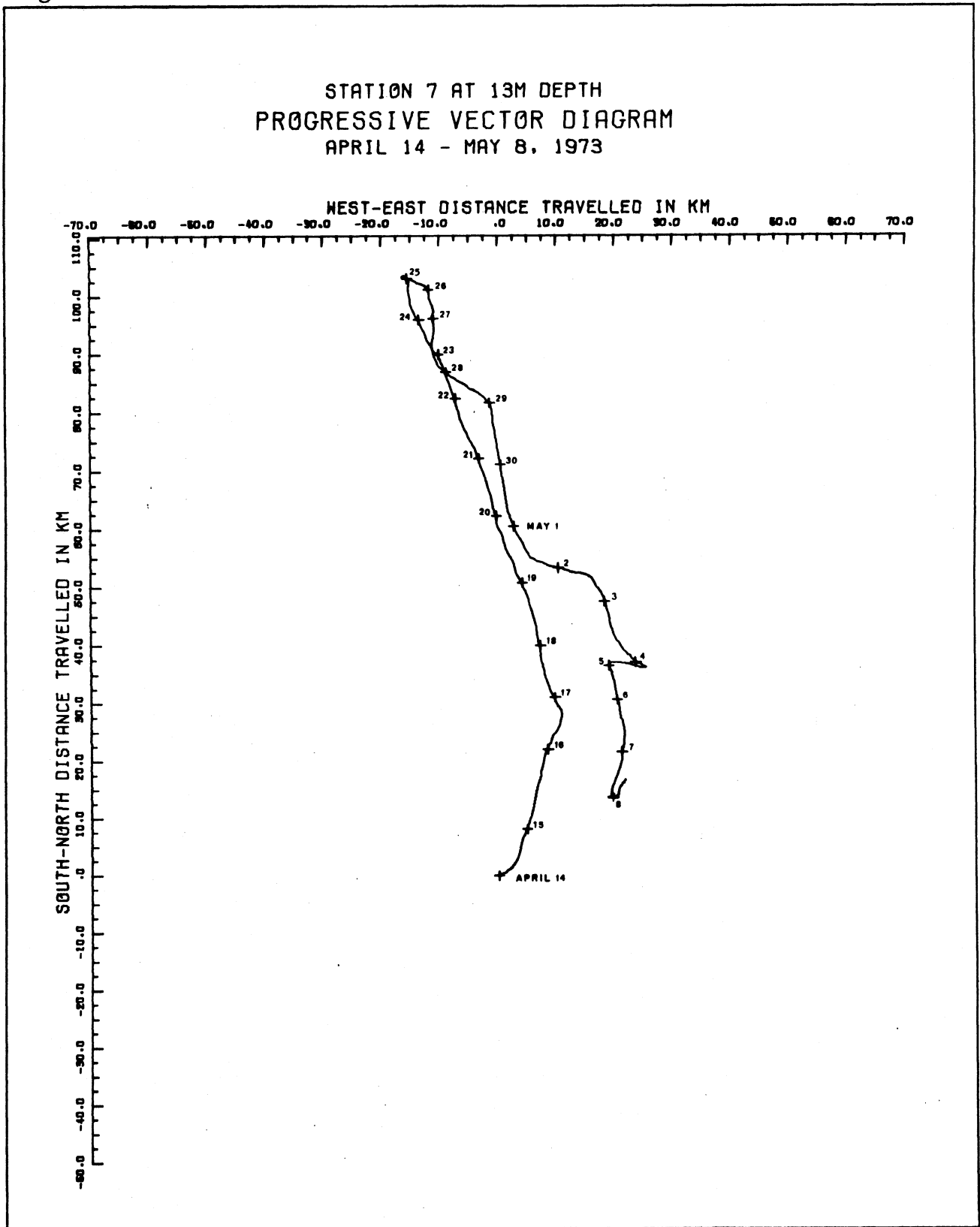


Figure 4.70



During June the winds were mainly offshore (toward E and NE, fig. 4.71) with some episodes of northwestward wind. Again, only the latter, onshore wind affected the current regime: northwestward flow at Station 2 (fig. 4.72); toward NNW at Station 4 (fig. 4.73); and toward the N to NW sector at Station 7 (fig. 4.75). It must be borne in mind, however, that Stations 4 and 7 were found to have been prematurely released, although they remained tethered at their stations. The effect of this on the current records cannot be precisely assessed. The instruments were riding higher in the water after release and may also have been influenced by wind-driven motions of the float, then at the surface.

#### Survey V, 17 July to 13 August 1973

The wind diagram for the latter half of July, at which time the Lake was fully stratified, showed strong winds toward three principal directions: WNW, NE and S (fig. 4.76). The stations in shallowest water showed the most direct response to wind with predominantly shore-parallel currents, e.g. toward SSE or NW at Station 1 (figs. 4.77 and 4.78). In somewhat deeper water at Station 4 (Fig. 4.79) the response was toward the south, and a "cusping" (see Chapter 1) of the progressive vector diagram (fig. 4.80) indicates the onset of a rotary current component. That component, produced by internal Poincaré wave activity, becomes more conspicuous as a "looping" at the stations in deeper water: Station 5 (fig. 4.82, particularly during the current reversal episode, 27 to 29 July) and Station 6 (figs. 4.84 and 4.86). This may provide part of the explanation of the direction scatter in the vector frequency diagram for Station 6 (figs. 4.83 and 4.85) and to a lesser extent for Station 5 (fig. 4.81). Note that the 1% frequency isopleth in the Station 6 diagrams reaches  $20 \text{ cm. s}^{-1}$  for various directions, with a maximum of about  $25 \text{ cm. s}^{-1}$  toward SSE at the 26 m level.

The August wind diagram (fig. 4.87) shows two frequency concentrations, the strongest toward NE and a lesser concentration toward SE. There is also a minor wind activity toward the NW, but as this is an onshore wind direction, the current response to this component is the strongest at Station 1 (fig. 4.88, 1-7 August) which also shows a response toward SSE. At Station 5

(fig. 4.89, 1-12 August) the response toward SSE is the strongest, but a substantial response toward NW is also present. The same is true for Station 6, 1-6 August, at both instrument depths (figs. 4.90 and 4.91) except that the response at that time at Station 6 was closer to northward. The speeds at Station 6 were higher during the first days of August than during previous months and higher than at other stations. A reduction in the speed scale was made on figures 4.90 and 4.91 to accommodate this. The strong current toward SSE starting on 2 August is illustrated in the progressive vector diagrams, figures 4.84 and 4.86. The rotary current component, causing conspicuous cusping and looping between 24 July and 2 August, is masked by the strong unidirectional flow after 2 August, but its influence can be inferred from the "meandering" course of the current track.

The vector diagrams for Stations 4 (fig. 4.80) and 5 (fig. 4.82) showed a sudden reversal from the strong south-southeastward current to a slower north-northwestward current on 7 August, a similar reversal having taken place at Station 1 (fig. 4.78) three days earlier.

#### Survey VI, 15 August to 7 November 1973

As Station 5 was the only station operating during this final survey, and as it was subject to premature release at an unknown time although remaining tethered, the value of vector frequency diagrams is open to question in this case. Therefore none were prepared. The progressive vector diagram (fig. 4.92) shows strong rotary components leading to persistent looping and clearly dominated by internal Poincaré wave motion during that month. For example, approximately three loops were completed between midnight on 19 August and one hour after midnight on 21 August, an average "period" of a little over 16 hours. Similarly then were three loops completed between about 1800 on 13 September and midnight on 16 September, an average period of 18 hours. These rough results strongly suggest near-inertial motion.

#### Persistence factors, spectra, and cross-spectra (deferred to Chapter 6)

Further analyses of current patterns and current/wind relationships are deferred to Chapter 6, of which the current spectra form a separate final section.

The remainder of the present chapter consists of figures only.

Figure 4.71

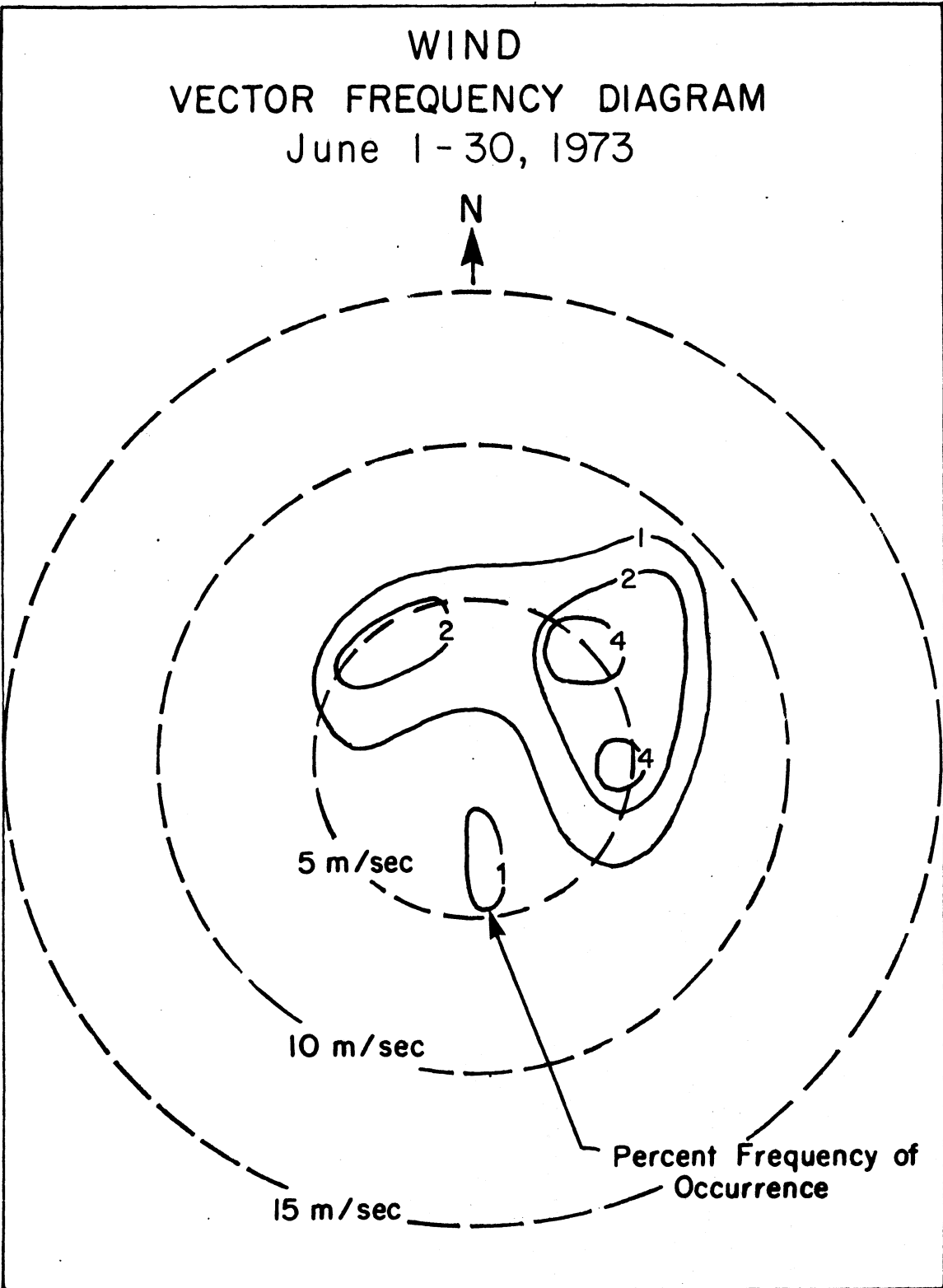


Figure 4.72 The corresponding progressive vector diagram is on page 227.

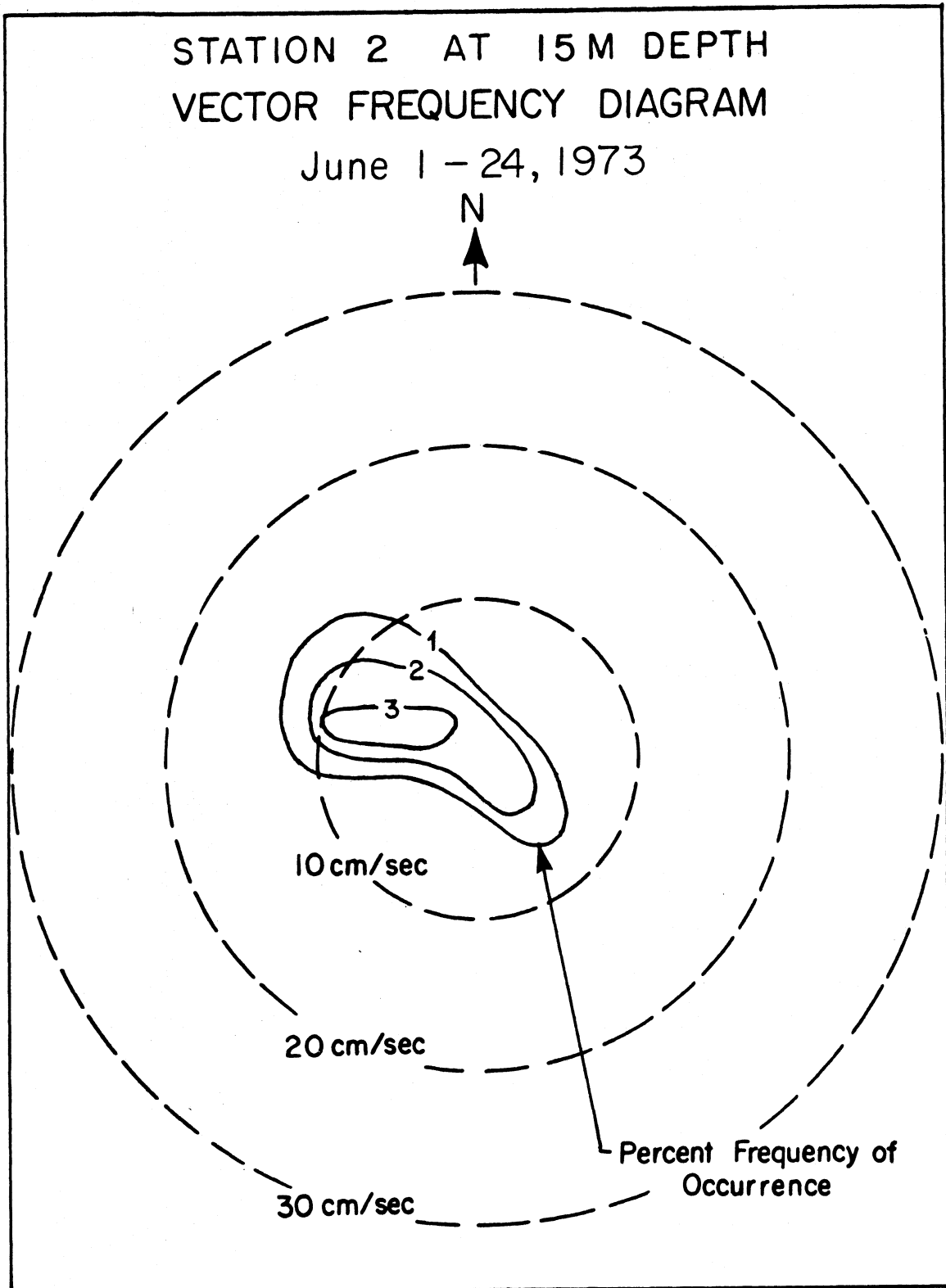


Figure 4.73

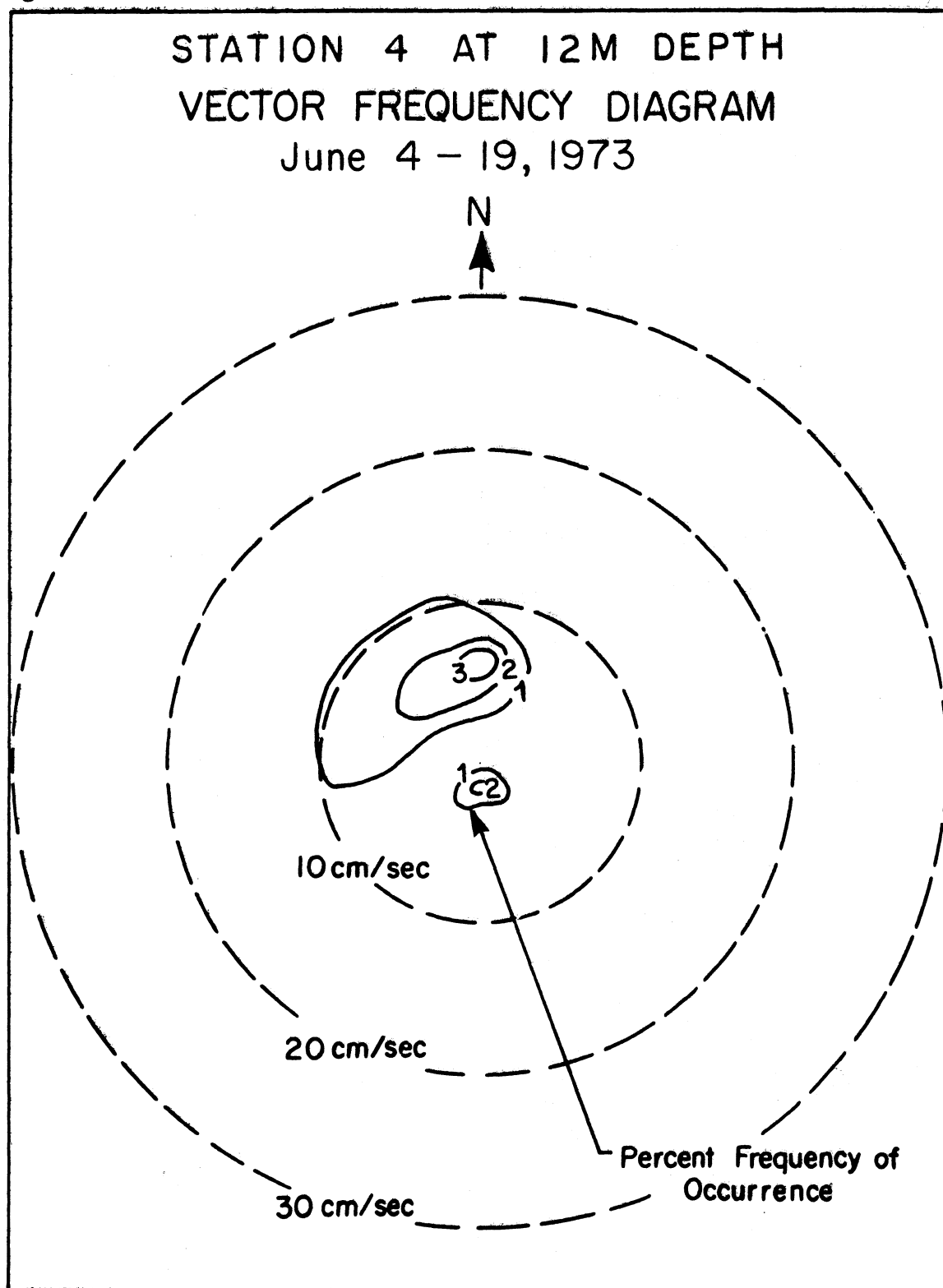


Figure 4.74

STATION 4 AT 12M DEPTH  
PROGRESSIVE VECTOR DIAGRAM  
JUNE 5 - 17, 1973

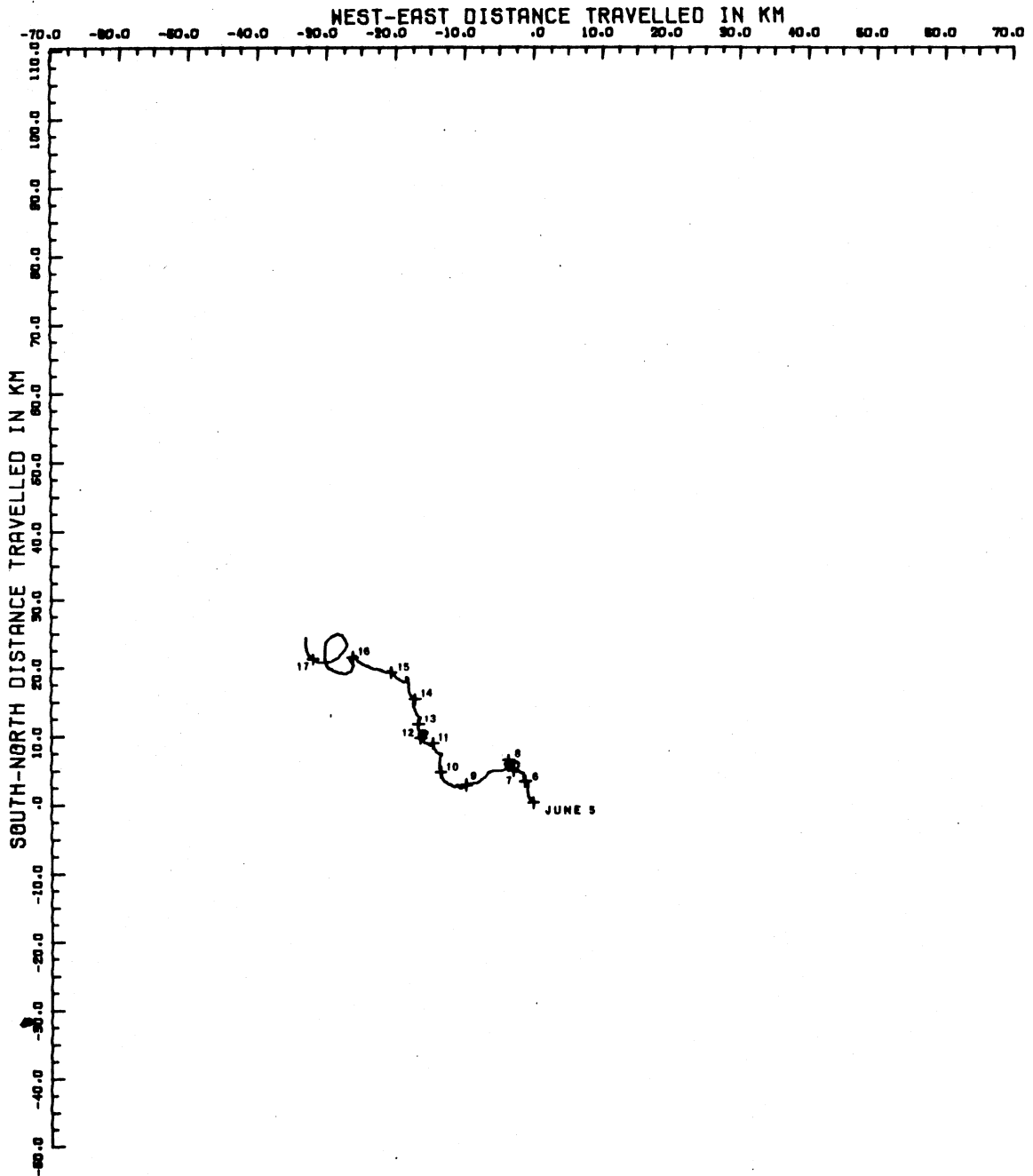


Figure 4.75

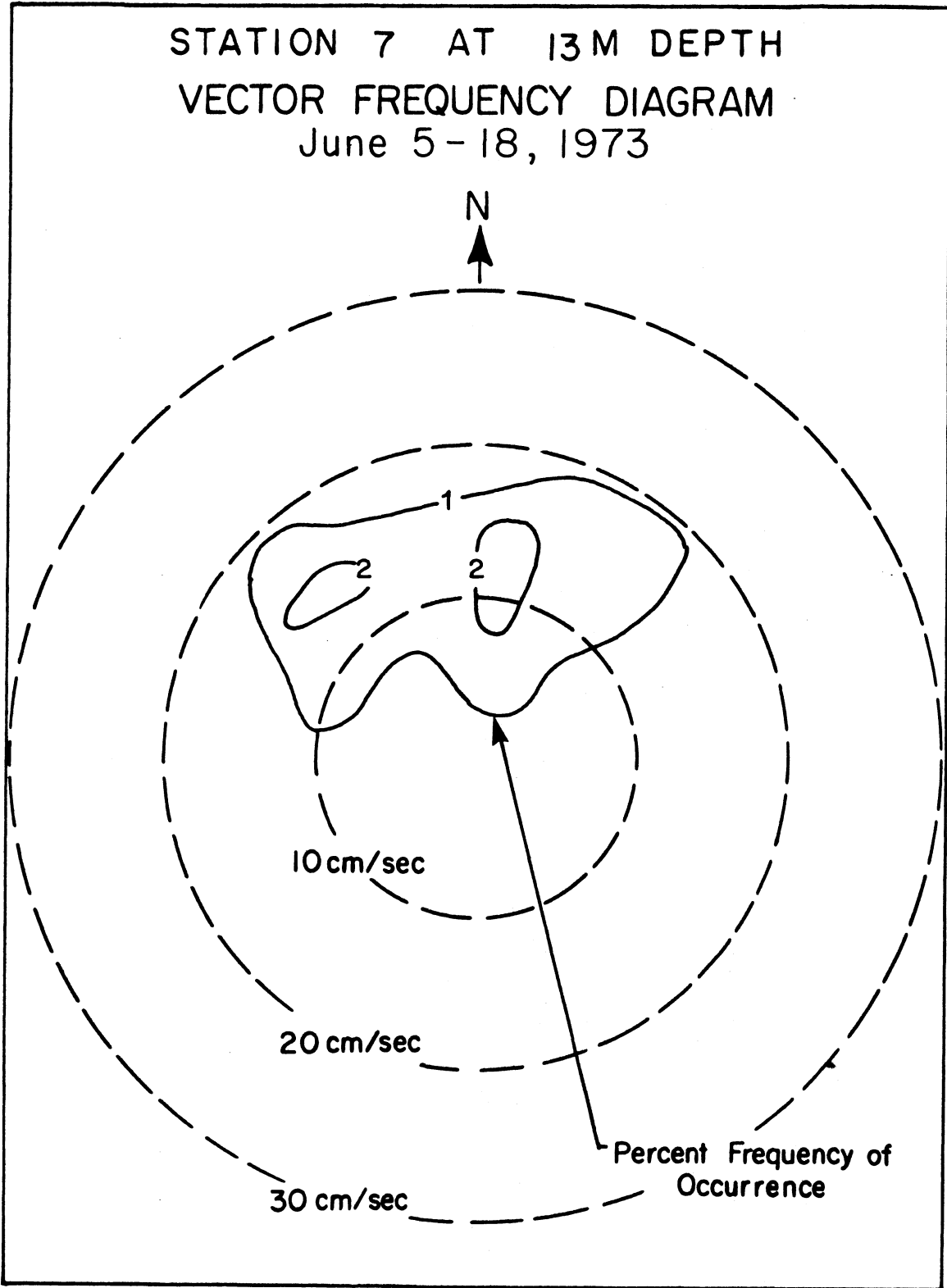


Figure 4.76

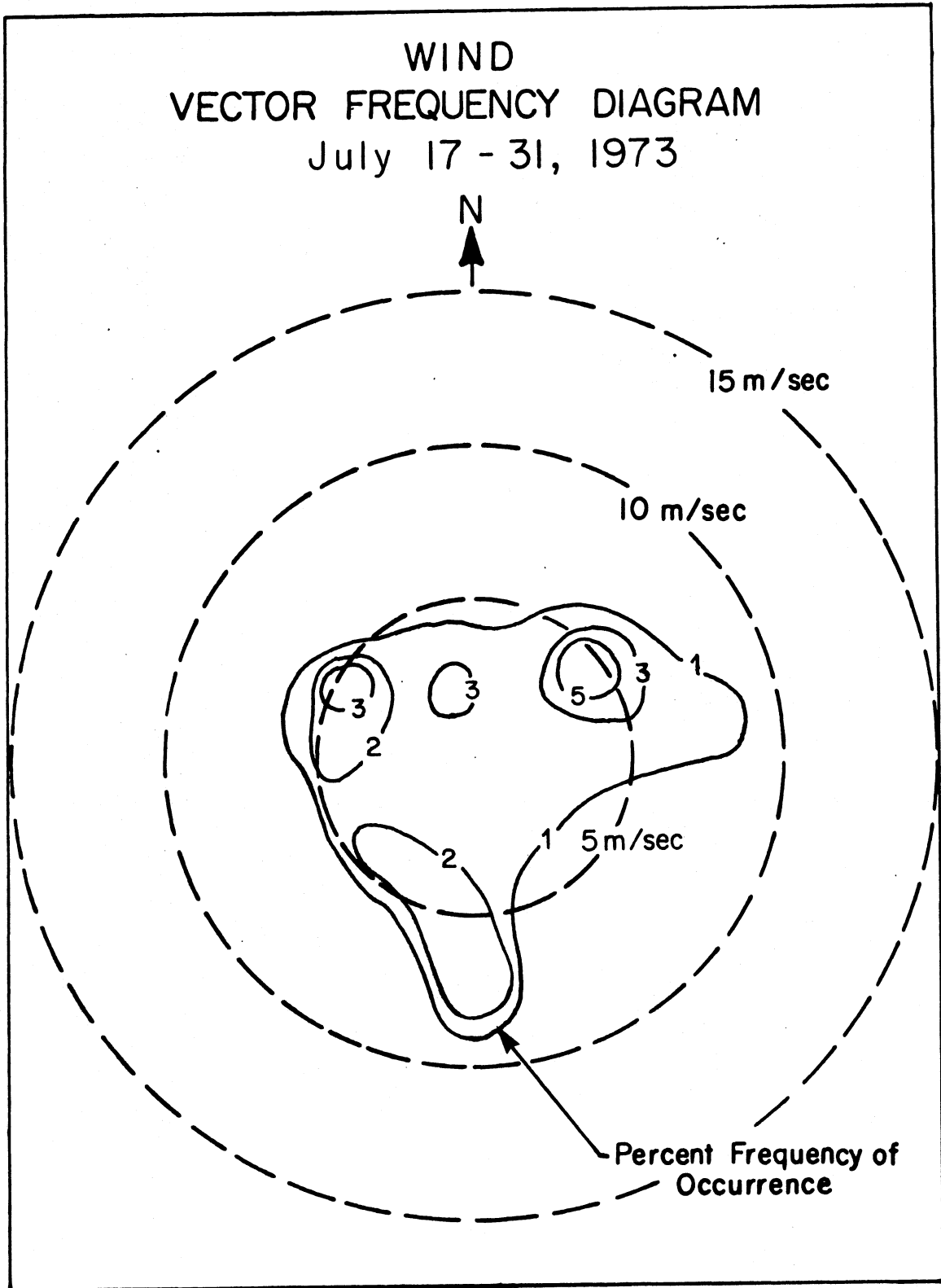


Figure 4.77

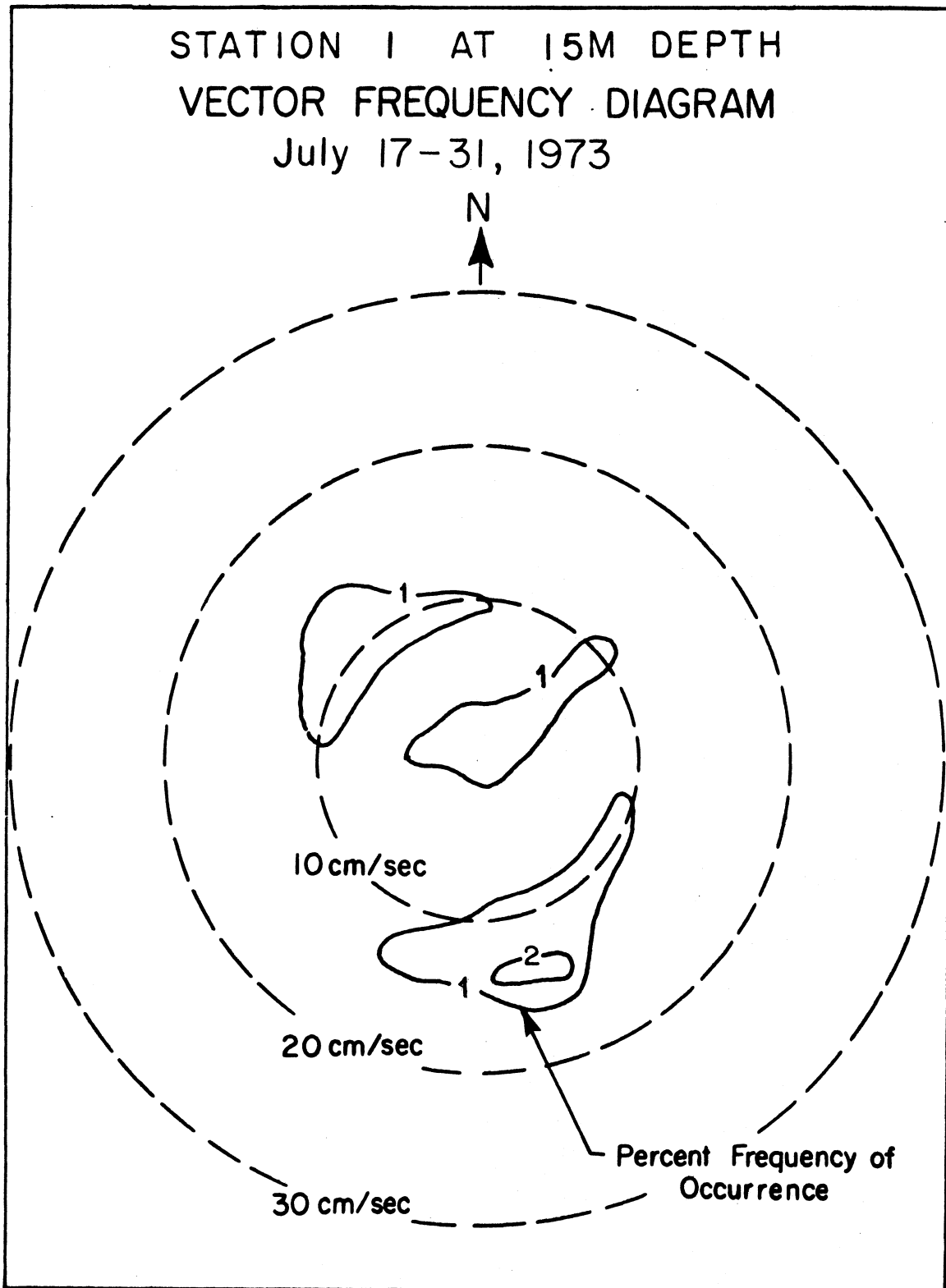


Figure 4.78

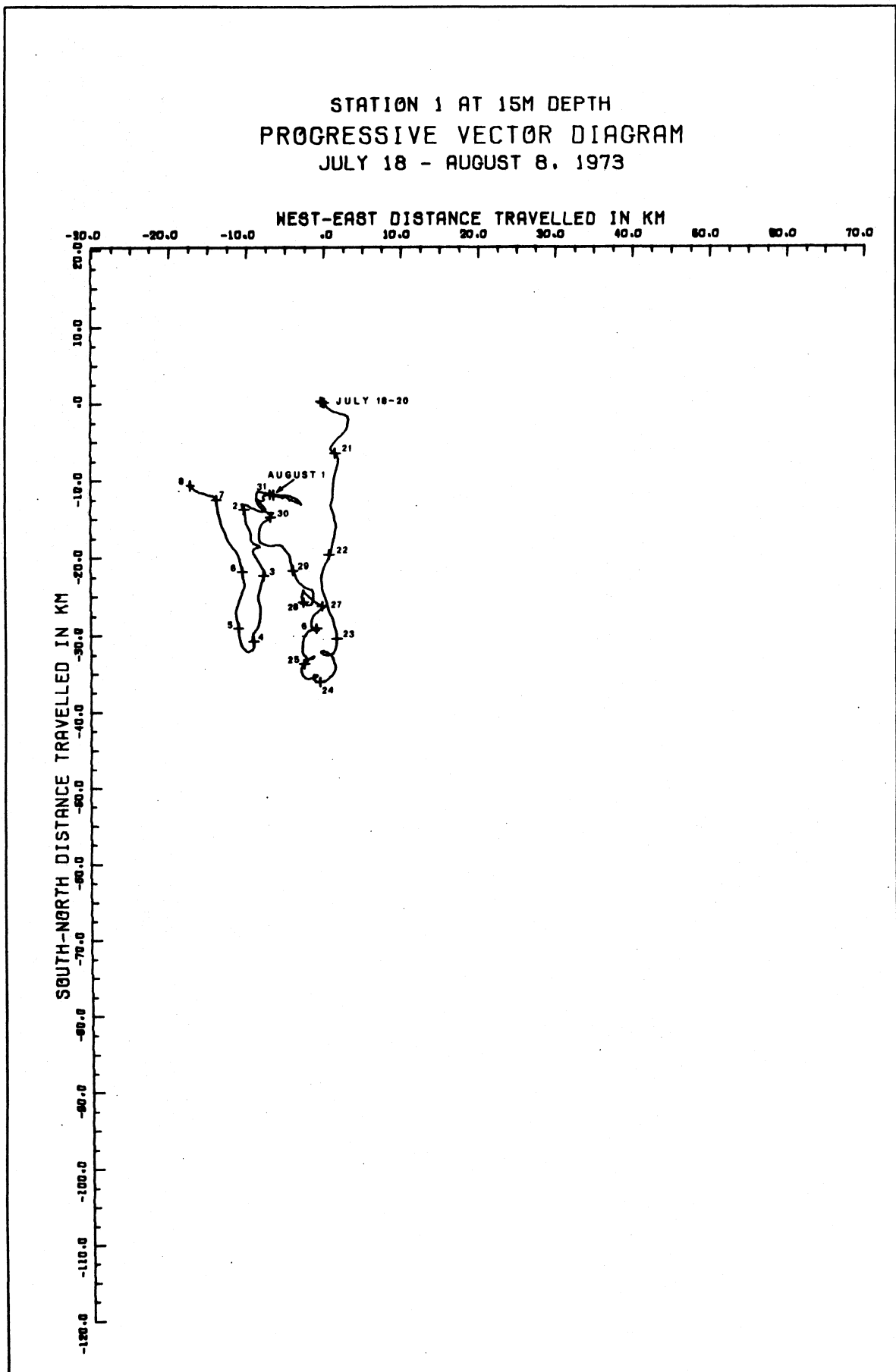


Figure 4.79

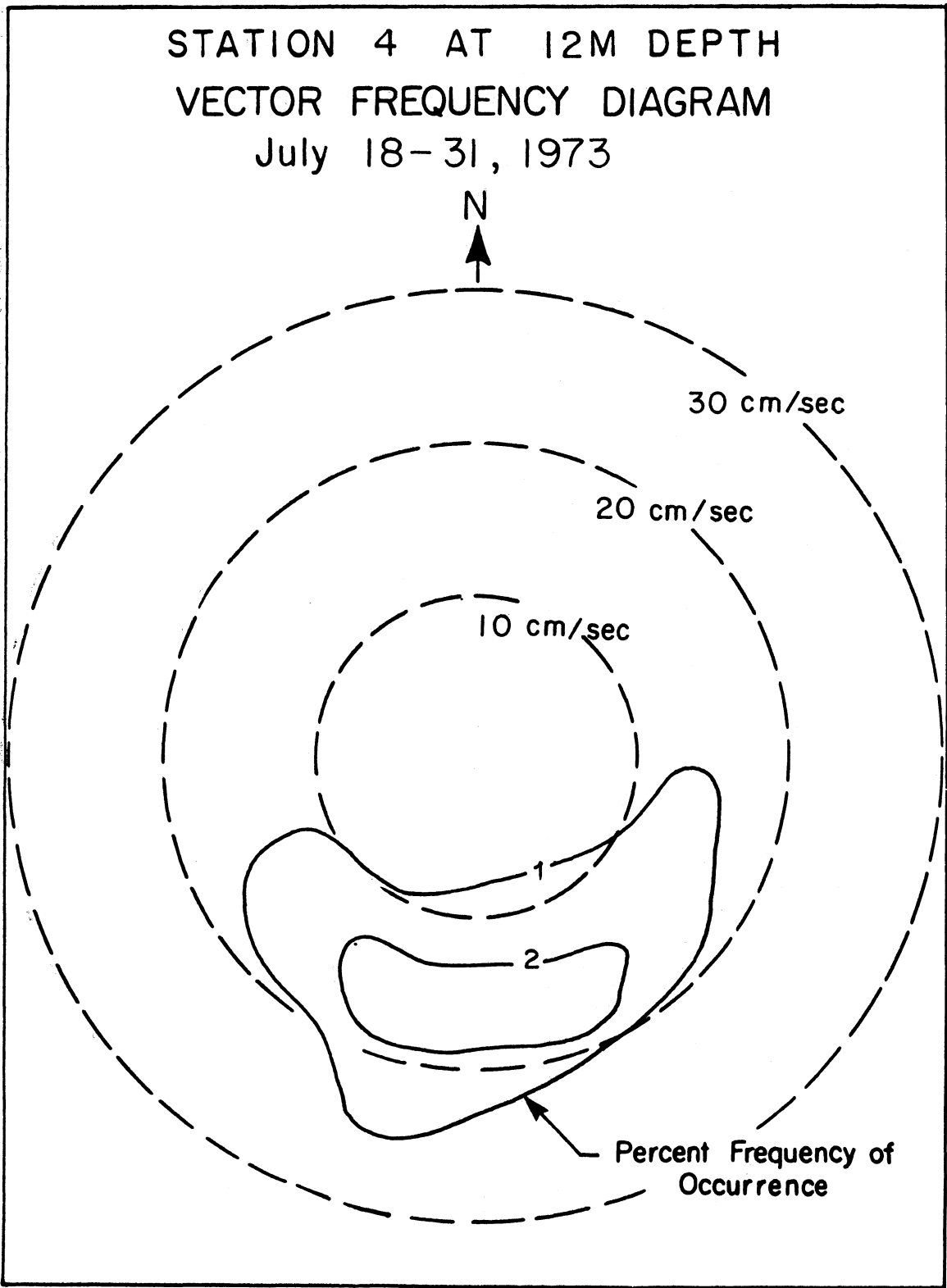


Figure 4.80

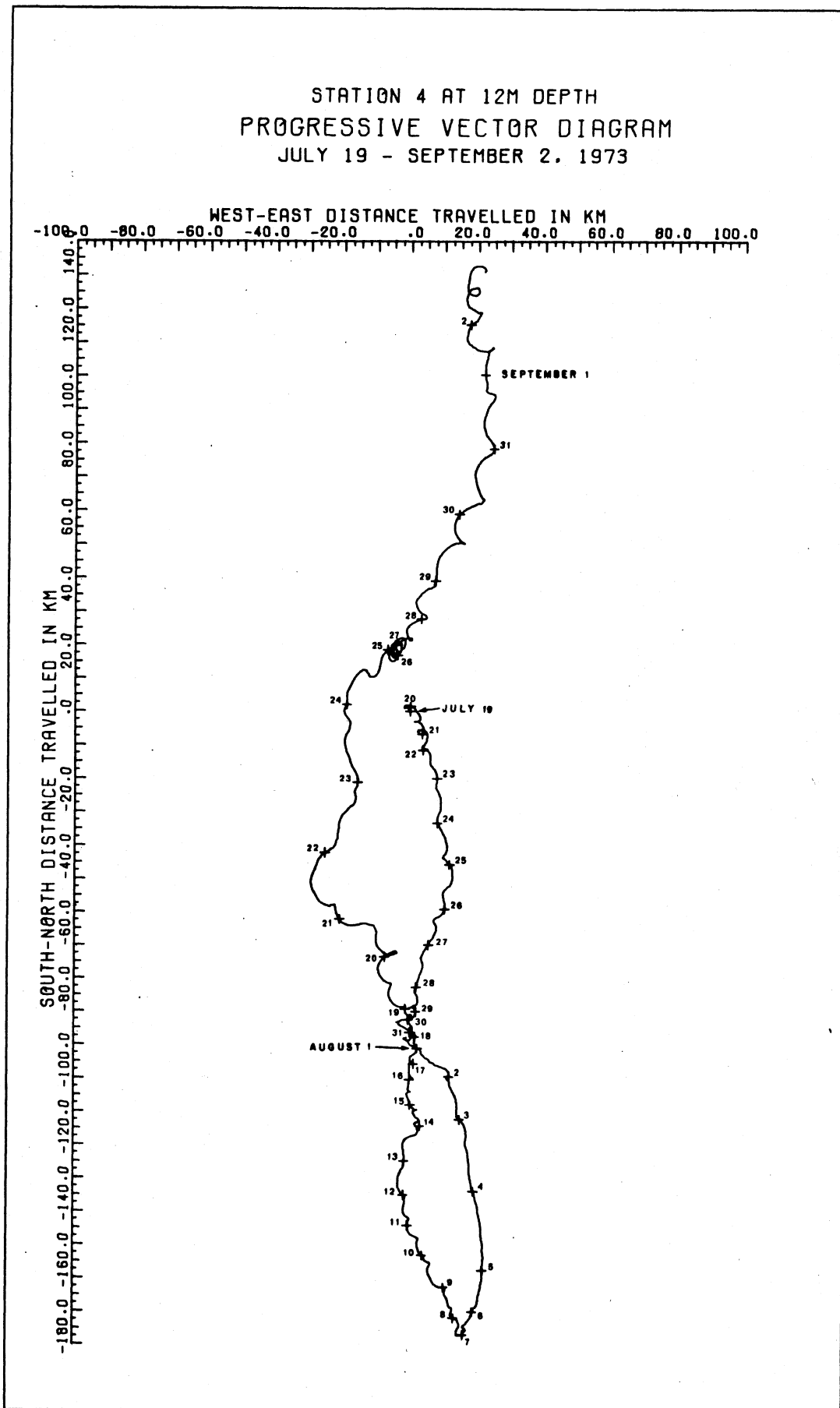


Figure 4.81

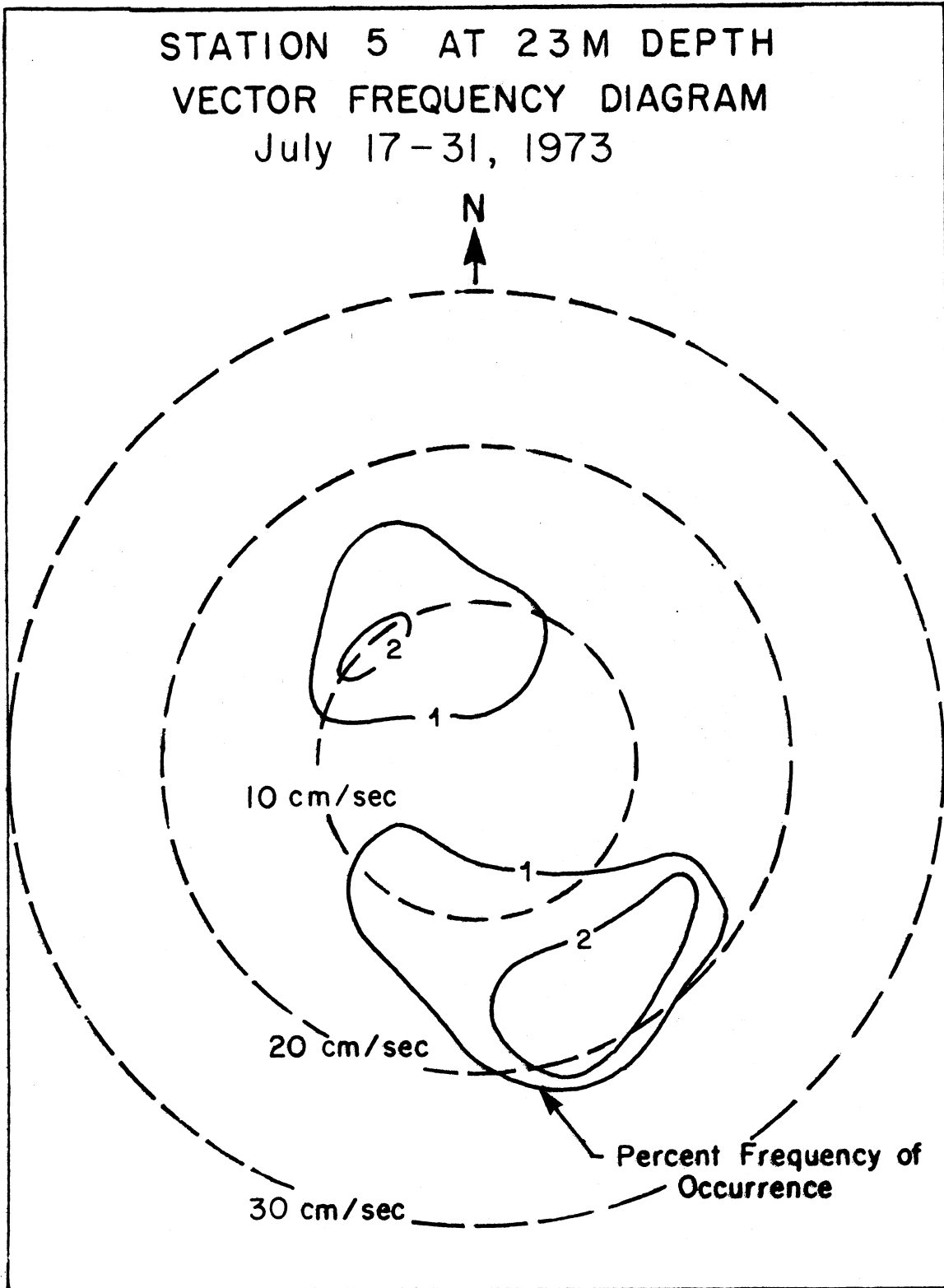


Figure 4.82

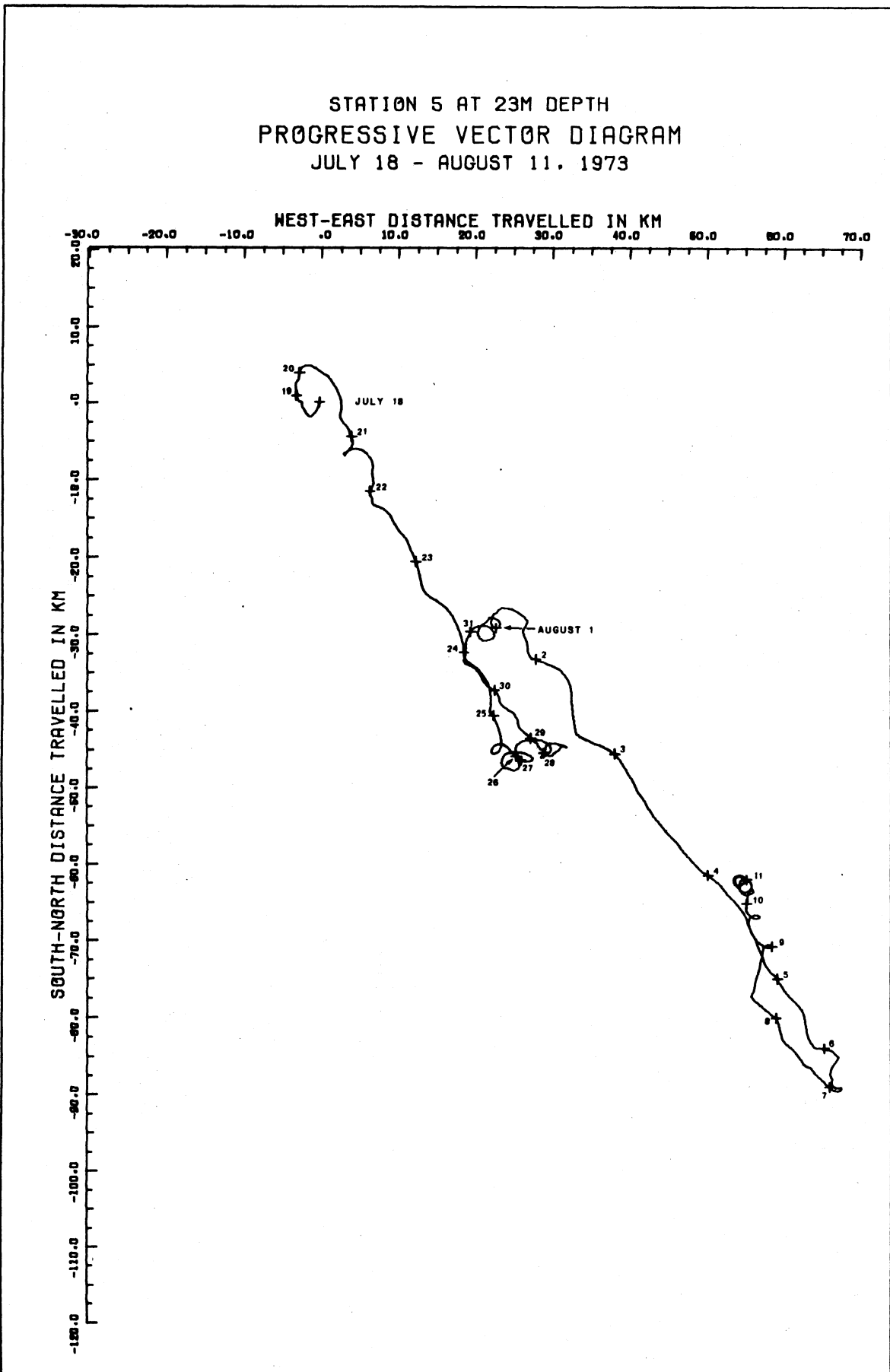


Figure 4.83

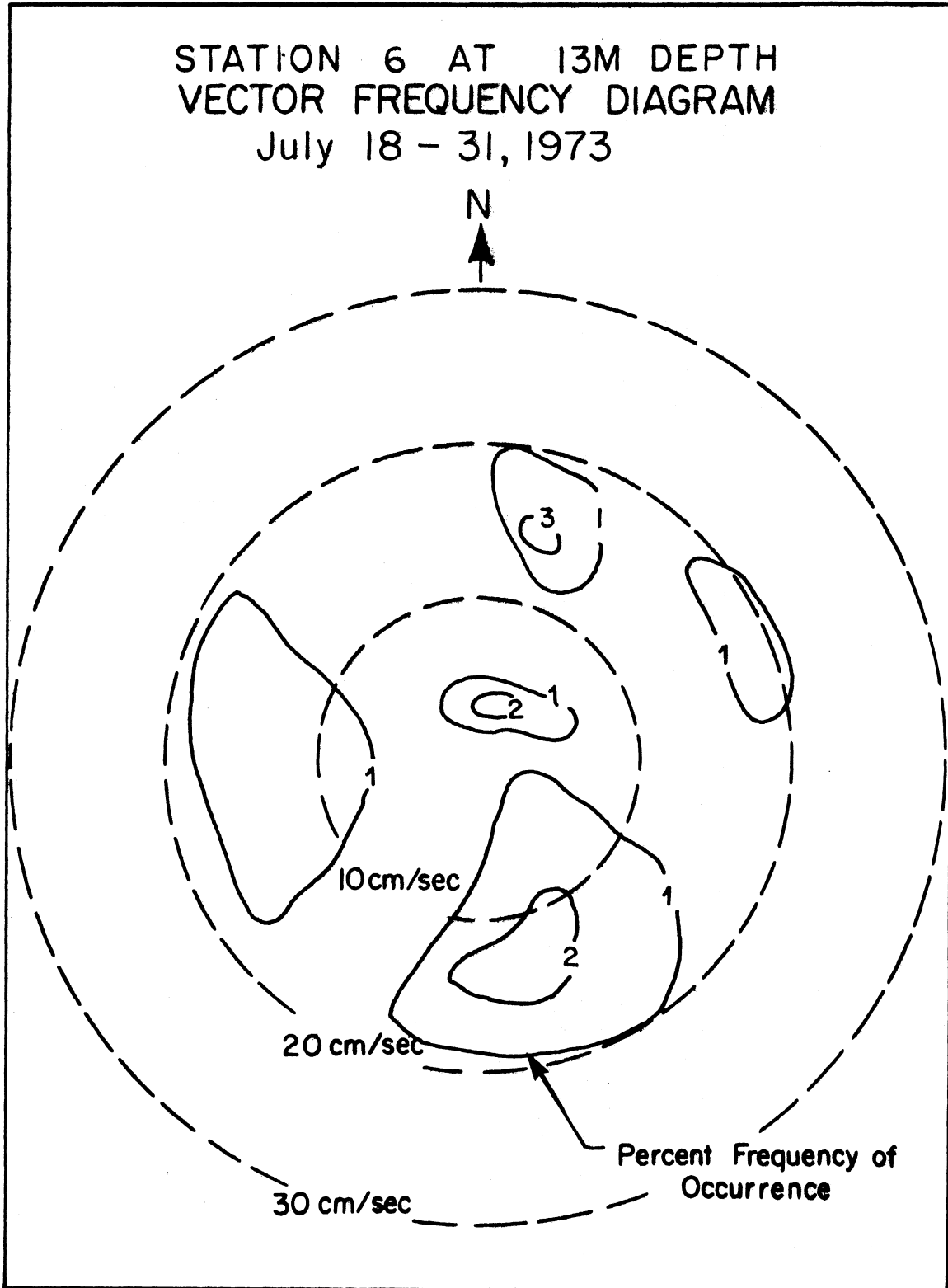


Figure 4.84

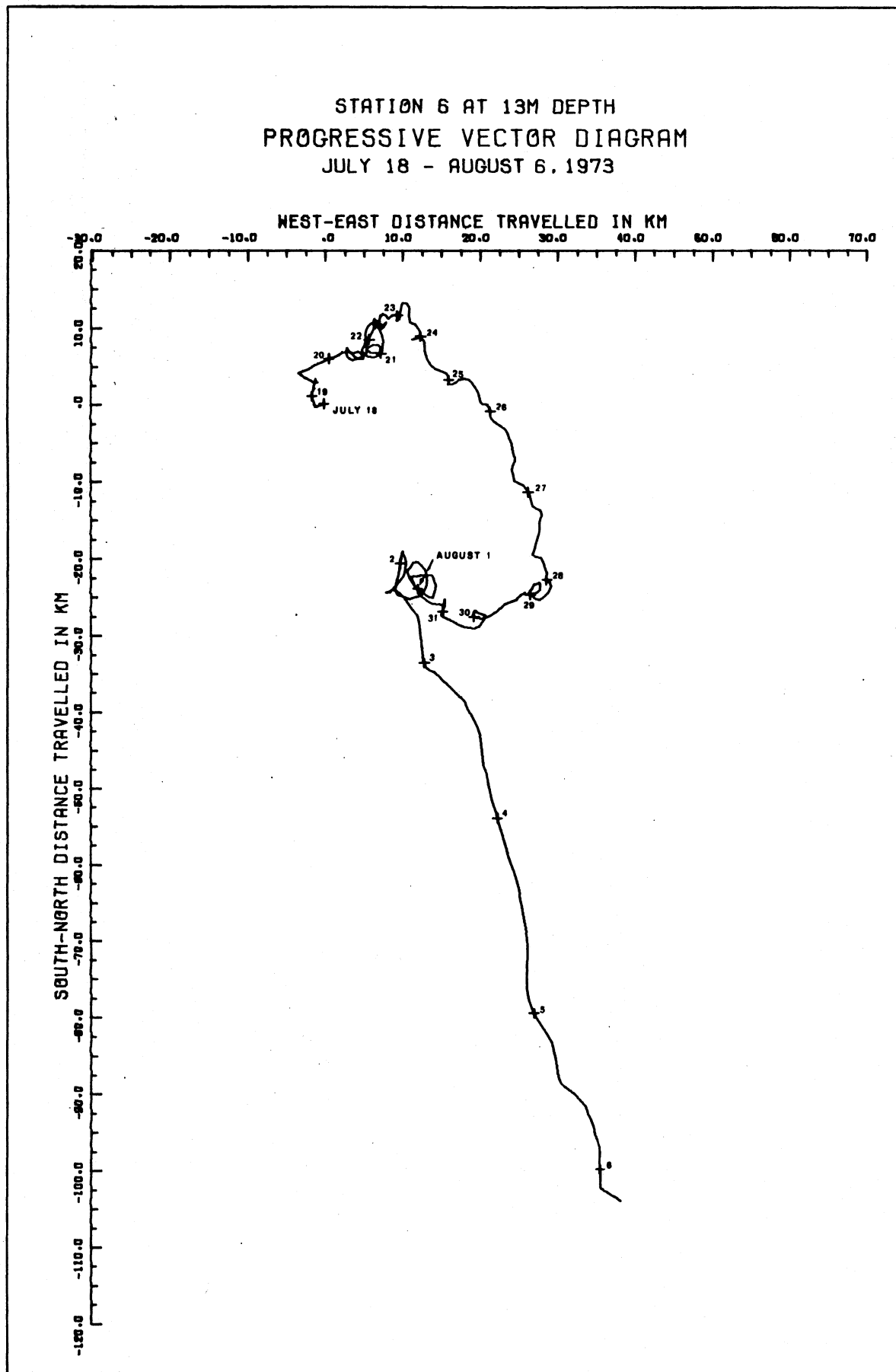


Figure 4.85

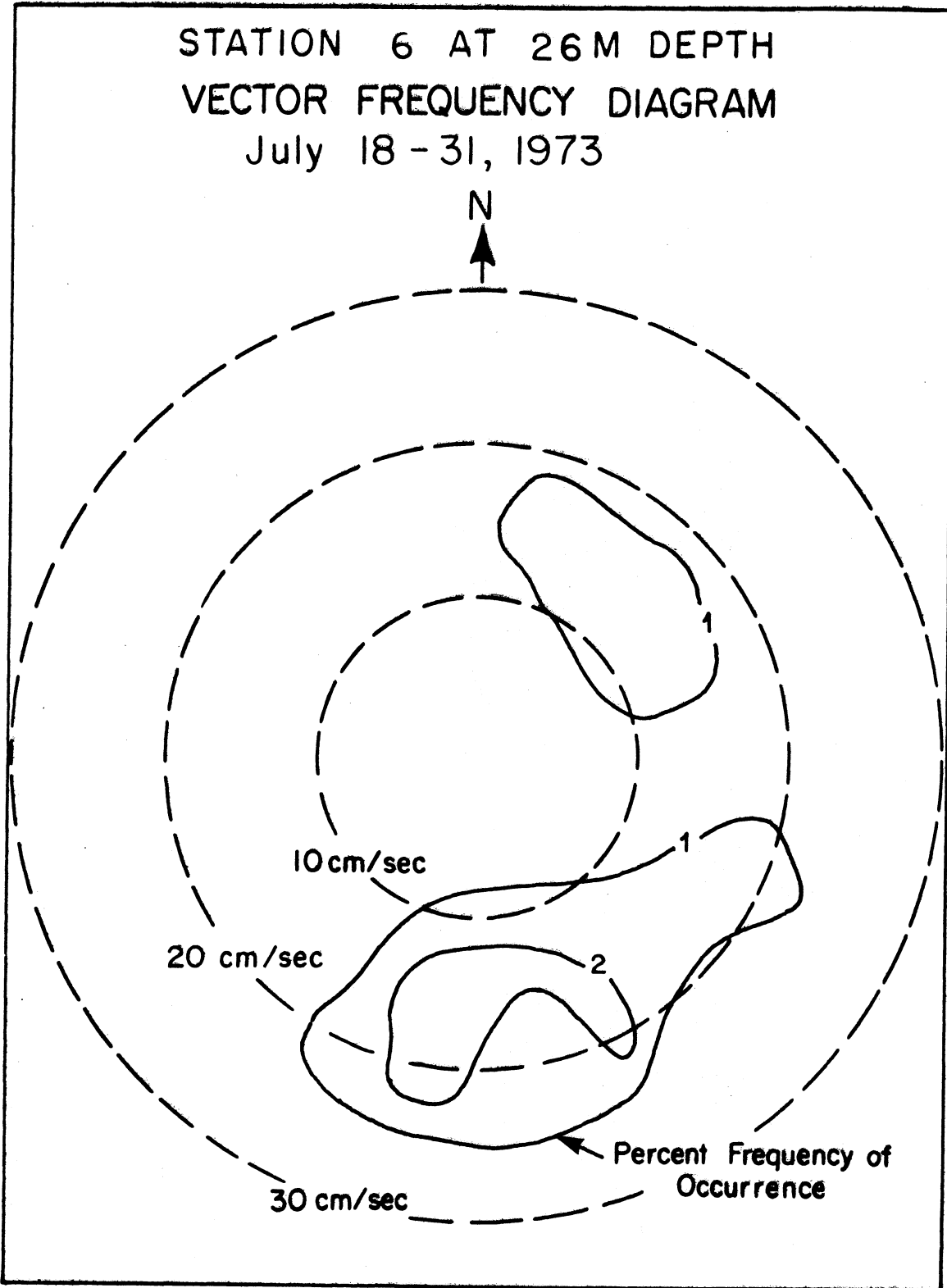


Figure 4. 86

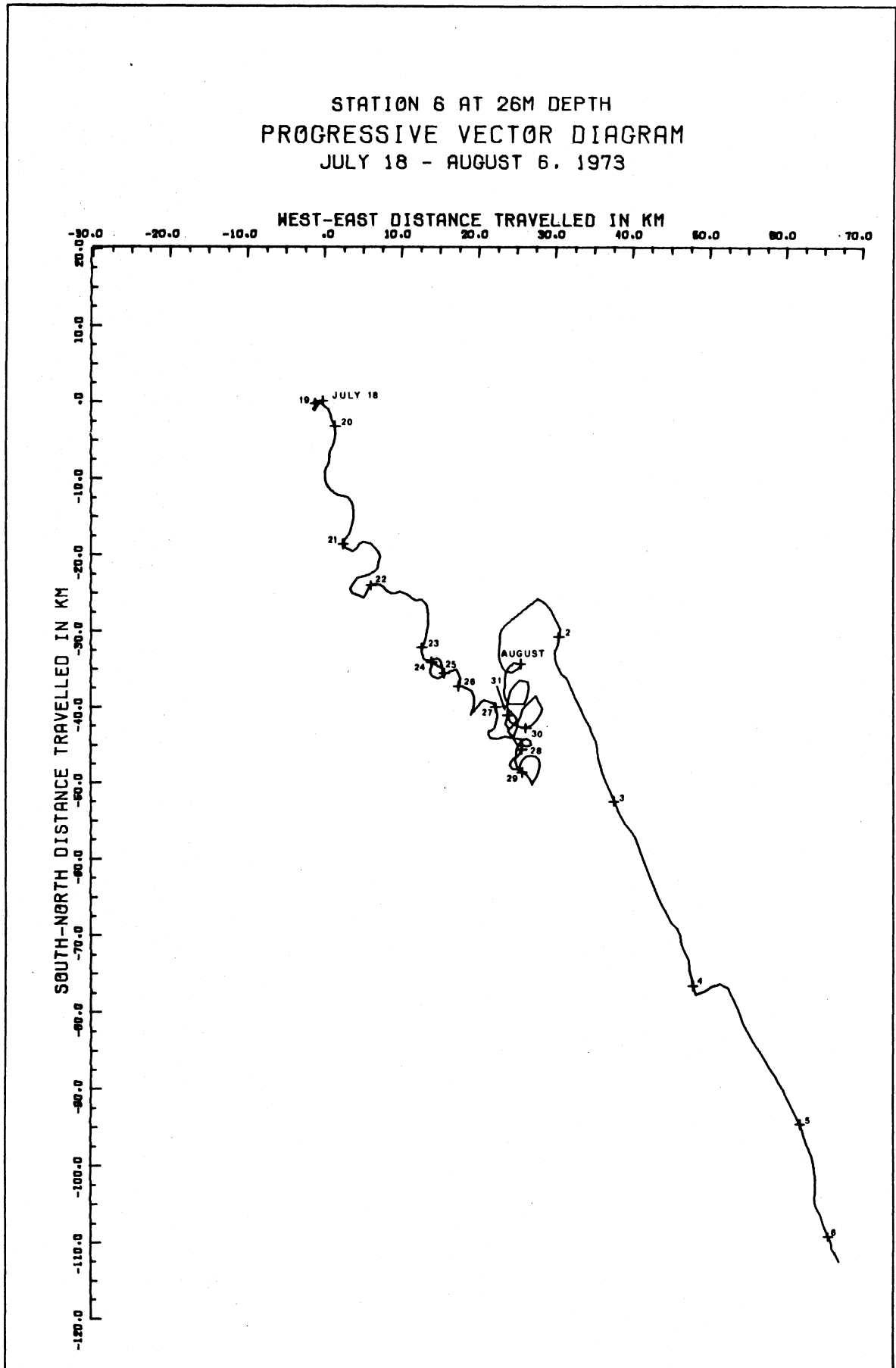


Figure 4.87

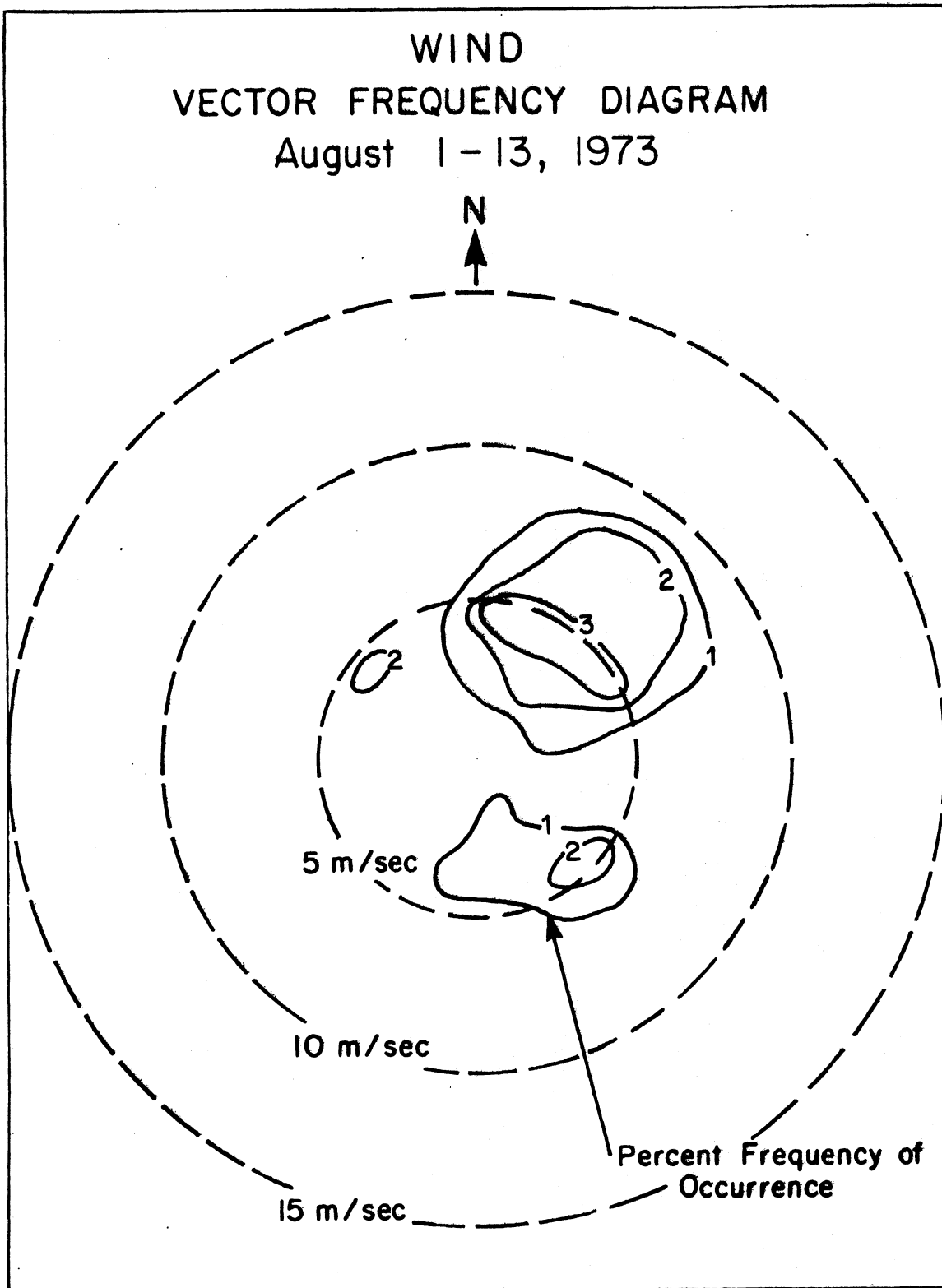


Figure 4.88

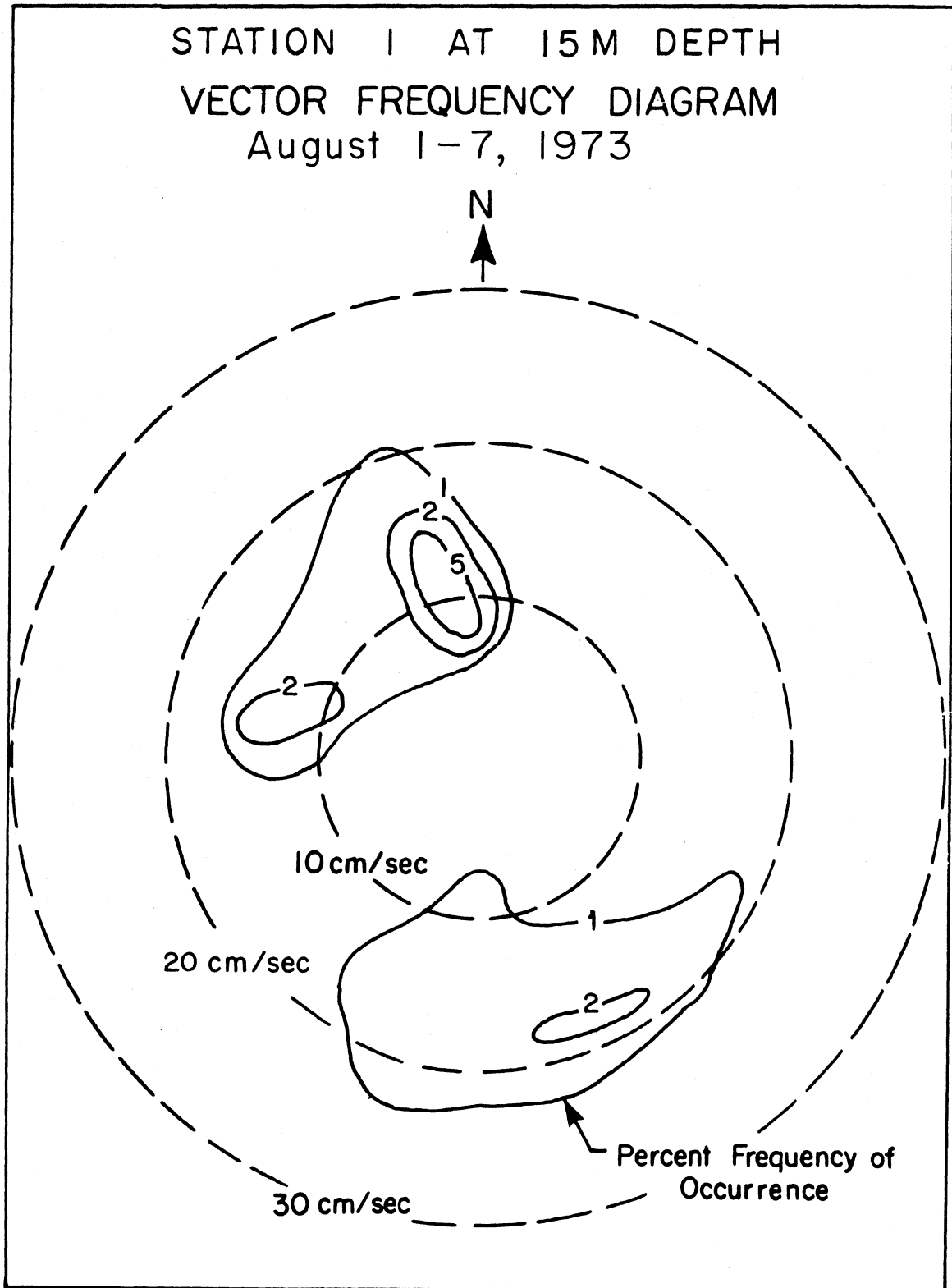


Figure 4. 89 The corresponding progressive vector diagram is on page 247.

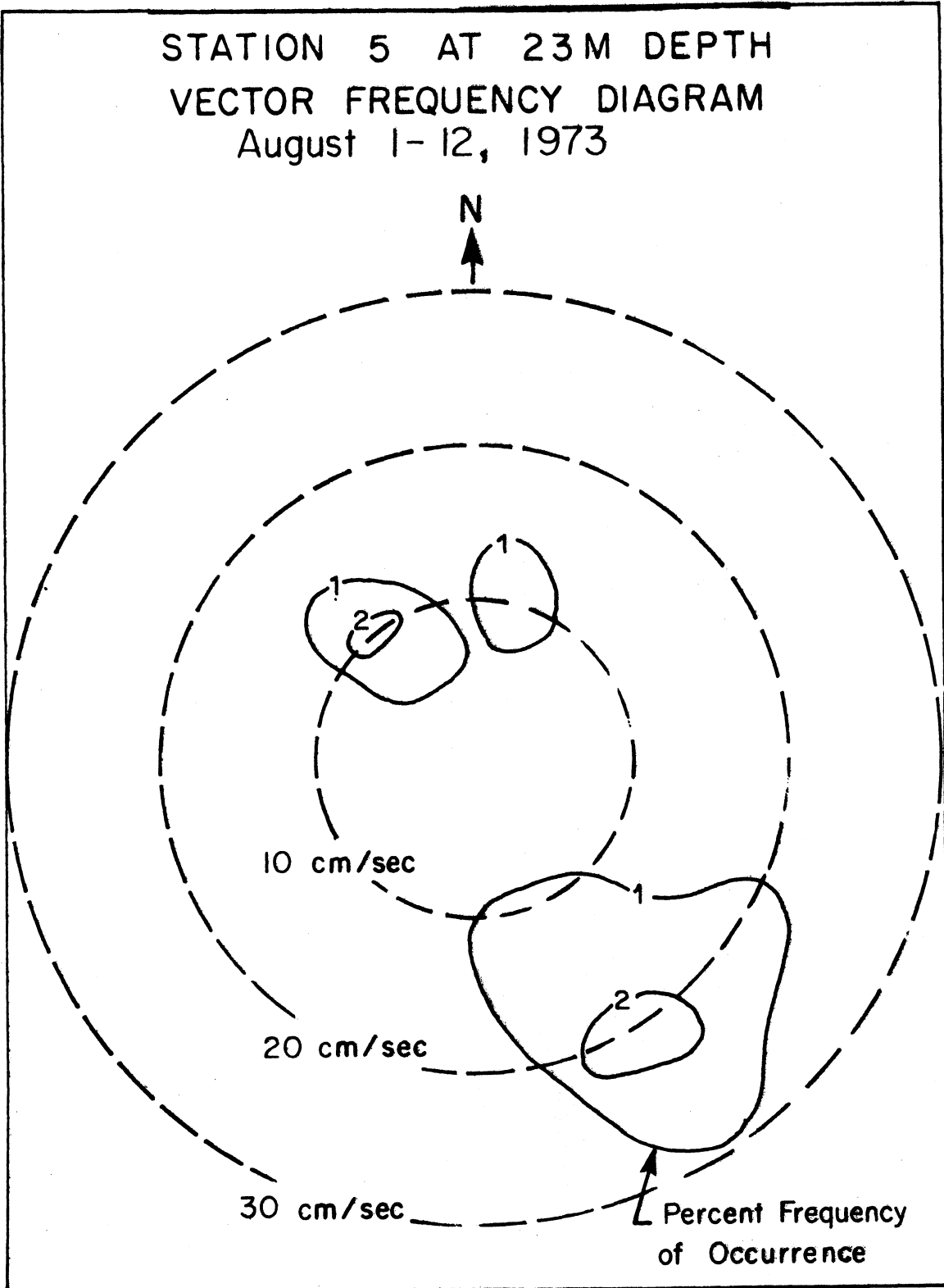


Figure 4.90 The corresponding progressive vector diagram is on page 249.

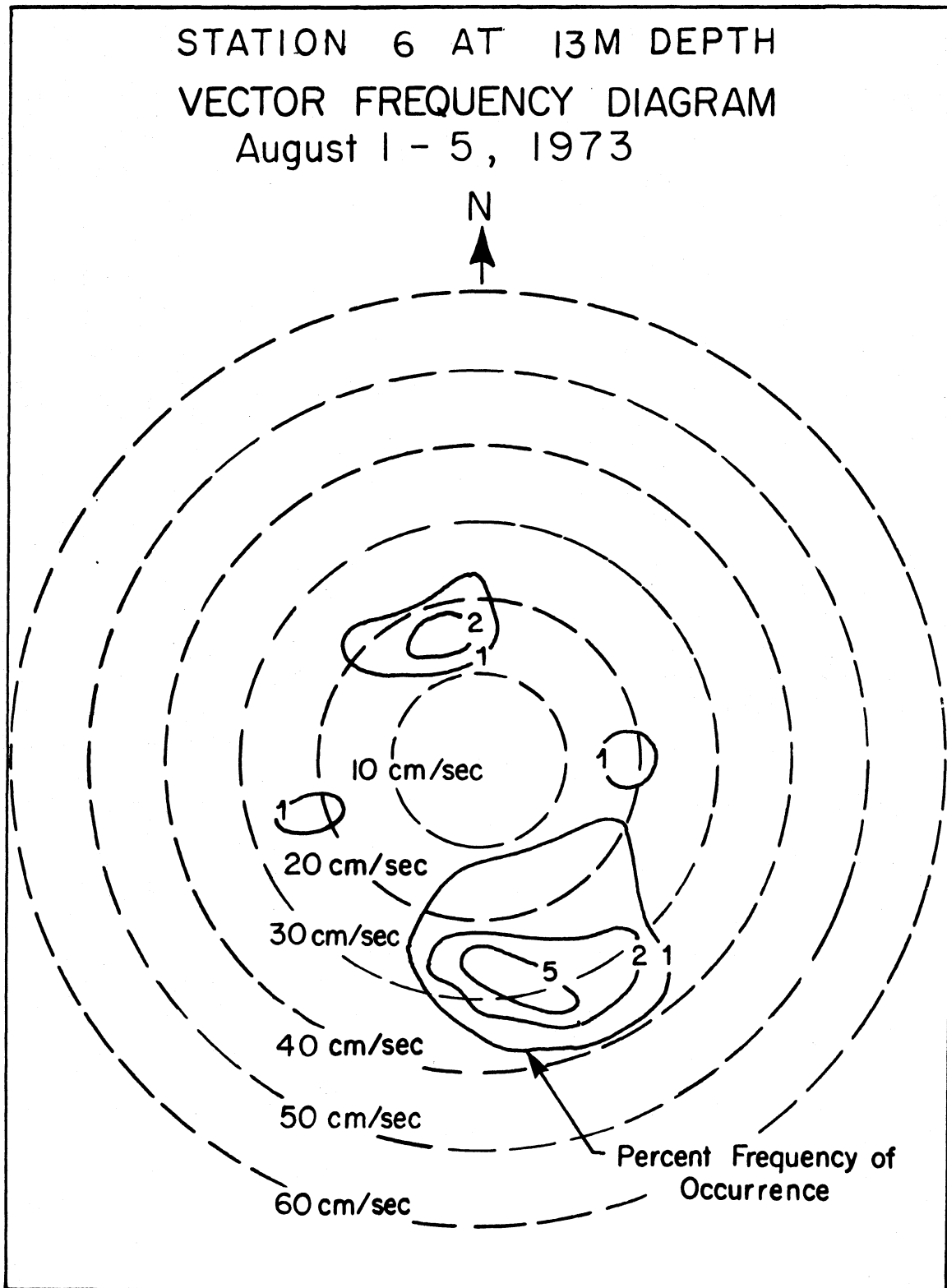
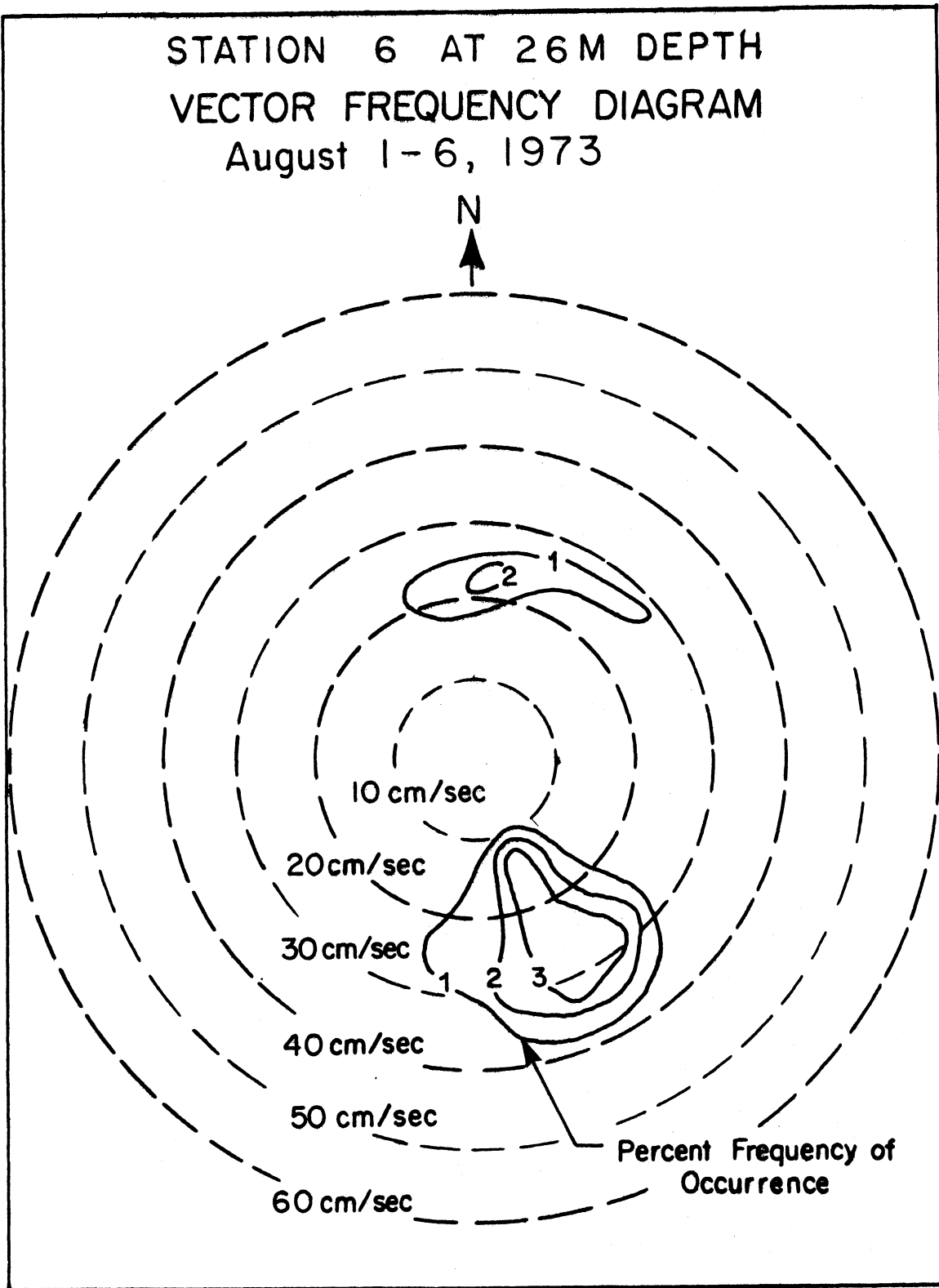


Figure 4.91 The corresponding progressive vector diagram is on page 251.





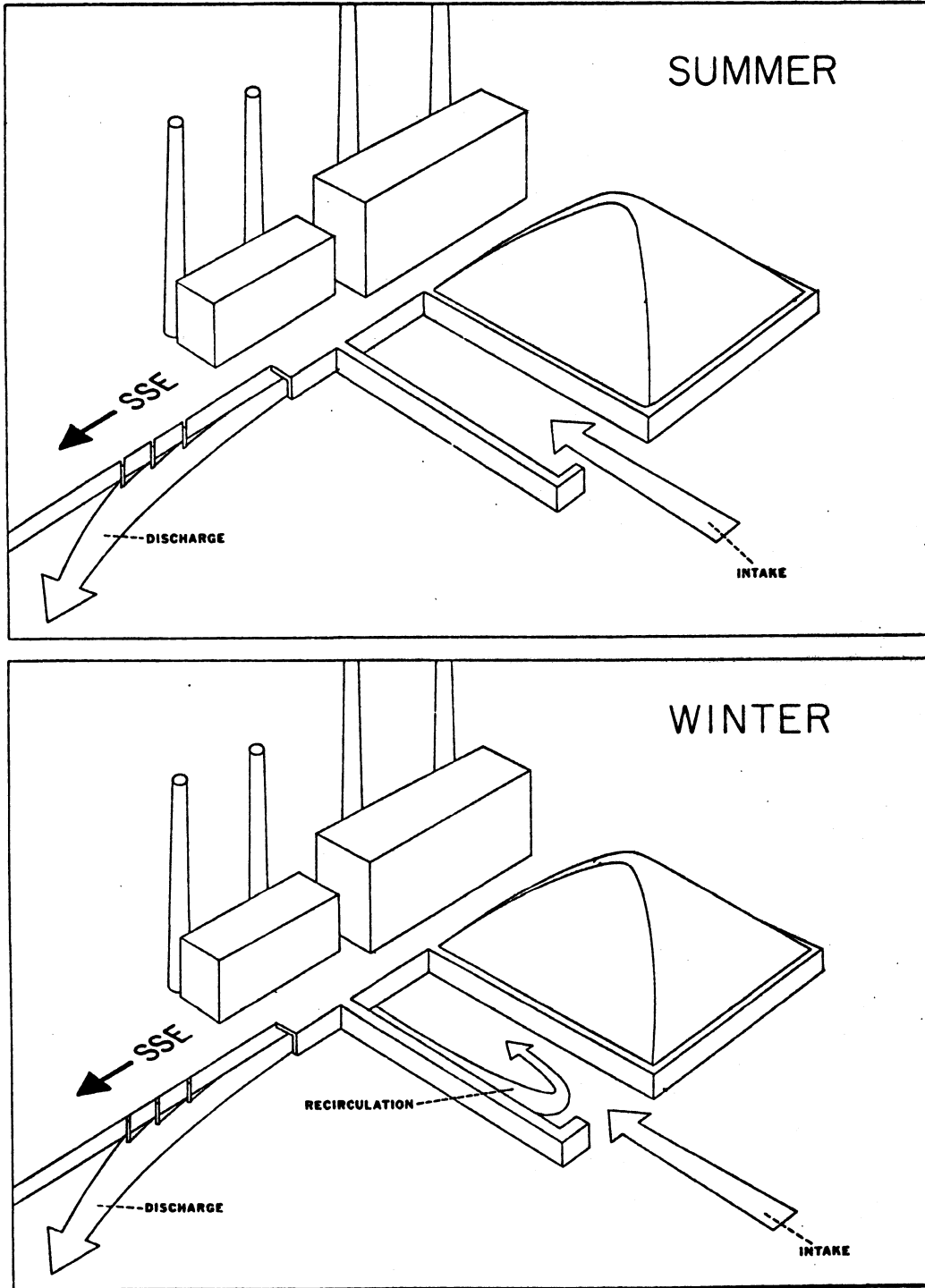


Figure 5.1 Water intake and discharge at the Oak Creek Power Plant in summer and winter (re-drawn from Limnetics, Inc. 1974).

## CHAPTER FIVE

### SINKING PLUMES

As the preceding chapters make clear, our principal efforts were devoted, not to a study of the behavior of the power station's effluent plume of warm water, but to a description of the dynamics of the coastal lake waters which receive that plume. Nevertheless, for reasons given below, we decided to devote some effort to little-investigated aspects of plume behavior in winter.

In general the plume consists of water warmed by passage through the plant plus water subsequently entrained from the receiving lake. The plume's limits are defined by an isothermal surface differing from ambient lake temperature by a selected small temperature difference. As long as the temperature of the receiving lake is  $4^{\circ}\text{C}$  or above, the plume is positively buoyant. It spreads as a relatively thin layer, floating on the lake surface, and it assumes a shape determined by the lake's current patterns at that particular time. As the currents change, so the plume shape changes. The geometry of the intake and outfall arrangements at the Oak Creek Power Plant is illustrated for a summer and winter condition in figure 5.1. The plume emerges from several outfalls and is directed south-southeastward along the shore. It normally continues in that general direction, hugging the shore, until the excess heat is dissipated by entrainment and exchanges with the atmosphere. Figure 5.3, to be described in detail later, provides an example of such a floating plume. At that time the ambient lake temperature was close to  $4.0^{\circ}\text{C}$ , i. e. the plume would float, and the wind was offshore but could not exert enough stress to deflect the plume away from the shore. This shore-hugging behavior is reinforced when the nearshore lake current is southward. On the other hand, with a northward current, the plume is turned out away from the shore and deflected northward, as shown in the infrared photograph, figure 5.8, which will also be discussed later. The considerable variability of areal extent and shape of the Oak Creek plume has been investigated by Limnetics, Incorporated (1974) and has been further explored in a series of infrared aerial photographs taken by Dr. Theodore Green III for the Wisconsin Electric Power Company, as yet unpublished.

When the temperature of the receiving lake is several degrees below the temperature of maximum density ( $4^{\circ}\text{C}$ ), the outer edges of the plume no longer float, because entrainment of lake water into plume water produces a mixture which is closer to the temperature of maximum density,  $4^{\circ}\text{C}$ , than either parent water mass. As also happens in a thermal bar (see Chapter One) the mixture sinks in the region of the  $4^{\circ}$  isotherm, which there runs nearly vertically. This "near  $4^{\circ}$ " water mass is continuously generated, as a sinking plume, and flows down the sloping lake bed to disperse or accumulate in deeper regions of the basin. The sinking plume is in contact with an area of lake bed, which would otherwise be a degree or two colder. Biologists (Great Lakes Fisheries Laboratory 1970, Edsall and Yocom 1972) have hypothesized -- but not yet demonstrated in Lake Michigan -- that the slightly higher bottom temperature would accelerate development of demersal (bottom-lying) fish eggs to produce a hatch too early in the season for the availability of natural planktonic food. This scenario has generated recent concern with sinking plumes, which prompted us to explore the winter situation at Oak Creek.

A thermistor probe (calibrated against a precision mercury thermometer in the range  $0^{\circ}$  to  $6^{\circ}\text{C}$ ) was used from a boat to survey the depth distribution of temperature along sections A to G in figure 5.3 and later figures, covering a roughly rectangular area, shown in figure 5.2, bounded by the shoreline immediately south of the plant, and with the approximate dimensions 1.7 km alongshore and 1.1 km offshore. We had planned to survey this area approximately every two weeks between November 1972 and March 1973, but because of adverse weather and lake conditions plume measurements were taken on a much more limited basis. Even on some calm days, surveys could not be conducted because heavy ice conditions in the harbour prevented the launching of a boat. Generally, surveys were limited to periods when winds were light and variable or light from the southwest to west and when currents were weak.

Temperature measurements were taken at one meter depth intervals and also at the bottom at the stations marked on the diagrams (figs. 5.3 and 5.4 to 5.7) and also at locations midway between these stations. Plant operating

# CURRENT METER STATION LOCATIONS

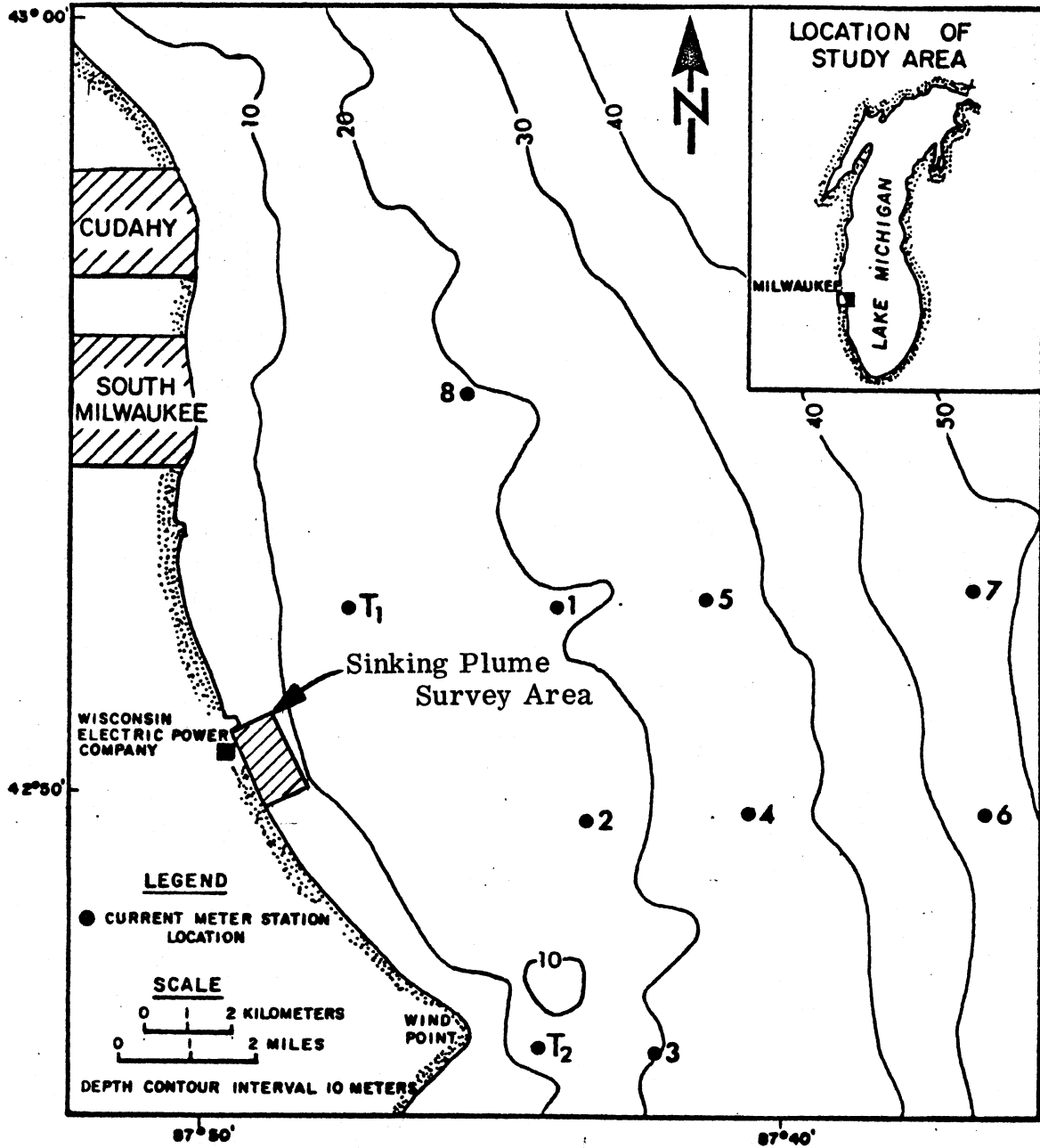


Figure 5.2 Repeat of figure 2.1 to show area covered by the plume surveys, illustrated in the six figures which follow.

# OAK CREEK POWER PLANT DISCHARGE PLUME THREE DIMENSIONAL VIEW AND DETAILED VERTICAL SECTIONS

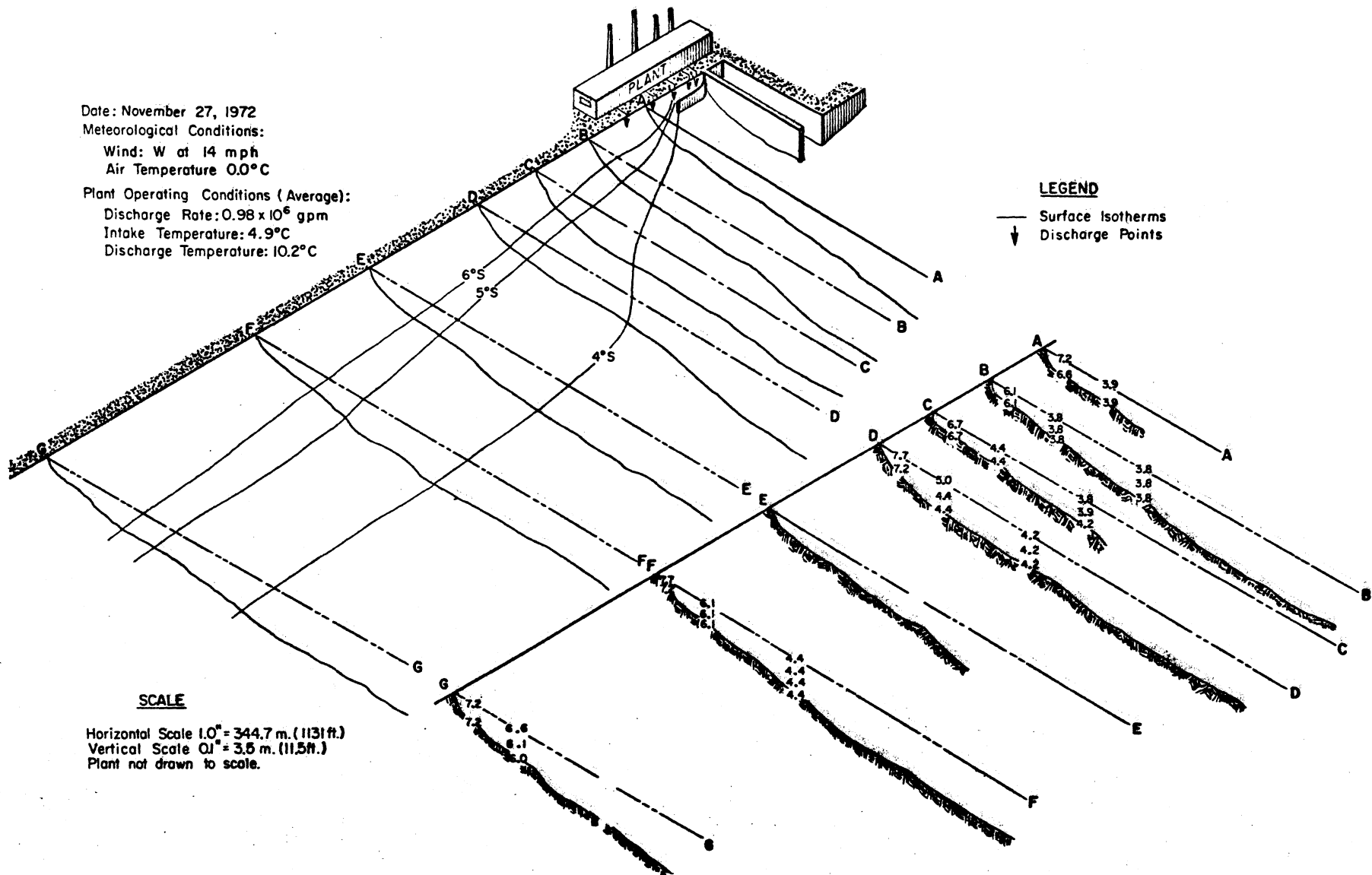


Figure 5.3 Thermal plume from the Oak Creek Power Plant, 27 November 1972.

-262-

conditions such as discharge rates, intake and discharge water temperature readings were kindly provided by the Wisconsin Electric Oak Creek Power Plant. The values presented on the diagrams were based on an average of hourly readings corresponding to the survey period. The air temperature was based on readings taken with the probe during the survey whereas the wind condition was obtained from General Mitchell Airport.

Based on the data from the five thermal plume surveys taken on 27 November 1972, and 25 January, 19 February, 28 February, and 8 March 1973, three dimensional views of the plume together with their vertical temperature sections were developed (figs. 5.3, 5.4, to 5.7) and used to illustrate the extent and shape of the sinking plume. Except in figure 5.3, only the 3° and 4° isotherms were drawn at the surface and at the middle and the bottom levels, to avoid cluttering the diagram. The 3° and 4° isotherm surfaces are shaded to illustrate the spreading of the sinking plumes with increasing distance from the discharge points.

In the vertical temperature sections, the values plotted show temperature readings at the surface, at every three-meter depth interval and at the lake bottom. Again, not all station values were plotted to avoid cluttering the diagram. Where appropriate, isotherms were drawn in the vertical sections to represent the general temperature patterns in the plume area.

#### Thermal plume survey, 27 November 1972 (fig. 5.2)

Temperature readings at the sampling stations during this survey ranged from 3.8° to 7.7°C. The intake and discharge temperatures were 4.9° and 10.2°C respectively. Since the ambient lake water temperature was greater than or close to the temperature of maximum density of water (on some sections temperatures slightly below 4° were found), no sinking plume was formed. The surface isotherms show that the plume had little lateral extent and traveled toward SSE along the shoreline out of the survey area. Westerly winds did little to spread the plume offshore. Figure 5.3 therefore represents the typical

# OAK CREEK POWER PLANT DISCHARGE PLUME THREE DIMENSIONAL VIEW AND DETAILED VERTICAL SECTIONS

Date: January 25, 1973  
 Meteorological Conditions:  
 Wind: W at 12 mph  
 Air Temperature: 4.4°C  
 Plant Operating Conditions (Average):  
 Discharge Rate:  $1.05 \times 10^6$  gpm  
 Intake Temperature: 3.4°C  
 Discharge Temperature: 8.1°C

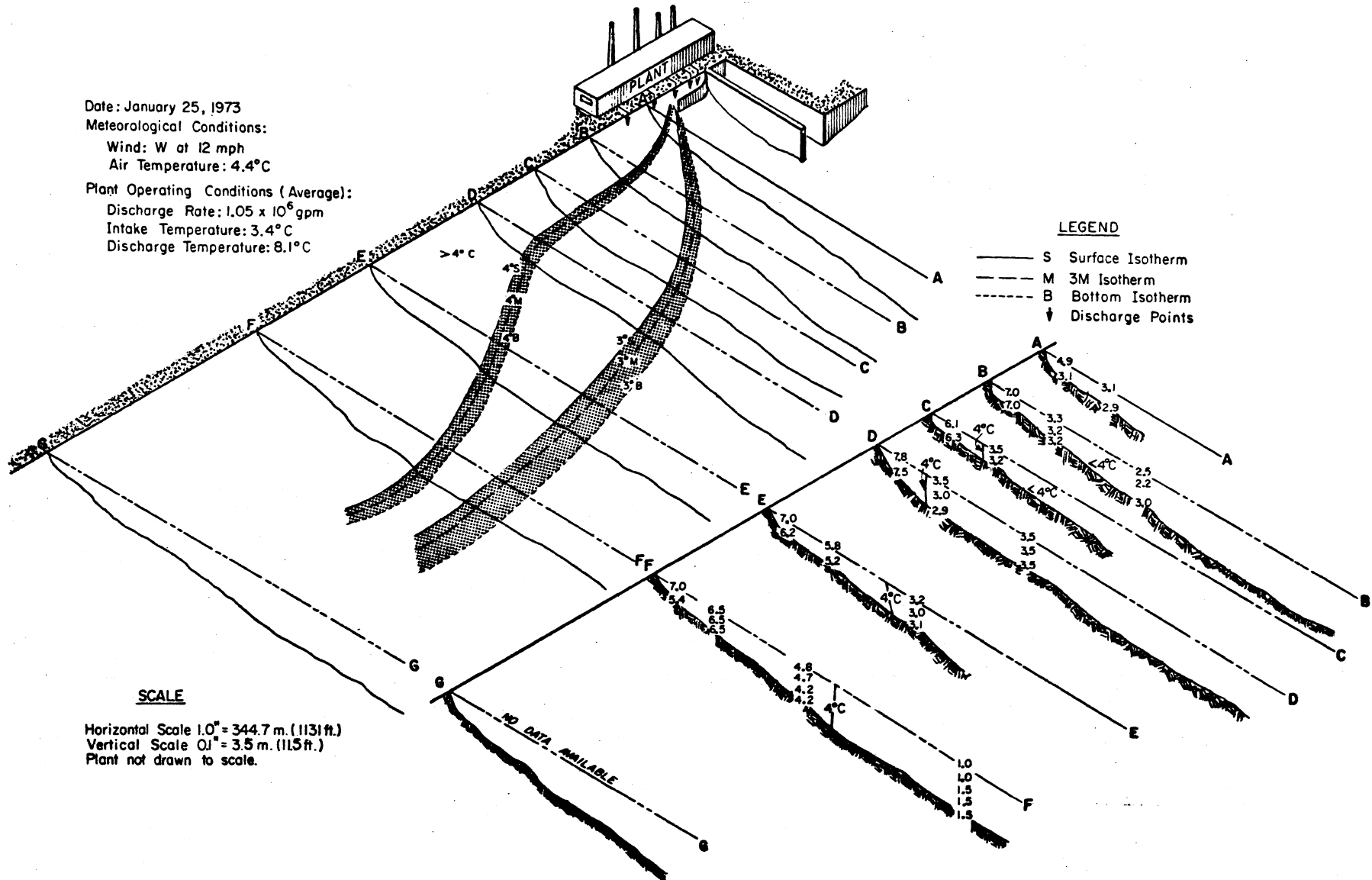


**Figure 5.4 Thermal plume from the Oak Creek Power Plant, 25 January 1973.**

shore-hugging and floating plume commonly found between May and November at the Oak Creek Plant (see Limnetics, Inc. 1974).

Thermal plume survey, 25 January 1973 (fig. 5.4)

By January, the ambient lake temperature had fallen to well below 4°C and to below 2° in some parts of the survey area. Under these conditions a sinking plume was produced by the mixing of warm discharge water at temperatures above 4°C with the cold lake water at temperatures less than 4°C. The resulting mixture was therefore at a density greater than either the density of the discharge, or the density of the ambient lake water; and the plume began to sink.

Winds were westerly at 12 mph and the air temperature was 4°C. Water temperature readings ranged from 1.0°C to 7.8°C. Unfortunately no data were available for line G-G because of instrument malfunction, so that the southern boundary of the plume could not be located. The 4° and 3° isotherm surfaces, nearly vertical, moved slowly away from the shore with increasing distance from the discharge. The configuration of the 4° and 3° isotherm surfaces indicates an actively sinking plume, with both isotherm surfaces forming nearly vertical curtains.

Thermal plume survey, 19 February 1973 (fig. 5.5)

By that date the lake water had cooled down 0.3°C, and it is during this month therefore that a strong development of sinking plumes is to be expected. The figure confirms that this was the case. The plume did not extend far along-shore in this case, possibly as a consequence of the moderately strong wind from the southwest at that time. The wind may also have enhanced mixing at the edges of the plume, which was bounded by an extensive spreading wedge of water contained between the 4° isothermal surface (nearly vertical) and the spreading "skirt" of the 3° isothermal surface (see sections B to F in fig. 5.5).

# OAK CREEK POWER PLANT DISCHARGE PLUME THREE DIMENSIONAL VIEW AND DETAILED VERTICAL SECTIONS

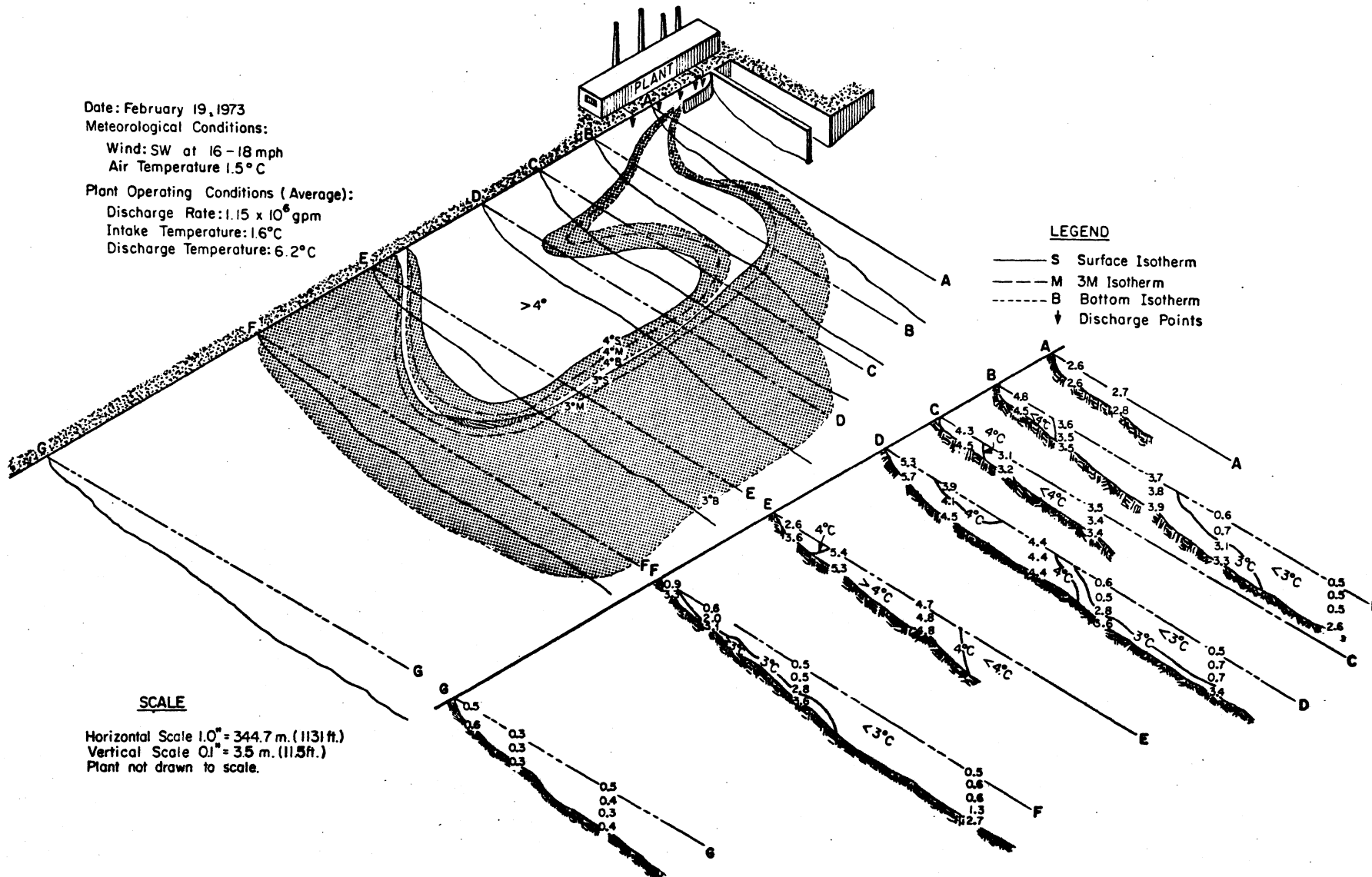


**Figure 5.5 Thermal plume from the Oak Creek Power Plant, 19 February 1973.**



### Thermal plume survey, 28 February 1973 (fig. 5.6)

During this survey winds were from the south at 7 mph and the air temperature was 1.1°C. Water temperatures ranged from 0.9°C to 5.9°C. The sinking plume was much more concentrated in area than were the plumes in previous surveys. The plume spread little in the offshore direction with the greatest offshore distance of the 3°C bottom isotherm being only 618 meters compared to 1030 meters during the 19 February survey. The southward extend of the 3°C bottom isotherm was slightly greater (1350 m) than that of the previous survey (1312 m). In this case both the 3° and the 4° isothermal surfaces assumed the "spreading skirt" form, indicating an increased rate of heat dissipation by sinking and spreading. This may have accounted for the relatively small surface area of this particular plume, although another factor may have been northgoing currents and mixing generated by the winds from SE on the previous day.

### Thermal plume survey, 8 March 1973 (fig. 5.7)

By March, the warming cycle in Lake Michigan had begun. The offshore station on line G-G showed a surface temperature of 1.8°C, compared to the temperature reading of 0.9°C at a station further inshore on 28 February. Winds were 10 mph from the west and the air temperature was 2.7°C. The intake and discharge temperatures were 3.3°C and 8.2°C respectively. The extent of the plume was considerably greater than during the two previous surveys -- the 3° isotherm at the lake bed extended nearly 1.6 km alongshore and 0.95 km offshore -- but the reasons for this are not clear. The intake and discharge temperatures were higher than during February. The winds were light and from the west, and therefore did not supply much energy to the mixing process. Another factor is the growing solar heat input at that time of year, which has the maximum temperature effect in shallow nearshore waters.

We were not able to determine how far into the spring the sinking plume condition persisted, but the April temperatures in 1972 (fig. 3.1) and 1973 (figs. 3.48, 3.50, and 3.52) suggest that sinking plumes would be found at least during the first half of April and would merge into the local "natural" thermal bar

# OAK CREEK POWER PLANT DISCHARGE PLUME

## THREE DIMENSIONAL VIEW AND DETAILED VERTICAL SECTIONS

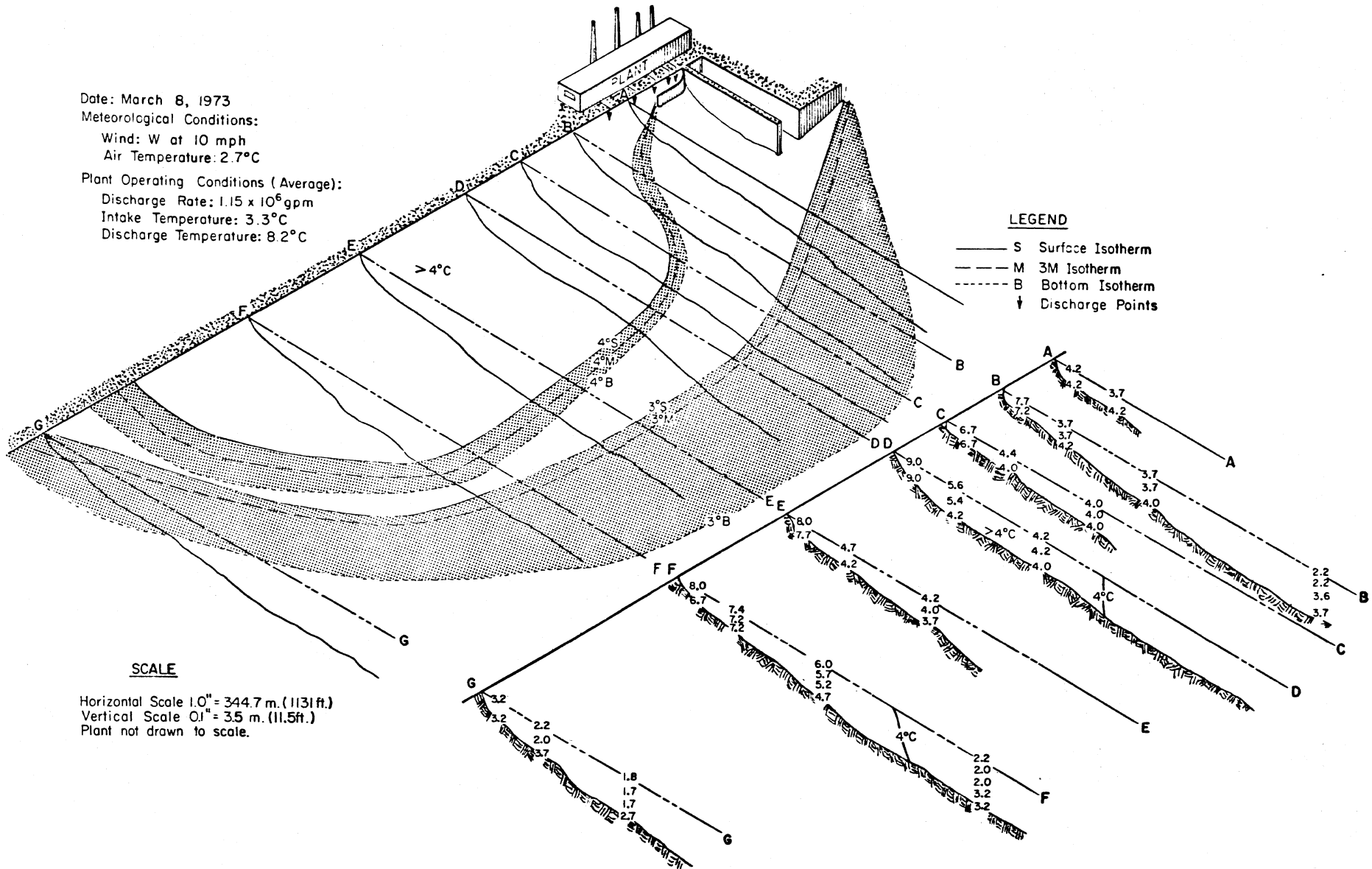
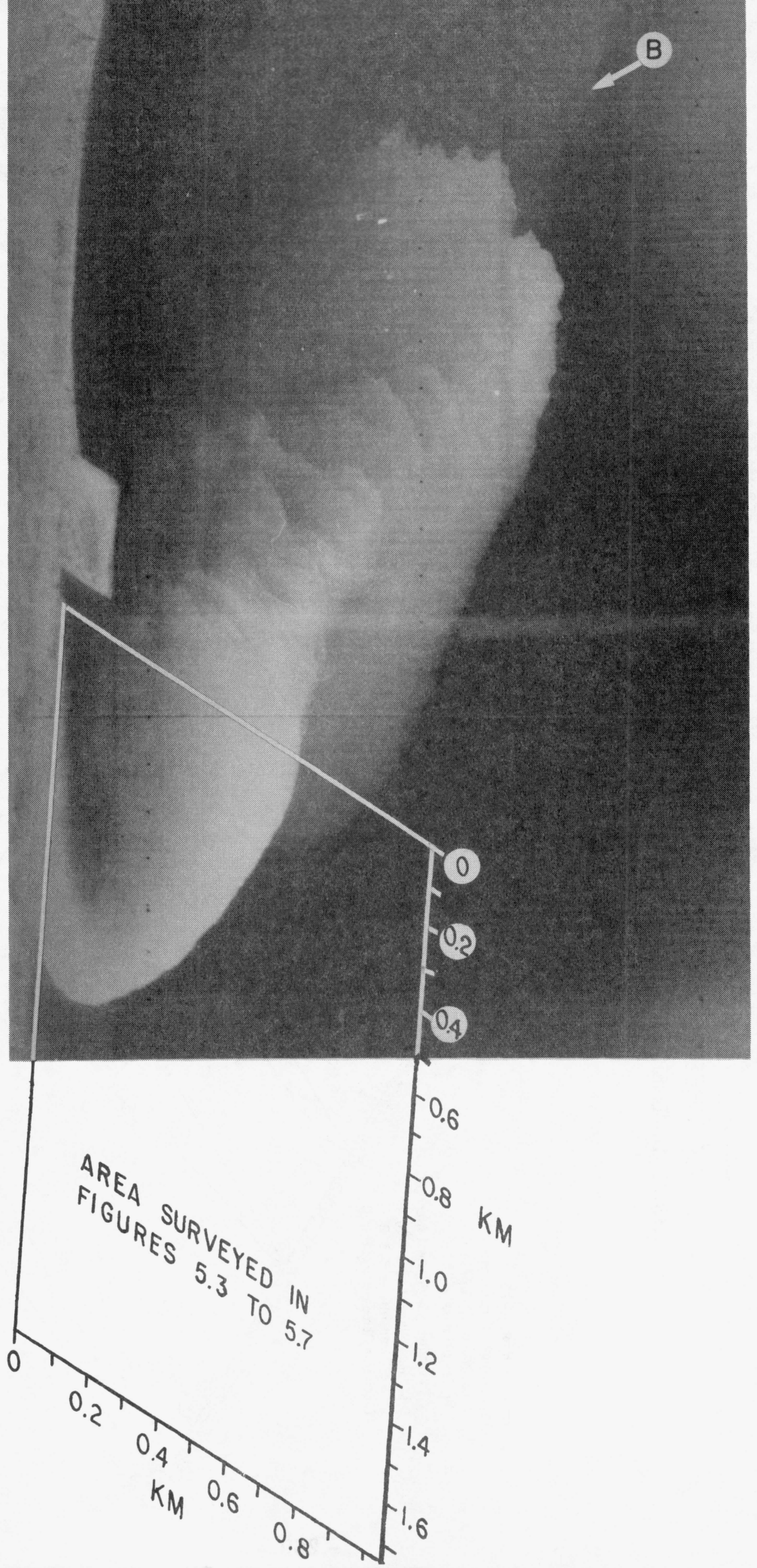


Figure 5.7 Thermal plume from the Oak Creek Power Plant, 8 March 1973.

Figure 5.8 Thermal plume at Oak Creek, WI (infrared imagery by Texas Instruments) 2 April 1968.

B perhaps indicates the edge of the natural thermal bar (by courtesy of Wisconsin Electric Power Co.).



beginning to develop at the end of that month.

### Thermal plume (infrared imagery) 2 April 1968

The sinking plumes illustrated in figures 5.4 to 5.7 all show a southward trend, probably the situation most commonly found because of the outfall configuration and because for most of the time the lake currents are either weak or southgoing. To force the plume to turn northward and away from the shore requires a strong wind from SE or SSE generating a strong northward current. Under those conditions of onshore wind it was too rough for us to survey with safety in winter; and therefore we were not able to record a north-turning, sinking plume. However, north-turning plumes have been recorded in summer (Limnetics, Inc. 1974), and they must also occur from time to time in winter. Figure 5.8 (for which we are indebted to the Wisconsin Electric Power Company) is an example. It was photographed on 2 April 1968 after several days of strong wind from S to SE, at a time when the natural thermal bar had probably begun to form in very shallow water. (Perhaps the faint discontinuity at B in figure 5.8 outlines the natural thermal bar.) The average discharge temperature at Oak Creek for unit 7 between 8 AM and 5 PM on 2 April 1968 was 13.0°C and the average intake temperature was 5.1°C. However, figure 5.8 suggests a strong probability that some plume water was recirculated into the intake. This probability and the low temperatures in early April of other years (figs. 3.1 and 3.48) suggest that offshore lake temperatures were well below 4°C and that the temperature of the plume-receiving water may have been 3°C or less. Figure 5.8 therefore probably illustrates a sinking plume, a supposition also borne out by its small surface extent compared with the floating plume illustrated in figure 5.3 and the summer plumes measured by Limnetics, Inc. (1974).

### Discussion of sinking plumes

Our findings -- discussed here and not in the following discussion chapter -- may be summarized as follows. A sinking plume is formed, as an artificial thermal bar, at Oak Creek whenever the warm water discharge mixes with lake water colder than 4°C. Between the warm plume water and colder

lake water lies a sinking region of 4°C water. The extent of the plume was dependent upon wind and ambient lake conditions. Under the influence of eastward winds, the plumes showed some tendency to spread offshore, whereas with northeastward winds the plumes apparently did not spread offshore as much. Northward winds increased the mixing of lake and discharge water, decreased the southward travel of the plume, and in some cases (fig. 5.8) caused it to turn northward.

Current and temperature structure are other factors which strongly affect the extent of the plume. Light or stagnant currents do little to dissipate the heat, whereas strong northward currents quickly decrease plume length. Lake water temperature also influences the dissipation of heat. Comparison of the surveys for 25 January and 8 March shows that under similar operating and atmospheric conditions the plume size was much greater on 8 March than on 25 January because the lake water temperature was higher on the latter date.

As mentioned earlier, our plume surveys were limited to conditions of calm wind and lake with no major build-up of ice in the harbor area. These conditions precluded any surveys when winds were from the northeast or southeast, i. e. when the current regime would be most active. It is difficult to predict the configuration of the plume under these circumstances except to suggest that the plume size would be smaller because of greater mixing between the discharge and lake waters.

The sinking plume differs from a thermal bar in that the plume's along-shore extent is much less. The continual sinking of the plume's "skirt" (4° water mass) represent an offshore transport mechanism which prevents the build-up of nutrients, pollutants, or other materials added to the discharge. Whereas the thermal bar also has an outer sinking edge, its most conspicuous dynamic feature in an alongshore, geostrophic current (Bennett 1971) which acts somewhat like a temporary river, in which materials will tend to be retained for some weeks. We conclude, therefore, that on open shorelines of Lake Michigan sinking plumes do not act as material traps during the winter, although they will of course contribute in a minor way to formation of the natural thermal bar in spring.

## CHAPTER SIX

### SUMMARIZING DISCUSSION AND ANALYSIS

Some discussion of our findings has already been embedded in previous chapters. We have noted that current directions are most commonly shore-parallel or nearly so. Current direction is strongly dependent on wind direction so that, when the wind direction changes, the current direction reverses after a few hours, more rapidly near shore. Current speed is also strongly positively correlated with wind speed; but -- as expected -- offshore winds, i. e. from SW to NW, produce much weaker responses in the form of currents than do winds with the greatest overwater fetch, namely from N to NE and from SE. A typical response to a burst of strong wind, after a delay of some hours, is a rapid increase in current speed representing an acceleration or a reversal of a previous current, followed by a slower decrease in speed after the wind has weakened. The delay in response tends to increase with increasing distance offshore; and in some cases a particular change in wind stress may fail to reverse the offshore currents -- because of their greater momentum in deeper water -- even though the nearshore currents, in shallower water, become reversed. In such situations, large horizontal shears are developed.

#### Persistence factors

It is difficult to summarize the episodic detail and the great variability of the current patterns, described in foregoing chapters. However, the prevalent wind fields, combined with shoreline geometry and lake bathymetry, generally imposed some regularity and some repeatability on the current responses. This repeatability, more clearly seen at some stations than at others, can be estimated by the calculation of persistence factors, as is done station by station and month by month in Tables 6.1 and 6.2. The persistence factor, defined in Chapter 2, is the (monthly) resultant mean current vector divided by the (monthly) mean current speed. The range of this factor is from zero (for example, currents divided equally between all possible directions and travelling at the same speed) and unity (for example, all currents travelling in the same direction for the whole month).

Table 6.1 Lake Michigan currents at Oak Creek, Wisconsin, 1972.  
Persistence factors and azimuth angles of monthly mean current vectors.

SURVEY	STATION	MONTH					
		APRIL		MAY		JUNE	
I	1	0.51	152°	0.43	169°	0.13	134°
	2	0.53	134°	0.59	154°	0.19	90°
	3			0.30	141°	0.46	165°
	4 upper meter			0.43	152°	0.70	173°
	4 lower meter			0.36	144°	0.58	153°
II		JUNE		JULY		AUGUST	
	3	0.56	142°	0.46	135°		
	4 upper meter	0.71	127°	0.57	112°		
	4 lower meter	0.81	152°				
	6 lower meter	0.58	166°	0.29	153°		
	8	0.67	156°	0.16	71°		
	T <sub>1</sub>	.55	163°	0.48	170°	0.48	136°
T <sub>2</sub>	0.94	170°	0.31	197°	0.48	148°	
III		AUGUST		SEPTEMBER		OCTOBER	
	T <sub>1</sub>	0.21	160°	0.38	184°		
	T <sub>2</sub>	0.54	181°	0.38	194°	0.32	122°
	T <sub>2</sub>	NOVEMBER					
		0.41	144°				

Table 6.2 Lake Michigan currents at Oak Creek, Wisconsin, 1973.  
Persistence factors and azimuth angles of monthly mean current vectors.

SURVEY STATION		APRIL	MAY	JUNE
IV	2	0.1 174°	0.1 203°	0.5 272°
	4	0.2 50°	0.3 134°	
	5	0.3 302°	0.2 250°	
	7 upper meter	0.3 24°	0.5 163°	
		JULY	AUGUST	
V	1	0.13 204°		
	5	0.25 146°		
	6 upper meter	0.23 152°	0.5 152°	
	6 lower meter	0.34 147°	0.5 150°	

No distinct seasonal variation of persistence factors were noted. Variation of persistence values would have to be investigated by including changes in wind structure, which plays a dominant role in generating and moderating nearshore currents.

Because of its proximity to Wind Point on the junction between two large "bays", Station 3 (operating only during 1972) tended to show lower persistence factors, arising from the greater variability in the current response at this station to changes in the wind. At most stations the persistence factors varied between 0.3 and 0.75. The higher value of 0.94 was obtained at Station T<sub>2</sub> for 14 to 30 June 1972 when, as the progressive vector diagram (fig. 4.43) shows, the currents were directed uniformly toward SSE from 14 to 24 June, with little motion until 1 July.

The monthly mean vector azimuth angles ranged from  $71^{\circ}$  to  $197^{\circ}$ . Most of these were in the shore-parallel direction. The lowest angle,  $71^{\circ}$ , was found at Station 8 during July 1972 when its currents were southeastward from 1 to 6 July and northward from 6 to 14 July. This shift in current direction resulted in a low persistence factor of 0.16 and a mean azimuth angle of  $71^{\circ}$ .

During 1973 (Table 6.2) persistence factors were lower than in 1972 because the current directions varied more. There were more frequent episodes of northerly currents, particularly during April 1972 (compare the progressive vector diagrams for April 1972 and 1973 for Station 2, figs. 4.3 and 4.58). Persistence factors ranged during 1973 from 0.1 to 0.65 with an average value of 0.31. Azimuth angles covered a wider range in 1973 than in 1972 because of the greater variability in current flow, as illustrated by comparison of progressive vector diagrams (for example, Station 2 in May 1972 and 1973, figs. 4.8 and 4.64).

#### Response to wind, particularly to wind reversals

A general inspection of the time series plots of wind and current in Chapter 3 discloses an alternation between episodes of strong, relatively persistent currents and episodes with current speeds of less than  $4 \text{ cm. sec}^{-1}$ , defined here as "very weak". The latter episodes, listed in Table 6.3, coincided with light and variable winds or with winds from west to southwest, for which the fetch was too small to permit the wind to exert much influence on water motion or to modify existing, near-geostrophic, shore-parallel currents which may have persisted from previous episodes of stronger wind.

The next step in analysis is provided by the vector frequency and progressive vector diagrams used in Chapter 4 to display the time history and changes of current speed and direction. For comparison, vector frequency diagrams were developed for wind data also. For onshore or alongshore winds -- the most effective generators of current -- there was in most months a prevalence of southwestward winds. These winds generated south-southeastward currents, a prevailing condition along this coast. There were also occasionally strong

Table 6.3 Lake Michigan currents at Oak Creek, Wisconsin, 1972 and 1973. Periods of very weak currents (speeds less than 4 cm. sec<sup>-1</sup>) during 1972.

STATION	APRIL	MAY	JUNE	JULY
1	26-30	1-5 14-29		
2	26-30	3-5 14-21		
3		2-5 14-28	27-30	5-6
4 upper meter		14-29	3-5 27-30	1-2
4 lower meter		16-25	28-29	
6 lower meter				
8			25-29	12-14
T <sub>1</sub>			25-30	1-2 4-23
T <sub>2</sub>			24-30	27-31 28-31
	AUGUST	SEPTEMBER	OCTOBER	NOVEMBER
T <sub>1</sub>	19-22 27-31	3-5 23-24	3-5 9-10 13-14 24-25	
T <sub>2</sub>	3-22 28-29	12-13 23-24		17-19

Periods of very weak currents (speeds less than 4 cm. sec<sup>-1</sup>) during 1973.

STATION	APRIL	MAY	JUNE	JULY	AUGUST
1				18-20	
2			5-7 11-14		
4 upper meter	22-24	14-15			25-27
5 lower meter					
6 upper meter					
6 lower meter					
7 upper meter	2	1	2-5	2	

winds directed northward or northwestward which produced northward currents. However only minor currents were associated with northeastward winds, because the fetch was too small to alter the existing current regimes. When the winds were light, the currents were very weak.

Monthly mean current speeds were about  $5 \text{ cm. sec}^{-1}$ , but this figure includes current speed readings from the weak current episodes which, in some months, occupied more than half of the time. During the active period current speeds ranged from 4 to  $30 \text{ cm. sec}^{-1}$ .

The analysis in Chapter 4 also exposes a systematic difference in the patterns disclosed by interstation comparisons during episodes of strong and weak current. The progressive vector diagrams, for example, show interstation similarities and prevalence of unidirectional flow during episodes of strong current, and the absence of a common, organized pattern during episodes of weak current. Also, as Table 6.3 shows, the timing and the duration of the weak current episodes sometimes differed markedly between shallow-water and deeper-water stations. The duration of the weak current episodes ranged from 1 to 21 days with an average value of 5 days. Occasionally the generally "stagnant" condition was interrupted by very short periods when currents were above  $4 \text{ cm. sec}^{-1}$ , but these interruptions were of minor significance. In contrast to episodes of active current, the weak current episodes were characterized by very low dispersion rates. Any pollutant introduced during periods of weak currents would diffuse only within the area of the discharge and would not be carried away downstream.

By contrast, during episodes of strong, persistent currents, different stations showed similar current behavior, with shore-parallel, near-geostrophic currents responding to winds from various along-shore or onshore directions. Over the whole recording interval southgoing (actually SSE) currents predominated, interrupted by occasional episodes of north-going currents. Under these circumstances, introduced waste materials must have been transported rapidly downstream from their source.

When the time series plots of wind and current are compared in Chapter 3, an important result appears, here amply documented for the first time. The current response to strong wind stress is rapid, with lag times of only a few hours. The decay in current speed is slower, once the wind has weakened or changed direction. Figure 6.1 illustrates examples.

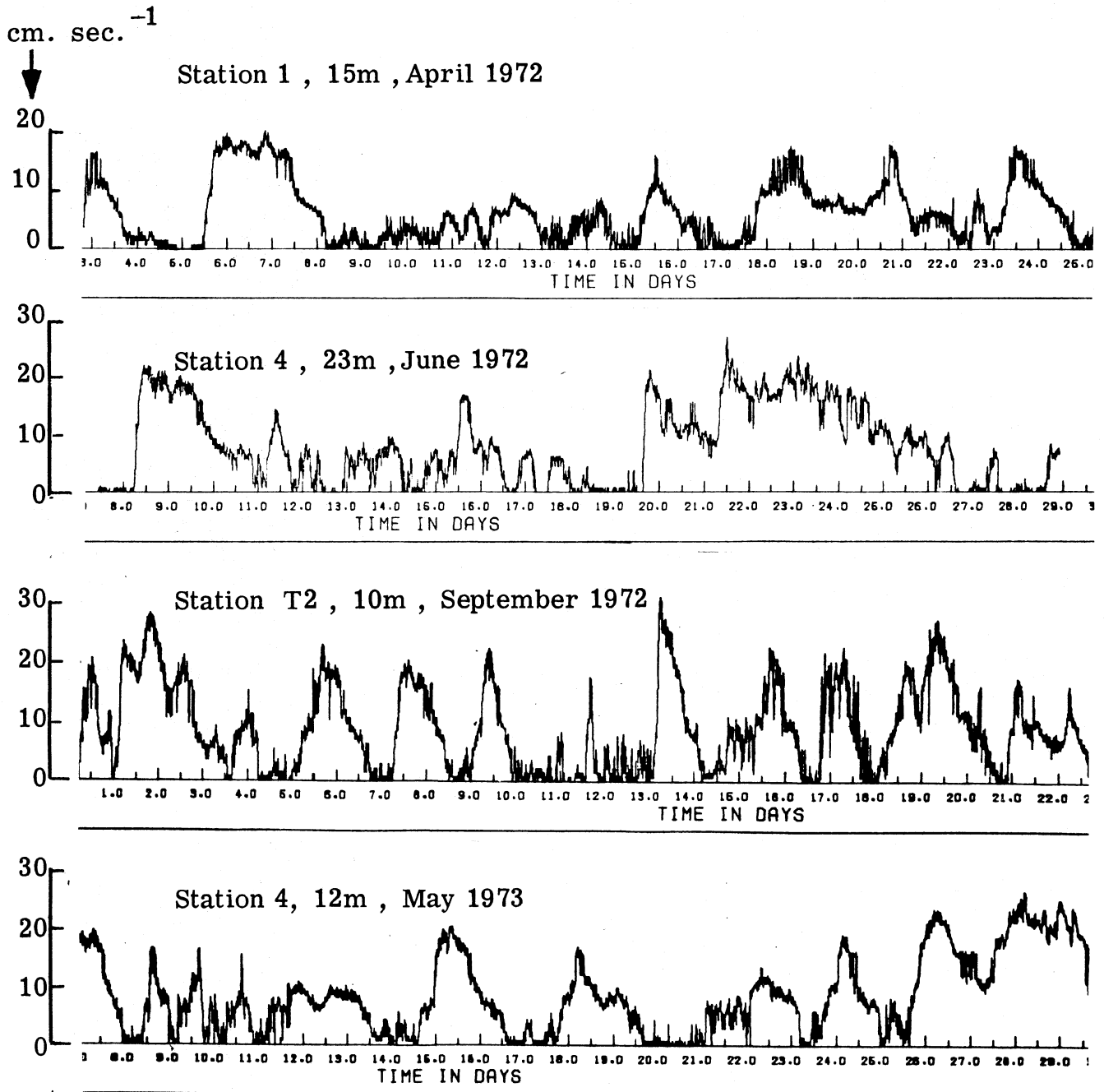


Figure 6.1 Characteristic current responses to changes in wind speed and/or direction (extracts from figures 3.2, 3.18, 3.41, and 3.56).

We have applied cross-spectral analysis to wind and current time series to investigate coherence and phase relationships between them, but the results of this analysis was not very revealing. A typical example is the spectral comparison in figure 6.2 of Station 2 data with wind data for April 1972. The current spectra showed no peaks except for a fairly large concentration of energy at 3 hour period. The wind spectra also did not contain any dominant peaks and most of its energy fell in the long-period region of the spectrum. Coherence between the two records was found to be fairly low (0.44) even at long periods. The five percent probability limit for this case was 0.38. In the other regions of the spectra coherence values were even lower. The phase diagram revealed little information on the relationship between wind and current. Since other cross-spectral analyses produced similar results, they are omitted. The reason for this initially surprising result is that coherence between wind and current records was low because winds had the greatest influence in generating and moderating nearshore currents when they were southwestward or northwestward. When the winds were northeastward they had little influence on the current structure. Under these circumstances the current regime became relatively stagnant or continued in the direction established during periods of strong winds. Cross-spectral coherence between wind and current would have been much higher if only episodes of strong current had been considered.

Since cross-spectral analysis revealed little information on the relationship between wind and current, we tried another approach which considered the time lag between current and wind reversals and the response of current to wind as a function of depth and distance from shore. The results are assembled in Tables 6.4 and 6.5.

MITCHELL AIRPORT WIND AND STATION 2 CURRENT AT 15M DEPTH  
 NORTH-SOUTH SPECTRA  
 APRIL 4 - APRIL 30, 1972

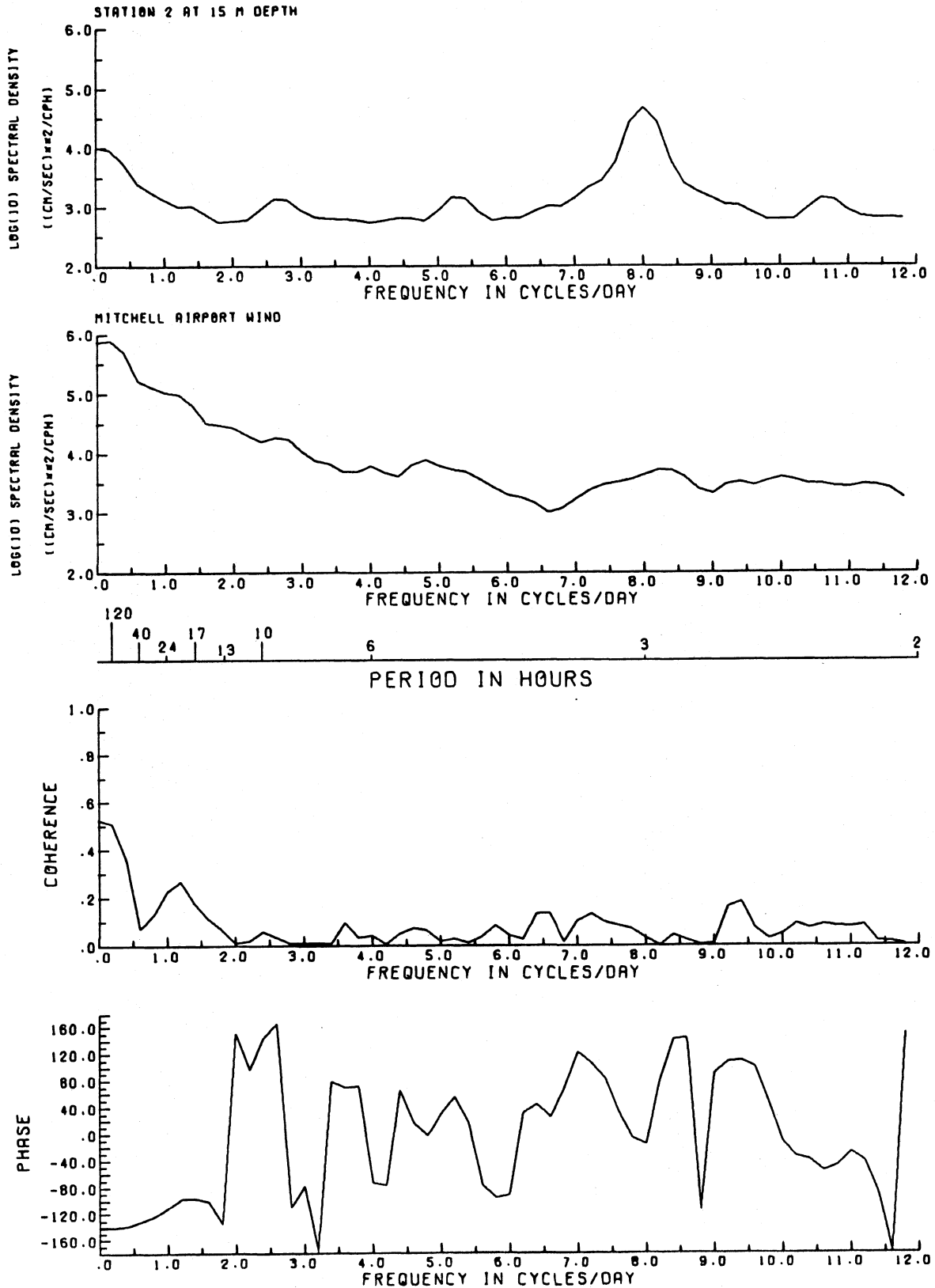


Figure 6.2 Spectra of N-S components of current (Station 2, 15 m) and wind (Mitchell Field) and coherence and phase difference between them.

Table 6.4 Lake Michigan 1972. Current reversal events at Oak Creek, Wisconsin. Lag time in hours between wind reversal and current reversal.

STATION	APRIL		MAY		JUNE	
	North-South Reversal	South-North Reversal	North-South Reversal	South-North Reversal	North-South Reversal	South-North Reversal
1		6, 4	3	15	—	
2		6, 4	3	15	—	
3	—		3, 2, 7, 2, 6, 3, 6, 8	8, 3, 5, 1, 5, 1, 3, 8, 5	8, 5, 2, 2, 1	5, 6, 2
4 upper meter	—		8	10, 3	11, 6	11
4 lower meter	—		9	15, 4	11, 6	11
6 lower meter	—		—			
8	—		—		2	12, 10

— indicates that no measurements were made at that station during that month.

Table 6.4, continued, Lake Michigan 1972. Current reversal events at Oak Creek, Wisconsin.  
Lag time in hours between wind reversal and current reversal.

STATION	JULY		AUGUST		SEPTEMBER	
	North-South Reversal	South-North Reversal	North-South Reversal	South-North Reversal	North-South Reversal	South-North Reversal
T <sub>1</sub>			11, 16	11, 14	6, 2, 7	12, 4, 5, 6
T <sub>2</sub>			21, 16	20, 24	3	2, 4, 3, 4
	OCTOBER		NOVEMBER			
	North-South Reversal	South-North Reversal	North-South Reversal	South-North Reversal		
T <sub>1</sub>	5, 8, 6, 3	5, 2, 2, 4	—			
T <sub>2</sub>	3, 8	5, 2, 2, 4	24, 9	11		

— indicates that no measurement was made at that station during that month.

Table 6.5 Lake Michigan 1973. Current reversal events at Oak Creek, Wisconsin. Lag time in hours between wind reversal and current reversal.

STATION	APRIL		MAY		JULY	
	North-South Reversal	South-North Reversal	North-South Reversal	South-North Reversal	North-South Reversal	South-North Reversal
1					3	
2	21, 3		4, 7, 6	9	3	
4	3		34, 6	25, 13	5	
5	5			26	12	
7	69					

Tables 6.4 and 6.5 list the lag times between wind reversal and current reversal for the principal events in each month. No systematic seasonal variations were found in the lag times. Current reversals associated with wind reversals were easier to identify during spring and summer before oscillatory, internal wave motion became superimposed on the unidirectional flow characteristics of nearshore currents. Nearshore and offshore differences occurred in the lag times as mentioned in Chapter 3. Nearshore stations showed shorter reversal times and a greater frequency of reversals. In some cases, currents at the deeper stations did not change direction after wind reversal, but maintained their previously established direction.

Comparison of lag times for Stations 1, 2, and 3 which were at similar depths showed that not only depth, but also station location was an important factor. Stations 1 and 2 were located 8 and 7 km from shore, respectively; whereas Station 3 was only 4 km from shore near Wind Point, where it was under the influence of current regimes in the bays north and south of Wind Point. Station 3 therefore exhibited a greater frequency of current reversal and the reversals involved shorter lag times than those at Stations 1 and 2.

No general differences were observed between north to south and south to north reversal categories. In each category, the lag duration was less dependent on whether the reversal was N-S or S-N than on such factors as wind and current speed before reversal and on station position and depth.

The rotary, near-inertial current component;  
definition of the "nearshore" zone

To the above-described, general picture of current response to wind, a particular complicating factor was added during the summer and fall seasons when the lake was stratified and when large-amplitude internal waves were formed on the thermocline. These waves are of two distinctive types (Mortimer 1974); the Kelvin type with greatest amplitude and shore-parallel currents near shore, i. e. in the region of our measurements; and the Poincaré type

which extends over the whole thermocline and which produces currents which rotate clockwise once every 15 to 17 hours. These rotary currents become very conspicuous in regions further offshore than in the area covered by our instruments, and their rotary influence decreases as the nearshore zone is approached. There, shore-parallel, wind-driven, or Kelvin wave currents, both geostrophic or near-geostrophic, become dominant. Because our outer instruments were in the transition zone between the nearshore and offshore current patterns, the general shore-parallel current responses were sometimes modified by the Poincare wave rotary component with a near-inertial period, close to 17 hours. The inner instruments in shallower water showed little or no response to the rotary component. There the responses were predominantly shore-parallel and the strongest currents were near-geostrophic during the stratified and unstratified seasons.

The nearshore zone may be defined as the region in which unidirectional shore-parallel current patterns predominate and in which the rotary current components although detectable, do not assume major importance, as they do in offshore regions. The nearshore zone is also the locale of upwelling and downwelling motions and the attendant geostrophic flows. Blanton (1974) has also shown that the nearshore zone, approximately 8 km wide in Lake Ontario, is the repository of most of the Lake's kinetic energy (see Chapter 1, fig. 1.13). Because our instrument array extended 15 km offshore, and because the most distant instruments recorded a mixture of unidirectional and rotary currents (figs. 3.76, 3.77), placing them in a transition between nearshore and offshore current regimes, the width of the nearshore zone at Oak Creek and perhaps in Lake Michigan generally appears to be considerably greater than Blanton's 8 km. This may be the result of a topographic difference, with depth increasing more rapidly with offshore distance in Lake Ontario than in Lake Michigan.

## Water temperature

The time series plots of temperature assembled in Chapter 3 show a slow and steady increase in temperature from a low of  $1.1^{\circ}\text{C}$  to  $10.2^{\circ}\text{C}$  during spring. As the lake began to warm, the nearshore stations became warmer than those in deeper water. During spring the temperature records showed no traces of internal near-inertial wave activity. Sudden temperature changes were caused by upwelling and downwelling events. Upwelling episodes were associated with north-going currents and downwelling episodes with south-going currents. Downwelling produced more prominent temperature changes because of the large temperature difference between the surface water and the water at instrument depth. Upwelling episodes were not so conspicuous on the record, because the temperature of water around the instrument did not differ greatly from the temperature of lower layers. A good example of a downwelling episode is the one which occurred on 30 May 1972. There was a sudden increase in temperature at all the stations with the greatest change at Station 3 (figs. 3.4, 3.7). Currents had become northerly during this episode.

After stratification had set in, some temperature records were characterized by oscillations of near-inertial frequency. Upwelling and downwelling events were again respectively accompanied by sudden decreases and increases in temperature. After the thermocline had begun to sink during the fall it became more difficult to observe downwelling events because of the small temperature difference between the surface layers and the layer at instrument depth. Temperature began to show a strong downward trend in November, heralding the beginning of the cooling cycle in the lake.

Since currents along the coastline at Oak Creek were generally directed towards the south, downwelling events were more often observed than upwelling events. However, upwelling and downwelling are both characterized by mass exchange between the nearshore and offshore waters; and this exchange is a powerful mechanism for dispersion of pollutants from nearshore into offshore.

The effects of man-made temperature perturbations, in the form of the sinking plume at Oak Creek in winter, are described and discussed in Chapter 5.

#### Spectral and cross-spectral analyses of currents (deferred from Chapter 4)

Using the method described by Munk, Snodgrass, and Tucker (1959) we applied spectral and cross-spectral analyses to the current and temperature records to disclose any dominant modes of oscillation and to study coherence and phase relationships between the upper and lower instruments at the same station and between different station pairs.

Few of the temperature and current spectra exhibited conspicuous peaks. Therefore dominant modes of oscillation were generally absent.

Typical examples of the spectra, derived from Station 4 records in May 1972 are presented in figures 6.3, 6.4 and 6.5. Spectra of the north-south current component for the upper and lower meters at Station 4 disclose a rapid decrease in the variance in the frequency range 0 to 4 cycles/day before levelling off at higher frequencies (fig. 6.3). Since there were no major peaks in the spectra, no dominant modes of oscillation existed. Coherence between the two records was high at the lowest frequencies and low elsewhere. The two records were in phase at the lowest frequencies; slightly out of phase in the region 2 to 5 cycles/day. Elsewhere coherence was too low to render the phase relationships significant, except in the region of 20 cycles/day.

The east-west component spectra for the same two meters were slightly different in character (fig. 6.4). The upper spectrum showed a slight peak at 12 hours period, whereas the lower spectrum showed a peak near 8 and 4 hours. The 12 hour peak could perhaps be attributed to the semidiurnal tide and the 8 hour peak motion to the first longitudinal free mode of oscillation in Lake Michigan. The coherence plot in figure 6.4 was more erratic than that in figure 6.3, showing surprisingly high values at frequencies above 12 cycles/day, and the phase diagram also showed differences.

[the text continues on page 292]

Figure 6.3 Spectra of N-S current components at Station 4, 15 and 23 m, and coherence and phase difference between them, 4 May to 4 June 1972.

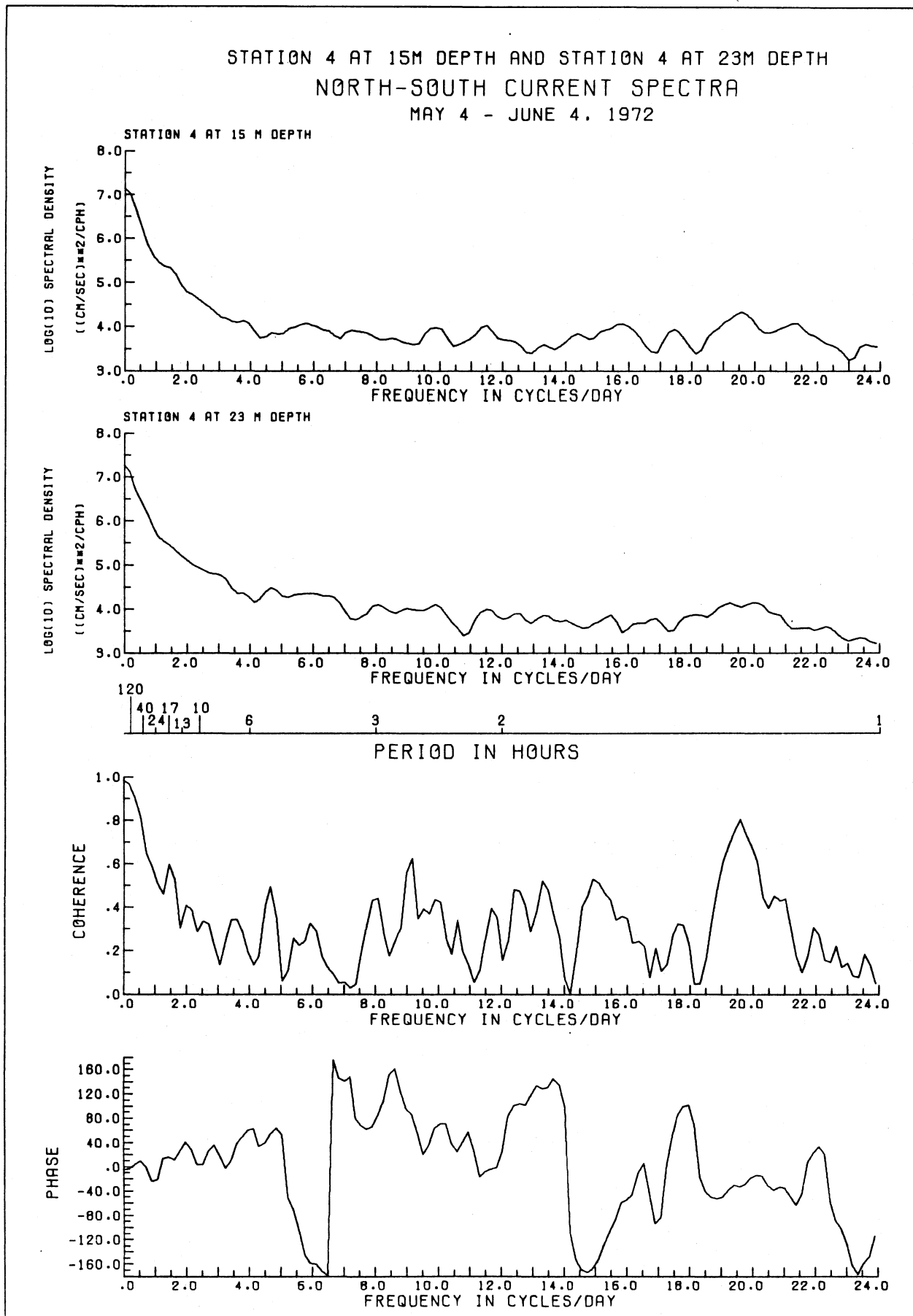


Figure 6.4 Spectra of E-W current components at Station 4, 15 and 23 m, and coherence and phase difference between them, 4 May to 4 June 1972.

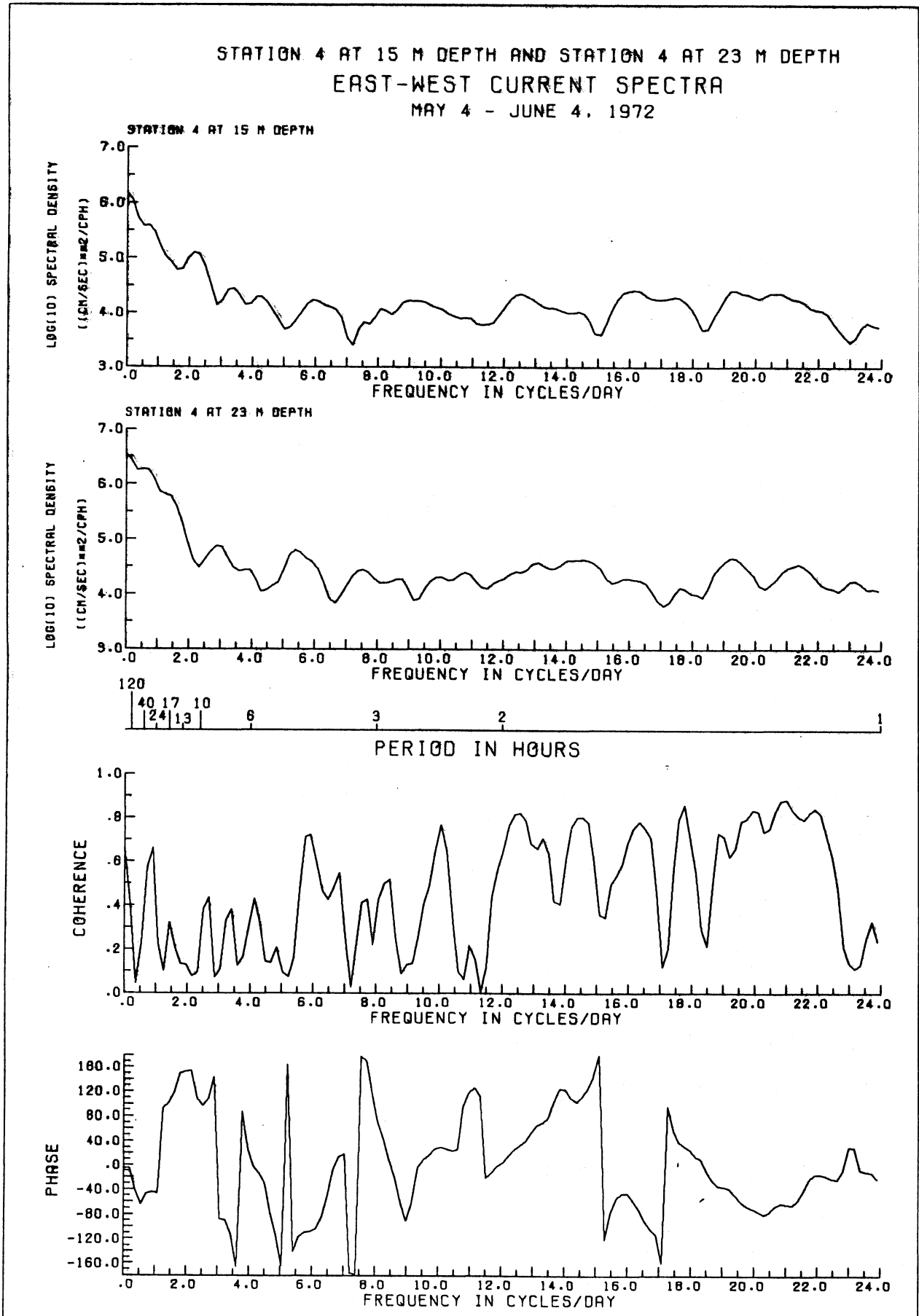
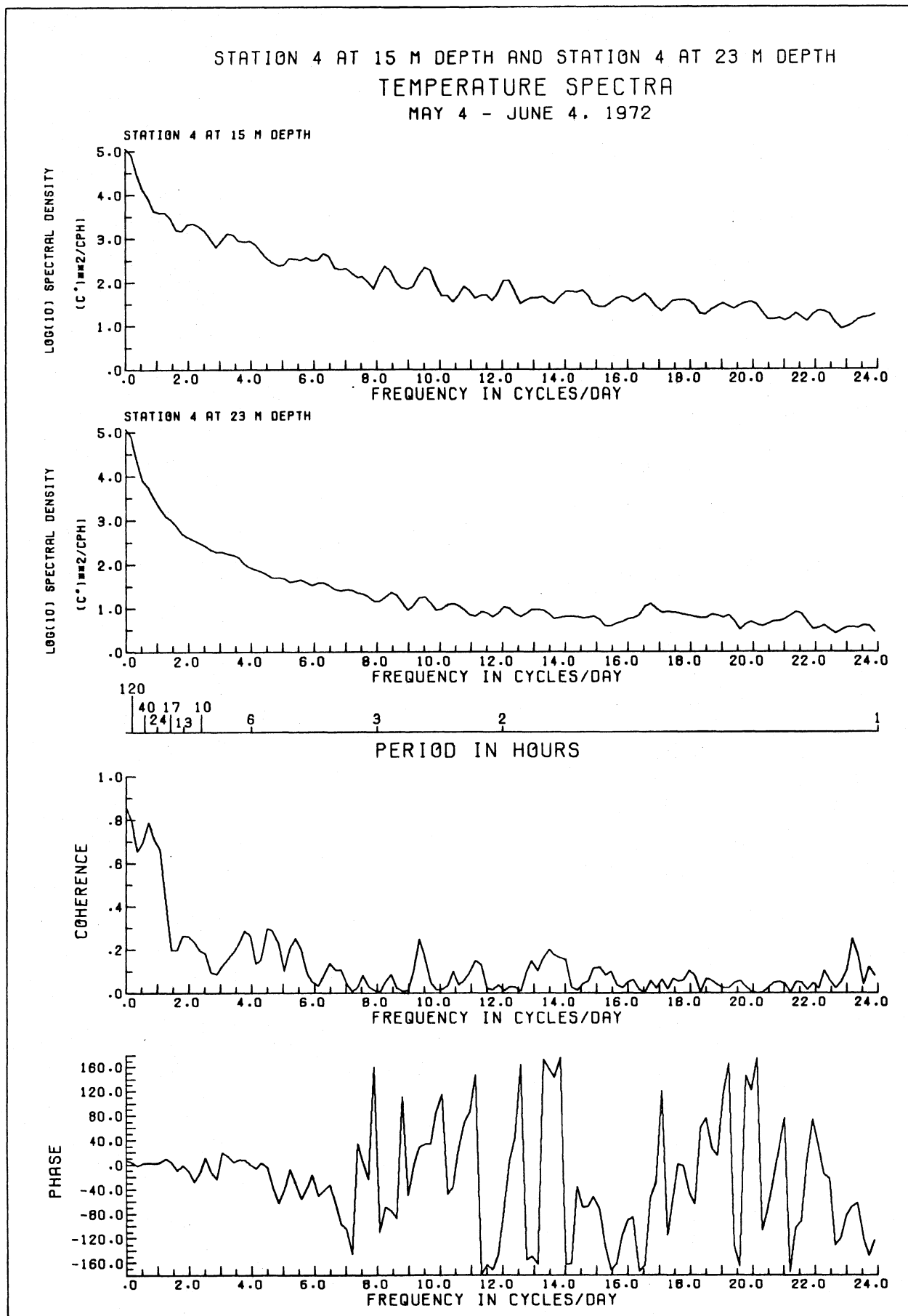


Figure 6.5 Spectra of temperature at Station 4, 15 and 23 m, and coherence and phase difference between them, 4 May to 4 June 1972.



The temperature spectra (fig. 6.5) for the two Station 4 depths were similar to those of the north-south current component. No distinct peaks were found. Coherence was high at the extreme low-frequency end of the spectrum, elsewhere very low. The two records were in phase in the high coherence region.

When a similar spectral comparison is made for Stations 2 and 3, 14-29 May, in figures 6.6, 6.7, and 6.8, an extremely low coherence appears (therefore the phase indications are without significance). This is the expected consequence of station position, Station 3 being near Wind Point and influenced by motions on both sides of that Point, as disclosed by earlier comparisons of the records in Chapter 3.

The June 1972 spectra and cross-spectral comparisons for instruments at the two depths at Station 4 (figs. 6.9, 6.10, and 6.11) are similar to the corresponding comparisons for May, except that a minor but distinct peak appears in the temperature spectra (fig. 6.11, in phase at 16 and 23 m) near the inertial frequency of 1.45 cycles/day. This signals the onset of thermal stratification and the beginning of internal Poincare wave activity. The same signal may also account for the broad peak near 1.5 cycles/day in the E-W current component spectra (fig. 6.10) but is absent or obscured in the N-S spectra (fig. 6.9). However, in the July 18-9 August 1973 spectra for both N-S and E-W components and for temperature at Stations 1 (15 m), 4 (12 m), and 5 (23 m), presented in figures 6.12 to 6.16, the near-inertial peaks or "shoulders" are more or less conspicuous. Otherwise the July-August 1973 cross-spectral comparisons in these figures show very low current coherences at frequencies higher than 1 cycle/day for both N-S and E-W components for Station pairs 5 (23 m)/4(12 m) and 1 (15 m)/5 (23 m) and low coherence at all frequencies for the temperature comparison 1 (15 m)/5 (23 m) in figure 6.16. As in previous spectral figures, most energy was concentrated in the frequency range below 2 cycles/day, with an in-phase relationship between station pairs in that range. An exception is the E-W current component comparison for 1 (15 m)/5 (23 m) in figure 6.15. In this case coherence is highest near the inertial frequency, at which there is a 40° phase difference.

[ the text continues on page 305 ]

Figure 6.6 Spectra of N-S current components at Stations 2 and 3, 17 and 13 m, and coherence and phase difference between them, 14 to 29 May 1972.

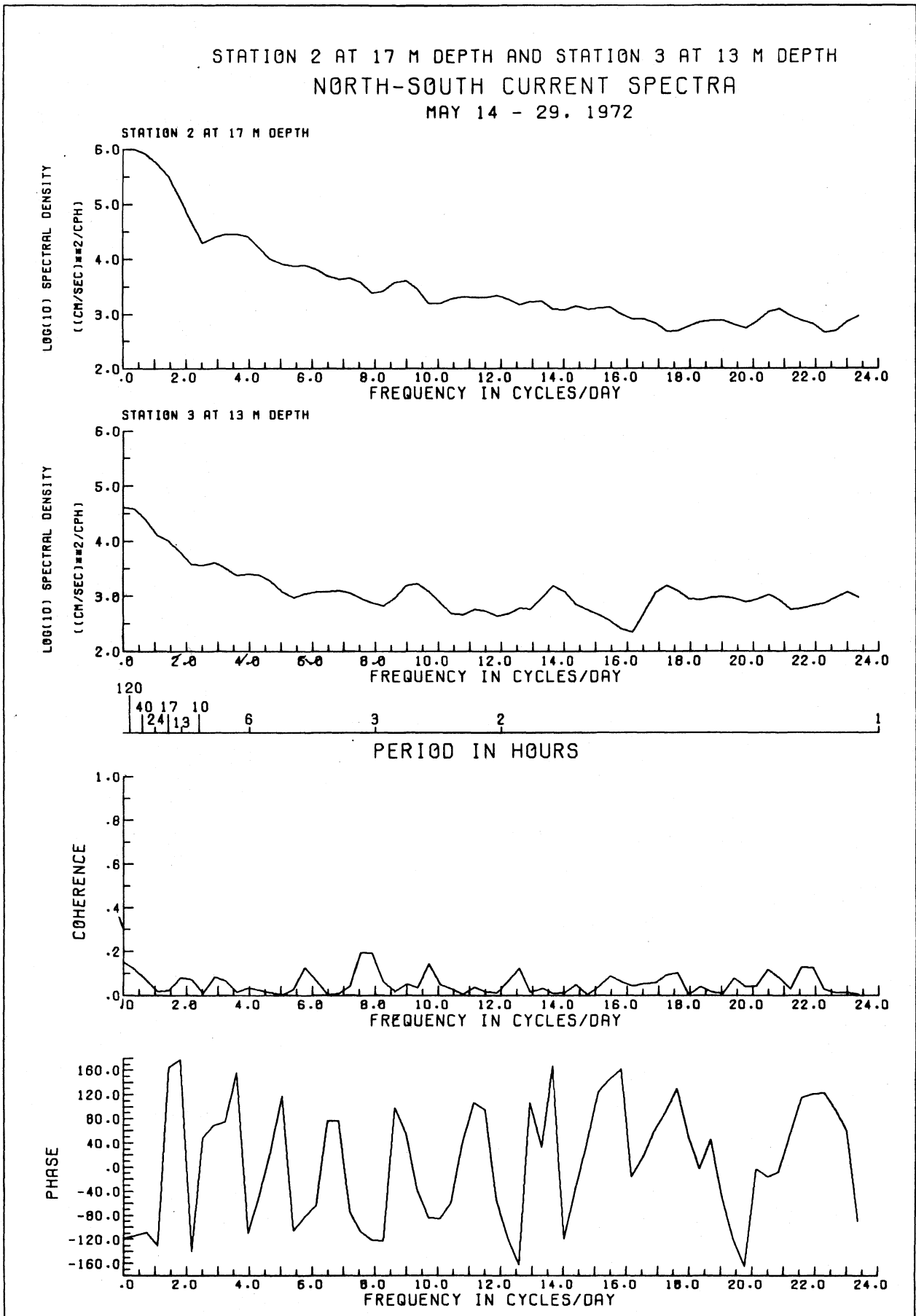


Figure 6.7 Spectra of E-W current components at Stations 2 and 3, 17 and 13 m, and coherence and phase difference between them, 14 to 29 May 1972.

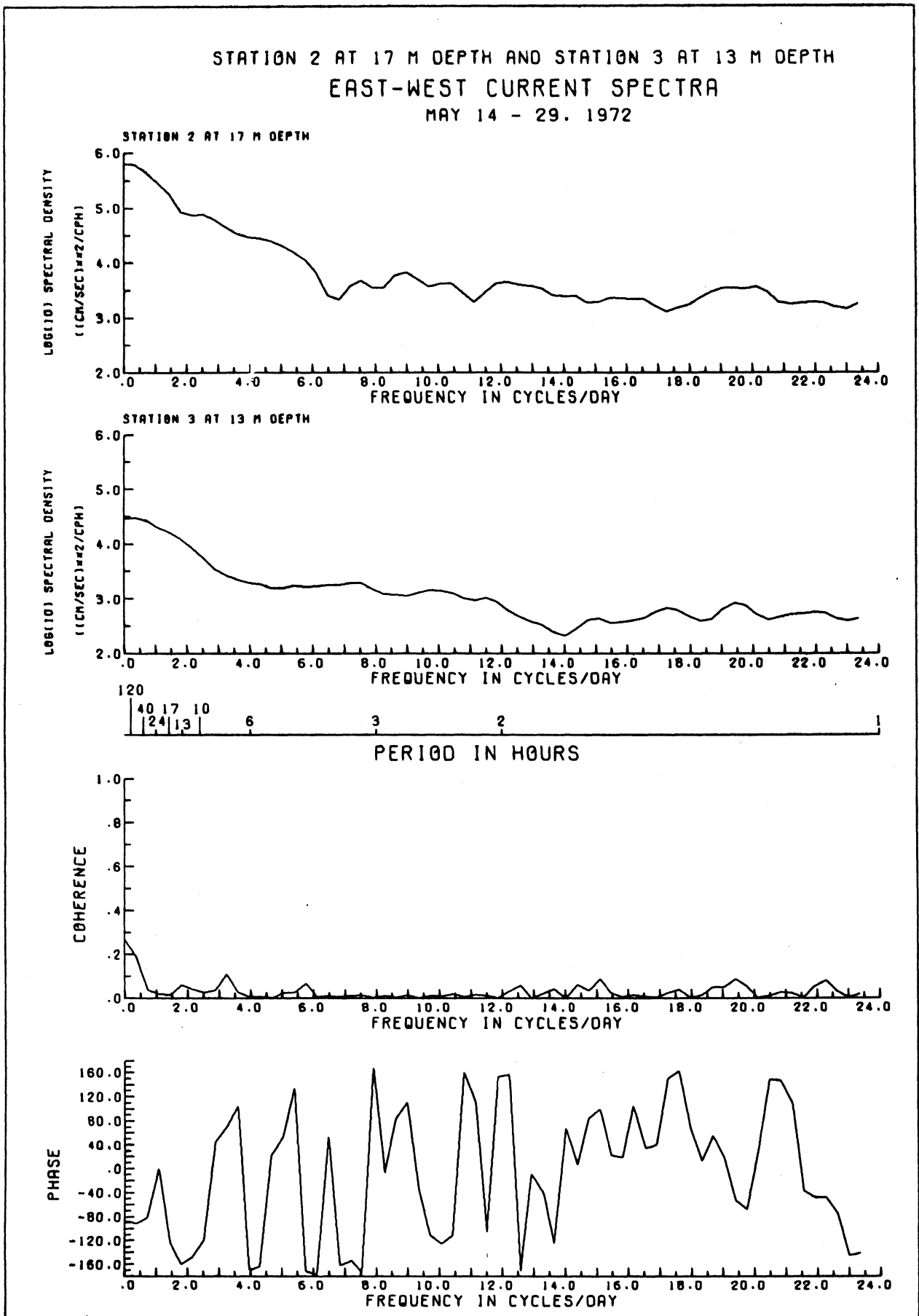


Figure 6.8 Spectra of temperature at Stations 2 and 3, 17 and 13 m, and coherence and phase difference between them, 14 to 29 May 1972.

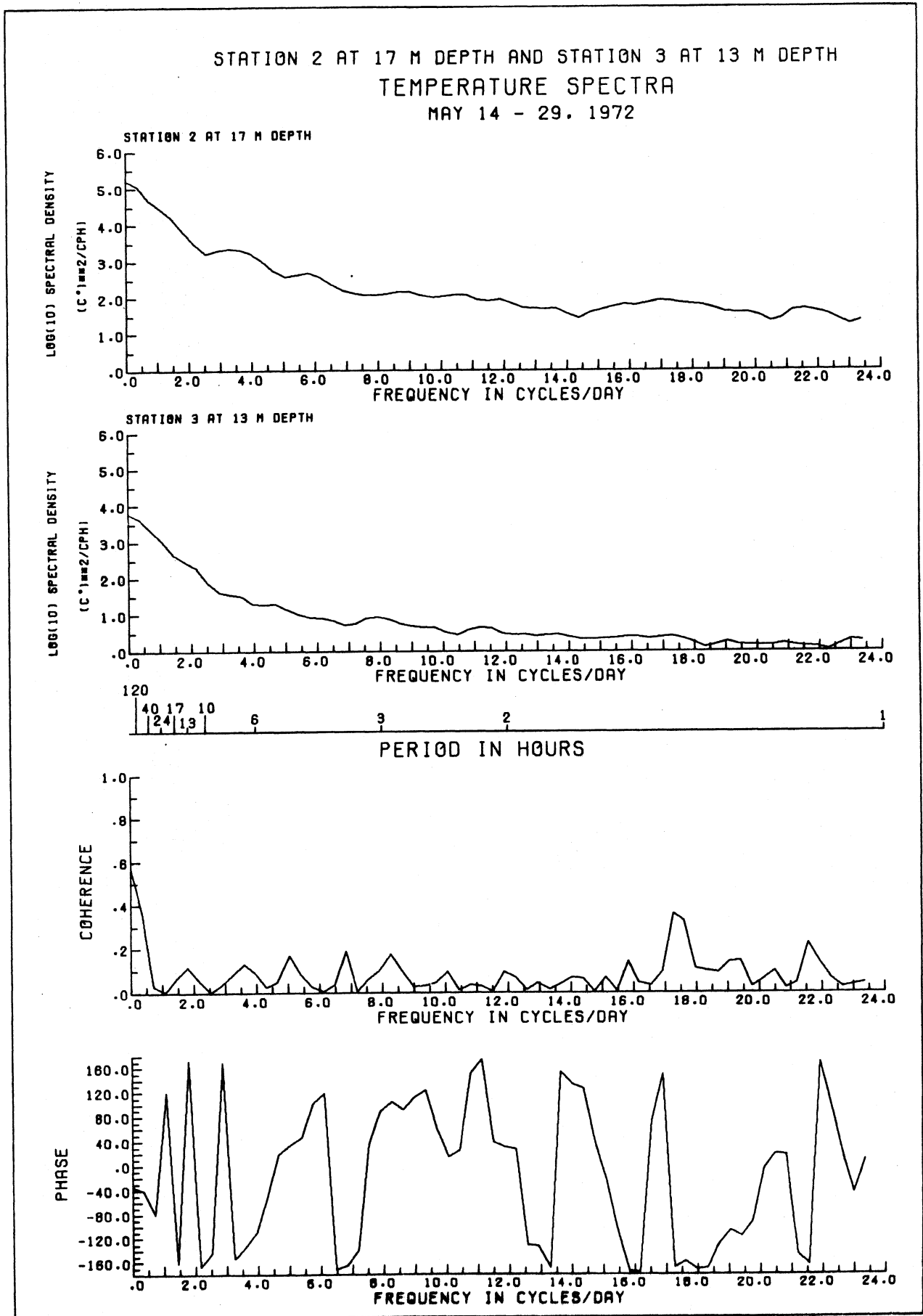


Figure 6.9 Spectra of N-S current components at Station 4, 16 and 23 m, and coherence and phase difference between them, 6 to 29 June 1972.

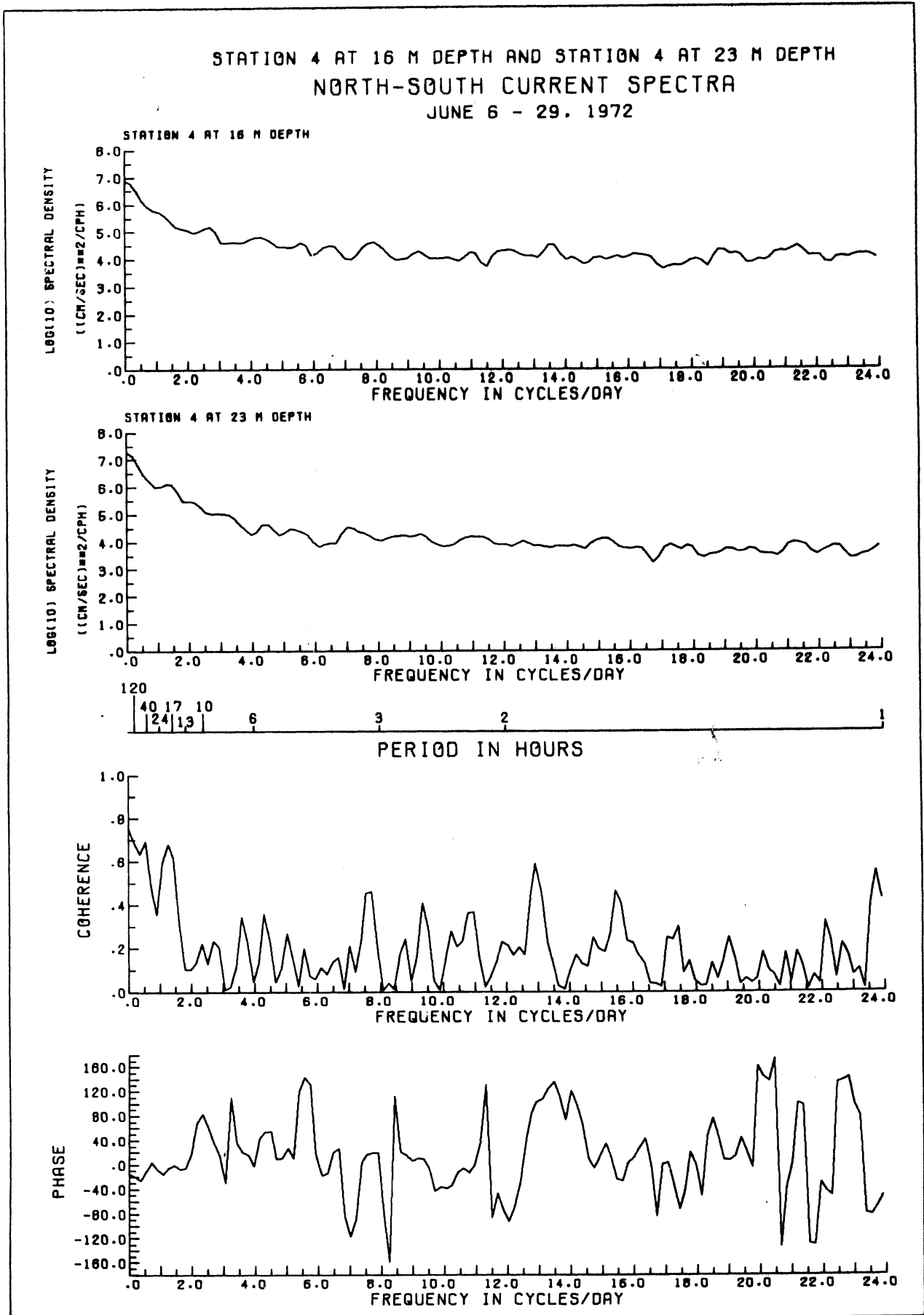


Figure 6.10 Spectra of E-W current components at Station 4, 16 and 23 m, and coherence and phase difference between them, 6 to 29 June 1972.

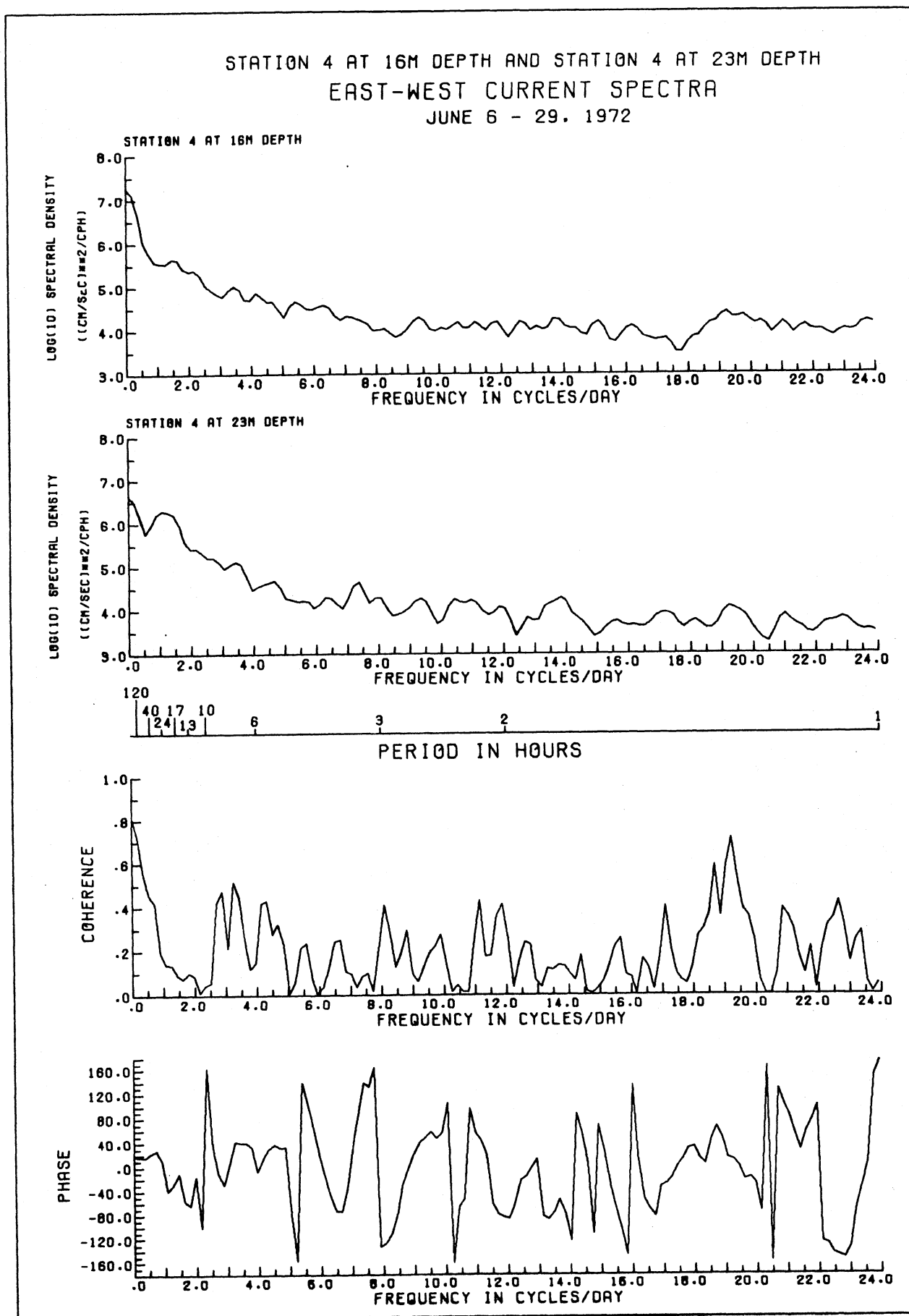


Figure 8.11 Spectra of temperature at Station 4, 16 and 23 m, and coherence and phase difference between them, 6 to 29 June 1972.

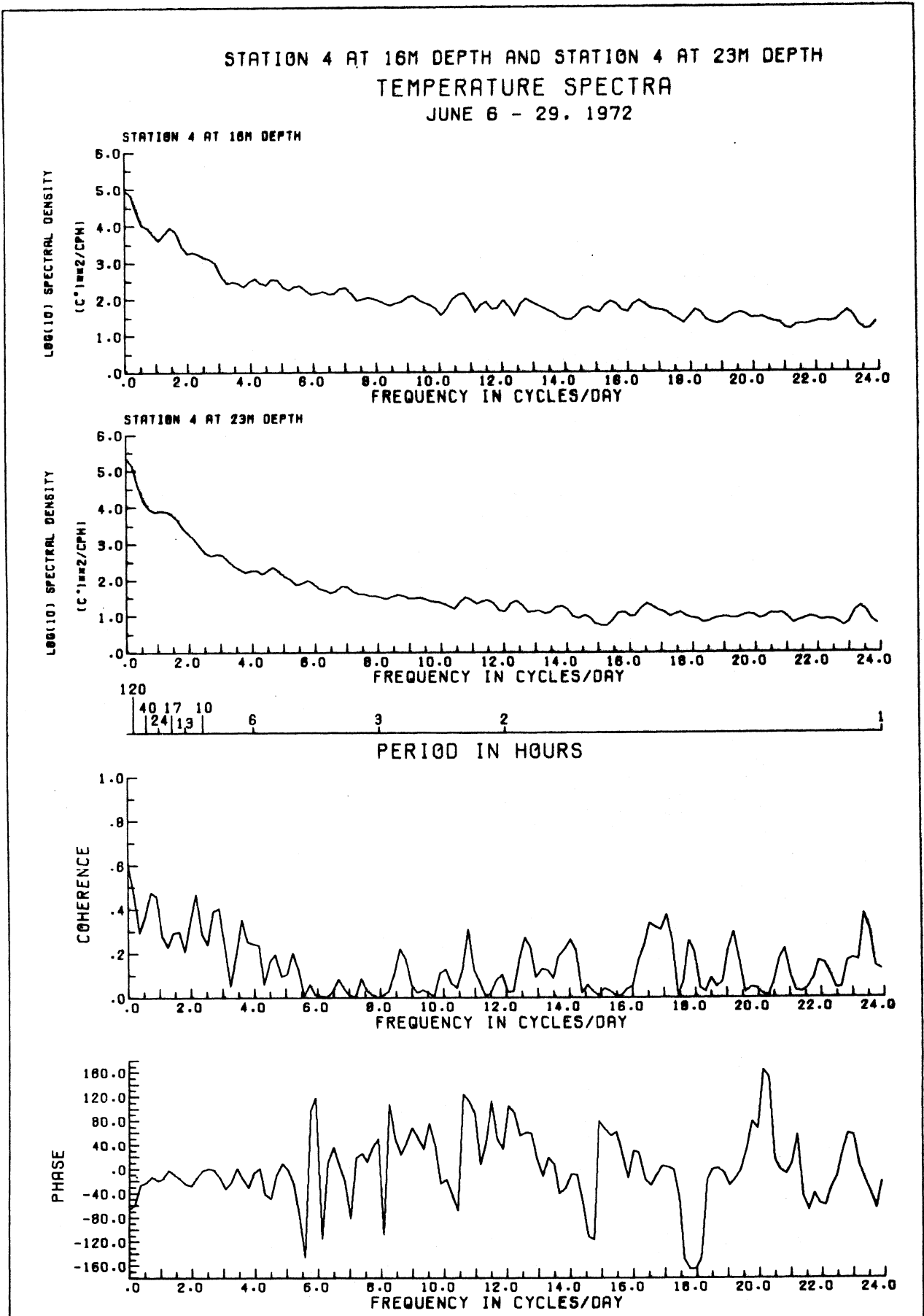


Figure 6.12 Spectra of N-S current components at Stations 5 and 4, 23 and 12 m, and coherence and phase difference between them, 18 July to 9 August 1973.

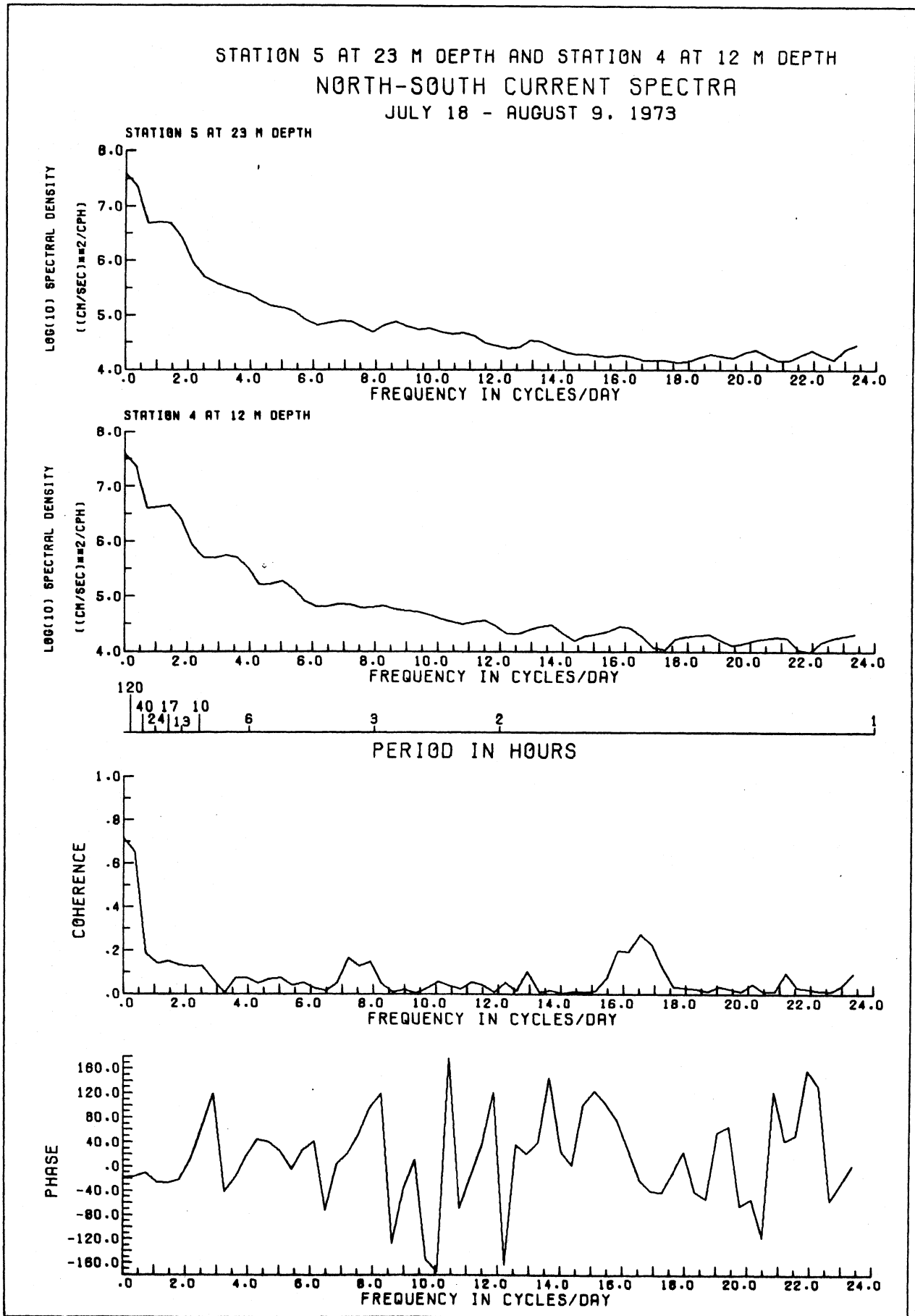
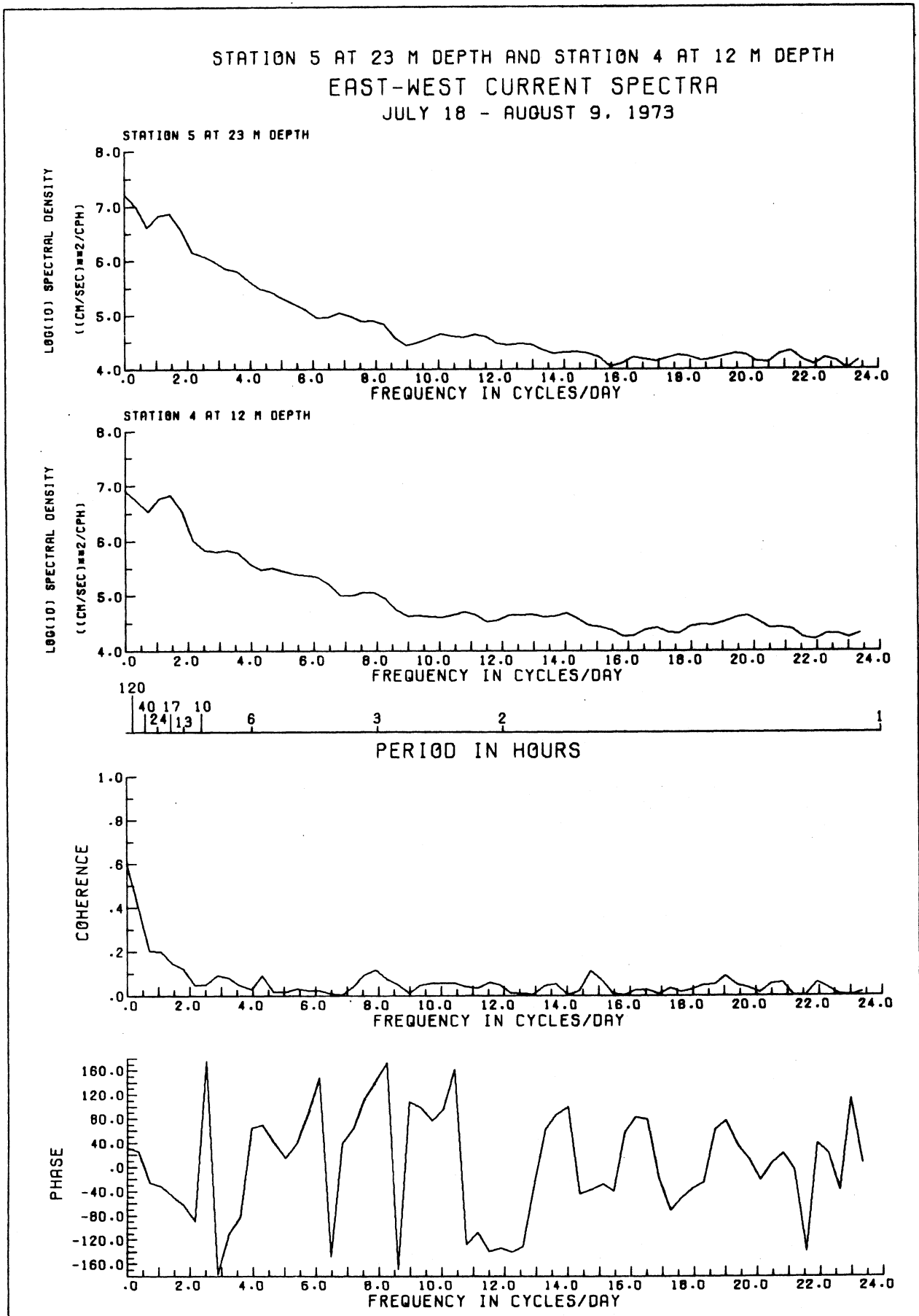


Figure 6.13 Spectra of E-W current components at Stations 5 and 4, 23 and 12 m, and coherence and phase difference between them, 18 July to 9 August 1973.



**Figure 6.14 Spectra of N-S current components at Stations 1 and 5, 15 and 23 m, and coherence and phase difference between them, 18 July to 8 August 1973.**

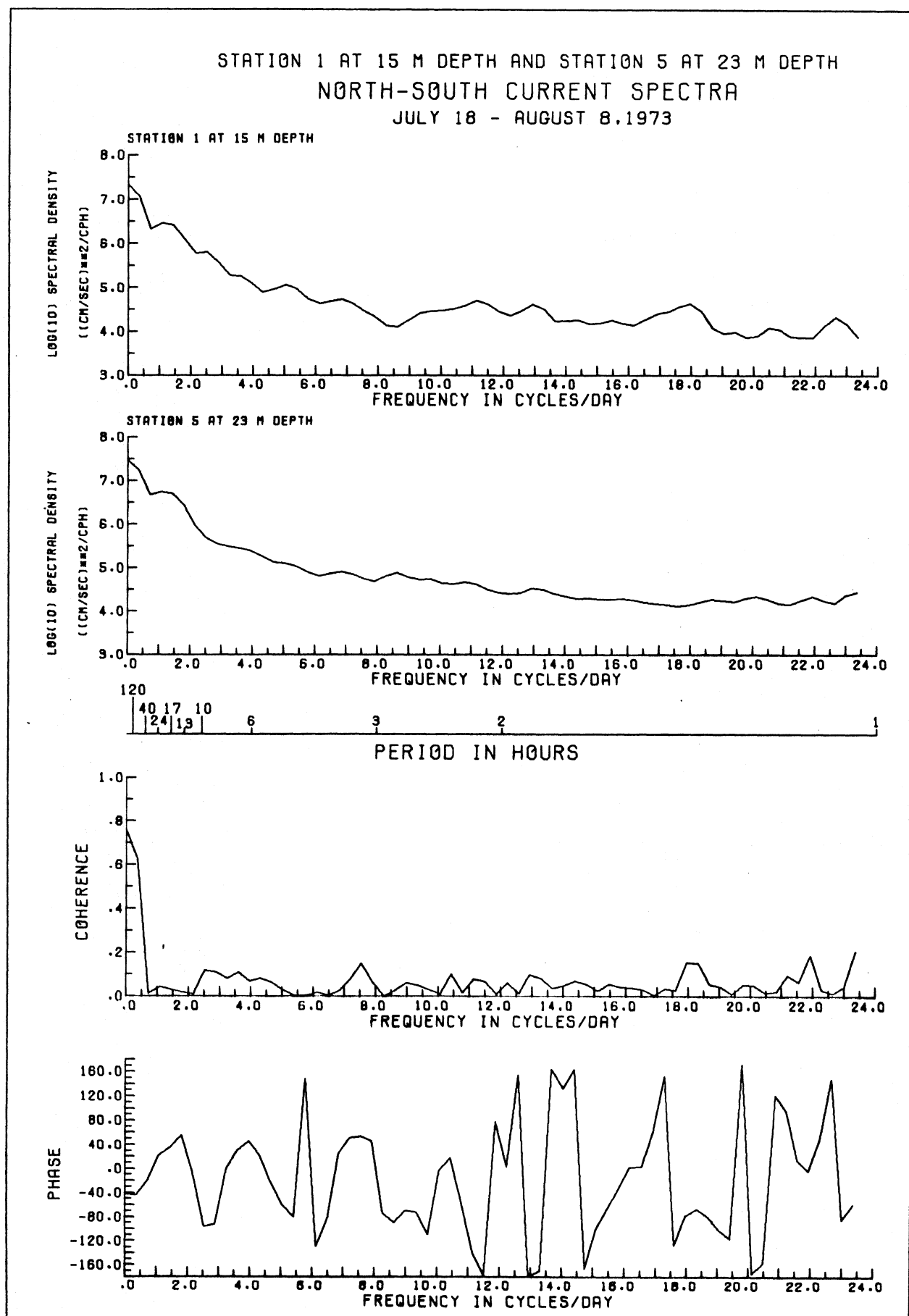


Figure 6.15 Spectra of E-W current components at Stations 1 and 5, 15 and 23 m, and coherence and phase difference between them, 18 July to 8 August 1978.

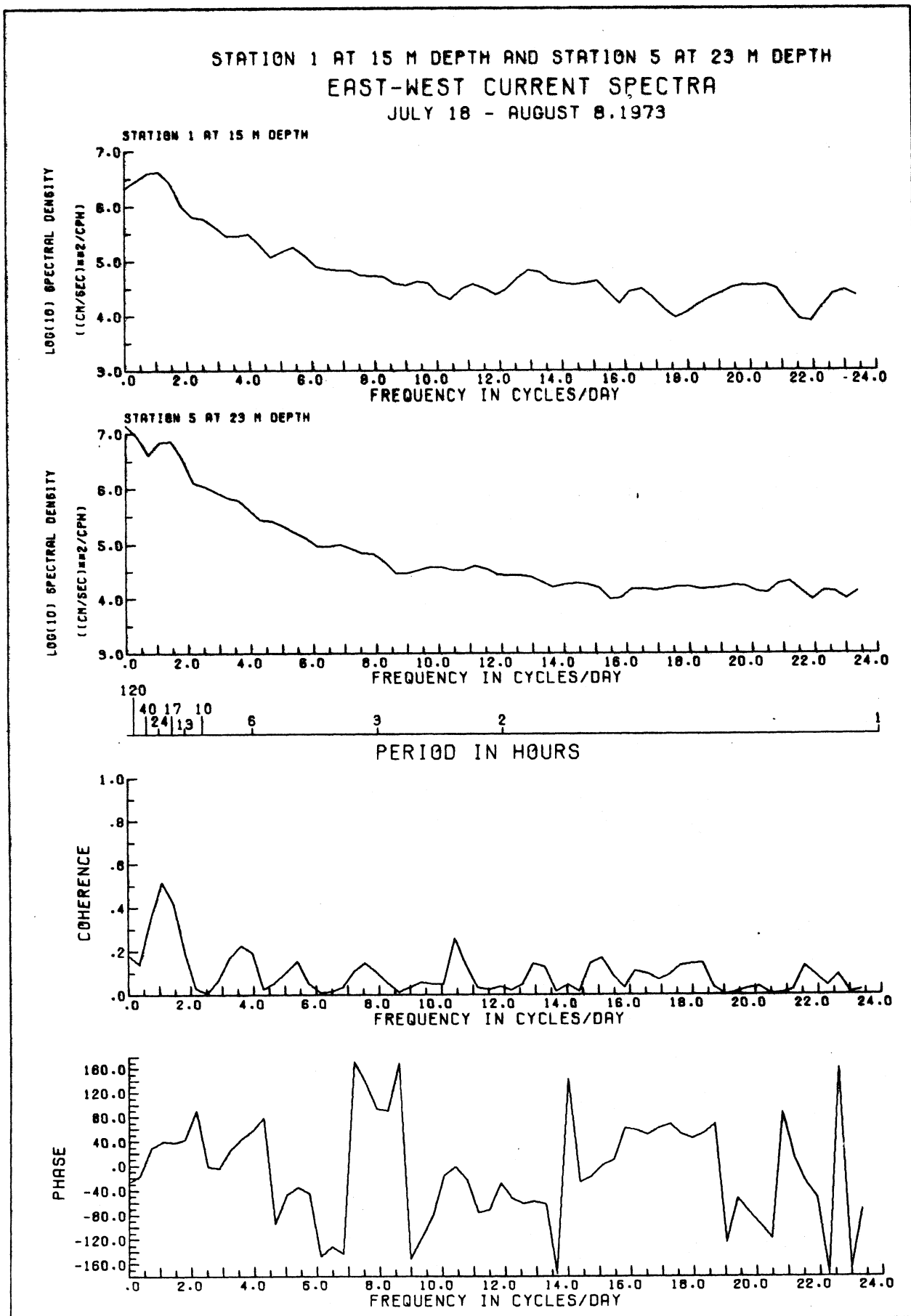
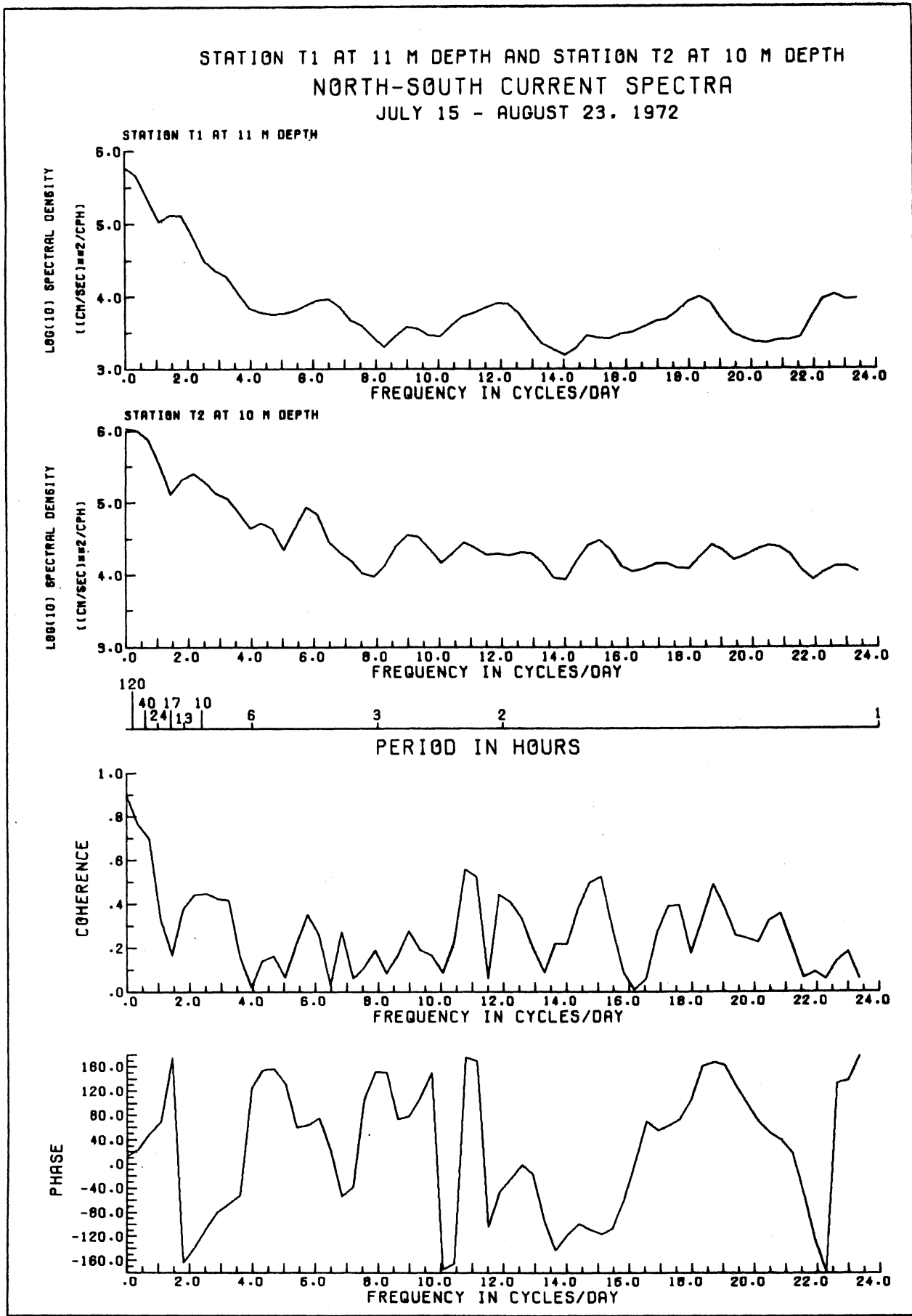




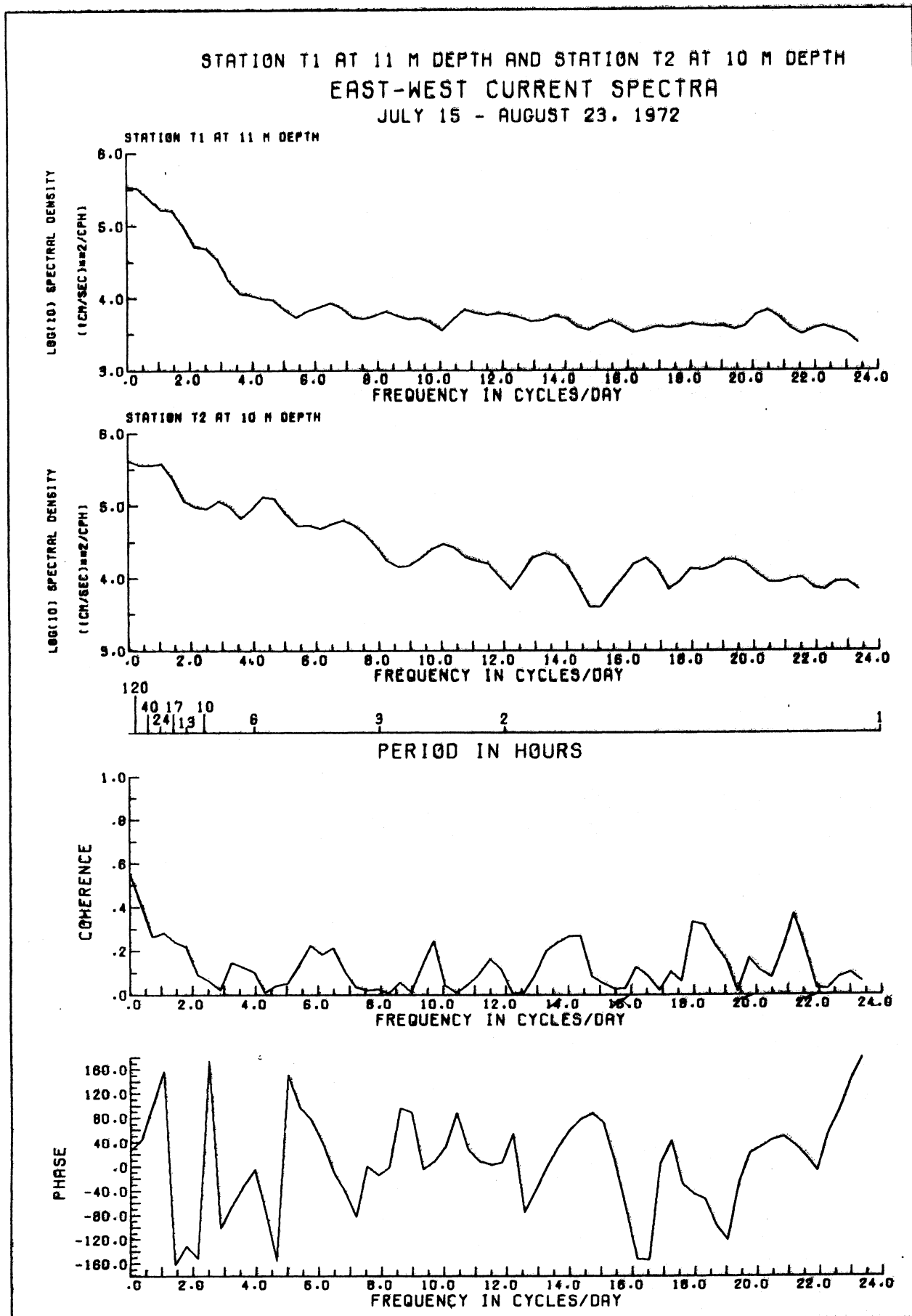
Figure 3.11 Spectra of N-S current components at stations 11 and 12, 11 and 10 m, and coherence and phase difference between them, 15 July to 23 August 1972.



For the mid-summer period in 1972 spectral comparisons are only available for Stations  $T_1$  (11 m) and  $T_2$  (10 m), N-S and E-W current components and temperature in figures 6.17 and 6.18, and 6.19 respectively. Near-inertial peaks or shoulders are absent from the spectra of these stations, an expected consequence of their shallow-water location. Again, spectral energy and interstation coherence is highest at the lowest frequency range, less than 1 cycle/day. The N-S current component (fig. 6.17) shows a subsidiary peak of possible tidal origin near 2.0 cycles/day, and out of phase between the stations, not shown by the E-W component or temperature.

In general, the concentration of spectral energy at the lowest frequencies and the lack of conspicuous or significant spectral peaks elsewhere is an indication of a long-period of quasi-steady current patterns with some "white noise" superimposed, but with no conspicuous or even recognizable high frequency modes of oscillation.

Figure 8.18 Spectra of E-W current components at stations T<sub>1</sub> and T<sub>2</sub>, 11 and 10 m, and coherence and phase difference between them, 15 July to 23 August 1972.





## REFERENCES

- Ayers, J. C., Chandler, D. C., Lauff, G. H., Powers, C. F. and E. B. Henson. 1958. Currents and water masses of Lake Michigan. Univ. Michigan, Great Lakes Res. Inst., Pub. No. 3.
- Beeton, A. M. and J. M. Barker. 1974. Investigation of the influence of thermal discharge from a large electric power station on the biology and nearshore circulation of Lake Michigan - Part A: Biology. Center for Great Lakes Studies, Univ. Wisconsin--Milwaukee, Spec. Rept. No. 18, 26 pp., 17 tables, 72 figs.
- Bellaire, F. R. 1963. Relation of winds, water levels and water temperatures, to currents in lower Lake Michigan. Proc. 6th Conf. Great Lakes Res., Univ. Michigan, Great Lakes Res. Div., Pub. No. 10, 219-230.
- Bennett, J. R. 1971. Thermally driven lake currents during the spring and fall transition periods. Proc. 14th Conf. Great Lakes Res., Internat. Assoc. Great Lakes Res., 535-544.
- \_\_\_\_\_. 1973(a). A theory of large-amplitude Kelvin waves. J. Phys. Oceanogr., 3: 57-60.
- \_\_\_\_\_. 1973(b). On the dynamics of wind-driven lake currents. Contr. No. 15, Marine Studies Center, Univ. Wisconsin--Madison, 85 pp.
- Birchfield, G. E. 1969. Preliminary numerical studies of wind-driven currents in the Lake Michigan-Huron basin. 12th Conf. Great Lakes Res., Ann Arbor, May, 1969, abstract only.
- \_\_\_\_\_ and V. E. Noble. 1969. Statistical analyses of currents at two near-by stations in Lake Michigan, Summer, 1967. Proc. 12th Conf. Great Lakes Res., Internat. Assoc. Great Lakes Res., 529-539.
- Blanton, J. O. 1974(a). Some characteristics of nearshore currents along the north shore of Lake Ontario. J. Phys. Oceanogr., 4: 415-424.
- \_\_\_\_\_. 1974(b). Nearshore lake currents measured during upwelling and downwelling of the thermocline in Lake Ontario (in press).
- \_\_\_\_\_ and C. R. Murthy. 1974. Observations of lateral shear in the nearshore zone of a Great Lake. J. Phys. Oceanogr., 4: 660-663.

- Boyce, F. M. 1974. Some aspects of Great Lakes physics of importance to biological and chemical processes. *J. Fish. Res. Bd. Canada*, 31: 689-730.
- Csanady, G. T. 1963. Turbulent diffusion in Lake Huron. *J. Fluid Mech.*, 17(3): 360-384.
- \_\_\_\_\_. 1967. Large-scale motion in the Great Lakes. *J. Geophys. Res.*, 72: 4151-4162.
- \_\_\_\_\_. 1970. Dispersal of effluents in the Great Lakes. *Wat. Res.*, 4: 79-114.
- \_\_\_\_\_. 1971(a). Baroclinic boundary currents and long edge-waves in basins with sloping shores. *J. Phys. Oceanogr.*, 1: 92-104.
- \_\_\_\_\_. 1971(b). On the equilibrium shape of the thermocline in the shore-zone. *J. Phys. Oceanogr.*, 1: 263-270.
- \_\_\_\_\_. 1972(a). Response of large stratified lakes to wind. *J. Phys. Oceanogr.*, 2: 3-13.
- \_\_\_\_\_. 1972(b). The coastal boundary layer in Lake Ontario: I, The spring regime; II, The summer and fall regime. *J. Phys. Oceanogr.*, 2: 41-53, 168, 176.
- \_\_\_\_\_. 1973. Wind-induced barotropic motions in long lakes. *J. Phys. Oceanogr.*, 3: 429-438.
- \_\_\_\_\_. 1974. Spring thermocline behavior in Lake Ontario during IFYGL. *J. Phys. Oceanogr.*, 4: 425-445.
- \_\_\_\_\_ and M. Mekinda. 1970. Rapid fluctuations of current direction in Lake Huron. *Proc. 13th Conf. Great Lakes Res.*, 397-412, Internat. Assoc. Great Lakes Res.
- \_\_\_\_\_ and B. H-G Pade. 1972. The coastal jet project, Annual Report, 1972. Report to the Dept. Environment, Canada Centre for Inland Waters, from the Environmental Fluid Mechanics Lab., Dept. Mechanical Engineering, Univ. Waterloo, Ontario, Canada.
- Davidson, D. R. and G. E. Birchfield. 1967. A case study of coastal currents in Lake Michigan. *Tech. Rept.*, Dept. Engineering Science, Tech. Inst., Northwestern Univ., Evanston, 14 pp., figs. and tables.

- Edsall, T. A. and T. G. Yocom. 1972. Review of recent technical information concerning the adverse effects of once-through cooling on Lake Michigan. U. S. Fish and Wildlife Sc., Great Lakes Fisheries Lab., Ann Arbor, Michigan (prepared for Lake Michigan Enforcement Conf., Sept., 1972, Chicago, Illinois).
- Great Lakes Fisheries Laboratory. 1970. Physical and ecological effects of waste heat on Lake Michigan. U. S. Bureau of Sport Fisheries and Wildlife in cooperation with U. S. Federal Water Quality Administration (prepared for Lake Michigan Enforcement Conf., 1970, Chicago, Illinois).
- Gunwaldsen, R. W., Brodfeld, B. and G. E. Hecker. 1971. Current and temperature surveys in Lake Ontario for James A. Fitzpatrick Nuclear Power Plant. Proc. 13th Conf. Great Lakes Res., Int. Assoc. Great Lakes Res. (in press).
- Hamblin, P. F. and G. K. Rodgers. 1967. The currents in the Toronto region of Lake Ontario. Great Lakes Inst., Univ. Toronto, PR 29, 133 mimeo. pp plus 10 plates.
- Harrington, M. W. 1894. Currents of the Great Lakes. U. S. Department of Agriculture, Weather Bureau, Bull., Washington, 6 pp plus 6 plates.
- Huang, J. C. K. 1971. The thermal current in Lake Michigan. J. Phys. Oceanogr., 1: 105-122.
- Johnson, J. H. 1960. Surface Currents in Lake Michigan 1954 and 1955. U. S. Fish and Wildlife Sc., Spec. Sic. Rept., Fish. No. 338.
- Kizlauskas, A. G. and P. L. Katz. 1973. A numerical model for summer flows in Lake Michigan. Arch. Met. Geophys. Bioklimatol., Wien (Vienna).
- Limnetics, Inc. 1974. An environmental study of the ecological effects of thermal discharges from Point Beach, Oak Creek, and Lakeside Power Plants on Lake Michigan (vols. 3 and 4). 4 vols. mimeo., commissioned by Wisconsin Electric Power Company.
- Malone, F. D. 1968. An analysis of current measurements in Lake Michigan. J. Geophys. Res., 73: 7065-7081.
- Monahan, E. C. 1973. Drogue measurements of the circulation in Grand Traverse Bay, Lake Michigan. Dept. Atmospheric and Oceanic Science, Sea Grant Program, Univ. Michigan, Tech. Rept. No. 35.

- Mortimer, C. H. 1963. Frontiers in physical limnology with particular reference to long waves in rotating basins. Proc. 5th Conf. Great Lakes Res., Univ. Michigan, Great Lakes Res. Div., Pub. No. 9: 9-42.
- \_\_\_\_\_. 1971. Large-scale oscillatory motions and seasonal temperature changes in Lake Michigan and Lake Ontario. Spec. Rept. No. 12, Center for Great Lakes Studies, Univ. Wisconsin--Milwaukee. Part I Text, 111 pp., Part II Illustrations, 106 pp., with the collaboration, in Chapter III on internal wave theory, of M. A. Johnson.
- \_\_\_\_\_. 1974. Lake hydrodynamics. Mitt. Intern. Ver. Limnol., 20: 124-197.
- Munk, W. H., Snodgrass, F. F. and M. J. Tucker. 1959. Spectra of low-frequency ocean waves. Bull. Scripps Inst. Oceanogr., La Jolla, California, U.S.A., 7: 283-362.
- Noble, V. E., Huang, J. C. and J. H. Saylor. 1968. Vertical current structure in the Great Lakes. Univ. Michigan Great Lakes Res. Div., Spec. Rept. No. 37.
- Palmer, M. D. 1973. Some kinetic energy spectra in a nearshore region of Lake Ontario. J. Geophys. Res., 78: 3585-3595.
- Ragotzkie, R. A. 1966. The Keweenaw current, a regular feature of summer circulation of Lake Superior. Tech. Rept. 29, Univ. Wisconsin--Madison, Dept. Meteorology, 30 pp.
- Rodgers, G. K. 1966. The thermal bar in Lake Ontario, spring 1965 and winter 1965-66. Proc. 9th Conf. Great Lakes Res., Univ. Michigan, Great Lakes Res. Div., Pub. No. 15: 369-374.
- Sato, G. K. 1969. Prediction of the time of disappearance of the thermal bar in Lake Ontario. M.A.S. thesis, School of Graduate Studies, Dept. Civil Engineering, Univ. Toronto.
- Scott, J. T. and L. Lansing. 1967. Gradient circulation in eastern Lake Ontario. Proc. 10th Conf. Great Lakes Res., Great Lakes Res. Div., Univ. Michigan, Pub. No. 60.
- \_\_\_\_\_. and D. Landsberg. 1969. July currents near the southern shore of Lake Ontario. 12th Conf. Great Lakes Res., Internat. Assoc. Great Lakes Res., 1969, 705-722.

- \_\_\_\_\_, Jekel, P. and M. W. Fenlon. 1971. Transport in the baroclinic coastal current near the south shore of Lake Ontario in early summer. Proc. 14th Conf. Great Lakes Res., Internat. Assoc. Great Lakes Res., 1971, 640-653.
- \_\_\_\_\_, Jekel, P., Landsberg, D. and V. Lemmin. 1973. U. S. IFYGL Coastal Chain Program: Report 1a: Basic data for the Oswego coastal chain. Atmospheric Sciences Res. Ctr., Rept. No. 227a. State Univ. New York at Albany, 1400 Washington Avenue, Albany, N.Y. 12222.
- Smith, N. P. and R. A. Ragotzkie. 1970. A comparison of computed and measured currents in Lake Superior. Proc. 13th Conf. Great Lakes Res., Internat. Assoc. Great Lakes Res., 1970, 969-977.
- Simons, T. J. 1973. Development of three-dimensional numerical models of the Great Lakes. Sci. Ser. No. 12, Canada Centre for Inland Waters, 26 pp.
- \_\_\_\_\_. 1974. Verification of numerical models of Lake Ontario: Part I, Circulation in spring and early summer. J. Phys. Oceanogr., 4: 507-523.
- Terrell, R. E. and T. Green. 1972. Investigations of the surface velocity structure of lake currents. Limnol. Oceanogr., 17: 158-160.
- Tikhomirov, A. I. 1963. The thermal bar in Lake Ladoga. Bull. (Izvestiya), All Union Geogr. Soc. 95: 134-142. (Amer. Geophys. Un. Trans., Soc. Hydrol., Collected Papers No. 2).
- U. S. Department of the Interior, FWPCA. 1967. Lake Michigan basin, lake currents. U. S. Dept. Interior, FWPCA, Great Lakes Region, Chicago, mimeo., 364 pp.
- Van Oosten, J. 1963. Surface currents of Lake Michigan, 1931 and 1932. Spec. Sci. Rept. -- Fish. No. 413, Fish and Wildl. Sc., U.S. Dept. Interior.
- Verber, J. L. 1966. Inertial currents in the Great Lakes. Proc. 9th Conf. Great Lakes Res., Univ. Michigan, Great Lakes Res. Div., Pub. No. 13: 375-379.

## FIGURE LEGENDS AND TABLE HEADINGS

In a report as bulky as this, unnecessary padding must be eschewed. Complete lists of figure legends and table headings are needed only when a manuscript is sent to a printer; but in this report the full legend is already typed or drawn on each of the 218 figures; and therefore all that is needed here is a classification by category and by individual page number reference.

Chapter 1. Currents observed or computed in other investigations: figures 1.1 to 1.14, pp. 3, 4, 6, 9, 10, 13, 14, 16, 18, 20, 21, 22, 26, 28.

Chapter 2. Map of station locations: figure 2.1, p. 34; equipment figures 2.2 to 2.8, 36/37, 39, 40, 43/44; flow charts of data reduction and analysis, figures 2.6 to 2.8, pp. 51, 56, 57, table 2.1 heading p. 46.

Chapter 3. Monthly diagrams of current speed and directions and water temperatures in Lake Michigan at Oak Creek, compared with wind speed and direction at Mitchell Field. See table 2.1. pp. 46 to 48, for information on which instruments were operating and when, during the following Surveys:

Survey I: figures 3.1 to 3.3, pp. 64 to 66, 3.4 to 3.6, pp. 68 to 70, 3.7 to 3.11, pp. 72 to 76.

Survey II: figures 3.12 to 3.24, pp. 78 to 90, 3.25 to 3.29, pp. 93 to 97, 3.30 to 3.35, pp. 99 to 104.

Survey III: figure 3.36, p. 106, figure 3.37, p. 107, figures 3.38 to 3.43, pp. 109 to 115, figures 3.44 to 3.46, pp. 117 to 119.

Survey IV: figures 3.47 to 3.53, pp. 121 to 127, 3.54 to 3.60, pp. 129 to 135, 3.61 to 3.64, pp. 138 to 141.

Surveys V and VI: figures 3.65 to 3.70, pp. 142 to 147, 3.71 to 3.77, pp. 149 to 155.

Chapter 4. Vector frequency diagrams of wind (VFW), vector frequency diagrams of current (VFC), and progressive vector diagrams of current (PVC). See table 2.1, pp. 46 to 48, for information on which instruments were operating and when, during the following Surveys:

Survey I: VFW figures 4.1, p. 160, 4.4, p. 163, 4.14, p. 174.

VFC figures 4.2, p. 161, 4.3, p. 162, 4.5, p. 164, 4.7, p. 166, 4.9, p. 168, 4.11, p. 170, 4.13, p. 172, 4.16 to 4.20, pp. 175 to 179.

PVC figures 4.6, p. 165, 4.8, p. 167, 4.10, p. 169, 4.12, p. 171, 4.14, p. 173.

Survey II: VFW figures 4.21, p. 181, 4.32, p. 192, 4.39, p. 200, 4.44, p. 206.

Chapter 4, Survey II (continued):

VFC figures 4.22, p. 182, 4.24, p. 184, 4.26, p. 186, 4.28 to 4.31, pp. 188 to 191, 4.33, p. 193, 4.34, p. 194, 4.35, p. 196, 4.37, p. 198, 4.40, p. 202, 4.42, p. 204, 4.44 to 4.46, pp. 206 to 208.

PVC figures 4.23, p. 183, 4.25, p. 185, 4.27, p. 187, 4.36, p. 197, 4.38, p. 199, 4.41, p. 203, 4.43, p. 205.

Survey III: VFW figures 4.47, p. 209, 4.52, p. 214, 4.55, p. 217.

VFC figures 4.48, p. 210, 4.50, p. 212, 4.53, p. 215, 4.54, p. 216, 4.56, p. 218.

PVC figures 4.49, p. 211, 4.51, p. 213.

Survey IV: VFW figures 4.57, p. 220, 4.62, p. 225, 4.71, p. 236.

VFC figures 4.58 to 4.61, pp. 221 to 224, 4.63, p. 266, 4.65, p. 228, 4.67, p. 230, 4.69, p. 232, 4.72, p. 237, 4.73, p. 238, 4.75, p. 240.

PVC figures 4.64, p. 227, 4.66, p. 229, 4.68, p. 231, 4.70, p. 233, 4.74, p. 239.

Surveys V and VI: VFW figures 4.76, p. 241, 4.87, p. 252.

VFC figures 4.77, p. 242, 4.79, p. 244, 4.81, p. 246, 4.83, p. 248, 4.85, p. 250, 4.88 to 4.91, pp. 253 to 256.

PVC figures 4.78, p. 243, 4.80, p. 245, 4.82, p. 247, 4.84, p. 249, 4.86, p. 251, 4.92, p. 257.

Chapter 5. Intake and discharge at power plant, figure 5.1, p. 258; map of area covered by sinking plume survey, figure 5.2, p. 261; plume surveys, figures 5.3 to 5.7, pp. 262, 264, 266, 267, 269; infrared image of plume, figure 5.8, p. 270.

Chapter 6. Representative current response to wind change, figure 6.1, p. 279; spectra and cross-spectra of wind and current components, figures 6.1, p. 281, 6.3 to 6.5, pp. 289 to 291, 6.6 to 6.17, pp. 293 to 304, 6.18, p. 306, 6.19, p. 307, table headings 6.1 to 6.5, pp. 274, 275, 277, 282, 284.



